The ‘fatus’ of East Timor: stratigraphy and structure

Aaron Benincasa

BSc (Hons)

Submitted in fulfilment of the requirements for the degree of Doctor of Philosophy of the University of Western Australia

School of Earth and Environment

Supervisors: Prof. Myra Keep, Prof. David W. Haig

Submitted: January 2015

Abstract

Timor Island, situated approximately 600 km north of northwest Australia, is the orogenic product of the collision of the northern edge of the Australian continental plate with the Banda volcanic arc. Collision has produced a complex fold and thrust belt comprising rocks of the Australian continental margin, rocks of Asiatic affinity, and more recent synorogenic deposits. East Timor occupies the eastern half of Timor Island.

Across Timor Island, a strike-parallel chain of steep-sided limestone massifs, known locally as 'fatus', form high peaks in both East and West Timor. Despite many early workers observing most 'fatu' limestones to be dominantly Triassic in age, most modern literature follows the reconnaissance mapping of Audley-Charles (1968) in interpreting the fatus of East Timor as coherent blocks of Miocene limestone. This study is based on 6 months of detailed field mapping on and around the major fatus of East Timor, including: Mount Mundo Perdido, Mount Laritame, the Builo Range, Mount Bibileu, the Paitchau Range and Lake Iralalaru region, the Matebian Range, Mount Taroman, Mount Loelako, the Saburai Range and the greater Maliana basin region.

Findings from this study differ markedly with most current stratigraphic and structural interpretations of the fatus. The central regions of all fatus studied are observed to comprise either Late Triassic or Early Jurassic shallow water limestones of Australian affinity, associated with a complex range of other lithologies including Triassic-Jurassic interior-rift basin deposits, Cretaceous to Oligocene pelagites, limestones and volcanics of Asiatic affinity, and Plio-Pleistocene synorogenic deposits.

Detailed structural mapping shows that the fatus of East Timor are dominated by recent, high angle, oblique-slip and strike-slip faults present at all scales, that have been active into the Pleistocene and control the present-day topography. The fault architecture and stratigraphic distributions in the study areas are comparable to pop-up structures and pull-apart basins developed at restraining and releasing bends or step-overs in zones of strike-slip, both in scaled sandbox models, and strike-slip systems elsewhere in the world.

Strike-slip faulting, common at convergent margins, has been postulated in East Timor by previous workers but this study is the first to detail and map extensive, recent, strike-slip deformation throughout the country. Interpretations of young strike-slip in East Timor correlate well with reports of young, left-lateral strike-slip deformation across the Timor Sea and Browse Basin of the adjacent North West Shelf of Australia.

The outcome of this study is a more detailed stratigraphic and structural interpretation of the fatus of East Timor, based on extensive field mapping and robust biostratigraphy, which makes an important contribution to the understanding of the stratigraphy and tectonics of the entire Timor region and the adjacent Banda Arc. The finding that the fatus are not Miocene in age, nor from the Banda side of the plate boundary, means that many tectonic models proposed for the region are incorrect. In addition, many previous models do not include the presence or effects of late, high-angle faulting, which dismembers any previous collision geometries. This study provides detailed mapping based on robust biostratigraphic ages to present a tectonic model for Timor that involves plate boundary-parallel strike slip as an active and important component of deformation along this segment of the Banda Arc.

Table of Contents

Appendix III – A. Benincasa, M. Keep & D. W. Haig (2012): A restraining bend in a young collisional margin: Mount Mundo Perdido, East Timor, Australian Journal of Earth Sciences: An International Geoscience Journal of the Geological Society of Australia, 59:6, 859-876

Including:

Mundo Perdido paper Appendix A - Lithostratigraphic units and age diagnostic fossils recognised at Mount Mundo Perdido

Mundo Perdido paper Appendix B - XRF analysis of volcanic and metamorphic samples.

Acknowledgements

This PhD was completed as part of the Eni Australia ex Eni Timor Leste funded project: *Petroleum Prospectivity of Timor Leste*, and I am grateful for their support. I also received an Australian Postgraduate Award and University of Western Australia Top-up Scholarship during my candidacy.

Thank you first and foremost to Myra Keep and David Haig, who have led the Timor research group at the University of Western Australia for the past decade. Myra's enthusiasm for the challenges of East Timorese geology during third year structural geology lectures is what started me down the path to this PhD nearly 7 years ago, and without her guidance and support I would never have been able to complete the journey. Thanks for always being there, even when I wasn't the easiest student. Thanks to David Haig for being a fount of expert geological knowledge, and for being so willing to share it with his students. He is one of the finest scientists I have known, and I suspect ever will.

This project involved many months of fieldwork in East Timor, often under less than ideal conditions, and I have numerous people to thank for helping me get the data from the rocks to this thesis. Thank you Norberta da Costa, Director, and all the staff at the National Directorate of Geology and Mineral Resources in the Secretariate for Energy and Natural Resources for your continuing support. Thanks to thanks to Tony Heynen and Jose Sabino at Eni Timor Leste for their assistance in Dili, and for being so helpful with storage, and ready access to, our field equipment. Thanks to all the staff at the Timor Leste Geological Survey, it was a real pleasure spending time in the field with such an enthusiastic group of geologists.

During my time in Timor I travelled through almost every district, and had fieldwork facilitated by the National Police of Timor Leste (PNTL), along with countless District Administrators, Sub-district Administrators, Suco Chiefs and Aldeia Chiefs, too many to name by person. I am incredibly grateful for all your help. I would particularly like to note the large number of Aldeia Chiefs who personally spent time with me in the field, and showed a keen interest in the science that we were doing, your enthusiasm for our work was extremely encouraging.

Thank you to everyone who worked with me in the field. Thanks to Eujay McCartain, who was with me for my first few days of fieldwork back in 2009, and showed me how a field trip to East Timor is done (and thanks also for your encouragement, and example, over the next few years!). Thanks to Gilsel Borges for your help and friendship, it was great taking on Mundo Perdido and Laritame together. Thanks to Manuel Hornai Gonsalves, who was with me every step of the way. Thanks to Atino Varela, for your help in the 2011 season. Thanks to Brendan Duffy for your friendship in the field, I'll never forget you helping me out of that landslide in 2010! Most of all, thanks to Andy Monteiro, who started as my assistant at the end of 2009, and became my dear friend. Without Andy I would not have been able to complete this fieldwork to the standard that I have, and I am so pleased that he has now gone on to pursue his own career in geology.

Back in Perth, thanks to Lorraine and Bill Wilson for your help in the UWA labs, and to Bill for facilitating the quarantine process for my many kilograms of rock samples.

Thanks to Dr Jack Grant-Mackie for helping me identify the brachiopods from Loelako.

Thank you to my employer of the past year, Shell Development Australia, for their support and understanding as I have attempted to finish this project. Thanks in particular to Lisa Thieme and Carsten Buker for their sustained encouragement, and for being so accommodating over the past few months during this final push to the finish line.

Thanks to my friends and family for all their support, even though the PhD has taken up so much of my time. Thanks in particular to Stephen French, whose unwavering belief that I would get this done was much stronger than my own a lot of the time.

Finally and most importantly, thanks to Louise, my wife and partner for the past 6 years. In many ways our relationship began in the mountains around Ossu, and my work in Timor has been a big part of our life (and my time) for our entire relationship. Thank you for your love, understanding and support, particularly over the last few months, I could not have done this without you. It's a little late, but I finally got you that paper anniversary gift.

1. Introduction

1.1 Introduction

Timor Island, formed at the collisional front between the northern edge of the Australian Plate and the Banda Arc (**Fig. 1**) provides an ideal setting to study the processes of recent orogenesis (e.g. Hall & Wilson 2000; Milsom 2000; Audley-Charles 2004; Harris 2006; Keep & Haig 2010). Collisional shortening juxtaposes rocks of the Australian continental margin against remnants of the pre-collisional arc and synorogenic deposits (Audley-Charles 2004; Harris 2006) (**Fig. 2**). Despite the resulting orogenic pile being described as "tectonic chaos" (Fitch & Hamilton 1974; Hamilton 1979) biostratigraphic analyses (e.g. Haig & McCartain 2007; Haig *et al.* 2007; Haig *et al.* 2008; Haig 2012a) have enabled documentation of three distinct orogenic phases (Keep & Haig 2010). These include initial shortening with associated diapirism (9.8–5.7 Ma), a tectonic quiet interval possibly representing the time of locking of the subduction zone

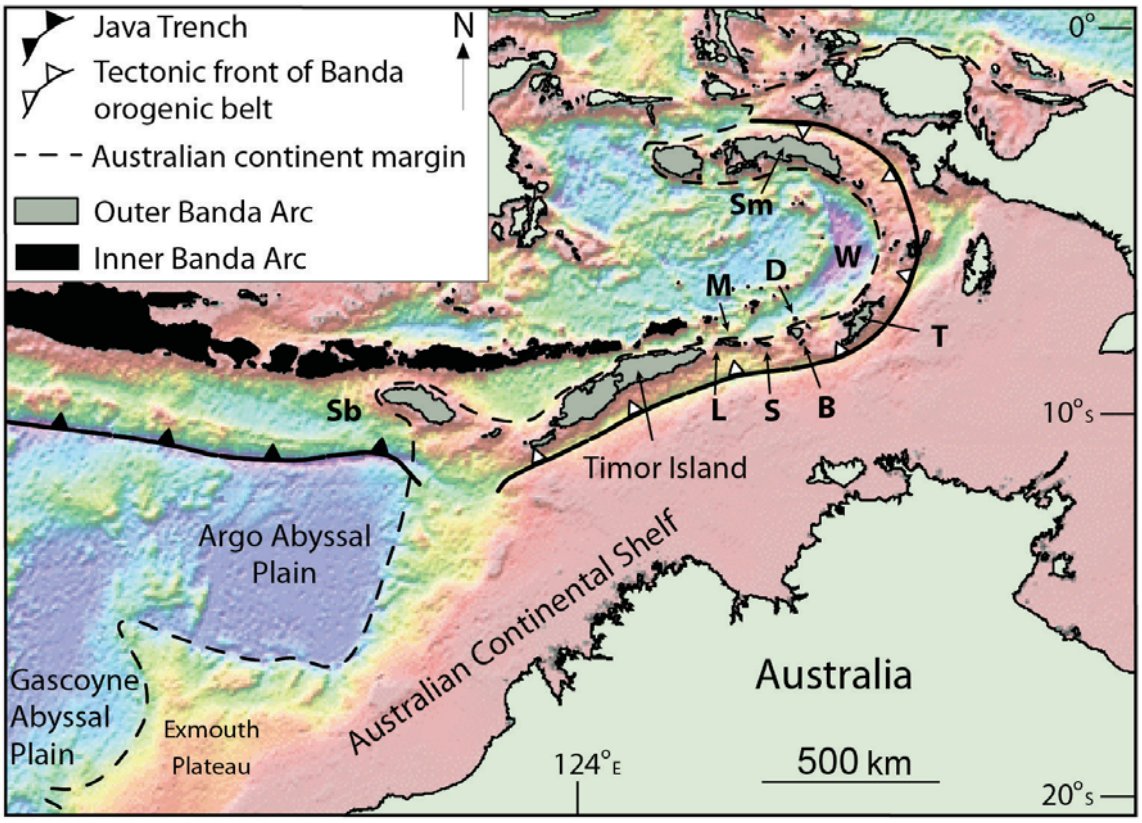

Fig. 1. Location map illustrating the tectonic setting of Timor Island and the main physiographic elements of the region. The dashed line around the Outer Banda Arc estimates the position of underthrust Australian continental crust in this region.

(5.7–4.5 Ma) and a post-4.5 Ma phase of uplift, unroofing and additional diapirism (Keep & Haig 2010; Haig 2012a). Structures developed through early thrusting during Phase 1 (e.g. Carter *et al.* 1976; Harris & Audley-Charles 1987) have since been overprinted by later high-angle faulting during Phase 3 (Chamalaun & Grady 1978; Charlton *et al.* 1991; Keep & Haig 2010).

Across Timor Island, a strike-parallel chain of steep-sided limestone massifs, known locally as 'fatus' (**Fig. 2**), form high peaks in both East and West Timor (e.g. Wanner 1913; De Roever 1940; Simons 1940; Tappenbeck 1940; van West 1941; Brouwer 1942; De Waard 1957; Audley-Charles 1968). Bahaman facies oolitic wackestones, packstones and grainstones common to many fatus were interpreted as shallow water Miocene deposits by Audley-Charles (1968, pp. 25–27) and included in the 'Cablac Limestone', which had its type locality at the Cablac Mountain Range (location 7 on **Fig. 2**). Following this interpretation the 'Cablac Limestone' fatus of East Timor have since been variably assigned to allochthonous thrust sheets of Asiatic affinity (Audley-Charles 2004; Harris 2006), carbonate build-ups on the outer Australian continental margin (Charlton 2002b), or in situ patch reefs formed after collision but before orogenesis (Audley-Charles & Carter 1972). More recent detailed field mapping (Haig *et al.* 2007; Haig *et al.* 2008; Keep *et al.* 2009) has documented a Late Triassic–Early Jurassic (i.e. not Miocene) age for the Bahaman facies at Cablac Mountain Range. This revision of the 'Cablac Limestone' at its type locality has prompted the present study: an examination of other mapped 'Cablac Limestone' fatus throughout East Timor, in order to assess their age and structural relationships. Investigating the development of the fatu chain may provide important insights into the structural evolution of Timor Island.

Fig. 2 → Schematic geological map of Timor Island, illustrating the generalised distribution of the main megasequences in East and West Timor prior to this study, modified from Haig et al. (2008). The locations of all 'Cablac Limestone' fatus investigated as part of this study are shown: Mount Mundo Perdido (1), Mount Laritame (2), the Matebian Range (3), the Builo Range (5), Mount Bibileu (6), Mount Taroman (9), and Mount Loelako (10), along with the Cablac Range (7), the site of previous investigations by Haig & Keep (Haig et al. 2007, 2008, Keep et al. 2009). This study also investigated two major fatus not originally mapped as 'Cablac Limestone': the Paitchau Range (4) and the Saburai Range (8), currently mapped as Triassic and Permian Australian affinity rocks respectively. Inset: the steep-sided, blocky, 'fatu'-style morphology of Mount Mundo Perdido (1) and Mount Laritame (2).

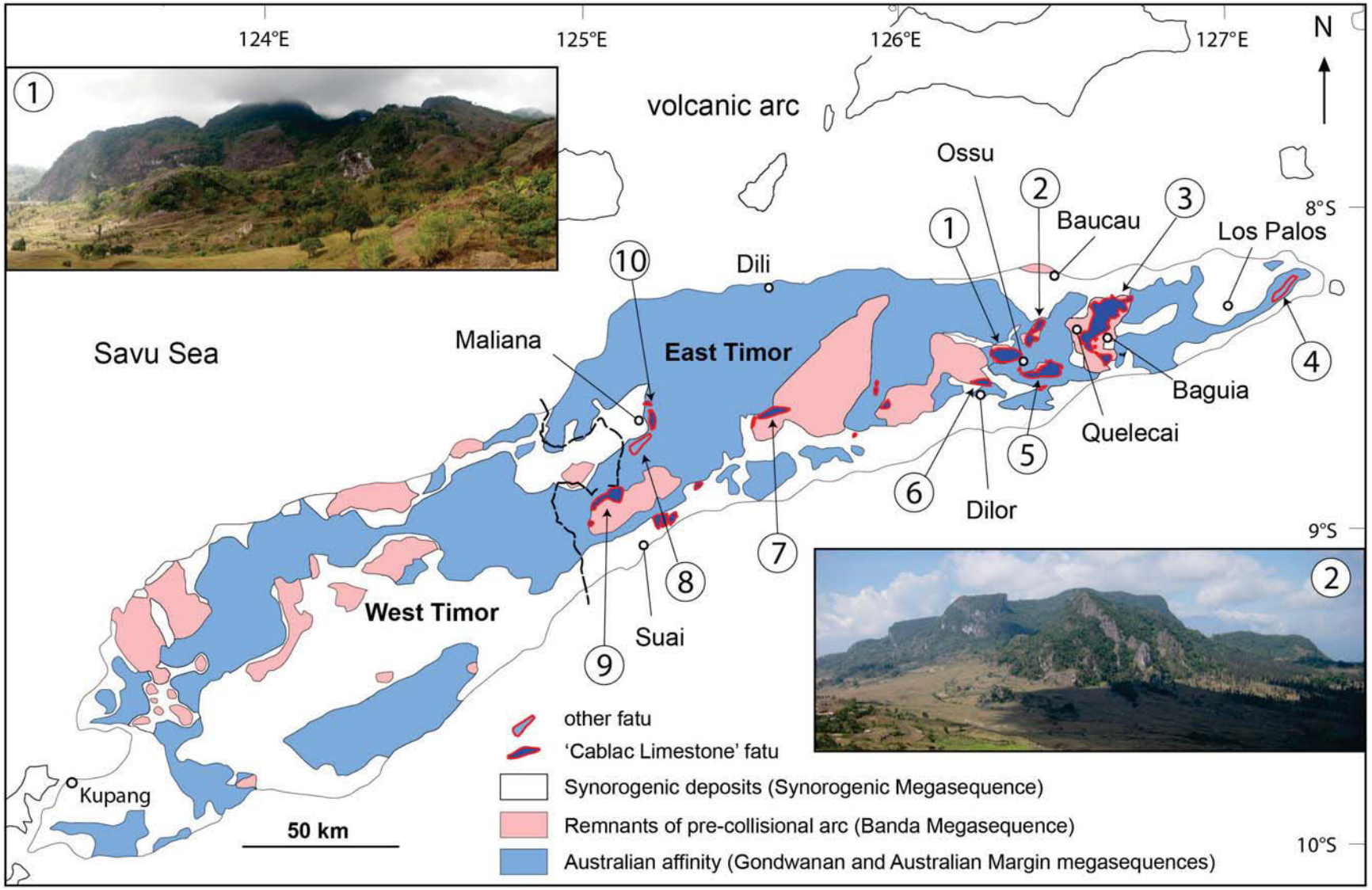
124°E
125°E
126°E
127°E
N
8°S
9°S
10°S
volcanic arc
Ossu
Baucau
Los Palos
Dili
Maliana
East Timor
Savu Sea
Baguia
Quelecai
Dilor
West Timor
Suai
Kupang
50 km
1
2
3
4
5
6
7
8
9
10
other fatu
'Cablac Limestone' fatu
Synorogenic deposits (Synorogenic Megasequence)
Remnants of pre-collisional arc (Banda Megasequence)
Australian affinity (Gondwanan and Australian Margin megasequences)

1.2 Objectives and aims

The aims of this study were to investigate the stratigraphy and structure of a number of under-explored fatus in East Timor, most of them currently mapped as 'Cablac Limestone'. In order to do this, the specific aims of this project were to:

1. **Conduct reconnaissance mapping of selected fatus in East Timor.** Reconnaissance mapping also extends to other areas of interest identified from aerial photographs, digital elevation models, and previous field observations.

2. **Choose a limited number of specific locations where the stratigraphy and structure of the fatus can be best observed and studied and map these areas in detail.** Locations were chosen not only on the basis of how much geological information they yielded, but also on practical considerations such as ease of access, in order to maximise the benefits of time spent in the field.

3. **Define the kinematics and timing of the structures controlling the uplift of the fatus.** Biostratigraphic techniques, along with geochemistry where necessary, were used to assign age and provenance to rocks within the study areas. Structural and stratigraphic data were synthesised to produce a structural model of each study area, and reveal the timing of deformation.

4. **Compare and integrate the findings with current structural models of East Timor and regional tectonics.** This involved an analysis of different models proposed for the structural evolution of East Timor in the context of the findings of this study, and an attempt to place the recent deformation within East Timor into a regional tectonic framework.

1.3 Methods

This thesis is based on 4 months of fieldwork conducted during 2010 and 2011. It follows and incorporates 2 months of initial field work completed in 2009 as part of a BSc Honours project at the University of Western Australia.

In 2009 field work was based in Ossu, Viqueque District (**Fig. 2**), and focused on detailed structural and stratigraphic mapping of Mount Mundo Perdido (**Fig. 2**). In 2010 fieldwork comprised reconnaissance and regional mapping of:

- Mount Laritame and the Builo Range (locations 2 and 5, **Fig. 2**), near Ossu
- Mount Bibileu, near Dilor (location 6 on **Fig. 2**)
- Mount Loelako and the Saburai Mountain Range (locations 8 and 10, **Fig. 2**), near Maliana;
- The Matebian Range, (location 3, **Fig. 2**) with mapping completed around Quelecai and Baguia
- The Paitchau Range (location 4, **Fig. 2**), east of Los Palos
- Mount Taroman (location 9, **Fig. 2**), northwest of Suai

Commonly three to seven days was spent at each location conducting systematic traverses from the flanks into the central regions of east fatu, collecting rock samples and structural data.

In 2011 fieldwork was based in Maliana (**Fig. 2**), with four weeks spent conducting more detailed geological mapping with traverses across the edges of the Maliana basin and into the surrounding fatus of Loelako and the Saburai Mountain Range (**Fig. 2**).

Most fatus, particularly in the eastern districts, are covered in dense jungle and access is difficult. Traverses through the foothills were often through gullies, which provide both reasonable outcrop and access, along with goat and buffalo tracks. Most traverses into the central regions of the fatus utilised the aid of local guides, and often required paths to be cut through with machetes.

Fieldwork was planned to coincide with the dry season, typically from May to November. However, 2010 was an unusually wet year in East Timor, with severe storms and flooding experienced throughout the normally dry months of June, July and August. Most fatus on which fieldwork had been planned remained clouded in, and very low visibility made geological observations, particularly judging outcrop relationships, quite challenging. Rain also hampered access as many paths up the mountains became too dangerous to pass. One of the largest difficulties was vehicular access, with many roads and bridges around East Timor washed out or impassable, preventing access to many locations where field work was planned. In July 2010, field work in the worst affected districts was postponed until later in the year. When fieldwork resumed in October weather conditions had improved slightly, however access remained difficult and some planned work remained incomplete. Dry weather returned in 2011, with field work around Mount Loelako and the Saburai range completed under more favourable conditions.

It was not the intention of this study to record detailed stratigraphic sections, as outcrop around the fatus is usually incoherent and dissected by high-angle faulting. This study focuses on identifying rock units, describing them, and mapping their relationships. At sampled stations along traverses, localities were marked with a Garmin GPS, lithologies were described and sampled, structures were measured and digital photographs were taken. Structural data collected included bedding orientation, fold measurements (type and orientation), and fault orientations. Where possible, movement sense on faults was determined using fault striae and a detailed examination of kinematic indicators on fault surfaces (e.g. criteria outlined by Petit 1987). GIS air photo data sourced from the National Mapping Advisor for East Timor was used to plot data and construct basic geological maps while in the field.

Field laboratories were set up at base camps with equipment for cutting limestones, disaggregation of mudstones and making acetate peels, enabling initial tectonostratigraphic determinations of rock samples in the field. Additional peels and thin-sections were made at the University of Western Australia, enabling biostratigraphic age determinations of limestone samples. Samples of the original rock, along with acetate peels, thin-sections and processed

mudstone residues, are housed in the collection of the Edward de Courcy Clarke Earth Science Museum at the University of Western Australia. Duplicates of each sample are stored in the Geological Laboratory of the Secretary of Energy and Natural Resources at Hera, East Timor.

1.4 Thesis outline

This thesis consists of six chapters. Following the Introduction (**Chapter 1**), the regional geology and tectonics of the Timor region are described in **Chapter 2**, along with an overview of the interpretation of the fatus of East Timor by previous workers. In **Chapter 3** I outline the tectonostratigraphic framework developed during this and associated work, followed by stratigraphic reconstructions of the various study areas. Structural observations and analysis are presented in **Chapter 4**, before being interpreted and discussed in **Chapter 5**. Finally, **Chapter 6** summarises the main findings of this study and provides recommendations for further work.

2. Regional geology and previous work

2.1 Regional Setting

Collision between continental crust of the Australian Plate and Southeast Asia commenced at approximately 25 Ma in the New Guinea region, colliding first with the North Sulawesi volcanic arc, and continuing diachronously westwards (Hall 2002; Keep *et al.* 2003). The age for collision in the Timor region has been reviewed by Keep and Haig (2010), Spakman and Hall (2010), Audley-Charles (2011), Hall (2011) and Haig (2012a). Detailed stratigraphic evidence (Haig & McCartain 2007; Keep & Haig 2010; Haig 2012a) suggests that continental crust, likely an outlying continental plateau (Timor Plateau) resembling present-day Exmouth Plateau (**Fig. 1**), entered the subduction zone in the Timor region during the Late Miocene between 9.8 Ma and 5.7 Ma. This caused disruption in Timor and eventual jamming of the subduction zone at approximately 5.7 Ma (Keep & Haig 2010). The cessation of subduction is evidenced by a present lack of deep seismic activity and a lack of active volcanism in the arc immediately north of Timor (Chamalaun & Grady 1978; with timing issues discussed by Ely *et al.* 2011, p. 492). Whilst this age for collision, after 9.8 Ma but before 5.7 Ma (Haig & McCartain 2007; Keep & Haig 2010; Haig 2012a) is older than some other estimates (e.g. 4 to 2 Ma, Audley-Charles 2004, 2011; Spakman & Hall 2010; Hall 2011), it is consistent with other evidence for a regional event at approximately 8 Ma from both Timor and the adjacent Australian North West Shelf (e.g. McCaffrey *et al.* 1985; Reed 1985; Berry & McDougall 1986; Fortuin *et al.* 1994; van der Werff *et al.* 1994; Richardson & Blundell 1996; Fortuin *et al.* 1997; Charlton 2000; Rutherford *et al.* 2001; Keep *et al.* 2002; Keep *et al.* 2003).

Since collision, Timor Island has undergone uplift and exhumation in excess of 5 km (Keep & Haig 2010) through processes of crustal thickening (Richardson & Blundell 1996) and isostatic rebound following a possible detachment of the down-going slab (Price & Audley-Charles 1987; Audley-Charles 2004; Ely *et al.* 2011). Its emergence possibly had begun by 5.7 Ma (Haig 2012a) and the island continues to undergo uplift of around 1.5 mm/ year (Audley-Charles 1986a).

The tectonostratigraphic framework (**Fig. 3**) of Timor includes:

1) Latest Carboniferous to Middle Jurassic Gondwana Megasequence deposited within interior basins of the East Gondwanan rift system (Harris *et al.* 1998; Harris 2006; Haig & McCartain 2007, 2010; Davydov *et al.* 2014);
2) Late Jurassic to early Late Miocene Australian Margin Megasequence deposited on the passive margin that, in the vicinity of Timor, subsided to middle bathyal water depths during the Early Cretaceous to form the 'Timor Plateau' (Haig & McCartain 2007; Keep & Haig 2010);
3) Middle Jurassic hemi-pelagic to pelagic deposits of the Indian Ocean Megasequence, emplaced during collision (Haig & Bandini 2013);
4) Jurassic to Early Miocene Banda Megasequence of Asian affinity, emplaced during collision (Audley-Charles & Harris 1990; Harris 2006; Haig *et al.* 2008); and
5) Synorogenic Megasequence (Haig & McCartain 2007; Roosmawati & Harris 2009; Haig 2012a).

The Bobonaro Melange (=Synorogenic Melange) recognised by Harris *et al.* (1998), Haig and McCartain (2007) and Haig *et al.* (2008) is no longer considered a coherent stratigraphic unit. It includes structural melange zones probably caused by diapirism (Barber *et al.* 1986; Harris *et al.* 1998) generated within Triassic clay units (Haig & McCartain 2010; see also Brunnschweiler 1978). However, in many areas, incipient diapirism has resulted in 'broken-formation' deformation (Harris *et al.* 1998) within units that can be identified as particular formations (e.g. much of the Babulu Formation recognised in this study). See **Chapter 3.1 Tectonostratigraphic framework** for detailed discussion.

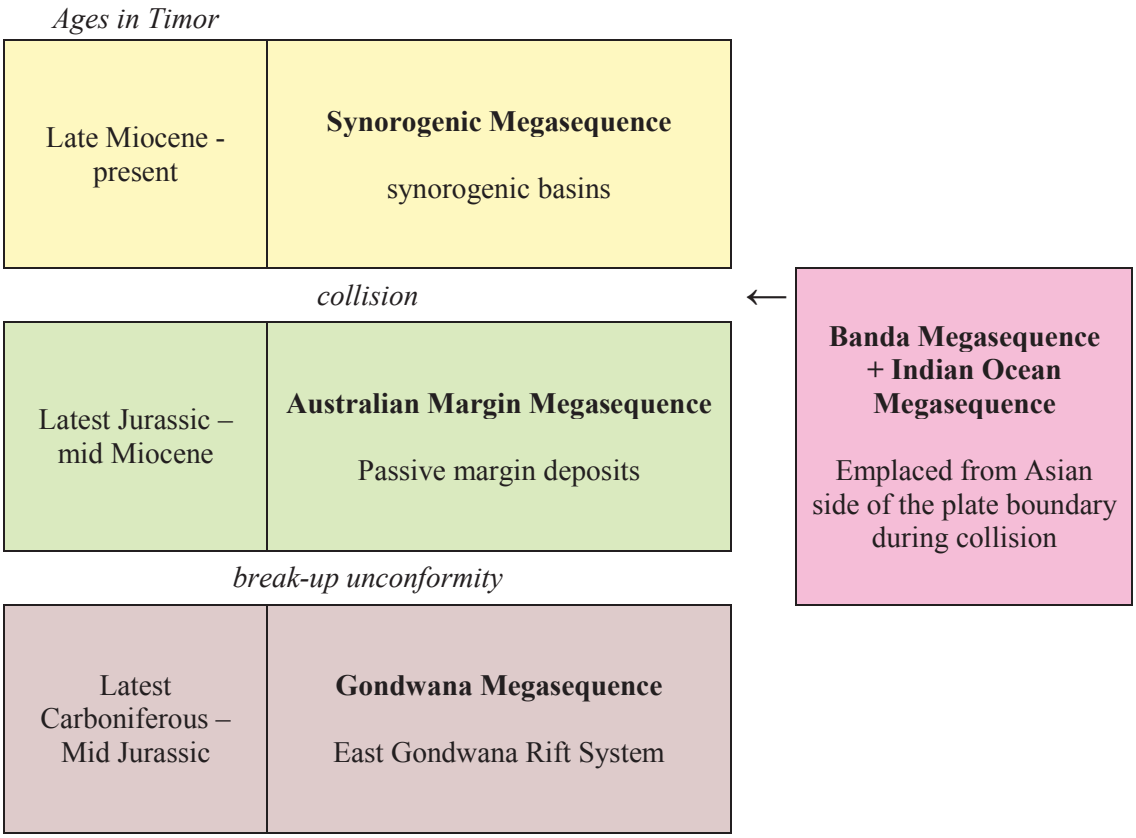

Fig. 3. An overview of the tectonostratigraphic framework of East Timor (Haig & McCartain 2007; Haig *et al.* 2007; Haig *et al.* 2008; Haig & McCartain 2010; Keep & Haig 2010; Haig 2012a; Haig & Bandini 2013; Davydov *et al.* 2014). See **Chapter 3.1 Tectonostratigraphic framework** for detailed discussion.

2.2 Tectonic history

2.2.1 Tectonic models

Timor has a complex tectonic history which has been the subject of much debate. East Timor is one of the best places in the world to study young arc-continent collision. However it is this young age which also confounds attempts to understand it, because very little of the orogen is exposed. Hamilton (1979) described the island as "a tectonic chaos", and Brunnschweiler (1978) noted that "Timor may well be an even more difficult case (than the European Alps) … because one suspects that what one sees is merely the top part of a very big pile of nappes which has only just begun to emerge from the sea."

Generally, most workers have agreed on the presence of crustal shortening and thrust tectonics in Timor (e.g. Hirschi 1907; Wittouck 1937; Grunau 1953; Gageonnet & Lemoine 1958; Marks 1961; Audley-Charles 1968; Carter *et al.* 1976; Barber *et al.* 1977; Brunnschweiler 1978; Audley-Charles 1981; Sopaheluwakan *et al.* 1989; Charlton *et al.* 1991; Harris 1991; Sani *et al.* 1995; Villeneuve *et al.* 1999; Keep *et al.* 2005). Audley-Charles (1968) attempted to describe the observations made during his field mapping (1959-1961) using Alpine-style terminology. His overthrust model (Audley-Charles 1968) proposes that large scale deformation and erosion of Australian continental margin sediments occurred during collision, followed by emplacement of thrust sheets from the Asian side of the plate boundary on to the developing orogen (**Fig. 4**). The model has undergone various modifications by Audley-Charles and others since then (Audley-Charles & Carter 1972; Audley-Charles *et al.* 1974; Carter *et al.* 1976; Barber *et al.* 1977; Audley-Charles 1978, 1985, 1986a, b; Price & Audley-Charles 1987; Audley-Charles & Harris 1990; Audley-Charles 1991, 2004), first to fit in with the paradigm shift to plate tectonics during the 1970s, and later to incorporate the results of ongoing field and geophysical studies.

Fitch and Hamilton (1974) and Hamilton (1979) interpreted Timor as a large accretionary prism, comprising imbricated blocks of Australian margin and Banda Arc material amidst a 'background' of Bobonaro Scaly Clay, which they interpreted as a tectonic melange (**Fig. 5**). Their model, derived using previous descriptions of the island (from previous workers) in conjunction with a deep-reflection seismic study, are not well supported by field observations (Audley-Charles 1986b). Mass balance calculations also show that the amount of material accreted is far too small to account for the entire island (Richardson & Blundell 1996), and geophysical studies have concluded that the Timor Trough is not a subduction zone (Chamalaun *et al.* 1976; Audley-Charles 1986b; Keep *et al.* 2003). Therefore, it is unlikely that this model is an accurate representation of the formation of Timor Island.

More recent overthrust models (e.g. Harris 2011) invoke a large scale decollement extending from the Timor Trough, over which the Australian margin is backthrust (**Fig. 6**). Harris (2011) shows the majority of Timor above this decollement dominated by a thick, stacked succession of duplexed Gondwana Megasequence lithologies, metamorphosed to the north, with

imbrication of Australian passive margin and more recent synorogenic deposits along southern edge of island. A large thickness of Banda Megasequence units have been overthrust from the north over a layer of melange, with the erosional remnants of this nappe now occupying high structural positions throughout the island.

Many authors however do not agree with the extent of interpreted thrusting for Timor. Based on field mapping, Grady (1975) and Grady and Berry (1977) determined that some previously mapped thrusts were in fact stratigraphic contacts. Grady and Berry (1977) also noted the ubiquity of high-angle Pliocene and Quaternary faults, which are not well incorporated into the overthrust or imbricate models (**Figs 4, 5**). Chamalaun and Grady (1978) proposed a 'rebound model' of Timor tectonics after incorporating these observations with additional gravity and seismic data (**Fig. 7**). The rebound model interprets Timor as entirely autochthonous, with uplift occurring as the result of isostatic rebound following detachment of the down-going slab. The model assumes that all transfer of exotic material across the plate boundary occurred as olistostromes carried by gravity sliding, resulting in the deposition of the Bobonaro Scaly Clay (sensu Audley-Charles 1968). The modern consensus is now that the 'Bobonaro Scaly Clay' (see also comments in Section 2.1) was emplaced via shale diapirism (Barber *et al.* 1986; Harris *et al.* 1998), and it is clear that some thrusting of exotic terranes over the plate boundary has occurred, as these have been mapped throughout East Timor (Audley-Charles 2004; Keep *et al.* 2009). However, the abundance of late-stage high-angle faults does point to some component of this model being active during late stage orogeny (Keep *et al.* 2009).

Along with Grady (1975), Grady and Berry (1977) and Chamalaun and Grady (1978), other authors have also noted the importance of high angle faults in East Timor. Schneeberger (1961) states in his report to Timor Oil that "systematic and careful investigations by the Company's geologists have conclusively shown that block faulting rather than overthrusting is the prevailing type of structural dislocation in Portuguese Timor." Similarly Romariz and Leme (1967) describe differential vertical movement about high angle faults as a strong influence on the present day topography of East Timor.

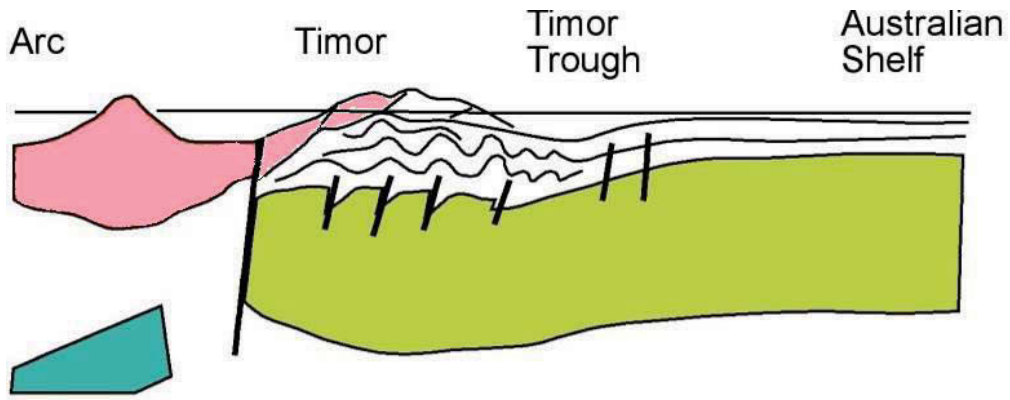

Fig. 4. The overthrust model. Deformation and erosion of Australian continental margin sediments occurs prior to emplacement of thrust sheets, which are mostly Asiatic in affinity. Figure modified from Richardson and Blundell (1996). Australian continental margin basement is coloured green, overlying Australian sedimentary units are white, rocks of Asiatic affinity are pink, and the down going slab is blue.

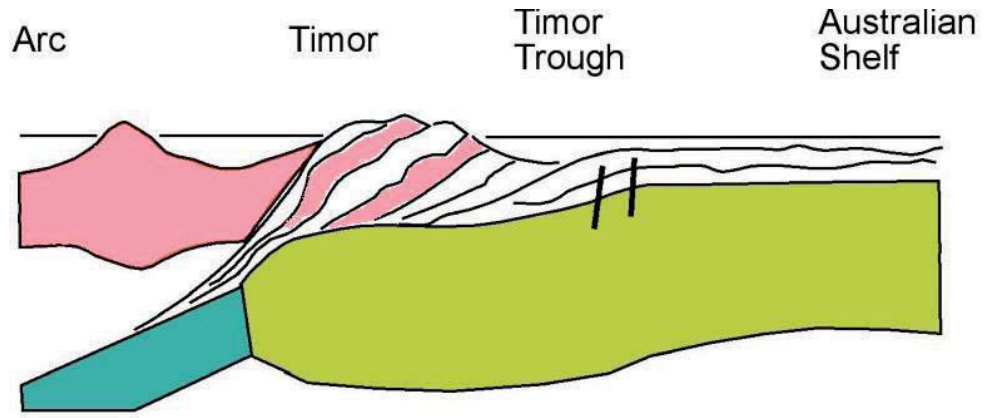

Fig. 5. The imbricate model. Timor is an accretionary prism consisting of blocks of both Australian and Asiatic affinity, forming a chaotic complex of imbricated blocks and melange. Figure modified from Reed *et al.* (1996). Australian continental margin basement is coloured green, overlying Australian sedimentary units are white, rocks of Asiatic affinity are pink, and the down going slab is blue.

And at the Cablac Mountain Range (**Fig. 2**), Haig *et al.* (2008) and Keep *et al.* (2009) interpret a high-angle fault separating units of Asian affinity from the overthrust limestone stack of Gondwana and Australian-Margin Megasequence units which make up the high, central regions of the Cablac Range.

Where these high-angle faults have been mapped in detail, workers have observed evidence of strike-slip movement. Berry and Grady (1981b) describe left-lateral movement on moderate to steeply-dipping faults which separate Aileu Formation metamorphic rocks on the northern coast

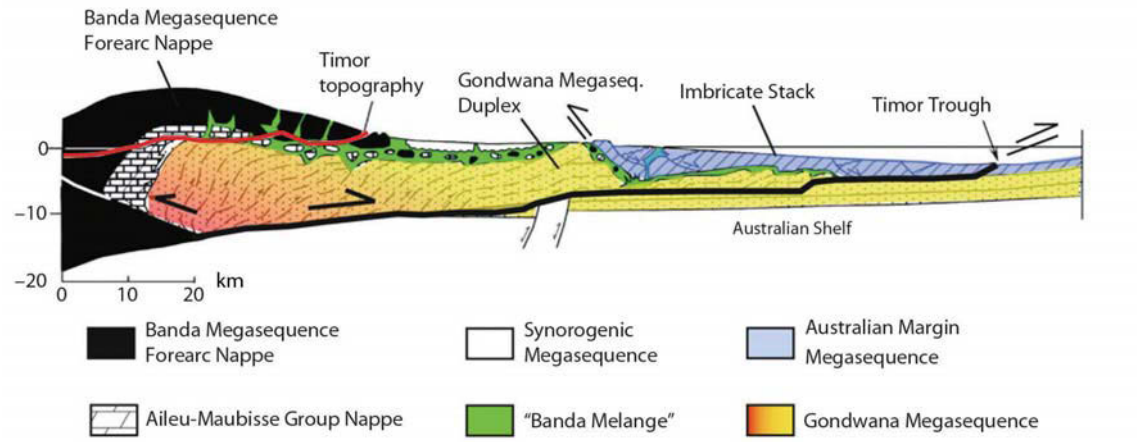

Fig. 6. An evolution of the overthrust model, from Harris (2011). It shows the imbrication of the Australian Margin Megasequence on the south coast, coupled with the thick, stacked succession of Gondwana Megasequence rocks which make up the bulk of the island, metamorphosed towards the north.

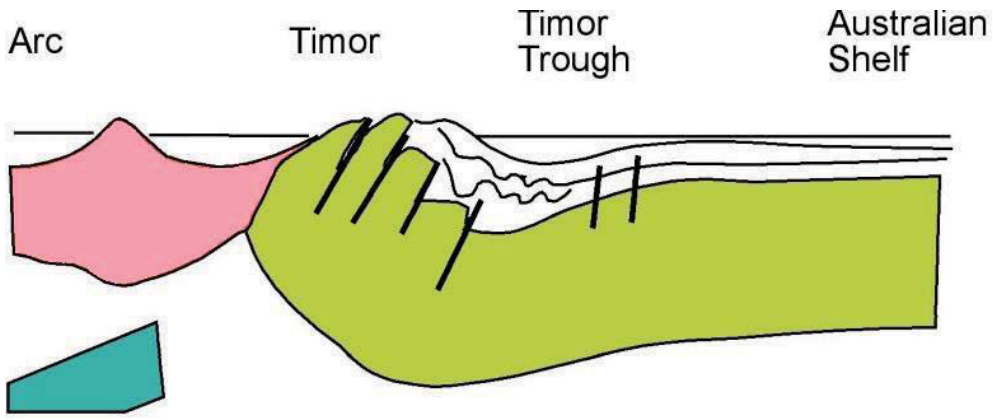

Fig. 7. The rebound model. Timor is derived almost entirely from the rocks of the Australian continental margin, with uplift accommodated by high angle faulting after slap break-off. All units of Asiatic origin were emplaced as olistostromes as the island was uplifted. Figure modified from Reed *et al.* (1996). Australian continental margin basement is coloured green, overlying Australian sedimentary units are white, rocks of Asiatic affinity are pink, and the down going slab is blue.

of East Timor with surrounding rock units. High angle, left-lateral structures have been mapped throughout West Timor striking north-northwest (e.g. Charlton 1990; Kaneko *et al.* 2007), and similar north-northwest striking strike-slip faults are sometimes interpreted in regional maps of East Timor (e.g. Audley-Charles 2004, fig. 1.). Benincasa *et al.* (2012) found strike-slip deformation ubiquitous throughout Mount Mundo Perdido (**Fig. 2**), and interpreted the mountain as a pop-up structure within a zone of east-west oriented left-lateral strike slip. Duffy *et al.* (2013) observed northwest-southeast oriented dextral-normal faults and northeast-southwest oriented sinistral-normal faults throughout East Timor. Duffy *et al.* (2013)

interpreted these intersecting fault systems to be related to orogen-parallel crustal extrusion accommodated by major east-northeast oriented strike-slip systems on the northern and southern sides of Timor.

2.2.2 Timing of collision

Audley-Charles and co-authors have suggested a Pliocene age for the collision between the Australian continental margin and the Banda Arc, which produced the island of Timor. The placing of the collision at younger than 4 Ma is largely based on unconformable relationships recognised by Audley-Charles within the Pliocene stratigraphy (Audley-Charles 2004, 2011). Audley-Charles (1968, 2004) and his colleagues (Audley-Charles & Carter 1972; Charlton & Wall 1994; Charlton 2002b) used the age of this interpreted unconformity as an age for collision. However, a recent review of paleontological work has found that the age of this unconformity cannot be supported by documented foraminiferal species (Keep & Haig 2010), and may be significantly older than first thought. If the unconformity does not exist or has been misidentified, the age of collision may be very different.

Haig & McCartain (2007) used detailed and robust biostratigraphy from Timor and comparisons the Australian North West Shelf to determine that, prior to collision, the Timor region was probably a broad submarine terrace similar to the present day Exmouth Plateau (**Fig. 2**), rather than being the continental slope suggested by Audley-Charles. This finding, in conjunction with other sedimentological evidence, has led to hypothesis of a much earlier, Miocene-age collision between 9.8 Ma and 5.7 Ma (Keep & Haig 2010; Haig 2012a).

This earlier date of collision is consistent with major deformational events recognised in the region (on both the Australian and Banda sides of the plate boundary) by many other workers (Hocking *et al.* 1987; Fortuin *et al.* 1997; Harris *et al.* 2000; Rutherford *et al.* 2001; Keep *et al.* 2002; Longley *et al.* 2002; Harrowfield *et al.* 2003). The proposed earlier age for collision also agrees with the collision dates determined via dating of Timorese metamorphic complexes (Berry & McDougall 1986), and mass balance calculations (Richardson & Blundell 1996). However, the older age of collision does not immediately fit with the ages of igneous rocks

from Wetar, which suggest that volcanism continued until 3 Ma, significantly younger than the proposed 9.8 Ma to 5.7 Ma collisional age (Honthaas *et al.* 1998). Ely *et al.* (2011) however cautioned that the timing relationship between the age of collision and end of volcanism and is not that straightforward. Because magma production in subduction zones occurs at depths of 65-130 km, there would be a significant delay between the time of collision (and resulting slab break-off) and the down-going slab passing through the magma-generation zone. Therefore, a cessation of volcanism at 3 Ma is not inconsistent with collision ending at 5.7 Ma. In addition, Keep and Haig (2010) note that volcanism on Wetar is not continuous but episodic, and link pulses of volcanism to stages in the deformation.

Keep and Haig (2010) and Haig (2012a) base the oldest possible age of collision on the age of the youngest deformed Australian margin sediments observed in East Timor, 9.8 Ma. They base the youngest possible age of collision at the onset of a period of pelagite deposition at 5.7 Ma, which they possibly attribute to the locking of the subduction zone. The collision age of 4-2 Ma proposed by Audley-Charles (2004) suggests that at 9.8 Ma the Banda Arc was still 600 km north of the Australian continental margin (Hall 2002) and therefore not in a position to collide. However, if a continental plateau was present, as suggested by Haig & McCartain (2007), it is possible that continental crust extended from 500 to 900 km further out towards the subduction zone (as currently occurs with the Wallaby Plateau on the Australian North West Shelf (Keep & Haig 2010), and collision would therefore be earlier (**Fig. 8**).

2.3 The 'fatus' of East Timor - previous work

In the early twentieth century, geologists working in Timor adopted the local word 'fatu' (derived from 'fatuk', meaning rock) to describe the steep sided limestone massifs that form high peaks in both West and East Timor.

Hirschi (1907) first described certain fatus in East Timor as resembling klippes, implying thrust deformation, and suggested that Timor Island has a complex tectonic history. Although attributing most limestones to the Triassic or late Paleozoic, Hirschi (1907) thought the stratigraphic position of the fatu limestones questionable, noting the unusual north-south orientation of several large fatus (e.g. Matebian, Loelako; Locations 4 and 10 respectively on

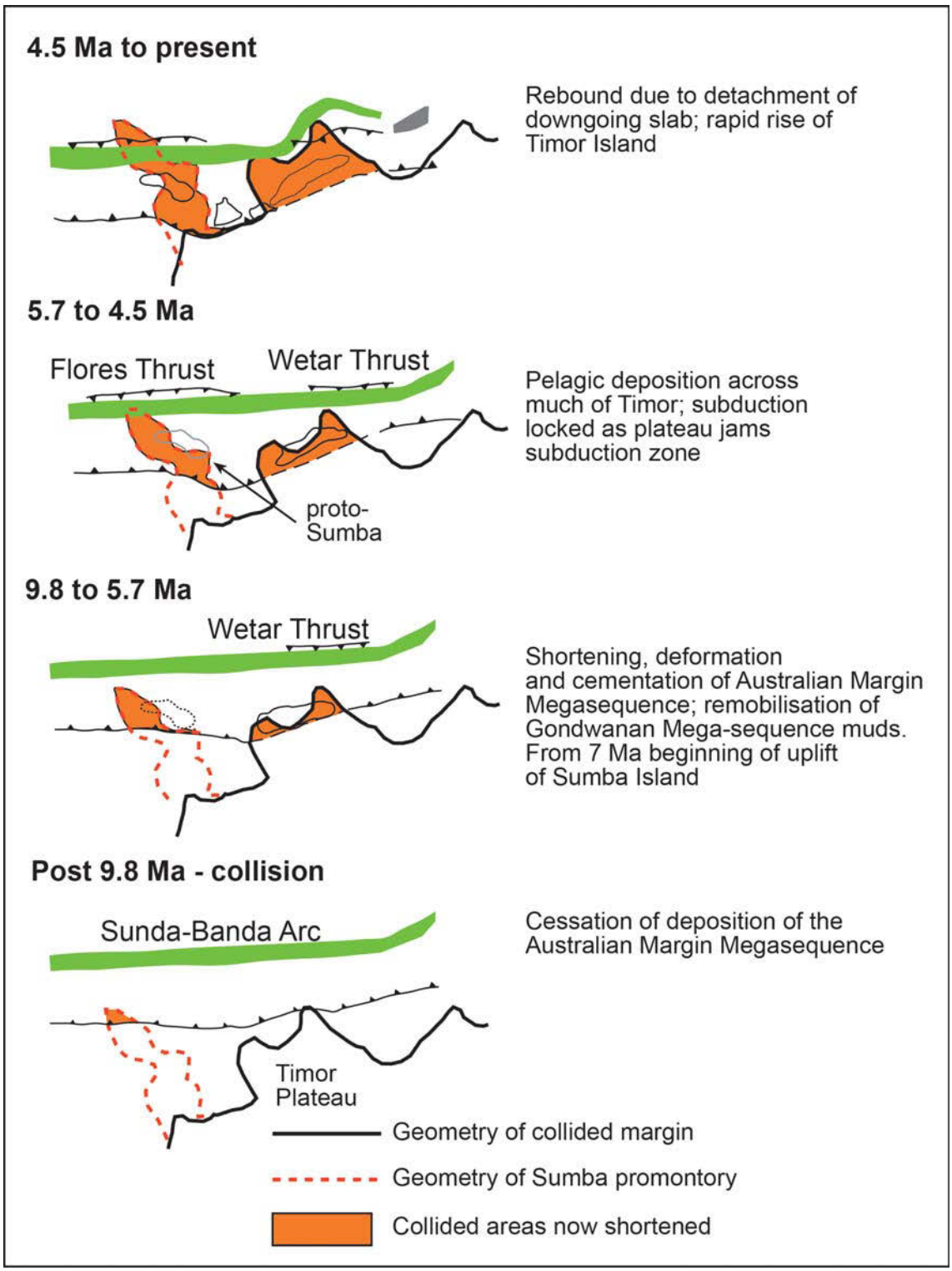

Fig. 8. Evolution of collision incorporating the current geometry of the continent-ocean boundary on Australia's North West Shelf, modified from Keep and Haig (2010). This shows that if the current plateaux (Wallaby and Exmouth, **Fig. 2**) are included in the margin geometry, as well as the proposed Timor Plateau (Haig & McCartain 2007), outliers of Australian continental crust would occur significantly outboard of the Australian margin at 9.8 Ma, allowing for an earlier age of collision. The existing irregular margin geometry, incorporating salient and embayments, reflects the underlying extensional geometries (Harrowfield & Keep 2005).

(**Fig. 2**), transverse to the main long-axis of the island.

Molengraaf (1912) described the fatus of West Timor as isolated limestone hills, separated from the surrounding, contrasting geology by vertical limestone cliffs. Molengraaf (1912) also observed that the fatus comprised many different rock types, most commonly Triassic ooilitic limestone but also Permian crinoid limestone, Tertiary limestone and igneous rocks. He suggested that the fatus were the remnants of a thrust sheet, which he dubbed the 'fatu-sheet.' However, he also noted evidence for 'mountain-forming movements' that had caused juxtaposition of fatus of different ages, observing "Permian fatus, an upper-Triassic fatu and Eocene fatus facing against each other."

Wanner (1913) distinguished the fatus of north-western Timor from the more gently-sloping, more vegetated 'netems,' or elongated ridges, and noted their striking resemblance to the cliffs of the European Alps and Carpathians. He described the fatus as mountains several kilometres long and wide, which rise with sharply sloping walls to "mighty peaks" 700 m above their surroundings (Wanner 1913). Fatu limestones sampled by Wanner were often ooilitic and described as being very similar to the Norian limestones of the eastern Alps (Krumbeck 1921). Wanner (1913) described the fatu limestones as "essentially a reef limestone facies of the upper-Triassic".

't Hoen and van Es (1925) noted the distinction between 'fatu' as a morphological concept, and its tectonic significance in describing overthrust units. They suggested that although fatu-type morphology was observed in rocks with ages ranging from Permian to Neogene, it was only the older Mesozoic and Paleozoic units that belonged to thrust sheets.

Brouwer made an expedition to West Timor in 1937 with several students, each mapping different regions, and described the fatus as conspicuous features in the topography formed by steep, isolated rock masses (Brouwer 1939). Brower's students studied several different regions of West Timor, with a number of papers published in from 1939 to 1941. Simons (1940) and van Voorthuysen (1940) both recorded fatu limestones of Triassic age in West Timor's northern regions. De Roever (1940) observed fatus comprising Triassic, often ooilitic, reef limestones

and lower Jurassic *Mytilus*-limestones in the south-western Mutis region of West Timor, and Tappenbeck (1940) placed most fatus in the south-central Mollo region in the Triassic, while also observing some of Permian age. van West (1941) also observed fatus of Triassic age in the eastern Miomaffo region of West Timor, and noted their high tectonic position. Brouwer (1939) suggested that the fatus had not reached their present positions by overthrusting alone, noting smaller blocks which appeared to have separated from the main fatus and reached their present position "by gliding on the surface."

Wittouck (1937, 1938) included the 'fatu type' as one of his three types of topography in East Timor (together with 'plateaux type' and 'igneous type'), describing them as long, flat-topped, limestone plateaux with steep, usually vertical sides, heavily eroded, with a general southwest-northeast direction (noting the exception of the north-south oriented Matebian Range; **Fig. 2**). He placed most fatu limestones within the Permian and Triassic (Wittouck 1937).

Subsequently Umbgrove (1938) briefly described the fatus in West Timor as prominent, steep-sided outcrops, strongly resistant to erosion. He characterised them as klippen, of Triassic age (Umbgrove 1938).

van Bemmelen (1949) described the 'Fatu Complex' as the highest overthrust unit in both West and East Timor. He also noted the presence of irregular block faulting in East Timor, quoting observations of the Allied Mining Corporation of fatus with huge, young scarps, evidencing large amounts of differential uplift.

De Waard (1957) discussed the nature of the fatus in depth, observing that although fatus with a range of different lithologies and ages are present in West Timor, the majority consist of massive limestone of Triassic age. Like 't Hoen and van Es (1925), he acknowledged the ambiguity that exists when using the word 'fatu' as both a morphological and geological term. De Waard (1957) gave examples of massive Triassic fatu limestones grading both vertically and laterally into well bedded limestones, marls and clays which form the surrounding lowlands. Following these observations, he suggested that a 'Fatu complex' does not exist as a separate tectonic unit. Rather, De Waard (1957) proposed that all fatu masses of Permian, Triassic and

Jurassic age represent local facies differences in the usually marly and clayey 'Sonnebait unit', widespread in West Timor.

In East Timor, Grunau (1953) used the term 'Fatu Limestone' to classify the rocks comprising the massifs surrounding Ossu, the Matebian Range, the Paitchau Range and others (**Fig. 2**). He interpreted the fatus as erosional remnants or klippen, despite admitting the absence of any observed thrust contacts, but noted that the fatus internally showed evidence of a considerably complicated tectonic history. Although many fatu localities visited by Grunau lacked age deterministic fossils, Grunau (1953) was able to attribute an age range of upper Cretaceous to upper Oligocene to the fatu limestones around Ossu, along with parts of the Matebian Range, based on the presence of foraminifera species *Globotruncana* and *Spriroclypeus*.

Wanner (1956) recorded Triassic fauna from several fatus in East Timor, including rich coral assemblages from certain localities, dating them as Carnian or Norian. Wanner (1956) disputed Grunau's (1953) interpretation of all fatu limestones belonging to a thrust sheet, giving examples where they observed a normal stratigraphic succession with surrounding lithologies. Wanner (1956) also disagreed with previous authors' interpretations of the fatu limestones being the highest tectonic element in Timor, describing localities where they have been overthrust by Permian units.

Gageonnet and Lemoine (1958) followed Grunau (1953) in attributing the fatu limestones in East Timor to the remnants of thrust sheets, based on the conspicuous geomorphology of the fatus as topographical highs distinct from their surroundings. They describe fatus with a wide range of ages, including Permian units, ooilitic Triassic limestones, pelagites of Cretaceous to Eocene age (based on the presence of foraminifera species *Globotruncana* and *Globorotalia*), and younger fossiliferous limestones attributed to the earliest Miocene (due to the presence of the larger foraminifera species *Spiroclypeus* and *Cycloclypeus*) (Gageonnet & Lemoine 1958).

Schneeberger, in his 1961 report to Timor Oil, stated that extensive overthrusting postulated by previous authors is not present in East Timor. He interpreted the distinctive fatu morphology as

produced by block faulting rather than overthrusting, and concluded that only one thrust nappe exists in East Timor, consisting of Permian sediments.

Romariz and Leme (1967) noted the stark relief of the fatus in East Timor amongst the surrounding landscape, describing abrupt walls, great altitude and sharp terminations. They also disagreed with the structural interpretations of many previous workers, noting a lack of basal thrust contacts or internal imbrications to indicate overthrusting. Romariz and Leme (1967) recognized that the fault architecture of the fatus was instead dominated by subvertical faults forming huge scarps, oriented in various directions and intersecting underlying units, and described differential vertical movement about these faults contributing to the present day morphology of the fatus. Romariz and Leme (1967) proposed that the fatus may have developed as isolated coral reefs on an ancient submarine relief during the Cenozoic. They do however record the presence of older, Cretaceous very fine grained carbonates, and note that many doubts remain concerning the origin and age of the fatu limestones.

Between 1959 and 1961, Timor Oil's resident geologist Michael Audley-Charles embarked on an extensive project of reconnaissance field mapping and analysis from which he produced a number of papers, culminating in his PhD thesis and his 1968 memoir 'The Geology of Portuguese Timor' (Audley-Charles 1968). This memoir provided the first regional description of the stratigraphy of East Timor along with a 1:250 000 map, and has since become the most common source for the regional geology and stratigraphy of East Timor, despite its reconnaissance nature. Audley-Charles mapped the majority of fatus in East Timor as Miocene 'Cablac Limestone', which had its type area at the Cablac Mountain Range, near Same in south-central East Timor (**Fig. 2**). He interpreted the Bahaman facies ooilitic wackestones, packstones and grainstones at the Cablac Mountain Range as shallow water deposits in depositional contact with underlying units, of Miocene age based on foraminifera within clasts of what was interpreted as a basal conglomerate (Audley-Charles 1968).

During the early 1970s additional fieldwork was conducted by Audley-Charles and several of his colleagues and students (Audley-Charles *et al.* 1974; Barber & Audley-Charles 1976; Carter

et al. 1976; Barber *et al.* 1977), however after the political situation in East Timor deteriorated in1975 the opportunity for fieldwork became very limited. Audley-Charles and others continued to publish papers as their ideas evolved, mostly relying on extrapolations from West Timor or new regional geophysical datasets. The 'Cablac Limestone' fatus were first thought to represent in-situ patch reefs formed on isolated shoals after collision but before orogenesis (Audley-Charles 1968; Audley-Charles & Carter 1972) but in later literature came to be most commonly interpreted as belonging to a thrust sheet of Asiatic affinity, emplaced during collision (Carter *et al.* 1976; Barber *et al.* 1977; Audley-Charles 1986a; Audley-Charles & Harris 1990; Sawyer *et al.* 1993; Milsom 2000; Audley-Charles 2004; Harris 2006; Standley & Harris 2009; Audley-Charles 2011).

Other authors with field experience in East Timor have since challenged the conclusions of Audley-Charles and associated workers. Grady (1975), Grady and Berry (1977) and Brunnschweiler (1978) found inconsistencies in Audley-Charles' field observations, most notably in the distribution and assigned ages of mapped units, and in the veracity of structural interpretations, particularly the mapped thrusts. Brunnschweiler (1978) states that "many fatu limestones are not simply Lower Miocene Cablac Limestone, but include Eocene, Upper Cretaceous and older elements."

Detailed field mapping studies at the Cablac Mountain Range (Haig *et al.* 2007; Haig *et al.* 2008; Keep *et al.* 2009) have concluded that the Bahaman facies lithologies comprising the 'Cablac Limestone' at its type area are Triassic-Early Jurassic carbonate platform deposits. Furthermore, field mapping at the Cablac Mountain Range in 2004 determined that rather than being of singular lithology, the mountain range comprises metamorphic, volcanic, shallow and deep marine sedimentary rocks, with ages ranging from Triassic to Pleistocene, dissected by recent, high-angle normal faults (Keep *et al.* 2009). The 'basal conglomerate' described by Audley-Charles (1968), containing clasts of Miocene age (from which Audley-Charles (1968) determined his age for the 'Cablac Limestone'), has been re-interpreted as a Plio-Pleistocene crush breccia in a high-angle fault zone (Haig *et al.* 2008; Keep *et al.* 2009).

2.4 Summary

Timor Island is the product of the collision between Australian continental crust and the Banda volcanic arc. There is a long history of geological work on the island, although most has been based on reconnaissance mapping with detailed fieldwork being very limited. As a result, some aspects of the geology remain controversial, particularly tectonic styles and the age of collision. The high, steep-sided limestone fatus are one of the most enigmatic and controversial features of Timorese geology. Although comprising a range of rock types and ages, most early workers observed Triassic limestone fatus as most common in both West and East Timor. However, since the 1960s most fatus in East Timor have been mapped as Lower Miocene 'Cablac Limestone', following the reconnaissance mapping of Audley-Charles (1968). Since detailed fieldwork in East Timor resumed in 2003, a re-evaluation of the 'Cablac Limestone' at its type area has led to important revisions in East Timorese stratigraphy, and prompted the present investigation of other fatus currently mapped as 'Cablac Limestone'.

3. Stratigraphic reconstructions

3.1 Tectonostratigraphic framework

Audley-Charles (1968) first mapped the geology of East Timor using Alpine-style terminology, grouping lithostratigraphic units into structural divisions of Para-Autochthon, Autochthon, and Allochthon. Since the 1970s new information and analyses have led to many changes in the interpretations of mapped units, dating, and the assignment of lithostratigraphic (Charlton *et al.* 1991) and tectonostratigraphic (Haig *et al.* 2007; Haig & Bandini 2013) names, however the following stratigraphic divisions have commonly been recognised:

1. **Permian to Middle Jurassic interior-rift basin deposits of Australian affinity**, extensively deformed by their interaction with the Banda Arc and the subduction zone during arc-continent collision. These belong to the *Para-Autochthon* of Carter *et al.* (1976) and Barber *et al.* (1977); and form the *Gondwana Sequence* of Harris *et al.* (1998; 2000), and the *Gondwana Megasequence* of Haig *et al.* (2007).
2. **Middle Jurassic, siliceous, hemi-pelagic to pelagic deposits with probable volcanic associations,** which have recently been recognised in East Timor from large blocks within a structural melange zone (Haig & Bandini 2013). Based on similarities in lithofacies and age to rocks previously described in West Timor, Haig and Bandini (2013) placed these rocks within the Noni Group (see Haig & Bandini 2013 pp 75-77). The lithofacies of the Noni Group are distinct from other stratigraphic units in Timor, and its facies, age, and probable volcanic association suggest deposition in a newly rifted Indian Ocean. As such, Haig and Bandini (2013) placed it within a separate megasequence designated the *Indian Ocean Megasequence*.
3. **Late Jurassic to early Late Miocene carbonate pelagic deposits of Australian affinity**, cemented and stylotised during collision. Isolated outcrops were originally described in structural terms as autochthonous or allochthonous (Audley-Charles 1968; Carter *et al.* 1976; Barber *et al.* 1977), these lithologies were later grouped stratigraphically as the *Kolbano Sequence* by Harris *et al.* (1998; 2000) and Haig and McCartain (2007), and the *Australian Margin Megasequence* by Haig *et al.* (2007).

4. **Rocks of Asiatic affinity** emplaced as thrust sheets as the forearc was carried over the Australian continental margin during collision. These belong to the *Allochthon* of Audley-Charles (1968), Carter *et al.* (1976) and Barber *et al.* (1977) and form the *Banda Terrane* of Harris *et al.* (1998; 2000), Harris (2006) and most following authors, and the *Banda Megasequence* of Haig (2012b).
5. **Synorogenic deposits** which formed during collision and subsequent orogeny. Part of the *Autochthon* of Audley-Charles (1968) and Carter *et al.* (1976) and sometimes referred to as 'synorogenic sedimentary units' (Harris *et al.* 1998; 2000) these units form the *Synorogenic Megasequence* of Haig *et al.* (2007).
6. **The Bobonaro Scaly Clay/Bobonaro Melange**, a basinal mud-dominated unit, in many areas characterised by broken-formation deformation (in the sense of Harris *et al.* 1998) in which dislocated blocks of well-bedded sandstone are incorporated into scaly clay, and in some places containing exotic blocks of varying lithology and age. This was mapped as a separate, widespread stratigraphic unit by Audley-Charles (1965a, 1968) called the 'Bobonaro Scaly Clay', and interpreted as a Miocene gravity slide deposit. Barber *et al.* (1986) first suggested that it was emplaced as overpressurised muds were forced to the surface as shale diapirs through fault zones during collision. The term 'Bobonaro Melange' has since been used by a number of authors (e.g. Harris *et al.* 1998; Harris & Long 2000; Charlton 2002b; Standley & Harris 2009). Haig and McCartain (2010) distinguished between zones of true tectonic melange, comprising blocks of varying lithology and age, and units characterised by broken-formation deformation, comprising dislocated blocks of sandstone or limestone within a clay contemporaneous in age – generally Late Triassic. They suggested that the tectonic melange should be mapped as structural zones rather than a stratigraphic unit, and where broken-formation deformation occurs within Late Triassic units it is more useful to map them by their parent rock types, either Babulu Group or Aitutu Group.

Recent studies by workers at the University of Western Australia have been refining a tectonostratigraphic framework for East Timor through detailed biostratigraphic investigations

(Haig *et al.* 2007, 2008; Haig & McCartain 2007, 2010, 2012; Keep & Haig 2010; Haig & Bandini 2013); the current state of knowledge is outlined in **Fig. 9**. The Permian to Middle Jurassic Gondwana Megasequence was deposited in interior-rift basins within the East Gondwanan rift system, and contains a number of facies including deep-water muds, deltaic sands, and carbonate shoals (Haig *et al.* 2007; Haig & McCartain 2010). After continental breakup at around 155 Ma, the now passive Australian continental margin subsided to form a continental terrace similar to Exmouth Plateau on which were deposited the deep water pelagites of the Australian Margin Megasequence, which range in age from Upper Jurassic to Neogene (Haig & McCartain 2007). Distal to the continental margin, in the Proto-Indian Ocean, siliceous argillites and radiolarites of the Indian Ocean Megasequence were deposited (Haig & Bandini 2013). The Banda Terrane of Asian affinity comprises a number of facies from metamorphic basement (the Lolotoi Metamorphic Complex), to overlying volcanics, siliciclastics, and shallow water carbonates ranging from Eocene to Miocene (Haig *et al.* 2008). These rocks were emplaced during the Neogene collision between the Banda Arc and the Australian continent. The relatively undeformed Synorogenic Megasequence was deposited from the latest Miocene to Pleistocene, and records the uplift and emergence of Timor as an island (Haig & McCartain 2007; Haig 2012a). Mapped distribution of megasequences and areas visited by this study are outlined in **Fig. 10**.

The 'Bobonaro Scaly Clay' or 'Bobonaro Melange' is not included in this framework. The field mapping of this study has confirmed the observations of previous authors: that where this unit is currently mapped outcrop often comprises Aitutu or Babulu Group successions that show 'broken- formation' deformation (Harris *et al.* 1998; Haig & McCartain 2010; Benincasa *et al.* 2012). Where outcrop of tectonic melange occurs, containing exotic blocks as a result of overpressured shale dispersion and diapirism, they are mapped in this study as structural melange zones, not a stratigraphic unit.

<table>
<tr><th>Systems</th><th colspan="2">Australian-Margin/Gondwana
Megasequences</th><th>Indian Ocean
Megasequence</th><th>Banda
Megasequence</th><th>Synorogenic
Megasequence</th></tr>
<tr><td>Quaternary</td><td colspan="2"></td><td></td><td></td><td>Neritic carbonate platform/coral reefs
Baucau Limestone
Mid-bathyal to outer neritic
mudstones/sandstones/turbidites
Viqueque Group</td></tr>
<tr><td>Neogene</td><td colspan="5">Late Miocene collision (after 9.8 Ma and before 5.7 Ma)</td></tr>
<tr><td>Paleogene</td><td rowspan="3">Australian-Margin Megasequence</td><td rowspan="2">Pelagite facies deposited on submerged continental plateau
Kolbano Group</td><td rowspan="2"></td><td>carbonate platform/outer neritic to upper bathyal mudstone/wackestone facies + volcanics
Booi Group (uppermost Oligocene to lowest Miocene)
Dartollu Group / Barique Volcanics
(Middle to Upper Eocene)
Uppermost Cretaceous outer neritic to upper bathyal argillites</td><td rowspan="8"></td></tr>
<tr><td>Cretaceous</td><td rowspan="2">siliceous argillites and radiolarites
(+ ? volcanics)
Noni Group</td><td rowspan="6">unconformable above Mutis/Lolotoi Metamorphic Complex (detrital zircon U/Pb age distribution spikes at 663, 120, 87 Ma; peak metamorphism from Lu-Hf analyses of garnet, 45.36±0.63 Ma; Standley and Harris, 2009)</td></tr>
<tr><td>Upper Jurassic</td><td>Neritic siliciclastic facies
Oebatt Group</td></tr>
<tr><td>Middle Jurassic</td><td colspan="2">Continental Breakup</td></tr>
<tr><td>Lower Jurassic</td><td rowspan="4">Gondwana Megasequence</td><td>outer neritic-upper bathyal mudstone facies
Wai Luli Group</td><td rowspan="5"></td></tr>
<tr><td>Triassic</td><td>carbonate platform / basin mudstone facies
Perdido Group / Wai Luli Group</td></tr>
<tr><td>Permian to uppermost Carboniferous</td><td>carbonate platform / basin / prodelta facies
Bandeira Group / Aitutu Group / Babulu Group</td></tr>
<tr><td>Below uppermost carboniferous</td><td>carbonate platform and volcanics / basin / prodelta facies
Maubisse Group / Cribas Group / Atahoc Group</td></tr>
<tr><td colspan="3">transitional to Aileu Metamorphics (sensu stricto*)
[*Based on type area in hills around Aileu (Audley-Charles, 1968). Peridotite bodies and perhaps some of the amphibolites along the north coast are exotic (Falloon et al., 2006)</td></tr>
</table>

In East Timor it is difficult to describe true formations with defined upper and lower boundary stratotypes, due to the structural complexity of the pre-collisional strata. As a result, this study will attempt to assign samples to broader lithostratigraphic groups, confined within chronostratigraphic limits based on biostratigraphy (**Fig. 9**). Note that **Appendix I** includes location details and specific coordinates for all sample numbers discussed in the text or shown in the figures. Coordinates in maps and appendices are given in latitude and longitude, WGS 84.

3.2 Mount Mundo Perdido

Mount Mundo Perdido is a 1750 m high fatu situated in the Viqueque district, approximately 1 km northwest of Ossu (**Figs 10, 12**). It forms an elongate, slightly rhomboidal massif approximately 10 km by 3 km, with its long axis in an east-west orientation. The following Mount Mundo Perdido results are based on field mapping completed in 2009 (Benincasa *et al.* 2012) and present a summary of that work, with interpretations updated and expanded in the context of this present study. Rock units are listed in ascending stratigraphic order and age.

3.2.1 Blue-grey mudstones with sandstone interbeds

Blue-grey mudstones form much of the lowlands around Mount Mundo Perdido (**Figs 12, 13a**). They contain medium to thick interbeds of laminated grey, micaceous, sandstone, often with well defined swaley and hummocky cross-bedding (**Fig. 13b**), however these beds are discontinuous and chaotically faulted (**Fig. 13c**). Both mudstones and sandstones contain well preserved palynomorphs (spores, pollen and rare acritarchs), along with rare nodosariid foraminifera (Benincasa *et al.* 2012), with the sandstones also containing abundant woody fragments and other carbonaceous material (**Fig. 13d**).

Lithologies suggest deposition in a prodelta setting, where muds, sands, micas and woody material from river systems settled on the sea floor below fair weather wave base, with

---

Fig. 9 ← Tectonostratigraphic framework of East Timor (modified from Haig & Bandini 2013 with results of this study).

hummocky cross-bedding formed during episodic higher energy storm conditions (Benincasa *et al.* 2012). Rare nodosariid foraminifera within the mudstone and sandstone units are consistent with a Middle or Late Triassic age. A mudstone sample from AB088 yielded a diverse and abundant palynomorph assemblage (see Benincasa *et al.* 2012, Appendix A for species list) which supports a marine interpretation and places it within the Norian, Late Triassic.

Triassic strata in East Timor were deposited during rifting within the East Gondwana rift system (Haig & McCartain 2010). Basinal facies associations suggest a complex array of depositional environments, with sediment input influenced by varying degrees from nearby carbonate platforms and terrestrial deltaic systems (Haig & McCartain 2010). Litho- and biostratigraphic evidence suggests a prodelta depositional setting for the blue-grey mudstones with sandstone interbeds at Mount Mundo Perdido (Benincasa *et al.* 2012), placing them within the Babulu Group (the Babulu Formation of Bird & Cook 1991) which forms part of the Gondwana Megasequence.

Fig. 10 → Mapped distribution of megasequences in East Timor. Geological boundaries are mostly after Geological Survey Indonesia maps compiled in the late 20th century (e.g. Rosidi *et al.* 1979; Partoyo *et al.* 1995, themselves based on the mapping of Audley-Charles 1968) with the geology in the study areas modified with the results of this study. Areas visited by this study are highlighted. Study areas contain most major fatus mapped as 'Cablac Limestone' by Audley-Charles (1968) and following authors: (1) Mount Mundo Perdido, (2) Mount Laritame, (5) the Matebian Range, (6) the Builo Range, (7) Mount Bibileu, (8) the Saburai Range, (9) Mount Taroman and (11) Mount Loelako. The Saburai Range and Mount Loelako form the eastern and south-eastern boundaries of (11) the Maliana basin. At the eastern tip of East Timor (3) Lake Iralalaru and its neighbouring fatu (4) the Paitchau Range – originally mapped as 'Aitutu Formation' (Audley-Charles 1968; Partoyo *et al.* 1995) – were also investigated by this study.

Fig. 11 →→ Aerial photograph of Mount Mundo Perdido illustrating sample points and 100 m topographic contours. Field work was based out of Ossu. Traverses were conducted into the central regions of the mountain from 4WD tracks which parallel the massif along its northern and southern flanks.

Fig. 12 →→→ Interpreted geological map of Mount Mundo Perdido, constructed using mapped outcrops and aerial photographs. See text for detailed descriptions of geology.

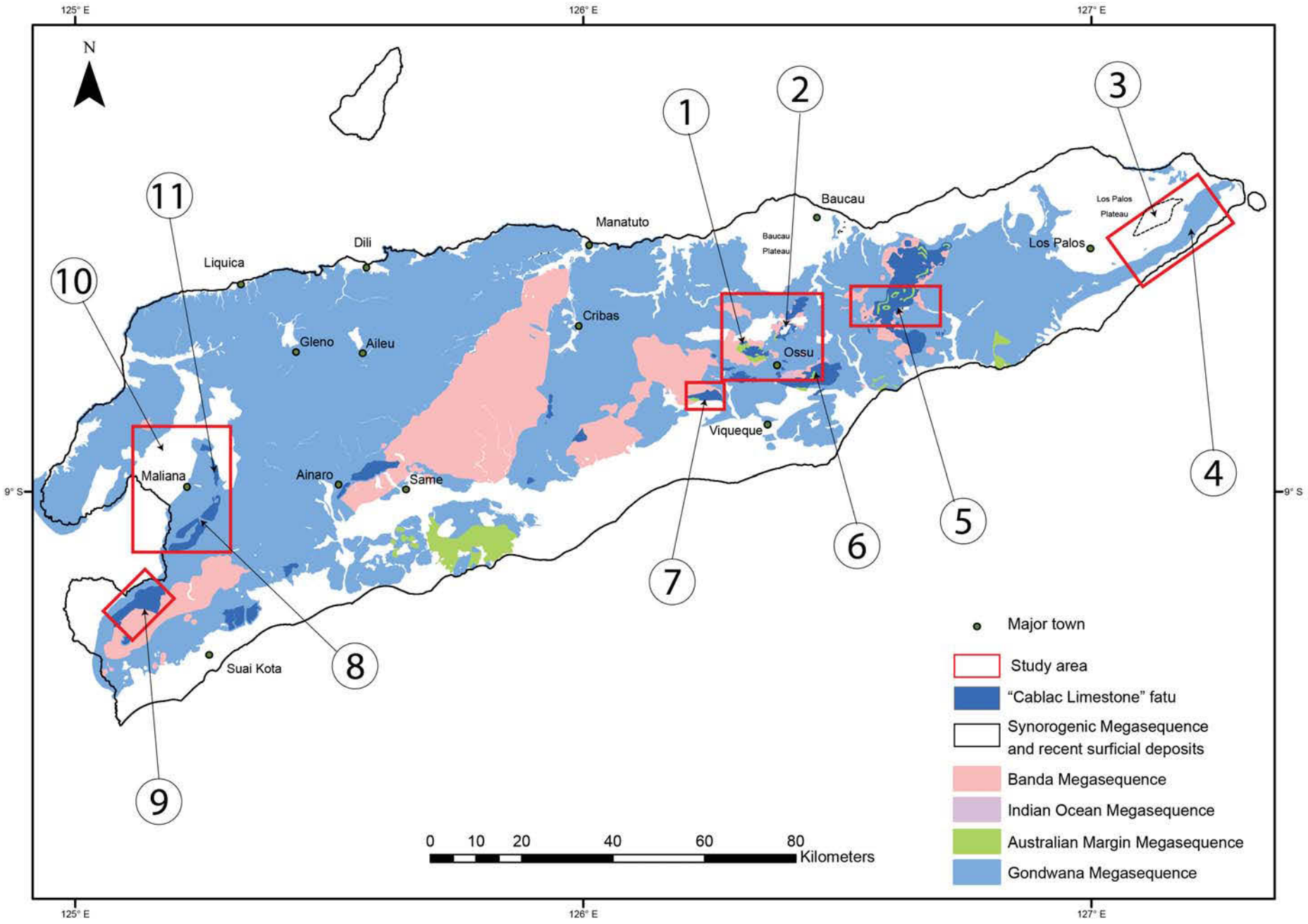
125° E
126° E
127° E
N
9° S
1
2
3
4
5
6
7
8
9
10
11
Baucau
Manatuto
Dili
Liquica
Cribas
Gleno
Aileu
Ossu
Viqueque
Baucau Plateau
Los Palos
Los Palos Plateau
Maliana
Ainaro
Same
Suai Kota
0 10 20 40 60 80
Kilometers
Major town
Study area
"Cablac Limestone" fatu
Synorogenic Megasequence and recent surficial deposits
Banda Megasequence
Indian Ocean Megasequence
Australian Margin Megasequence
Gondwana Megasequence

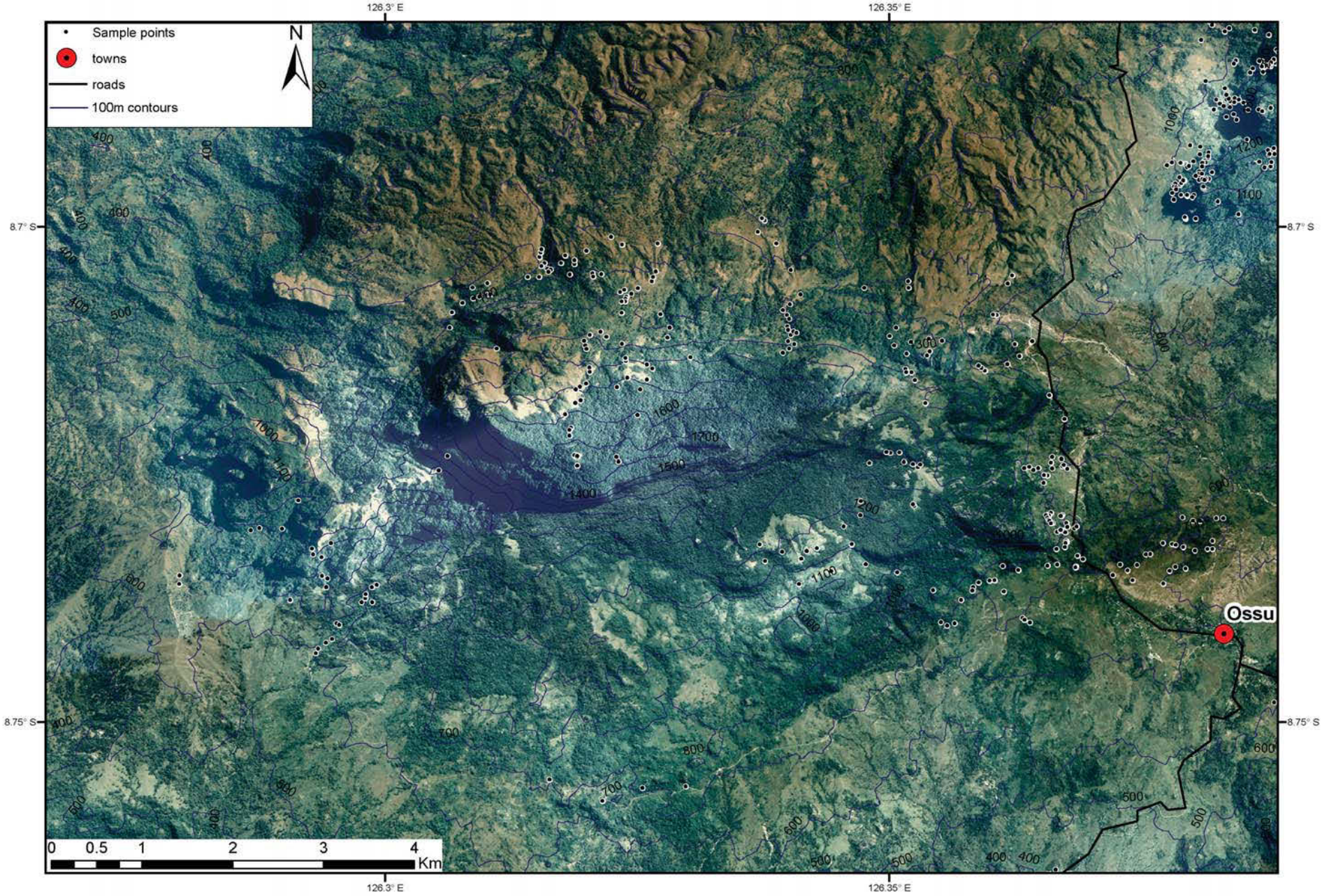
126.3° E
126.35° E
8.7° S
8.75° S
Sample points
towns
roads
100m contours
N
Ossu
0 0.5 1 2 3 4
Km

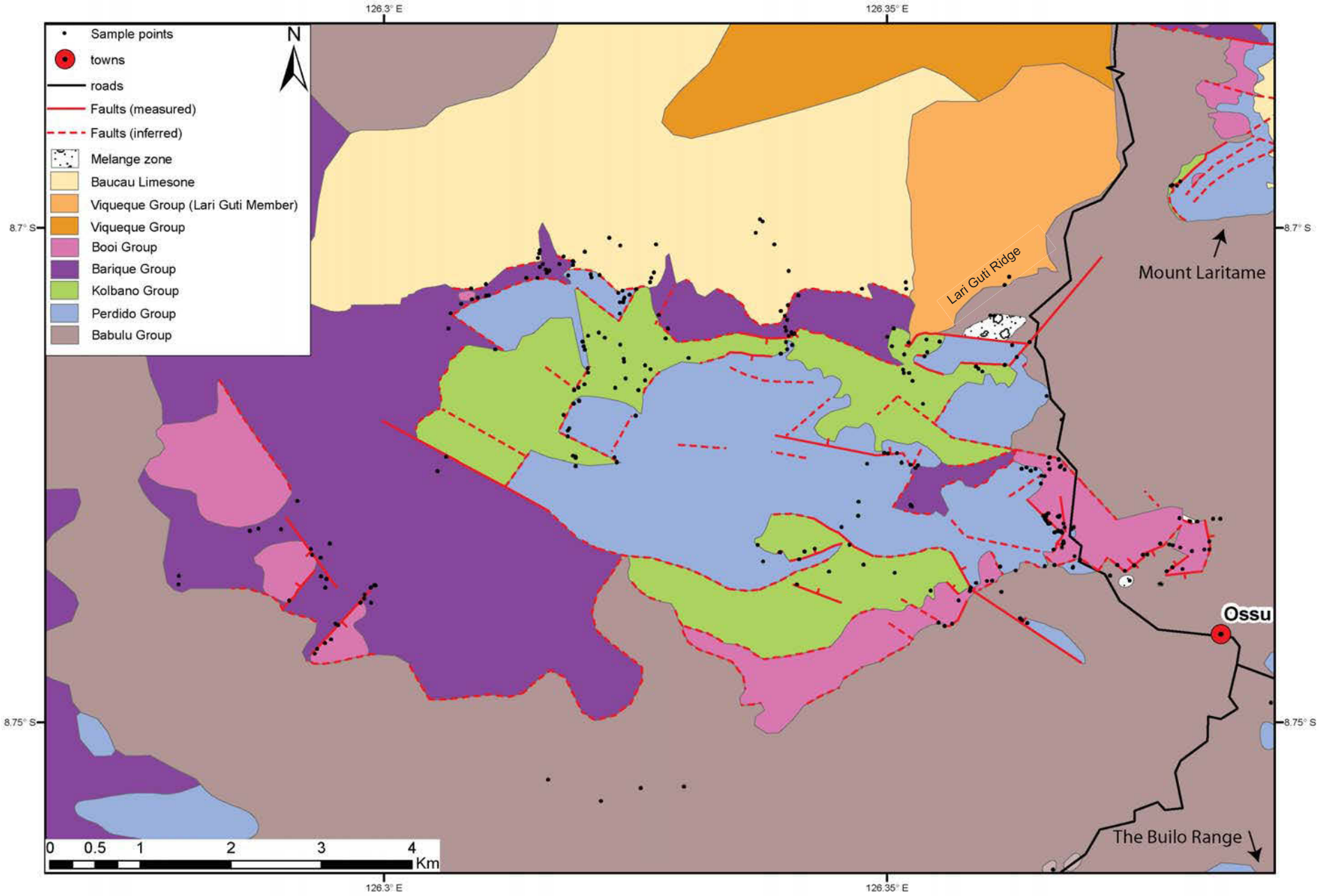
126.3° E
126.35° E
8.7° S
8.75° S
N
Sample points
towns
roads
Faults (measured)
Faults (inferred)
Melange zone
Baucau Limesone
Viqueque Group (Lari Guti Member)
Viqueque Group
Booi Group
Barique Group
Kolbano Group
Perdido Group
Babulu Group
Lari Guti Ridge
Mount Laritame
Ossu
The Builo Range
0 0.5 1 2 3 4
Km

The mudstones surrounding Mount Mundo Perdido were originally mapped as a melange, the 'Bobonaro Scaly Clay' of Audley-Charles (1968). This study has found melange containing an assortment of lithologies to be confined to distinct structural zones, particularly around the south-eastern end of the massif (**Fig. 12**). In most areas originally mapped as Bobonaro Scaly Clay the only rock types present are Babulu Group mudstones and sandstones (Benincasa *et al.* 2012). Mudstones predominate, with the sandstone beds faulted and displaced in 'broken-formation' style (Harris *et al.* 1998).

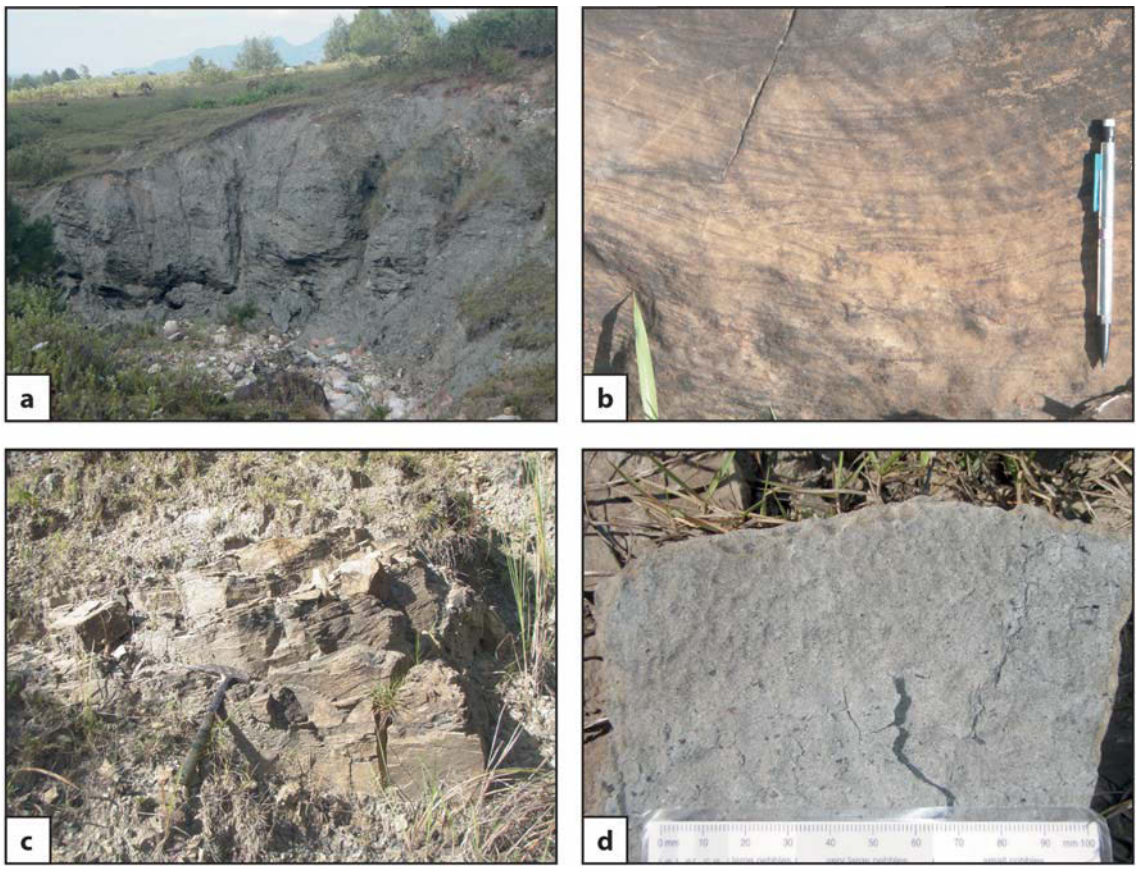

Fig. 13. (a) Thick, deformed Babulu Group mudstone beds near AB117, note horses in top left for scale. (b) Swaley cross-bedding within a Babulu Group sandstone block from AB110, pen for scale. (c) A faulted and broken sandstone bed within the Babulu Group at AB089, hammer for scale. (d) A sample of carbonaceous sandstone from the Babulu Group at AB089. The black flecks are woody fragments. Scale at base of frame = 10 cm.

3.2.2 Radiolarian limestones

Four samples of grey, fine grained, well bedded radiolarian limestone were collected at Mount Mundo Perdido, two outcropping on the southern side of the mountain (AB058 - **Fig. 14**,

AB133) and two found in scree on the mountain's northern flank (AB124, AB154).Radiolaria, calcispheres, spicules and rare nodosariids are visible in acetate peels, along with *Halobia*-type shell "filaments" in one sample (**Fig. 14b**). Some samples contain lenses of reworked peloidal grainstone (Benincasa *et al.* 2012). Due to their limited occurrence at Mount Mundo Perdido they have not been broken out as a separate mapping unit (**Fig. 12**).

Slow sedimentation of radiolarian mud requires low energy, deep water environments and the presence of *Halobia*-type shell filaments suggests an oxygen deficient, basinal setting (McRoberts 1993), with nearby inner neritic carbonate platforms providing lenses of peloids and rare benthic foraminifera transported downslope. The benthic foraminifera species *Siphovalvulina variabilis* suggests a Late Triassic or Early Jurassic age.

Triassic radiolarian limestones have long been recognised within the Gondwanan rocks of Timor (Grunau 1953; Gageonnet & Lemoine 1958) and were placed within the Aitutu Formation by Audley-Charles (1968). This study similarly places the Triassic radiolarian limestones at Mount Mundo Perdido within the Aitutu Group of the Gondwana Megasequence. Like other Triassic units they were deposited within the East Gondwana rift system, with radiolarian muds deposited in the deeper, restricted parts of the rifted basins with minimal deltaic input (Haig & McCartain 2010). Lenses of peloidal grainstone in some samples from Mount Mundo Perdido, along with its close spatial association with the ooid and oncoidal limestones in outcrop, suggest nearby carbonate platform environments.

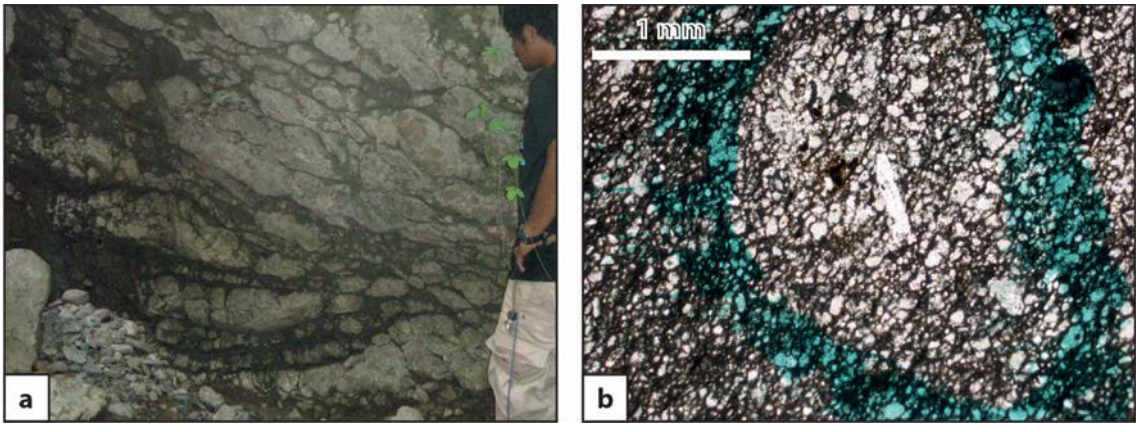

Fig. 14. (a) An outcrop of Aitutu Group limestone at AB058. (b) Image from an acetate peel of a fine-grained radiolarian limestone from the Aitutu Group, found in scree at AB124. The small spherical grains are mostly radiolaria, with the elongate grain in the centre possibly a *Halobia*-type bivalve fragment.

3.2.3 Ooid and oncoidal limestones

These comprise ooid wackestone, packstone and grainstone, oncoid packstone and wackestone, peloid grainstones, and intraclastic limestone (including breccia), (**Fig. 15a, b**). Bedding is difficult to determine, with outcrops appearing highly deformed, usually massive, blocky, well-indurated grey limestone (**Fig. 15a**). Bedding orientation can sometimes be established in the field where grainsize variations are visible, but this is rare. Jointing and stylobedding, common in some exposures, should not be confused with sedimentary bedding. Outcrop is heavily fractured, stylolitized and often dolomitised. In many places, the wackestone includes common thaumatiporellacean algae, dasyclade algae, and carbonate-cemented agglutinated foraminifera. At some sites, the thaumatiporellaceans are cryptoendolithic within cavities of dasyclades (similar to those described by Schlagintweit & Velić 2012, from the Tethyan platform of eastern Europe). Gastropods, shell fragments of bivalves and brachiopods, corals, echinoid spines, and ostracods are rare. These rocks form most of the high cliffs of Mount Mundo Perdido particularly at high structural levels in the central region of the massif (**Fig. 12**).

These limestones resemble modern Bahaman carbonate-bank deposits (Purdy 1963a, b; Bathurst 1975) with low diversity fossil assemblages (see Benincasa *et al.* 2012, Appendix A). The differences in rock types are due to slight differences in depositional environments. The packstones and wackestones suggest deposition in low energy conditions (e.g. **Fig. 15b**), with the grainstones deposited under higher energy conditions where the mud fraction has been winnowed out. At some localities the presence of the foraminifera *Everticyclammina* sp., *Planisepta compressa, Meandrovoluta asiagoensis* and the dasyclade algae *Palaeodasycladus mediterraneus* indicates a late Sinemurian to Pleinsbachian age (Early Jurassic) for at least part of the formation (following age ranges of these species discussed by Septfontaine 1988; Fugagnoli & Broglio 1998; Boudagher-Fadel *et al.* 2001; Fugagnoli *et al.* 2003; Boudagher-Fadel 2008). Other fossil evidence, although indicating the possibility of a broader age range, is also consistent with the late Sinemurian or Pleinsbachian determination. The more widespread occurrence, particularly in fine grainstones and wackestones, of *Siphovalvulina* and/or *Duotaxis* points to a Late Triassic or Early Jurassic age (Haig *et al.* 2007). The thaumatoporellacean algae

Thaumatoporella ?parvovesiculifera is common in many samples constraining these as no older than Middle Triassic and no younger than Cretaceous (Schlagintweit & Velić 2012).

Haig *et al.* (2007) gives similar Bahaman facies carbonates collected from the Cablac Mountain Range a Gondwanan provenance, based on palynological and foraminiferal evidence, and a correlation to platform limestones found on the Exmouth Plateau and in New Guinea. The age and shallow water, metahaline facies of these rocks suggest that carbonate banks were developing on isolated, submerged topographic highs as seas flooded newly rifted basins during the breakup of Gondwana (Haig *et al.* 2007). On Mundo Perdido, these rocks are associated with small isolated outcrops of the Aitutu Formation, some of which contain reworked peloidal sediment derived from similar Bahaman-type facies. These units belong within the Upper Triassic and/or Lower Jurassic and are considered to be part of the Gondwana Megasequence. In central parts of Mundo Perdido, ooid and oncoidal limestones are also closely associated with latest Jurassic to Oligocene carbonate pelagites attributed to the Australian Margin Megasequence (Haig & McCartain 2007), with the oldest unit of the pelagite succession (uppermost Jurassic-lowest Cretaceous) close to the contact (probably faulted).

Audley-Charles (1968) originally mapped the Bahaman-type ooid and oncoidal limestones at Mount Mundo Perdido as 'Cablac Limestone' of Early Miocene age, which has its type locality at the Cablac Mountain Range. At the type locality he confused different limestones of different ages and grouped them as 'Cablac Limestone', a name widely used in Timor literature (Haig & McCartain 2007; Haig *et al.* 2007, 2008 p. 375; Keep *et al.* 2009). Haig *et al.* (2008, p. 375-376) suggested that 'Cablac Limestone' should not be used to designate the Early Miocene shallow-water limestone lacking the 'Bahamite facies' included by Audley-Charles (1968, p. 25-27, table 1) in the 'Cablac Limestone'. Haig *et al.* (2008) re-designated the Early Miocene unit as the 'Booi limestone' (revised to 'Booi Group' in the present study).

Because of the confusion obvious in Audley-Charles's (2011) discussion of the 'Cablac Limestone' this name should be abandoned. Benincasa *et al.* (2012) mapped the 'bahamite

facies' at Mount Mundo Perdido as the Perdido Group, which is of Early Jurassic and possible Late Triassic age, and this study will continue with that nomenclature.

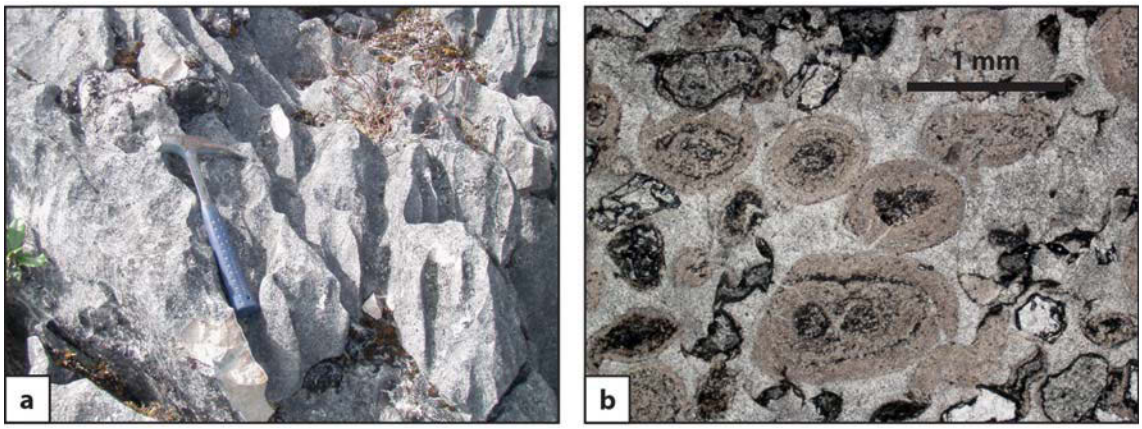

Fig. 15. (a) The weathered surface of a massive, blocky outcrop of Perdido Group limestone at AB276, hammer for scale. (b) Image from an acetate peel of a dolomitised Bahaman-facies ooid packstone/wackestone of the Perdido Group from AB301. Scale bar = 1 mm.

3.2.4 Carbonate pelagites

These dense wackestones with scattered planktonic foraminifera form many of the high cliffs on the northern and southern flanks of the Mundo Perdido massif (**Fig. 12**). Massive, blocky outcrops (**Fig. 16a**) are usually pink to white or grey, while two samples of a Late Paleocene or earliest Eocene unit have a distinctive red colour and finely laminated appearance. Outcrops are extensively stylotised and deformed, with the older, Cretaceous rocks frequently containing elongate chert nodules parallel to bedding (Benincasa *et al.* 2012). On gentle slopes where soil has formed over this lithology vegetation is distinctive and often consists of eucalypts and grasses, in contrast to the dense jungle frequently found over other limestone types.

The oldest unit lacks planktonic foraminifera but the presence of a possible calpionellid tentatively identified as *Calpionella alpina*, associated with *Inoceramus* bivalve prisms, may indicate a latest Jurassic or earliest Cretaceous age. Remaining units can be assigned Early Cretaceous, Late Cretaceous (e.g. **Fig. 16b**) or Paleogene ages based on planktonic foraminiferal assemblages (Benincasa *et al.* 2012, Appendix A). The predominance of planktonic foraminifera over benthic types within a very fine carbonate mud matrix lacking

other sand sized skeletal elements suggests that deposition of these limestones took place within the middle bathyal to abyssal zone (500-3000 m water depth).

Late Jurassic to Middle Miocene sediments were deposited unconformably over the Gondwana Megasequence as the now passive Australian margin subsided to middle to lower bathyal depths after the breakup of Gondwana, with evidence for deposition on a submerged continental terrace similar to the Exmouth Plateau (Haig & McCartain 2007; Keep & Haig 2010). Originally deposited as carbonate ooze, the sediment became indurated, deformed, and extensively stylotised during collision, in contrast to the carbonate pelagites of the basal Synorogenic Megasequence which remain relatively undeformed friable chalk (Haig & McCartain 2007). Previously mapped as the 'Kolbano Sequence' (Harris *et al.* 2000), Haig *et al.* (2008) proposed the term Australian Margin Megasequence to describe this succession, which includes both the Kolbano Group pelagite facies and the Late Jurassic siliciclastic shallow marine Oebatt Group. Lithofacies and biofacies of the pelagites mapped at Mount Mundo Perdido correlate directly to known units within the Kolbano Group (Haig & McCartain 2007).

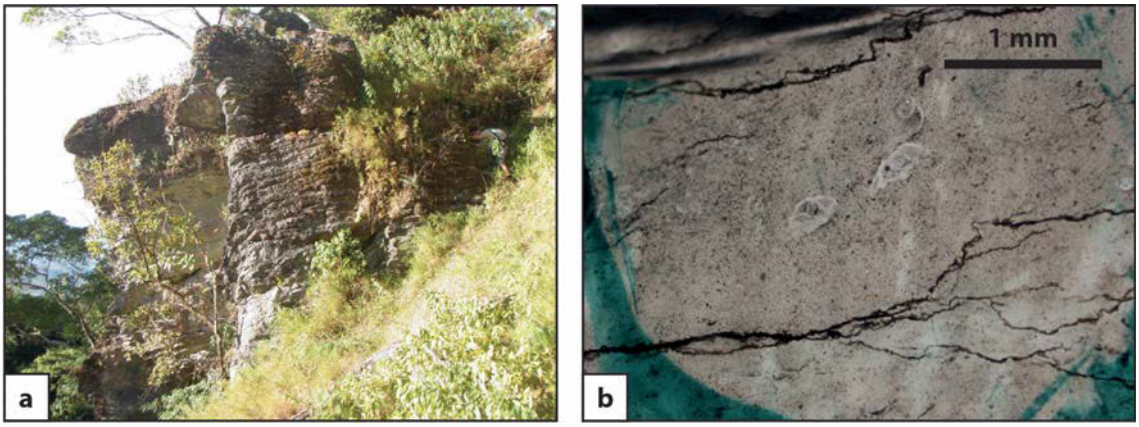

Fig. 16. (a) Well bedded, white Kolbano Group limestone of Cretaceous age at AB163, note geologist under outcrop in top right for scale. (b) An acetate peel taken from Kolbano Group limestones at AB138. The keeled foraminiferal species highlighted, *Dicarinella* sp., is diagnostic of a Turonian age. Scale bar = 1 mm.

3.2.5 Igneous and metamorphic rocks

Igneous rocks include gabbros, breccias (**Fig. 17a**), and undifferentiated volcanic sediments (**Fig. 17b**), whereas metamorphic rocks include mainly schists (**Fig. 17c, d**). These rocks

dominate the geology in the southwest corner of Mount Mundo Perdido (**Fig. 12**) where they outcrop in an area over 2 km^2 of high, rolling hills, covered with sparse vegetation consisting mainly of grasses, and extend around the western edge of the mountain to its northwest corner. Isolated outcrops are also observed within gullies along Mount Mundo Perdido's southern flank, and as blocks within zones of tectonic melange at the eastern tip of the massif (Benincasa *et al.* 2012).

Petrological and geochemical analyses suggest that the igneous rocks at Mount Mundo Perdido share the same source, most likely originating in an island arc type environment (Benincasa *et al.* 2012, Appendix B). Benincasa *et al.* (2012) attributes the metamorphic rocks to the same terrane based on outcrop relationships. At AB234 these rocks are associated with red mud containing clasts of mafic volcanics and a foraminiferal assemblage of Mid-Late Eocene age.

Audley-Charles (1968) mapped volcanic rocks in the northwest and southwest corners of Mount Mundo Perdido as Barique Formation, composed of tuffs with the occasional lava, and interpreted as autochthonous Oligocene extrusive rocks. As structural models developed the Barique Formation was later recognised as Asiatic in origin, having been emplaced as part of thrust sheets, equivalent to pre-Eocene volcanic rocks within West Timor (Audley-Charles *et al.* 1974).

Petrological and geochemical analyses suggest island arc affinities for the volcanics and volcaniclastics mapped at Mount Mundo Perdido (Benincasa *et al.* 2012) which is consistent with geochemical studies of the Barique Formation elsewhere in East Timor (Standley & Harris 2009). This study places the igneous and metamorphic rocks at Mount Mundo Perdido within the Barique Group, which forms part of the Banda Megasequence.

Although no contacts were observed, field relationships suggest that the Barique Group is always faulted against or stratigraphically below the earliest Miocene foraminiferal limestones at Mount Mundo Perdido (**Fig. 18**), similar to relationships observed in the Booi region of West Timor (Tappenbeck 1940). These island arc volcanics and shallow water limestones may

represent the remains of an old Paleogene arc emplaced as part of the Banda Terrane during collision.

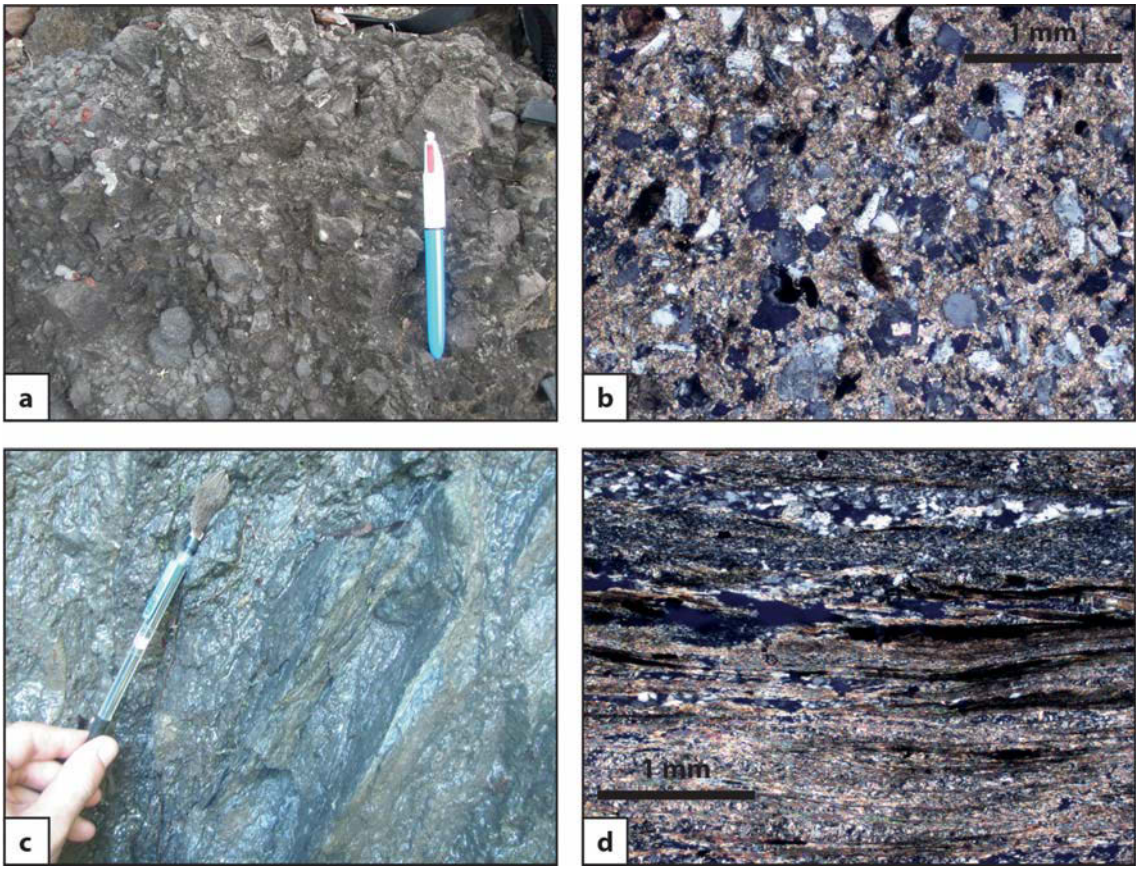

Fig. 17. (a) A volcanic breccia at Mount Mundo Perdido, consisting of large mafic clasts within a matrix of fine-grained volcanic sediment, hammer for scale. (b) A photomicrograph with crossed-polars from AB286, a volcanic sediment of intermediate composition, containing angular grains of quartz and plagioclase within a fine-grained matrix. The matrix is almost completely recrystallised to calcite in this sample. Scale bar = 1 mm. (c) A schist outcropping in a gully at AB216 in the south-western corner of Mount Mundo Perdido, pen for scale. (d) In thin section most schists from Mount Mundo Perdido are observed to be composed of compositionally layered quartz and calcite. This sample is from AB256, viewed with crossed-polars. Scale bar = 1 mm.

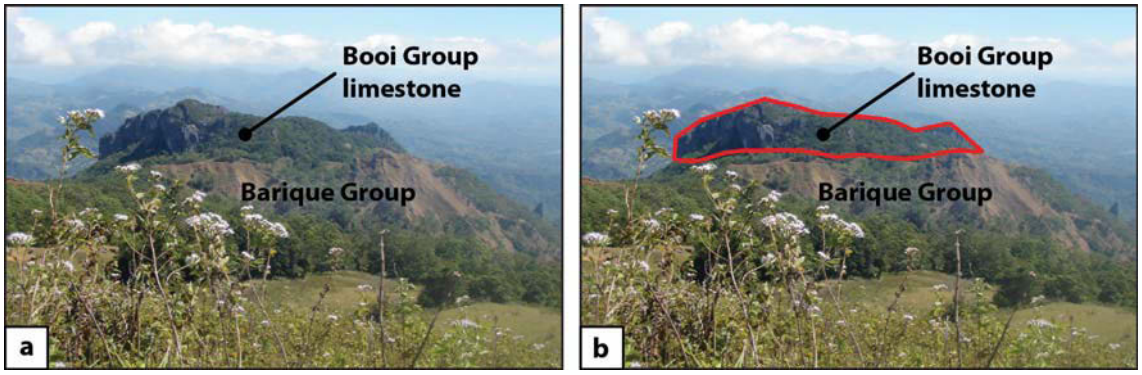

Fig. 18. (a, b) Looking south, from high on the southern flank of the massif, over southern exposures of the Banda Megasequence. Field relationships, most commonly in the northwest and southwest of the study area, often have blocks of Booi Group limestone (highlighted in red on the right) subhorizontally overlying mafic volcanics of the Barique Group, which may be a stratigraphic contact.

3.2.6 Calcareous sandstones with red mudstone interbeds

Calcareous sandstones with red mudstone interbeds (**Fig. 19a**) were observed at only one locality, within a fault zone on the eastern edge of Mount Mundo Perdido. They occur as large blocks on average 5 – 10 m in size, within a blue grey mud matrix. The bedding within these blocks is chaotically folded in similar style to blocks found within structural melange zones elsewhere in East Timor e.g. at Viqueque, 12 km south of Ossu (**Fig. 10**). Sandstone and mudstone beds contain abundant planktonic foraminifera (**Fig. 19b**).

Planktonic foraminiferal assemblages suggest an upper bathyal depositional setting and place these rocks within the Lower or Middle Eocene (Benincasa *et al.* 2012, Appendix A).

These well bedded outer neritic to upper bathyal mudstones and sandstones have no match to coeval rocks within the Australian Margin Megasequence in East Timor, or on the current Australian continental margin, where Eocene lithogies comprise pelagites of deeper, middle to lower bathyal facies. As a result, this study places them within the Banda Megasequence. Found at Mount Mundo Perdido only as blocks within a melange zone, similar Eocene bathyal mudstones have since been observed in situ at Mount Laritame and Mount Bibileu associated with Barique Group volcanics. As a result, this study tentatively places the calcareous sandstones with red mudstone interbeds of Mount Mundo Perdido within the Barique Group of the Banda Megasequence.

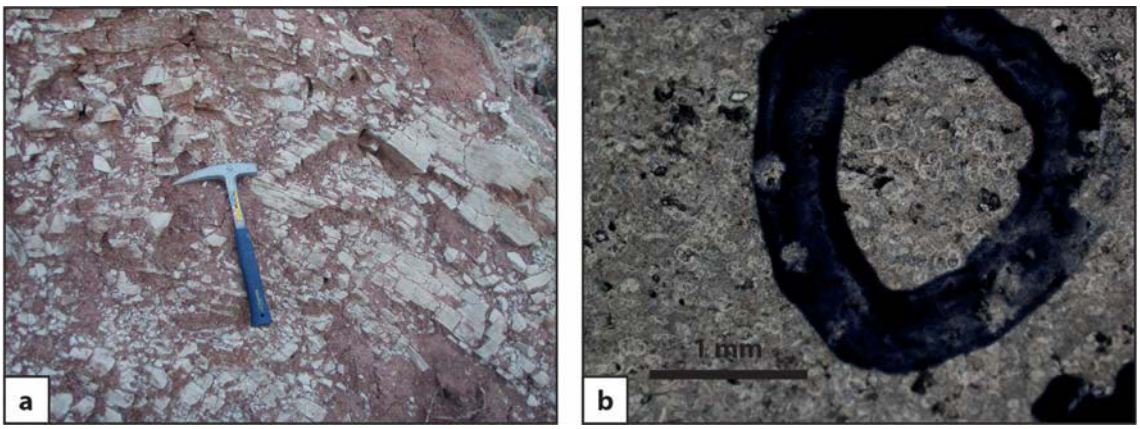

Fig. 19. (a) Calcareous sandstone with red mudstone interbeds at AB061, most likely belonging to the Barique Group, hammer for scale. (b) An acetate peel of the calcareous sandstone from AB061 showing abundant planktionic foraminifera including *Acarinina sp.* and *Morozovella sp.*. Scale bar = 1 mm.

3.2.7 Foraminiferal limestones and associated mudstones and sandstones

Limestones are foraminiferal packstones and wackestones, white to pale grey in colour, containing abundant large benthic foraminifera along with minor coralline algae and other coral debris, echinoid spines, and rare mollusc debris. Outcrop appears as medium bedded to massive and blocky (**Fig. 20a**), and can occasionally have a slight reddish tinge. Larger benthic foraminifera (**Fig. 20b**) are often greater than 1 cm in size, aiding identification of this unit in the field. These rocks make up much of the limestone cliffs at lower structural levels, particularly around the southern and eastern edges of the mountain, although outcrop is also found in the northwest corner (**Fig. 12**). Grey mudstones with thin (<5 cm) sandstone interbeds are also observed associated with the packstones (**Fig. 20c**). Mudstones contain abundant planktonic foraminifera (**Fig. 20d**), with rare leaf impressions and gastropods in some beds. Sandstones consist mainly of fine grained quartz (Benincasa *et al.* 2012).

Planktonic foraminifera within the mudstones suggest outer neritic to upper bathyal deposition. The presence of corals and abundance of larger hyaline benthic foraminifera within the limestones suggests deposition in clear water, neritic environments, and foraminiferal assemblages indicate an earliest Miocene age (Benincasa *et al.* 2012).

Haig *et al.* (2008) determined that the Lower Miocene larger foraminiferal limestones of East Timor were of Asiatic affinity, based both on the absence of any transitional facies between these shallow water sediments and the coeval deep water pelagites of the Australian Margin Megasequence, and the absence of any similar shallow water faunal assemblages of the same age elsewhere on the Australian margin. Lower Miocene foraminiferal limestones of East Timor are of similar facies to Lower Miocene limestones of the Booi region in West Timor (Tappenbeck 1940), which are associated with volcanic and metamorphic rocks of likely Asiatic origin (Wensink & Hartosukohardjo 1990; Harris 2006), and Haig *et al.* (2008) designated the Lower Miocene foraminiferal limestones ‘Booi Limestone’. This study places the Lower Miocene foraminiferal limestones and associated mudstones and sandstones at Mount Mundo Perdido within the Booi Group, of the Banda Megasequence.

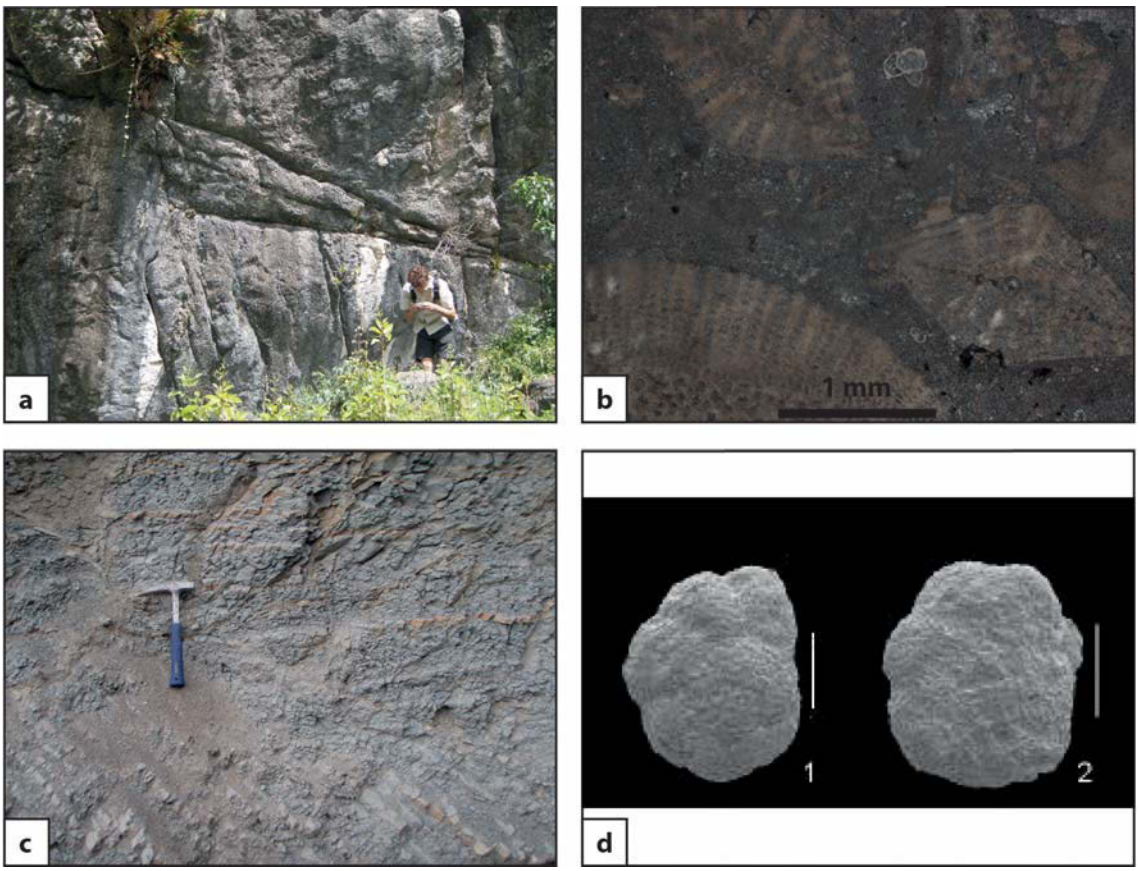

Fig. 20. (a) A medium to thickly bedded outcrop of Booi Group limestone at AB007. (b) An acetate peel from AB173 showing larger benthic foraminifera including *Lepidocyclina*, typical of Te5 Letter Stage, earliest Miocene. Scale bar = 1 mm. (c) Grey Booi Group mudstone beds with thin sandstone interbeds at AB284, hammer for scale. (d) Scanning electron microscope images of planktonic foraminifera *Globorotalia kugleri* from Booi Group mudstone beds at AB284. Scale bar = 0.1 mm.

3.2.8 Limestones and mudstones of the Lari Guti ridge

Thinly bedded foraminiferal packstones and grainstones with thick beds of coral rudstone are found on Mount Mundo Perdido's north-eastern side, near the Lari Guti ridge (**Fig. 12**). Mudstones at the base of the ridge consist of grey mud and sandy mud (**Fig. 21a**), containing abundant planktonic and benthic foraminifera (**Fig. 21b**), (Benincasa *et al.* 2012).

Foraminiferal assemblages in the mudstones at the base of the ridge suggest a depositional environment in the middle bathyal zone, and indicate an age of Zone 21 of the Late Pliocene to Early Pleistocene. Bedded units from the face of the ridge have foraminiferal assemblages which suggest deposition in the upper bathyal to outer neritic zone, and indicate an age of Zone

22 of the Early Pleistocene (Benincasa *et al.* 2012). Audley-Charles (1968) originally interpreted these rocks as a near-shore coral reef succession, the 'Lari Guti Limestone'. However, based on foraminiferal assemblages Haig (2012b) considers these rocks to be deeper water deposits, with the thick coral-rich beds interpreted as debris slides rather than *in situ* reef deposits.

Synorogenic deposits are widespread throughout Timor Island (Audley-Charles 1968; De Smet *et al.* 1990; van Marle 1991a, b; Haig & McCartain 2007; Haig 2012a). They were deposited mainly in marine settings after collision, unconformably overlying older, deformed terranes. They remain relatively undeformed by folding and thrusting, preserving an important record of the post collisional history of the island. The synorogenic Viqueque Group begins with initial pelagic deposition followed by a progressive increase in both sedimentation rate and lithogenic input, recording the uplift and emergence of Timor Island (Haig & McCartain 2007; Keep & Haig 2010; Haig 2012a). Middle bathyal mudstones at the Lari Guti ridge transition into upper bathyal units interrupted by gravity slides of coral reef debris brought down from reefs developed in shallow water on adjacent steep scarps. Similar successions of bathyal mudstones alternating with shallow water sediments transported downslope are found in the Viqueque Group elsewhere in East Timor (Haig & McCartain 2007).

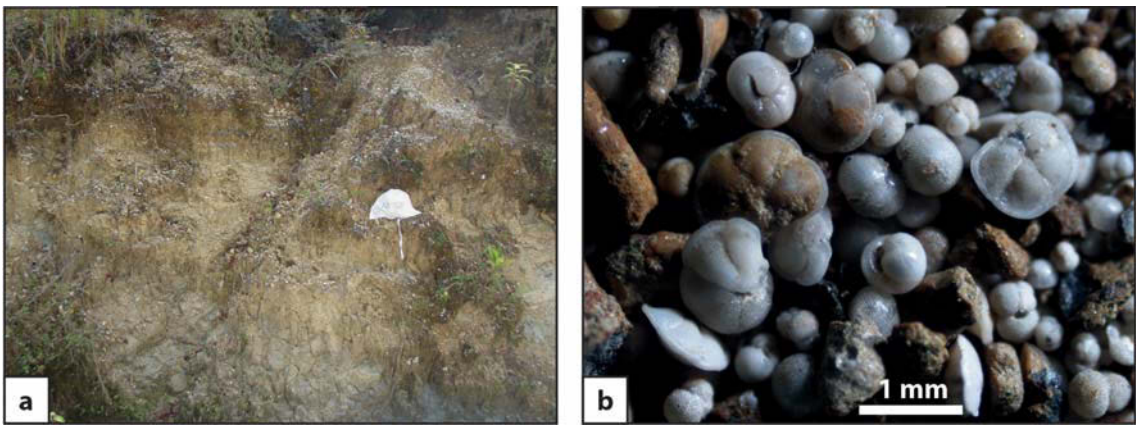

Fig. 21. (a) A thick, friable Viqueque Group synorogenic mudstone on the north-eastern side of Mount Mundo Perdido, near the Lari Guti Ridge. Sample bag for scale. (b) Washed mudstone residue from a synorogenic mudstone at AB085, near the Lari Guti Ridge, containing abundant planktonic foraminifera. Scale bar = 1 mm.

This study places the limestones and mudstones of the Lari Guti Ridge within the Viqueque Group, which forms part of the Synorogenic Megasequence. The bioclastic debris slide deposits within bedded foraminiferalpackstones and grainstones comprise the Lari Guti Member of the Viqueque Group.

3.2.9 Medium bedded limestones of northern Mundo Perdido

Medium to thick-bedded, yellow to white, porous, vuggy packstones and grainstones are found on the lower northern flank of Mount Mundo Perdido (**Fig. 22a**), where the Baucau Plateau (**Fig. 10**) abuts the massif (**Fig. 12**). They contain abundant planktonic and benthic foraminifera, along with echinoid spines, fragments of coralline algae, bryozoan and mollusc debris, and large in situ corals (**Fig. 22b**). Some samples also contain small clasts of mafic igneous rock (Benincasa *et al.* 2012).

Foraminiferal assemblages suggest a Pleistocene age for these lithologies, with depositional environments defined as inner, middle or outer neritic (Benincasa *et al.* 2012, Appendix A). This shallow depositional environment, the diverse, abundant and often fragmented biota, along with the presence of in situ corals suggest that these units may be a succession of near shore coral reefs and reef debris beds (Benincasa *et al.* 2012).

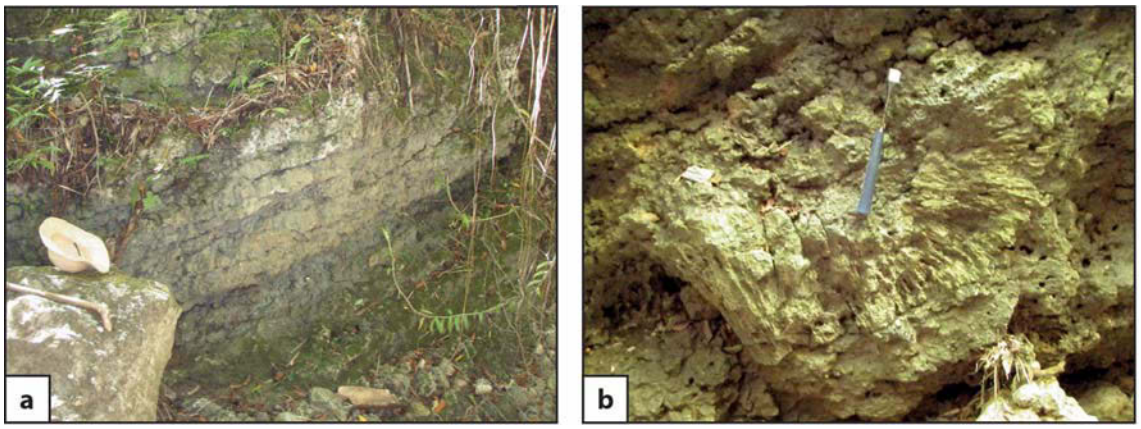

Fig. 22. (a) Medium bedded synorogenic Baucau Limestone within a gully on the north side of Mount Mundo Perdido, at AB129. Note hate at left of frame for scale. (b) A large in situ coral approximately 1 m in diameter within the Baucau Limestone at AB219, hammer for scale.

Lithofacies and ages of the medium bedded limestones from the northern edge of the mapping area are identical to the Baucau Limestone of Audley-Charles (1968), which has its type locality at Baucau (**Fig. 10**), where a series of terraced reef limestones rise up from the coast marking stages of uplift of Timor Island through the Quaternary. From the top of these terraces the Baucau Plateau, 700 m in height, extends south until it abuts the northern flanks of Mount Mundo Perdido and Mount Laritame (**Fig. 10**).

3.3 Mount Laritame

Mount Laritame is a 1390 m high fatu situated near the northern border of the Viqueque district, approximately 5 km north of the town of Ossu and 3 km northeast of Mount Mundo Perdido (**Fig. 10**). The massif has a rhomboidal outline, approximately 2.5 km by 4.5 km, with its long axis oriented northeast-southwest (**Figs 23, 24**). Mount Laritame exhibits a squat profile, with near vertical sides terminating in extensive flat plains which occupy the top of the fatu (**Fig. 23**).

These results are based on mapping completed in 2010 in conjunction with G. Borges, some of which is presented in his 2010 honours thesis (Borges 2010). Rock units are listed in ascending stratigraphic order and age.

3.3.1 Blue-grey mudstones with sandstone interbeds

Blue-grey mudstones with sandstone interbeds occupy much of the lowlands between Mount Mundo Perdido and Mount Laritame (**Fig. 25a, b**), extending up to the southern edges of the Mount Laritame massif (**Fig. 24**). As at Mount Mundo Perdido, medium to thick sandstone interbeds are micaceous, carbonaceous, and exhibit swaley and hummocky cross-bedding. Bedding is discontinuous and chaotically faulted.

Fig. 23 → Aerial photograph of Mount Laritame illustrating sample points and 100 m topographic contours. Mount Mundo Perdido is situated just out of the bottom left of frame.

Fig. 24 →→ Interpreted geological map of Mount Laritame, constructed using mapped outcrops and aerial photographs. See text for detailed descriptions of geology.

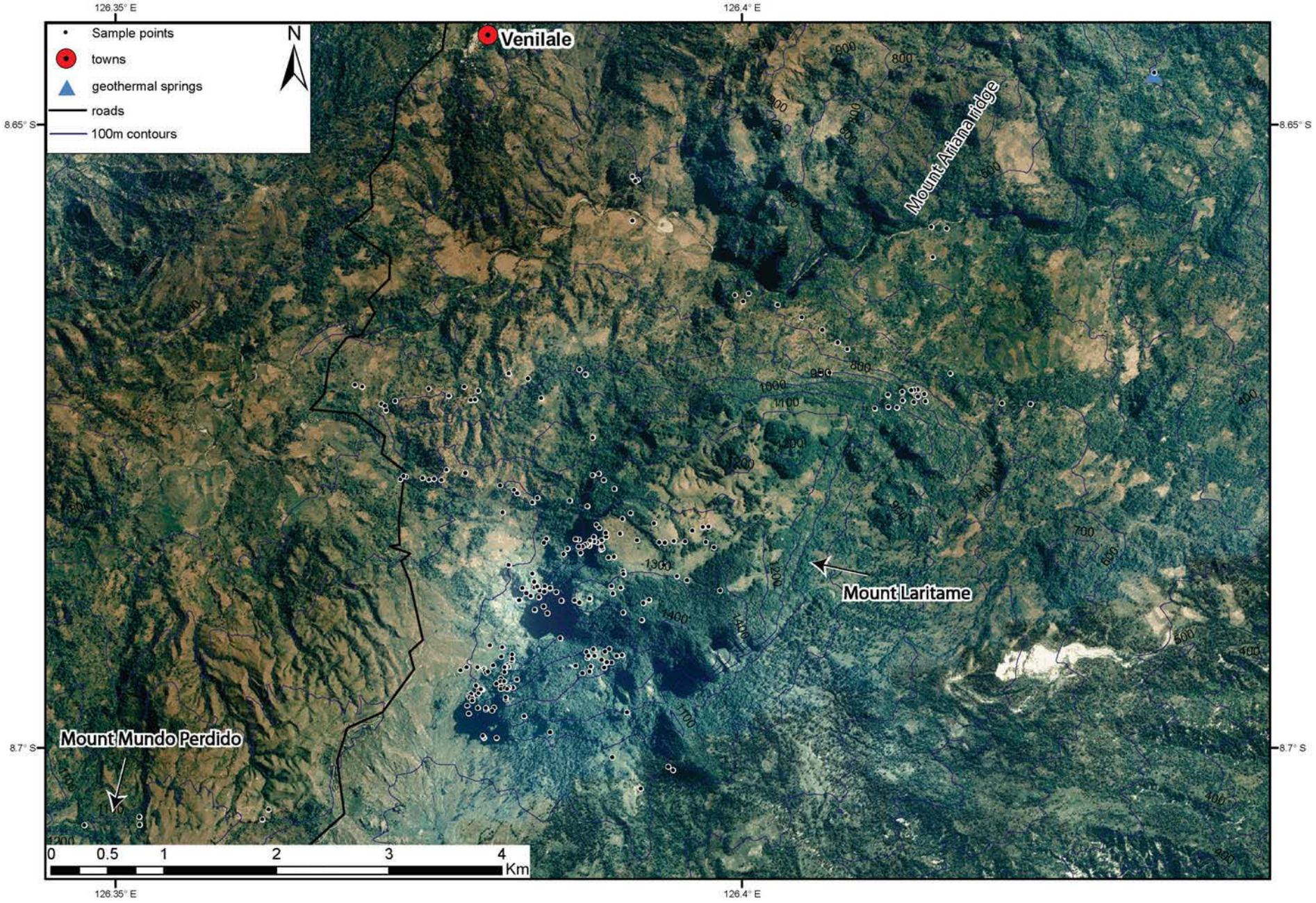
126.35° E
126.4° E
8.65° S
8.7° S
Sample points
towns
geothermal springs
roads
100m contours
N
Venilale
Mount Ariana ridge
Mount Laritame
Mount Mundo Perdido
0 0.5 1 2 3 4
Km

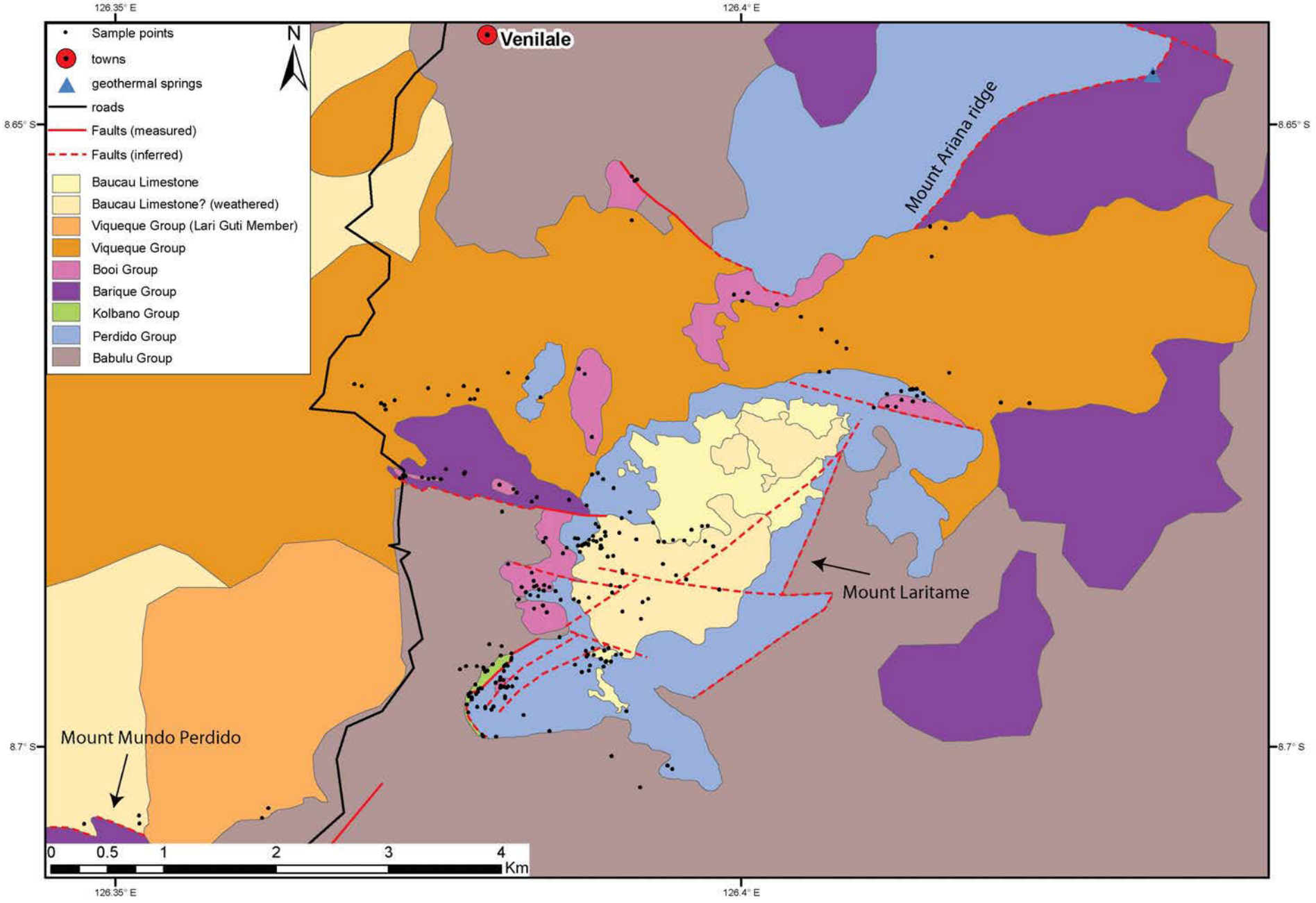
126.35° E
126.4° E
8.65° S
8.7° S
Sample points
towns
geothermal springs
roads
Faults (measured)
Faults (inferred)
Baucau Limestone
Baucau Limestone? (weathered)
Viqueque Group (Lari Guti Member)
Viqueque Group
Booi Group
Barique Group
Kolbano Group
Perdido Group
Babulu Group
N
Venilale
Mount Ariana ridge
Mount Laritame
Mount Mundo Perdido
0 0.5 1 2 3 4
Km

Lithologically identical to the blue-grey mudstones at Mount Mundo Perdido, this unit is interpreted as a pro-delta facies deposited in a shallow rift basin setting. A Norian age of the Late Triassic is assigned following palynology from samples at Mount Mundo Perdido (Benincasa *et al.* 2012).

This unit is lithologically identical and contiguous in outcrop to the Babulu Group mapped at Mount Mundo Perdido, and is similarly assigned to the Babulu Group of the Gondwana Megasequence. Around the southern margins of Mount Laritame, all areas originally mapped as Bobonaro Scaly Clay (Audley-Charles 1968) are found to be occupied by the Babulu Group, no melange zones containing exotic blocks were observed.

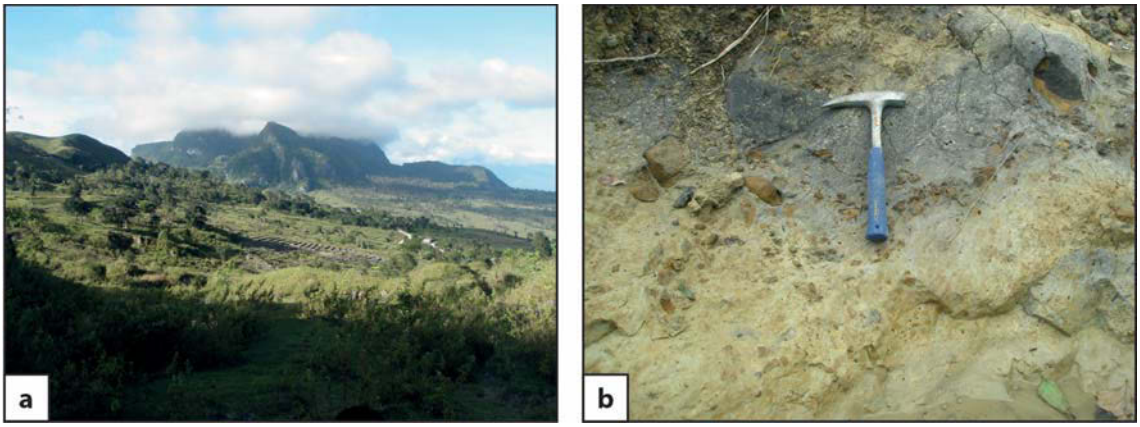

Fig. 25. (a) Facing northeast from the eastern end of Mount Mundo Perdido, Babulu Group mudstones form much of the lowlands between the two fatus. (b) Small blocks of sandstone within weathered Babulu Group mudstones near the south-western corner of Mount Laritame, hammer for scale (image courtesy of G. Borges).

3.3.2 Ooid and peloidal limestones

Ooid wackestones, ooid grainstones and peloidal grainstones are all observed at Mount Laritame where, as at Mount Mundo Perdido, they comprise the central core of the massif and most of the high cliffs (**Fig. 26a**). Outcropping in similar massive, blocky styles, bedding is difficult to distinguish from jointing and fractures, although it was sometimes determined when obvious changes in grainsize were observed. These limestones are extremely well indurated, with extensive recrystallization and calcite veining common, and some dolomitisation occurring within zones of deformation. Similar fossil assemblages to those at Mount Mundo Perdido were

observed, containing chambered sponges, calcareous algae, gastropods, ostracods, echinoid spines, with rare carbonate-cemented agglutinated forams in the wackestones (Borges 2010).

These rocks exhibit identical Bahaman-type facies to the ooid limestones at Mount Mundo Perdido (**Fig. 26b**). Further evidence supporting a Late Triassic to Early Jurassic age for these rocks is observed at Mount Laritame, including the presence of foraminiferal species *Duotaxis metula* Kristan, *Siphovalvulina variabilis* Septfontaine, and *Endoteba* sp. ex. gr. *E. obturata* (Haig *et al.* 2007), and the appearance of Solenoporacean red algae (Borges 2010). The appearance of *Lituosepta* sp. in some samples confines these rocks at least in part to the Sinemurian-Pleinsbachian, following the stratigraphic range outlined by Septfontaine (1988) (Borges 2010).

Ooid and peloidal limestones at Mount Laritame share the same Bahaman-type facies as those at Mount Mundo Perdido (Benincasa *et al.* 2012) and the Cablac Mountain Range (Haig *et al.* 2007), and foraminiferal assemblages indicate the same Late Triassic – Early Jurassic age. Therefore, these rocks at Mount Laritame are similarly placed within the Perdido Group of the Gondwana Megasequence.

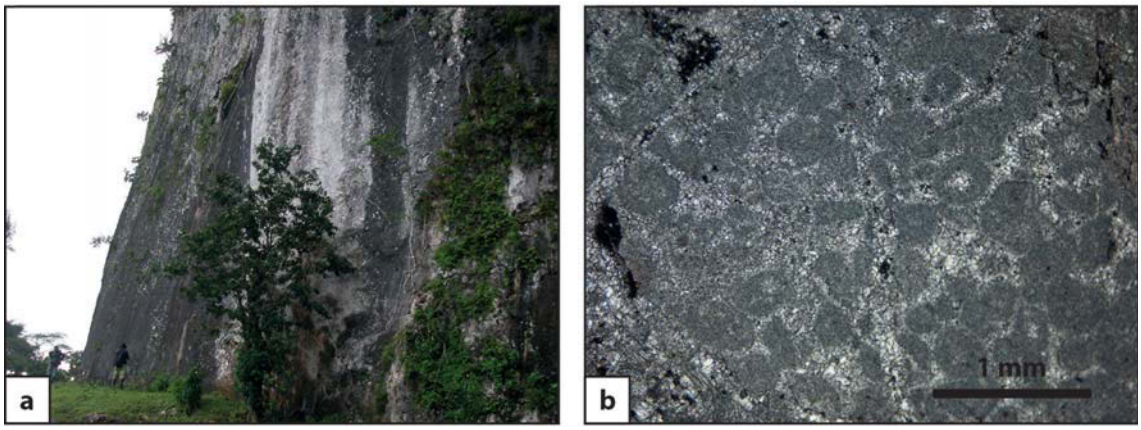

Fig. 26. (a) A large, subvertical, northwest facing cliff of Perdido Group limestone near AB444, on the western edge of Mount Laritame (image courtesy of G. Borges). (b) Acetate peel of a Perdido Group Bahaman-facies ooid packstone from Mount Laritame near AB404. Scale bar = 1 mm.

3.3.3 Carbonate pelagites

Carbonate pelagites occur at Mount Laritame as indurated, pink or white wackestones containing scattered planktonic foraminfera (**Fig. 27a, b**). Outcrop often exhibits pervasive stylotisation resulting in a foliated appearance suggestive of bedding; although this 'stylo-bedding' is not necessarily parallel to depositional structures. As at Mount Mundo Perdido, bedding is best observed in older, Cretaceous pelagite units which often contain elongate, bedding-parallel chert nodules (**Fig. 27**). Extensive veining and recrystallization is common, particularly near zones of deformation. These units are much less common at Mount Laritame than at Mount Mundo Perdido, with observed outcrop confined to the lower slopes of the south-west corner of the massif, where it is faulted against Perdido Group limestones (which form the cliffs above) about high-angle reverse faults.

Similar to the carbonate pelagites found at Mount Mundo Perdido, those at Mount Laritame comprise a very fine carbonate mud matrix with scattered planktonic foraminifera predominant over benthic types, suggesting deposition within the middle bathyal to abyssal zone. A range of Cretaceous ages can be determined based on planktonic foraminifera, including: Late Aptian – Early Albian (late Early Cretaceous), based on the presence of *Blefuscuiana* and *Globigerinelloides*; Late Cenomanian (early Late Cretaceous), based on the presence of *Praeglobotruncana gibba* and *Rotalipora greenhornensis*; and Turonian (Late Cretaceous), based on the presence of indeterminate species of *Dicarinella* and *Marginotruncana* (Borges 2010). It is also likely that some pelagites sampled are of Oligocene age, based on the presence of large globigerinid species including bulbous chambered forms of *Globigerina* sp. including *Globigerina venezuelana – G. tripartita* and *Dentoglobigerina*, and the absence of species diagnostic of an older or younger age within these samples (Borges 2010).

Carbonate pelagites sampled at Mount Laritame correlate with the Cretaceous and Oligocene age carbonate pelagites observed at Mount Mundo Perdido (Benincasa *et al.* 2012) and

elsewhere in East Timor (Haig & McCartain 2007), and are similarly placed within the Kolbano Group of the Australian Margin Megasequence.

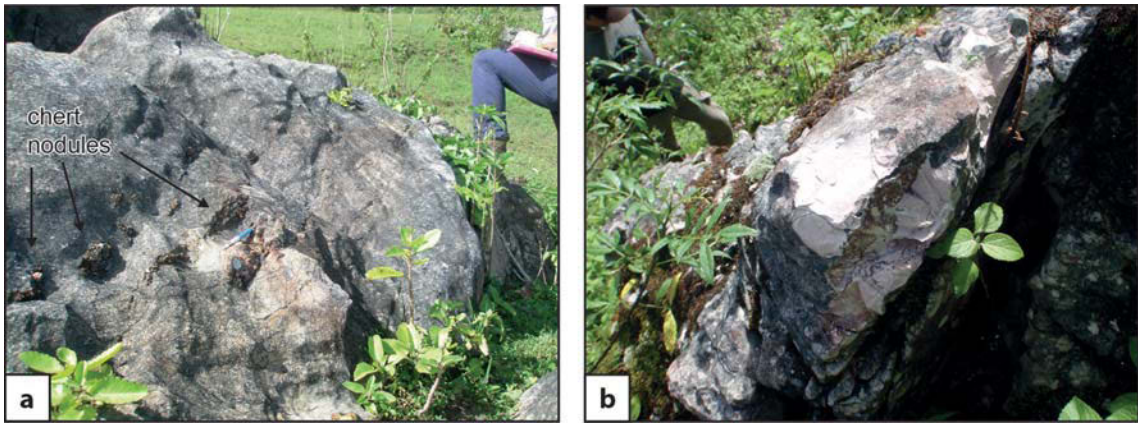

Fig. 27. (a) A large boulder of Kolbano Group limestone from beneath Kolbano Group limestone cliffs in the south-western corner of Mount Laritame. Chert nodules are generally aligned with original bedding planes. Note geologist on right of frame for scale (image courtesy of G. Borges). (b) A fresh surface of this boulder exposes a dense, white, fine grained wackestone. Note geologist in top left of frame for scale (image courtesy of G. Borges).

3.3.4 Igneous and metamorphic rocks

These include schists and volcanic sediments. Schists are green-grey, chloritic, highly deformed, and extensively weathered. Volcanic sediments comprise mostly mafic volcanic breccias with angular clasts (**Fig. 28a**), interspersed with some finer grained volcanic sandstone. At Mount Laritame, observations of these units were confined to a narrow ridge which extends 1.5 km in a westerly direction from the north-west corner of the massif (**Fig. 24**).

Volcanic breccias at Mount Laritame comprise poorly sorted, angular, basaltic clasts in a very fine grained matrix and are likely the pyroclastic deposits of explosive eruptions. This is consistent with detailed geochemical and petrological investigations of identical breccias at nearby Mount Mundo Perdido which suggested that they are the products of island arc volcanism. Metamorphic rocks, where observed, are closely associated with the volcanics and are attributed to the same terrane, most likely representing the basement rock on to which the volcanics were erupted. An interbedded fine sandstone and mudstone unit (**Fig. 28b**) outcrops in the lowlands at the western edge of the ridge containing the volcanic and metamorphic rocks.

This unit is dated as Early Eocene based on planktonic foraminifera (Haig 2009), similar to but slightly older than the Mid-Late Eocene ages determined for sediments associated with the volcanic rocks at Mount Mundo Perdido.

Igneous and metamorphic rocks at Mount Laritame exhibit very similar lithologies and associations to those at nearby Mount Mundo Perdido, and this study also places them within the Barique Group of the Banda Megasequence. The presence of Eocene sediments associated with these rocks at both fatus suggests the Barique Group is, at least in part, of Eocene age in the Ossu region. At Mount Laritame the Barique Group appears to be stratigraphically below the earliest Miocene foraminiferal limestones of the Booi Group, echoing observations previously made at Mount Mundo Perdido and supporting the interpretation of these groups as the remains of an old Paleogene arc emplaced during collision.

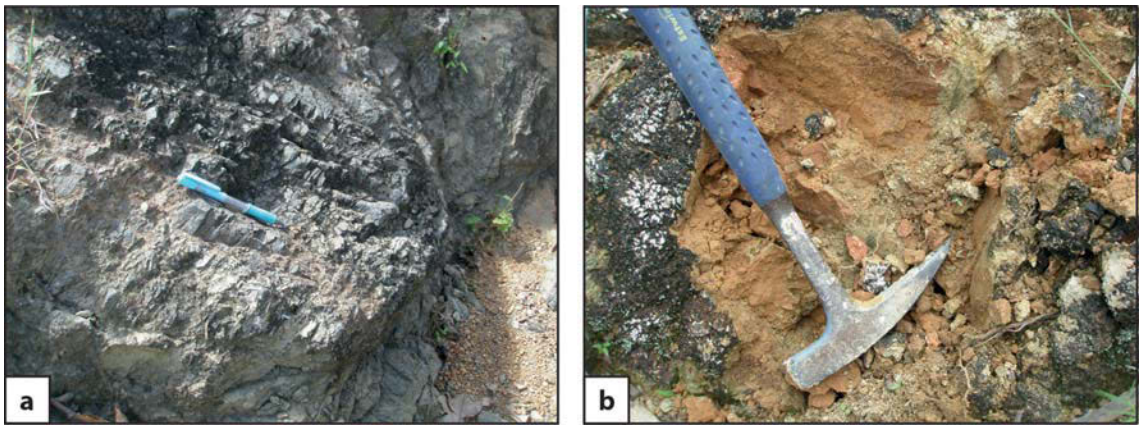

Fig. 28. (a) Barique Group volcanic breccia at AB443, part of a ridge of Banda Megasequence lithologies which extends west from the northwest corner of Mount Laritame, pen for scale (image courtesy of G. Borges). (b) Fine sandstones and mudstones associated with Barique Group volcanics on this ridge contain planktonic foraminiferal assemblages of Eocene age, hammer for scale (image courtesy of G. Borges).

3.3.5 Foraminiferal limestones and associated sandstones and sandy mudstones

Limestones are wackestones and packstones containing abundant larger benthic foraminifera, minor coralline algae and other coral debris. Outcrop is white to pale grey, medium bedded to massive and blocky (**Fig. 29a, b**), with rare interbeds of friable volcaniclastic sandstone. Distribution of these limestones is similar to that at Mount Mundo Perdido, comprising some of

the high cliffs at lower structural levels (**Fig. 24**). At Mount Laritame they are observed most commonly around the northern and western edges of the massif, and appear to stratigraphically overly the igneous and metamorphic rocks where they outcrop on the aforementioned west-trending ridge. Towards the western end of this ridge a quarry was observed containing fossiliferous, brown, sandy mudstone with interbeds of matrix supported conglomerate comprising clasts of limestones, sandstones, mafic volcanics, and abundant macrofossils dominated by colonial coral and gastropod debris (**Fig. 29b, c**), (Borges 2010). Bedding within this unit is indistinct and chaotic.

The presence of corals and abundant large, hyaline benthic foraminifera within the limestones suggests deposition in clear water, neritic environments, with proximity to active volcanism evidenced by volcaniclastic interbeds. The chaotically bedded conglomerates and sandy mudstones likely represent debris slides. A larger benthic foraminiferal assemblage dominated by *Spiroclypeus* sp., *Lepidocyclina* (*Nephrolepidina*) spp. with rare *Lepidocyclina (Eulepidina)* place the limestones within the upper Te Stage of the earliest Miocene.

The foraminiferal limestones at Mount Laritame are identical in age and facies to the Lower Miocene foraminiferal limestones at Mount Mundo Perdido, and this study similarly places them within the Booi Group of the Banda Megasequence. As at Mount Mundo Perdido, they are found stratigraphically above the volcano-sedimentary Barique Group. This relationship, along with the presence of rare volcaniclastic beds within the Booi limestones at Mount Laritame, further supports a volcanic island arc interpretation for the Barique and Booi groups.

3.3.6 Foraminiferal mudstones, sandy mudstones and conglomerates

The lowlands surrounding the northern half of the Mount Laritame massif are dominated by grey to yellow-grey friable mudstones, sandy in places, containing abundant, mainly planktonic, foraminifera (**Fig. 30a, b**). Rare conglomerates and turbidites, commonly containing coral debris, are observed within the mudstone succession. Outcrop is gently dipping and relatively undeformed in comparison to much of the surrounding geology.

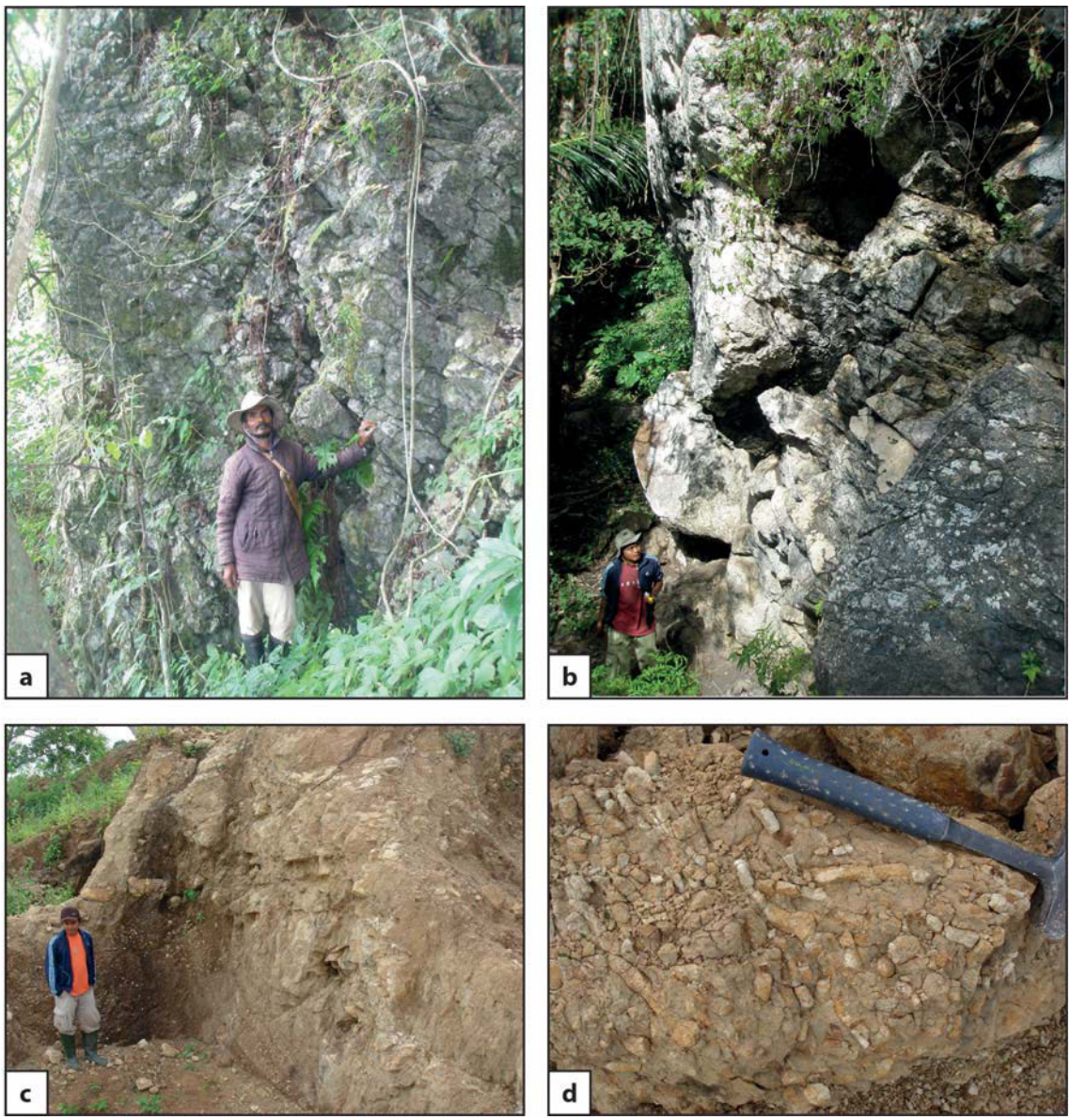

Fig. 29. (a) Outcrop of medium bedded Booi Group limestone forming lower cliffs on the western edge of Mount Laritame. (b) Medium bedded Booi Group limestone outcropping to the north of Mount Laritame, between Mount Laritame and the Mount Ariana ridge (**Fig. 24**). (c) Fossiliferous brown, sandy mudstone in a quarry near AB442, on the ridge of Banda Megasequence lithologies which extends west from the northwest corner of Mount Laritame. (d) Interbeds of matrix supported conglomerate within the mudstone are dominated by colonial coral and gastropod debris, hammer for scale (images courtesy of G. Borges).

Foraminiferal assemblages from the mudstones suggest a bathyal depositional environment and indicate an age range of N20 to N22 of Late Pliocene to Early Pleistocene (Borges 2010). Conglomerates and turbidites containing coral debris represent debris slides sourced from nearby shallow water environments.

The age and lithofacies of the foraminiferal mudstones north of Mount Laritame place them within the Viqueque Group of the Synorogenic Megasequence (Audley-Charles 1968; De Smet *et al.* 1990; van Marle 1991a, b; Haig & McCartain 2007; Haig 2012a). They include similar N21-N22 mid bathyal mudstones and debris slides to those at Mount Mundo Perdido (Benincasa *et al.* 2012) which record the uplift and emergence of Timor Island. However at Mount Laritame older, deeper N20 bathyal mudstones with little to no lithogenic component are also present, which record an earlier stage of post-collisional deposition before Timor Island was emergent. (The earliest evidence for emergence occurs in the Viqueque Group elsewhere in East Timor in the form of turbidite beds low in Zone N21, dated at approximately 3.1 Ma (Haig & McCartain 2007; Keep & Haig 2010; Haig 2012a), containing displaced inner neritic benthic foraminifera). Consistent with the Synorogenic Megasequence elsewhere in East Timor, the Viqueque Group at Mount Laritame remains relatively undeformed compared with older, underlying units.

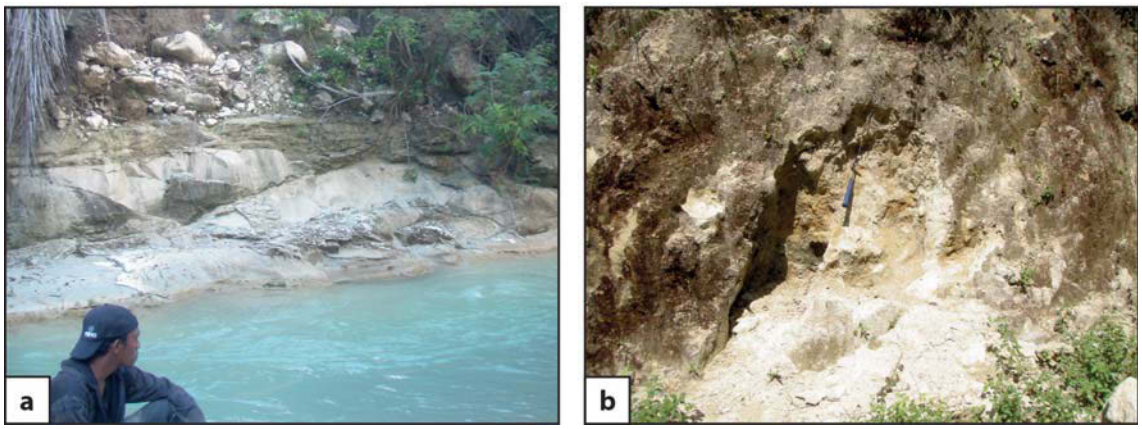

Fig. 30. (a) Well bedded, foraminiferal, fine grained sandstones and mudstones of the Viqueque group exposed in a river bank at AB437, north of Mount Laritame near the Mount Ariana ridge. (b) Foraminiferal, sandy mud of the Viqueque Group at AB436, just below the north-eastern tip of Mount Laritame, hammer for scale.

3.3.7 Medium bedded coralline limestones

Medium to thick-bedded, white to yellow-orange, porous, vuggy, coralline rudstones are widespread at Mount Laritame. They form the broad, horizontal plateaus at the top of Mount Laritame (**Fig. 31a-d**) and extend down the sides of the massif to an altitude of approximately

1100 m, effectively ‘capping’ the massif in a series of flat lying terraces 200 m in thickness (**Fig. 24**). In places these rocks consist of in-situ corals surrounded by an orange, muddy, sandy matrix comprising abundant foraminifera, coralline algae and mollusc debris. Similar orange matrix material is sometimes observed infilling fractures in the older, underlying Gondwana Megasequence limestones. Friable, weathered, red mud is often found associated with this unit on the plateau at the top of the Laritame massif. It has the consistency and appearance of saprolitic clay, and may represent a weathering product of the limestones.

Foraminiferal assemblages within these limestones suggest a neritic depositional environment, and indicate an age within Zone N22 of the Early Pleistocene (Borges 2010). This shallow depositional environment, the diverse, abundant biota including in situ corals, and their occurrence at Mount Laritame as a series of regular, flat-lying terraces, suggests that these rocks represent a near-shore coral reef succession, similar to the Pleistocene reef limestones at Mount Mundo Perdido.

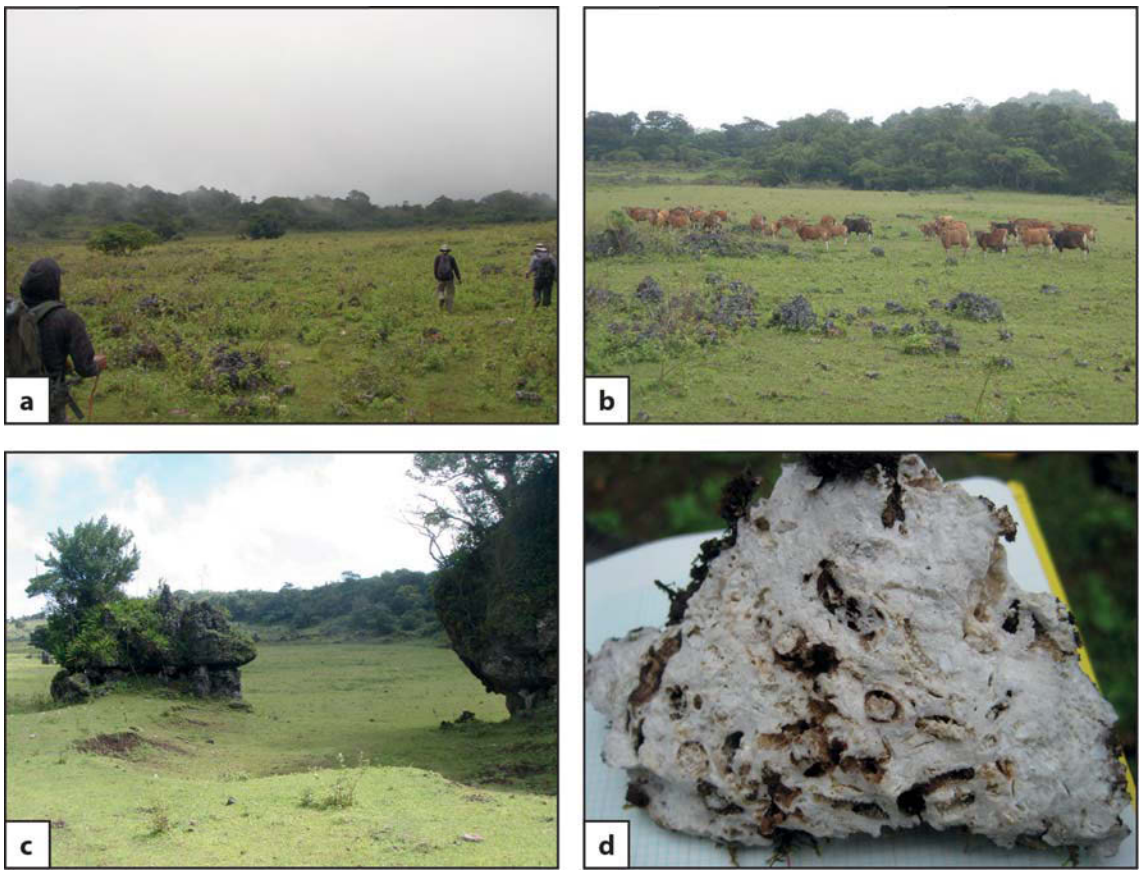

Fig. 31. (a, b) The broad, flat-lying Baucau Limestone plateaus at the top of Mount Laritame. (c) Pinnacles of weathered Baucau Limestone protrude from the plateau in places. (d) Close-up of freshly broken white, fossiliferous, vuggy Baucau Limestone from the top of Mount Laritame. 2 mm grid under sample for scale.

This Early Pleistocene near-shore coral reef succession correlates with the Baucau Plateau (Audley-Charles 1968) and the reef limestones of northern Mount Mundo Perdido (Benincasa *et al.* 2012), and is similarly placed within the Baucau Limestone, of the Synorogenic Megasequence. Deposited at similar paleo-water depths of 40-80 m, the flat lying terraces of Mount Laritame (~1400 m a.s.l.) are now separated from the flat lying terraces of the Baucau Plateau (~700 m a.s.l.) by 700 m of vertical displacement.

3.4 The Builo Range

The Builo Range is an elongate massif situated in the Viqueque District approximately 5 km south west of Ossu, and together with the Mundo Perdido and Laritame massifs effectively encircles the town (**Fig. 10**). Lower and broader than its neighbouring Ossu massifs, the Builo Range has an unusual stretched-S shaped morphology, with two steep sided east-south-east trending ridges joined by a wider, more gently sloping, north-east trending central portion (**Figs 32, 33**). Its highest point at 1235 m is situated on the eastern ridge, but most of the range is less than 900 m above sea level.

Only two days were spent conducting reconnaissance mapping at the Builo Range in 2010, and this brief time was further hindered by very heavy rains and local politics. As such, sampling was confined to near the road that parallels the northern front of the range, and only a small number of samples were collected (**Figs 32, 33**). Rock units are listed in ascending stratigraphic order and age.

Fig. 32 → Aerial photograph of the Builo Range illustrating sample points and 100 m topographic contours. Field mapping and sampling was conducted along the northern front of the range.

Fig. 33 →→ Interpreted geological map of the Builo Range. Field mapping and sampling was conducted along the northern front of the range, with the geology in this area constructed using outcrop data and aerial photographs. Geology outside of the mapped field extent is modified after Partoyo *et al.* (1995) using aerial photographs. See text for detailed descriptions of geology.

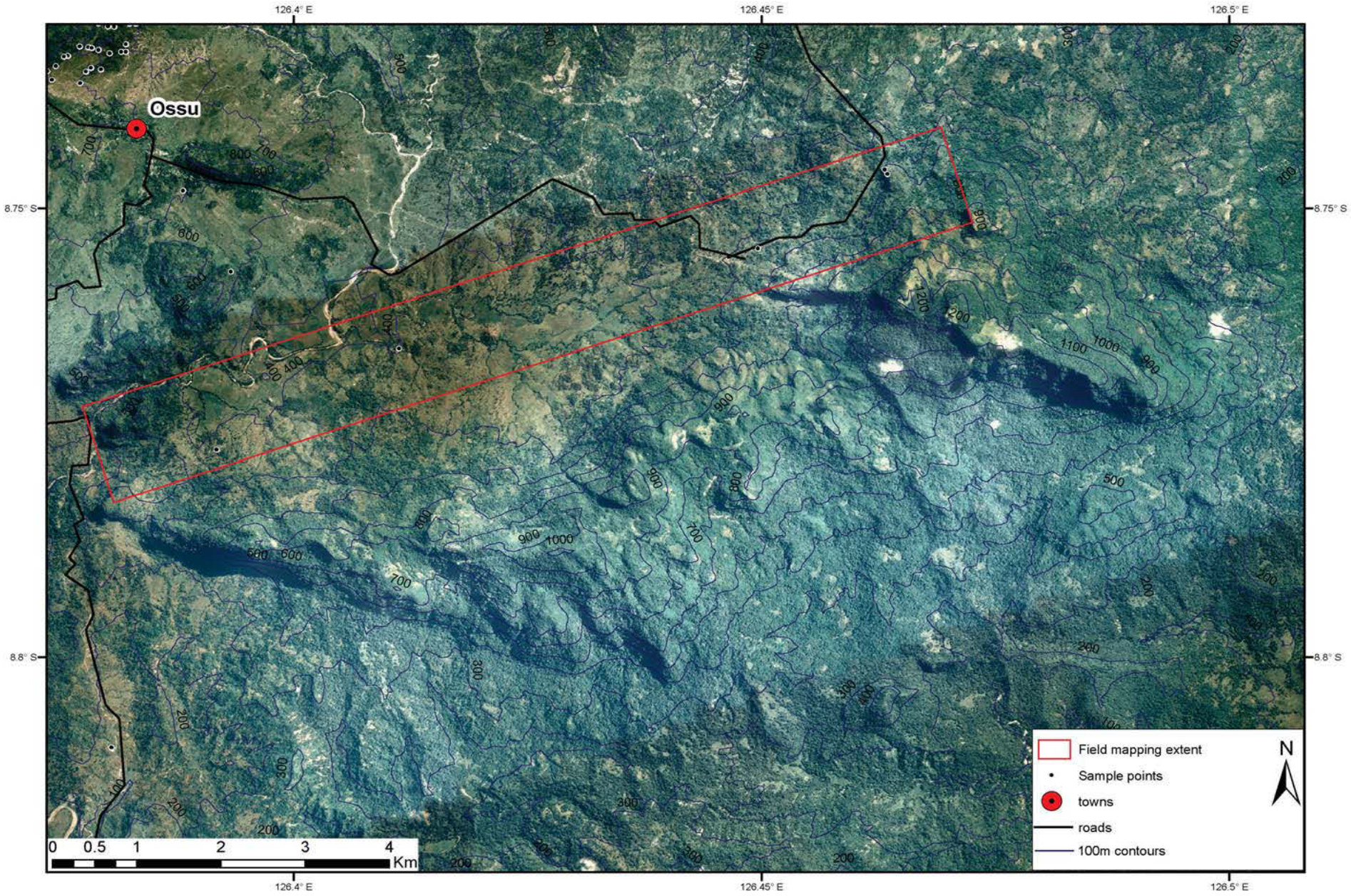
126.4° E
126.45° E
126.5° E
8.75° S
8.8° S
Ossu
0 0.5 1 2 3 4 Km
Field mapping extent
Sample points
towns
roads
100m contours
N

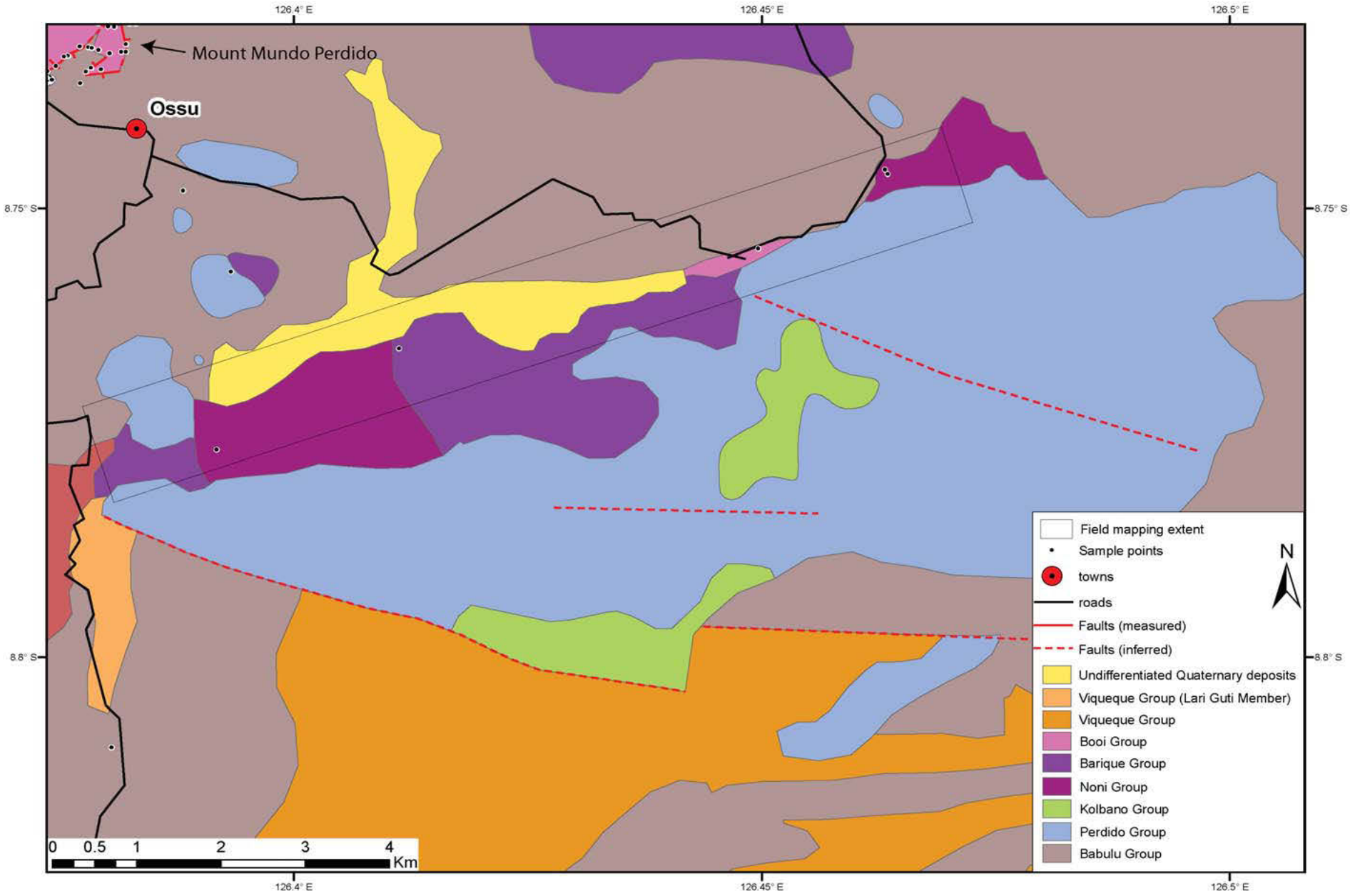
126.4° E
126.45° E
126.5° E
Mount Mundo Perdido
Ossu
8.75° S
8.8° S
Field mapping extent
Sample points
towns
roads
Faults (measured)
Faults (inferred)
Undifferentiated Quaternary deposits
Viqueque Group (Lari Guti Member)
Viqueque Group
Booi Group
Barique Group
Noni Group
Kolbano Group
Perdido Group
Babulu Group
N
0 0.5 1 2 3 4
Km

3.4.1 Blue-grey mudstones with sandstone interbeds

Extending south from the bases of Mount Mundo Perdido and Mount Laritame, blue-grey mudstones with sandstone interbeds also form the lowlands north of the Builo Range (**Fig. 33**). Lithologies are consistent with those sampled at the other Ossu massifs, with faulted and discontinuous medium to thick bedded micaceous, carbonaceous, cross-bedded sandstone (**Fig. 34a, b**).

Contiguous with other blue-grey mudstones occupying the lowlands around Ossu, these rocks are interpreted as the same pro-delta facies, and a Norian age of the Late Triassic is therefore assigned following palynolgy from samples at Mount Mundo Perdido (Benincasa *et al.* 2012). Benthic foraminifera *Pseudonodosaria* sp. in the mudstones at Builo are also consistent with a Triassic age.

Contiguous with and identical to the other blue-grey mudstones mapped in the lowlands around Mound Mundo Perdido and Mount Laritame, these rocks belong to the Babulu Group of the Gondwana Megasequence.

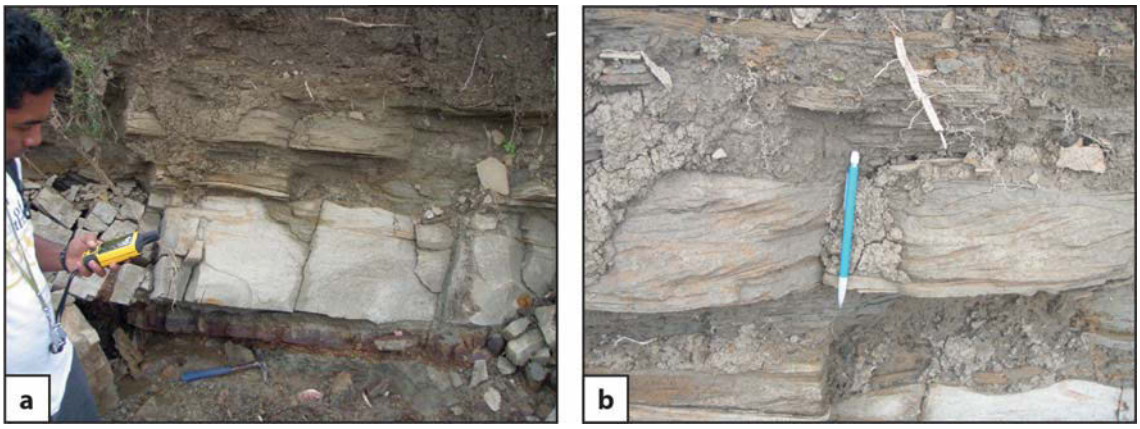

Fig. 34. (a) Interbedded Babulu Group mudstone and sandstone at AB489, just north of the Builo Range. (b) Swaley cross-bedding in Babulu Group sandstone beds at AB489, pen for scale.

3.4.2 Ooid limestones

Ooid wackestones and packstones were observed forming a few small, isolated peaks between Ossu and the northern edge of the Builo Range (**Fig. 35a**). These peaks are generally less than 1

km in width, and rise to a height of 100-300 m above the surrounding blue-grey mudstones. Outcrop styles are typical of ooid limestones in the Ossu region, appearing as massive, blocky, highly indurated grey limestone. Ooid limestones have previously been observed forming the high western peaks of the Builo Range (**Fig. 35b**) (Haig pers. comm. 2012), however this study was unable to sample the interior of the range.

These rocks are identical Bahaman-type facies shallow water carbonate platform deposits as the ooid limestones at Mount Mundo Perdido and Mount Laritame. Biostratigraphic dates were not obtained for these samples but they are similarly placed within the late Triassic – Early Jurassic based on lithofacies correlation.

These rocks share the same Bahaman-type facies as the ooid limestones at Mount Mundo Perdido (Benincasa *et al.* 2012) and the Cablac Mountain Range (Haig *et al.* 2007) and are similarly placed within the Perdido Group of the Gondwana Megasequence.

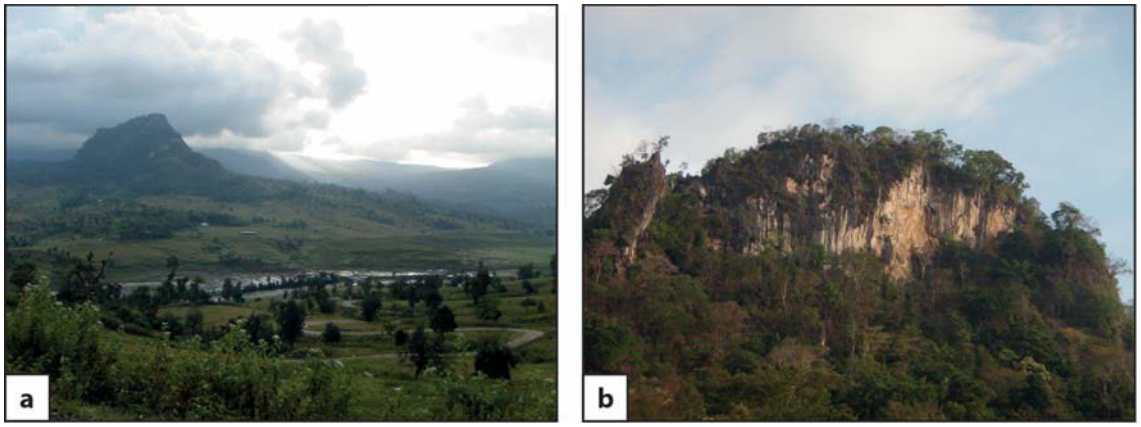

Fig. 35. (a) Facing north from the northern edge of the Builo Range. Small pinnacle hills of Perdido Group limestone, 100-200 m high, form isolated peaks between the Builo Range and Ossu. (b) The high, western peaks of the Builo Range comprise Perdido Group ooid limestones.

3.4.3 Interbedded mudstones and radiolarites

These rocks were observed in roadside outcrop low on the northern slope of the western Builo Range. They comprise interbedded red-grey mudstone; white, friable, porous radiolarite; and red siliceous radiolarian chert (**Fig. 36a, b**). Bedding is thin to medium (5-15 cm) and outcrop is

extensively folded and faulted (**Fig. 36a**). White friable porous layers comprise almost entirely radiolaria, with rare radiolaria also observed within the mudstone beds and chert (**Fig. 36c**).

These radiolarian rich lithogies represent pelagic sedimentation. The lack of carbonates in the succession may suggest a deep abyssal depositional environment, and the absence of a lithogenic component suggests deposition distal to terrigenous influence. Radiolarian species suggest an Early Cretaceous (probably Aptian) age based on a radiolarian assemblage including *Archaeodictyomitra*, *Stichomitra*, *Podobursa*, *Sethocapsa* and *Wrangellium* (Haig pers. comm. 2013)

Similar thin to medium bedded, red, radiolarian rich cherts and shales have been previously described from West Timor (Tappenbeck 1940; van West 1941; Haile *et al.* 1979), where they were dated as Late Jurassic or Early Cretaceous (Haile *et al.* 1979), and elsewhere in the outer Banda Arc at Sulawesi (Bücking 1902; von Steiger 1915, p. 200; 't Hoen & Ziegler 1917, pp. 241-2; Haile 1974; Haile *et al.* 1979). Observed at both locations resting unconformably on schists and gneisses of continental origin, Haile *et al.* (1979) suggested that these rocks represented a previously detached margin of Asia, emplaced on to islands of the outer Banda Arc during collision with the Australian continent. Radiolarian cherts have since been described from East Timor (Haig & Bandini 2013), where they are observed as large blocks within a structural melange zone at Viqueque, approximately 9 km south of the Builo Range. Haig and Bandini (2013) date the Viqueque cherts as Middle Jurassic (late Bathonian – early Callovian), and following Haile *et al.* (1979) suggest that these rocks represent a continental fragment rifted from the Asian margin, and isolated from terrigenous influence at bathyal depth within the Proto-Indian Ocean during the late Jurassic. Haig and Bandini (2013) refer to these deep-sea radiolarian rich deposits as the Noni Group (named for the Noil Noni River in which they outcrop in West Timor), which belongs to the Indian Ocean Megasequence. The deep-sea Indian Ocean Megasequence was emplaced on to Timor, along with the island-arc Banda Megasequence, during Neogene collision with the Australian continent. This study places the radiolarian rich cherts and mudstones of the Builo Range within the Noni Group of the Indian Ocean Megasequence, which extends the known range of the Noni Group in East Timor into the

Early Cretaceous. It is evident in the geological map that the lower northern slope of the Builo Range is a narrow strip 1-1.5 km wide comprising rocks of the Noni Group, the Booi Group, and previously mapped Barique Group (Partoyo *et al.* 1995), which extends parallel to the entire length of the mountain range (**Fig. 33**). These associations may hint at spatial relationships prior to and during collision and warrant further field mapping to clarify.

3.4.4 Interbedded wackestones and cherts

The vertical cliffs at the eastern end of the northern range front were the highest points sampled at the Builo Range, approximately 700 m above sea level. These cliffs comprise thin to medium bedded, pink-white to grey limestones with abundant chert nodules, and interbedded grey chert beds (**Fig. 36d, e**). The limestones are micritic wackestones containing very fine grained skeletal fragments (**Fig. 36f**); mainly bivalves, ostracods, and rare benthic foraminifera. Radiolaria are also present, more abundant within cherty layers.

These rocks also represent pelagic sedimentation; however an abundance of carbonate along with rare benthic foraminifera suggests shallower depths. Once again, the absence of any lithogenic component indicates no terrigenous influence. The presence of Lagenids (*Nodosaria*, *Lenticulina*) and rare carbonate cemented agglutinated foraminifera including *Duotaxis* and *Siphovalvulina* suggest a Late Triassic or Early Jurassic age.

Although more carbonate rich than the Noni Group rocks described above, these rocks are similar deep-sea pelagites of Jurassic age, representing a slightly shallower facies than the radiolarites. This study also places them within the Noni Group of the Proto-Indian Ocean Megasequence.

Fig. 36 → (a) On the northern edge of the Builo Range a thick succession of interbedded red-grey mudstone, friable, white porous radiolarite, and red radiolarian chert is observed at AB487 – these lithologies belong to the Noni Group of the Indian Ocean Megasequence. Hammer for scale. (b) Close-up of siliceous radiolarian chert beds at AB487, pen for scale. (c) An acetate peel of a radiolarite sample from AB487 illustrating an abundant and diverse radiolarian assemblage. Scale bar = 0.5 mm. (d) Steeply dipping, interbedded wackestones and cherts of the Noni Group at AB485, at the eastern tip of the northern range front. (e) Thin chert beds within white wackestone in a sample taken from AB486, also at the eastern tip of the northern range front. (f) An acetate peel from the AB486 sample shows a rare nodosariid foraminifera test within a very fine grained carbonate mud matrix.

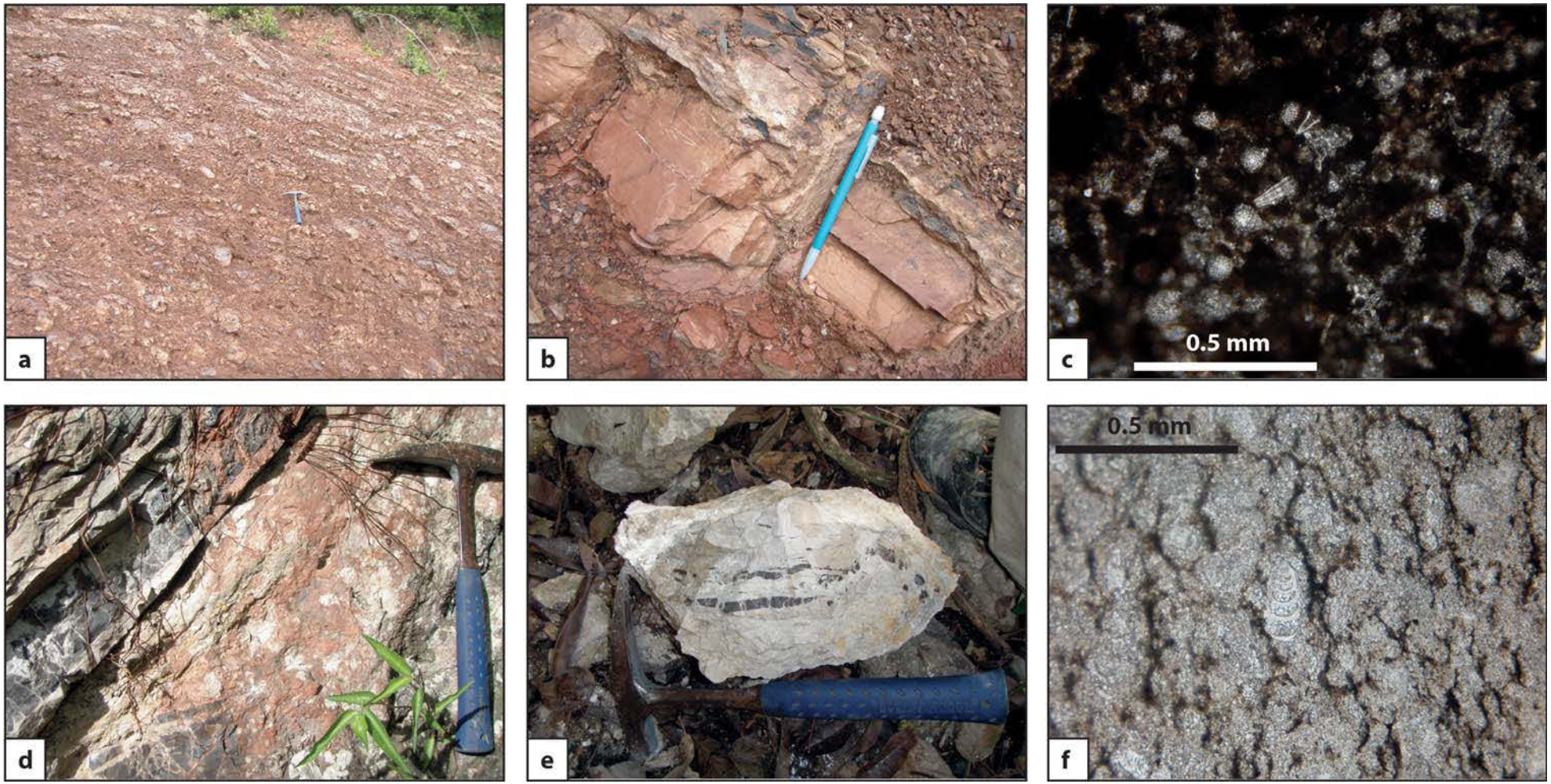
a
b
c
0.5 mm
d
e
f
0.5 mm

At the Builo Range they are observed at the north-eastern end of the strip of Asiatic affinity lithologies (Indian Ocean and Banda Megasequences), in close proximity to Early Miocene mudstones of the Booi Group.

3.4.5 Foraminiferal mudstones

Grey-brown mudstones are observed in roadside outcrop on the northern slope of the Builo Range, at the tip of the easternmost east-south-east trending ridge. Outcrop is massive and appears deformed with abundant veins and small faults (**Fig. 37a, b**). The mudstone contains abundant planktonic foraminifera.

The planktonic foraminiferal assemblage within the mudstones suggests an outer neritic to upper bathyal depositional environment. The presence of foraminiferal species *Globigerinoides triloba* suggests a Miocene age.

These mudstones are a similar lithology and share the same facies and age to the mudstones of the Booi Group, previously observed associated with Lower Miocene larger foraminiferal limestones at Mount Mundo Perdido and Mount Laritame. This study also places the Miocene mudstones of the Builo Range within the Booi Group of the Banda Megasequence. At the Builo Range they are observed proximal to Barique Group and Noni Group rocks, also of Asiatic affinity.

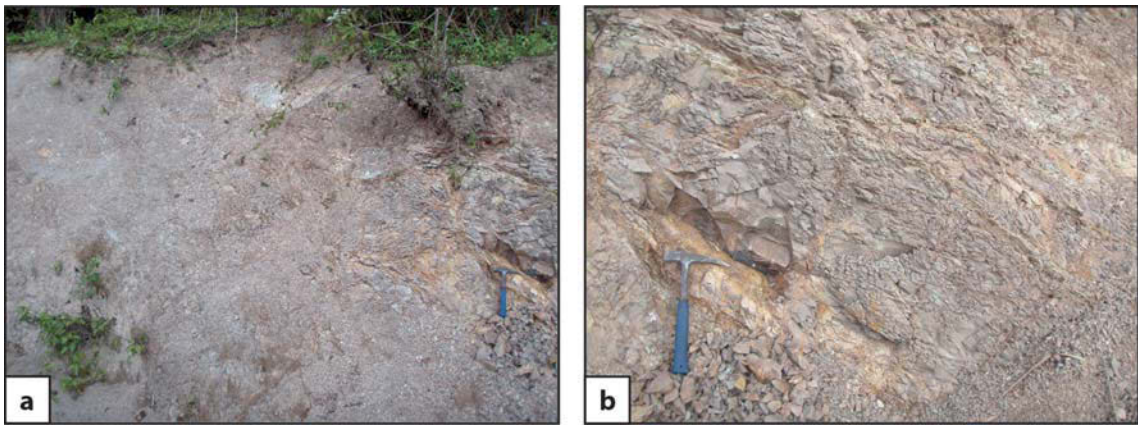

Fig. 37. (a, b) Massive, grey-brown, foraminiferal Booi Group mudstones at AB484, on the northern edge of the Builo Range. Outcrop is extensively veined and faulted. Hammer for scale.

3.5 Mount Bibileu

Mount Bibileu is situated in the Viqueque District, approximately 15 km west of the Builo Range (**Fig. 10**) and 2.5 km northwest of the village of Dilor (**Fig. 38**). It is a small, elongate fatu, approximately 6 km long and 1.5 km wide, with its long axis oriented east-west (**Figs 38, 39**). Mount Bibileu reaches a maximum altitude of 968 m, and its southern edge is bounded by a steep scarp (**Fig. 38**). Two days were spent reconnaissance mapping at Mount Bibileu in 2010, comprising one transect northeast from Dilor to sample the high cliffs on the fatu's southern scarp, and one transect northwest from Dilor to investigate geothermal springs past the western end of the massif. Rock units are listed in ascending stratigraphic order and age.

3.5.1 Ooid limestones

The high south-facing cliffs at the western end of Mount Bibileu comprise medium bedded, white to purple-grey ooid packstones and grainstones (**Fig. 40a, b**). Outcrop is deformed and extensively recrystallised, however abundant large shell debris are visible in acetate peels of some samples including gastropods, ostracods and pectin bivalves. Rare outlines of foraminifera are visible however the samples are too recrystallised to make accurate species determinations.

These rocks are the same shallow water Bahaman-type facies carbonate deposits as the ooid limestones observed at Mount Mundo Perdido, Mount Laritame and the Builo Range. Foraminifera were too poorly preserved to enable a biostratigraphic age determination, however based on lithofacies correlation with the ooid limestones sampled at the fatus surrounding Ossu this study tentatively places them within the Late Triassic or Early Jurassic.

Based on lithofacies correlation with the Bahaman-type facies ooid limestones at Mount Mundo Perdido (Benincasa *et al.* 2012), the Cablac Mountain range (Haig *et al.* 2007) and sampled elsewhere in this study, the ooid limestones at Mount Bibileu are also placed within the Perdido Group of the Gondwana Megasequence.

3.5.2 Carbonate pelagites

Further east on the southern scarp of Mount Bibileu, approximately 1.2 km east of the sampled ooid limestones, the high cliffs comprise pink to white fine grained wackestones (**Fig. 41a**). These rocks have undergone extensive stylotisation which has resulted in a pervasive centimetre-scale foliation, or 'stylobedding', throughout the outcrop (**Fig. 41b, c**). The wackestones contain abundant well preserved planktonic foraminifera and radiolaria in a carbonate mud matrix. These rocks are also abundant in scree on the lowlands between Dilor and the Bibileu massif.

These carbonate pelagites are a similar facies to those found at Mount Mundo Perdido and Mount Laritame, with predominantly planktonic foraminifera within a very fine carbonate mud matrix suggesting deposition within the middle bathyal to abyssal zone. The presence of planktonic foraminifera species *Acarinina* sp. and *Morozovella* sp. (e.g. **Fig. 41d**) suggests an age of Early to Middle Eocene.

Carbonate pelagites sampled at Mount Bibileu correlate with Eocene age carbonate pelagites observed elsewhere in East Timor (Haig & McCartain 2007), and are similarly placed within the Kolbano Group of the Australian Margin Megasequence.

Fig. 38 → Aerial photograph of Mount Bibileu illustrating sample points and 100 m topographic contours. Field mapping and sampling was conducted around the western end of the fatu, north of Dilor.

Fig. 39 →→ Interpreted geological map of Mount Bibileu. Field mapping and sampling was conducted around the western end of the fatu, north of Dilor, with the geology in this area constructed using outcrop data and aerial photographs. See text for detailed descriptions of geology. Geology outside of the mapped field extent is modified after Partoyo *et al.* (1995) using aerial photographs. Lithologies outside of the mapped field extent not described in the text include the Dilor Conglomerate (Conglomerates and coarse sands in the upper part of the Viqueque Group – Audley-Charles, 1968) and the Lolotoi Metamorphic Complex (metamorphic basement rocks of the Banda Megasequence – see **Fig. 9**).

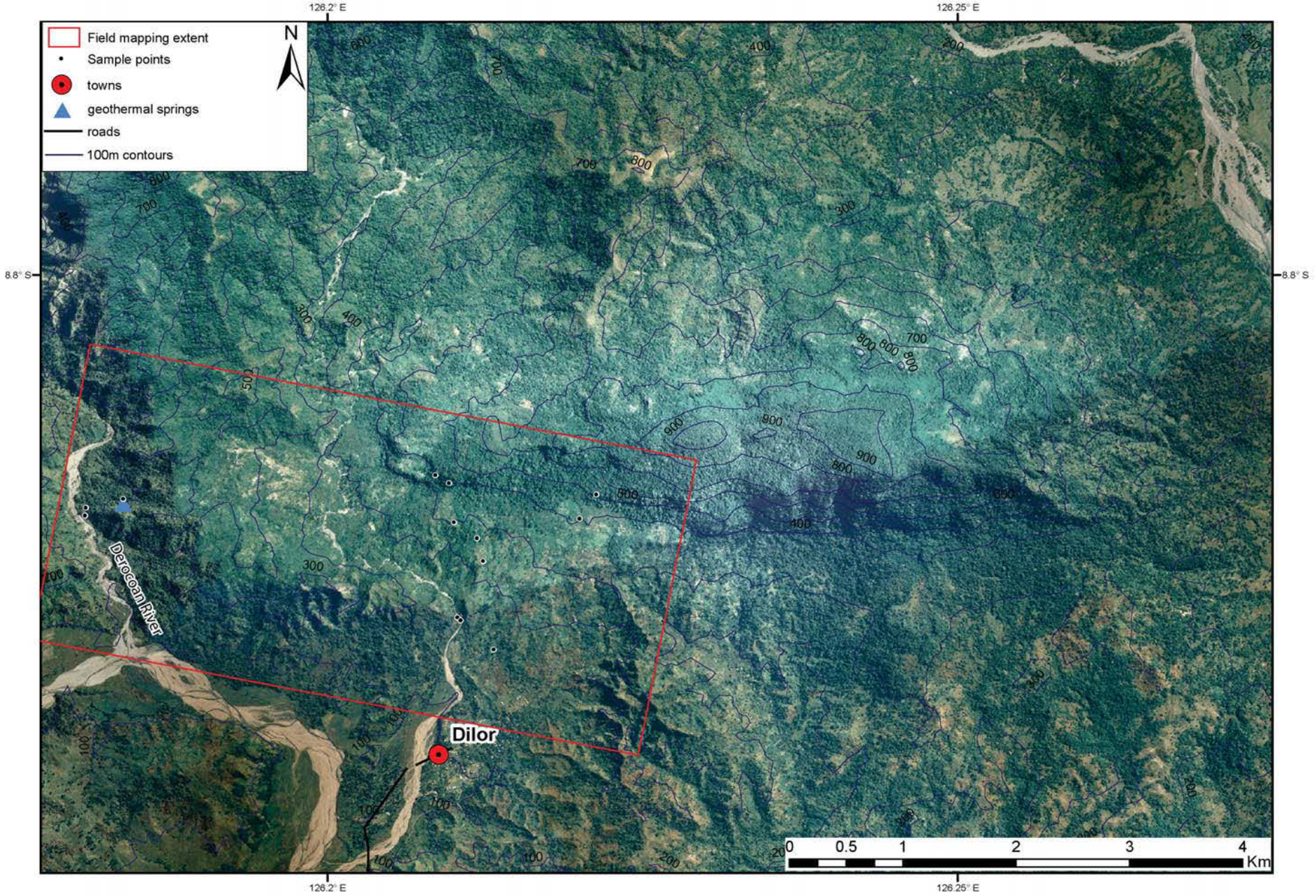
126.2° E
126.25° E
8.8° S
Field mapping extent
Sample points
towns
geothermal springs
roads
100m contours
N
Dilor
Darocoan River
0 0.5 1 2 3 4
Km

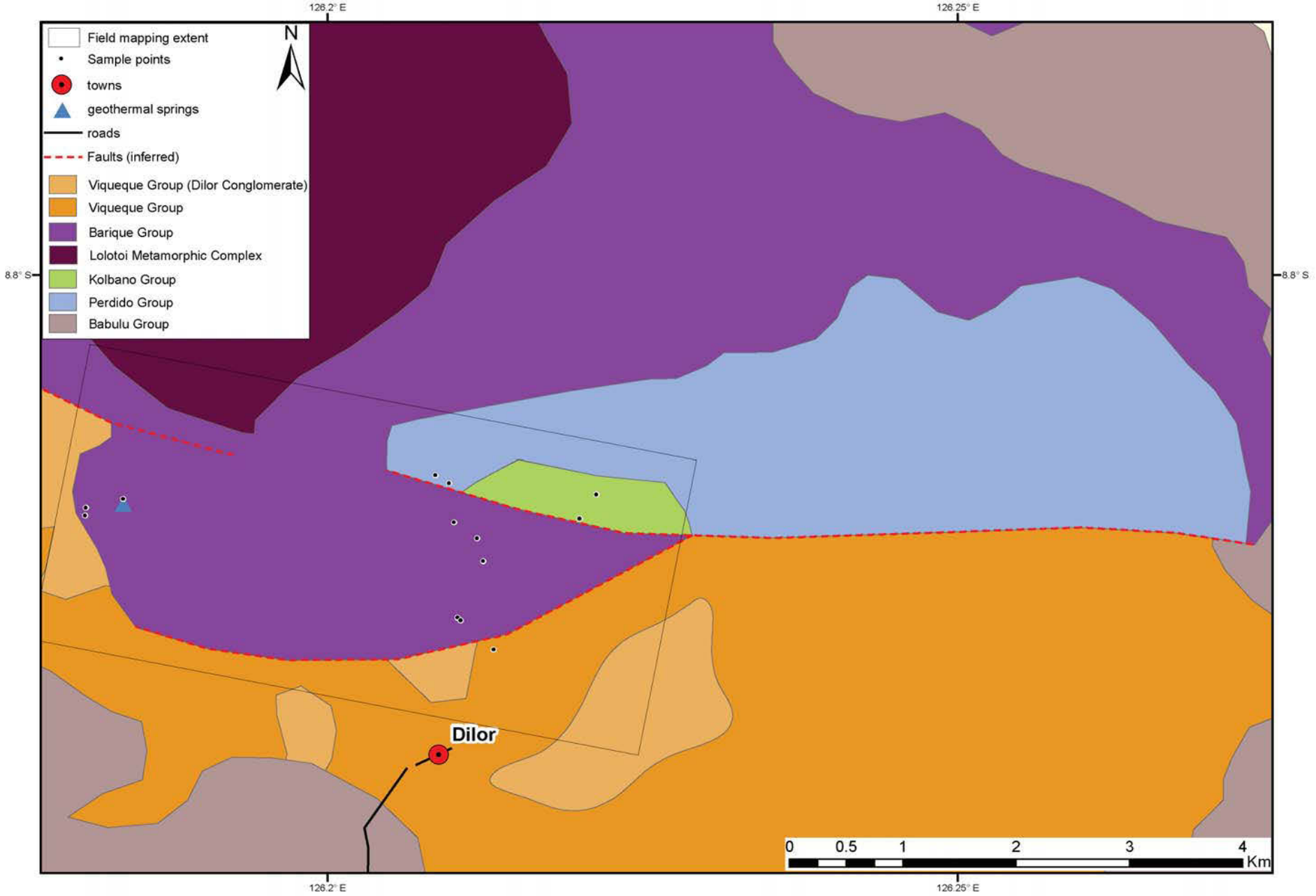
126.2° E
126.25° E
8.8° S
N
Field mapping extent
Sample points
towns
geothermal springs
roads
Faults (inferred)
Viqueque Group (Dilor Conglomerate)
Viqueque Group
Barique Group
Lolotoi Metamorphic Complex
Kolbano Group
Perdido Group
Babulu Group
Dilor
0 0.5 1 2 3 4
Km

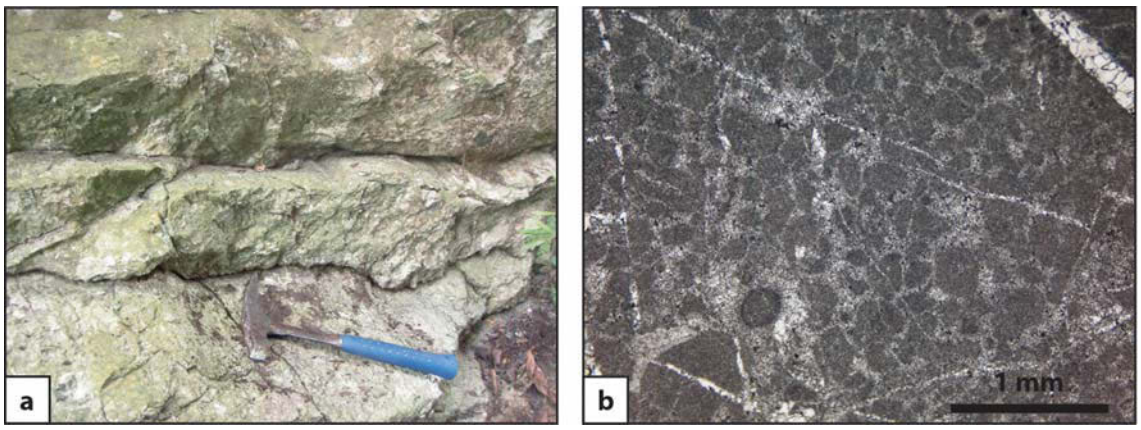

Fig. 40. (a) White, medium bedded Perdido Group limestone from the high south-facing cliffs at the western end of Mount Bibileu at AB542. Hammer for scale. (b) Image from an acetate peel of a Bahaman-facies ooid packstone of the Perdido Group from AB541. Scale bar = 1 mm.

Fig. 41. (a) Kolbano Group carbonate pelagites comprising high cliffs on the southern scarp of Mount Bibileu at AB543. (b) Pervasive centimetre-scale foliation, or 'stylobedding', in Kolbano Group limestones at AB543, a result of extensive stylotisation. Pen in bottom-left of frame for scale. (c) Pink, early-middle Eocene Kolbano Group carbonate pelagite at AB544, with 'stylobedding' visible on the fresh surface. Pen for scale. (d) Image from an acetate peel of a sample from AB543, illustrating extensive recrystallisation in bottom left of frame. A foraminiferal test of *Morozovella* sp. is present in the centre of frame, indicative of early-middle Eocene age. Scale bar = 0.5 mm.

3.5.3 Volcanic breccia

The low hills surrounding the western end of the Bibileu fatu are mostly covered soil and very little outcrop was observed. However, mafic volcanic material is abundant in scree throughout this area, comprising mainly volcaniclastic sandstones and breccias. Volcanic breccias were observed in situ in rare locations within incised river gullies. These outcrops are very weathered, comprising poorly sorted, highly angular clasts of mafic volcanic material 1-20 cm in size (**Fig. 42a**).

At AB545 a small, poorly preserved outcrop of brown-white, porous, friable, fine to medium grained sandstone was observed in the path leading up from the eastern bank of the Derocoan River, surrounded by soil and volcanic scree. It contains a range of grain types including subangular to subrounded quartz, mafic lithic fragments, and abundant foraminifera (**Fig. 42b**).

Although observations were limited to heavily weathered outcrop and scree, the poorly sorted, angular volcaniclastic breccias suggest that these rocks are at least in part pyroclastic deposits, though some of the finer grained rocks found in scree may represent epiclastic material. Associated sandstones at AB545 are of latest Paleocene to Early Eocene age, based on the presence of the planktonic foraminiferal species *Morozvella* sp.

The volcanic breccias appear very similar to those observed in the Barique Group at Mount Mundo Perdido (Benincasa *et al.* 2012) and Mount Laritame and although little outcrop was observed at Mount Bibileu, the rounded, low, soil covered hills are typical of the easily weathered Barique Group lithologies. Eocene sediments associated with the volcaniclastic rocks are consistent with observations of the Barique Group at Mount Mundo Perdido, Mount Laritame and the Barique Group type area near Barique (Haig pers. comm. 2012). The Barique Group has previously been mapped north and east of Mount Bibileu (as Barique Formation – Audley-Charles 1968; Partoyo *et al.* 1995), and this study increases its extent south around the tip of Mount Bibileu.

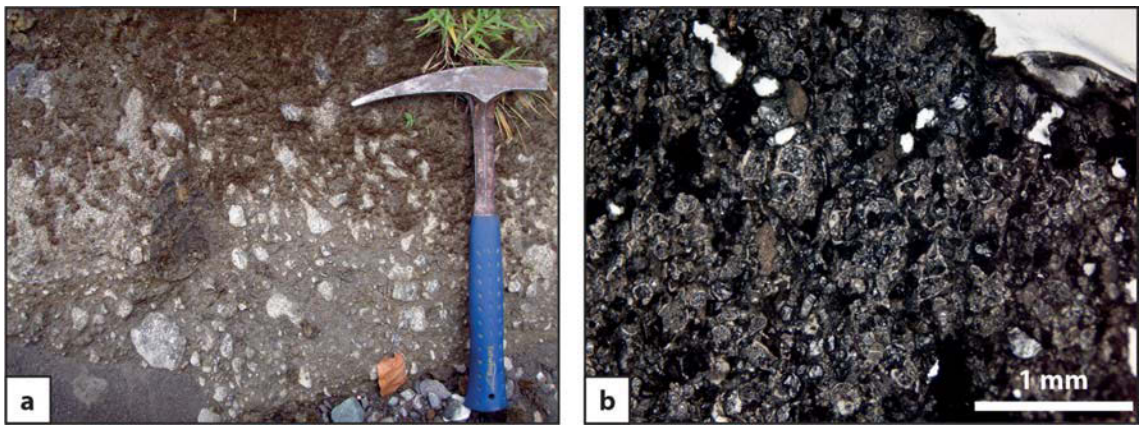

Fig. 42. (a) A weathered volcanic breccia at AB536, approximately 1.2 km north of Dilor, with angular mafic clasts measuring 1-20 cm in size. Hammer for scale. (b) Image of an acetate peel taken from a sandstone sample from AB545, illustrating abundant foraminifera including *Morozvella* sp. Scale bar = 1 mm.

3.5.4 Foraminiferal limestones

Distinctive larger foraminiferal limestones were collected in scree from the Cauhoa River, 1.2 km north of Dilor (**Fig. 43a**). They are muddy wackestones containing many large benthic foraminifera up to 10 mm in size within a grey-brown, muddy sandy matrix. Foraminiferal species include *Nummulites* sp. (**Fig. 43b**) and *Alveolina* sp. (**Fig. 43c, d**), along with assorted rotalid and miliolid forms.

The abundance of larger benthic foraminifera indicates inner neritic deposition, most likely on a shallow carbonate platform. The presence of *Alveolina* sp. and *Nummulites* sp. suggests an Eocene age.

These Eocene inner neritic deposits are placed within the Banda Megasequence as they have no correlation with the much deeper pelagites of the Eocene Australian Margin Megasequence. Similar *Alveolina* sp. and *Nummulites* sp. bearing wackestones were described by Audley-Charles (1968) and placed within his Dartollu Formation. He observed them to be commonly associated with Barique Group volcanics (Audley-Charles 1968), as they are at Mount Bibileu. This study places the foraminiferal limestones of Mount Bibileu within the Dartollu Group, of the Banda Megasequence. The Dartollu Group likely represents shallow water carbonate platforms developing proximal to Barique Group volcanic arc islands during the Eocene.

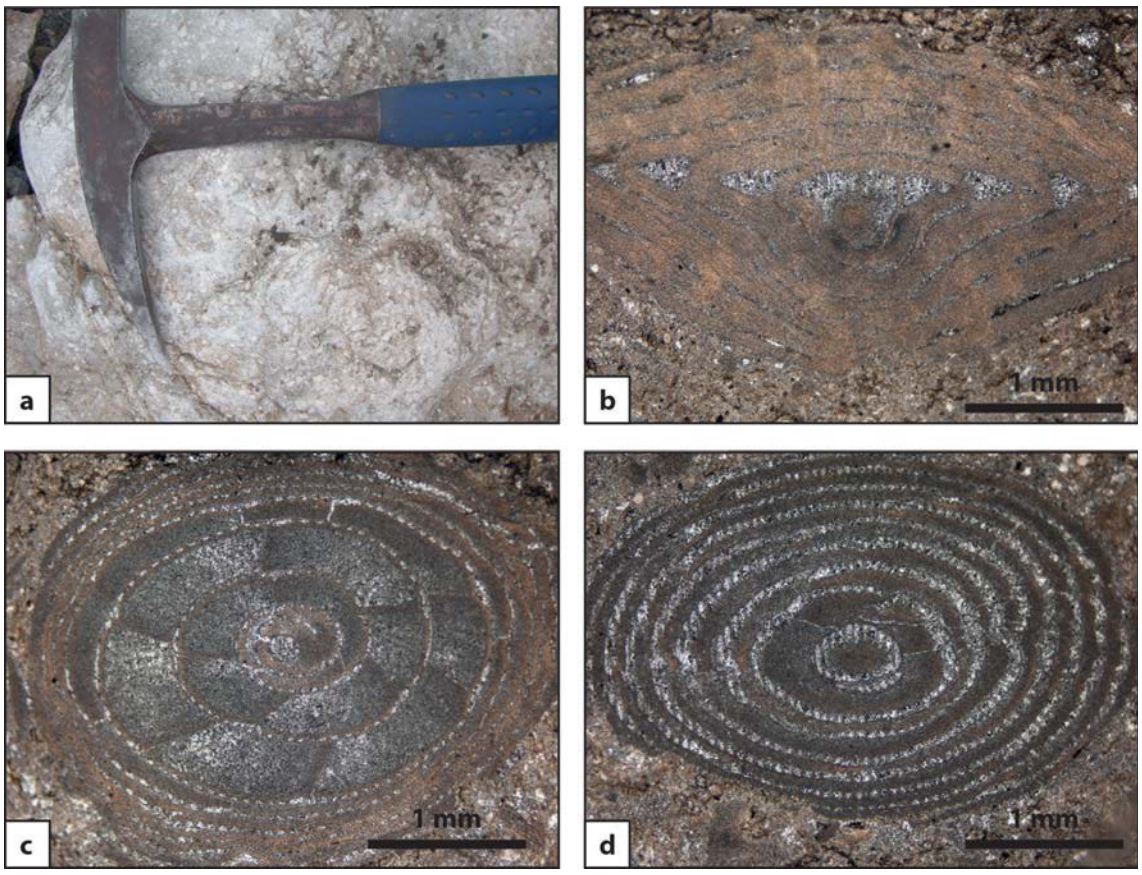

Fig. 43. A sample of scree from the Cauhoa River, approximately 1.2 km north of Dilor at AB537. Circular outlines of larger benthic foraminifera are visible on the surface of the rock. Hammer for scale. Abundant larger benthic foraminifera in this sample include (b) *Nummulites* sp. and (c, d) *Alveolina* sp.. Scale bar = 1 mm.

3.6 The Paitchau Range

The Paitchau Range is situated at the eastern end of Timor Island, in Lautem District, 2.5 km south of Lake Iralalaru (**Figs 10, 44**). It comprises a series of two to three long, narrow ridges, striking northeast and dipping north, which increase in prominence from northwest to southeast. The south-eastern ridge has a strike length of approximately 10 km, and reaches an altitude of 995 m above sea level. The ridges are largely continuous except for at the north-eastern end of the range, where they are dissected by faults into a small group of separated hills. The Paitchau Range runs parallel to the shore of the Timor Sea, situated approximately 3 km to the south (**Figs 44, 45**).

The Paitchau Range is within East Timor's only national park, and vehicular access is prohibited, requiring long treks from nearby towns in order to reach the mountains.

Furthermore, Lake Iralalaru experienced extensive flooding during our 2010 field season, requiring sections of these treks through waist deep water. Due to these complications with access, along with difficulties locating outcrop within the dense jungle cover of the Paitchau Range, only three days were spent mapping in this area. Rock units are listed in ascending stratigraphic order and age.

3.6.1 Fossiliferous packstones, wackestones and bindstones

The high ridges of the Paitchau Range comprise thickly bedded, grey wackestones, packstones and algal bindstones (**Fig. 46a, b**). Outcrop is highly indurated, and sometimes brecciated and recystallised, particularly at the north-eastern end of the range. These rocks are extremely fossiliferous, with medium to coarse grains comprising gastropods and other shell debris, tubiphytes, benthic foraminifera, ooids (some samples) and abundant algal nodules (**Fig. 46c, d**). Algal films are observed encrusting grains throughout these rocks and forming bindstones in some samples.

The presence of foraminiferal species *Duostomina* sp. and *Aulotortus* spp., along with abundant Thaumatoporellacean algae, indicate a Late Triassic age. The presence of ooids along and abundant large shell debris suggests deposition in a shallow, moderate to high energy environment. An association of ooids, Thaumatoporellacean algae and tubiphytes are typical of carbonate platform margin environments during the Late Triassic (Flügel 2004).

Like the Perdido Group limestones, the age and shallow water facies of these rocks suggest that carbonate banks were developing on isolated, submerged topographic highs within newly rifted basins during the breakup of Gondwana. Whereas biostratigraphic evidence suggests a likely Early Jurassic, Sinemurian-Pliensbachian age for the Perdido Group limestones (**Chapter 3.2.3 Mount Mundo Perdido – Ooid and oncoidal limestones**), the carbonate platform facies at the Paithchau Range represent older, Late Triassic deposits. Other important differences exist between these rocks and the Perdido Group limestones. Carnian-Norian shallow water carbonates at the Paitchau Range, and elsewhere in East Timor (Haig 2012b), show a more diverse range of fauna including various foraminifera, tubiphytes, crinoids, echinoids,

brachiopods, gastropods, bryozoans, sponges, ooids and peloids. The Perdido Group is much less diverse, containing a more limited range of foraminifera, echinoids, mollusc shell fragments, ooids, oncoids and peloids. This suggests that the Perdido Group facies were deposited in more restricted, possibly higher salinity environments. Furthermore, whilst the shallow water carbonates of the Paitchau Range often contain ooids as a minor component, Perdido Group limestones are usually ooid dominated, with ooid packstones and grainstones common. Haig (2012b) recognised similar diverse Carnian-Norian shallow water carbonates in the Bandeira Gorge, near Atsabe in western East Timor, placing them within the Bandeira Group of the Gondwana Megasequence as these rocks were previously not described. This study also places the Carnian-Norian shallow water carbonates of the Paitchau Range within the Bandeira Group. At the Bandeira Gorge, large sections of less indurated mudstones, muddy wackestones, and sandstones were observed situated between thick, highly indurated limestone units. It is possible that a similar stratigraphic succession is responsible for the distinctive morphology of the Paitchau Range, with the less indurated units forming the recessive valleys between the prominent, indurated limestone ridges.

Fig. 44 → Aerial photograph of the eastern tip of East Timor, including the Paitchau Range and Lake Iralalaru, illustrating sample points and 100 m topographic contours. Field mapping and sampling was conducted between the south-eastern banks of Lake Iralalaru and the northwest facing slopes of the Paitchau Range, extending in places into the central parts of the range. Mapping and sampling was also completed around Tutuala.

Fig. 45 →→ Interpreted geological map of the eastern tip of East Timor, including the Paitchau Range and Lake Iralalaru. The extent of field mapping and sampling is outlined with boxes, with the geology in these areas constructed using outcrop data and aerial photographs. See text for detailed descriptions of geology. Geology outside of the mapped field extent is modified after Partoyo *et al.* (1995) using aerial photographs. Lithologies outside of the mapped field extent not described in the text include the Poros Limestone (Thinly bedded, vuggy algal limestone overlying the Baucau Limestone – Audley-Charles, 1968) and the Cribas Group (Permian basinal facies of the Gondwana Megasequence – see **Fig. 9**).

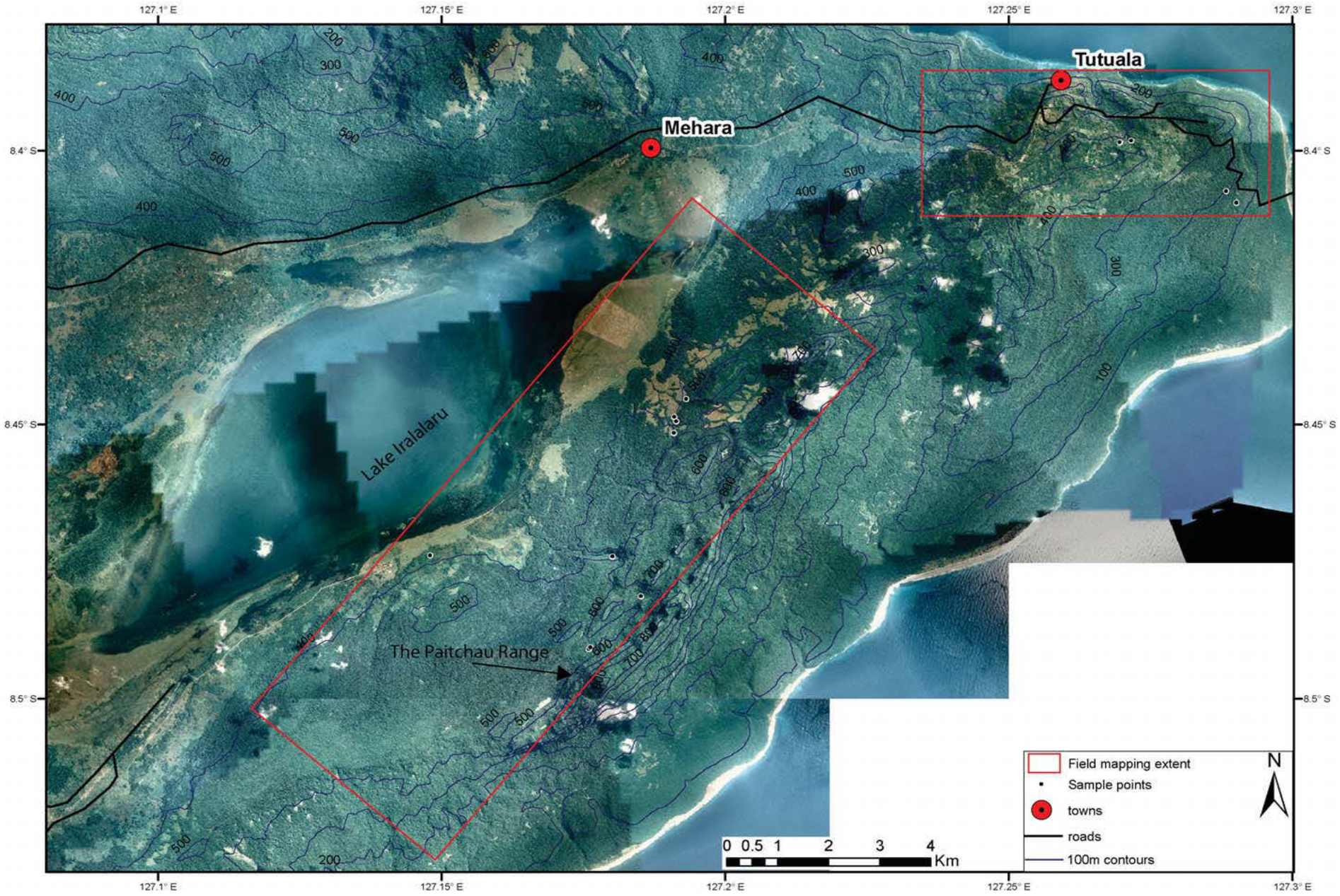
127.1° E
127.15° E
127.2° E
127.25° E
127.3° E
8.4° S
8.45° S
8.5° S
Tutuala
Mehara
Lake Iralalaru
The Paitchau Range
Field mapping extent
Sample points
towns
roads
100m contours
N
0 0.5 1 2 3 4
Km

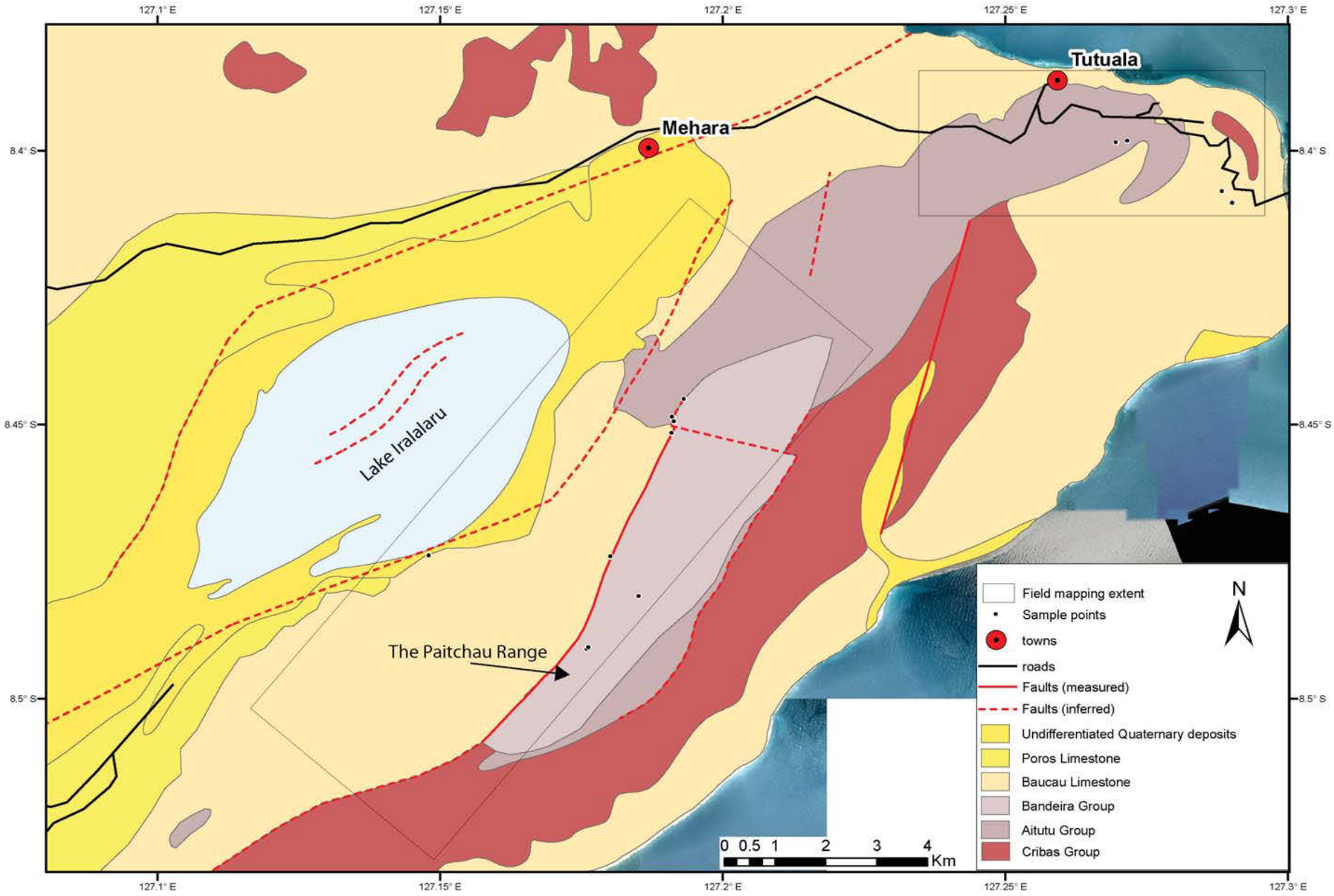
127.1° E
127.15° E
127.2° E
127.25° E
127.3° E
8.4° S
8.45° S
8.5° S
Tutuala
Mehara
Lake Iralalaru
The Paitchau Range
Field mapping extent
Sample points
towns
roads
Faults (measured)
Faults (inferred)
Undifferentiated Quaternary deposits
Poros Limestone
Baucau Limestone
Bandeira Group
Aitutu Group
Cribas Group
N
0 0.5 1 2 3 4
Km

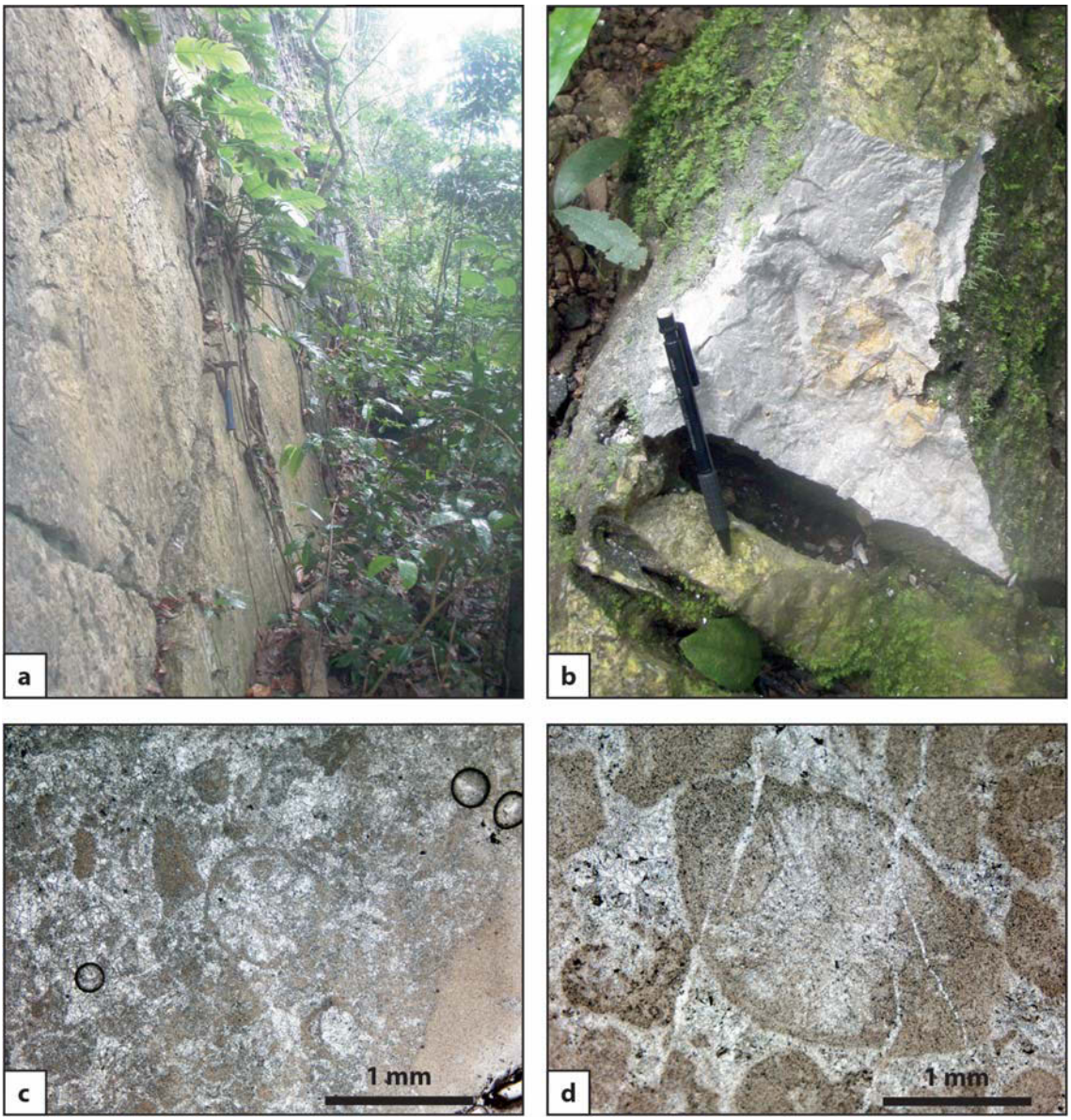

Fig. 46. (a) Highly indurated Bandeira Group limestones form all of the high cliffs that were sampled at the Paitchau Range, including this example at the north-eastern end of the range at AB559. Hammer for scale. (b) A freshly broken sample of Bandeira Group limestone at AB551, in the high central region of the Paitchau Range. Pen for scale. (c) Image of an acetate peel taken from the limestone at AB551. The rock is a packstone comprising algal nodules and growths, ooids, large shell fragments and abundant foraminifera. Scale bar = 1 mm. (d) Image of an acetate peel taken from Bandeira Group limestone from AB557, in the north of the Paitchau Range. The large grain in the centre of frame is a benthic foraminiferal test, most likely *Aulotortus* spp.. Scale bar = 1 mm.

3.6.2 Medium bedded grey wackestones

Whilst visiting administrators and scouting for access east of the Paitchau Range, near Tutuala, medium bedded grey wackestones were observed in rare roadside outcrops (**Fig. 47a**). They comprised very well bedded grey wackestone, bedding 10-30 cm, with thin interbeds of chert and mudstone less than 10 cm. The wackestone contained radiolaria and thin *Halobia*-type bivalve filaments, with rare nodosariid and lagenoid foraminifera (**Fig. 47b**).

Very fine grained carbonate mud containing radiolaria suggests a deep water, low energy environment, while the presence of *Halobia*-type bivalves suggest an oxygen deficient, basinal setting. The presence of primitive nodosariid foraminifera and *Halobia* is suggestive of a Triassic age, but not definitive.

Medium bedded radiolaria and *Halobia* bearing wackestones are typical of the Aitutu Group elsewhere in Timor (e.g. Audley-Charles 1968; Charlton *et al.* 2009; Haig 2012b, **Chapter 3.2.2 Mount Mundo Perdido – Radiolarian limestones**) and are distinctive in outcrop. This study places the medium bedded wackestones sampled east of the Paitchau Range within the Aitutu Group of the Gondwana Megasequence on the basis of lithofacies correlation.

The Paitchau Range itself was mapped as 'Aitutu Formation' by Audley-Charles (1968) and since followed by other authors (e.g. Partoyo *et al.* 1995). Charlton *et al.* (2009) differentiated the limestones of the Paitchau Range from the basinal Aitutu facies, describing them informally as 'Pualaca Facies' after finding similarities with Late Triassic shallow water carbonates previously observed around Pualaca, in central East Timor (Hirschi 1907; Grunau 1956). He described the shallow water limestones in the Tutuala/Paitchai area as successions several hundred metres thick, grading laterally into basinal Aitutu-like facies (Charlton *et al.* 2009).

This study has observed similar vertical and lateral gradational relationships between the Bandeira Group and Aitutu Group elsewhere in East Timor (most strikingly at Mount Loelako, see **Chapter 3.8**). Although not observed directly, this study agrees with previous mapping and observations (Audley-Charles 1968; Partoyo *et al.* 1995; Charlton *et al.* 2009) that the Bandeira

Group shallow water carbonates of the Paitchau Range most likely have gradational contacts with the surrounding Aitutu Group.

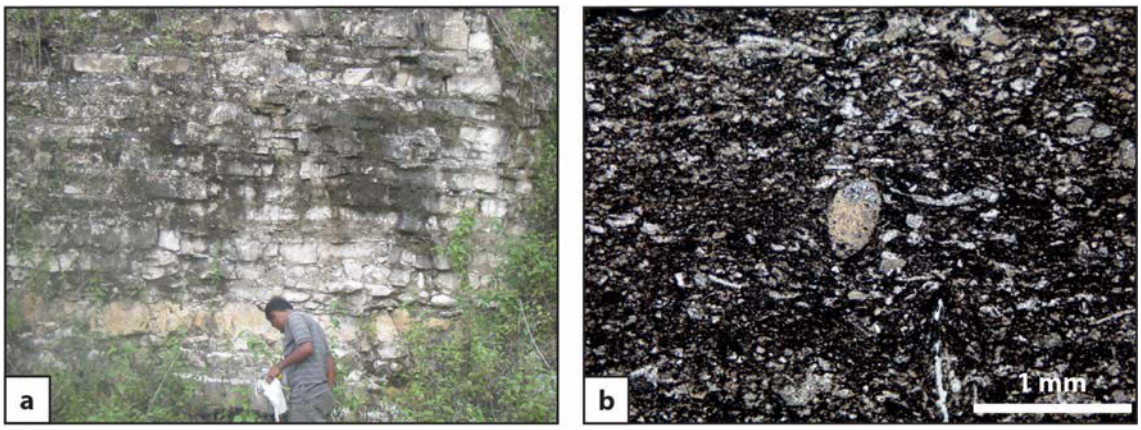

Fig. 47. (a) Well bedded Aitutu Group limestone in a roadside outcrop at AB555, near Tutuala. (b) Image of an acetate peel taken from AB555 illustrates a radiolaria and *Halobia*-type bivalve rich facies typical of the Aitutu Group in East Timor. Scale bar = 1 mm.

3.6.3 Carbonate pelagites

Carbonate pelagites were observed in a single roadside outcrop near Tutuala, and also in loose, metre-scale boulders lying on flat ground between the hills of the north-eastern end of the Paitchau Range. The roadside outcrop is medium bedded, white-brown to pink wackestone containing abundant planktonic foraminifera in a very fine grained carbonate mud matrix, with some thin cherty beds less than 5 cm. Examples found in scree are yellow-white wackestones with abundant planktonic foraminifera, and a pervasive, centimetre scale, stylolitic foliation (**Fig. 48a**).

Similar to carbonate pelagites found at other fatus, predominantly planktonic foraminifera within a very fine carbonate mud matrix suggests deposition within the middle bathyal to abyssal zone. Abundant *Morozovella* sp. within the roadside outcrop samples suggests an early to middle Eocene age. *Globorotalia limbata* and *Dentoglobigerina altispira* within the Paitchau Range boulder samples suggests a younger, Miocene age (**Fig. 48b**).

Carbonate pelagites sampled at the Paitchau Range correlate with Eocene and Miocene age carbonate pelagites observed elsewhere in East Timor (Haig & McCartain 2007), and are similarly placed within the Kolbano Group of the Australian Margin Megasequence. These rocks have not previously been mapped in the Paitchau area, and from their very limited observation in this study it is difficult to map their occurrence. It can be said that the Kolbano Group boulders found at the base of the Paitchau Range were not sourced from the cliffs above, as these were observed to comprise Triassic Bandeira Group limestones. The Kolbano Group belongs to a thin pelagite succession deposited unconformably above the Gondwana Megasequence, and these boulders may represent the isolated remnants of a previously eroded landscape.

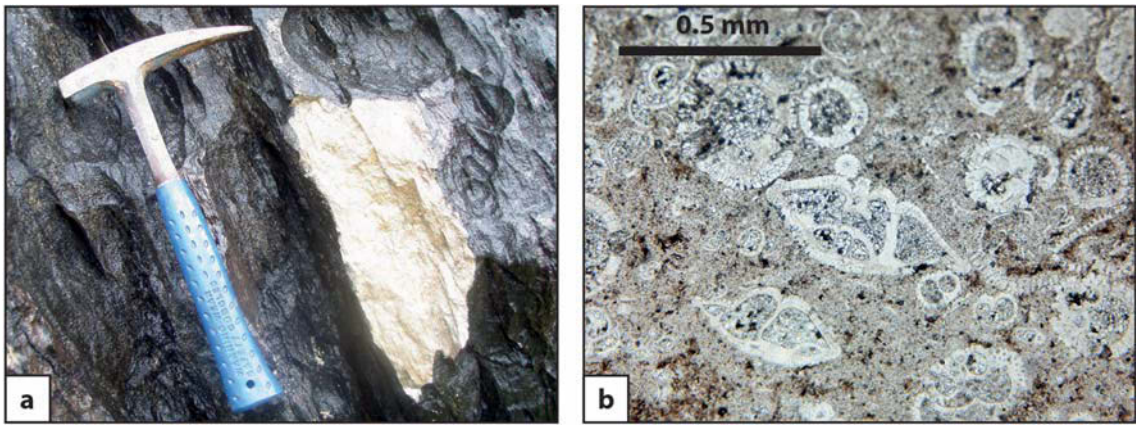

Fig. 48. (a) A boulder of foliated Kolbano Group limestone found between the hills of the north-eastern end of the Paitchau Range. A fresh surface exposes the yellow-white carbonate pelagite. Hammer for scale. (b) Image of an acetate peel taken from this rock, illustrating foraminiferal species *Globorotalia limbata* of Middle Miocene age. Scale bar = 0.5 mm.

3.6.4 Vuggy coralline limestones

Lake Iralalaru sits within a broad depression (**Fig. 44**) which on the south side is bounded by small limestone cliffs 15-20 m high (**Fig. 49a**). These cliffs comprise yellow, vuggy, coralline limestone, which forms a fairly flat, thickly vegetated plateau that extends over 3 km southeast towards the base of the Paitchau Range. Outcrop is rare, and where sampled is highly altered and karstified.

However, diverse and abundant fossils are still visible (**Fig. 49b**), including abundant planktonic and benthic foraminifera, along with echinoid spines, fragments of coralline algae, bryozoan and mollusc debris, and large in situ corals. The contact of the vuggy limestones with the indurated wackestones comprising the range is obscured by jungle, however based on the change in composition of scree float the contact appears very close to the abrupt change in topographic gradient at the base of the main Paitchau ridges.

The diverse, abundant and often fragmented biota, along with the presence of in situ corals, suggests a shallow, high energy depositional environment, likely a near shore coral reef. Due to the highly altered nature of all observed outcrop a biostratigraphic age determination was not possible on the samples collected.

Lithofacies of these rocks are identical to the synorogenic, coralline limestones of the Baucau Plateau (Audley-Charles 1968), Mount Mundo Perdido (Benincasa *et al.* 2012) and Mount Laritame (**Chapter 3.3.7 Mount Laritame – Medium bedded coralline limestones**), and the vuggy coralline limestones of the Paitchau Range are placed within the Baucau Limestone of the Synorogenic Megasequence based on lithofacies correlation. Like its occurrences elsewhere in East Timor, the Baucau Limestone at the Paitchau Range forms a broad, flat topped plateau, having undergone vertical uplift with little tilting since deposition in the Pleistocene.

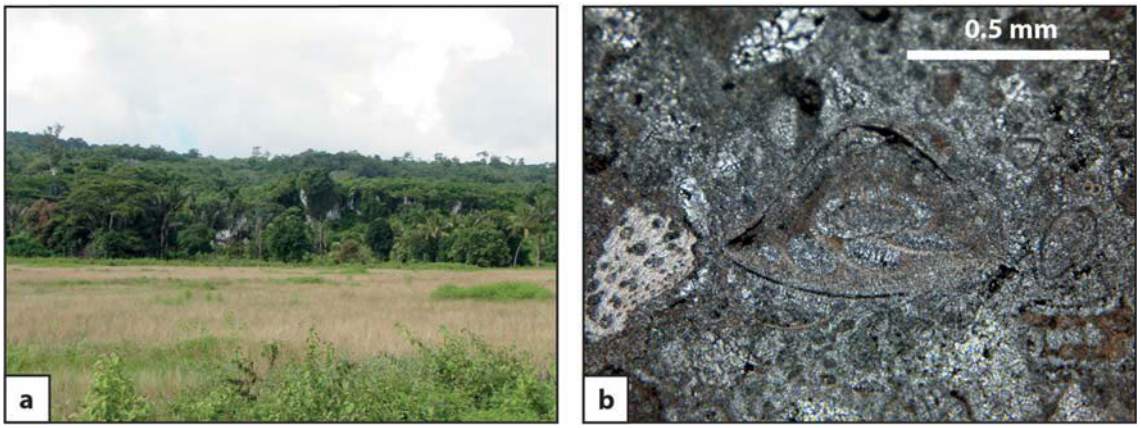

Fig. 49. (a) Near the southern banks of Lake Iralalaru, facing south-southwest. The Baucau Limestone forms a small cliff 10-20 m high which extends for several kilometres along the southern boundary of the Lake Iralalaru basin. (c) An image from an acetate peel taken from a sample of this cliff at AB405 illustrates diverse and abundant biota.

With the possible exception of the cliffs bounding the Lake Iralalaru basin, well defined terraces are not observed at the Paitchau Range as they are elsewhere, however they are most likely obscured by extensive karstification and extremely dense vegetation.

3.7 The Matebian Range

The Matebian Range (also known as Mata Bia) is one of East Timor's highest mountains, and at over 20 km long and 7 km wide it is the largest of all the fatu-style massifs. Situated in Baucau District in eastern East Timor, it forms a dramatic north-northeast striking ridge which almost bisects the narrow island from the north to south coast (**Fig. 10**). The Matebian Range is bounded by extremely steep scarps along its north-western edge, while slopes on its south-eastern flank, though still steep, are more irregular (**Figs 50, 51**). There are two main peaks: the lesser, northern peak is Matebian Mane, at around 1500 m, while Matebian Feto, to the south, rises to an altitude of 2376 m.

Reconnaissance mapping around the Matebian Range in 2010 was based first out of Quelecai, a small village 4 km west of Matebian's western scarp (**Figs 50, 51**). Four days were spent here conducting transects east towards the range; however access was repeatedly blocked by swollen rivers and flash flooding, preventing us from sampling the high limestone cliffs comprising the western scarp.

Fig. 50 → Aerial photograph of the Matebian Range, illustrating sample points and 100 m topographic contours. The extent of field mapping by this study is highlighted around Quelecai, beneath the high, west facing cliffs of the Matebian range, and around Baguia, on Matebian's eastern flank.

Fig. 51 →→ Interpreted geological map of the Matebian Range. The extent of field mapping and sampling is outlined around Quelecai and Baguia, with the geology in these areas constructed using outcrop data and aerial photographs. See text for detailed descriptions of geology. Geology outside of the mapped field extent is modified after Partoyo *et al.* (1995) using aerial photographs. Banda Megasequence rocks belonging to the Lolotoi Metamorphic Complex and Barique Group (see **Fig. 9**) have been widely mapped around the outskirts of the Matebian Range by Audley-Charles (1968) and following authors (e.g. Partoyo *et al.* 1995; Standley & Harris 2009), outside of the mapped field extent of this study. It is possible that some limestone mapped as Perdido Group here after Partoyo *et al.* (1995) and aerial photographs may belong to the Booi Group of the Banda Megasequence – particularly those outcrops at lower structural levels associated with other Banda Megasequence lithologies. This would be consistent with geological distributions seen around the Ossu fatus and Mount Bibileu.

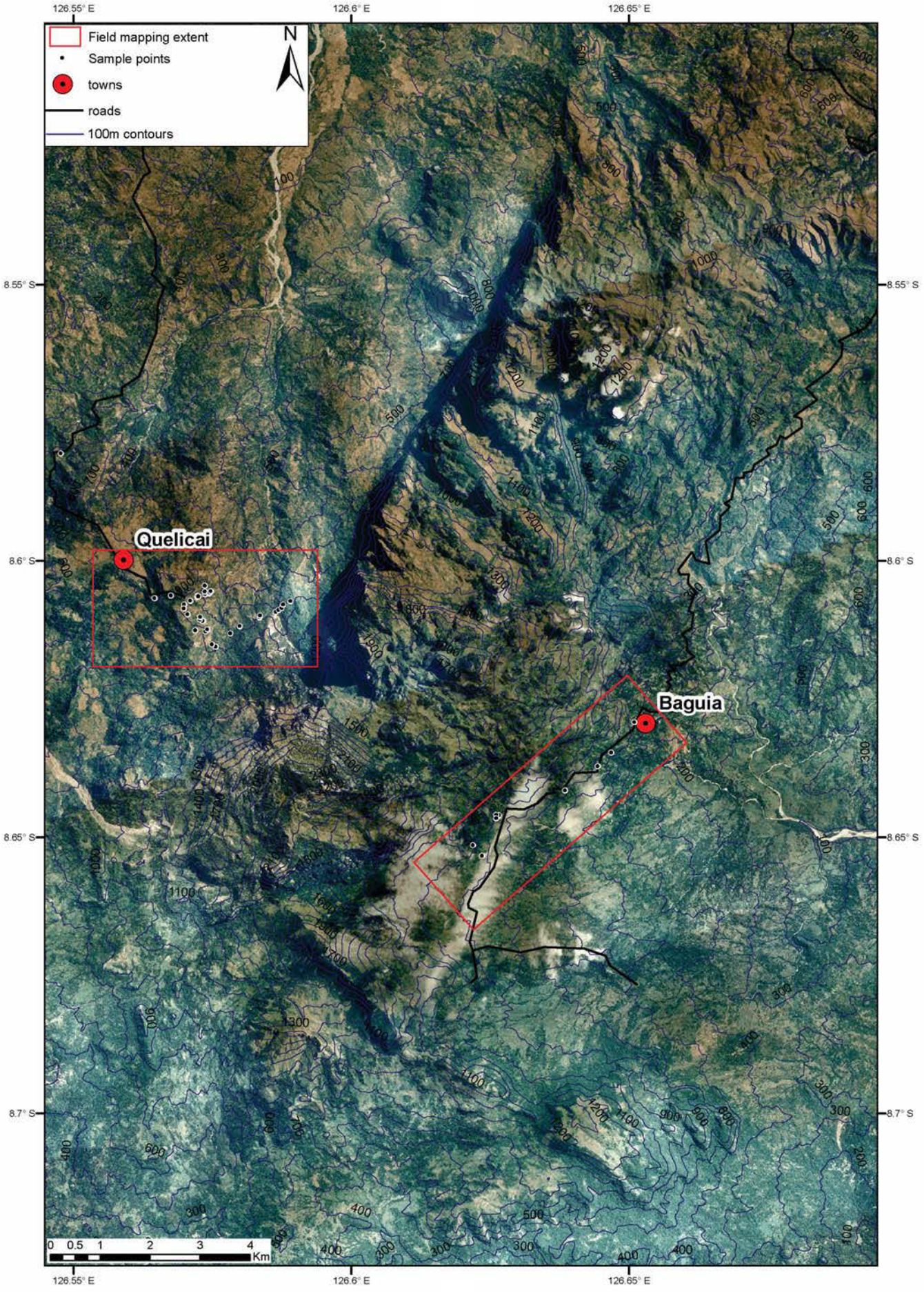
126.55° E
126.6° E
126.65° E
8.55° S
8.6° S
8.65° S
8.7° S
Field mapping extent
Sample points
towns
roads
100m contours
N
Quelicai
Baguia
0 0.5 1 2 3 4
Km

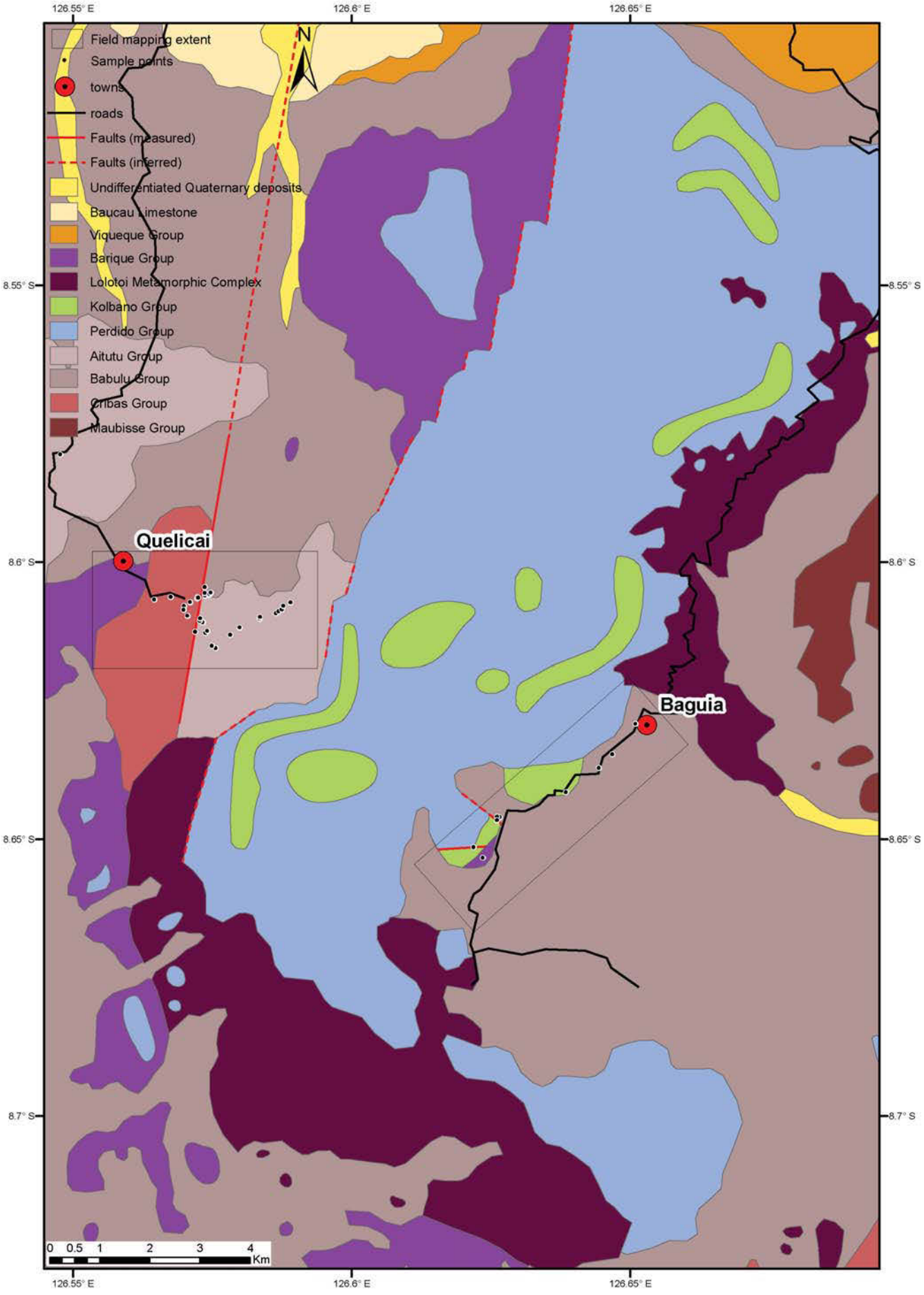
126.55° E
126.6° E
126.65° E
N
Field mapping extent
Sample points
towns
roads
Faults (measured)
Faults (inferred)
Undifferentiated Quaternary deposits
Baucau Limestone
Viqueque Group
Barique Group
Lolotoi Metamorphic Complex
Kolbano Group
Perdido Group
Aitutu Group
Babulu Group
Cribas Group
Maubisse Group
8.55° S
8.6° S
8.65° S
8.7° S
Quelicai
Baguia
0 0.5 1 2 3 4
Km

We then moved to Baguia, nestled in the lower cliffs on the eastern side of the mountain (**Figs 50, 51**). Unfortunately, our time here was cut short after just one day. The only road in to the village was being washed away by heavy rain and landslides, and we were advised by the local police to either leave immediately or risk being trapped in Baguia until the end of the wet season. Despite these difficulties, our brief reconnaissance mapping around the lower flanks of the Matebian Range, particularly around Quelecai, yielded many interesting observations. Rock units are listed in ascending stratigraphic order and age.

3.7.1 Thinly bedded mudstones, sandstones and turbidites

Much of the hilly farmland immediately east of Quelecai comprises dark grey mudstones and siltstones with thin sandstone interbeds (**Fig. 52a**). The mudstones and siltstones are micaceous and have a pervasive, slatey cleavage (**Fig. 52b**). Fossil material includes rare radiolaria and echinoid spines, and some samples contain abundant sulphides. The mudstones contain thin interbeds of fine to very fine sandstone, predominantly less than 5 mm but up to centimetre scale. Sandstones are red-green and appear to have a large mafic-volcanic component.

Higher up in the succession are found medium grained sandstones (**Fig. 52c**) and very well graded turbidite beds fining up from conglomerates to fine sandstone (**Fig. 52d**). The medium grained sandstones are medium bedded, poorly sorted, and comprise subangular grains of quartz and mafic lithic fragments. The graded beds range in thickness from 5-40 cm. They grade from coarse grained biogenic and lithogenic clasts in a muddy, sandy matrix at the base into very fine grained sandstone containing rare bivalve filaments and other fine grained skeletal fragments. Lithogenic components include subangular clasts of limestone, mudstone, and volcanic sandstone. Biogenic components include bivalves, rhynchonellid brachiopods, crinoids, echinoids, bryozoans and very well preserved specimens of benthic foraminifera *Colaniella* sp (**Fig. 52e, f**).

The presence of radiolaria within the mudstones suggests slow, pelagic sedimentation, and pyrite in some samples is indicative of locally anoxic conditions. Thin volcanic sandstone interbeds represent pulses of sediment supply from a nearby volcanic source. The turbidite beds

contain abundant shallow water fauna, these deposits likely represent debris slides sourced from nearby shallow carbonate platforms. The sequence possibly represents volcanic influenced, marine, pro-delta and slope deposits. The presence of the larger foraminiferal species *Colaniella* sp. suggests a Late Permian age.

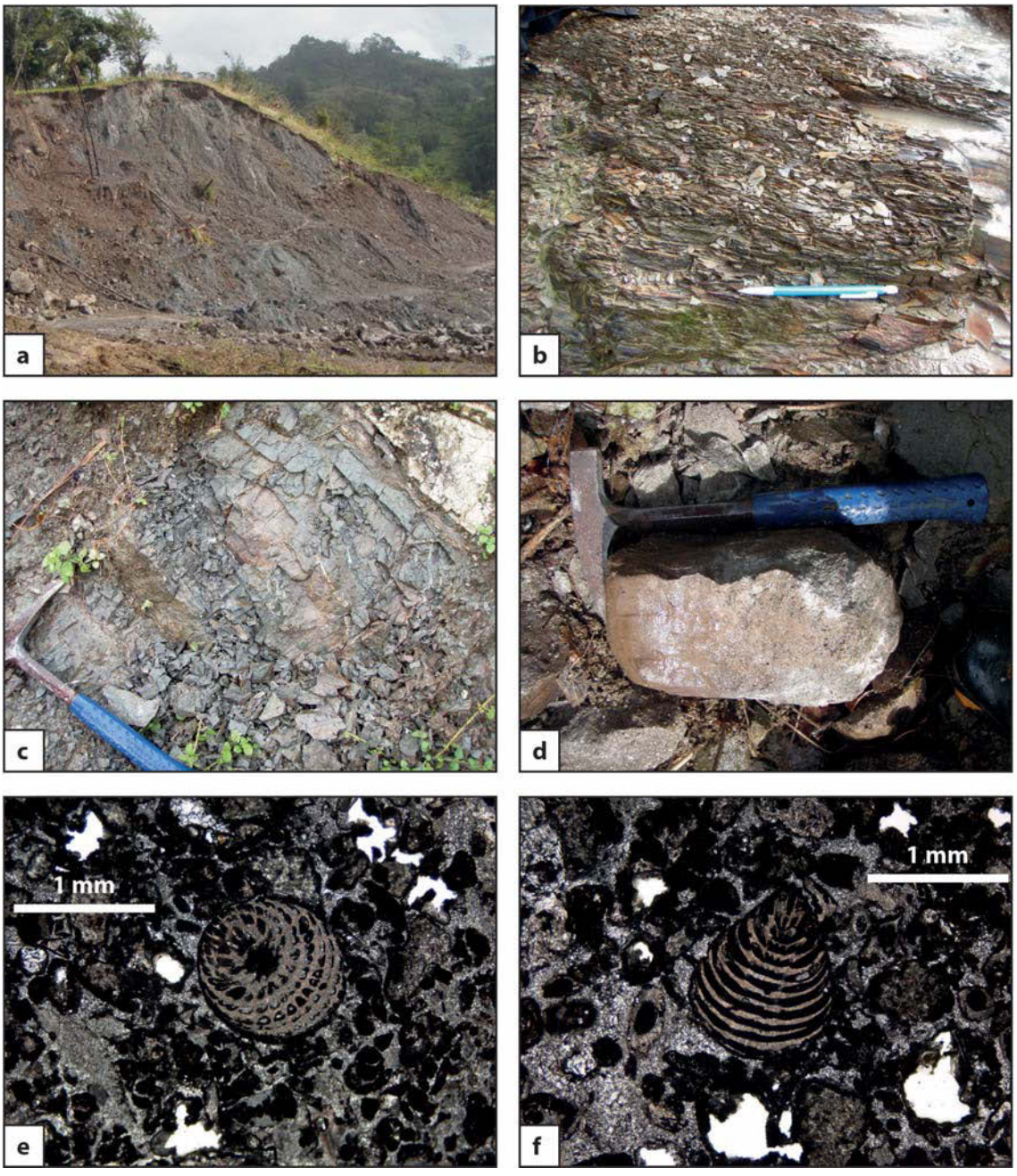

Fig. 52. (a) Dark grey Cribas group mudstones exposed by a large landslip approximately 2 km southeast of Quelecai. Exposed vertical thickness here is approximately 30 m. These mudstones comprise much of the hilly farmland immediately east of Quelecai (b) Slatey cleavage in Cribas Group mudstone at AB492, pen for scale. (c) Interbedded Cribas Group mudstones and sandstones at AB491, hammer for scale. (d) A sample of a turbidite bed taken from AB494. Grain size in this sample fines up from right to left of frame. Hammer for scale. (e, f) Very well preserved specimens of benthic foraminifera *Colaniella* sp. are abundant in samples from AB494, suggesting a Permian age. Scale bar = 1 mm.

Throughout the Permian the Timor region was undergoing active extension (Charlton *et al.* 2002). By the late Permian when the mudstones, sandstones and turbidites of Quelecai were deposited, there existed a broad intercratonic sea between the Australian craton and an uplifted landmass to the northwest (Bird & Cook 1991), which had rifted from Gondwanaland after the end of the early Permian (Metcalfe 2011). Permian strata observed in Timor has two main end member groups, the carbonate dominated shallow water Maubisse Group and the siliciclastic dominated basinal Cribas Group, with volcanics interbedded in both groups. Within the Cribas Group, differences are observed between strata proximal to shallow-water carbonates and distal to siliciclastic input and vice versa i.e. strata proximal to siliciclastic input and distal to shallow-water carbonates (Haig 2012b).

The upper and lower Cribas Series of Grunau (1956) and Gageonnet and Lemoine (1958) were defined as the Atohoc Formation and Cribas Formation respectively by Audley-Charles (1968). The Atohoc Formation comprises a monotonous sequence of hard, black shales, with massive to thick bedded quartz sandstone at its base, with the top of the formation taken arbitrarly as the top of an amygdaloidal basalt layer in its type area, which coincides with the appearance of the bivalve *Atomodesma exarata* (Audley-Charles 1968). The Cribas Group of Haig (2012b) removes the arbitrary differentiation of Atohoc and Cribas Formations and describes the entire succession as the Cribas Group, with the thick basal sandstones of the Atohoc Formation referred to as the Atahoc beds. The remainder of the Cribas Group comprises micaceous shales and siltstones with interbedded sandstones and marls (Audley-Charles 1968). Fine to very fine sandstone layers grade upwards into coarser clastic units in the upper part of the sequence, where arenite beds are up to several metres thick, and are characterised by fining up sequences (Charlton *et al.* 2002).

The mudstones, sandstones and turbidites found around Quelecai are placed within the Cribas Group by this study on the basis of their Late Permian age and lithological correlation to the Cribas Formation described elsewhere in East and West Timor (Grunau 1956; Gageonnet & Lemoine 1958; Audley-Charles 1968; Bird & Cook 1991; Charlton *et al.* 2002). They were deposited within an active Permian basin, with fine clastic and volcaniclastic sediments

prograding out from the basin margins, and debris slides transporting shallow water fauna from proximal carbonate platforms or shoals. Around Quelecai they are commonly associated with pillow basalts and breccias; common products of rift volcanism.

3.7.2 Igneous rocks

Igneous rocks are common around Quelecai, most commonly pillow basalts and pillow breccias. Pillow basalts are abundant but are generally not found in situ; they are most commonly observed as large, loose boulders 1-5 m in size (**Fig. 53a, b**). Small, vesicular pillows range in size from 10 cm to 1 m, but are generally less than 50 cm. Pillow breccias were observed both in float and in situ, where they form small, erosion resistant topographic highs overlying interbedded mudstones and sandstones. They comprise subangular to subrounded basalt clasts and fragmented pillows 2-20 cm (**Fig. 53c, d**).

Pillow lavas are submarine in origin, and are consistent with a rift basin setting. Pillow breccias are commonly associated with pillow lavas, and may represent the base of the advancing lava flow. Where observed in situ, the pillow breccias belong to the succession of mudstones, sandstones and turbidites, and they assigned a Late Permian age based on this association. Pillow basalts are common within the Permian of East Timor (Haig 2012b).

Volcanics are observed throughout the Permian stratigraphy in East Timor (Haig 2012b) although they are usually more common within the Maubisse Group succession (Audley-Charles 1968; Charlton *et al.* 2002). Generally basaltic in composition, they include abundant pillow lavas, current structures and other evidence of deposition in a mostly subaqueous volcanic environment (Charlton *et al.* 2002). Likewise, basaltic pillow lavas and breccias are encountered around Quelecai, where they are associated with the Permian Cribas Group. On this basis, the igneous rocks sampled on the western side of the Matebian Range are placed within the Cribas Group, of the Gondwana Megasequence, and are the volcanic products of active Permian rifting. Barkham (1993) described very similar pillow lavas within the Upper Permian of West Timor, occurring with small, vesicular pillows and interbedded pillow breccias.

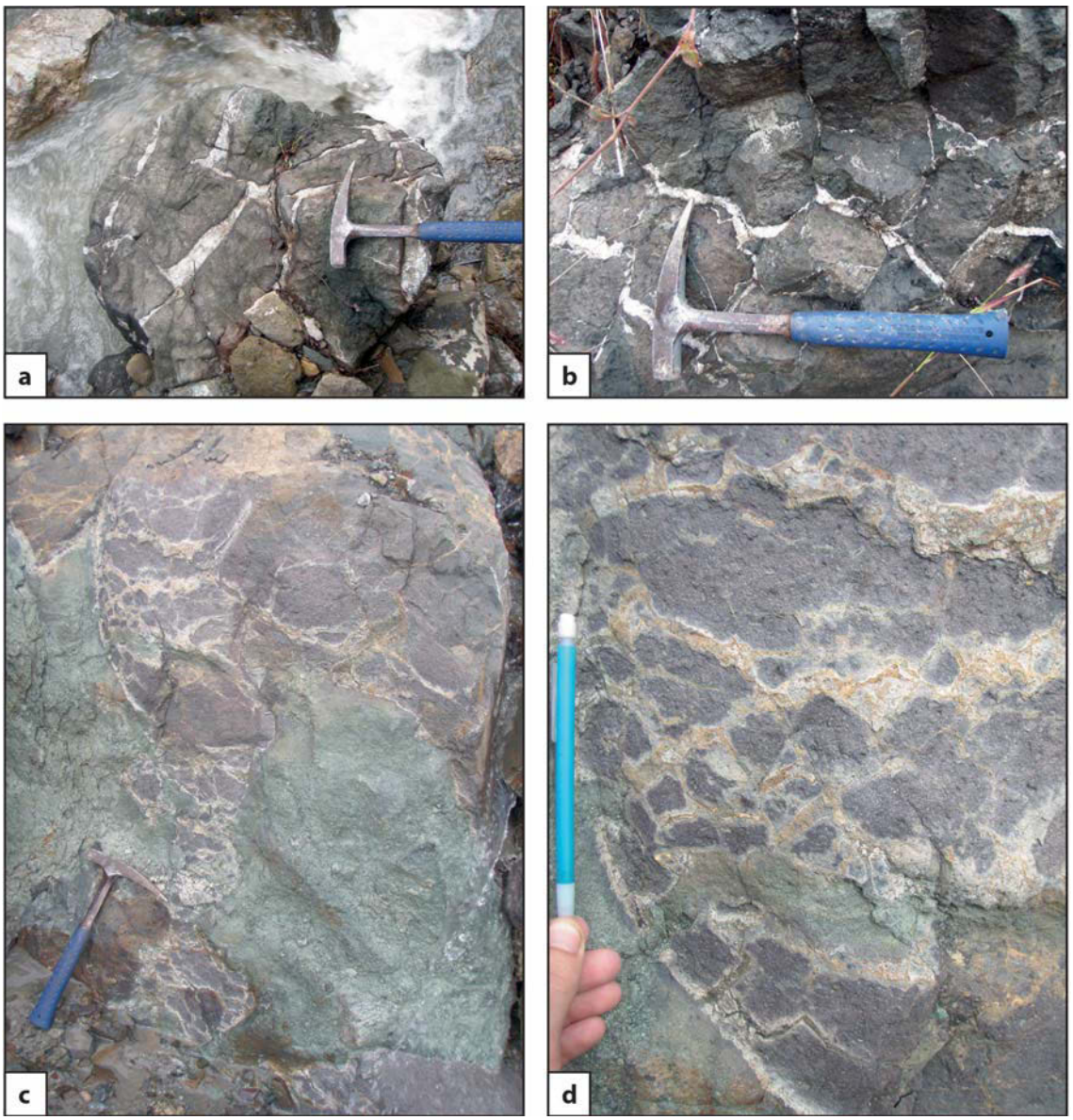

Fig. 53. (a) A boulder of pillow basalt at AB499, hammer for scale. (b) Pillow basalt at AB503, hammer for scale. (c) Pillow breccia at AB498, hammer for scale. These pillow breccias are associated with Cribas Group mudstones and sandstones in the field area. (d) Close-up of pillow breccia at AB498, pen for scale.

3.7.3 Medium bedded limestones and mudstones

Heading towards the Matebian Range, at approximately 1.5 km east of Quelecai lithologies change from mudstones and sandstones to interbedded mudstones and limestones (**Fig. 54a-d**). Mudstone beds are dark grey, medium to thickly bedded (mostly less than 70 cm) and contain rare small forams including *Dentalina* sp. and *Cryptoseptida* sp. Limestone interbeds are 5-30 cm, grey, highly indurated wackestones containing abundant radiolaria, thin *Halobia*-type

bivalve filaments usually concentrated in beds, rare echinoid fragments and rare small forams including *Nodosaria* sp., *Lenticulina* sp., *Atsabella* sp. and undifferentiated miliolids (e.g. **Fig. 54e**). Rare ooid packstone interbeds were observed within this succession (**Fig. 54f**) comprising ooids, peloids, assorted skeletal fragments and many small forams including *Lenticulina* sp. and *Opthalmidium* sp. These packstones also contain rip up clasts of mudstone above the mudstone-packstone contact.

Very fine grained carbonate mud containing radiolaria suggests a deep water, low energy environment, while the presence of *Halobia*-type bivalves suggest an oxygen deficient, basinal setting. Rare beds of ooid packstone with rip-up clasts at their base most likely represent debris slides transporting shallow water fauna to down on to the basinal mudstones. An age of Late Triassic is assigned to these rocks based on the presence of foraminiferal species *Lenticulina* sp., *Opthalmidium* sp. and unornamented species of *Dentalina* sp. and *Cryptoseptida* sp.

Medium bedded radiolaria and *Halobia* bearing wackestones are typical of the Aitutu Group elsewhere in Timor (e.g. Audley-Charles 1968; Charlton *et al.* 2009; Haig 2012b, **Chapter 3.2.2 Mount Mundo Perdido – Radiolarian limestones**, **Chapter 3.6.2 The Paitchau Range – Medium bedded grey wackestones**) and this study places the medium bedded limestones sampled at Mount Matebian within the Aitutu Group of the Gondwana Megasequence on the basis of their Triassic age and lithofacies correlation. Some limestone beds within the Aitutu Group at Mount Matebian represent debris slides containing ooids and shallow water foraminifera typical of the coeval Bandeira Group, indicating proximity to nearby carbonate platforms.

3.7.4 Peloid packstones

Peloid packstones were observed approximately 4 km south west of Baguia, comprising some of the lower cliffs of the Matebian Range at around 1000 m above sea level. Orange-grey and massive in outcrop (**Fig. 55a**), these peloids packstones are extensively micritised. Rare small forams, mainly Lenticulina sp., and rare skeletal fragments are observed in acetate peels (**Fig. 55b**).

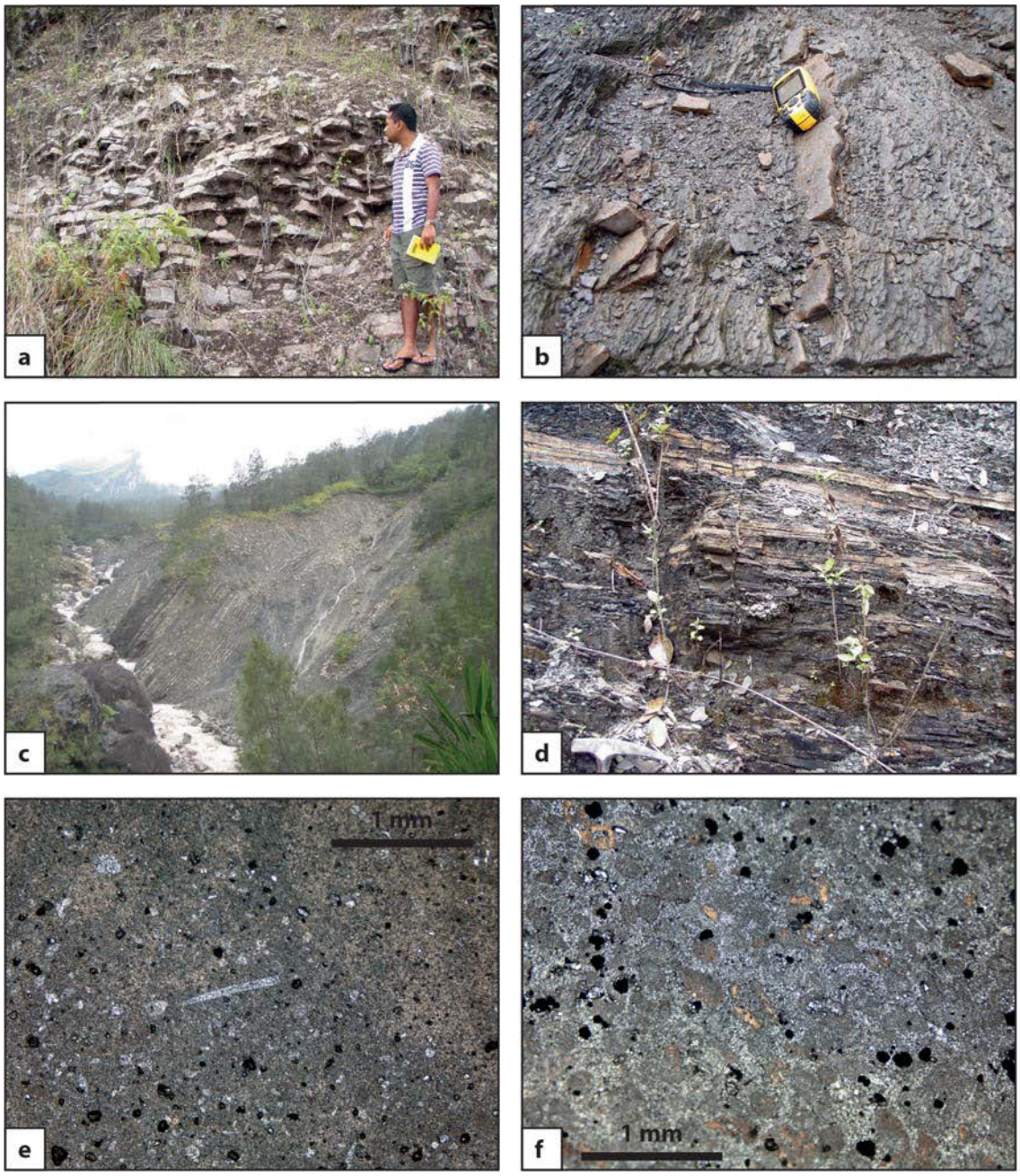

Fig. 54. (a) Very well bedded Aitutu Group limestone at AB525. Limestone beds at this location are very siliceous and contain abundant radiolaria. (b) Thin beds of Aitutu Group limestone at AB510, handheld GPS for scale. (c) Steeply dipping interbedded Aitutu Group limestone and mudstone at AB502, approximately 1 km west of the western scarp of the Matebian Range. (d) The Aitutu Group at AB521 is mud rich with thin limestone beds. Note hammer at bottom-left of frame for scale. (e) Image of an acetate peel taken from a sample at AB497. This rock is a wackestone containing abundant radiolaria and some *Halobia*-type bivalve filaments in a matrix of carbonate mud – a facies typical of the Aitutu Group in East Timor. Scale bar = 1 mm. (f) Image of an acetate peel taken from a rare ooid packstone bed at AB513. These rare fossiliferous beds within the Aitutu Group at the Matebian Range most likely represent debris slides transporting shallow water fauna to down on to the basinal Aitutu Group mudstones. Scale bar = 1 mm.

The predominance of peloids suggests these sediments have their origin in the well-agitated, shallow water of an open lagoon or shelf. However, the muddy matrix and rare and fragmented skeletal debris suggest that the peloids have perhaps been transported and deposited in slightly deeper water on the edge or slope of a carbonate platform. There is not enough fossil data for a distinct biostratigraphic age, but the presence of primitive Lenticulina sp. is consistent with the Mesozoic.

Mesozoic shallow water carbonates may belong to the Bandeira Group or Perdido Group of the Gondwana Megasequence, and peloid grainstones have been observed within both groups. Outcrop of peloids grainstones at AB530 is massive and more similar in style to the Perdido Group, whereas the Bandeira Group is usually medium to thick bedded (although can also be, more rarely, massive). However, without a more definitive biostratigraphic age determination it is not possible to conclusively classify this sample.

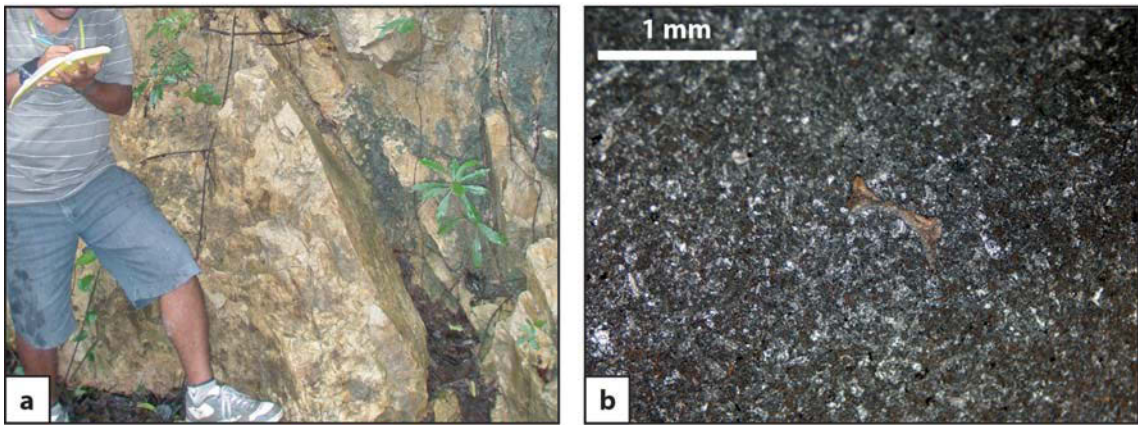

Fig. 55. (a) Outcrop of massive, orange-grey peloids packstone at AB530, where these rocks comprise the lower cliffs southwest of Baguia. (b) Image of an acetate peel taken from a sample of this same outcrop at AB530. The rock comprises micritised peloids with rare small foraminifera and shell fragments. Scale bar = 1 mm.

3.7.5 Interbedded red mudstone and chert

An outcrop of thinly bedded (5-10 cm) red mudstone and red chert was observed on the steep, lower, south-eastern slopes of the Matebian Range, at approximately 750 m above sea level (**Fig. 56a, b**). The red chert beds contain abundant radiolaria and rare bivalve filaments (**Fig. 56c, d**). The mudstone has an unusual oily sheen, but contained no visible biogenic grains.

These radiolarian rich lithologies represent pelagic sedimentation, and the absence of any lithogenic component suggests deposition distal to terrigenous influence.

These rocks have a very similar lithology and outcrop style to the thin to medium bedded, red, radiolarian rich cherts and shales observed at the Builo Range (see **Chapter 3.4.3 The Builo Range – Interbedded mudstones and radiolarites**) and are tentatively placed within the Noni Group on the basis of lithofacies correlation. Unfortunately only cursory sampling around Baguia was possible, and more detailed mapping would be required to support this assignment.

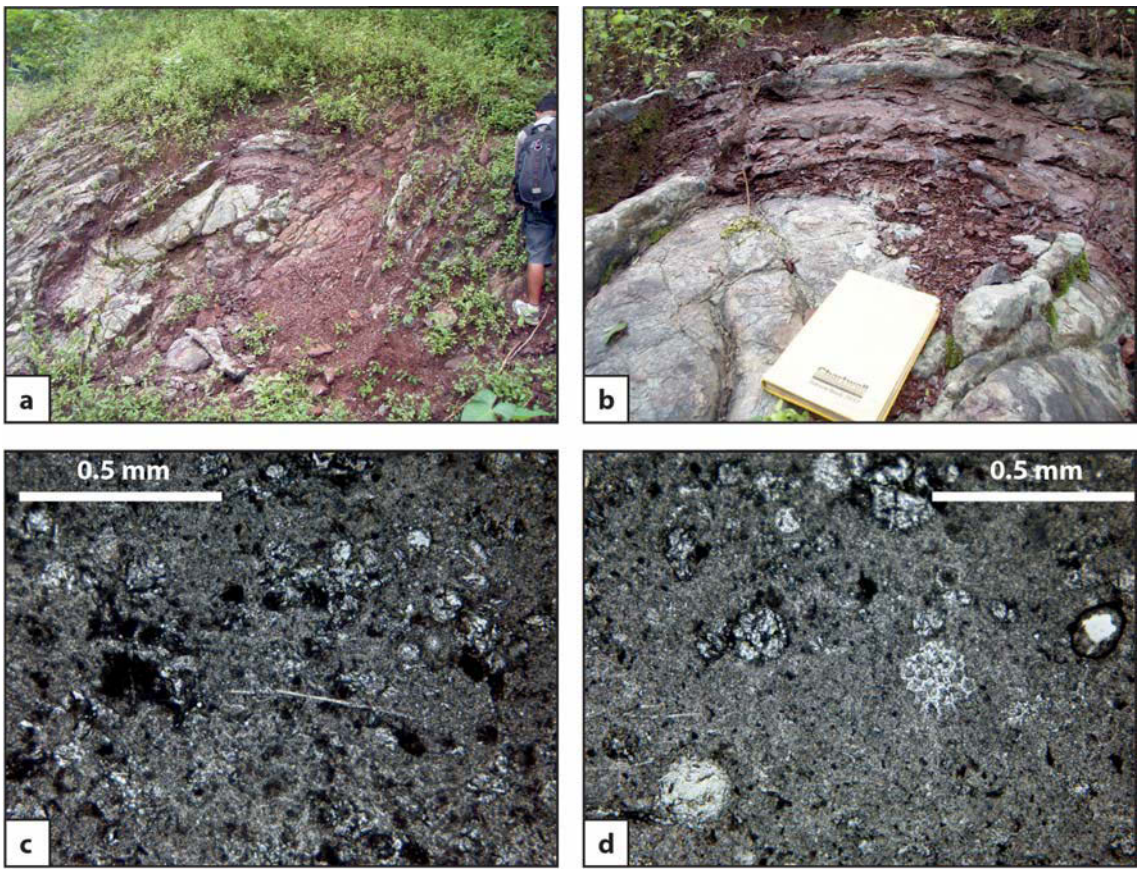

Fig. 56. (a) Outcrop of thinly bedded red mudstone and radiolarian chert at AB526, on the lower, south-eastern slopes of the Matebian Range. (b) Mudstone beds in this outcrop have an unusual oily sheen. A5 notebook for scale. (c, d) Images of acetate peels taken from chert beds at AB526. Samples contain abundant radiolaria and rare bivalve filaments.

3.7.6 Carbonate pelagites

Two outcrops of carbonate pelagites were observed in roadside outcrop along the track that leads southwest from Baguia into the lower reaches of the Matebian Range. AB528 is situated approximately 3.5 km southwest of Baguia, where it comprises the northeast facing cliffs above the road (**Fig. 57a**). Extensively recrystallised and stylotised, only small clasts of the original rock remain within a stockwork of calcite veins. These clasts are wackestone containing abundant planktonic foraminifera including *Morozovella* sp. and *Acarinina* sp. (**Fig. 57b**). AB531 is situated approximately 2 km southwest of Baguia, and comprises massive, yellow-white wackestone (**Fig. 57c**) with abundant, well preserved radiolaria and planktonic foraminifera including *Globigerinoides* sp. (**Fig. 57d**), and some small, centimetre scale chert nodules. Planar fractures gave this outcrop the appearance of thick bedding but these were difficult to distinguish from jointing (**Fig. 57b**).

Similar to carbonate pelagites facies elsewhere, these comprise predominantly planktonic foraminifera within a very fine carbonate mud matrix, suggesting deposition within the middle bathyal to abyssal zone. Based on planktonic foraminiferal assemblages AB528 is assigned an age of Early Eocene, and AB531 is placed tentatively within the Oligocene.

Carbonate pelagites sampled at the Matebian Range southwest of Baguia correlate with Eocene and Oligocene age carbonate pelagites observed elsewhere in East Timor (Haig & McCartain 2007), and are similarly placed within the Kolbano Group of the Australian Margin Megasequence. Isolated outcrops of carbonate pelagites at the Matebian Range have previously been mapped by Audley-Charles (1968 – as 'Borolalo Limestone'), who interpreted them as klippen, and more extensively by Partoyo *et al.* (1995).

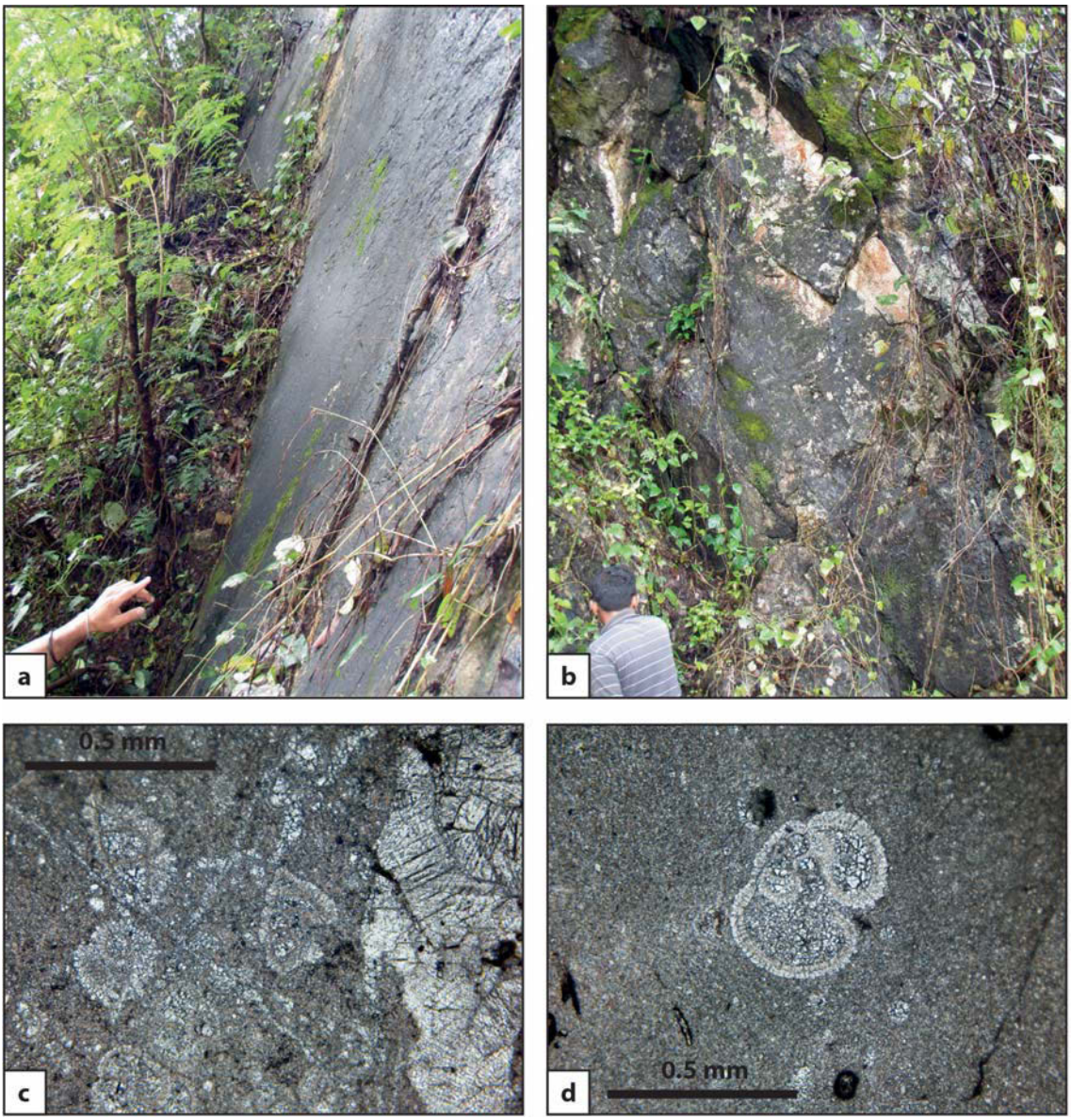

Fig. 57. (a) Kolbano Group limestone forms steep, northeast facing cliffs southwest of Baguia at AB528. (c) Massive, yellow-white Kolbano Group wackestone at AB531. Planar fractures give the appearance of thick bedding but these are difficult to distinguish from jointing. Note geologist in bottom-left of frame for scale. (c) Image of an acetate peel taken from Kolbano Group limestones at AB528. The rock is extensively recrystallised but clasts of the original wackestone contain abundant planktonic foraminifera including *Morozovella* sp. and *Acarinina* sp. Scale bar = 0.5 mm (d) Image of an acetate peel taken from a sample at AB531. A well preserved planktonic foraminifera, possibly *Dentoglobigerina* sp., sits at centre of frame, in a very fine grained carbonate mud matrix. Scale bar = 0.5 mm

3.8 Mount Loelako

Mount Loelako, in Bobonaro District, is one of the most distinctive and impressive landforms in East Timor. It is situated 6 km west of Maliana, East Timor's third largest city, which sits within a large, 15 km wide basin approximately 100-200 m above sea level (**Fig. 10**). Mount Loelako comprises a spectacular north-south trending fatu which bounds the Maliana basin's eastern edge, the upper part of which forms a remarkable limestone 'crest', approximately 6 km long but no more than 1 km wide at its base, and bounded on both sides by near vertical cliffs several hundred metres high (**Fig. 58**). The top of this crest reaches a maximum altitude of 1920 m above sea level and is extremely narrow, only a few metres wide at some points. The west-facing cliffs of the massif have their base at approximately 1400 m above sea level, where the topography changes from sheer cliffs to a more modest slope which descends into the basin 1200 m below over a distance approximately 5 km (**Fig. 58**). The eastern side of the massif is taller still, with the cliffs here beginning at 1000-1100 m above sea level, making the east-facing cliffs of Mount Loelako some of the largest in East Timor. Mount Loelako is distinctive not only for its spectacular morphology, but also because its north-south orientation is unlike any other fatu in East Timor, which all tend to trend either east-west (Mount Mundo Perdido, Mount Bibileu, the Builo Range), or northeast-southwest (Mount Laritame, the Paitchau Range, Mount Matebian, Mount Taroman, the Saburai Range) (**Fig. 10**).

1 km north of Mount Loelako is smaller, secondary massif also investigated by this study, known as Mount Lesululi (**Figs 58, 59**). Approximately 2.5 km wide east to west and less than 1 km from north to south, it rises to a maximum altitude of 1244 m. Almost triangular in shape, it has a gently dipping north-facing slope but high cliffs on its southern and western edges.

Fig. 58 → Aerial photograph of Mount Loelako, Mount Lesululi, and the surrounding area, illustrating sample points, 100 m topographic contours, and main geomorphic features. The Bulubo River runs along the eastern edge of the Maliana basin.

Fig. 59 →→ Interpreted geological map of Mount Loelako, constructed using mapped outcrops and aerial photographs. See text for detailed descriptions of geology. The Dilor Conglomerate (Conglomerates and coarse sands in the upper part of the Viqueque Group – Audley-Charles, 1968) is included in the northwest corner of the mapping area after Partoyo *et al.* (1995), as this area was not sampled by the present study.

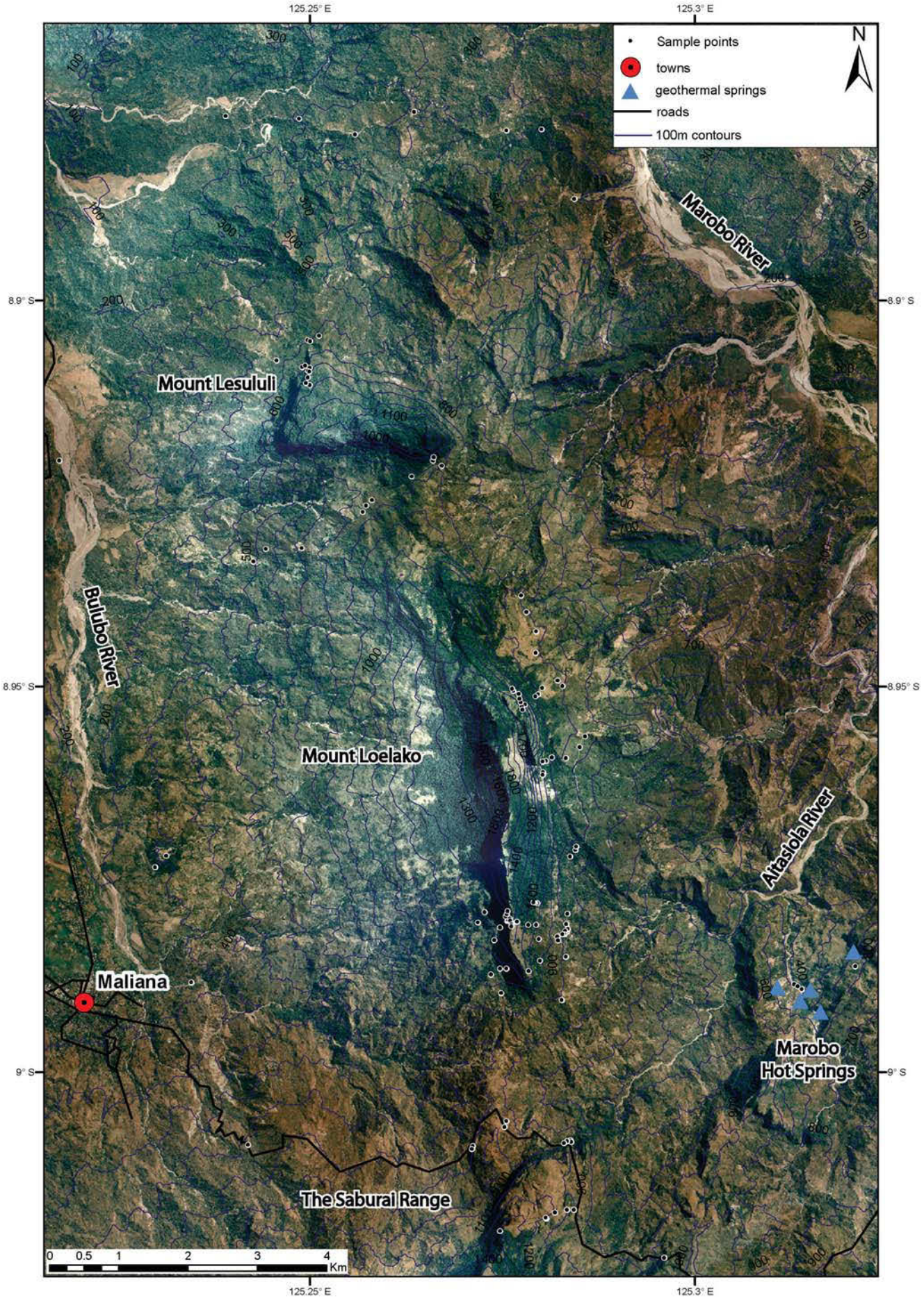
125.25° E
125.3° E
8.9° S
8.95° S
9° S
Sample points
towns
geothermal springs
roads
100m contours
N
Marobo River
Mount Lesululi
Bulubo River
Mount Loelako
Aitasiola River
Maliana
Marobo
Hot Springs
The Saburai Range
0 0.5 1 2 3 4
Km

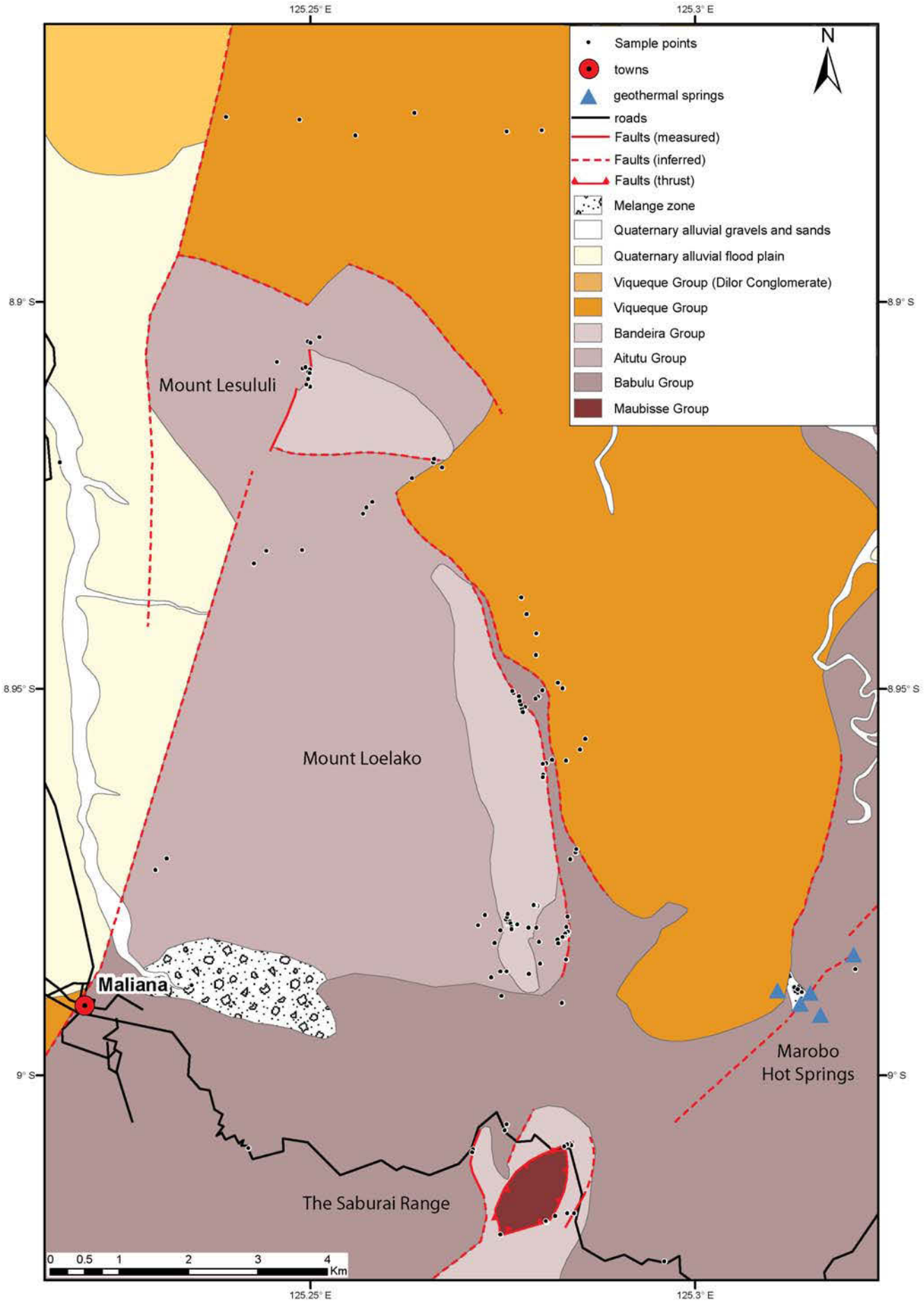
125.25° E
125.3° E
8.9° S
8.95° S
9° S
N
Sample points
towns
geothermal springs
roads
Faults (measured)
Faults (inferred)
Faults (thrust)
Melange zone
Quaternary alluvial gravels and sands
Quaternary alluvial flood plain
Viqueque Group (Dilor Conglomerate)
Viqueque Group
Bandeira Group
Aitutu Group
Babulu Group
Maubisse Group
Mount Lesululi
Mount Loelako
Maliana
Marobo
Hot Springs
The Saburai Range
0 0.5 1 2 3 4
Km

3 km east of Mount Loelako is the Aitasiola River, which runs north into the larger Marobo River east of Mount Lesululi (**Fig. 58**). Numerous hydrothermal springs are found along the banks of the Aitasiola River, including the well-known Marobo Hot Springs.

Six days were spent conducting reconnaissance mapping at Mount Loelako in 2010, based in Maliana, and although travel to the northern parts of the massif were blocked by landslides, access and weather conditions proved much better here than at other 2010 field localities. These factors, along with fairly good outcrop, interesting geology, and the logistical benefits of working near a major town influenced our decision to make the Maliana area the focus of more detailed mapping in 2011. A further six days were spent mapping Mount Loelako and Mount Lesululi in 2011 as part of this more comprehensive study including the Maliana basin and the Saburai Range. Rock units are listed in ascending stratigraphic order and age.

3.8.1 Thinly bedded, folded sandstones and mudstones

Much of the lower hills around the southern tip of Mount Loelako comprise interbedded sandstones and mudstones, with thin bedding generally 2-5 cm (**Fig. 60a, b**). Sandstones are brown to grey, fine grained, comprising mostly subrounded quartz, feldspar and lithic fragments, with no visible biogenic grains. Mudstones are orange to grey, micaceous, and sometimes fissile. These units show extensive deformation close to the southern tip of the massif, with pervasive close to tight recumbent folding which appears almost chaotic in places (e.g. **Fig. 60b**). Further north at AB646, 350 m from the base of the cliffs on the eastern side of Mount Loelako, a purple-grey mudstone unit was observed with centimetre scale mudstone beds interbedded with thin sandstone laminae and rare thin sandstone beds (**Fig. 60c, d**). This mudstone contains abundant mica and black, carbonaceous woody flecks less than 1 mm in size, and also appears chaotically deformed.

Uniform thin bedding and fine grain size suggests deposition from weak, low density pulses of sediment supply, and there is no evidence of cross-bedding or grading. The abundance of wood and mica and the absence of any carbonate component suggest a strong terrigenous influence. It is possible that these deposits may represent the most distal parts of a deltaic system, with the

mudstone dominated unit representing a very low energy environment only receiving rare pulses of fine sediment. Samples collected yielded no fossil material to allow a biostratigraphic age determination. However siliciclastic sediments with tight, recumbent folding and chaotic deformation are generally only observed within the Gondwana Megasequence in East Timor, so it is likely that these sandstone and mudstone units belong somewhere within the Permian to Jurassic succession.

Thinly interbedded, siliciclastic sandstones and shales of the Gondwana Megasequence may be found within the Permian Cribas Group or the Triassic Babulu Group (Haig 2012b) and samples collected at Mount Loelako yielded little information to distinguish between the two. At Mount Loelako these rocks form a monotonous siliciclastic sandstone and shale succession; limestone or volcanic beds that may be suggestive of the Cribas Group (Charlton *et al.* 2002; Haig 2012b) were not observed. Furthermore, all other Gondwana Megasequence rocks at Mount Loelako are Triassic, and belong to either the Aitutu Group (**Chapter 3.8.2 Mount Loelako – Interbedded limestones and mudstones**) or Bandeira Group (**Chapter 3.8.3 Mount Loelako – Fossiliferous wackestones, floatstones and bindstones**). On this basis, this study tentatively places the thinly bedded, folded sandstones and mudstones at Mount Loelako within the Triassic Babulu Group of the Gondwana Megasequence.

3.8.2 Interbedded limestones and mudstones

Interbedded limestones and mudstones are common at Mount Loelako. These rocks form much of the lower ground immediately underneath the high cliffs of both Loelako and Lesululi (e.g. **Fig. 61a**), including the saddle between them, and on the western side they extend down the lower slope of the Lolelako massif into the Maliana basin below. They are also observed on the northern side of Lesululi, where the gentle northern slope of that massif appears to be a dip slope formed by bedding planes within this unit (e.g. **Fig. 61b**).

Limestone beds comprise mostly grey, rarely orange, wackestones with bedding 5-50 cm (**Fig. 61a, b**). They contain abundant radiolaria and *Halobia*-type bivalve filaments with rare ostracods, calcispheres, echinoid debris and benthic foraminifera including *Nodosaria* sp. and

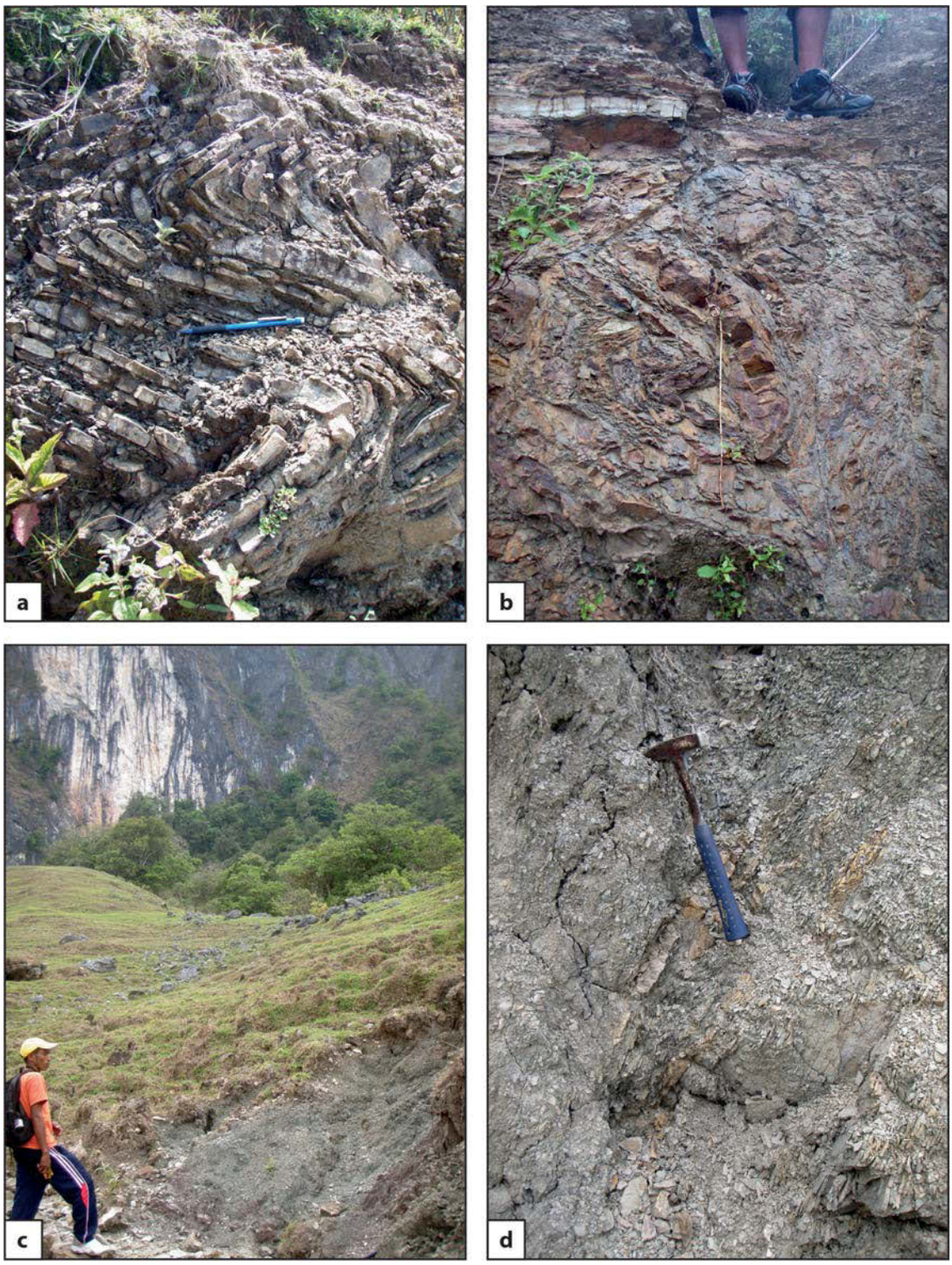

Fig. 60. (a) Tightly folded, thin beds of Babulu Group sandstones and interbedded mudstones at AB420, approximately 400 m southeast of the southern tip of Mount Loelako. Pen for scale. (b) Highly deformed interbedded sandstones and mudstones of the Babulu Group at AB450, approximately 250 m southwest of the southern tip of Mount Loelako. Note feet in top of frame for scale. (c) Facing west, at AB646 beneath high cliffs on the eastern side of Mount Loelako. The Babulu Group here comprises purple-grey mudstones with thin sandstone laminae. (d) Close up of the mudstone rich Babulu Group facies at AB646 illustrating closely spaced sandstone laminae and rare, thin sandstone beds in centre of frame. Hammer for scale.

Lenticulina sp. (**Fig. 61c**). A rare shelly bed was sampled at AB478 which contains abundant large brachiopods (**Fig. 61d, e**) of the genus *Halorella* (Grant-Mackie pers. comm. 2012). Cherty nodules are sometimes visible, and many outcrops, particularly closer to the cliffs, are extensively stylotised and veined. Grey mudstones beds range in thickness from 5-100 cm. Washed mudstone residues are mostly barren but contain some rare foraminifera test fragments, with AB477 containing abundant fine grained feldspar.

Moving closer to the massif, mudstone beds decrease in size and limestone beds get thicker and more fossiliferous. This is particularly evident in a transect conducted up the western slope of the massif, where recessive, predominantly mudstone units grade upwards into thickly bedded limestone 'caps', which become more frequent moving upwards on the slope (**Fig. 61f, g & h**). Limestone beds are up to 100 cm thick and separated by thin mudstone beds. They comprise wackestones and packstones containing abundant, but usually fragmented, fauna including bivalves, brachiopods, gastropods, crinoids, ostracods, calcispheres, benthic foraminifera and rare algal material. Foraminifera include *Nodosaria* sp. including *Nodosaria lagenoides*, *Lenticulina* sp. (diverse but not ornamented forms), and *Endothyra* sp..

Fig. 61 → (a) Well bedded Aituti Group limestone beneath the high east-facing cliffs towards the southern end of Mount Loelako, at AB477. Hammer for scale. (b) North-dipping Aitutu Group limestone beds at AB710, on the northern slope of Mount Lesululi. (c) Image of an acetate peel from Aitutu Group limestone at AB741, near the eastern edge of the Maliana basin. This sample exhibits a typical Aitutu group wackestone facies comprising abundant radiolaria and *Halobia*-type bivalve filaments in a matrix of very fine grained carbonate mud. Scale bar = 1 mm (d, e) Samples of a brachiopod rich bed observed in the Aitutu Group at AB478. The brachiopods belong to the genus *Halorella*, suggesting a Late Triassic age. Centimetre ruler and pen for scale. (f) Facing north, approximately 1 km west of Mount Loelako, the slopes which connect the Maliana basin to the base of Mount Loelako comprise Aitutu Group rocks. Heading towards Mount Loelako limestone beds get thicker and more abundant, and mudstone rich units lower on the slopes grade upwards into thickly bedded limestone 'caps' in the topography – seen here in the centre of frame. In the background, right of frame, are the 200-300 m high cliffs which form the southwest corner of Mount Lesululi. (g) Facing east, directly under and looking up at one of the limestone 'caps' on the western slopes beneath Mount Loelako, at AB630. Prolific limestone scree is shed downslope. (h) Limestone beds at the top of thickening-upwards bedding sequences, such as here at AB630, are thick and fossiliferous, and represent a transitional facies between the basinal radiolarian wackestones of the Aitutu Group and the shallow-water carbonate platform deposits of the Bandeira Group which comprise the Mount Loelako fatu.


a


b

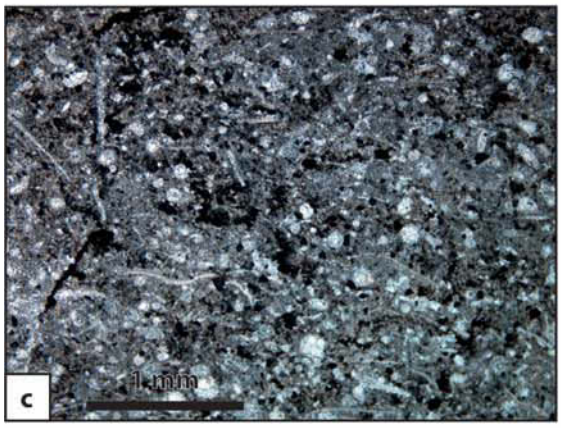
1 mm
c


celco
d


e


f


g


h

Abundant radiolaria within a very fine grained carbonate mud may suggest a deep water, low energy environment, while the presence of *Halobia*-type bivalves suggests an oxygen deficient, basinal setting. Rare lenses and beds containing ooids and shallow water fauna within this basinal carbonate facies have been previously sampled at Mount Mundo Perdido and the Matebian Range; however at Mount Loelako fossiliferous beds containing abundant shallow water fauna are thicker and more frequent, with thickening-upwards bedding sequences clearly visible in outcrop (e.g. **Fig. 61h**). These represent a transitional facies between the basinal radiolarian wackestones and the shallow-water carbonate platform deposits, comprising fossiliferous wackestones, floatstones and bindstones, described below. They may have been deposited on a slope between platform and basin, frequently receiving sediment shed from the developing carbonate platform above. The presence of the brachiopod *Halorella* sp. indicates a Late Triassic age (Grant-Mackie pers. comm. 2013), which is also consistent with the benthic foraminiferal assemblages within these rocks.

Late Triassic basinal carbonate deposits in East Timor, such as the interbedded limestones and mudstones of Mount Loelako, belong to the Aitutu Group of the Gondwana Megasequence (e.g. Audley-Charles 1968; Charlton *et al.* 2009; Haig 2012b). Observations of the Aitutu Group at Mount Loelako support observations made at the Paitchau Range by this author and others (**Chapter 3.6.2 The Paitchau Range – Medium bedded grey wackestones**; Audley-Charles 1968; Partoyo *et al.* 1995; Charlton *et al.* 2009) of lateral and vertical gradations between, and interfingering of, deep water Aitutu Group facies and shallow water Banderia Group facies in the Triassic of East Timor. These groups are best considered end-members, with a range of transitional facies present between them.

3.8.3 Fossiliferous wackestones, floatstones and bindstones

The high cliffs of Mount Loelako and Mount Lesululi comprise well bedded to massive, grey to white, fossiliferous wackestones, floatstones and bindstones (**Fig. 62a-d**). Medium to thick bedding 30-200 cm is common in the southern half of Loelako, with more massive outcrop more frequently observed in the northern parts of Loelako, and at Lesululi. Around the cliff

faces these rocks are extensively recrystallised and dolomitised, with fossils overprinted by a white, crystalline sugary texture. However, well preserved samples contain a diverse and abundant faunal assemblage including gastropods, punctate brachiopods, echinoids, ostracods, crinoids, coral fragments, and benthic foraminifera (**Fig. 62e, f**). Ooids are common along with abundant algal material in the form of encrustations and large nodules up to 30 mm. Benthic foraminifera include *Aulotortus* sp., *Duostomina* sp., *Duotaxis* sp., *Endoteba* sp., *Gandinella* sp., *Karaburunia* sp. and *Nodosaria* sp..

The presence of large skeletal grains, ooids, corals and abundant algae suggests deposition in shallow water, while common, muddy wackestone and floatstone lithologies indicate a low energy environment, and these rocks are consistent with a shallow water, lagoonal facies on a carbonate platform. Benthic foraminiferal assemblages suggest a Carnian age of the Late Triassic.

These rocks are the same age and represent similar shallow water carbonate platform facies to the Triassic wackestones and bindstones at the Paitchau Range, and this study similarly places them within the Bandeira Group of the Gondwana Megasequence on the same bases (**Chapter 3.6.1 The Paitchau Range – Fossiliferous packstones, wackestones and bindstones**). They represent carbonate banks developing on isolated, submerged topographic highs within newly rifted basins during the breakup of Gondwana, and at Mount Loelako, are seen to grade into surrounding slope and basin facies.

3.8.4 Foraminiferal mudstones and sandstones

Foraminiferal mudstones and sandstones are widespread around the east and north of Mounts Loelako and Lesululi (**Fig. 63**). These rocks overlie all other units and appear little deformed, with shallow dips that are variable over the wide extent of the unit but are generally locally consistent. Outcrop runs alongside the eastern edge of Mount Loelako, generally beginning 200-500 m east of the base of the high cliffs, and extends east towards the Aitasiola River where it is observed at the top of the river gorge. This unit is also observed very close to the eastern edge of Mount Lesululi, and outcrop is extensive to the north of this smaller massif.

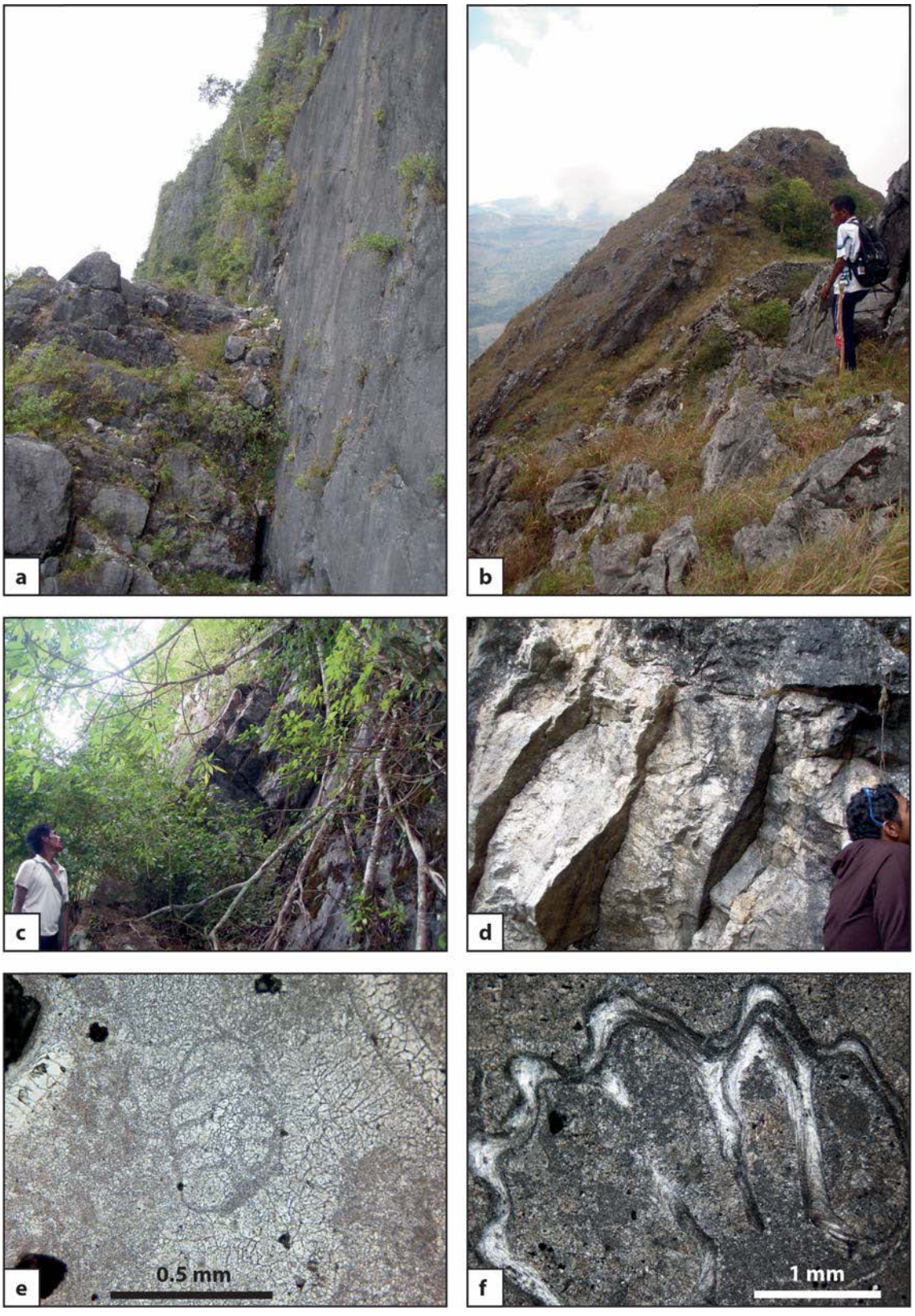
a
b
c
d
e
0.5 mm
f
1 mm

Lithologies comprise friable, grey, interbedded mudstone and muddy sandstone. Around Loelako, outcrop is generally medium bedded, with sandstone beds 5-40 cm, though rarely up to 100 cm, with thin mudstone interbeds less than 10 cm (**Fig. 63a, b**). North of Lesululi these units are more commonly mud dominated, comprising grey mud with thin sandstone interbeds approximately 1-2 cm (**Fig. 63c, d**). Sandstones are fine to medium grained, comprising subangular to more rarely subrounded quartz, mica and lithic fragments including abundant schist, with rare planktonic foraminifera including *Globorotalia* sp. and the benthic *Pseudorotalia* sp.. Mudstones contain very abundant and diverse benthic and planktonic foraminifera. At AB706 a 1 m thick bed of melange was observed within 5-30 cm interbedded sandstone and mudstone (**Fig. 63e**). The melange comprises very poorly sorted pebbles, cobbles and boulders within a mud matrix.

On the eastern side of Mount Loelako the friable sandstone and mudstone succession grades upwards into an indurated interbedded sandstone and gravel/pebble/cobble conglomerate unit, which forms a series of small cliffs near the road (**Fig. 63f**). Clasts within the conglomerate are mainly very fine grained igneous material, but also contain schist, mudstone and various limestone clasts belonging to both the Aitutu Group and Bandeira Group.

Planktonic foraminifera within the mudstones suggest an upper bathyal depositional environment for the muddy lithologies north of Mount Lesululi, and an outer neritic to upper bathyal depositional environment for the more sandstone rich sequences closer to Mount

---

Fig. 62 ← (a) Facing south at AB475, with the high eastern cliffs of Mount Loelako extending into the distance. The sub-vertical cliff faces are bedding planes of medium to thickly bedded Bandeira Group limestones. (b) At the top of Mount Loelako, facing south, at AB655. Medium bedded Bandeira Group limestones dip steeply to the east, the broken ends of bedding planes forming the jagged top of the Mount Loelako ridge. (c) Facing south, at the base of the east-facing cliffs of Mount Loelako, near the fatu's southern end, at AB469. Babulu Group limestones dip steeply to the east, with bedding planes forming the cliff face. The Babulu Group facies at AB469 is radiolarian rich and abundant chert nodules are visible in outcrop, aligned with bedded. This facies may be transitional between the Bandeira Group and the Aitutu Group, which outcrops beneath the cliffs in the south-eastern corner of Mount Loelako. (d) Thickly bedded Bandeira Group limestones dipping steeply to the east on the eastern side of Mount Loelako, at AB482. (e) Many Bandeira Group rocks at Mount Loelako are extensively recrystallised, however foraminifera tests are still clearly visible in acetate peels, such as this duostominid from an acetate peel of sample AB474. Scale bar = 0.5 mm. (f) Bandeira Group rocks at Mount Loelako often contain large skeletal grains, such as this punctate brachiopod fragment in an acetate peel from sample AB658. Scale bar = 1 mm.

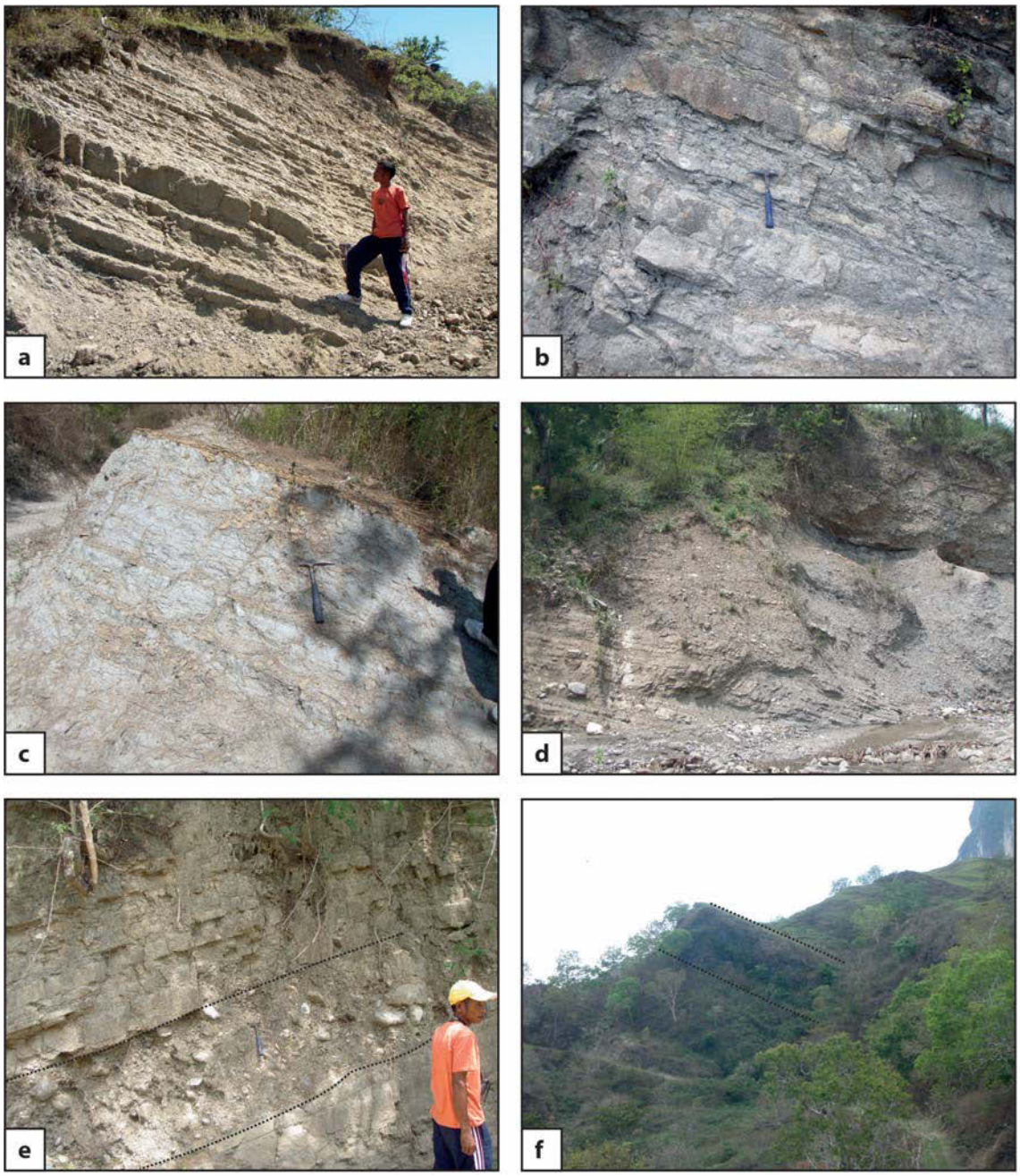

Fig. 63. (a) Interbedded foraminiferal sandstones and mudstones of the Viqueque Group at AB640, 650 m east of the high eastern cliffs of Mount Loelako. Bedding dips 25° towards east-southeast (b) Viqueque Group sandstones and mudstones at AB641, approximately 1.4 km north-northeast of AB640 and 600 m from the high eastern cliffs of Mount Loelako. Bedding here dips 26° to the northwest. Hammer for scale. (c) Mud dominated Viqueque Group facies at AB703, north of Mount Lesululi. Hammer for scale (d) More mud dominated Viqueque Group at AB707, northeast of Mount Lesululi. Some coarse grained pebble rich beds are visible high in the succession, top right of frame. (e) A bed of melange approximately 1 m thick (outlined) within 5-30 cm interbedded Viqueque Group sandstones and mudstones at AB706. Hammer for scale. (f) Facing south, approximately 500 m east of Mount Loelako at its northern end, the high cliffs of the fatu visible top-right of frame. The Viqueque Group here dips southwest, towards Mount Loelako. Stratigraphy grades upwards from sandstones and mudstones to a gravel/pebble/cobble conglomerate unit several metres thick, outlined centre of frame. Locality AB644.

Loelako (Haig pers. comm. 2013). Broad foraminiferal species are consistent with a Neogene to Quaternary age (Appendix 1), with more specific assemblages confining some samples to N21-N22 of the latest Pliocene to Early Pleistocene.

The age and lithofacies of the foraminiferal mudstones and sandstones of Mount Loelako place them within the Viqueque Group of the Synorogenic Megasequence (Audley-Charles 1968; De Smet *et al.* 1990; van Marle 1991a, b; Haig & McCartain 2007; Haig 2012a). At Mount Loelako these rocks are seen to overlie all older lithologies, and their friable texture and consistent, shallow dips are typical of the Synorogenic Megasequence in East Timor. They represent slow deposition of muds and planktonic foraminifera in deep water, periodically interrupted by pulses of sediment shed from an emerging island.

3.9 The Saburai Range

As Mount Loelako bounds the eastern edge of the Maliana basin, so does the Saburai Range bound the basin's south-eastern edge (**Figs 10, 64**). Rising to a similar height as Mount Loelako, slightly over 1900 m above sea level, it is a much longer and broader massif, measuring 15 km along its southwest-northeast oriented long axis, and a little over 4 km across its widest point, towards the southern end of the range (**Figs 64, 65**). The massif comprises one narrow ridge in the north, and two parallel ridges side-by-side in the south, all oriented southwest-northeast, with the northern and southern sections separated by a saddle at approximately 1500 m altitude (**Fig. 64**). The saddle extends south into narrow basin between the two southern ridges, around 4 km long but no more than 1 km wide, which sits at an altitude of 1500-1600m above sea level (**Fig. 64**). The Saburai Range has steep cliffs along both its north-western and south-eastern edges, but those on the northwest are the largest, rising over 600 m from their base near Saburai village to the top of the north-western ridge. From the base of the cliffs, muddy lowlands descend gently into the Maliana basin over a distance of approximately 5 km.

The northern tip of the Saburai Range was sampled briefly in 2010 as part of reconnaissance mapping around Mount Loelako, and during travel to and from Mount Taroman reconnaissance

mapping and sampling were conducted along the road which runs along the south-eastern edge of the range. A further seven days were spent mapping the Saburai Range in 2011 as part of a more comprehensive study including Mount Loelako and the Maliana basin. Rock units are listed in ascending stratigraphic order and age.

3.9.1 Coarse grained sandstones and breccias

The northern tip of the Saburai Range is capped by a 50-60 m thick package of coarse grained sandstones and breccias (**Fig. 66**). They overlie well bedded fossiliferous limestones, which comprise the bulk of the Saburai massif, along a shallow, mostly north-dipping thrust fault (**Fig. 66a, b & c**), forming a klippe at the tip of the range approximately 1.5 km long and 750 m wide (**Fig. 65**). Red-grey, medium bedded sandstones (**Fig. 66d**) comprise poorly sorted, medium to very coarse grains of mainly volcanic material. Grains are very well rounded, and appear to be formed of iron rich basalt, black or weathered brown to red, in which small feldspar laths are occasionally visible. Occasional biogenic material is observed, including calcareous green algae, crinoids and bryozoans, including fenestrate types (**Fig. 66e**). Breccias are reddish-green to grey, massive to thickly bedded and comprise very poorly sorted angular volcanic clasts 5-50 mm in size within a sandy matrix. This matrix appears similar in composition to the coarse grained sandstones, although biogenic grains are less frequent, comprising mainly small fragments of calcareous algae.

The faunal assemblage within these rocks suggests marine deposition, while the large, well rounded grains within the sandstones suggest a high energy environment. A proximal volcanic terrane has supplied the majority of sediment comprising the sandstone, with eruptive events likely providing the large, angular clasts within the breccias. These rocks would be consistent with a shallow, high energy shoreline environment with nearby active volcanism.

Fig. 64 → Aerial photograph of the Saburai Range illustrating sample points and 100 m topographic contours. The southern tip of Mount Loelako is visible top right of frame.

Fig. 65 →→ Interpreted geological map of the Saburai Range, constructed using mapped outcrops and aerial photographs. See text for detailed descriptions of geology.

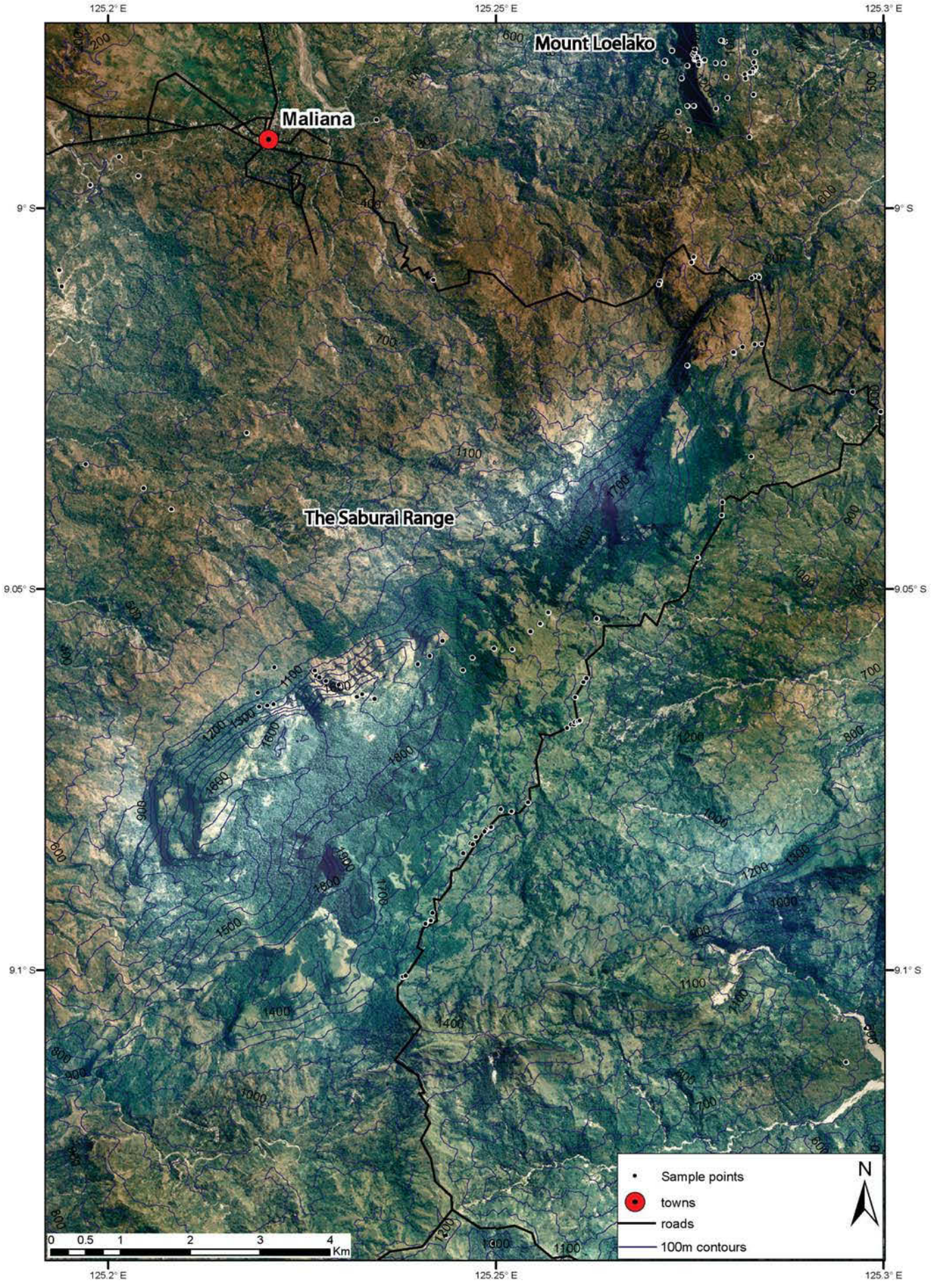
125.2° E
125.25° E
125.3° E
9° S
9.05° S
9.1° S
Mount Loelako
Maliana
The Saburai Range
Sample points
towns
roads
100m contours
N
0 0.5 1 2 3 4
Km

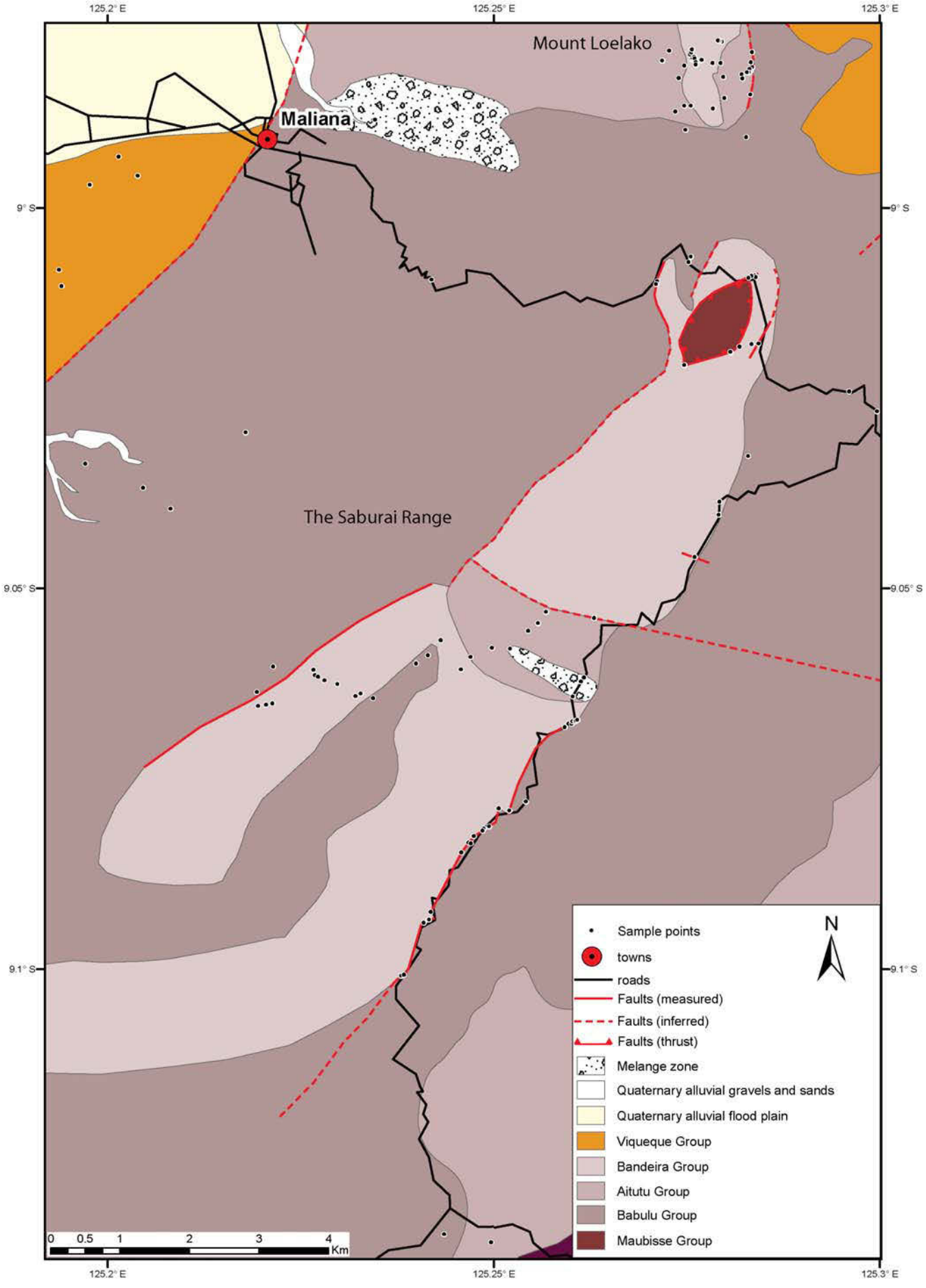
125.2° E
125.25° E
125.3° E
Mount Loelako
Maliana
9° S
9.05° S
9.1° S
The Saburai Range
Sample points
towns
roads
Faults (measured)
Faults (inferred)
Faults (thrust)
Melange zone
Quaternary alluvial gravels and sands
Quaternary alluvial flood plain
Viqueque Group
Bandeira Group
Aitutu Group
Babulu Group
Maubisse Group
N
0 0.5 1 2 3 4
Km

The limited fossil assemblage is not sufficient for a definitive age determination, but reddish coloured limestones and biocalcarenites with abundant crinoids and fenestrate bryozoans are typical of the latest Carboniferous and Permian in Timor (Audley-Charles 1968; van Bemmelen 1970; Hamilton 1979; Bird & Cook 1991; Charlton *et al.* 2002; Davydov *et al.* 2013, 2014; Haig *et al.* 2014).

Permian strata in Timor has two main end member groups, the carbonate dominated shallow water Maubisse Group and the siliciclastic dominated basinal Cribas Group, with volcanics interbedded in both groups (Haig 2012b). The coarse grained sandstones and breccias from the Saburai Range are very similar to the volcaniclastic sands of the Maubisse Group described by Bird (1987) from West Timor. Rocks described by Bird (1987) "have the texture of grainstones", with well-rounded volcanic clasts of high sphericity, in hand specimen resembling black ooliths. Each clast is formed of weathered iron rich basalt with visible interlocking feldspar laths, and the rocks are rich in bioclasts including brachiopod shell debris, echinoderm plates and spines, and small benthic foraminifera (Bird 1987). Based on their probable Permian age, and very close lithofacies correlation to the Maubisse volcaniclastic sands of Bird (1987), this study places the coarse grained sandstones and breccias of the Saburai Range in the Maubisse Group of the Gondwana Megasequence. They were likely deposited proximal to volcanism, within a shallow, high energy shoreline environment in an actively spreading Permian basin.

The Saburai Range has been mapped by most previous studies as a massive nappe of Permian limestone (e.g. Gageonnet & Lemoine 1958; Audley-Charles 1968; Partoyo *et al.* 1995). This is likely due to the fact that the most accessible part of the mountain is the northern tip, so most previous mapping has sampled these Permian volcaniclastics and biocalcarenites which have then been extrapolated to the rest of the massif. This study confirms that there is a nappe of Permian rocks present, sitting on a clearly visible low angle thrust, however it is confined to the northern 1.5 km of the Saburai Range, the majority of which comprises Triassic lithologies.

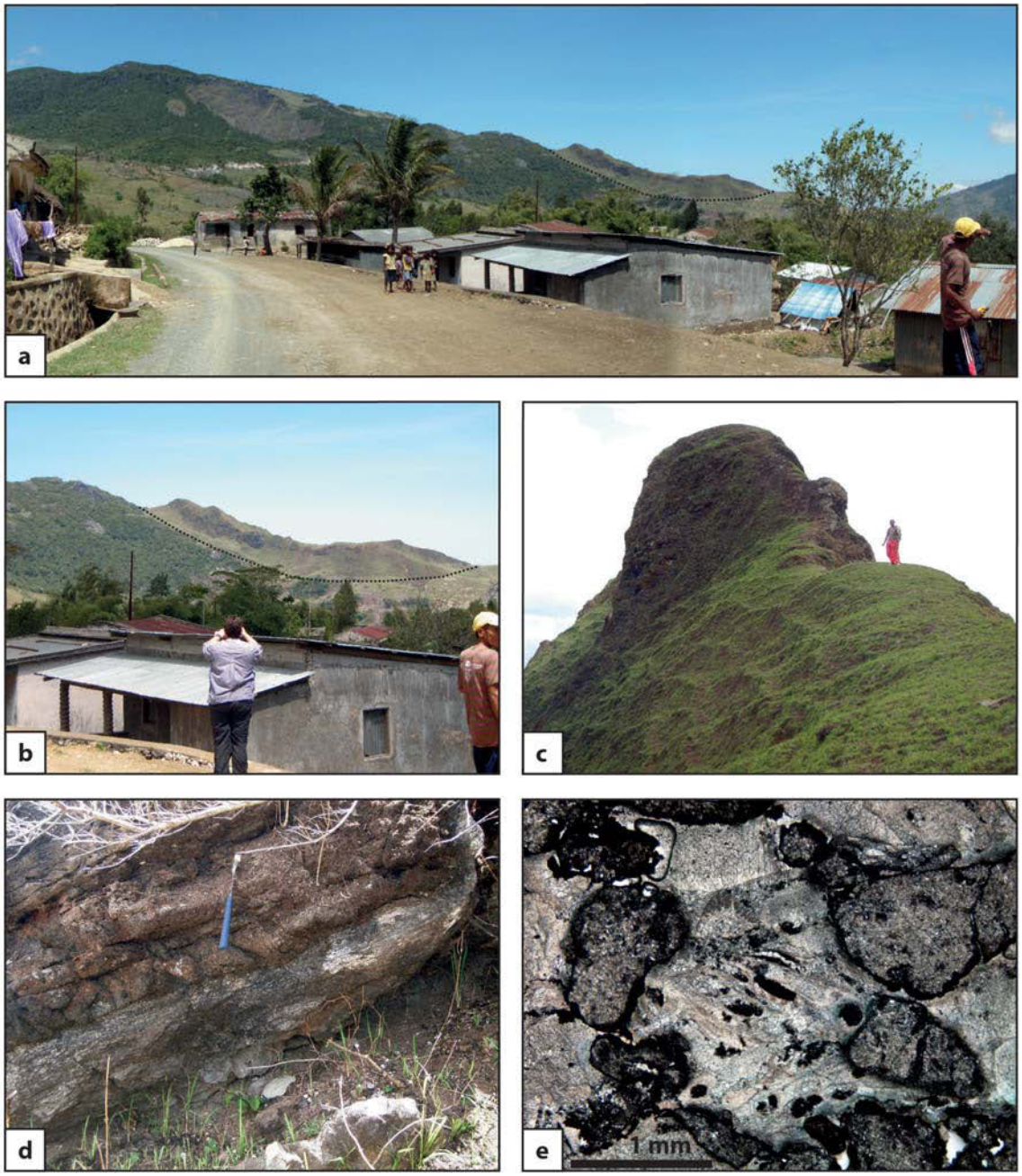

Fig. 66. (a) Facing northwest towards the northern tip of the Saburai Range, approximately 2 km southeast of the mountain. Sitting over the northern tip of the range, centre-right of frame, is a 50-60 m thick package of coarse grained sandstones and breccias of the Maubisse Group, overlying well bedded fossiliferous limestones which make up the bulk of the Saburai Range on a low angle thrust fault (interpreted on the image with a dashed line). The difference in lithologies between the klippe and the underlying limestones is evident even from this distance. The Maubisse Group rocks have weathered into rounded profiles, in contrast to the blocky, angular limestones elsewhere on the range, and the grassy vegetation cover of the klippe sits in stark contrast to the thick jungle foliage growing over the Saburai Range to the south. (b) Close-up image of the Maubisse Group klippe from the same vantage point of the previous photograph. The interpreted, mostly north dipping thrust is again shown with a dashed line. (c) Photographer standing near the southern thrust contact of the Maubisse Group with underlying Bandeira Group limestones, at AB739, facing south looking out over the klippe. The rounded morphology and grassy vegetation cover is very different to the blocky limestone and thick jungle elsewhere on the Saburai Range (d) Outcrop of medium bedded, course grained Maubisse Group sandstone from AB738, on the eastern side of the klippe. Hammer for scale. (e) Image of an acetate peel taken from AB738, illustrating lithic and biogenic grains in the rock framework. A large bryozoan fragment sits at centre of frame. Scale bar = 1 mm.

3.9.2 Grey mudstones with sandstone interbeds

There is little outcrop within the high basin between the two southern ridges of the Saburai Range, but most subcrop appears to be recessive orange/grey mudstone (**Fig. 67a**). The best outcrop was observed at AB753, close to the northern end of the basin, which comprises thinly interbedded grey siliciclastic mudstone and grey, fine grained micaceous sandstone (**Fig. 67b**), with *Chondrites* trace fossils evident within the mudstone beds. Washed mudstone residues yield radiolaria, *Bathysiphon* sp. (with dark colour indicating high temperatures due to burial),

and rare foraminifera including *Ammodiscus* sp. and ?*Carteriella manelobasensis* (Haig & McCartain 2010). Just north of, and slightly below, the elevated basin, large sandstone boulders are observed strewn chaotically within the saddle that separates the southern and northern ridges of the Saburai Range (**Fig. 67c**). They comprise medium to thinly bedded fine sandstone with minor cross-bedding (**Fig. 67d**) and occasional thin mudstone laminae less than 1 mm (**Fig. 67e**). These likely represent the erosional remains of a previous landscape, and may be related to the mudstones and sandstones observed to the south within the basin, perhaps representing thick sandstone packages within the succession which have been the most resistant to weathering. Micaceous mudstones with thin sandstone interbeds are also observed down on the lower slopes of the Saburai Range, towards the base of the massif well below the high limestone cliffs, on both the north-western (**Fig. 67f, g**) and south-eastern (**Fig. 67h**) edges of the range. These mudstones contain abundant sulphides, mostly in the form of internal moulds of very small (< 150 μ) gastropods and bivalves. *Chondrites* trace fossils indicate anoxic conditions within the mudstones, which is supported by the presence of abundant sulphides. This is consistent with deposition in a deep water, low energy environment. Sandier facies however display some minor cross-bedding, evidence of deposition above storm wave base, and the thick sandstone packages were probably deposited in shallower water within the offshore transition zone. Benthic foraminiferal species are consistent with a Late Triassic age.

Siliciclastic mudstone and sandstone successions of the Triassic in Timor belong to the Babulu Group of the Gondwana Megasequence (Haig 2012b). They were deposited as terrestrially

derived sediment from river systems infilled basins within the East Gondwanan Rift System. Siliciclastic Babulu Group rocks appear to overlie Bandeira Group limestones (**Chapter 3.9.4 The Saburai Range – Fossiliferous wackestones, floatstones and bindstones**) at the top of the Saburai Range, implying that they are at least in part younger deposits. Similar relationships have been observed at the Bandeira Gorge and elsewhere in East Timor (Haig pers. comm. 2013).

3.9.3 Interbedded grey limestones and mudstones

The saddle separating the northern and southern ridges of the Saburai Range comprises medium bedded, grey limestones and mudstones (**Fig. 68a**). 10-30 cm beds of highly bioturbated, muddy wackestone are interbedded with thinner mudstone beds generally less than 5 cm thick (**Fig. 68b, c**). Wackestones contain abundant radiolaria, *Halobia*-type shell filaments, and some benthic foraminifera, mainly *Lenticulina* sp. (**Fig. 68d**).

On the south-eastern flank of the Saburai range, approximately 1.5 km south of the saddle but at a similar 1500 m altitude, similar interbedded, grey limestones and mudstones are observed, however with generally thicker limestone beds 10-100 cm interbedded with fissile, grey mudstone beds 1 to 30 cm (**Fig. 68e**). Limestones show similar extensive bioturbation but are far more fossiliferous than those sampled within the saddle, containing fragments of echinoids, crinoids, bryozoans and punctate brachiopods, and a more diverse foraminiferal assemblage including *Nodosaria* sp., *Lenticulina* sp. and *Pamula* sp. (e.g. **Fig. 68f**).

Fig. 67 → (a) Recessive orange/grey Babulu Group mudstone found is throughout the high basin between the two southern ridges of the Saburai Range, locality photographed here is AB754. Hammer for scale. (b) Steeply dipping, fine grained, micaceous sandstone and grey mudstone at AB753, hammer for scale. (c) Large sandstone boulders within the saddle that separates the southern and northern ridges of the Saburai Range at AB696, most likely representing the erosional remains of a previous landscape (d) Sandstones at AB696 display swaley cross bedding typical of Babulu Group sandstones elsewhere in East Timor. A5 notebook for scale. (e) Close up of a sandstone sample from AB696 showing thin mudstone laminae, pen for scale (f) Babulu Group micaceous mudstones with thin sandstone interbeds at AB731, beneath the north-western corner of the Saburai Range. (g) Sulfide-rich, grey Babulu Group mudstone with thin to medium sandstone interbeds at AB419, also beneath the north-western corner of the Saburai Range. (h) Grey, micaceous mudstones of the Babulu Group at AB611, at the southern end of the Saburai Range's south-eastern flank. Hammer for scale.


a
b
c
d
e
f
g
h

Abundant radiolaria with *Halobia*-type bivalves within a very fine grained carbonate mud suggests a deep water, low energy, oxygen deficient basinal setting. As at Mount Loelako, thick, fossiliferous beds containing abundant shallow water fauna are sometimes found within this sequence at the Saburai Range. These may represent a transitional facies between the basinal radiolarian wackestones and the shallow-water carbonate platform deposits which comprise the high cliffs of the Saburai massif (see below, **Chapter 3.9.4 Fossiliferous wackestones, floatstones and bindstones**). Benthic foraminiferal assemblages within these rocks are consistent with a Late Triassic age.

Along with similar Late Triassic basinal carbonate deposits in East Timor (e.g. Audley-Charles 1968; Charlton *et al.* 2009; Haig 2012b), the interbedded grey limestones and mudstones of the Saburai Range belong to the Aitutu Group of the Gondwana Megasequence. As at Mount Loelako, thicker, fossiliferous limestone beds with abundant shallow water fauna within the succession may represent transitional facies between the basinal Aitutu Group and the shallow water, carbonate platform Bandeira Group.

3.9.4 Fossiliferous wackestones, floatstones and bindstones

With the exception of the sandstones and breccias at the northern tip, all of the high cliffs of the Saburai Range comprise fossiliferous limestones (**Fig. 69a-d**). Sampled outcrops comprise most commonly wackestones, floatstones and bindstones, with subordinate packstones and grainstones also observed. These limestones are highly indurated, grey to white in colour and medium to thickly bedded, most commonly 30 cm to 3 m (**Fig. 69a, b & c**), although sometimes appear massive, particularly high on the northwest facing cliffs in the south of the range. Extensive recrystallization and dolomitisation are common, with dolomite sometimes appearing in outcrop as mottled, black, 30-100 cm thick bands of small rhombic crystals (**Fig. 69d**).

Wackestones, floatstones and bindstones contain a diverse and abundant fossil assemblage including gastropods, brachiopods, echinoids, ostracods, bryozoans and thaumatoporellacean algae. Diverse benthic foraminifera include *Aulotortus* sp., *Duostomina* sp., *Endothyra* sp., *Gandinella* sp., *Karabarunia* sp., *Lenticulina* sp. and *Siphovalvulina* sp. (**Fig. 69e-h**).

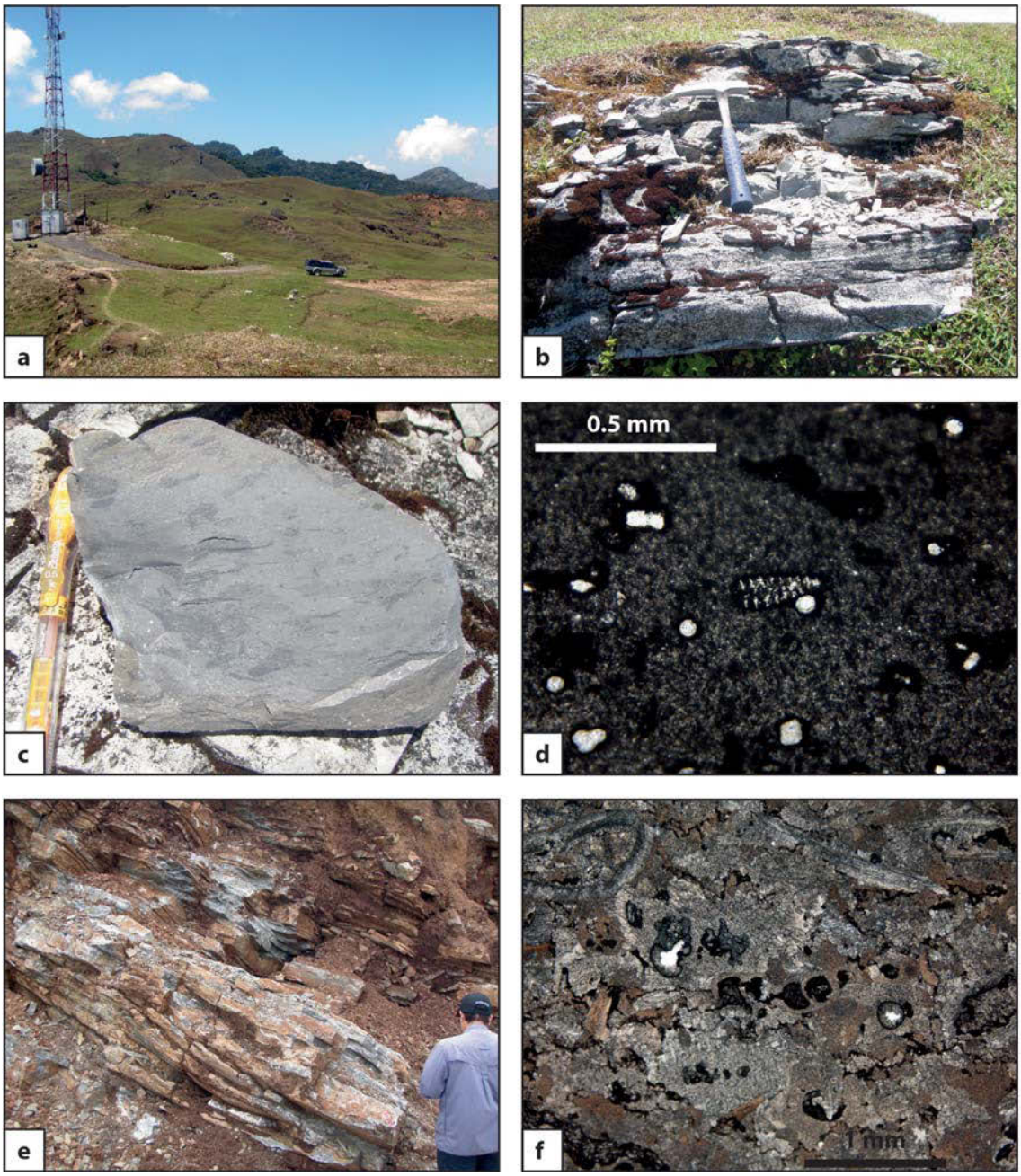

Fig. 68. (a) Looking out over the saddle that separates the northern and southern ridges of the Saburai Range, near AB686. This saddle comprises Aitutu Group interbedded limestones and mudstones. (b)Aitutu Group limestone beds jut out from surrounding recessive mudstones at AB686 (c) A limestone sample from AB686 shows extensive bioturbation. (d) Image from an acetate peel taken from an Aitutu Group limestone at AB686. The peel contains radiolaria and rare, small foraminifera in a carbonate mud matrix. Scale bar = 0.5 mm. (e) Well bedded Aitutu Group limestones on the south-eastern flank of the Saburai Range at AB759, approximately 1.5 km southeast of the saddle (f) Image from an acetate peel of a limestone sample from AB759. Some Aitutu Group beds at AB759 are extremely fossiliferous. Like similar fossiliferous Aitutu Group beds at Mount Loelako, these may represent transitional facies between the basinal Aitutu Group and the shallow water, carbonate platform Bandeira Group that comprises the fatu above.

Rare ooids are observed in the muddier wackestones and floatstones but are far more abundant within packstones and grainstones, where they form the dominant grain type (**Fig. 69e-h**).

Like the wackestones, floatstones and bindstones at Mount Loelako, the presence of large skeletal grains, ooids, corals and abundant algae suggests deposition in shallow water, while a large carbonate mud component indicates a fairly low energy environment. This is consistent with deposition in shallow water, lagoonal facies on a carbonate platform. Rarer ooid packstones and grainstones would have been deposited in higher energy conditions, where wave or tide action has winnowed out the mud component, and these lithologies most likely represent shallower or less restricted parts of the carbonate platform. Benthic foraminiferal assemblages are consistent with a Late Triassic age.

These rocks belong to the same Late Triassic shallow water carbonate platform facies as the wackestones, floatstones and bindstones sampled at the Paitchau Range and Mount Loelako, and this study places them within the Bandeira Group of the Gondwana Megasequence on the same basis (**Chapter 3.6.1 The Paitchau Range – Fossiliferous packstones, wackestones and bindstones**). They represent carbonate banks developing on isolated, submerged topographic highs within newly rifted basins during the breakup of Gondwana. Reconnaissance mapping has previously interpreted these rocks as Permian Maubisse Formation (e.g. Gageonnet & Lemoine 1958; Audley-Charles 1968; Partoyo *et al.* 1995), however as described above (**Chapter 3.9.1 The Saburai Range – Coarse grained sandstones and breccias**) this is most

---

Fig. 69 → (a) Facing southeast, looking up towards the high limestone cliffs of the Saburai Range from locality AB680. These cliffs comprise medium to thickly bedded Bandeira Group limestones. Here, bedding appears to dip shallowly to the right of frame (southwest) (b) Facing southwest at AB749, looking out along the top of the Bandeira Group limestone cliffs in the previous photograph. The cliffs drop away into the Maliana basin to the right of frame. (c) Fossiliferous Bandeira Group limestone at AB699, in the central region of the Saburai Range at approximately 1600 m above sea level. Hammer for scale. (d) A large boulder which has fallen from the high, northwest facing cliffs of the Saburai Range, at AB748. The dark bands in the rock are formed by layers of dolomitisation, which appear to be parallel to bedding (although this boulder has fallen and bands are now at right angles to their original, shallowly dipping orientation in the cliff, see **Fig. 69a**). Note field assistant at top of boulder for scale. (e) Image of an acetate peel from a Bandeira Group ooid packstone at AB679. Scale bar = 1 mm (f) Thaumatoporellacean algae in an acetate peel taken from a Bandeira Group ooid packstone at AB699 (g) Image of an acetate peel from a Bandeira Group ooid packstone at AB699. A small foraminifera sits at centre of frame, possibly *Aulotortus* sp.. Scale bar = 0.5 mm (h) A duostominid foraminifera in an image of an acetate peel taken from AB699. Scale bar = 0.5 mm.

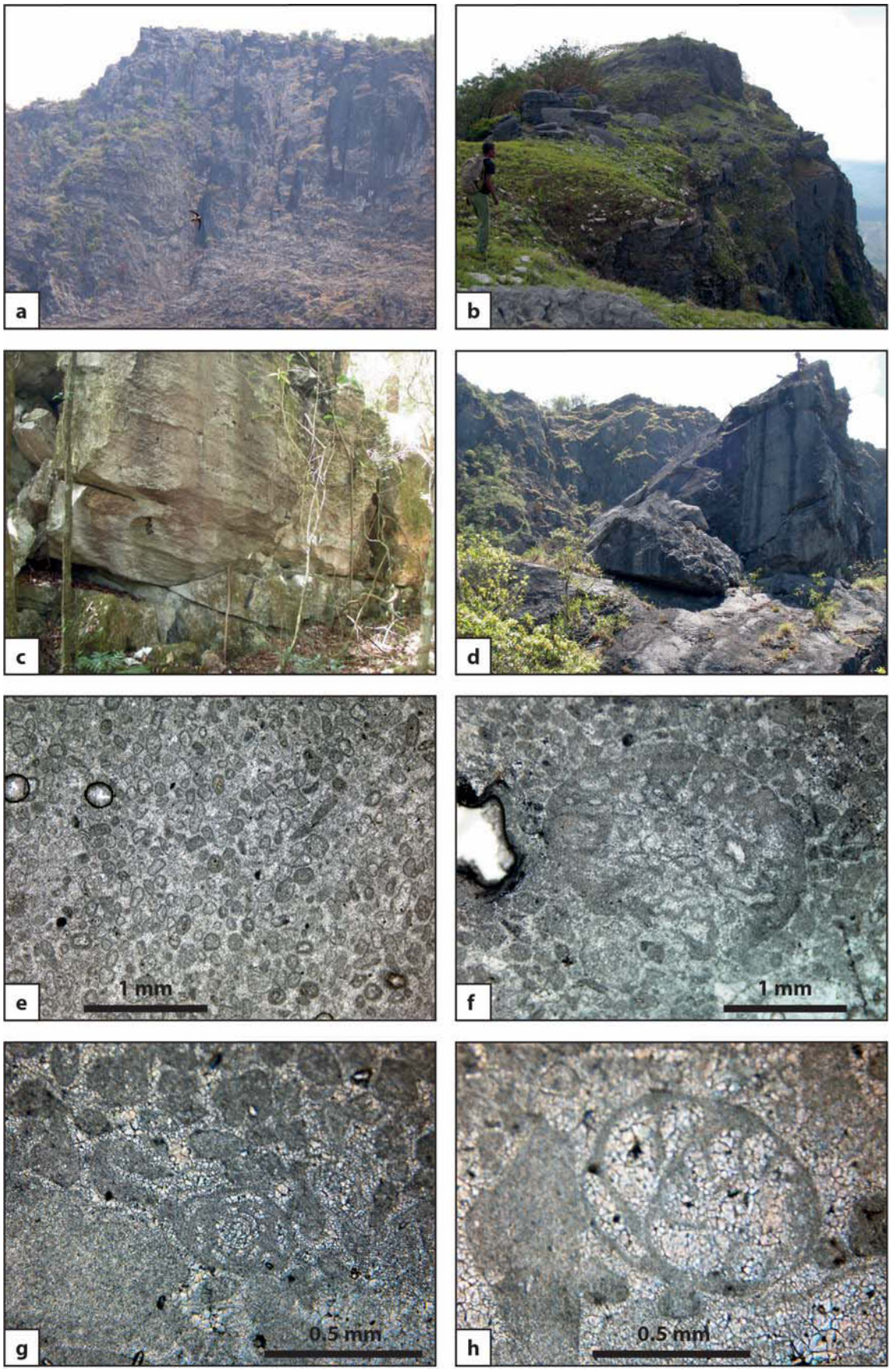
a
b
c
d
e
1 mm
f
1 mm
g
0.5 mm
h
0.5 mm

likely due to previous sampling being limited to Permian outcrops on the northern tip of massif. This study shows that the Saburai Range comprises predominantly Triassic, Bandeira Group limestones.

3.9.5 Igneous rocks

A small zone of igneous rocks is observed low on the south-eastern flank of the Saburai Range, below the saddle, comprising volcanic cobbles and boulders up to 3 m in size within a matrix of red/green/grey scaly mud (**Fig. 70a, b**). The road which parallels the massif along its south-eastern flank cuts through this zone for approximately 300 m, with bedded limestones and mudstones outcropping to the north and south. A very similar outcrop is observed 1 km west-northwest of this zone, approximately 200 m higher up the mountain within the saddle of the Saburai Range. Here are found the same volcanic boulders, though mostly smaller in size at less than 1 m, within a matrix of red-brown mud (**Fig. 70c**). Most volcanic rocks sampled within this zone are green-grey, fine grained vesicular basalts (**Fig. 70e**), with prominent striations observed on the sides of many blocks.

The vesicular texture of these rocks indicates that they were originally formed by eruptions of basaltic magma at or near the surface. Now outcropping as chaotic boulders within a scaly mud matrix, with prominent striations evidence of shearing and movement among blocks, these vesicular basalts have since been incorporated into a tectonic melange zone. Such zones are common throughout Timor, as fluid-saturated Gondwana Megasequence mudstones, overpressured during collision, have been brought to the surface via fault zones and shale diapirism, bringing with them exotic blocks of many different lithologies (Barber *et al.* 1986; Harris *et al.* 1998). No geochemical analysis has been carried out on these blocks, and in the absence of any coherent stratigraphy it is not possible to provide these melange blocks with a definitive age determination.

Rocks of a variety of ages and tectonostratigraphic affinities are observed incorporated into zones of tectonic melange in East Timor (Harris *et al.* 1998). Volcanics within melange at the Saburai Range have potentially been sourced from either volcanic sequences within the

Gondwana Megasequence or Banda Megasequence (**Fig. 9**). Vesicular basalts are most commonly observed within the Permian in Timor (de Roever 1942; Audley-Charles 1968; Barkham 1993; Sawyer *et al.* 1993), however there is no reason that they should not also occur within younger, Barique Group volcanics of the Banda Megasequence, which have been observed incorporated into melange zones at Mount Mundo Perdido (**Chapter 3.2.5 Mount Mundo Perdido – Igneous and metamorphic rocks**).

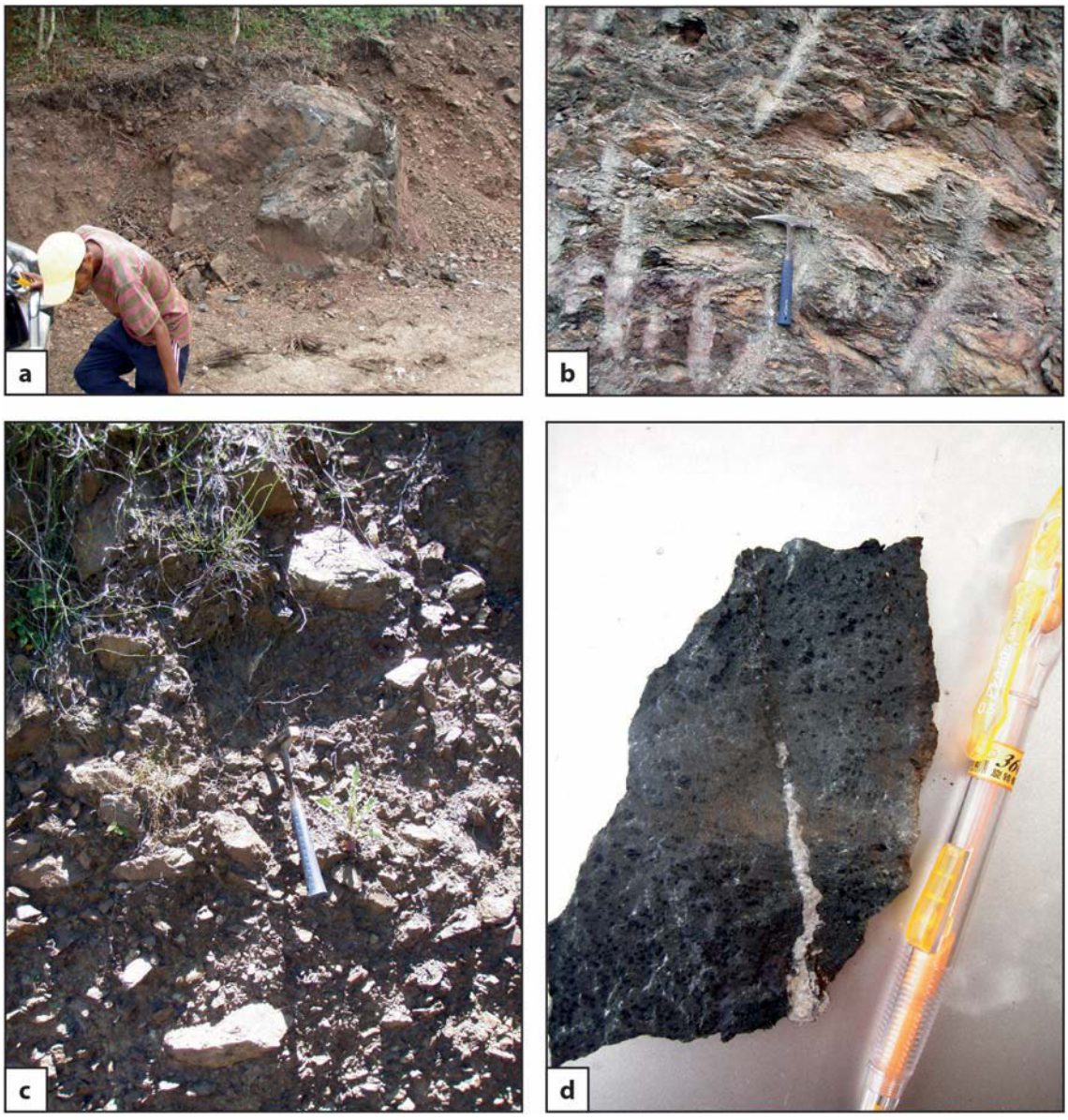

Fig. 70. (a) A large mafic volcanic boulder within a matrix of red/green/grey scaly mud at AB692, part of a tectonic melange zone. (b) Many smaller volcanic cobbles are also present within the mud matrix in this zone. This photograph is at AB693, 300 m northwest along the road from AB692. Hammer for scale. (c) 1 km west-northwest of this zone, and 200 m higher up the mountain, similar outcrop of volcanic cobbles within a matrix of red-brown mud is present at AB697. Hammer for scale. (d) A sample of a volcanic cobble from AB693 illustrating its fine grained, vesicular texture. Pen for scale.

However, if the melange at the Saburai Range is a result of overpressured muds rising to the surface through fault zones (Barber *et al.* 1986; Harris *et al.* 1998), it would be expected that the exotic blocks incorporated in them would be sourced from the underlying stratigraphy.

At the Saburai Range, this particular melange zone occurs within Triassic Bandeira Group limestones, and it is more likely that the volcanic blocks came from underlying Permian units rather than the Banda Megasequence which occurs as thrust sheets at high structural levels (Harris 2006). Therefore, the igneous rocks within the melange zone at the Saburai Range most likely originated in either the Maubisse or Cribas groups of the Gondwana Megasequence.

3.10 The Maliana basin

Timor Island has a boomerang-shaped outline, with the Maliana basin situated right at the bend, where the northeast strike of West Timor changes abruptly to the east-northeast strike of East Timor (**Fig. 2**). Approximately 15 km wide, the floor of the basin is strikingly flat, although it has a slight gradient from 200 m above sea level in the southeast to less than 100 m in the northwest (**Fig. 71**). Outside of the coastal plains it is by far the lowest, flattest expanse of land in East Timor.

Fig. 71 → Aerial photograph of the Maliana basin region illustrating sample points, 100 m topographic contours, and main geomorphic features. Mount Loelako and the Saburai Range are situated on the right and bottom right of the map, respectively. The bottom left of the map is Indonesian territory for which this study has no geological or geographical data.

Fig. 72 →→ Interpreted geological map of the Maliana basin region, constructed using mapped outcrops and aerial photographs. See text for detailed descriptions of geology. Areas not sampled by this study (e.g. the central north portion of the map) are modified after Partoyo *et al.* (1995) using aerial photographs. Lithologies in these areas not described in the text include the Dilor Conglomerate (Conglomerates and coarse sands in the upper part of the Viqueque Group – Audley-Charles, 1968) and the Aileu metamorphics (metamorphosed lower Gondwana Megasequence rocks, see **Fig. 9**. Aileu metamorphics were observed by this study in the mapped area on a reconnaissance traverse but not sampled).

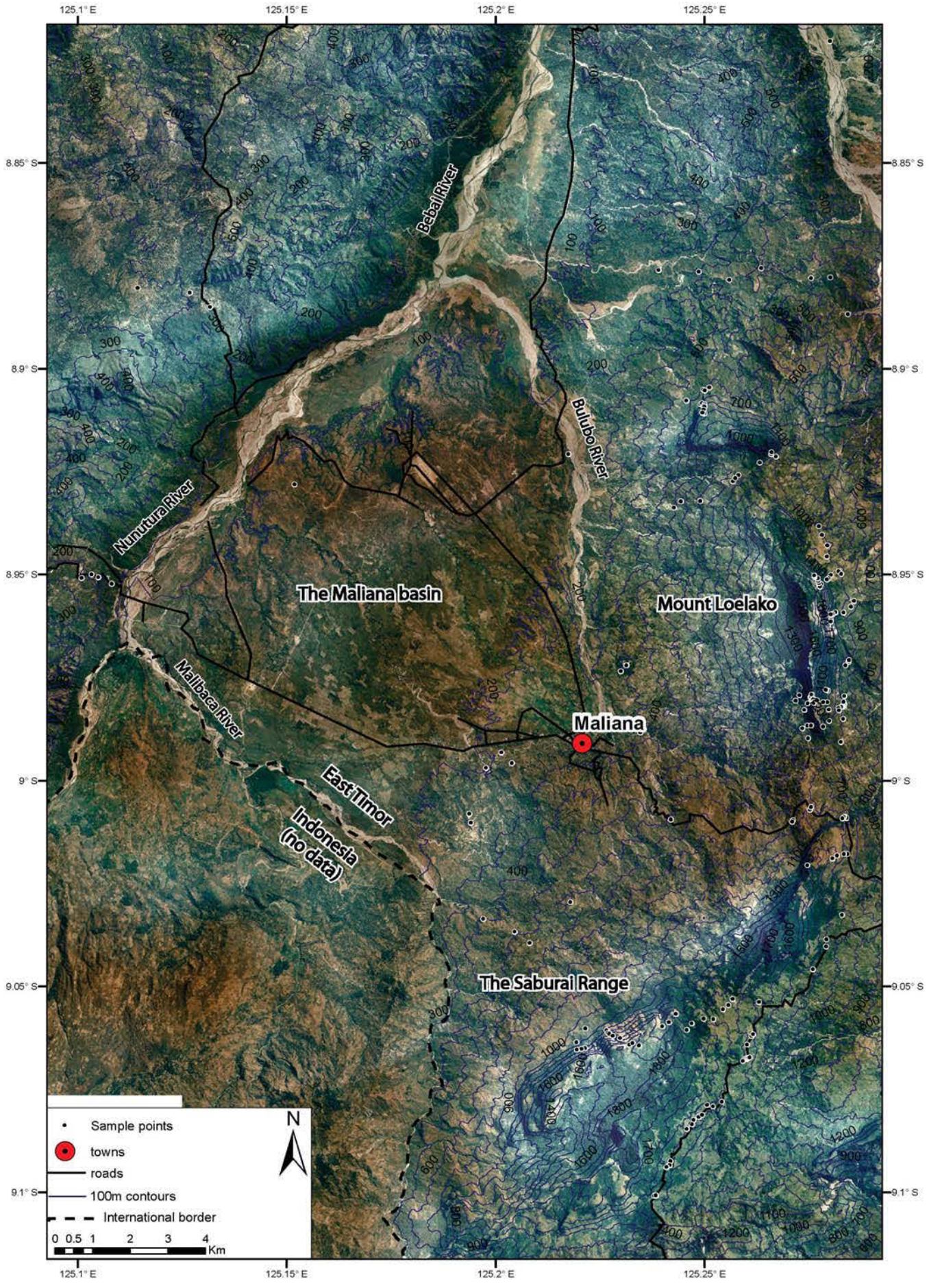
125.1° E
125.15° E
125.2° E
125.25° E
8.85° S
8.9° S
8.95° S
9° S
9.05° S
9.1° S
Bebal River
Bulubo River
Nunutura River
Mallbaca River
The Maliana basin
Mount Loelako
Maliana
East Timor
Indonesia
(no data)
The Saburai Range
Sample points
towns
roads
100m contours
International border
0 0.5 1 2 3 4
Km
N

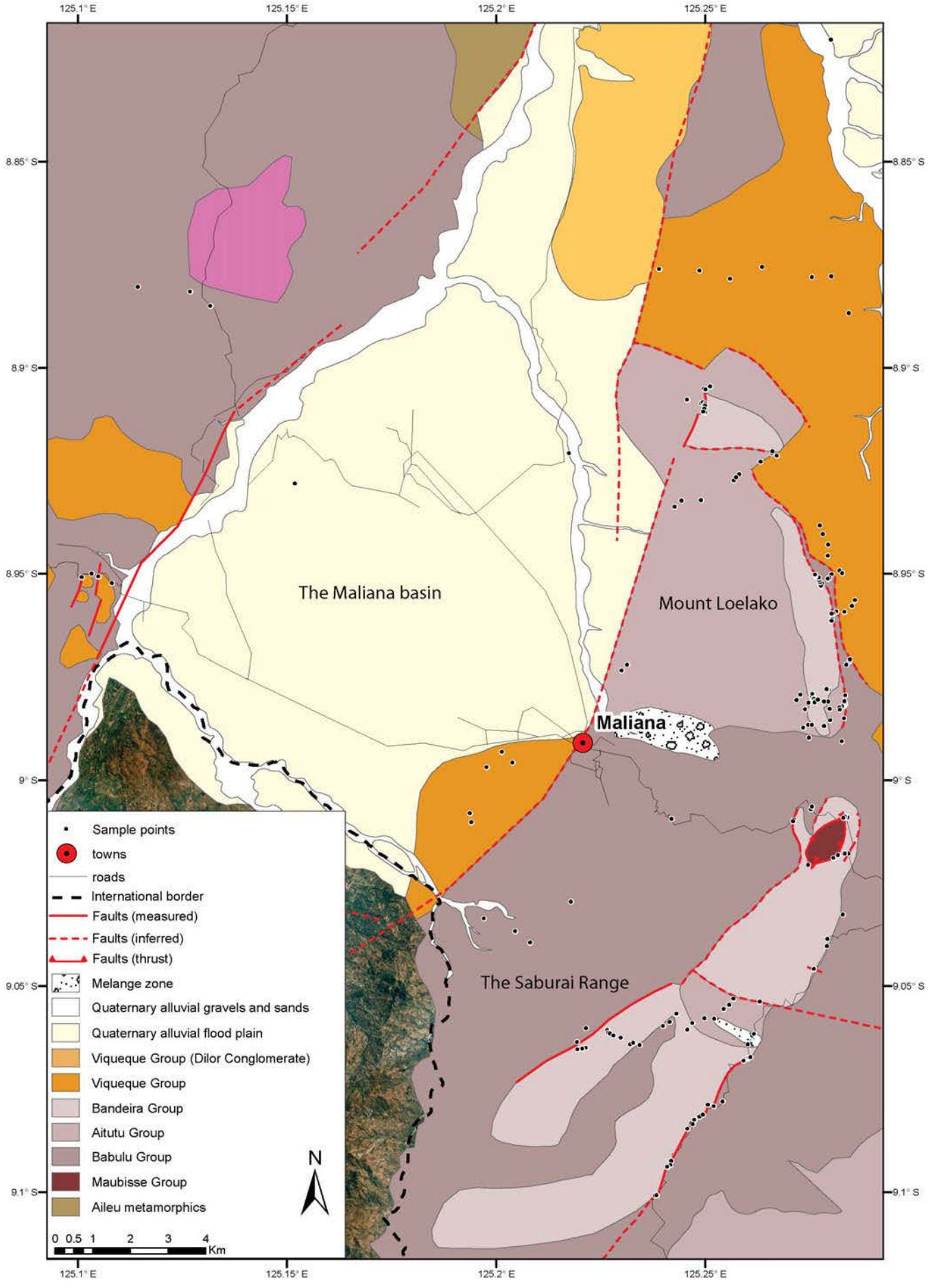
125.1° E
125.15° E
125.2° E
125.25° E
8.85° S
8.9° S
8.95° S
9° S
9.05° S
9.1° S
The Maliana basin
Mount Loelako
Maliana
The Saburai Range
Sample points
towns
roads
International border
Faults (measured)
Faults (inferred)
Faults (thrust)
Melange zone
Quaternary alluvial gravels and sands
Quaternary alluvial flood plain
Viqueque Group (Dilor Conglomerate)
Viqueque Group
Bandeira Group
Aitutu Group
Babulu Group
Maubisse Group
Aileu metamorphics
N
0 0.5 1 2 3 4
Km

The basin is bounded by the high limestone ridges of Mount Loelako and the Saburai Range to the east and southeast (**Figs 71, 72**). The southern and western edges of the basin are also sharply defined but comprise much lower, rounded hills of mudstone and other more friable lithologies (**Figs 71, 72**).

The basin is bounded by large rivers on all sides which are coincident with the well-defined change in topography at the basin margins (**Fig. 71**). The Malibaca River runs northwest close to the basin's southern boundary, before meeting the Nunutura River at the basin's western edge, and forms part of the border of East Timor and Indonesia. The Bulubo River runs north below Mount Loelako, along the eastern boundary of the Maliana basin, before it also meets the Nunutura River at the basin's northern tip. The Nunutura River defines the north-western boundary of the Maliana basin, before merging with the Bulubo to form the Bebai River. At its northern tip the boundaries of the Maliana basin narrow to a gap approximately 3-4 km wide, allowing the Bebai to exit and eventually drain into the Timor Sea (**Fig. 71**).

Several days were spent investigating the eastern and south-eastern boundaries of the Maliana basin as part of mapping around Mount Loelako and the Saburai Range in 2011. A further two days were spent investigating the western and northern extents of the basin, and the hills beyond, by vehicle transects at the end of the 2011 field season. The southern edge of the basin is situated across the border in Indonesia and was not accessible. Rock units are listed in ascending stratigraphic order and age.

3.10.1 Grey mudstones with discontinuous sandstone interbeds

These rocks comprise the majority of the western margin of the Maliana basin, forming the eroded hilly landscape immediately west of the Nunutura River (**Fig. 73a-d**), and are sometimes observed faulted against friable chalks of the synorogenic Viqueque Group. They consist of grey mudstones containing blocks up to 2 m thick of laminated fine to medium grained, micaceous quartz sandstone. The sandstone blocks often contain swaley and hummocky cross-bedding (**Fig. 73d**), and are faulted and disjointed in 'broken-formation facies' style (Harris *et al.* 1998), (**Fig. 73a**). Similar grey to reddish-grey mudstones are observed at AB743 on the

southern margin of the Maliana basin, 3.5 km northwest of the Saburai Range (**Fig. 73e, f**). Outcrops here have much thinner sandstone interbeds, generally 1-2 cm, which are more continuous but extensively folded.

Equivalent to the 'broken formation facies' mudstones and sandstones found near the Ossu fatus (Benincasa *et al.* 2012), these rocks were likely deposited in a prodelta setting where terrigenous muds, sands, and micas from river systems were deposited within the offshore transition zone, with cross-bedding formed during episodic high energy storm conditions. These outcrops were not sampled for biostratigraphy.

On the western boundary of the Maliana basin these units are lithologically identical to the 'broken formation facies' Babulu Group mudstones and sandstones mapped around Ossu (Benincasa *et al.* 2012) and this study places them within the Babulu Group of the Gondwana Megasequence based on lithofacies correlation. The folded, thinly bedded mudstones and sandstones outcropping at AB743 show more similarity to the folded Babulu Group units at the bases of Mount Loelako and the Saburai Range (**Chapters 3.8.1 Thinly bedded, folded sandstones and mudstones, 3.9.2 Grey mudstones with sandstone interbeds**) and outcrop is possibly contiguous with these units along the lower western flank of Saburai.

3.10.2 Thinly bedded limestones and mudstones

Thinly bedded limestones and mudstones were observed in roadside outcrop just beyond the south-western boundary of the Maliana basin, as the flat topography of the basin begins to slope upwards towards the base of the Saburai Range, approximately 3.5 km northwest of the massif. These rocks comprise thinly bedded soft, grey mudstone with indurated white to brown limestone beds generally less than 10 cm (**Fig. 74a**). The limestone beds are wackestones which show evidence of burrowing and bioturbation. They contain abundant radiolaria and thin, *Halobia*-type bivalve filaments concentrated in thin layers (**Fig. 74b**).

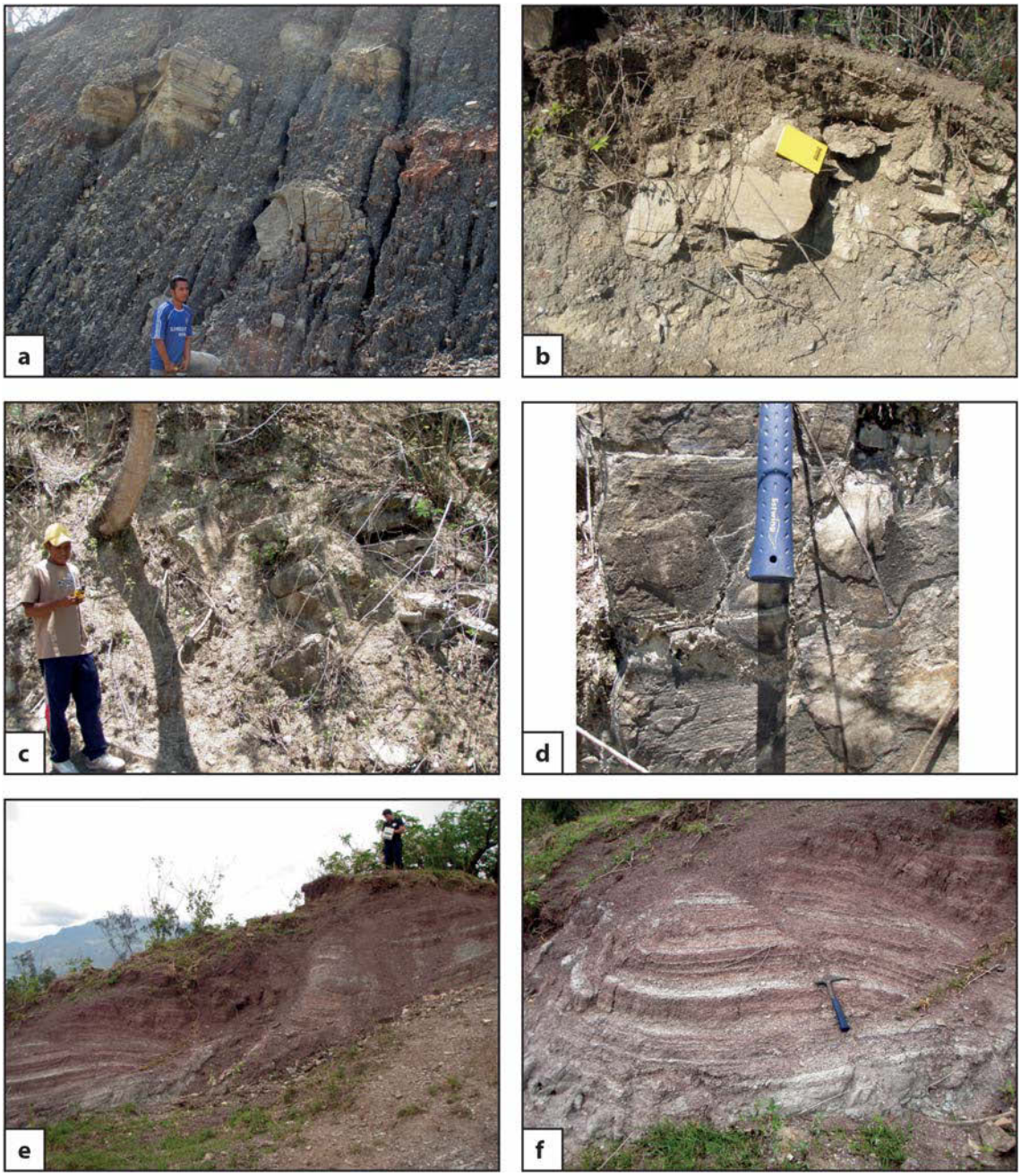

Fig. 73. (a) The Babulu Group in the western margin of the Maliana basin, near the intersection of the Malibaca and Nunutara rivers, comprises metre-scale blocks of broken and disjointed well bedded sandstones within grey mudstones, in 'broken-formation facies' style (Harris *et al.* 1998). Outcrop pictured is approximately 300 m east of AB626 (b) At AB775, approximately 3 km west of the north-western corner of the Maliana basin, the Babulu Group comprises similar 'broken-formation' facies sandstones and mudstones, although outcrop here is more weathered. A5 notebook for scale. (c) Interbedded sandstones and mudstones of the Babulu Group at the northern tip of the Maliana basin at AB770 (d) Swaley cross-bedding typical of Babulu Group sandstones is visible in outcrop at AB770. Hammer for scale (e, f) Mud rich Babulu Group facies at AB743 on the southern margin of the Maliana basin. Outcrop here is extensively folded. Geologist and hammer for scale respectively.

Abundant radiolaria with *Halobia*-type bivalves within a very fine grained carbonate mud suggests a deep water, low energy, oxygen deficient basinal setting. No foraminifera were observed in this sampled outcrop to provide an age determination, however the radiolaria-*Halobia* bivalve facies of these rocks appears typical of the Late Triassic in Timor.

The radiolarian-*Halobia* wackestone facies of these rocks is identical to that of the Aitutu Group observed elsewhere in Timor (e.g. Audley-Charles 1968; Charlton *et al.* 2009; Haig 2012b; **Chapters 3.2.2 Mount Mundo Perdido – Radiolarian limestones, 3.6.2 The Paitchau Range – Medium bedded grey wackestones, 3.7.3 The Matebian Range – Medium bedded limestones and mudstones, 3.11.1 Mount Taroman – Cherty limestones, 3.8.2 Mount Loelako – Interbedded limestones and mudstones; 3.9.3 The Saburai Range – Interbedded grey limestones and mudstones**), and its outcrop style is very similar, although the bedding at AB674 is slightly thinner than the medium bedding usually observed closer to fatus. This study places the thinly bedded limestones and mudstones sampled in the Maliana basin within the Aitutu Group of the Gondwana Megasequence on the basis of lithofacies correlation.

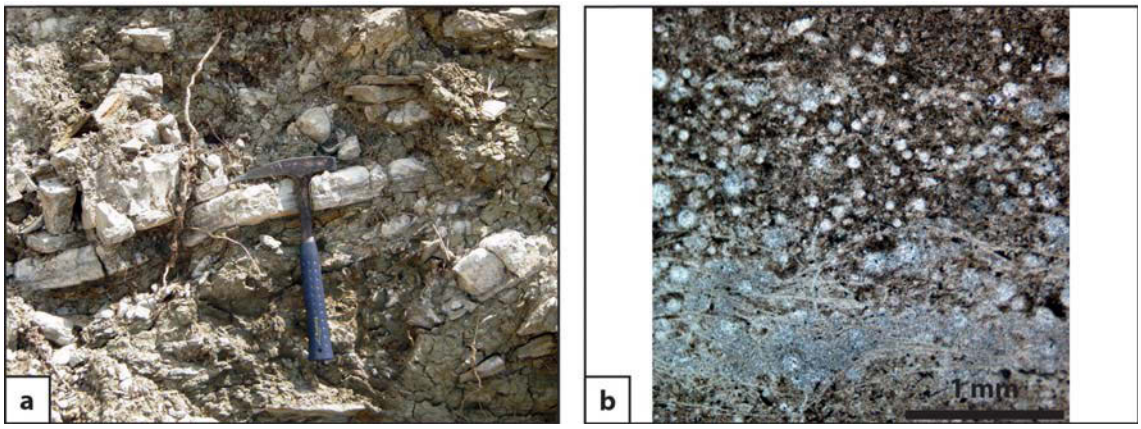

Fig. 74. (a) Thinly bedded Aitutu Group limestones and mudstones at AB674, in the south-eastern corner of the basin just as the topography begins to slope upwards towards the Saburai Range. Limestone beds here are thinner than those usually observed within the Aitutu Group. Hammer for scale. (b) Microfacies at AB674 are typical of the Aitutu Group. Seen here in an acetate peel, they comprise *Halobia*-type bivalve filaments concentrated in thin beds and abundant radiolaria within a fine grained carbonate mud matrix. Scale bar = 1 mm.

3.10.3 Foraminiferal limestones

Samples of two different foraminiferal limestone lithologies were collected as scree shed from a small, heavily vegetated hill approximately 2.5 km northwest of the north-western margin of the Maliana basin (**Fig. 75a, b**), both samples comprising white wackestones with abundant larger benthic foraminifera. AB776A is a muddy wackestone containing abundant benthic foraminifera *Alveolina* sp. (**Fig. 75c**), along with rare, small planktonic forms and shelly debris. AB776B is a wackestone containing more diverse benthic foraminifera including *Spiroclypeus* sp., *Lepidocyclina* (*Nephrolepidina*) spp. with rare *Lepidocyclina (Eulepidina* sp.*)*, along with rare small planktonic foraminifera, and mollusc and coral fragments (**Fig. 75d**).

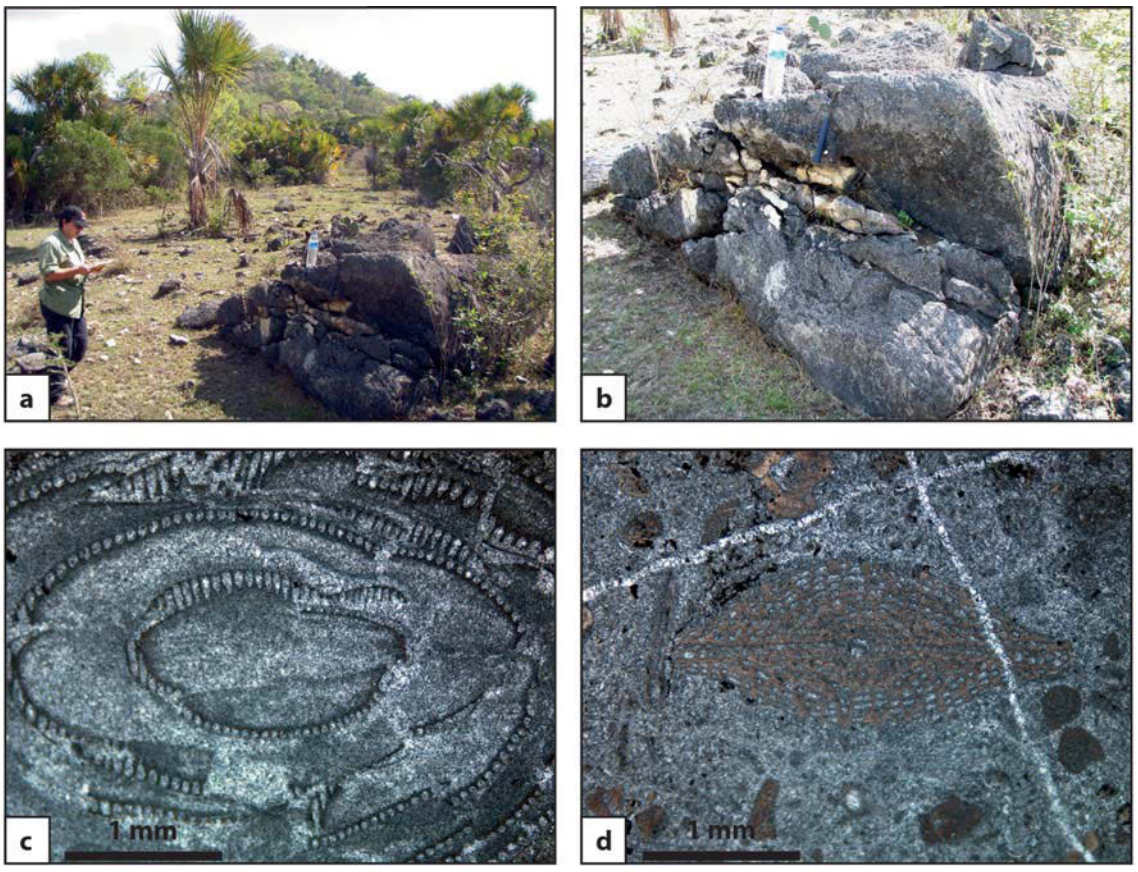

Fig. 75. (a) Facing south, limestone scree (foreground) is shed from a heavily vegetated hill (background) at AB776, approximately 2.5 km northwest of the north-western margin of the Maliana basin (b) Close up of one of the boulders in scree, this particular sample comprises Booi Group limestone. Hammer for scale. (c) Image from an acetate peel taken from sample AB776A, showing a large benthic foraminifera *Alveolina* sp.. Scale bar = 1 mm (d) Image from an acetate peel taken from sample AB776B. Centre of frame is the larger benthic foraminifera *Lepidocyclina* sp., typical of Booi Group limestones in East Timor. Scale bar = 1 mm.

The presence of corals and abundance of larger hyaline benthic foraminifera within the limestones suggests deposition in clear water, neritic environments. The presence of *Alveolina* sp. within AB776A suggests an Eocene age, while a larger benthic foraminiferal assemblage dominated by *Spiroclypeus* sp., *Lepidocyclina* (*Nephrolepidina*) spp. with rare *Lepidocyclina (Eulepidina)* places sample AB776B within the upper Te Letter Stage of the earliest Miocene.

AB776A is a similar Eocene, neritic, *Alveolina* rich facies to the Dartollu Formation of Audley-Charles (1968) and the Dartollu Group limestones sampled at Mount Bibileu (**Chapter 3.5.4 Mount Bibileu – Foraminiferal limestones**), and are on the same basis placed within the Dartollu Group of the Banda Megasequence. AB776B is identical in age and facies to the Lower Miocene larger foraminiferal limestones found at Mount Mundo Perdido and Mount Laritame (**Chapters 3.2.7 Mount Mundo Perdido – Foraminiferal limestones and associated mudstones and sandstones, 3.3.5 Mount Laritame – Foraminiferal limestones and associated sandstones and sandy mudstones**), and is similarly placed within the Booi Group of the Banda Megasequence. The close association in outcrop of these two samples supports their attribution to the same tectonostratigraphic terrane.

3.10.4 Friable mudstones, muddy sandstones and sandstones

These were observed outcropping in the incised banks of small streams and rivers within the south-eastern parts of the Maliana basin, where the floor of the basin is topographically highest, approximately 200-250 m above sea level (**Fig. 71**). They comprise well bedded mudstones with 2-20 cm thick interbeds of friable sandstones and muddy sandstones (**Fig. 76a-f**). The friable sandstones contain mostly subangular quartz and lithic fragments, predominantly schist. Washed mudstone residues yield abundant biota, including diverse and abundant planktonic foraminifera, rarer benthic foraminifera, gastropods, bivalves and in one sample a crab claw. These rocks show little evidence of deformation and have a constant, shallow dip of 20-30° towards the northwest (e.g. **Fig. 75a, c, & e**). Moving further south towards the Saburai Range, dips increase to over 40° with a dip direction closer to the north (e.g. **Fig. 75f**).

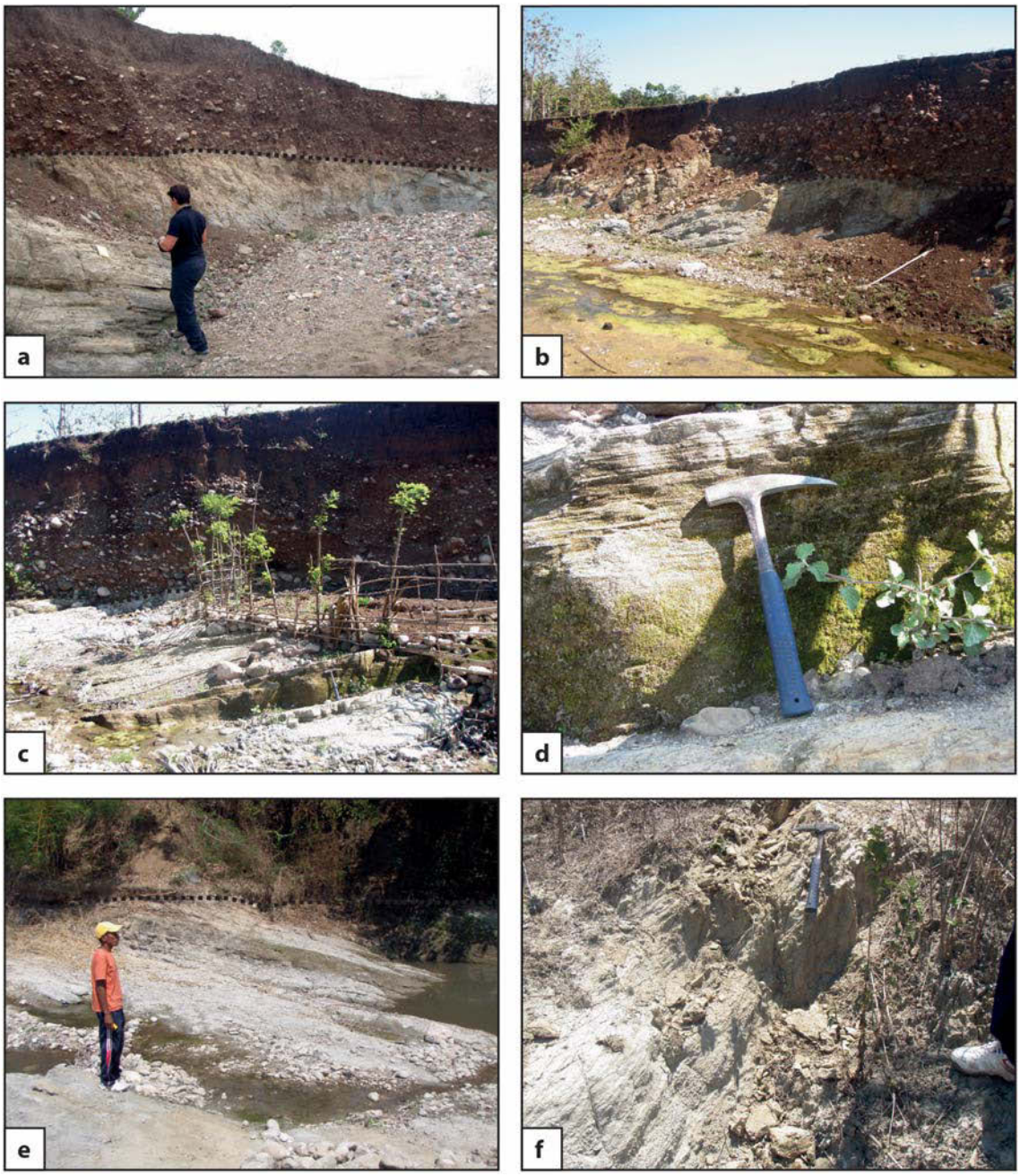

Fig. 76. (a) AB744, approximately 2 km south-southwest of Maliana, in the southeast corner of the Malian basin. Well bedded, brown-grey Viqueque Group sandstones and mudstones are exposed alongside many small rivers and streams in this area. Interpreted with a dashed line is the unconformity between the Viqueque Group and overlying Quaternary alluvial deposits. (b) The Viqueque Group similarly outcropping beneath alluvial deposits in a stream bank at AB659, approximately 400 m northwest of AB744. Unconformity again interpreted with a dashed line. (c) Another perspective at AB659, illustrating the well bedded, gently dipping strata of the Viqueque Group. Note hammer for scale in bottom right of frame. (d) Close-up of a sandstone bed at AB659, which shows a fining up in grainsize and thin mudstone laminae at the top of the bed. Hammer for scale. (e) The Viqueque group at AB670 dips gently to the northwest. This outcrop is approximately 600 m southwest of AB744. (f) Viqueque Group at AB672, 2 km southwest of AB744. Beds dip approximately 45° at this outcrop, and dip in the Viqueque Group appears to increase closer to the Saburai Range. Hammer for scale.

AB672 is the stratigraphically lowest point sampled in the north to northwest dipping succession, and is mud dominated with very little sand. Its foraminiferal assemblage comprises approximately 80% planktonic and 20% benthic forms, suggesting a bathyal depositional environment, and the presence of *Globorotalia tosaensis* and *Globorotalia truncatulinoides* suggests an age of N22 of the Early Pleistocene. Moving north up through the succession sandstone beds become thicker and more abundant, and an increase in benthic foraminifera along with abundant gastropods, bivalves and shallow water faunal debris suggests a progressively shallowing depositional environment.

The age and lithofacies of the friable mudstones, muddy sandstones and sandstones in the Maliana basin place them within the Viqueque Group of the Synorogenic Megasequence (Audley-Charles 1968; De Smet *et al.* 1990; van Marle 1991a, b; Haig & McCartain 2007; Haig 2012a). The friable lithologies and consistent, shallow dips are typical of the Synorogenic Megasequence in East Timor, and consistent with the Viqueque Group observed at Mount Mundo Perdido, Mount Laritame, and Mount Loelako. The Maliana basin has previously been mapped as Quaternary to recent alluvial deposits (Gageonnet & Lemoine 1958; Audley-Charles 1968; Partoyo *et al.* 1995), however this study shows that in the highest, south-eastern parts the basin fill is much older. It is possible that the Maliana basin has occupied a low structural position since at least the Early Pleistocene, accumulating sediment shed from the emerging island. Uplift and tilting has since exposed these deposits in the southeast, but it is possible that the Viqueque Group underlies more recent alluvial deposits throughout much of the basin.

3.11 Mount Taroman

Mount Taroman is a large massif situated in the southwest corner of East Timor, approximately 15 km northwest of Suai and directly south of the Indonesian border (**Fig. 10**). Parallel to the south coast of Timor Island at this point, it measures 15 km along its long axis from southwest to northeast (**Figs 77, 78**).

Mount Taroman is completely encircled by the Maubui and Tafara Rivers to the west and east, and the Nahamauk River to the south, which create a distinctive moat-like topography around the base of the massif (**Fig. 77**). Slopes rise comparatively gently from these rivers to around 1000-1200 m above sea level, where topography changes to steep gradients and cliffs which reach a maximum altitude of 1762 m above sea level (**Fig. 77**). The north eastern section of Mount Taroman is broad, approximately 5 km across, but close to the midpoint of the massif the steep upper section of the mountain narrows into a 1 km wide ridge, which then extends out to the southwest (**Figs 77, 78**).

Three days were spent conducting reconnaissance mapping at Mount Taroman in 2010, based out of the small village of Fatululik on the north-eastern edge of the massif (**Fig. 77**). The first two days were spent investigating the high cliffs above the north-western flank, and the third day we attempted to travel as far as possible by vehicle along the southern flank of the massif, sampling mainly roadside outcrop. Rock units are listed in ascending stratigraphic order and age.

3.11.1 Cherty limestones

Pink to grey cherty limestones were observed on the north-western flank of Mount Taroman, just below the high limestone cliffs approximately 1150 m above sea level. They appear to be large limestone blocks 5-10 m in size within a zone of structural melange, appearing together with other blocks of assorted lithology and tectonostratigraphic affinity within a highly deformed matrix of strained shale (**Fig. 79a-d**). The limestones blocks themselves are highly deformed and recrystallised, but some limestone clasts are visible in acetate peels amongst a stockwork of calcite and quartz veins. AB572I is a wackestone containing abundant radiolaria

with rare recrystallised ostracods, bivalve filaments and primitive *Lenticulina*-type foraminifera (**Fig. 79e**). AB 573 comprises mainly micritised peloids (**Fig. 79f**). Similar cherty limestones have also been observed at the south-western tip of Mount Taroman at AB567 (**Fig. 79g**), similarly containing abundant radiolaria along with *Halobia*-type bivalve filaments concentrated in thin beds (**Fig. 79h**).

Abundant radiolaria suggest a deep water, low energy environment, while thin beds of *Halobia*-type bivalves suggest an oxygen deficient, basinal setting. Peloids within AB573 suggest a shallower, moderate energy environment. Primitive *Lenticulina*-type forams are consistent with a Mesozoic age.

Wackestones containing radiolaria and *Halobia* are typical of Aitutu Group facies elsewhere in Timor (e.g. Audley-Charles 1968; Charlton *et al.* 2009; Haig 2012b, **Chapter 3.2.2 Mount Mundo Perdido – Radiolarian limestones, Chapter 3.6.2 The Paitchau Range – Medium bedded grey wackestones, Chapter 3.7.3 The Matebian Range – Medium bedded limestones and mudstones**) and this study places the cherty, radiolarian rich limestones sampled at AB567 and AB572I within the Aitutu Group of the Gondwana Megasequence based on lithofacies correlation.

Fig. 77 → Aerial photograph of Mount Taroman illustrating sample points and 100 m topographic contours. The areal extent of field mapping at the fatu is highlighted in red.

Fig. 78 → Interpreted geological map of Mount Taroman. Field mapping and sampling was conducted around the northern edge of the fatu, with the geology in these areas constructed using outcrop data and aerial photographs. See text for detailed descriptions of geology. Geology outside of the mapped field extent is modified after Partoyo *et al.* (1995) using aerial photographs. The Dartollu Group (Eocene shallow water limestones of the Banda Megasequence, see **Chapter 3.5.4 Mount Bibileu – Foraminiferal limestones**) has been illustrated on maps around the southern margin of Mount Taroman since Audley-Charles (1968). This study attempted to reach these outcrops however access was prevented as roads had been washed away by bad weather. The extent of the Dartollu Group on this map therefore is modified after Partoyo *et al.* (1995).

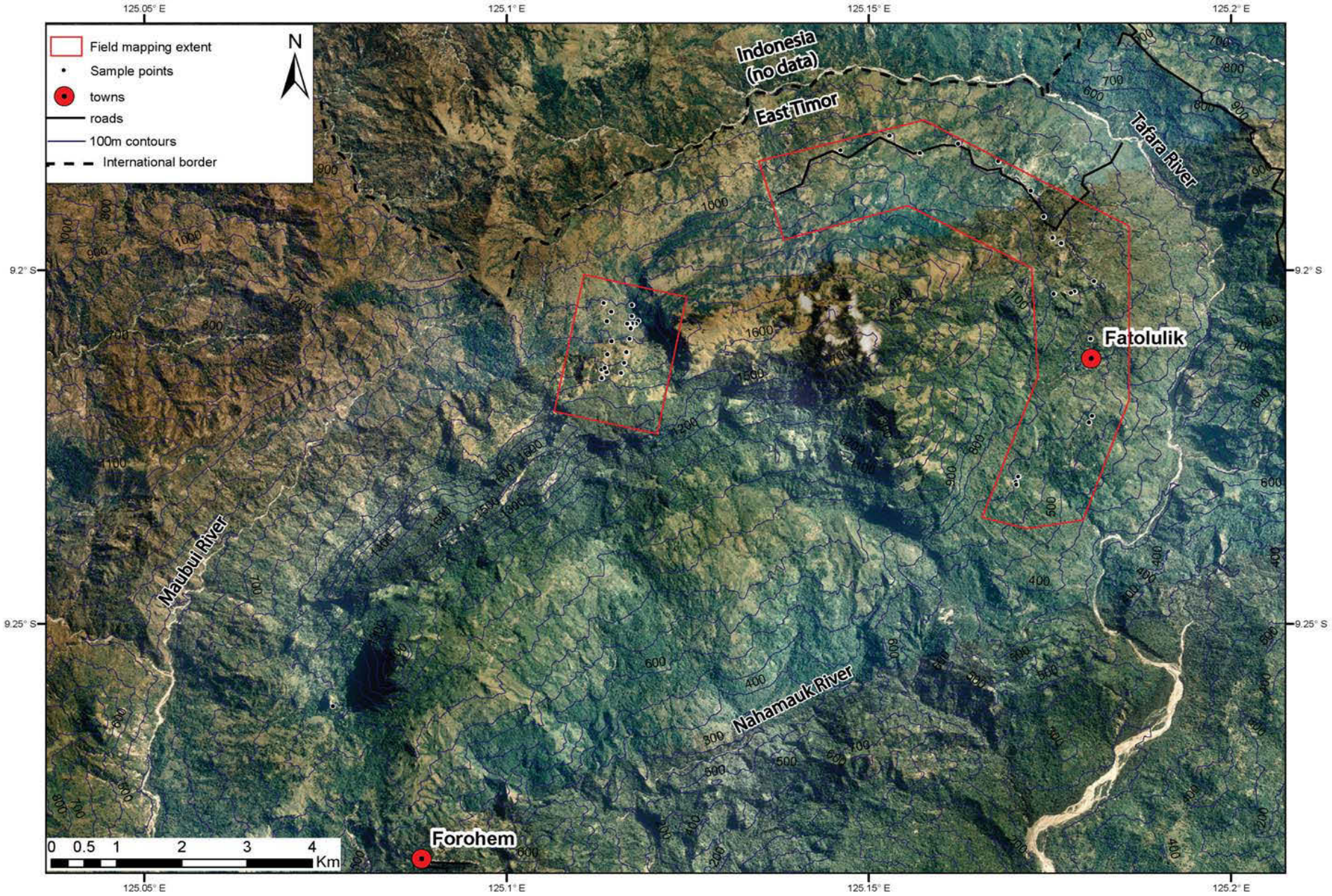
125.05° E
125.1° E
125.15° E
125.2° E
9.2° S
9.25° S
Field mapping extent
Sample points
towns
roads
100m contours
International border
N
Indonesia
(no data)
East Timor
Tafara River
Fatolulik
Maubul River
Nahamauk River
Forohem
0 0.5 1 2 3 4
Km

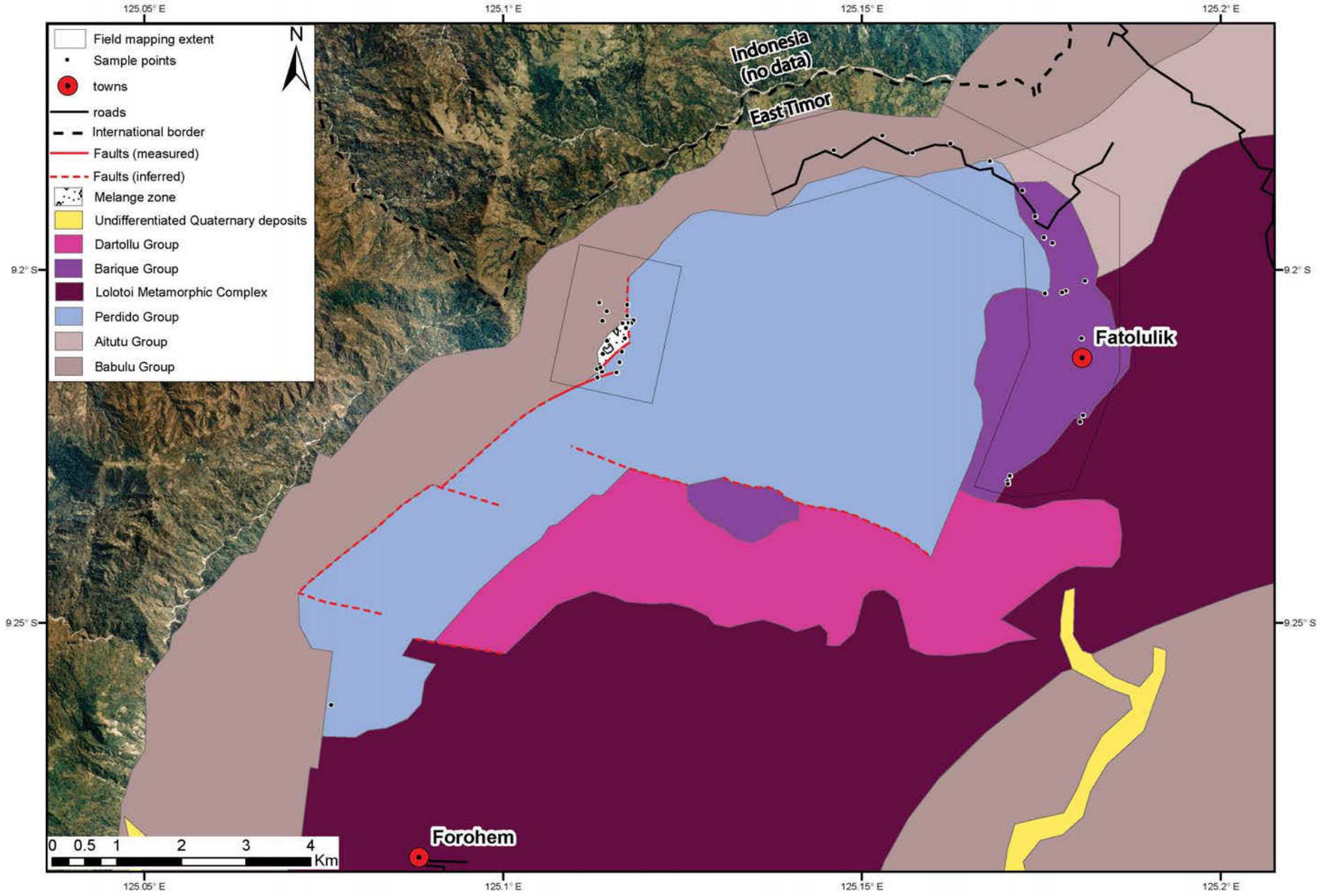
125.05° E
125.1° E
125.15° E
125.2° E
9.2° S
9.25° S
N
Field mapping extent
Sample points
towns
roads
International border
Faults (measured)
Faults (inferred)
Melange zone
Undifferentiated Quaternary deposits
Dartollu Group
Barique Group
Lolotoi Metamorphic Complex
Perdido Group
Aitutu Group
Babulu Group
Indonesia
(no data)
East Timor
Fatolulik
Forohem
0 0.5 1 2 3 4
Km

The peloid bearing rocks at AB573 appear superficially similar in outcrop to AB572I, with similar cherty nodules and layers. The peloids may represent down-slope transport of shallow water sediments into basinal, Aitutu-type facies, as observed within the Aitutu Group at Mount Mundo Perdido and Mount Matebian. These peloids beds may have been most resistant to strain since the limestone blocks were incorporated within the melange, and therefore are most visible within these extensively veined and recrystallised samples. Alternatively, AB573 could represent a dissimilar, shallow water facies. This may be less likely as chert is uncommon in most shallow water facies of East Timor.

3.11.2 Interbedded sandstones and mudstones

Below the high limestone cliffs on the north-western flank of Mount Taroman, between altitudes of approximately 800-1100 m, most outcrops comprise interbedded sandstones and mudstones (**Fig. 80a-f**). Sandstone beds are grey, fine to medium grained, often micaceous, with bedding 5-30 cm (e.g. **Fig. 80a, b & c**). Grains are subrounded to subangular and include a variety of types including quartz, feldspar, lithic fragments, with occasional small foraminifera and very fine grained shell fragments visible in AB574. Minor cross bedding is observed in some outcrops. Mudstone beds are medium to thick, generally 20-60 cm (e.g. **Fig. 80d**), and dark grey to red in colour. Mudstone at AB574 yielded abundant small foraminifera including *Dentalina* sp., *Pseudonodosaria* sp. and *Glomospirella* sp. along with rare ostracods and conodonts. At AB575, 30 m north of AB574, thick beds of grey, muddy sandstone up to 1 m are observed, interbedded with medium beds of grey mudstone 20-30 cm (**Fig. 80e, f**). Sand sized particles comprise predominantly bryozoan and crinoid debris.

The abundance of mica and lithic grains sandstones suggests a terrestrial influence, perhaps deposition from a deltaic system, while the presence of cross bedding – generally a result of oscillation currents – indicates a depth above storm wave base. This is consistent with deposition in the offshore transition zone, where muds, micas and terrigenous sands from river systems settled on the sea floor in quiet water below fair weather wave base, periodically interrupted by higher energy storm conditions.

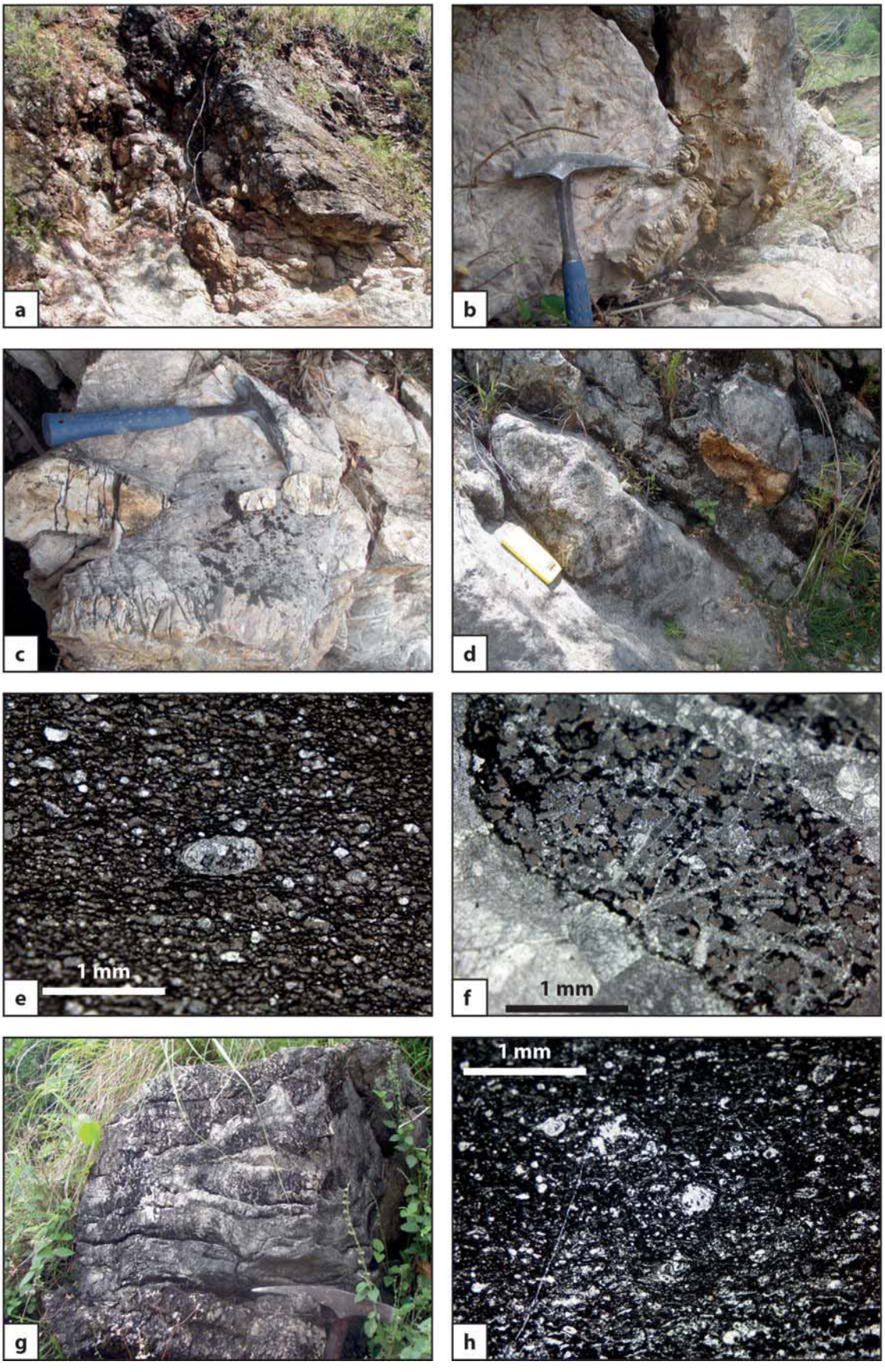
a
b
c
d
1 mm
e
1 mm
f
1 mm
g
h

The thick beds of muddy sandstone at AB575 (**Fig. 80e, f**) possibly represent transport and fragmentation of bryozoan and crinoid debris from nearby carbonate banks. Foraminiferal assemblages within the mudstone units are consistent with a Late Triassic age.

Lithofacies and biofacies correlations place these Late Triassic, likely pro-delta siliciclastic deposits within the Babulu Group (Benincasa *et al.* 2012; Haig 2012b; née Babulu Formation of Bird & Cook 1991) . However, the thick calcarenite beds observed at some localities and have not been previously recorded within the Babulu Group (Bird & Cook 1991), and suggest a nearby carbonate source.

The north-western flank of Mount Taroman has previously been mapped as the Wai Luli Formation (Audley-Charles 1968; Partoyo *et al.* 1995). Grunau (1953) and Gageonnet and Lemoine (1958) did not distinguish the Jurassic from the Triassic mudstone dominated units, however Audley-Charles differentiated the Jurassic as the Wai Luli Formation, which had its type locality in the Wai Luli Valley, north of the Cablac Mountain Range, comprising marls, calcilutites and calcareous shales. The Wai Luli Formation at its type section has since been found to comprise Permian Cribas Group, Triassic Babulu Group, as well as Jurassic calcareous shales and marls (McCartain *et al.* 2006; Haig *et al.* 2007). Haig (2012b) defined the Wai Luli Group as Lower Jurassic, but notes that bioturbated marl facies within the Wai Luli Group extend down into the Upper Triassic.

This study places the medium bedded sandstones and mudstones of Mount Taroman within the

---

Fig. 79 ← (a) A block of cherty Aitutu Group limestone several metres in size within a structural melange zone on the north-western flank of Mount Taroman, at AB571. (b) Another block of Aitutu Group cherty limestone with the same melange zone. This block, at AB572I, has abundant chert nodules visible on a weathered face. Hammer for scale. (c) Close-up of chert nodules in sample AB572I. Hammer for scale. (d) In the same melange zone, another block of Aitutu Group limestone at AB573 shows well defined medium bedding. A5 notebook for scale. (e) Typical radiolarian rich Aitutu Group microfacies in an acetate peel taken from sample AB572I. An ostracod sits centre of frame. Scale bar = 1 mm. (f) Image of an acetate peel taken from Aitutu Group limestone at AB573, illustrating a peloid packstone clast surrounded by recrystallised calcite. Scale bar = 1 mm. (g) Cherty Aitutu Group limestone at AB567, on the south-western tip of Mount Taroman, observed during reconnaissance mapping north of Fohorem (**Fig. 78**). Hammer for scale. (h) Image of an acetate peel from AB567, illustrating a typical Aitutu Group radiolarian-rich microfacies with *Halobia*-type bivalve filaments. Scale bar = 1 mm.

Babulu Group of the Gondwana Megasequence. However, it is likely that some of the rocks here may represent the Triassic Wai Luli type facies as noted by Haig (2012b), transitional between the siliciclastic Babulu Group and the more carbonate influenced Wai Luli Group.

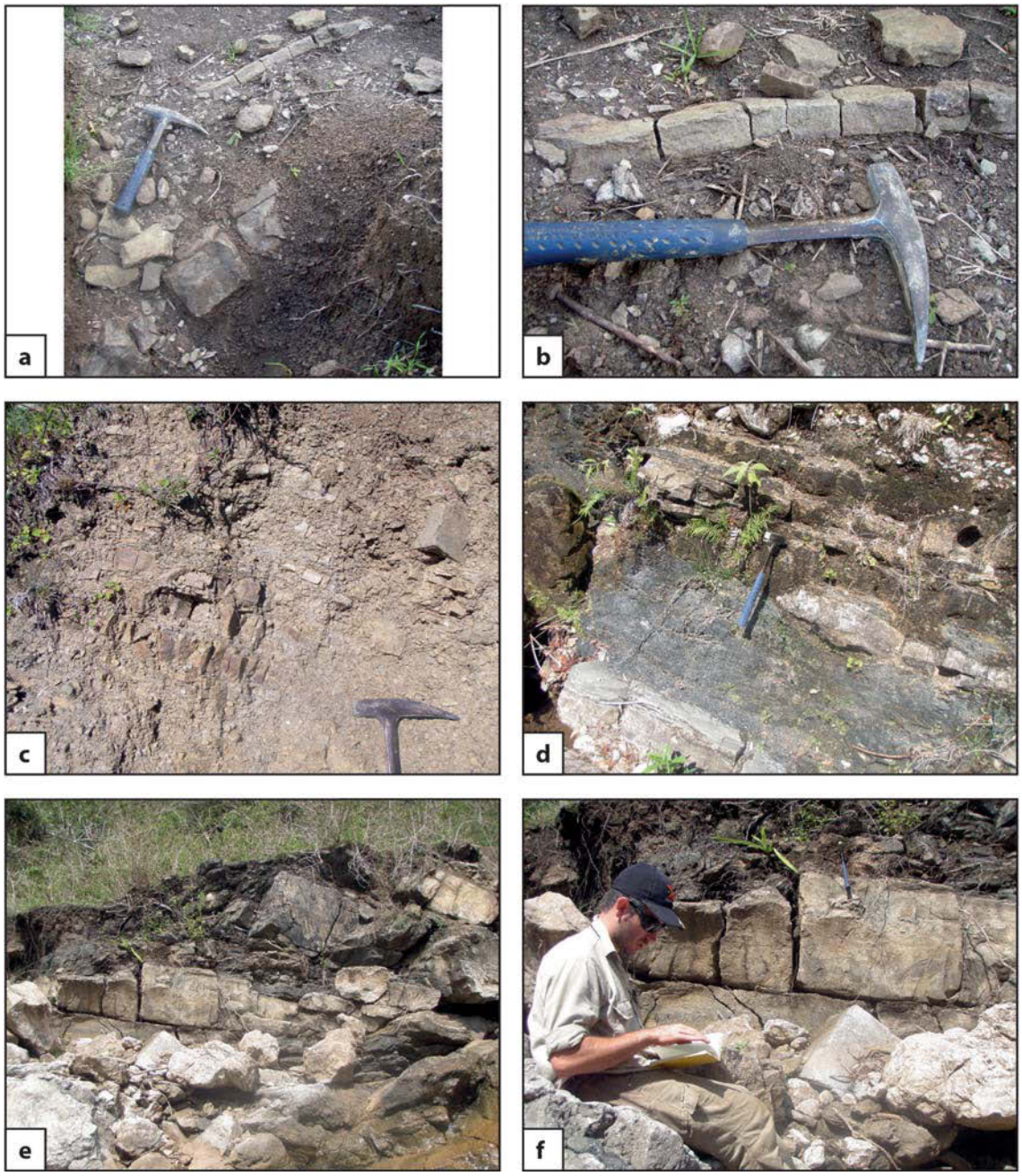

Fig. 80. (a) Babulu Group grey-brown mudstone with thin to medium interbeds of sandstone at AB590, on the north-western flank of Mount Taroman. Hammer for scale. (b) Close-up of a thin sandstone bed in the Babulu Group at AB590. Hammer for scale. (c) Weathered outcrop of interbedded Babulu Group mudstones and sandstones at AB592, at the very northern end of the north-western flank of Mount Taroman. Hammer for scale (d) Interbedded Babulu Group mudstones and sandstones at AB574, on the north-western flank of Mount Taroman. Hammer for scale. (e) Thick beds of thick beds of grey, muddy sandstone containing abundant bryozoan and crinoid debris at AB575, approximately 30 m south of AB574. (f) Close up of one of the thick, muddy sandstone beds at AB575.

3.11.3 Ooid limestones

All the high cliffs sampled on the north-western side of Mount Taroman comprise ooid packstones and grainstones, with rare ooid wackestones. Outcrop is grey, indurated and massive, and bedding was not observed (**Fig. 81a, b**). Rocks chiefly comprise ooids, up to 10 mm in size in some samples, with rare gastropods and large shell fragments of bivalves and brachiopods (**Fig. 81c-f**). AB596 also contains layered algal growths around larger grains (**Fig. 81f**). Most samples are extensively dolomitised, predominantly within cement (e.g. **Fig. 81d**).

These ooid packstones, grainstones and wackestones appear to be the same shallow water Bahaman-type facies as the ooid limestones observed at Mount Mundo Perdido, Mount Laritame, the Builo Range and Mount Bibileu. Most samples are grainstones or packstones with very little mud, suggesting high energy depositional environments (e.g. **Fig. 81c, d**), while the muddy wackestone at AB596 represents a lower energy environment where mud has not been winnowed out (**Fig. 81e, f**). Due to extensive dolomitisation and recrystallisation of the samples collected at Mount Taroman, foraminifera were too poorly preserved to enable a biostratigraphic age determination. This study tentatively places them within the Late Triassic or Early Jurassic based on lithofacies correlation with Bahaman-type facies limestones elsewhere in Timor.

Based on lithofacies correlation with the Bahaman-type facies ooid limestones at Mount Mundo Perdido (Benincasa *et al.* 2012), the Cablac Mountain range (Haig *et al.* 2007) and sampled elsewhere in this study, the ooid limestones at Mount Taroman are also placed within the Perdido Group of the Gondwana Megasequence.

3.11.4 Carbonate pelagites

Clasts of carbonate pelagites were observed within the same structural melange as the chert limestones (**Chapter 3.11.1 Mount Taroman – Cherty limestones**) as small blocks generally less than 20 cm in size (**Fig. 82a, b**). They are yellow/white foraminiferal packstones containing abundant planktonic foraminifera, mostly *Acarinina* sp. and *Morozovella* sp. (**Fig. 82c, d**).

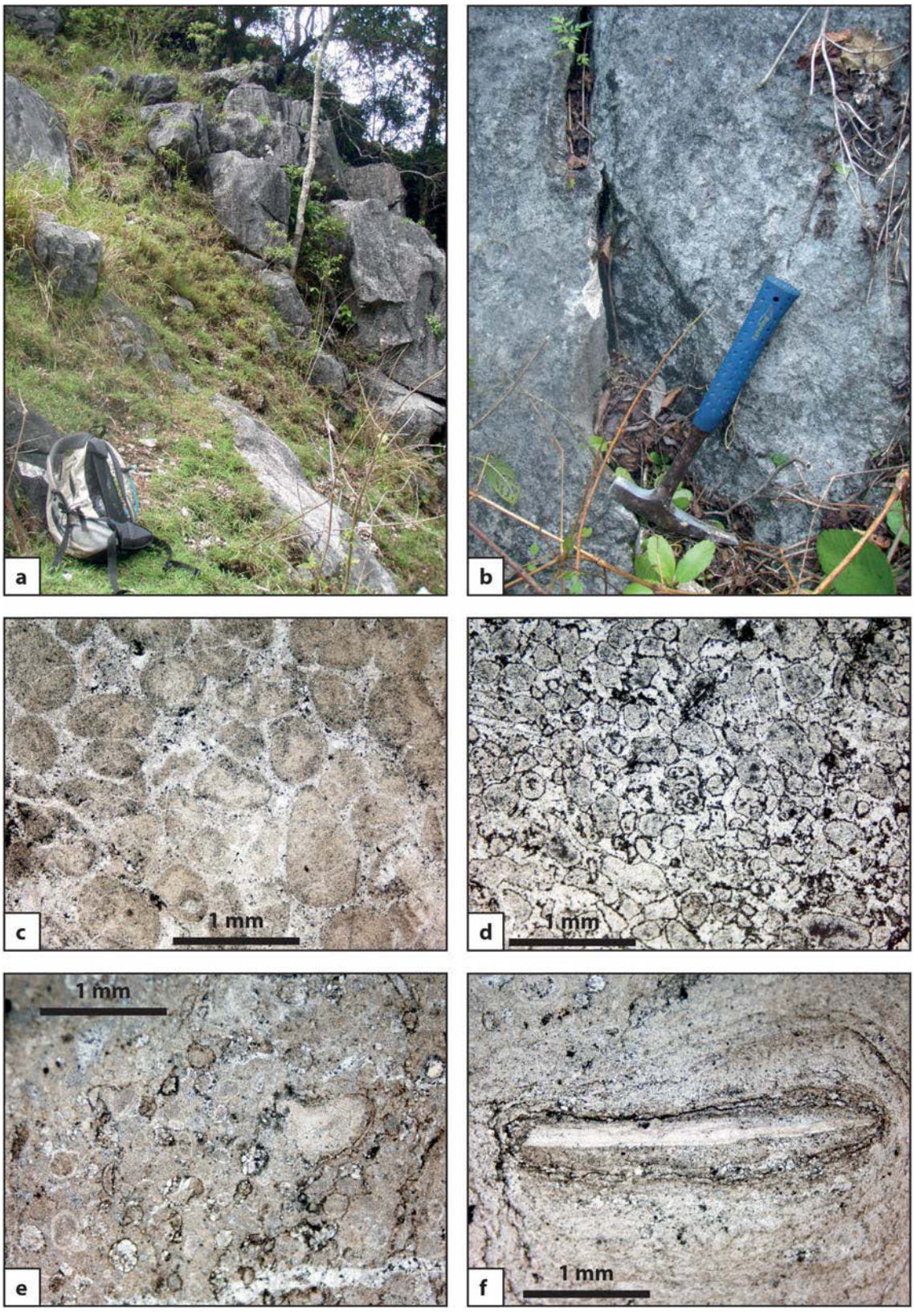
a
b
c
1 mm
d
1 mm
1 mm
e
f
1 mm

As with carbonate pelagites found elsewhere in Timor, the predominance of planktonic over benthic foraminifera within a very fine carbonate mud matrix suggests deposition within the middle bathyal to abyssal zone. Based on planktonic foraminiferal assemblages the samples from Mount Taroman are placed within the Early to Middle Eocene.

Carbonate pelagites sampled at Mount Taroman correlate with Eocene age carbonate pelagites observed elsewhere in East Timor (Haig & McCartain 2007), and are similarly placed within the Kolbano Group of the Australian Margin Megasequence.

3.11.5 Igneous and metamorphic rocks

Igneous and metamorphic rocks are widespread around the eastern flank of Mount Taroman between altitudes of approximately 600-1000 m, below the steep cliffs of the upper section of the massif. Igneous lithologies include mafic to intermediate volcanic sediments, mainly volcanic sandstones and breccias, and fine grained basalts including pillow basalts (**Fig. 83a-d**). Metamorphic rocks are less common and comprise dark green to black chloritic schists. Outcrop is often deeply weathered. Similar igneous and metamorphic lithologies were also encountered as blocks in melange zones on the north-western flank of Mount Taroman (**Fig. 83e-h**).

Volcanic breccias at Mount Taroman generally comprise poorly sorted, angular, basaltic clasts in a very fine grained, tuffaceous matrix (e.g. **Fig. 83d**), similar to those found at Mount Mundo Perdido and Mount Laritame, which suggests they may be pyroclastic deposits of explosive eruptions. Pillow basalts are also present (e.g. **Fig. 83c**), indicating subaqueous volcanic activity.

Fig. 81 ← (a) Massive, grey-white ooid limestone outcropping AB586, at the base of the northwest facing cliffs of Mount Taroman. Backpack for scale. (b) Another ooid limestone outcrop at AB569, approximately 1100 m northeast of AB586, hammer for scale. (c) An acetate peel of a limestone sample taken from AB586. The rock is an ooid packstone with very little mud, suggesting a high energy depositional environment. Scale bar = 1 mm. (d) Image of an acetate peel taken from AB586. This sample is an ooid packstone/grainstone which shows extensive dolomitisation around grain boundaries. Scale bar = 1 mm. (e) Image of an acetate peel of an ooid wackestone from AB596, at the base of the cliffs at the north-eastern tip of Mount Taroman. The muddier facies in this sample represents a lower energy environment than the samples at AB586 and AB569. Scale bar = 1 mm. (f) Another image of an acetate peel from AB596, illustrating algal growths around a large skeletal grain. Scale bar = 1 mm.

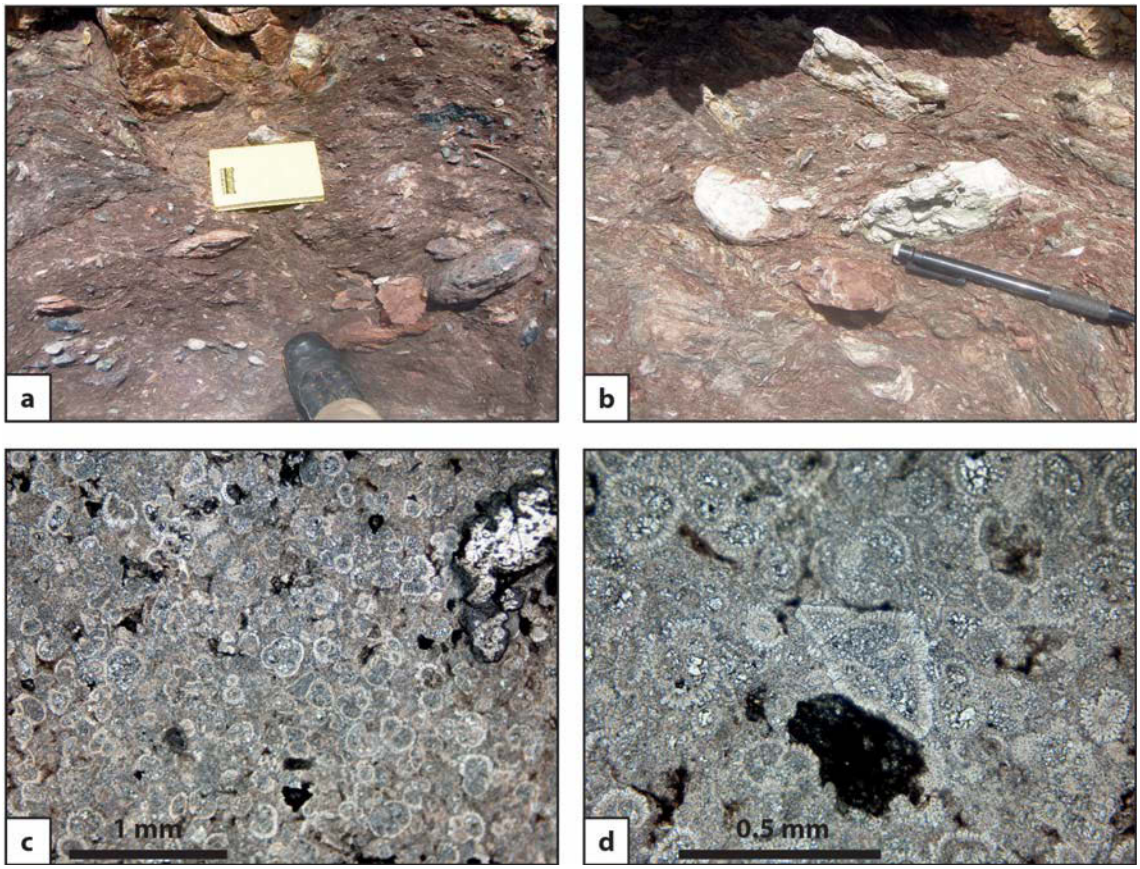

Fig. 82. (a) A sheared zone of melange at AB572, comprising rocks of assorted ages and tectonostratigraphic affinities within a highly deformed matrix of strained shale. The melange contains blocks from centimetre scale to several metres in size. A5 notebook for scale. (b) Most of the carbonate pelagites observed within this melange zone came from smaller blocks, such as the two white blocks pictured here, centre of frame, pen for scale. (c) Image of an acetate peel taken from sample AB572G, showing abundant planktonic foraminifera. Scale bar = 1 mm. (d) A smaller scale image of an acetate peel from sample AB572G. Visible centre of frame is the foraminifera *Morozovella* sp. suggesting an Early to Middle Eocene age. Scale bar = 0.5 mm

---

Fig. 83 → (a) A large outcrop of mafic volcanic rock at AB600, on the eastern flank of Mount Taroman (b) The surface of the outcrop at AB600 is extensively fractured. Hammer for scale. (c) Some remnant pillow outlines visible in the outcrop at AB600. Tip of hammer bottom right of frame for scale. (d) An outcrop of volcanic breccia at AB602, approximately 1600 m south-southeast of AB600. Hammer for scale. (e) A large block of schist within a melange zone on the north-western flank of Mount Taroman, at AB588. Hammer for scale. (f) Close-up of the schist at AB588. Evidence of shearing on this sample is present in the form of large striations on the rock surface. Hammer for scale. (g) Close up of one of the smaller mafic volcanic clasts in the melange zone at AB572. A5 notebook for scale. (h) Another small mafic volcanic clast at AB572, pen for scale.

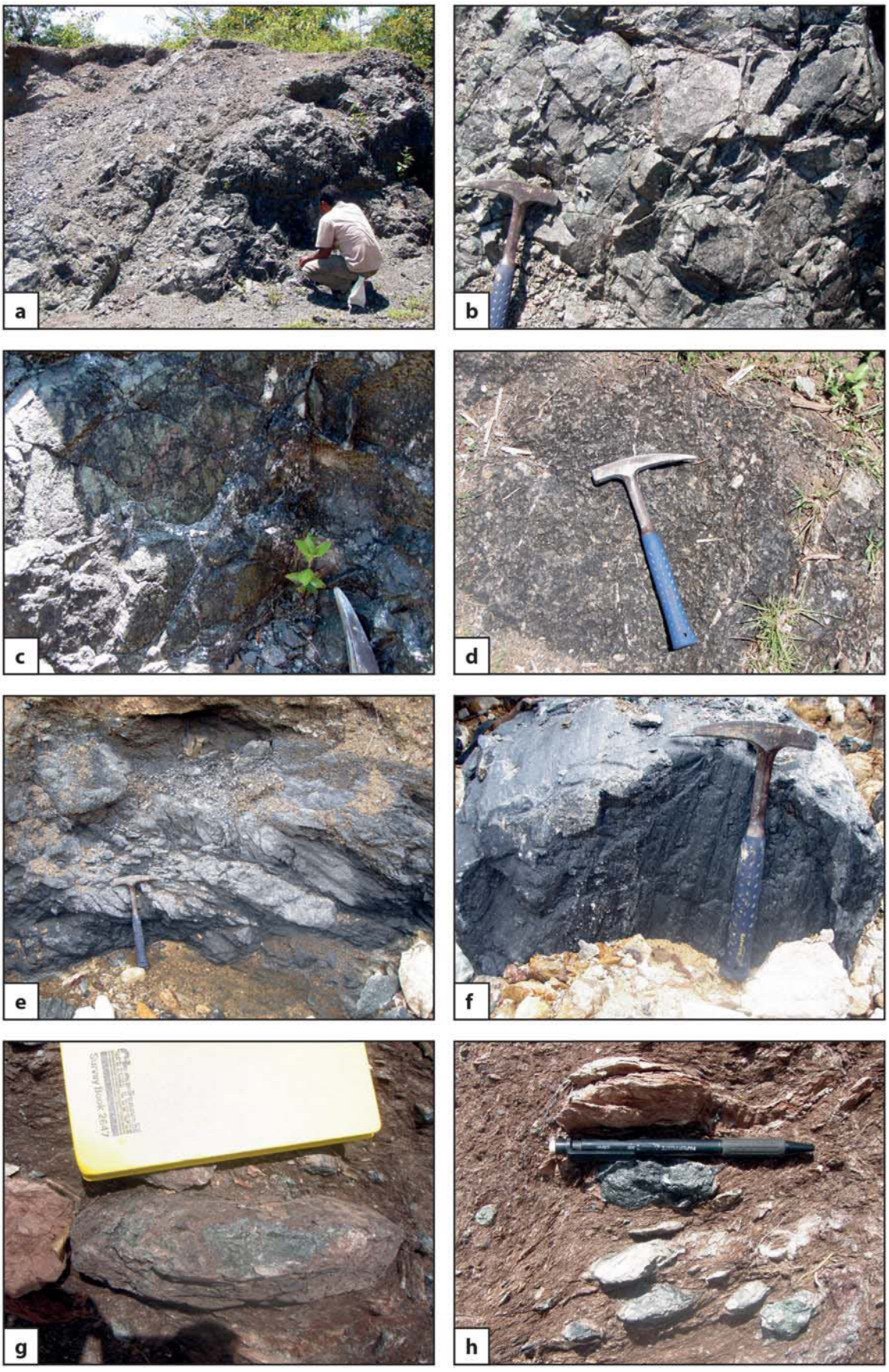
a
b
c
d
e
f
g
h

No sediments were found associated with the igneous rocks to enable a biostratigraphic age determination; however volcanics in Timor commonly belong to either the Permian Maubisse and Cribas Groups or Eocene Barique Group (Haig 2012b).

The schists appear mafic in hand specimen, although thin section analysis shows them to be extremely altered, with quartz and calcite the only minerals with a grainsize large enough to allow identification. They are always found in isolated outcrops surrounded by volcanics, although no contacts were observed. As such, this study attributes them to the same terrane. They may represent pieces of the metamorphic basement on which the volcanics have been deposited, exposed due to faulting, or xenoliths brought towards the surface by rising magma. Alternatively, they may represent distinct tectonic zones of shear within the volcanic units.

Although volcanic breccias and pillow basalts are found within both the Banda Megasequence Barique Group and the Gondwana Megasequence Cribas and Maubisse Groups, the breccias observed at Mount Taroman appear to be pyroclastic breccias similar to those of the Barique (Benincasa *et al.* 2012) rather than flow breccias or basalt-limestone breccias common in the Cribas and Maubisse (**Chapter 3.7.2 The Matebian Range – Igneous rocks**; Charlton *et al.* 2002) . Furthermore, Permian volcanics are not associated with metamorphic rocks, whereas the Barique Group volcanics have a close association with the Lolotoi Metamorphic Complex, which represent the basement rocks of the Banda Megasequence (Standley & Harris 2009).

This study places the igneous rocks found at Mount Taroman within the Barique Group of the Banda Megasequence. The schists may either belong to the Lolotoi Metamorphic Complex, or alternatively they may be discretely sheared zones within the Barique Group Volcanics. The Lolotoi Metamorphic Complex and Barique Group have both been mapped around the southern and western edges of Mount Taroman by previous studies (Audley-Charles 1968; Partoyo *et al.* 1995; Standley & Harris 2009). This study increases the mapped extent of the Barique Group around the eastern flank of the massif.

3.12 Summary

This study has re-evaluated most major fatus in East Timor that appear on current geological maps as Miocene, Asiatic affinity 'Cablac Limestone' (e.g. Audley-Charles 1968; Rosidi *et al.* 1979; Partoyo *et al.* 1995). Detailed geological mapping has been completed around the Ossu region (Mount Mundo Perdido and Mount Laritame) and the Maliana basin (Mount Loelako and the Saburai Range), with less detailed, regional geological mapping and sampling completed around the Matebian Range, the Builo Range, Mount Bibileu and Mount Taroman. Mapping was also completed at the eastern tip of East Timor around Lake Iralalaru and the Paitchau Range, a fatu originally mapped as Triassic 'Aitutu Formation' of Gondwanan affinity by Audley-Charles (1968) and following authors.

Miocene limestones of the Banda Megasequence (here placed within the Booi Group after Haig *et al.* 2008; Haig 2012b) have been observed around the Ossu fatus, forming some of the smaller cliffs at lower structural levels. However, the high, central regions of all fatus visited by this study comprise much older, Australian affinity limestones. Mount Mundo Perdido, Mount Laritame, the Builo Range, Mount Bibileu, Mount Taroman, and most likely the Matebian Range comprise mainly Early Jurassic (? Late Triassic) Bahaman-facies ooid limestones of Australian affinity – the 'Perdido Group' after Benincasa *et al.* (2012) – with subordinate Cretaceous to Miocene carbonate pelagites of the Kolbano Group. The Paitchau Range, Mount Loelako and the Saburai Range comprise Late Triassic (Carnian-Norian) fossiliferous wackestones, packstones, floatstones and algal bindstones of Australian affinity – the 'Bandeira Group' after Haig (2012b). See **Table 1** for summary of stratigraphy in the study areas.

Figure 84 outlines how the stratigraphic groups in the study areas fit into the tectonostratigraphic framework of East Timor.

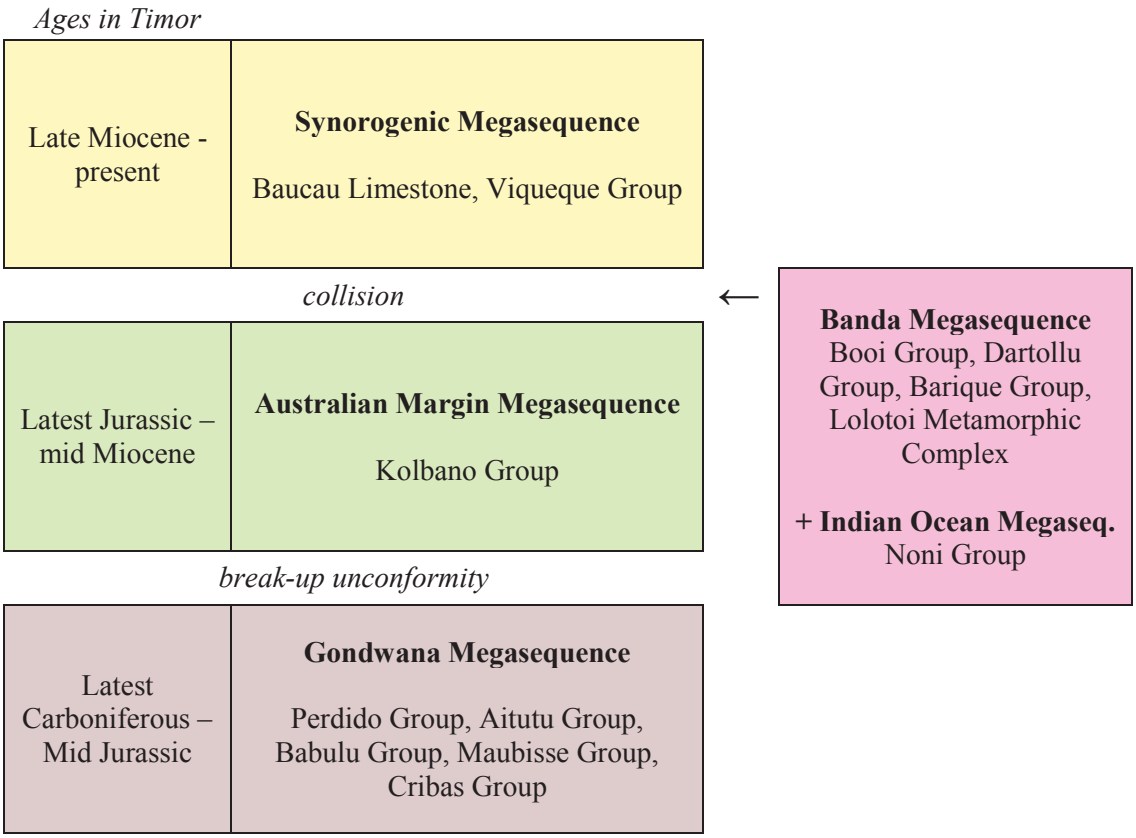

Fig. 84. Stratigraphic groups in the study areas within the tectonostratigraphic framework of East Timor.

Table 1. Main rock types recognised in the study areas. See **Appendix I** for detailed location co-ordinates.

Group	Geographical distribution in study areas	Rock types	Sedimentary structures	Fossils	Facies	Age	Thickness	Contact relationships	Chapter references
Baucau Limestone	At the Ossu fatus these rocks abut Mount Mundo Perdido on its lower northern flank, and form flat-lying terraces overlying Mount Laritame. At Lake Iralalaru the Baucau Limestone is widespread and forms a broad elevated plateau which occupies much of the north-eastern tip of East Timor, surrounding the lake	Yellow to white, porous, vuggy, packstones and grainstones.	Medium to thick bedded. At Mount Laritame forms flat-lying terraces tens of metres in thickness	Abundant corals, coralline algae, and larger rotaliid benthic foraminifera	Neritic carbonate platform associated with coral reefs	Pleistocene	Up to 200 m at Mount Laritame	Faulted against the Barique Group and Perdido Group at Mount Mundo Perdido, and against the Bandeira Group at the Paitchau Range. Unconformably overlies the Perdido Group at Mount Laritame	Chapter 3.2.9 Chapter 3.3.7 Chapter 3.6.4
Viqueque Group	At the Ossu fatus the Viqueque Group is observed to the north of Mount Mundo Perdido and Mount Laritame, and to the south of Mount Bibileu and the Builo Range. In the Maliana region these rocks comprise the thick synorogenic basin fill of the Maliana and Marobo basins.	Grey mud, sandy mud and muddy sandstone. Rare conglomerates and turbidites. At Mount Mundo Perdido the Lari Guti Member comprises thin to thick-bedded yellow to white vuggy foraminiferal packstones and grainstones with thick beds of coral rudstone in cut and fill channels.	Thin to thick bedded. Sandstone beds increase in thickness and frequency with younging. Occasional thick beds (>1 m) of poorly sorted melange and debris slides.	Diverse and abundant planktonic foraminifera, rarer benthic foraminifera, occasional gastropods and bivalves	Mid-bathyal to outer neritic	Late Pliocene–Early Pleistocene (planktonic foraminiferal zones N20–N22).	Over 700 m in the Maliana region	Faulted against Gondwana Megasequence limestones and mudstones at the Ossu fatus and in the Maliana region	Chapter 3.2.8 Chapter 3.3.6 Chapter 3.8.4 Chapter 3.10.4
Booi Group	Occupies lower structural levels around the outskirts of Mount Mundo Perdido, Mount Laritame, the Builo Range. Isolated outcrop northwest of the Maliana basin. Possibly present at lower structural levels at the Matebian Range (see chapter 4.4.1 The Matebian Range - Distribution of stratigraphy)	White to pale grey foraminiferal packstones and wackestones. Grey mudstones with thin sandstone interbeds.	Medium bedding in limestones, thin bedding in mudstones and sandstones.	Limestones contain abundant large benthic foraminifera along with minor coralline algae and other coral debris, echinoid spines, and rare mollusc debris. Mudstones contain abundant planktonic foraminifera with rare leaf impressions and gastropods in some beds	Limestones are neritic; mudstones are outer neritic to upper bathyal	Latest Oligocene–earliest Miocene (Upper Te Letter Stage and ?P22–N4–?N5 planktonic foraminiferal zones)	Greater than 50 m at the Ossu fatus	Faulted against the Perdido Group, the Babulu Group, the Kolbano Group, and the Barique Group. Field observations imply that it may stratigraphically overly the Barique Group at the Ossu fatus.	Chapter 3.2.7 Chapter 3.3.5 Chapter 3.4.5 Chapter 3.10.3
Dartollu Group	Observed in scree below Mount Bibileu and at one locality north-west of the Maliana basin	White to grey-brown muddy wackestones with abundant larger benthic foraminifera in a muddy, sandy matrix	Sampled from scree – no sedimentary structures observed	Abundant larger benthic foraminifera including *Alveolina* sp. and *Nummulites* sp.	Inner neritic, shallow carbonate platform	Middle Eocene	Sampled from scree – thickness unknown	Associated in all locations with other Banda Megasequence lithologies (Booi and Barique Groups)	Chapter 3.5.4 Chapter 3.10.3
Barique Group	Found at lower structural levels around the outskirts of the Ossu fatus and Mount Bibileu. Associated with the Lolotoi Metamorphic Complex on the eastern flank of Mount Taroman. Possibly present at lower structural levels at the Matebian Range (see chapter 4.4.1 The Matebian Range - Distribution of stratigraphy)	Undifferentiated volcanic sandstone and breccia, associated red mudstone, schist, and gabbro.	Undifferentiated volcanic sandstone and breccia, associated red mudstone, schist, and gabbro. Sandstone contains lithic fragments in a matrix of angular plagioclase crystals and glass, and in places displays flow layering.	Absent	Basaltic to intermediate calc-alkaline plutonic and volcanic rocks of island arc affinity; mudstones are upper bathyal to outer neritic	No age determinations made of volcanic and igneous rocks in map areas. Red mudstone at Mount Mundo Perdido is late Middle Eocene (within planktonic foraminiferal zones E11–E13) (Benincasa *et al.* 2012)	Possibly hundreds of metres based on the height of volcanic hills in the southwest of Mount Mundo Perdido	Faulted against the Perdido Group, the Babulu Group, the Kolbano Group, the Booi Group the Viqueque Group and the Baucau Limestone. Field observations around the Ossu fatus imply that it may sit stratigraphically beneath the Booi Limestone. Associated with the Lolotoi Metamorphic Complex at Mount Taroman.	Chapter 3.2.5 Chapter 3.2.6 Chapter 3.3.4 Chapter 3.5.3 Chapter 3.11.5
Kolbano Group	Forms many of the high cliffs on the northern and southern flanks of Mount Mundo Perdido. Also observed forming parts of Mount Loelako, Mount Bibileu and the Matebian Range, in isolated outcrop and scree at the Paitchau Range, and incorporated into a structural melange zone at Mount Taroman.	Pink, white and grey wackestones	Chert nodules aligned to bedding in places	Most samples contain abundant planktonic foraminifera. Oldest unit lacks planktonic foraminifera, but has calpionellids, inoceramid prisms, and rare belemnite guards.	Latest Jurassic or earliest Cretaceous beds: upper bathyal. Aptian and younger units: Middle Bathyal to Abyssal (within 500–3000 m water depth)	Ages range from latest Jurassic or earliest Cretaceous through to Miocene (N14-N15 planktonic foraminiferal zones)	Possibly several hundreds of metres.	Faulted against the Perdido Group, the Babulu Group, the Booi Group and the Barique Group. Field observations suggest that it stratigraphically overlies the Perdido Group at Mount Mundo Perdido and the Matebian Range	Chapter 3.2.4 Chapter 3.3.3 Chapter 3.5.2 Chapter 3.6.3 Chapter 3.7.6 Chapter 3.11.4
Noni Group	Observed along the northern edge of the Builo Range, and possibly on the eastern flank of the Matebian Range near Baguia.	Interbedded red-grey mudstone; white, friable, porous radiolarite; and red siliceous radiolarian chert. Thin to medium bedded, pink-white to grey micritic wackestones with interbedded grey chert beds.	Thin to medium bedded. Limestones contain abundant chert nodules, generally aligned to bedding.	Abundant radiolaria. Wackestones contain very fine grained skeletal fragments; mainly bivalves, ostracods, and rare benthic foraminifera.	Abyssal	Jurassic to Early Cretaceous	Observed to be several tens of metres in isolated outcrop but likely to be several hundred metres	Associated with Banda Megasequence lithologies (Booi and Barique Groups). Likely to be faulted against the Perdido Group at the Builo Range.	Chapter 3.4.3 Chapter 3.4.4 Chapter 3.7.5

Table 1 (cont.). Main rock types recognised in the study areas. See **Appendix I** for detailed location co-ordinates

Group	Geographical distribution in study areas	Rock types	Sedimentary structures	Fossils	Facies	Age	Thickness	Contact relationships	Chapter references
Perdido Group	Observed to form the high peaks in the central regions of Mount Mundo Perdido, Mount Laritame, Mount Bibileu and Mount Taroman. Most likely also occupies similar structural positions at the Builo Range (see chapter 3.4.2 Ooid Limestones) and the Matebian Range (see chapter 4.4.1 The Matebian Range - Distribution of stratigraphy)	Grey oolitic, oncoidal, peloidal, and intraclastic grainstone, packstone and wackestone.	Outcrop generally massive, with bedding only observed in rare outcrops where grainsize variations are visible.	Main bioclasts include carbonate-cemented agglutinated foraminifera, dasycladale algae and Thaumatoporellacean algae (including cryptoendolithic types—following Schlagintweit & Velic´ 2012).	Inner neritic carbonate platform with restricted marine conditions including higher than normal salinities (Bahaman facies)	Early Jurassic (? Late Triassic). Where the unit can be dated with precision it is Sinemurian–Pleinsbachian.	Possibly many hundreds of metres based on the size of large, blocky outcrops.	Faulted against the Booi Group, the Barique Group, the Kolbano Group and the Booi Group. Field observations suggest that it stratigraphically underlies the Kolbano Group at Mount Mundo Perdido and the Matebian Range	Chapter 3.2.3 Chapter 3.3.2 Chapter 3.4.2 Chapter 3.5.1 Chapter 3.7.4 Chapter 3.11.3
Babulu Group	Comprises the majority of the low-lands around and between the Ossu fatus, the low-lands surrounding the Saburai Range, and the lower slopes along the north-western flank of Mount Taroman. Also observed in a high structural position occupying the saddle between the two main ridges of the south-western Saburai Range (see chapter 3.9.2 3.9.2 Grey mudstones with sandstone interbeds)	Around the Ossu fatus the Babulu Group comprises grey mudstone incorporating, in places, small blocks, up to ~2 m thick, of laminated fine to medium quartz sandstone. In the Maliana region and at Mount Taroman the Babulu Group comprises interbedded mudstones and sandstones. Sandstone beds are grey, fine to medium grained, comprising mostly subrounded quartz, feldspar lithic fragments and mica.	Sandstone beds generally have well defined swaley and hummocky cross-bedding, and occasional thin mudstone laminae. Bedding is medium to thick at the Ossu fatus, medium at Mount Taroman, and thin to medium at the Saburai Range and thin at Mount Loelako	Well preserved palynomorphs (spores, pollen and rare acritarchs), along with rare nodosariid foraminifera. Sandstones contain abundant woody fragments and carbonaceous material.	Prodelta facies (in shallow rift-basin setting)	Late Triassic (Carnian-Norian). Palynomorph assemblage at Mount Mundo Perdido is probably lowest Minutosaccus crenulatus Zone, Norian (Benincasa *et al.* 2012)	Difficult to determine due to extensive ductile deformation of mudstones, but probably in the order of thousands of metres based on observed outcrop extent	Can be observed to be in faulted contact with most other lithologies in East Timor. Possibly stratigraphically overlies the Bandeira Group at the Saburai Range.	Chapter 3.2.1 Chapter 3.3.1 Chapter 3.4.1 Chapter 3.8.1 Chapter 3.9.2 Chapter 3.10.1 Chapter 3.11.2
Bandeira Group	Comprises the indurated limestone ridges which form the high cliffs of the Paitchau Range, Mount Loelako, Mount Lesululi, and the Saburai Range.	Grey to white grey wackestones, packstones floatstones and algal bindstones	Generally medium to thick bedded, massive in places	Extremely fossiliferous with medium to coarse grains comprising gastropods, punctate brachiopods, echinoids, ostracods, crinoids, coral fragments, tubiphytes, benthic foraminifera, ooids and abundant algal nodules. Algal films are observed encrusting grains throughout and forming bindstones in some samples.	Shallow, moderate to high energy, carbonate platform and platform margin	Late Triassic (Carnian-Norian).	A cross section through Mount Loelako contains approximately 800 m of continuous stratigraphic section	In faulted contact with the Babulu Group in the Maliana Region, and appears to be stratigraphic below the Babulu Group at the Saburai Range. Faulted against the Baucau Limestone at the Paitchau Range. Transitional contacts with the Aitutu Group are observed in several locations.	Chapter 3.6.1 Chapter 3.8.3 Chapter 3.9.4
Aitutu Group	Widespread in East Timor and observed occupying low structural positions beneath the high cliffs of many fatus, including Mount Mundo Perdido, the Paitchau Range, the Matebian Range, Mount Loelako and the Saburai Range, and also incorporated into a melange zone at Mount Taroman	Dark grey radiolarian-rich bioturbated wackestone and interbedded mudstone. Can be limestone or mudstone dominated. Lenses of reworked fossiliferous shallow water facies in places	Very well defined bedding, with limestone beds generally 5-50 cm and mudstones beds 2-100 cm. Thin interbeds of chert in some localities.	Abundant *Halobia*-type pelagic bivalve filaments. Common radiolaria particularly in cherty beds. Rare ostracods, calcispheres, echinoid debris and benthic foraminifera	Basinal facies (outer neritic or upper bathyal in rift-basin setting)	Late Triassic or Early Jurassic. Elsewhere in Timor, the formation has a ?Anisian, Ladinian to Early Jurassic age (Haig & McCartain 2010)	Difficult to determine due to extensive folding but likely to be at least several hundred metres	Faulted against the Permian Cribas Group at the Matebian Range on a major strike-slip fault (see chapter 4.4 The Matebian Range). Transitional contacts with the Bandeira Group are observed in several locations.	Chapter 3.2.2 Chapter 3.6.2 Chapter 3.7.3 Chapter 3.8.2 Chapter 3.9.3 Chapter 3.10.2 Chapter 3.11.1
Maubisse Group	Observed as a small klippe overlying the northern tip of the Saburai Range	Red-grey, coarse grained volcanic sandstones and breccias	Sandstones are medium bedded, breccias are thickly bedded to massive.	Rare calcareous green algae, crinoids and bryozoans	Shallow, high energy shoreline with nearby active volcanism	Permian based on lithofacies correlation (see Chapter 3.9.1 Coarse grained sandstones and breccias)	50-60 m at the Saburai Range, known to be much thicker elsewhere in Timor (Audley-Charles 1968; Bird & Cook 1991; Charlton et al. 2002)	Overlies Bandeira Group limestones on a shallow, north-dipping thrust.	Chapter 3.9.1 Chapter 3.9.5
Cribas Group	Comprises much of the hilly farmland immediately east of Quelecai, approximately 4 km west of Matebian's western scarp	Mostly dark grey mudstones and siltstones with thin sandstone interbeds, with medium grained sandstones and very well graded turbidites observed higher in the stratigraphic succession. Sandstones appear to have a large mafic-volcanic component.	Mudstones contain thin sandstone interbeds >5 mm-10 mm, with abundant sulphides in some samples. Sandstone and turbidite beds are 5-40 cm	Mudstones contain rare radiolaria and echinoid spines, Sandstones contain bivalves, brachiopods, crinoids, echinoids, bryozoans and very well preserved benthic foraminifera *Colaniella* sp.	Volcanic influenced, marine, pro-delta and slope deposits.	Late Permian	At least several hundred metres where mapped east of Quelecai	Faulted against the Triassic Bandeira Group at the Matebian Range on a major strike-slip fault (see chapter 4.4 The Matebian Range).	Chapter 3.7.1 Chapter 3.7.2 Chapter 3.9.5

4. Deformation

4.1 The Ossu fatus: Mount Mundo Perdido, Mount Laritame and the Builo Range

Mount Mundo Perdido, Mount Laritame and the Builo Range dominate the landscape around the town of Ossu (**Figs 85, 86**). North of Ossu, Mount Mundo Perdido and Mount Laritame share typical fatu-style morphology, with steep-sided, blocky profiles dominated by high, near vertical cliffs up to hundreds of metres high (**Fig. 85a, b**). The Builo Range to the south of Ossu is the lowest and broadest of the Ossu fatus, and while its two narrow, east-south-east trending ridges exhibit typical steep sided fatu-style profiles, the wider, north-east trending central portion of the range is more gently sloping and lacks prominent limestone scarps (**Fig. 85c**). All of the Ossu fatus display rhomboidal geometries in map view, which is most apparent on a digital elevation model (**Fig. 87**). The Builo Range shows the most extreme asymmetry with its distinctive stretched-S shaped outline. To the north of Laritame, a limestone ridge known as Mount Ariana extends over 6 km to the northeast, and has similarly been mapped in the past as Miocene 'Cablac Limestone' (Audley-Charles 1968; Partoyo *et al.* 1995). A hot spring adjacent to Mount Ariana forms one of a series of such springs that extends along strike to the NE across East Timor; see **Chapter 4.1.4** for further discussion.

4.1.1 Distribution of stratigraphy

From field mapping and stratigraphic re-evaluation during the present study (**Table 1**), both Mount Mundo Perdido and Mount Laritame display a broadly antiformal distribution of stratigraphic units (**Fig. 88**). Triassic–Jurassic Gondwana Megasequence limestones dominate the structurally highest, central regions of the fatus. At Mount Laritame these older rocks are capped by a veneer of flat-lying Pleistocene reef terraces. Younger Cretaceous to Oligocene limestones of the Australian Margin Megasequence form the high cliffs on the northern and southern flanks of Mundo Perdido, and are also present at the south-western tip of Mount Laritame.

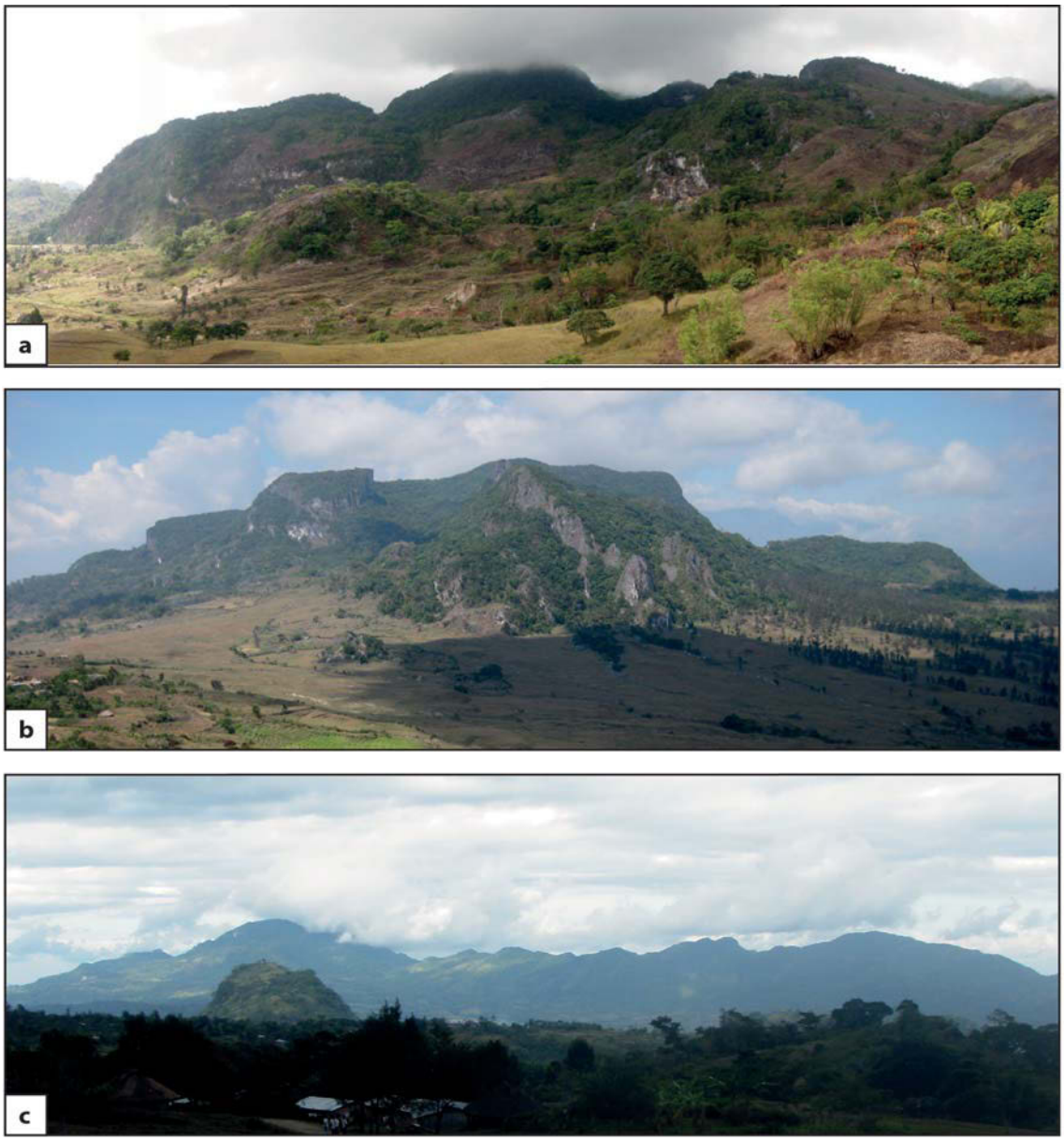

Fig. 85 ↑ The steep sided, blocky profiles of Mount Mundo Perdido (a, facing west) and Mount Laritame (b, facing east-northeast). Builo Range (c, facing south) displays similar morphology at its eastern and western ends, but these are separated by a low, broad, gently sloping central section.

Fig. 86 → Digital elevation model of East Timor outlining the main fatus and other geomorphic features investigated by this study. (DEM in this figure, and throughout this chapter, courtesy of the University of Melbourne SRTM landform atlas at http://jaeger.earthsci.unimelb.edu.au/Images/Landform/landform.html)

Fig. 87 →→ (a) Aerial photo of the Ossu fatus with interpreted structure. (b) Digital elevation model of the Ossu fatus with interpreted structure. Faults shown with solid lines have been observed and measured in the field; those shown with dashed lines have been interpreted from aerial photographs. Arrows indicate fault striae where observed and measured on major faults.

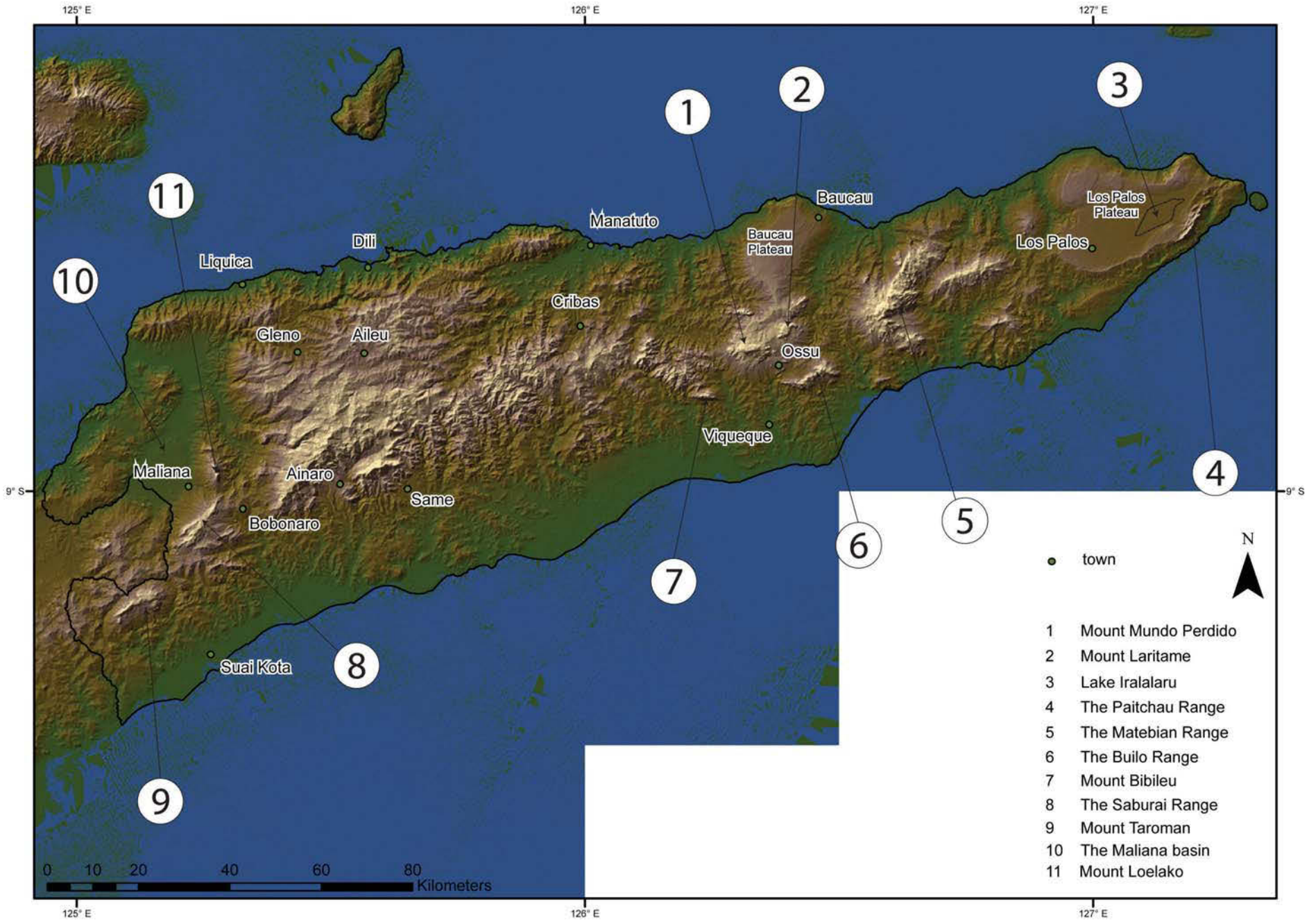
125° E
126° E
127° E
9° S
Baucau
Manatuto
Dili
Liquica
Baucau Plateau
Los Palos
Los Palos Plateau
Cribas
Gleno
Aileu
Ossu
Viqueque
Maliana
Ainaro
Same
Bobonaro
Suai Kota
1
2
3
4
5
6
7
8
9
10
11
town
N
1 Mount Mundo Perdido
2 Mount Laritame
3 Lake Iralalaru
4 The Paitchau Range
5 The Matebian Range
6 The Builo Range
7 Mount Bibileu
8 The Saburai Range
9 Mount Taroman
10 The Maliana basin
11 Mount Loelako
0 10 20 40 60 80
Kilometers

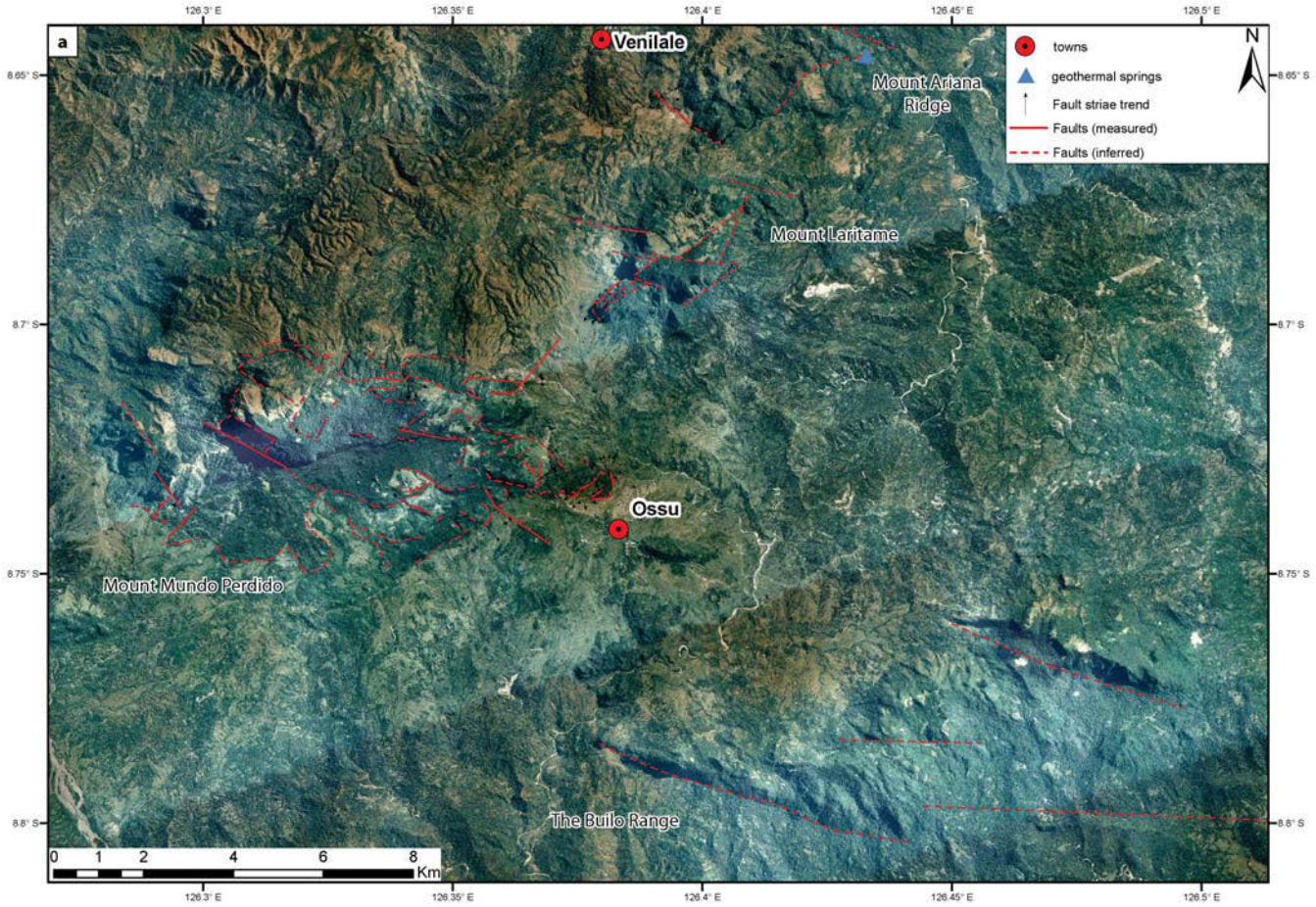
a
Venilale
Mount Ariana Ridge
Mount Laritame
Ossu
Mount Mundo Perdido
The Builo Range
towns
geothermal springs
Fault striae trend
Faults (measured)
Faults (inferred)
N
126.3° E
126.35° E
126.4° E
126.45° E
126.5° E
8.65° S
8.7° S
8.75° S
8.8° S
0 1 2 4 6 8
Km

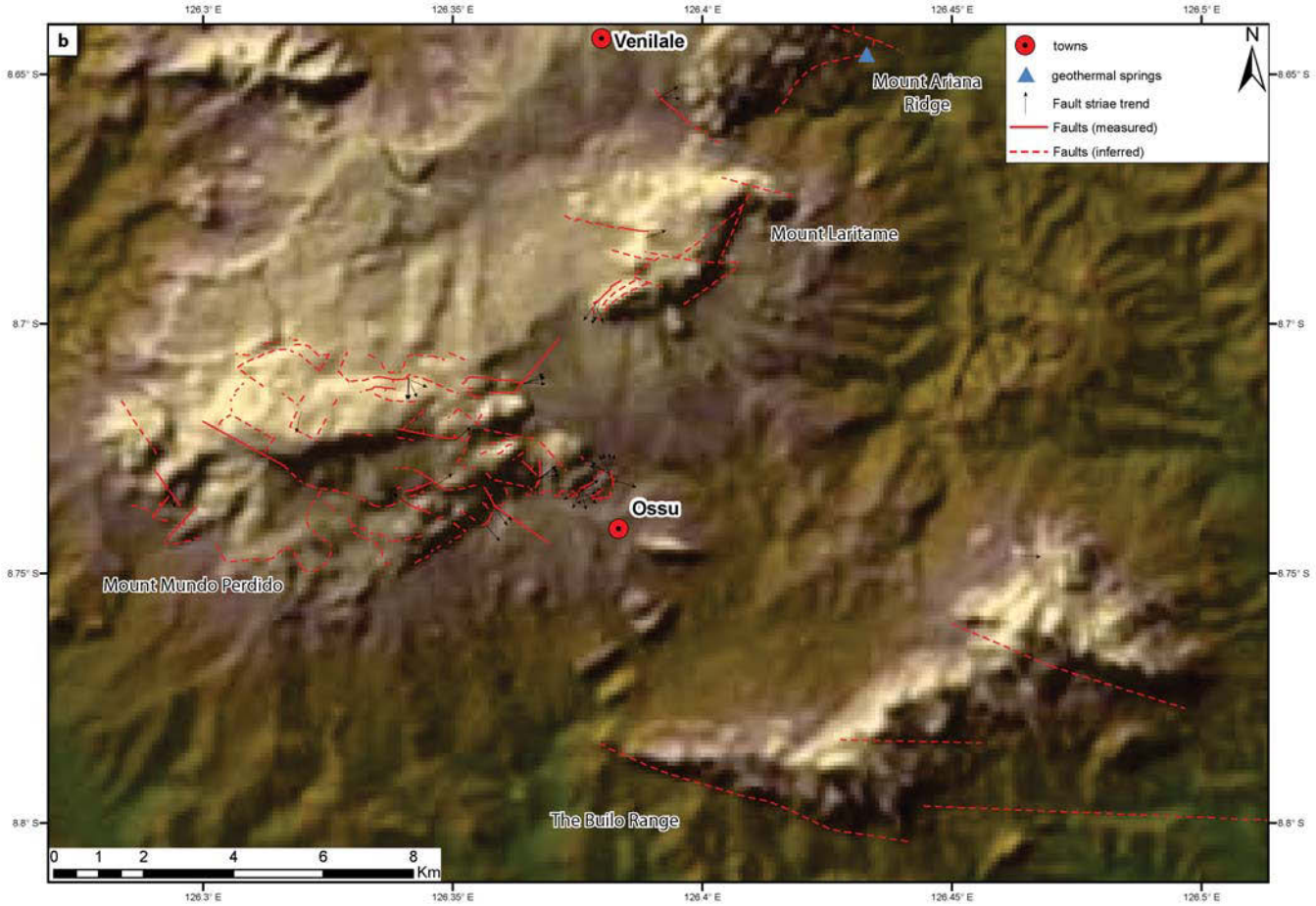
b
Venilale
Mount Ariana Ridge
Mount Laritame
Ossu
Mount Mundo Perdido
The Builo Range
towns
geothermal springs
Fault striae trend
Faults (measured)
Faults (inferred)
N
126.3° E
126.35° E
126.4° E
126.45° E
126.5° E
8.65° S
8.7° S
8.75° S
8.8° S
0 1 2 4 6 8
Km

Banda Megasequence units occupy the foothills and lower cliffs around both massifs at lower structural levels, extending up into higher levels only on the eastern side of Mount Mundo Perdido. Therefore, Banda Megasequence units emplaced on to the top of the structural pile through shortening during arc-continent collision (Audley-Charles 2004; Harris 2006) now occur only at lower topographic/structural levels around the Ossu fatus. High-angle, oblique-slip faults juxtapose the Banda Megasequence rocks against the older Australian-affinity rocks in the higher, central regions of the fatus (**Fig. 88**) and form the steep-sided limestone cliffs that dominate the topography (e.g. **Fig. 85**) (Benincasa *et al.* 2012). Pliocene–Pleistocene limestones and mudstones of the Synorogenic Megasequence, the youngest units in the study area, abut Mount Mundo Perdido and Mount Laritame on their northern flanks. Flat-lying terraces of Pleistocene Baucau Limestone (**Fig. 84**) are found at the top of Mount Laritame at 1400 m above sea level. Similar terraces of corresponding age are found immediately north of Mount Mundo Perdido at up to 1100 m above sea level, and also comprise the vast, flat expanse of the Baucau Plateau, situated 10 km north of Mount Laritame, which rises to a maximum altitude of 700 m above sea level (**Fig. 86**).

The Builo Range displays a similar distribution of stratigraphy to Mount Mundo Perdido and Mount Laritame, however rather than a single antiformal distribution it displays an antiformal stratigraphic distribution in both its two narrow ridges, which are each surrounded by younger rocks. The oldest, and structurally highest, rocks of the range are located within the pair of east-south-east trending ridges which, like the cores of Mount Mundo Perdido and Mount Laritame, are dominated by Triassic–Jurassic Gondwana Megasequence limestones (Perdido Group) (**Fig. 88**). Younger Cretaceous-age limestones of the Australian Margin Megasequence (Kolbano Group) have previously been mapped within the low, central section of the Builo Range, and forming the high cliffs on Builo's south-western tip (; the 'Borolalo Limestone' of Audley-Charles 1968; Partoyo *et al.* 1995), although these areas were not sampled by the present study which was confined to the northern edge of the Builo Range.

Consistent with the other Ossu massifs, Banda Megasequence units also occupy the foothills and lower cliffs at the Builo Range, and are mapped extensively at lower structural levels along

the northern edge of the range by the present study and previous authors (e.g. Partoyo *et al.* 1995). Similar to the northern edges of Mount Mundo Perdido and Mount Laritame, synorogenic limestones abut the Builo Range on its southern edge (Audley-Charles 1968; Partoyo *et al.* 1995).

Around the Ossu fatus, there is a marked difference in structural style between the more highly deformed Gondwana- and Australian Margin Megasequence limestone units and the Booi Group limestones of the Banda Megasequence. The former generally have steeply inclined bedding of variable strike that in many places are folded and disrupted by small-scale faulting and fracturing. The less deformed Booi Group limestones show more consistency in bedding, commonly dipping between 20–50° S at Mount Mundo Perdido where most measurements were made (**Fig. 88**), and are less internally deformed.

4.1.2 Faulting

At the regional scale, late, high-angle faults dominate the topography of Mount Mundo Perdido, Mount Laritame, and the high east and west ridges of the Builo Range. These faults obscure structures associated with early shortening, which is now evidenced around Ossu only by the abrupt juxtaposition of rocks of the Gondwana- and Australian Margin megasequences against those of the Banda Megasequence. These high-angle faults produce near vertical cliffs extending up to several hundred metres in height and up to several kilometres in length for some fault strands (Grunau 1953; Gageonnet & Lemoine 1958; Romariz & Leme 1967) (**Fig. 85**). Mapped both in the field and also from aerial photography, these cliffs occur along three dominant trends, a 030°– 050° trend, a 060°– 070° trend and a 100°– 120° trend, with a subordinate fourth trend of 160°–170° (**Fig. 88** – inset).

Fig. 88 → Interpreted geological map of the Ossu region, showing the distribution of lithologies and main geological structures (modified from Partoyo *et al.* 1995; Borges 2010; and Benincasa *et al.* 2012). SM = Synorogenic Megasequence, BM = Banda Megasequence, IM = Indian Ocean Megasequence, AM = Australian Margin Megasequence, GM = Gondwana Megasequence. Faults shown with solid lines have been observed and measured in the field; those shown with dashed lines have been interpreted from aerial photographs. Strike and dip of bedding is shown where measured. Inset – rose diagram showing the orientations of all measured faults at the Ossu fatus. Perimeter = 10%. (In this and following rose diagrams of faults in this thesis, the unique strike value of faults is calculated from the dip direction using the right hand rule)

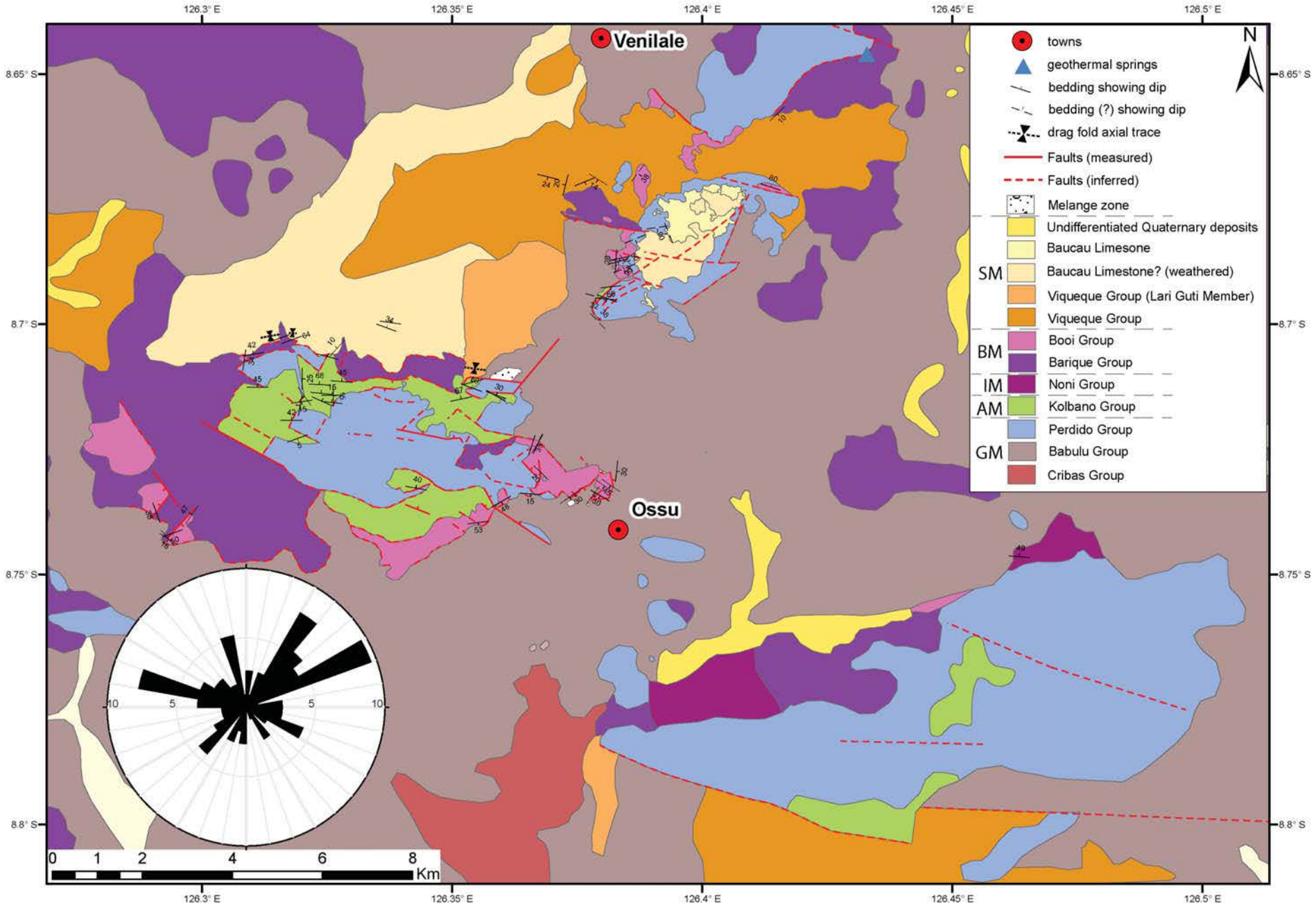
126.3° E
126.35° E
126.4° E
126.45° E
126.5° E
8.65° S
8.7° S
8.75° S
8.8° S
Venilale
Ossu
N
towns
geothermal springs
bedding showing dip
bedding (?) showing dip
drag fold axial trace
Faults (measured)
Faults (inferred)
Melange zone
Undifferentiated Quaternary deposits
Baucau Limesone
SM
Baucau Limestone? (weathered)
Viqueque Group (Lari Guti Member)
Viqueque Group
BM
Booi Group
Barique Group
IM
Noni Group
AM
Kolbano Group
Perdido Group
GM
Babulu Group
Cribas Group
10
5
5
10
0 1 2 4 6 8
Km

The 030°– 050° orientation is best seen in the trends of Mount Laritame and the Mount Ariana ridge, particularly their fault-bounded eastern scarps, and is also evident in major through-going faults within both massifs (**Figs 87, 88**). One of these faults (**Fig. 89**) extends between the northeast corner of Mount Mundo Perdido and the southwest corner of Mount Laritame, and may be responsible for apparent left-lateral separation between two half-dome structures, which have prominent aligned scarps facing southeast at Mount Mundo Perdido and northwest at Mount Laritame .

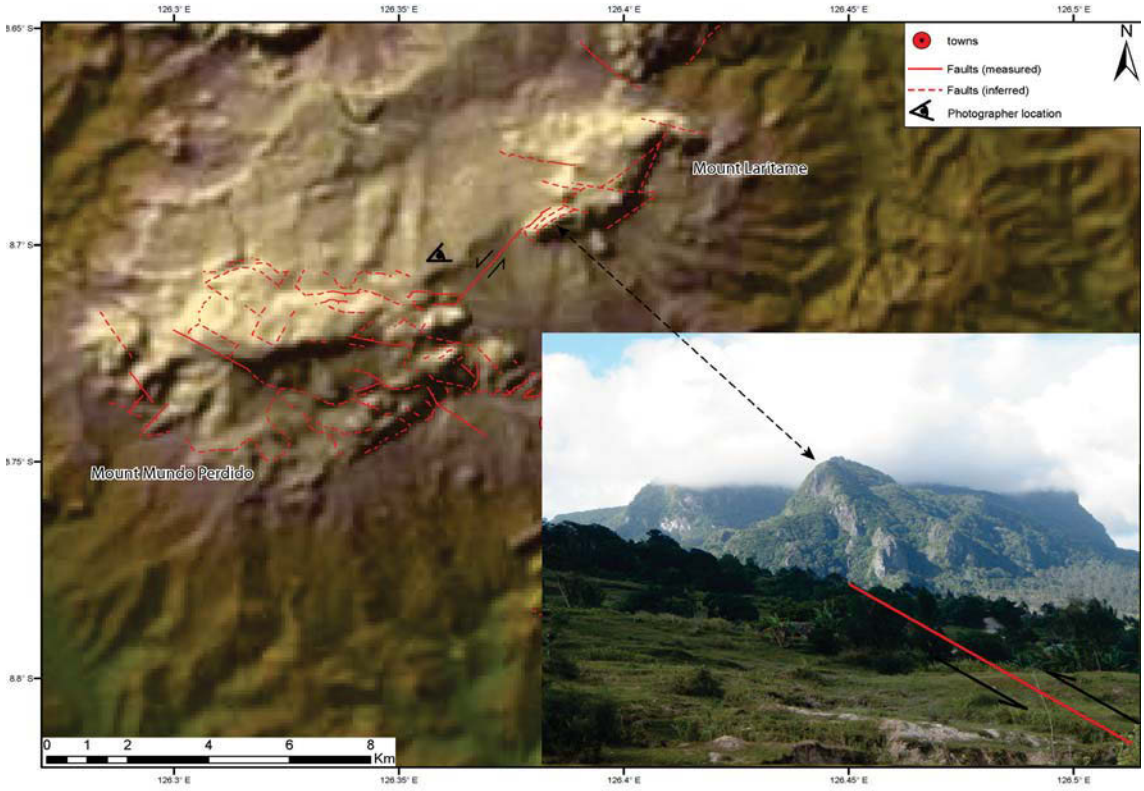

Fig. 89. Digital elevation model of the Ossu area showing apparent left lateral offset between prominent half dome structures in the northeast corner of Mount Mundo Perdido and the southwest corner of Mount Laritame. Both scarps are aligned with a northeast trending fault that extends between the two fatus. Photograph inset is the northwest-facing face of the half dome at Mount Laritame, viewed from Mount Mundo Perdido. Eye indicates photographer location.

The 060°– 070° and 100°– 120° trends form the bounding faults of Mount Mundo Perdido, and are most evident in the trends of the high cliffs on the mountain's southern edges, facing southeast and southwest respectively. The 100°– 120° trend is also clearly evident in the dominant fault scarps of the main ridges of the Builo Range, and in through-going faults within

the Mundo Perdido and Laritame fatus. The 160°–170° trend is less obvious at map scale, being found in mostly outcrop-scale faults.

The lateral extent of the largest faults was mapped from aerial photographs. Traces of these structures cut across topography, indicating steep dips, which are verified by field observations of sub-vertical fault planes throughout the study area. Where the lower reaches of these vertical faults were accessible, fault orientations and striae were measured directly on the fault planes (**Table 2**). The surfaces yielded fault striae (e.g. **Fig. 90**), often with multiple orientations, including both gently- and steeply-plunging, indicating multiple phases of slip on these surfaces. Almost all striae are oblique to dip, indicating some component of strike-slip (**Table 2**). At the outcrop scale we identified 123 fault surfaces from smaller-scale faults that displayed both steep and shallow dips (**Table 2**). Fault striae enabled slip direction interpretations on 86 of the 123 observed fault surfaces, with fault steps and other kinematic indicators allowing kinematic interpretations on an 44 of those 86 faults (**Table 3**). The majority of faults at both outcrop- and map-scale indicate mainly oblique-slip movement (**Table 2, 3**).

Slip data from over 100 regional- and outcrop-scale fault surfaces in the study area (**Table 2, 3**) therefore indicates a strong strike-slip component to the faulting, for multiple slip events, both on steeply- and shallowly-dipping fault surfaces. Further, these strike-slip indicators show a change in movement sense between the highest and lowest structural levels at Mount Mundo Perdido and Mount Laritame, with higher structural levels showing reverse-oblique indicators, contrasting normal-oblique motion at lower structural levels (**Fig. 91**). The highest mapped fault structure at Mount Mundo Perdido, at ~1350 m above sea level (the highest sample was at ~1760 m above sea level), indicates reverse-oblique movement (**Fig. 91**). Likewise, reverse-oblique faults were observed at Mount Laritame at ~1000 m above sea level in the southwest corner of the fatu, where the Jurassic Perdido Group (Gondwana Megasequence) has been faulted over Cretaceous Kolbano Group limestone (Australian Margin Megasequence) about moderate to high angle, south-east dipping sinistral-reverse faults (**Fig. 92**). Confirmed normal oblique faults were all observed at lower structural levels, mainly in the southeast corner of Mount Mundo Perdido ~600 m above sea level (**Fig. 91**).

Table 2. Classification of major, mappable faults at the Ossu fatus. Fault striae indicate a movement direction on 32 of the measured fault surfaces. Kinematic indicators allow a shear sense to be determined on a further 18; indicators included steps and crescentic fractures on limestone fault surfaces, asymmetric deformed clasts within fault zones, and s-c type shear fabrics developed within mudstones. Faults are classified as oblique-slip when striae indicate a movement vector with an obliquity greater than 10° from pure strike-slip or pure dip-slip.

Total	Movement indicators		Dip-slip		Strike-slip		Oblique-slip			
	Striae	Kinematic indicators	Normal	Reverse	Dextral	Sinistral	Dextral Normal	Sinistral Reverse	Dextral Reverse	Sinistral Normal
56	32	18	5		2		17		8	
			2	2	0	1	3	7	1	2

Table 3. Classification of all measured fault surfaces in outcrop at the Ossu fatus. Fault striae indicate a movement direction on 86 of the measured fault surfaces. Kinematic indicators allow a shear sense to be determined on a further 44; indicators included steps and crescentic fractures on limestone fault surfaces, asymmetric deformed clasts within fault zones, and s-c type shear fabrics developed within mudstones. Faults are classified as oblique-slip when striae indicate a movement vector with an obliquity greater than 10° from pure strike-slip or pure dip-slip

Total	Movement indicators		Dip-slip		Strike-slip		Oblique-slip			
	Striae	Kinematic indicators	Normal	Reverse	Dextral	Sinistral	Dextral Normal	Sinistral Reverse	Dextral Reverse	Sinistral Normal
123	86	44	9		3		38		36	
			3	2	0	2	10	14	7	6

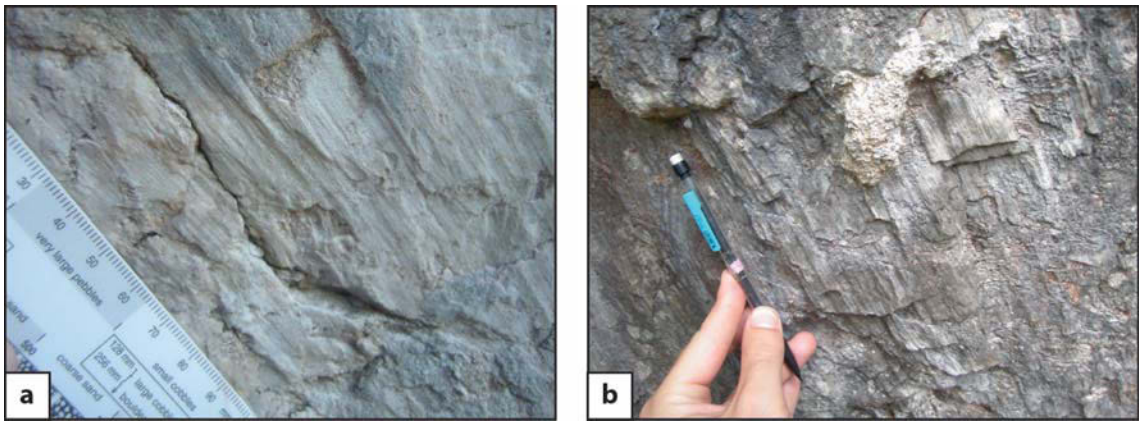

Fig. 90. (a) Fault striae recording oblique-slip within limestone of the Booi beds, which form the lower cliffs at the eastern end of the Mount Mundo Perdido. (b) Fault striae and steps on the hanging wall surface of an oblique-reverse fault developed within Australian Margin Megasequence foraminiferal wackestones, on the northern flank of Mount Mundo Perdido.

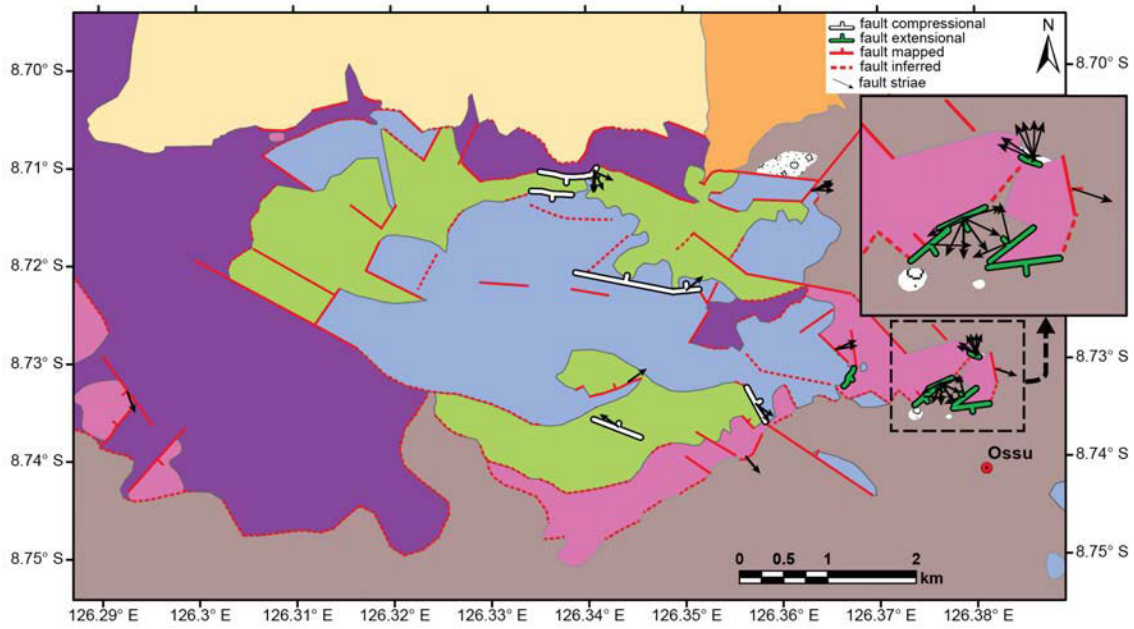

Fig. 91. Geological map of Mount Mundo Perdido, showing the distribution of major compressional and extensional faults, modified after Benincasa *et al.* (2012). Confirmed reverse-oblique faults (white, showing dip direction) are most common at high structural levels, where they dip towards the central east–west axis of Mount Mundo Perdido and the northeast-southwest axis of Mount Laritame. Confirmed normal-oblique faults (green, showing dip direction) are most common at lower structural levels in the southeast corner of Mount Mundo Perdido, where they dip away from the central axis of the massif. Inset shows detail of striae recording multiple directions of oblique slip on extensional faults in the southeast corner of the Mount Mundo Perdido.

Given the relatively young age of deformation, as evidenced by the fault-controlled present-day topography, the ~700 m elevation difference equates to an equivalent structural thickness.

In addition, dip domains identified in fault attitude data indicate that at lower structural levels (i.e. in the foothills of Mount Mundo Perdido, ~600 m above sea level) faults generally dip away from the elongate east–west axis of the mountain, whereas at higher structural levels (~1000 m to ~1350 m above sea level at Mount Mundo Perdido and Mount Laritame), faults dip towards the axis of elongation of both massifs (Benincasa *et al.* 2012, fig. 4).

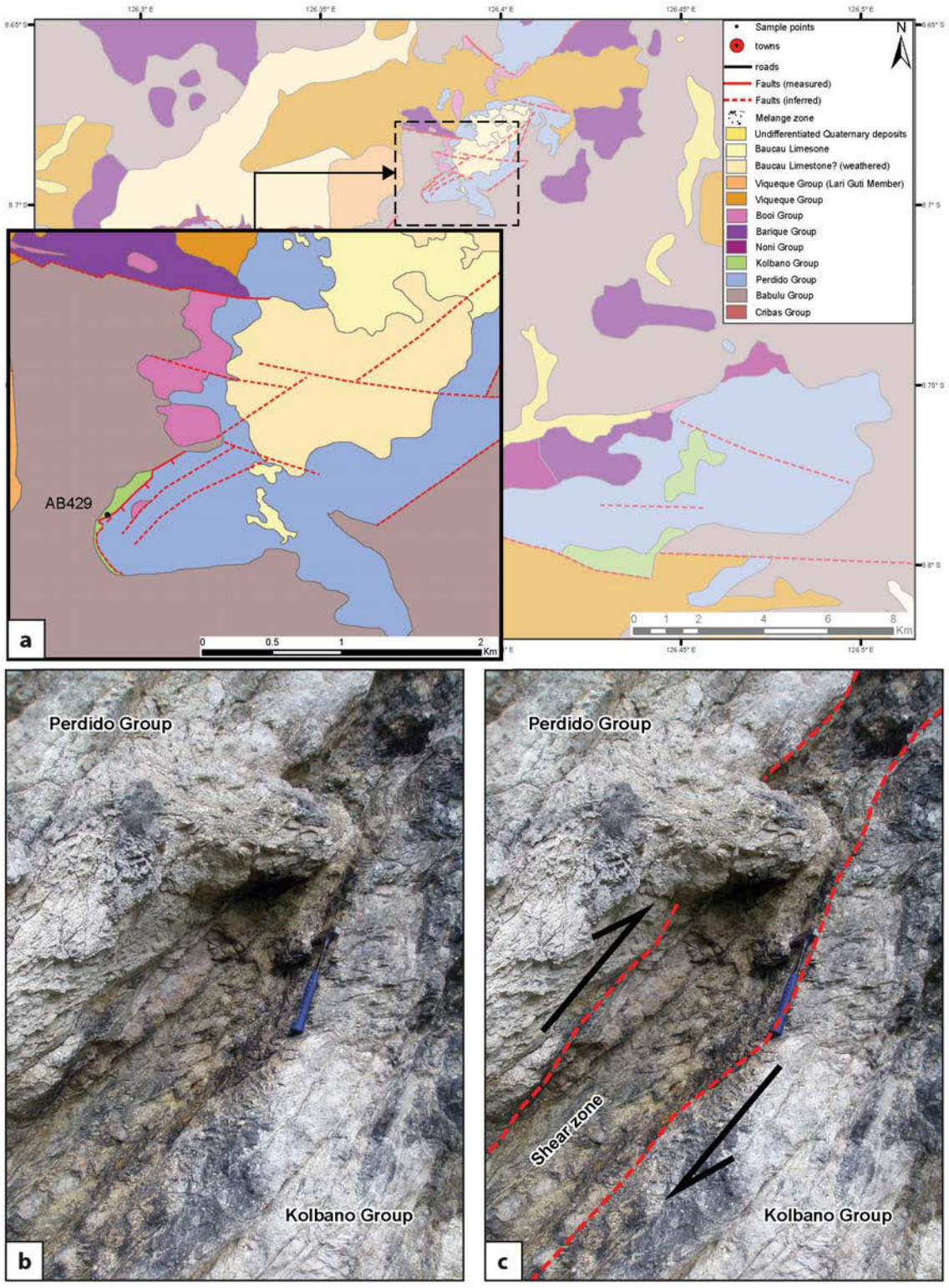

Fig. 92. (a) At the southwest corner of Mount Laritame, moderate to high angle, south-east dipping, reverse-oblique faults juxtapose Jurassic Perdido Group limestone (Gondwana Megasequence) over Cretaceous Kolbano Group limestone (Australian Margin Megasequence). (b) Uninterpreted and (c) interpreted outcrop photograph of one of these faults at AB429, showing Perdido Group and Kolbano Group limestones separated by a high angle, southeast-dipping brittle-shear zone approximately 30-40 cm in width. Hammer for scale.

The oblique-slip interpretations from striae on both regional- and outcrop-scale fault surfaces are supported by the discovery of a multi-domainal strike-slip fault at outcrop scale at Mount Mundo Perdido (**Fig. 93**) (Benincasa *et al.* 2012). This structure, approximately 3 m in height by 5 m in width, shows domains of overall shortening, overall extension and overall pure strike-slip. The top of the outcrop preserves a positive flower structure, indicating a reverse-oblique sense of displacement. In middle of the structure the multiple strands of the flower merge into a single dominant strand, with a near-vertical dip. Towards the base of the structure, the single

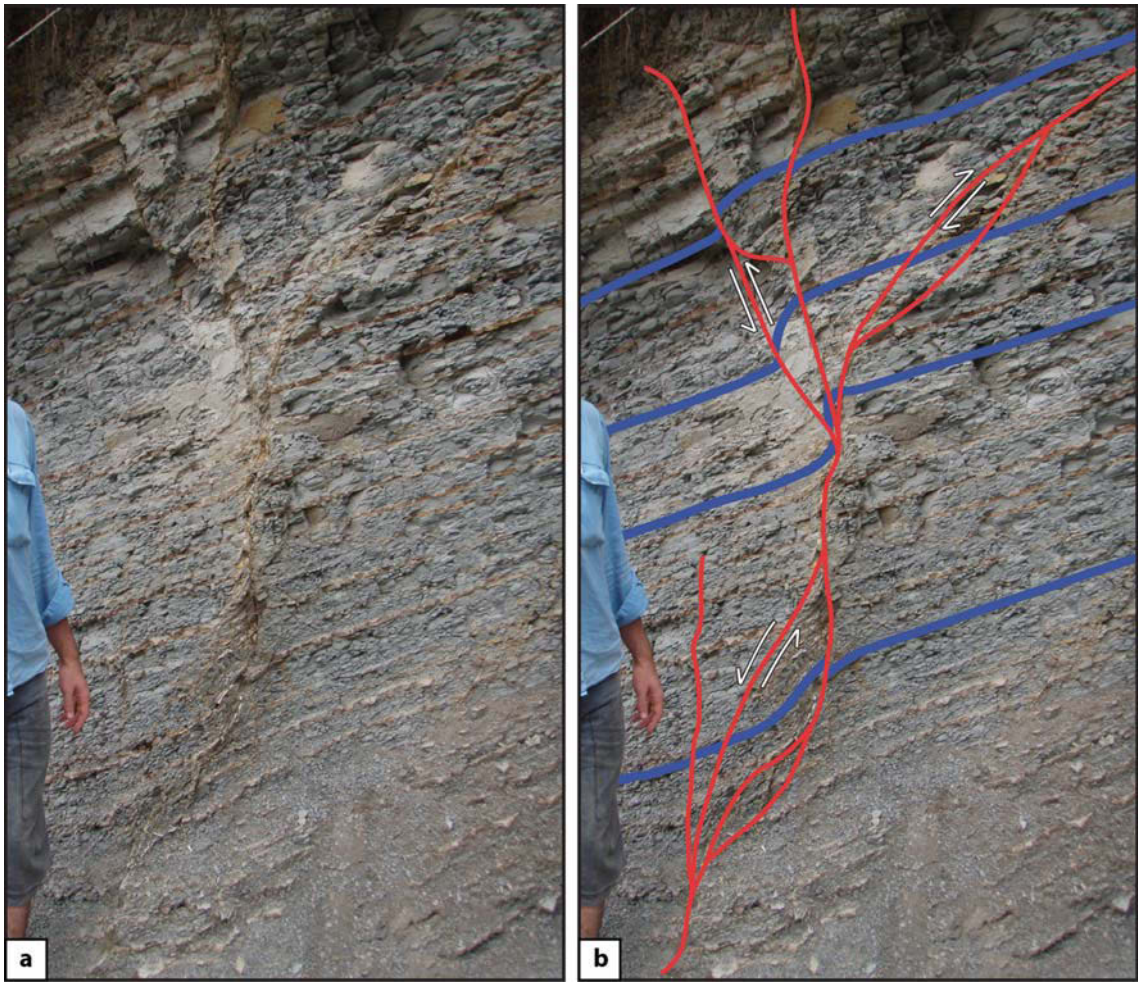

Fig. 93. Uninterpreted (a) and interpreted (b) figures of a large, asymmetric flower structure at location AB293, produced by strike-slip movement within grey Banda Terrane mudstones with thin sandstone interbeds. Note the large number of steeply dipping, upwardly diverging fault splays at high structural levels. Corresponding bed-sets have been marked on the outcrop with faults highlighted in red; following bed-sets through the fault zone allows fault movement to be determined. Reverse movement is observed on fault splays at higher structural levels, forming a pop-up structure, while normal movement is observed around the main fault strand at lower structural levels. Drag folds formed against the fault splays in outcrop (b) are replicated at map scale (**Fig. 95a, b**) where the Synorogenic Megasequence is faulted against the older rocks of the massif.

strand splays out into a number of smaller faults, with overall net normal displacement, becoming a single steep strand again at the base of the outcrop. The finely-bedded nature of the rocks and the numerous contrasting marker layers accentuate the sense of slip at both the upper- and lower-levels of this structure. The reverse-oblique motion at higher structural levels contrasts the net normal (normal-oblique) sense of displacement at the lowest structural levels of the outcrop, separated by a domain of a single-strand, high angle fault (**Fig. 93**). Movement senses in this outcrop-scale strike-slip fault mimic relationships described above at a larger scale, with faults at high structural levels showing indication of reverse-oblique motion, contrasting interpreted normal-oblique motion at significantly lower structural levels. The presence of these relationships at both scales within the study area, coupled with the hundreds of fault striae measurements, suggest that overall a significant component of strike-parallel slip has dominated movement on these young faults at all scales. Fault planes show evidence of both left-lateral and right-lateral movement (**Table 3**), however the right-lateral faults are concentrated strongly at the 100° trend and 040°– 070° (220°– 250°) trend (**Fig. 94b**), while left lateral faults are concentrated around the 030°– 050°, 060°– 070° and 160°– 170° (340°– 350°) trends (**Fig. 94c**).

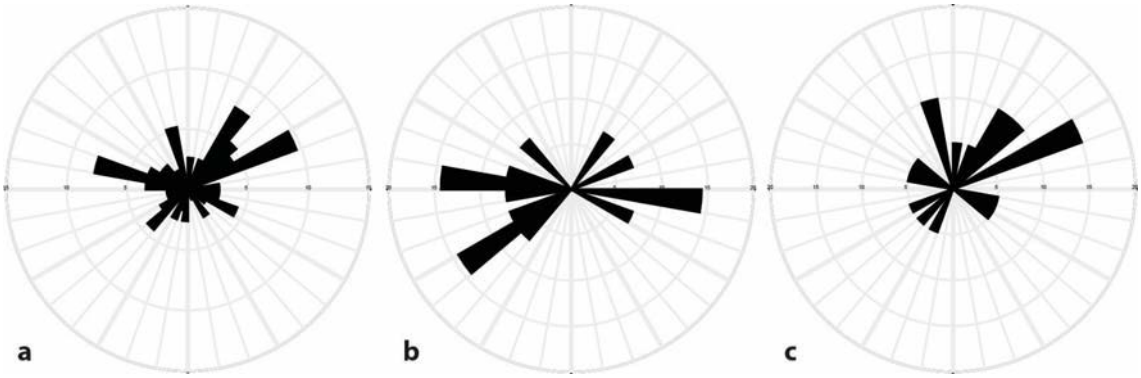

Fig. 94. Rose diagrams showing the orientations of measured faults at the Ossu fatus. (a) All measured faults. The most common fault orientations at the Ossu fatus are a 030°– 050°, a 060°– 070° and 100°– 120°, with a subordinate fourth trend of 160°–170° (b) Right lateral faults. These are most common at the 100° (280°) trend and 040°– 070° (220°– 250°) (c) Left lateral faults. These are most common at the 030°– 050°, 060°– 070° and 160°– 170° (340°– 350°) trends.

4.1.3 Folding

Map-scale drag folds have developed within rocks of the Synorogenic Megasequence (Baucau Limestone, Viqueque Group) on the northern side of Mount Mundo Perdido (**Fig. 88**) where these young units are faulted against the older Triassic to Miocene rocks of the fatu. At AB263 on Mount Mundo Perdido's northern side bedding within the Baucau Limestone (**Fig. 84**) changes from steeply dipping (64°→340°) adjacent to the fault, to 37°→340° 100 m further north, producing a drag fold with an east-west striking axial plane (**Fig. 95a, b**). On the north-eastern side of the fatu where the Pleistocene Lari Guti Member of the Viqueque Group (Synorogenic Megasequence) is faulted against Cretaceous pelagites of the Australian Margin Megasequence (**Fig. 88**), a large drag fold is observed of similar style, at this location striking east-southeast. The presence of these drag folds attests to the relative upwards movement of the older rocks that make up the central bulk of the fatu, where they are faulted against the younger units that surround them on the lowlands. Similar outcrop-scale drag folds are seen around the bounding faults of flower structures observed in outcrop (**Fig. 93**) and are consistent with reverse-oblique movement.

Minor, outcrop-scale, open, upright-to-inclined folds within pelagites of the Australian Margin Megasequence were observed occasionally on Mount Mundo Perdido (**Fig. 93 c–f**). Axial plane strikes vary and include strikes of 005°, 030° and 090°, with dips ranging from moderate to steep, and plunges ranging from shallow to moderate (Benincasa *et al.* 2012). From their limited exposure it is not clear whether these small-scale folds are related to early contraction or are coeval with more recent strike-slip deformation.

4.1.4 Melange zones and geothermal springs

Barber *et al.* (1986) suggested that much of the melange in Timor is formed as hydrous Triassic mudstones at lower structural levels become overpressured due to shortening, and that pressure is released through vertical faults which cut through the overthrust units. Observations around Ossu support that hypothesis, as most of the area originally mapped as 'melange' (Audley-Charles 1968) actually comprises Triassic mudstones and sandstones of the Babulu Group

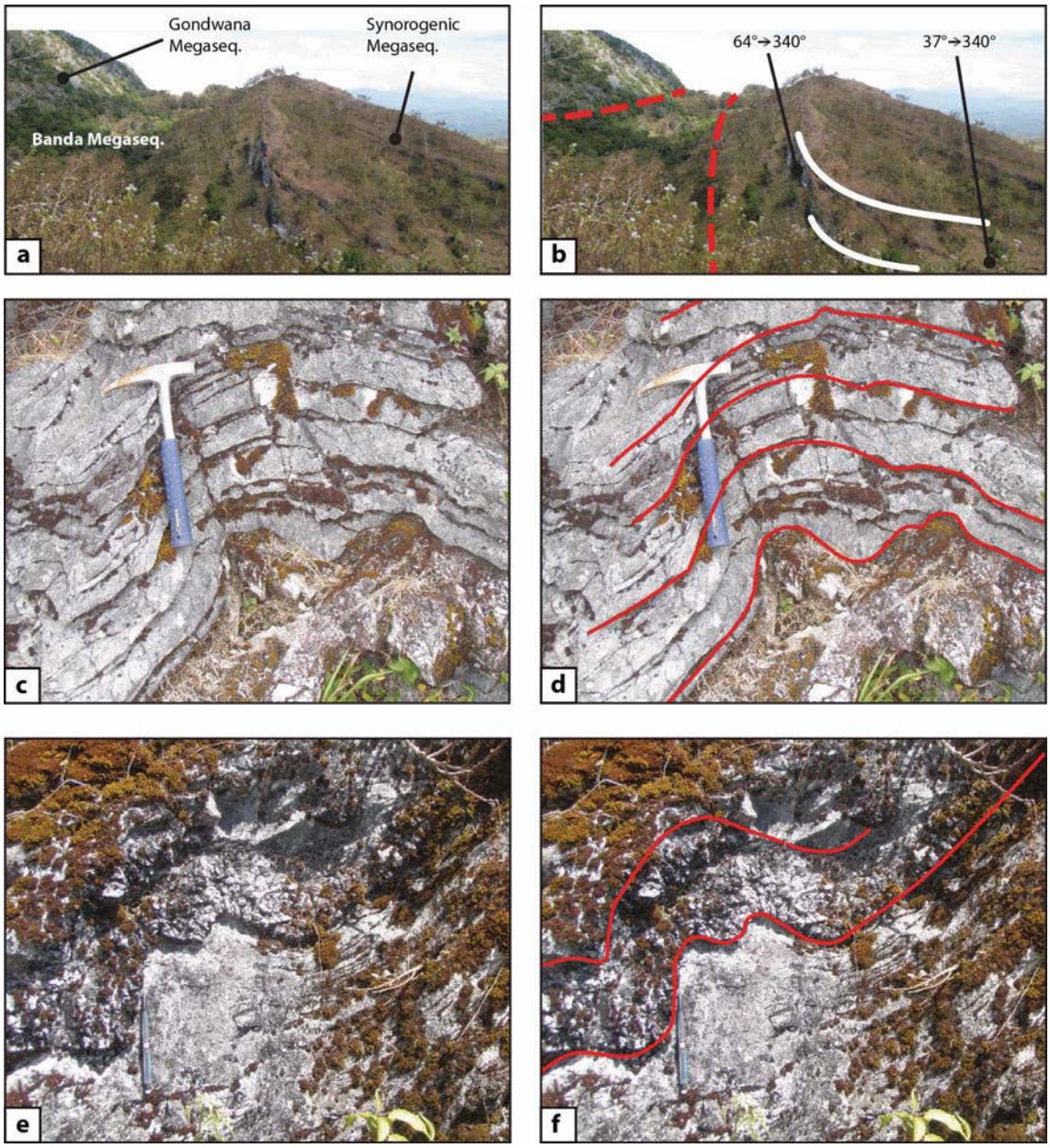

Fig. 95. Facing west, uninterpreted (a) and interpreted (b) images of the northern edge of Mundo Perdido show Triassic–Jurassic Gondwana Megasequence limestones of the massif in the top left corner of the frame. They are faulted against volcanics of the Banda Terrane (occupying the gully), which are in turn faulted against much younger Pliocene–Pleistocene synorogenic limestones of the Baucau Limestone (right of frame). Dashed red lines show the interpreted surface traces of the faults on either side of the gully. The measured change in the dip of bedding in the synorogenic units moving north from the fault trace describes a drag fold (white). These large drag folds form a series of small hills that parallel the northern edge of the mountain. Uninterpreted (c) and interpreted (d) images of open, upright folding within an outcrop of Turonian Australian Margin Megasequence pelagite at 144821. Of note is the 'M' fold developed in the fold hinge within the cherty bed at the base of outcrop. Uninterpreted (e) and interpreted (f) images of open, moderately inclined, moderately plunging folding within an outcrop of similar pelagite at 144814. Folding is well defined within cherty layers.

(see **Chapter 3.2.1 Mount Mundo Perdido – Blue-grey mudstones with sandstone interbeds**). However, this study recognises that zones of actual tectonic mélange containing an assortment of exotic blocks (as opposed to Babulu Group with 'broken formation' deformation – see **Chapter 3.1 Tectonostratigraphic framework**), are restricted to areas proximal to extensional/transtensional structures in the southwest corner of Mount Mundo Perdido (**Fig. 88**); their locations appear to be strongly structurally controlled.

A handful of local geothermal springs are described by Ossu residents, although only one was located by this study. It is situated on the eastern flank of the Mount Ariana ridge (**Figs 86, 87, 88**), where hot water is observed flowing from highly fractured and hydrothermally altered Perdido Group limestone over a broad area, with no specific single source identifiable. This spring is situated along strike of the major northeast-trending faults that bound the eastern edge of the Laritame fatu, and are interpreted to extend along strike to form the parallel eastern edge of the Mount Ariana ridge (**Fig. 88**). According to existing maps (Partoyo *et al.* 1995) the spring is situated at the contact between the Barique Group and the Perdido Limestone, although this contact was not observed in the field.

4.1.5 Structural model

(Benincasa *et al.* 2012) found that Mount Mundo Perdido is dominated by high-angle faults, with oblique-slip observed on the majority of surfaces. The fatu has an antiformal distribution of stratigraphy and a similarly antiformal bedding pattern. Positive flower structures are observed on strike-slip faults in outcrop, the fault architecture and kinematics of which strongly mimic that observed throughout Mount Mundo Perdido at map scale. As a result, Benincasa *et al.* (2012) suggested that deformation at Mount Mundo Perdido was the result of uplift in a restraining bend or step-over in a zone of strike-slip, and that the fatu represents a pop-up structure within that system. This is supported by striking similarities of the morphology, fault architecture and stratigraphic distribution of Mount Mundo Perdido with those of structures developed within analogue models of restraining bends (see Benincasa *et al.* 2012, fig. 9), and within restraining bends in documented active and ancient strike-slip systems (see Benincasa *et*

al. 2012, fig 11b). Similar evidence suggests that Mount Laritame and the Builo Range may also be the result of strike-slip dominated processes.

Mount Laritame is similarly dominated by high angle faults, producing a blocky morphology even more extreme than that of Mount Mundo Perdido (**Fig. 85**) (also see observations of Keep & Haig 2010; Duffy *et al.* 2013). Oblique-slip is again observed on the majority of fault surfaces (**Table 2, 3**). The bounding faults of the fatu, observed in the southwest corner of Mount Laritame, are southeast-dipping reverse faults which juxtapose Jurassic Perdido Limestone over younger limestones of the Kolbano Group (**Fig. 92**). Bounding faults along the eastern edge of Mount Laritame and the Mount Ariana ridge host geothermal springs in the Mount Ariana region (**Fig. 88**). This water is heated by the geothermal gradient alone, as Timor is not a volcanically active island; therefore these bounding faults that likely provide conduits for fluid flow are necessarily deep structures. Mount Laritame also has an antiformal distribution of stratigraphy; a high central core dominated by Gondwana Megasequence limestones is surrounded by younger units belonging to the Australian Margin and Banda megasequences at lower structural levels, separated by high angle faults (**Fig. 88**). The central region of Mount Laritame, capped by flat lying terraces of Pleistocene Baucau Limestone, is now topographically 700 m higher than corresponding terraces 10 km north on the Baucau Plateau. The Laritame fatu appears to have quite literally 'popped up' since the Pleistocene, with no folding or tilting observed.

All these characteristics are consistent with pop-up structures formed within strike-slip zones, and like Mount Mundo Perdido, Mount Laritame shows a strong similarity to transpressional structures developed in analogue models of restraining fault stepovers. Modelled deformation above restraining stepovers typically results in the formation of rhomboidal or lozenge shaped uplifts or 'pop-ups'. These pop-ups are bounded by oblique-slip reverse faults, with their upper surfaces dissected by synthetic and antithetic oblique-slip and strike-slip faults (Dooley *et al.* 1999; McClay & Bonora 2001). The distribution of stratigraphy in plan view has the oldest strata at the centre, with a succession of progressively younger strata exposed towards the margins of the popup structure. Bedding dips away from the centre of the structure, and rotation

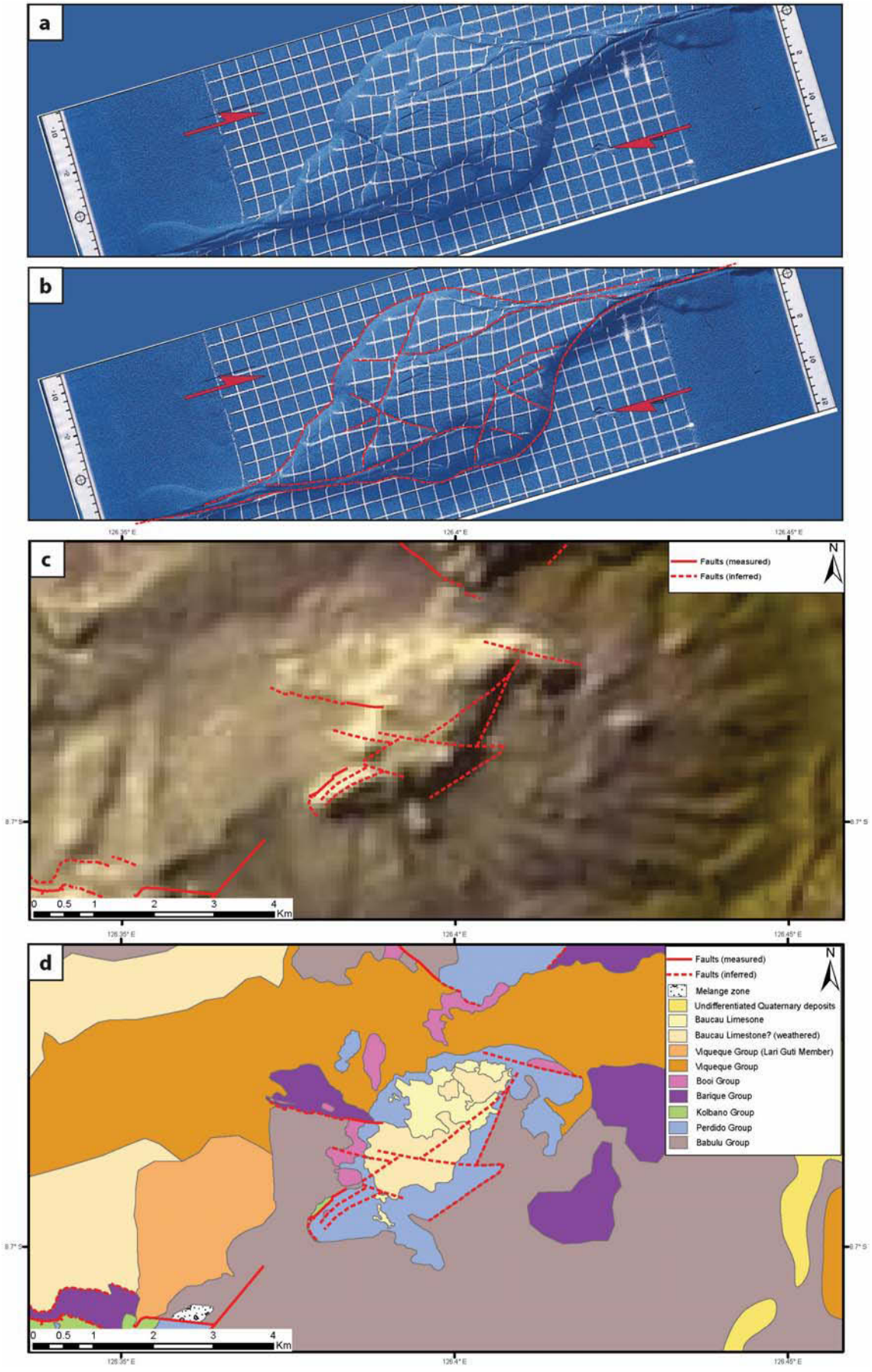
a
b
c
Faults (measured)
Faults (inferred)
N
0 0.5 1 2 3 4 Km
d
Faults (measured)
Faults (inferred)
Melange zone
Undifferentiated Quaternary deposits
Baucau Limesone
Baucau Limestone? (weathered)
Viqueque Group (Lari Guti Member)
Viqueque Group
Booi Group
Barique Group
Kolbano Group
Perdido Group
Babulu Group
126.35° E
126.4° E
126.45° E
8.7° S

Fig. 96 ← (a) Uninterpreted and (b) interpreted plan view of a pop-up developed in a sandbox model of a 90° restraining stepover, modified from McClay and Bonora (2001). The structure is a short, rhomboidal to slightly sigmoidal, S-shaped pop-up, crosscut by a network of dextral and sinistral strike-slip faults. A digital elevation model (c) and geological map (d) of Mount Laritame shows that the fatu has a very similar S-shaped morphology. Both the analogue model and the fatu also show similarities in orientations of main fault trends.

---

is observed within some fault bounded blocks (McClay & Bonora 2001). Mount Laritame most strongly resembles a pop-up developed at a 90° restraining stepover (**Fig. 96**). This produces a short, rhomboidal to slightly sigmoidal pop-up with maximum uplift over the centre of the stepover, crosscut by a network of dextral and sinistral strike-slip faults. Curved, oblique-slip reverse faults bound the structure, which form above the basement stepover and converge at depth (McClay & Bonora 2001).

Based on asymmetries in morphology and orientation of dominant fault trends Benincasa *et al.* (2012) suggested an overall left-lateral movement sense around the structure at Mount Mundo Perdido, which is consistent with the overall north-northeast convergence direction of Australia with respect to the Pacific and Eurasian plates (Genrich *et al.* 1996). Within a left-lateral strike-slip fault zone, a fault stepover will usually result in a z-shaped pop-up, such as Mount Mundo Perdido, when the fault steps to the right and an s-shaped basin when the fault steps to the left. The opposite is true of a right-lateral fault zone, which should produce a z-shaped basin when the fault steps left and an s-shaped pop-up when the fault steps right (**Fig. 97**). The s-shaped asymmetry of Mount Laritame (**Fig. 96**) suggests a structure formed within a step-over with a right-lateral movement sense, opposite to that of Mount Mundo Perdido.

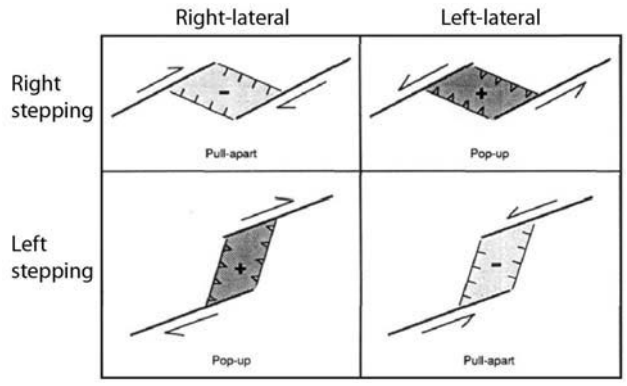

Fig. 97. Theoretical structural asymmetries developed within a strike-slip fault zone. Within a right-lateral fault zone, a right fault stepover produces a z-shaped basin, while a left fault stepover produces an s-shaped pop-up. Within a left-lateral fault zone, a right fault stepover produces a z-shaped pop-up, while a left fault stepover produces an s-shaped basin. (modified after Richard *et al.* 1995)

This apparently anomalous asymmetry may be the result of transpressional stress across the fault zone rather than pure strike slip. Analogue models produced by González *et al.* (2012) investigate structures developed at paired fault stepovers. When a modelled paired fault stepover undergoes pure strike-slip movement, left lateral movement will produce a z-shaped pop-up over a right fault stepover and a slightly smaller, s-shaped basin over a left fault stepover (**Fig. 98a**). However when convergence is incorporated across the paired fault stepover a basin will not form. A left fault stepover which produces an s-shaped rhomboidal basin at 0° of convergence will produce a similarly s-shaped rhomboidal pop-up with as little as 30° convergence across the fault zone (**Fig. 98b**). Structures developed within a model of a paired fault stepover within a left-lateral strike slip zone with 30° convergence are consistent with the morphology and relationships of the Mundo Perdido and Laritame fatus (**Fig. 98c, d**). A large, elongate z-shaped pop-up – comparable to Mount Mundo Perdido – is produced over the right fault stepover while a slightly smaller, more rhomboidal s-shaped pop-up – comparable to Mount Laritame – is produced over the left fault stepover.

Within the model the two pop-up structures appear to be separated by an apparent left lateral displacement around faults which cross the axis of the PDZ at a high angle (**Fig. 98b**). This may be equivalent to the northwest trending fault that runs between the north-eastern corner of Mount Mundo Perdido and the south-western corner of Mount Laritame, and which appears to produce left lateral displacement between the two fatus (**Fig. 89**).

Fig. 98 → (a) Analogue model of a paired fault stepover experiencing pure strike-slip movement, modified after González *et al.* (2012). The fault steps to the right on the left-hand side of the model, and to the left on the right-hand side of the model. With 0° of convergence a z-shaped pop-up forms where the fault steps right, and a slightly smaller, s-shaped basin forms where the fault steps left. (b) the same paired fault stepover undergoing left-lateral strike-slip with 30° of convergence across the fault zone, modified after González *et al.* (2012). A similar z-shaped pop-up is produced over the right fault stepover at 30° convergence, however it is larger and more elongate than the 0° convergence model. Over the left fault stepover at 30° convergence a pop-up now forms instead of a basin, though it has a similar small, rhomboidal s-shaped morphology to the basin in the 0° convergence model. The morphology of these two pop-up structures and the spatial relationship between them are very similar to those of Mount Mundo Perdido and Mount Laritame seen in (c) digital elevation model and (d) geological map.

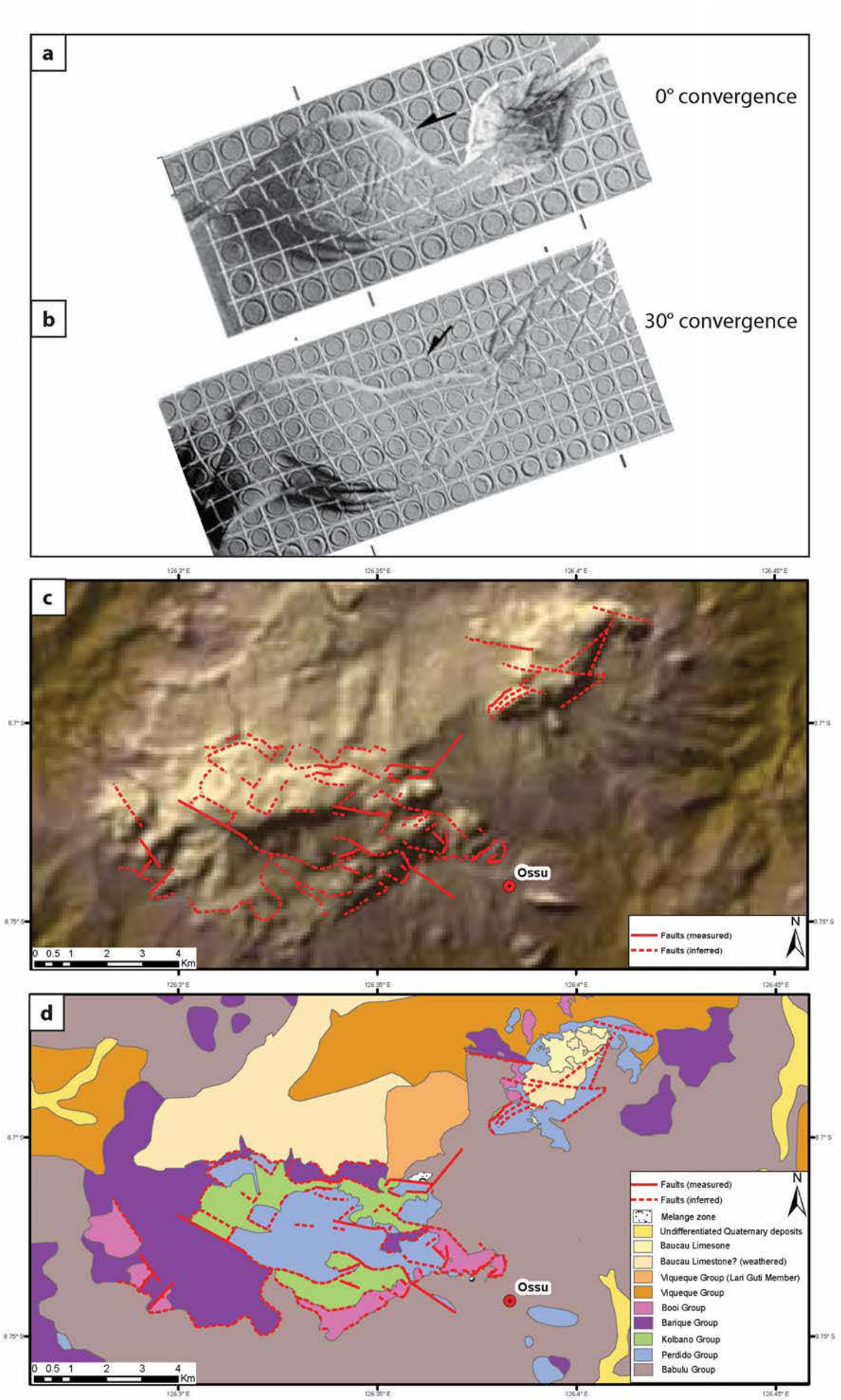
a
0° convergence
b
30° convergence
c
Ossu
0 0.5 1 2 3 4 Km
Faults (measured)
Faults (inferred)
N
d
Ossu
0 0.5 1 2 3 4 Km
Faults (measured)
Faults (inferred)
Melange zone
Undifferentiated Quaternary deposits
Baucau Limesone
Baucau Limestone? (weathered)
Viqueque Group (Lari Guti Member)
Viqueque Group
Booi Group
Barique Group
Kolbano Group
Perdido Group
Babulu Group
N

The Builo Range shares certain characteristics with Mount Mundo Perdido and Mount Laritame. The high eastern and western ridges are consistent with the 110° fault trend observed throughout the Ossu fatus, and are parallel with the south-western edges of Mound Mundo Perdido and Mount Laritame (**Fig. 87**). Likewise the lower, central portion of the Builo Range strikes at 050°, consistent with the 030°– 050° fault trend and sub-parallel to the strikes of Mount Laritame and the Mount Ariana ridge (**Fig. 87**). The Builo Range also has a striking asymmetry in plan view, typical of structures developed within strike-slip fault zones and consistent with the z-shaped and s-shaped asymmetries of Mount Mundo Perdido and Mount Laritame respectively. The stretched-s shaped asymmetry of the Builo Range compares favourably to similar stretched-s shaped pop-up structures developed in analogue models of restraining, overlapping, fault stepovers (**Fig. 99a**). However, uplift at the Builo Range has been greatest at the eastern and western ridges, where the rocks are stratigraphically oldest and topographically highest. This is not consistent with uplift over a restraining stepover, which is always greatest at the centre of a pop-up structure (McClay & Bonora 2001).

One way of producing the 'paired antiformal' stratigraphic distribution of the Builo Range is with uplift above a double basement strike-slip fault. Analogue experiments by Schellart and Nieuwland (2003) investigate structures developed above two parallel basement faults experiencing the same amount and sense of pure strike-slip deformation. These models produce elongate, rhombic pop-up structures above the parallel faults. However, detailed surface observations show that maximum uplift occurs at either end of the elongate pop-up, with uplift zones which trend sub-parallel to the P-shear direction (**Fig. 99b**).

Fig. 99 → (a) Plan view of a pop-up developed in a sandbox model of a restraining, overlapping, fault stepover, modified after McClay and Bonora (2001). The structure has a similar stretched-S shaped morphology to the Builo Range, however it has its greatest uplift at the centre, rather than at the end ridges as at the Builo Range. Furthermore, the right-lateral displacement sense of this structure is not consistent with local and regional kinematics at the Builo Range. (b) Plan view of a pop-up structure developed in an analogue model of a left-lateral double basement strike-slip fault, modified after Schellart and Nieuwland (2003). This structure has a pair of uplift zones which parallel the P-shear direction (see Riedel shear model, inset), and compares favourably to the 'paired-antiformal' uplift pattern of the Builo Range seen in (c) digital elevation model and (d) geological map.

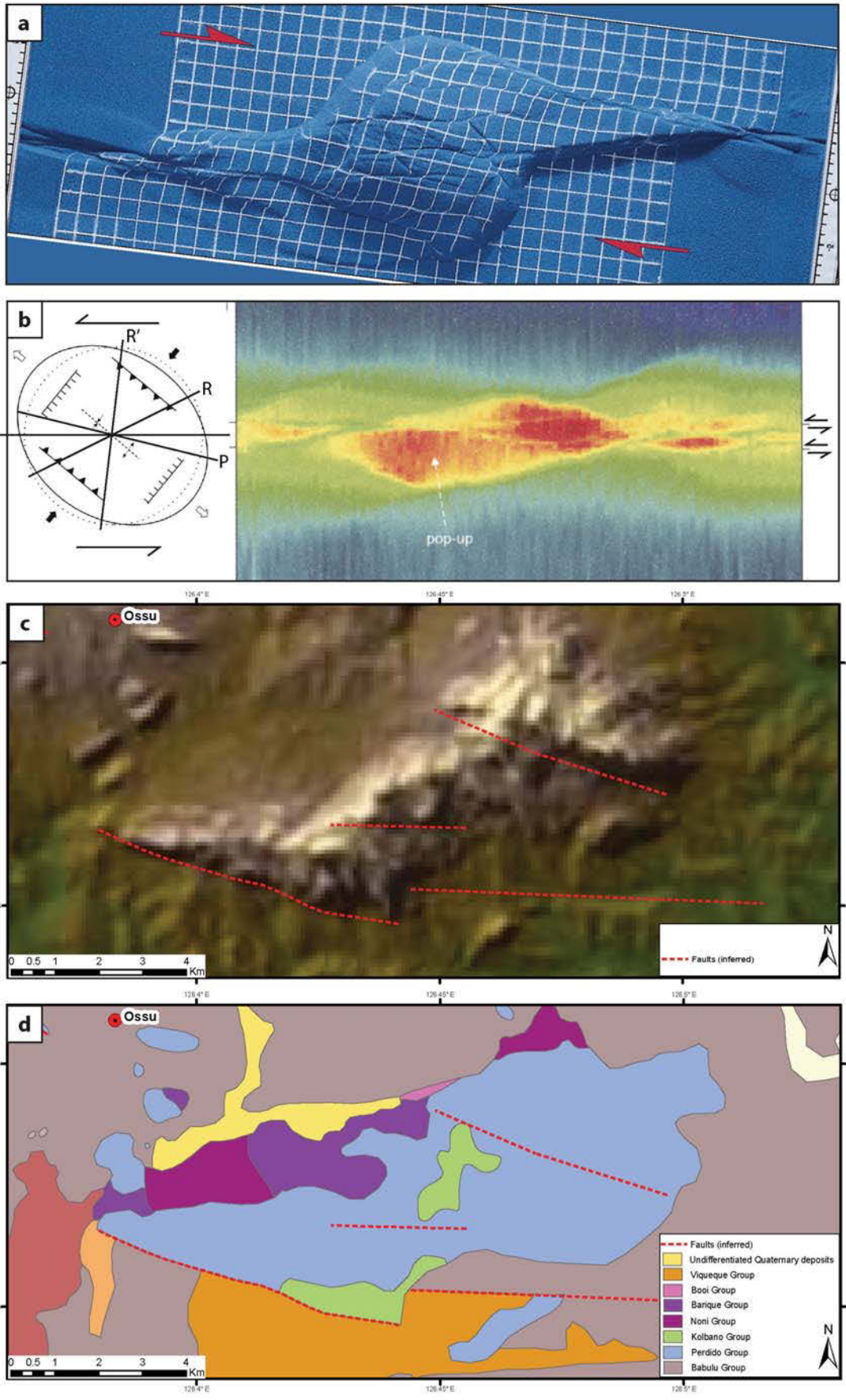
a
b
R′
R
P
pop-up
c
Ossu
0 0.5 1 2 3 4
Km
Faults (inferred)
N
d
Ossu
Faults (inferred)
Undifferentiated Quaternary deposits
Viqueque Group
Booi Group
Barique Group
Noni Group
Kolbano Group
Perdido Group
Babulu Group
N

These are joined by a slightly lower central section trending sub-parallel to the long axis of the rhomb, creating a stretched-s pattern of maximum uplift.

A comparison of the uplift pattern developed over an analogue model of a double basement strikes slip fault with the topography of the Builo Range shows striking similarities in major fault orientations and morphology of zones of maximum uplift (**Fig. 99c, d**). If a double basement strike-slip fault was responsible for uplift at the Builo Range, the high eastern and western ridges would be expected to develop parallel to the P-shear orientation. This would indicate an overall left-lateral displacement, consistent with interpreted kinematics at the other Ossu fatus, and across the plate boundary.

Ultimately a definitive structural model for the Builo Range cannot be developed with the little relatively small amount of field data collected here. Future structural mapping at the Builo Range needs to be undertaken to see if field data supports this structural model, or if uplift at the Builo Range is the result of a different mechanism.

4.2 Mount Bibileu

Situated approximately 9 km southwest of Mount Mundo Perdido and 15 km west of the Builo Range (**Fig. 86**), Mount Bibileu is an elongate, east-west trending fatu. A very steep southern scarp is dominated by east-west striking vertical limestone cliffs 300-400 m high in typical fatu-style morphology, while a more gentle topography slopes off to the north, northeast and northwest (**Fig. 100**).

Fig. 100 → (a) Aerial photo of Mount Bibileu with interpreted structure. (b) Digital elevation model of Mount Bibileu with interpreted structure. Faults shown with solid lines have been observed and measured in the field; those shown with dashed lines have been interpreted from aerial photographs.

Fig. 101 →→ Interpreted geological map of Mount Bibileu, showing the distribution of lithologies and main geological structures. Geology outside of mapped areas is modified after Partoyo *et al.* (1995) using aerial photographs. SM = Synorogenic Megasequence, BM = Banda Megasequence, AM = Australian Margin Megasequence, GM = Gondwana Megasequence. Faults shown with solid lines have been observed and measured in the field; those shown with dashed lines have been interpreted from aerial photographs. Strike and dip of bedding is shown where measured.

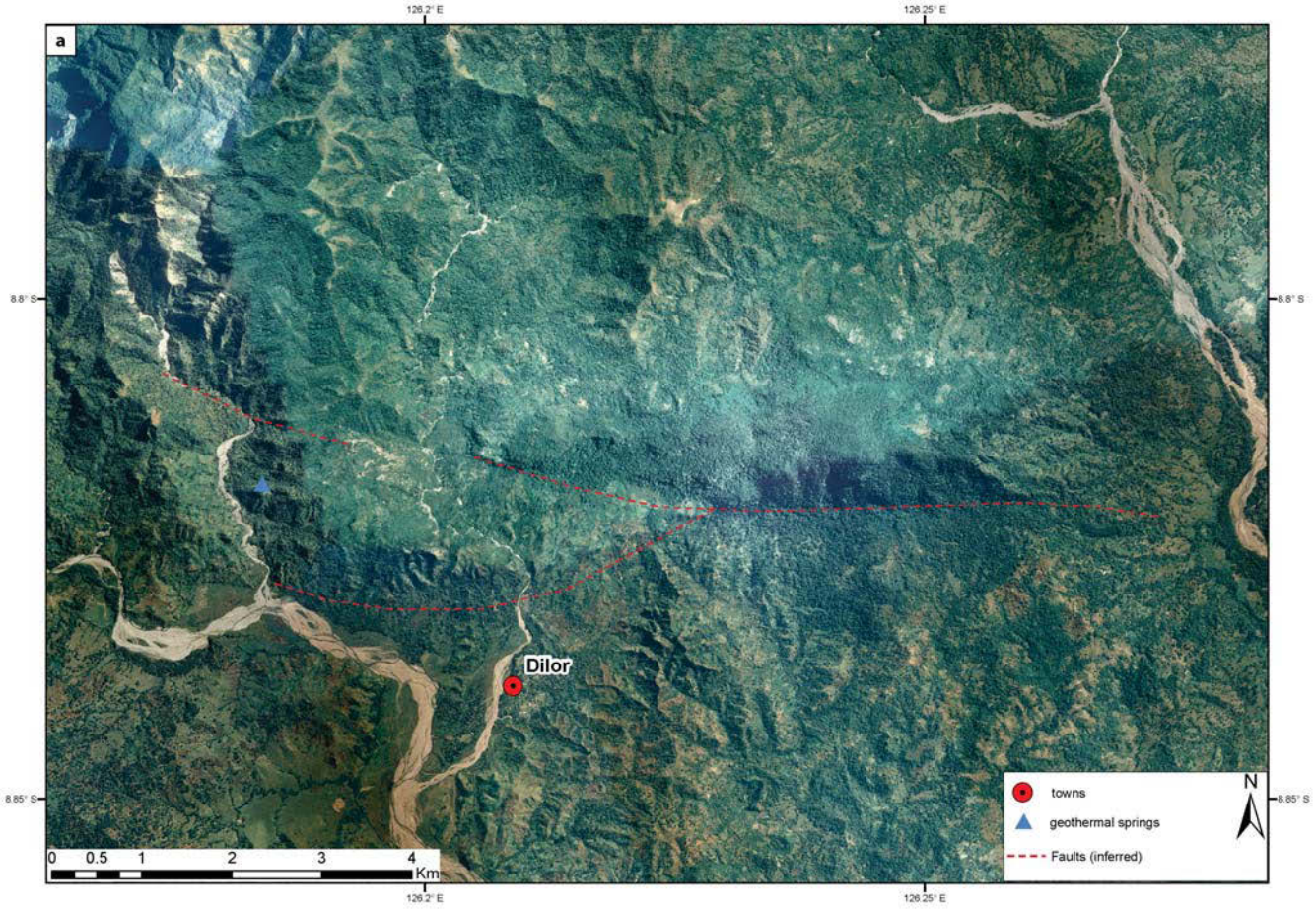
a
126.2° E
126.25° E
8.8° S
8.85° S
Dilor
towns
geothermal springs
Faults (inferred)
N
0 0.5 1 2 3 4
Km

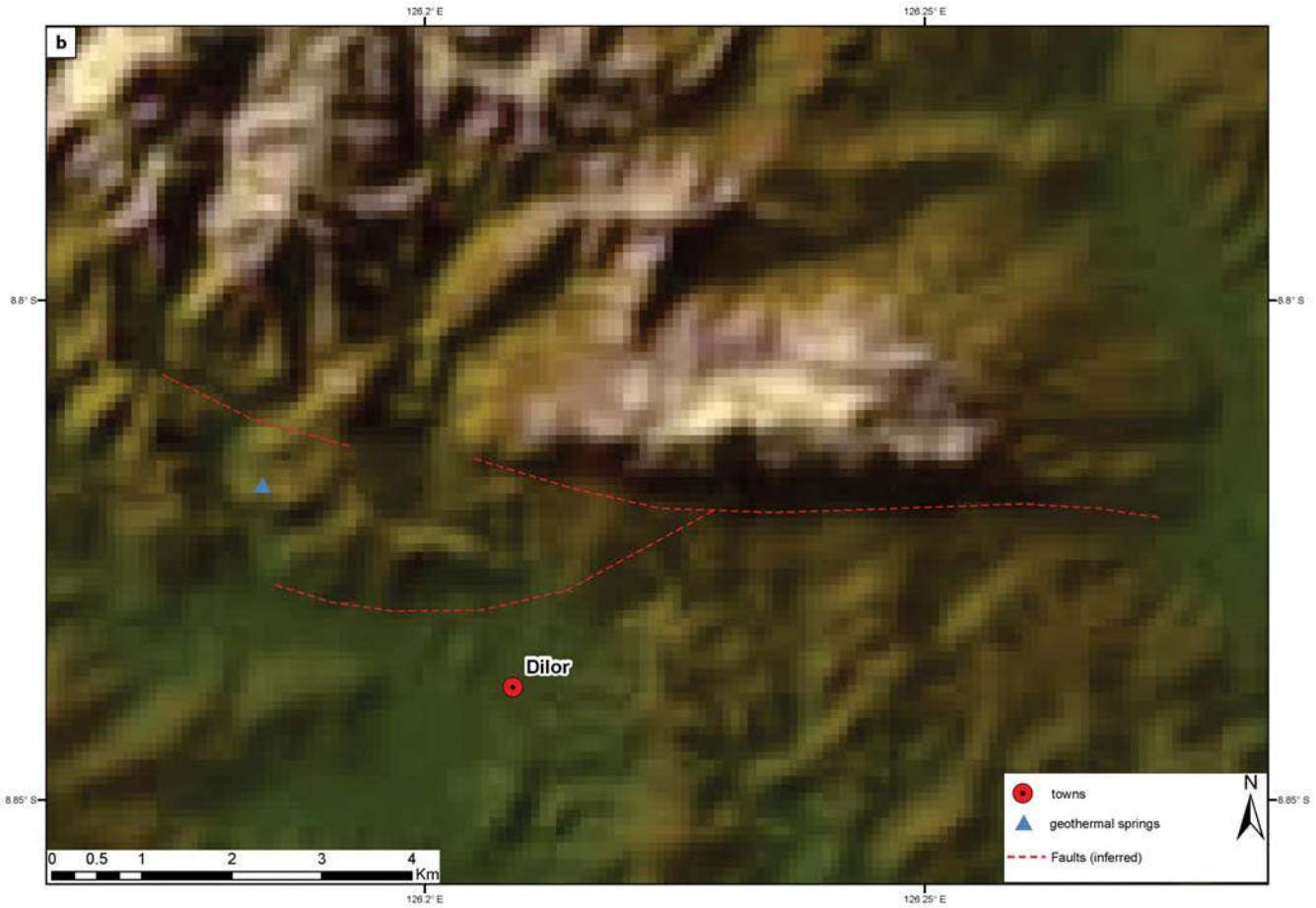
b
126.2° E
126.25° E
8.8° S
8.85° S
Dilor
towns
geothermal springs
Faults (inferred)
N
0 0.5 1 2 3 4
Km

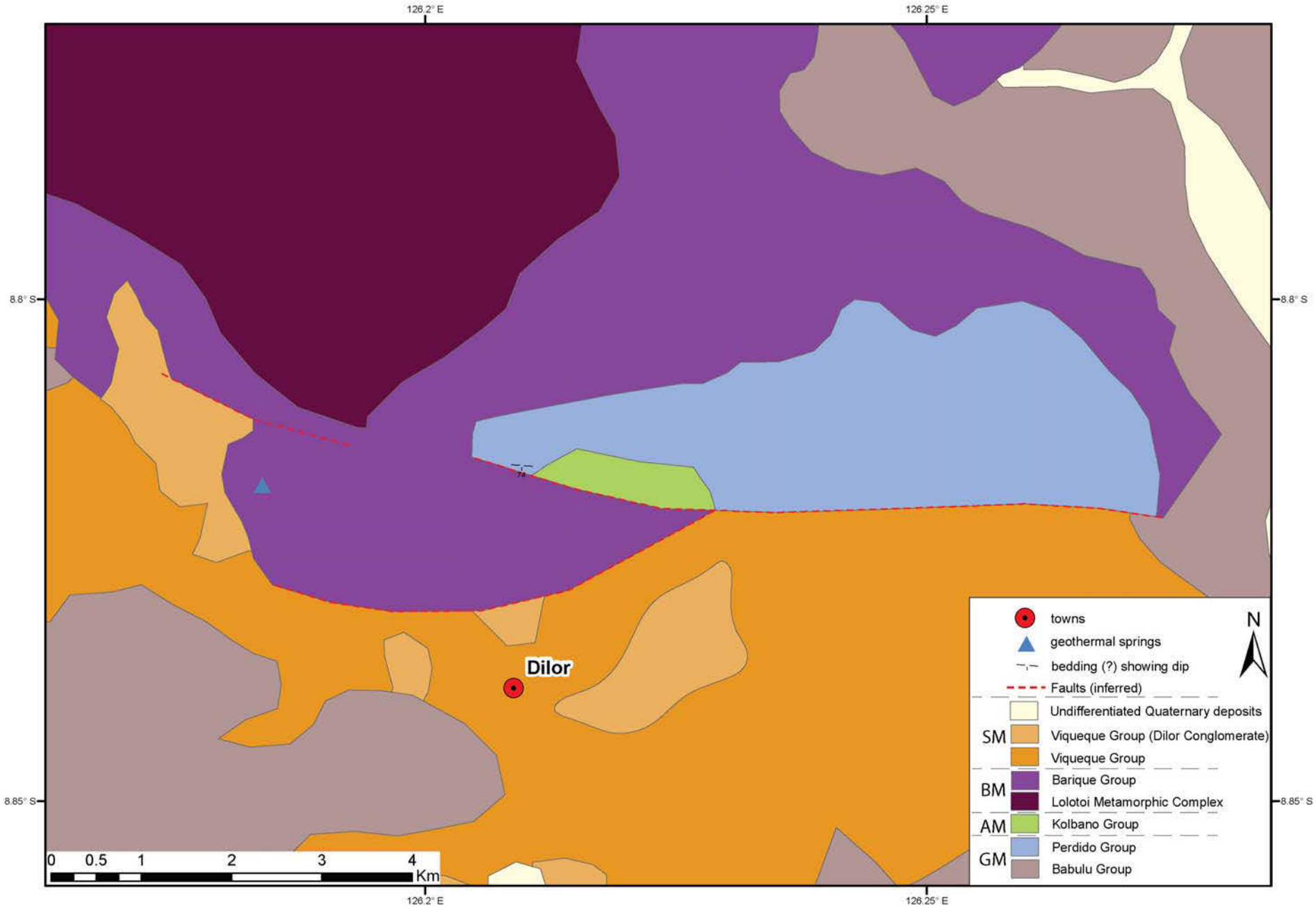
126.2° E
126.25° E
8.8° S
8.85° S
Dilor
74
towns
geothermal springs
bedding (?) showing dip
Faults (inferred)
Undifferentiated Quaternary deposits
SM
Viqueque Group (Dilor Conglomerate)
Viqueque Group
BM
Barique Group
Lolotoi Metamorphic Complex
AM
Kolbano Group
GM
Perdido Group
Babulu Group
N
0 0.5 1 2 3 4
Km

4.2.1 Distribution of stratigraphy

Sampling at Mount Bibileu was restricted to the high cliffs at Mount Bibileu's western end and the lowlands below. Lithologies sampled from the cliffs comprise either Jurassic Perdido Group limestones of the Gondwana Megasequence, or Eocene Kolbano Group Limestones of the Australian Margin Megasequence (**Fig. 101**). No reliable bedding surfaces were observed along the cliff faces. Although sampling was limited it may be reasonable to assume that like the nearby Ossu fatus, Perdido Group and Kolbano Group limestones also dominate most of the high, central regions of Mount Bibileu. Lithologies sampled from the foothills below the high cliffs at the western end of Mount Bibileu comprise Banda Megasequence lithologies – either Barique Group volcanics and sandstones or Dartollu Group limestones (**Fig. 101**). Barique Group rocks have also previously been mapped encircling the northern limits of the fatu (Partoyo *et al.* 1995). The Plio-Pleistocene Viqueque Group (Synorogenic Megasequence) has previously been mapped extending up from the Viqueque basin in the south to abut Mount Bibileu along its southern scarp (Audley-Charles 1968; Partoyo *et al.* 1995). Although the Viqueque Group was not observed at the very western end of the fatu, this study has found no evidence to contradict this relationship elsewhere.

Overall, the distribution of stratigraphy at Mount Bibileu appears similar to that of the Ossu fatus. High, central regions are dominated by Gondwana and Australian Margin Megasequence limestones (Perdido Group and Kolbano Group), with Banda Megasequence lithologies found around the lower foothills, and Synorogenic Megasequence lithologies in the lowlands, in places extending up to the steep, bounding cliffs of the fatu.

4.2.2 Faulting

The most prominent structural feature of Mount Bibileu is its southern scarp, which extends uninterrupted for approximately 7 km along the southern edge of the fatu (**Fig. 100**). This fault scarp strikes 090° along the eastern two thirds of the fatu, before curving slightly to strike approximately 100° at the western end of the fatu. The 100° striking western section juxtaposes the Gondwana and Australian Margin Megasequence limestones of the fatu (Perdido Group and

Kolbano Group) against the Banda Megasequence lithologies of the foothills. The main, 090° oriented length of the fault juxtaposes the Australian affinity limestones of the fatu against recent, Plio-Pleistocene Viqueque Group synorogenic deposits.

Although obvious on a DEM or aerial photograph, outcrop evidence of the main Bibileu Fault was not observed in the field by the limited mapping of this study. The very linear nature of the fault trace implies that it is a steeply dipping fault. In his Timor Oil Report on Geology, Audley-Charles (1962) observed the Bibileu Fault to be a steep-angled major reverse fault where it juxtaposes the fatu limestones against the Viqueque Group. This is consistent with steep-angled reverse faults observed by this study that bound the nearby Ossu fatus.

4.2.3 Folding

No evidence of folding was observed at Mount Bibileu, perhaps due in part to the limited amount of work in this region.

4.2.4 Melange zones, petroleum seeps and geothermal springs

Geothermal springs are present approximately 2 km west of Mount Bibileu, along strike of the main Bibileu Fault (**Fig. 101**). We were guided to within a few hundred metres of the springs; however we were not allowed to view their source due to local cultural sensitivities. Runoff from the springs was very warm to the touch, and likely much hotter at the source. Lawless *et al.* (2005) described springs from very near to this locality, which he was also not able to reach (Laclota Springs). However, he describes reports of the Indonesian Army using these springs to cook noodles, implying a temperature of at least 60°C. These springs are most likely related to meteoric water circulating through the Bibileu Fault, and like other geothermal springs in Timor, implies that this fault extends to significant depths.

4.2.5 Structural model

Although limited structural data was gathered during the brief time spend at Mount Bibileu by this study, the fatu appears similar in lithology, stratigraphic distribution and structural style to the nearby Ossu fatus of Mount Mundo Perdido, Mount Laritame and the Builo Range. The fatu

itself comprises the same Perdido Group and Kolbano Group limestones that dominate the high, central parts of the Ossu fatus. The foothills likewise comprise Banda Megasequence lithologies, which are juxtaposed against the Australian affinity rocks of the fatu by high-angle, reverse faults. It may be reasonable to assume that Mount Bibileu, at least at its southern margin, has been exhumed along a high angle, probably transpressional fault, producing uplift similar to the pop-up structures at Mount Mundo Perdido, Mount Laritame and the Builo Range. However, much more extensive mapping would need to be carried out in order to create a well-defined structural model.

4.3 The Paitchau Range and Lake Iralalaru

The eastern tip of Timor Island is dominated by the Lautem Plateau, a flat expanse comprising over 500 km^2 of Pleistocene Baucau Limestone (**Fig. 84**) and younger overlying sediments, which now lie approximately 400-500 m above sea level (**Fig. 86**). The south-eastern edge of the Lautem Plateau abuts the Paitchau Range, which comprises a series of two to three long narrow ridges striking approximately 030° for over 10 km (**Fig. 102**). The northernmost ridge closest to the plateau is smallest, and the ridges increase in both length and height moving southeast across the range. All of the highest peaks of the Paitchau Range, situated at over 900 m above sea level, occur on the south-easternmost ridge. The ridges appear to dip northwest, having gentler slopes on their north-western sides and steeper, more irregular scarps on their southeast. At the north-eastern end of the Paitchau Range the ridges become discontinuous and are separated into a series of hills.

Lake Iralalaru is situated in the eastern end of the Lautem Plateau, less than 2 km northwest of the Paitchau Range (**Fig. 102**). It forms an almost perfectly rhomboidal east-northeast striking basin, slightly elongate in the southwest-northeast direction. Its western and eastern edges measure approximately 7 km and strike at 020°-030°, while its northern and southern edges measure approximately 9 km and strike at 070°. In the dry season the lake is reduced to a narrow, elongate, spindle-shaped water body situated in the basin's centre, approximately 2 km

long and just a couple of hundred metres wide, with an S-shape that mirrors the asymmetry of the larger basin.

4.3.1 Distribution of stratigraphy

The ridges of the Paitchau Range comprise indurated Triassic limestones of the Bandeira Group (Gondwana Megasequence), most likely with units of less indurated mudstones, muddy wackestones and sandstones occupying the recessive valleys between them (**Chapter 3.6 The Paitchau Range**), (**Fig. 103**). Bedding in the massive limestones is difficult to determine in the field but a Google Earth DEM shows that the ridges appear to be dipping northwest, towards the plateau (**Fig. 104**). Aitutu Group mudstones and limestones (**Fig. 84**) have previously been mapped at the Paitchau Range (Audley-Charles 1968; Partoyo *et al.* 1995). This study agrees with these interpretations in some of the lower areas along the edges of the range, particularly around its north-eastern and south-western ends, but suggests that the Aitutu Group may have gradational contacts with the Bandeira Group limestones that comprise the main ridges of the range (**Chapter 3.6 The Paitchau Range**). Although not sampled by this study, Permian Cribas Group rocks (**Fig. 84**) have been mapped extensively along the south-eastern edge of the Lautem Plateau by previous authors, surrounding the Paitchau Range on all but its north-western edge (Audley-Charles 1968; Partoyo *et al.* 1995).

The Lautem Plateau (**Fig. 86**) abuts the Paitchau Range along the length of its north-western edge. The Plateau consists of a series of uplifted Baucau Limestone coral reef terraces, deposited in shallow water during the Pleistocene and now situated 400-500 m above sea level.

Fig. 102 → (a) Aerial photo of the Paitchau Range and Lake Iralalaru with interpreted structure. (b) Digital elevation model of the Paitchau Range and Lake Iralalaru with interpreted structure. Faults shown with solid lines have been observed and measured in the field; those shown with dashed lines have been interpreted from aerial photographs.

Fig. 103 →→ Interpreted geological map of the Paitchau Range and Lake Iralalaru, showing the distribution of lithologies and main geological structures. Geology outside of mapped areas is modified after Partoyo *et al.* (1995) using aerial photographs. SM = Synorogenic Megasequence, GM = Gondwana Megasequence. Faults shown with solid lines have been observed and measured in the field; those shown with dashed lines have been interpreted from aerial photographs. Strike and dip of bedding is shown where measured.

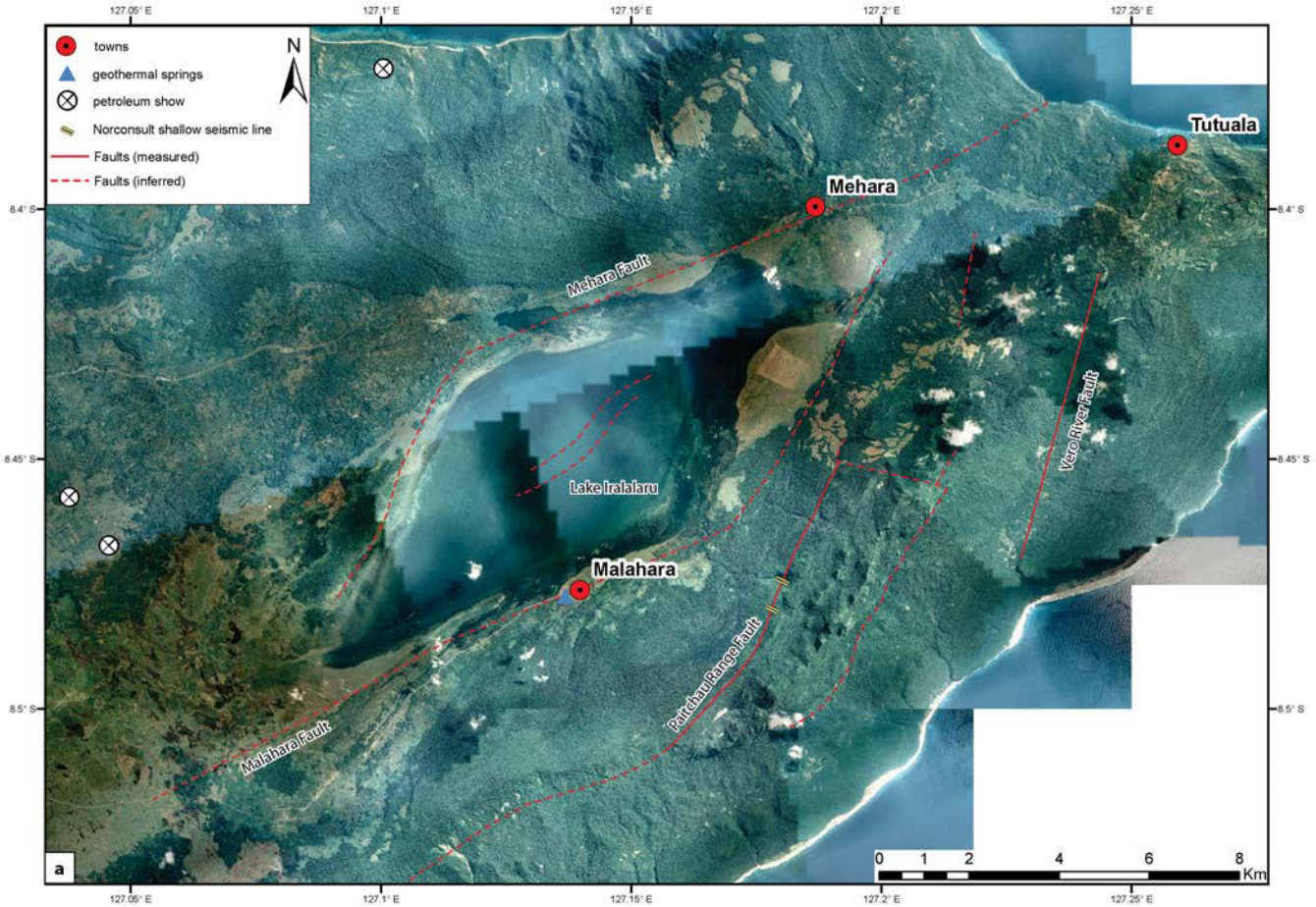
towns
geothermal springs
petroleum show
Norconsult shallow seismic line
Faults (measured)
Faults (inferred)
N
Tutuala
Mehara
Malahara
Lake Iralalaru
Mehara Fault
Vero River Fault
Paitchau Range Fault
Malahara Fault
127.05° E
127.1° E
127.15° E
127.2° E
127.25° E
8.4° S
8.45° S
8.5° S
0 1 2 4 6 8 Km
a

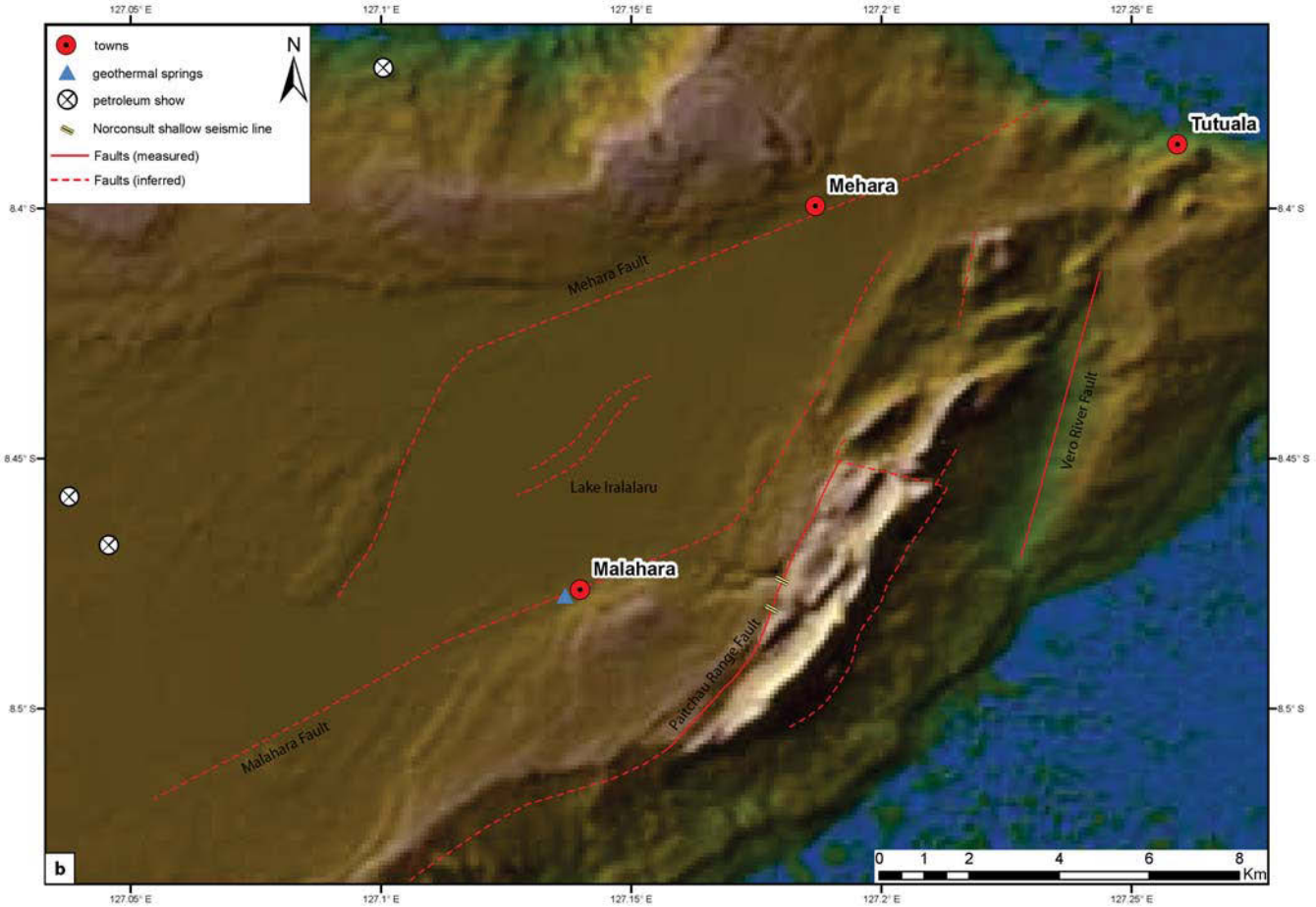
towns
geothermal springs
petroleum show
Norconsult shallow seismic line
Faults (measured)
Faults (inferred)
N
Tutuala
Mehara
Malahara
Lake Iralalaru
Mehara Fault
Vero River Fault
Paitchau Range Fault
Malahara Fault
127.05° E
127.1° E
127.15° E
127.2° E
127.25° E
8.4° S
8.45° S
8.5° S
0 1 2 4 6 8 Km
b

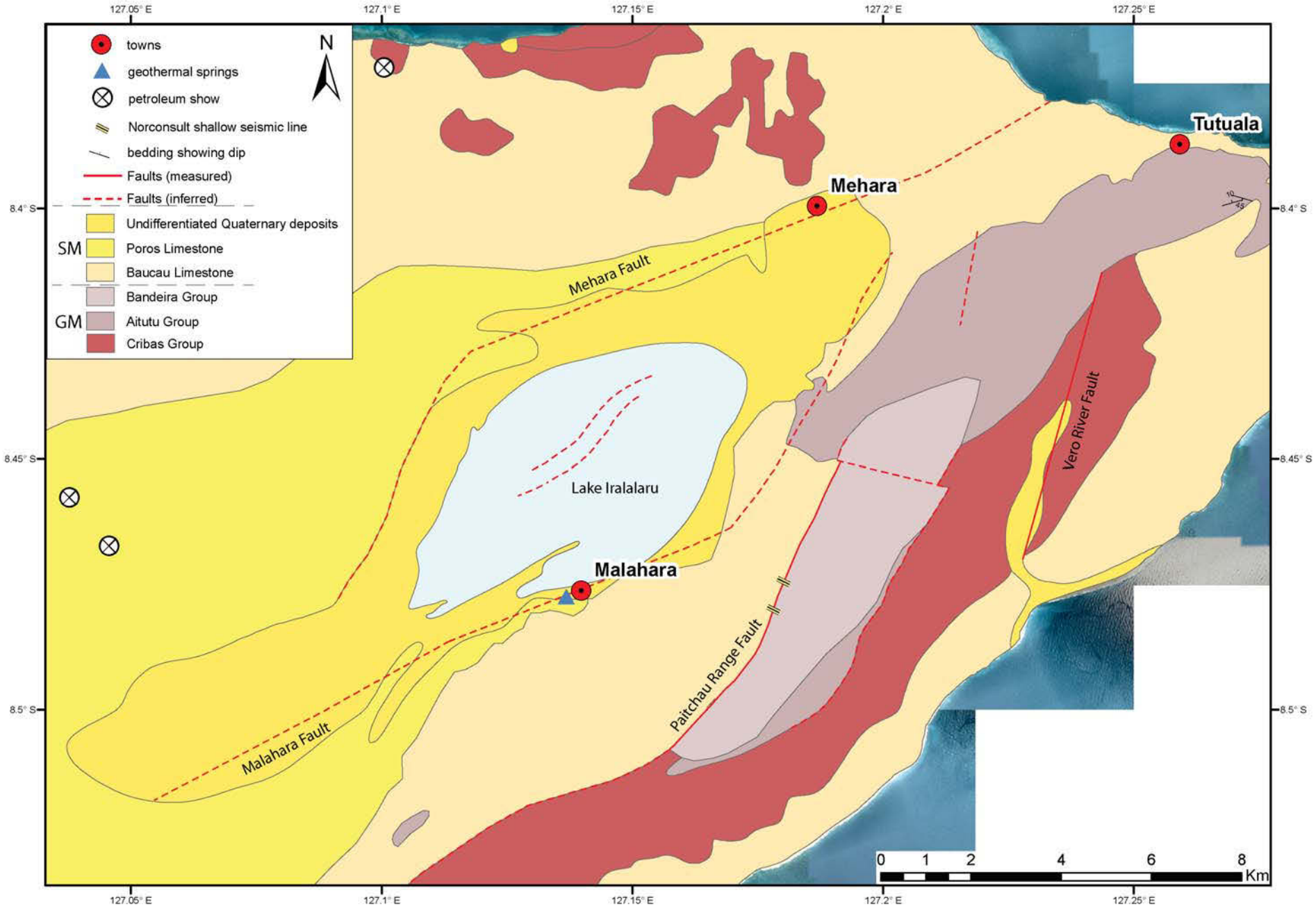
towns
geothermal springs
petroleum show
Norconsult shallow seismic line
bedding showing dip
Faults (measured)
Faults (inferred)
Undifferentiated Quaternary deposits
SM
Poros Limestone
Baucau Limestone
Bandeira Group
GM
Aitutu Group
Cribas Group
N
Tutuala
Mehara
Malahara
Lake Iralalaru
Mehara Fault
Malahara Fault
Paitchau Range Fault
Vero River Fault
127.05° E
127.1° E
127.15° E
127.2° E
127.25° E
8.4° S
8.45° S
8.5° S
0 1 2 4 6 8
Km

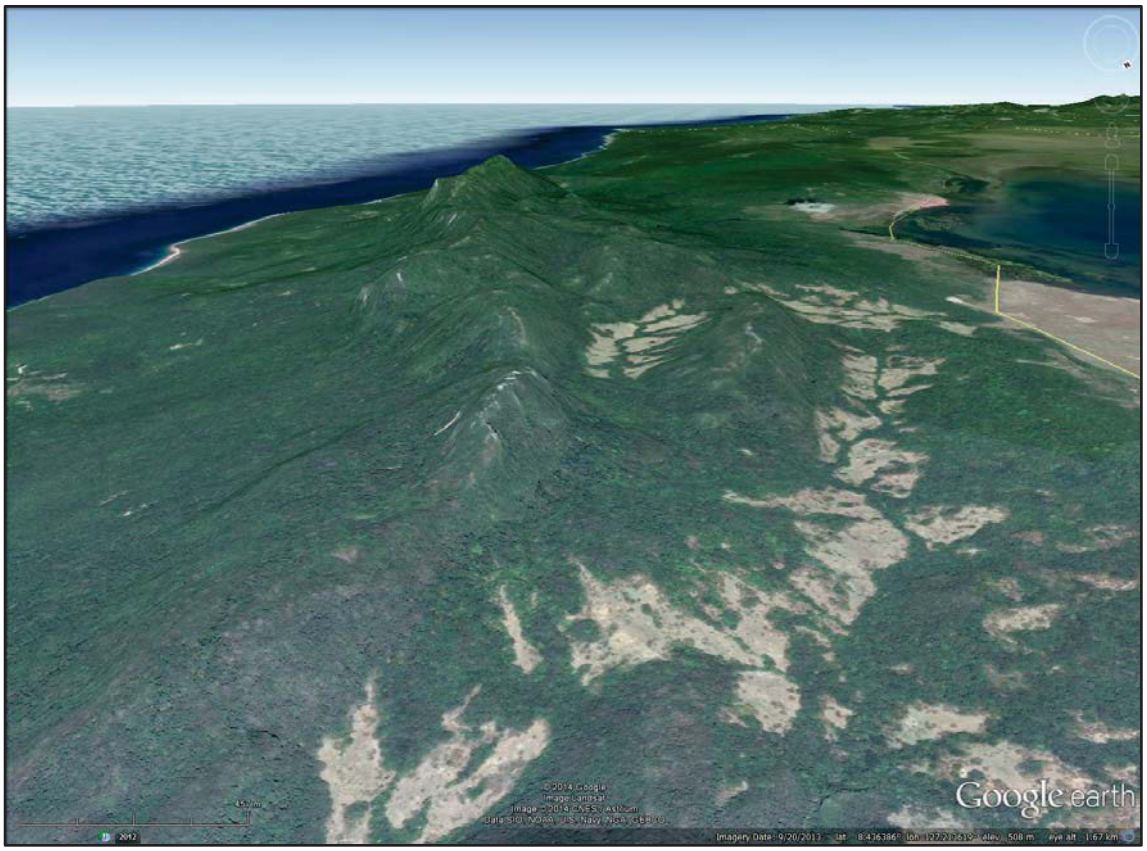

Fig. 104. Aerial photography and digital elevation model from Google Earth, looking southwest along strike of the Paitchau Range, eye altitude = 1.67 km. The Bandeira Group limestone ridges that comprise the Paitchau Range appear to dip northwest, towards the Lautem Plateau (right of frame), displaying steep southeast facing cliffs (left of frame) and more gentle, northwest facing dip-slopes (right of frame).

Younger, Pleistocene to Holocene lacustrine limestones (Poros Limestone of Audley-Charles 1968) and overlying gravels, sands and muds (Suai Formation of Audley-Charles 1968) occupy a large basin in the centre of the southern part of the Lautem Plateau, and are most likely related to the paleo-extent of Lake Iralalaru, which is now confined to the south-eastern end of this basin.

4.3.2 Faulting

Lake Iralalaru displays a striking rhomboidal geometry with unusually linear boundaries inferring structural control. Several regional scale lineaments are evident in aerial photographs and digital elevation models that most likely represent major structures around Lake Iralalaru and the Paitchau Range (**Fig. 102**).

Benincasa *et al.* (2012) proposed that Lake Iralalaru is bound along its northern and southern edges by sinistral normal faults that strike east-northeast, parallel to the long axis of the lake. These northern and southern faults strike 070°, while the western and eastern edges of the lake strike 025°-030° parallel to the Paitchau Range.

The Paitchau Range is bound by major northeast striking lineaments along its north-western and south-eastern edges, parallel to the ridges of the range, and these linear structures may represent steeply dipping faults. The north-western structure, striking 025°, now juxtaposes the synorogenic Pleistocene Baucau Limestone of the Lautem Plateau against the older Gondwanan Megasequence rocks of the Paitchau Range, and may be interpreted as a northwest dipping normal fault. The south-eastern lineament is sub-parallel, striking approximately 030°, and may represent a similar, southeast dipping normal fault, exhuming the Paitchau Range as a horst block between normal faults on either side. Alternatively, this lineament may be due to lithological differences between the indurated Triassic limestones of the Paitchau Range and underlying mud dominated Permian units. At the north-western end of the Paitchau Range the ridges of the range are offset to the left along an east-southeast striking lineation (**Fig. 102**). This discontinuity and offset may be interpreted as high angle fault striking approximately 115°, accommodating left-lateral strike-slip movement.

At the Paitchau Range, limited structural data was gathered in the field by this study due to difficulties in access during the 2010 field season, and field data for this remote area of Timor is rare in the literature. However, some reconnaissance mapping was completed by a Norwegian consultancy around the Paitchau Range in 2003/2004 as part of the pre-feasibility study for a proposed Hydropower Project in the area (Norconsult 2006). The Norconsult study also included a small number of boreholes drilled to gather geotechnical data, and some shallow seismic surveys. Norconsult (2006) field evidence supports the interpretation that the Paitchau Range is bound by steeply-dipping southwest-northeast striking normal faults. Fault planes associated with the north-western normal fault were observed in the field, striking 023°and dipping 60° northwest (Norconsult 2006). Related damage zones are noted within several drill holes (slickensides and breccia) although drill hole locations and depths are not given. Two

shallow seismic lines on the north-western side of the Paitchau Range also show steep scarps in the interpreted bedrock profile and corresponding low velocity zones where they intersect the interpreted north-western fault trace (**Fig. 105**). Norconsult (2006) also interprets a southeast dipping normal fault along the south-eastern boundary of the Paitchau Range, although does not describe field evidence for this fault. Two kilometres southeast of the south-eastern Paitchau normal fault Norconsult (2006) describes the Vero normal fault, which strikes 015°, sub-parallel to the Paitchau normal faults, from the south coast of Timor Island over 6 km inland (Norconsult 2006). The Vero River drains along the fault trace and fault scarps are observed at the river in the field (Norconsult 2006). Norconsult (2006) also contains observations of two smaller-scale dextral strike-slip faults, one on the northern and one on the southern side of the Paitchau Range.

Orientations and detailed localities of these faults however are not provided, and the present study was unable to verify these faults in the field. Norconsult (2006) reaches a similar conclusion to Benincasa *et al.* (2012) regarding Lake Iralalaru as being bound by linear faults along its northern and southern edges. They name the northern and southern faults the Mehara Fault and Malahara Fault respectively, describing the faults as forming a graben structure that controls the occurrence of the lake. This study observed a large scarp in the Baucau Limestone on the south side of Lake Iralalaru, approximately 10-20 m in height, which extends for several kilometres and corresponds with the trace of the Malahara Fault (**Fig. 106**).

4.3.3 Folding

Some of the older literature (e.g. Audley-Charles 1965b) interprets a northeast striking syncline extending through the Lautem Plateau, with the fold axial trace passing through the long axis of Lake Iralalaru, and the Paitchau Range representing the southern limb of the fold. However there is little direct evidence to support such an interpretation, aside from the north-western dip of the Paitchau Range. Given the highly unusual rhomboidal geometry and linear banks of Lake Iralalaru, along with the evidence for large scale faulting in the area, it is more likely that recent

brittle deformation is responsible for the distinctive morphology of the Paitchau/Iralalaru region.

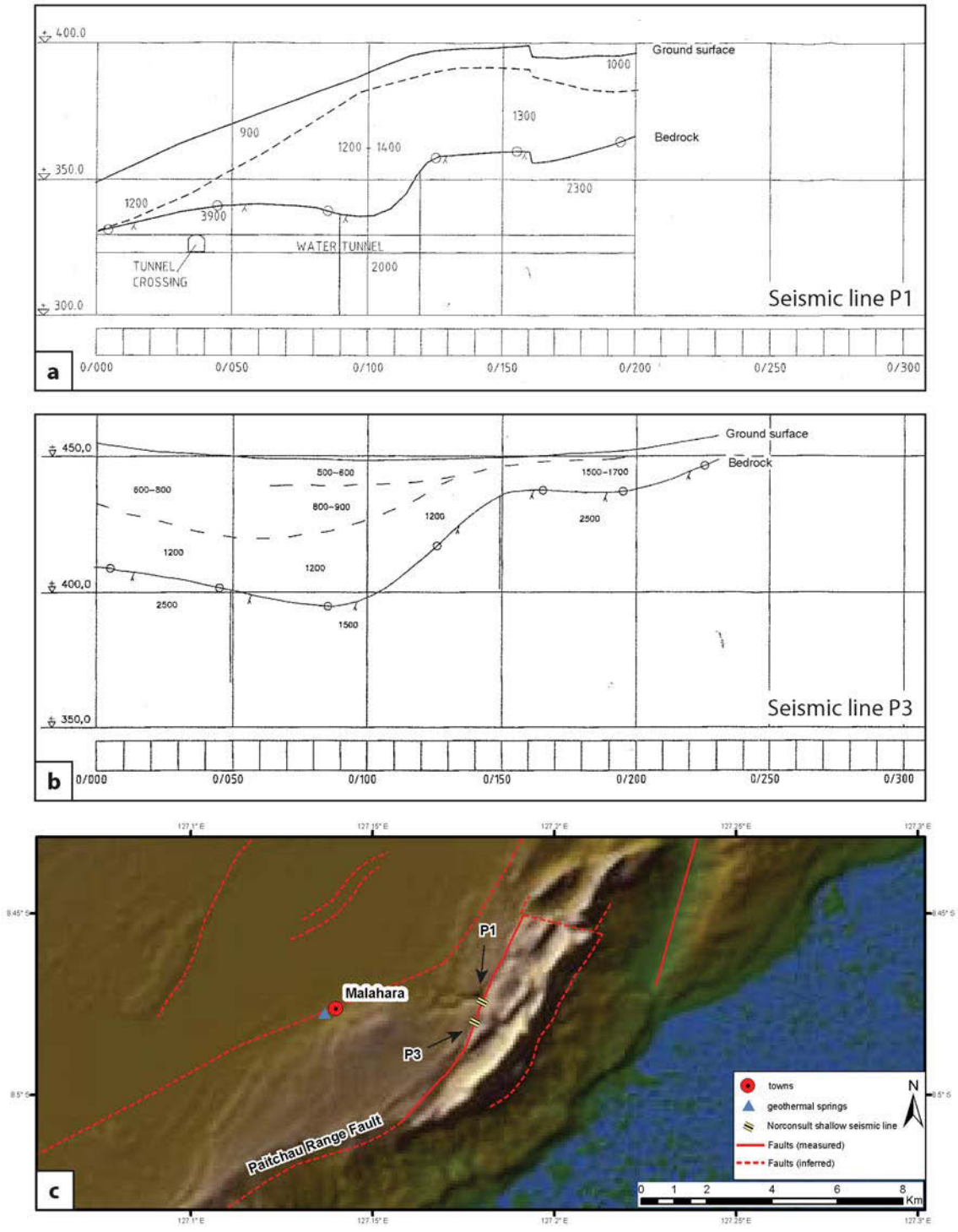

Fig. 105. Norconsult (2006) shallow seismic lines P1 (a) and P3 (b) both cross the interpreted trace of the Paitchau Range Fault (c). Vertical and horizontal scales are in metres with velocity zones in the subsurface shown in ms^{-1}. Both seismic sections show steep scarps where they cross the interpreted fault trace. Section P1 also shows a zone of low velocity below the scarp, which may be associated with a fault zone.

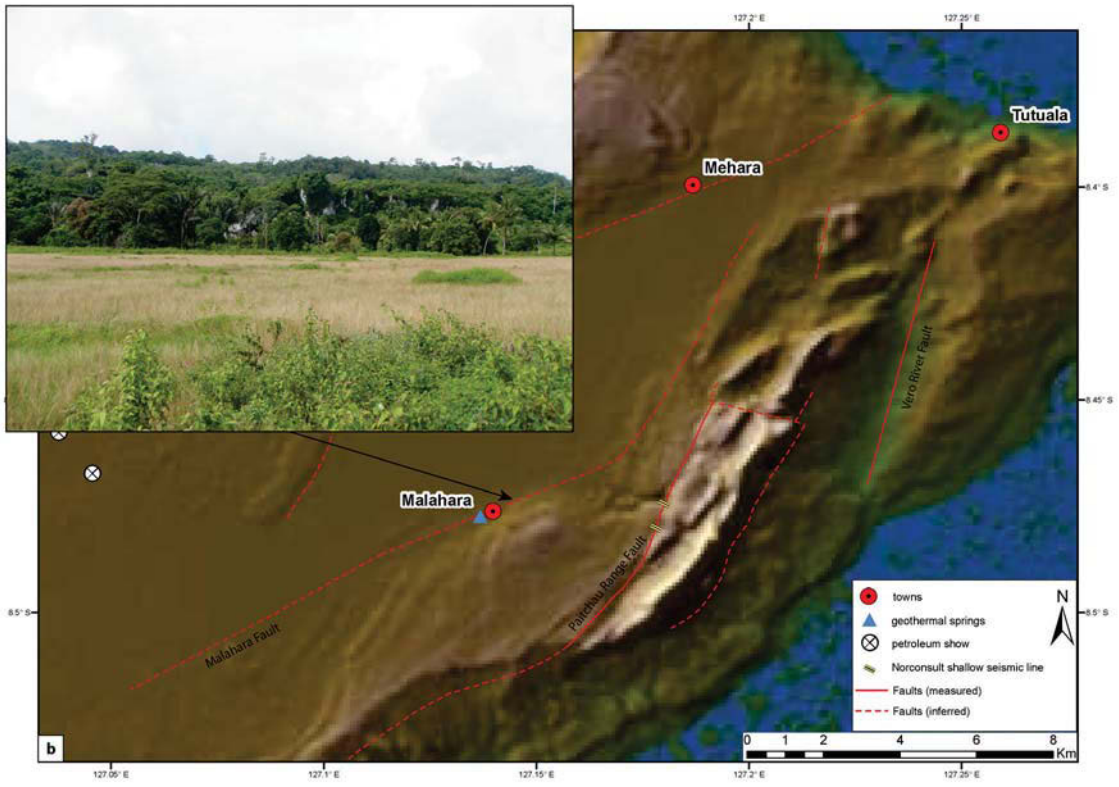

Fig. 106. Facing south, a 10-20 m high scarp developed within Pleistocene Baucau limestone situated on the southern edge of the Lautem Plateau, at AB405. The scarp extends for several kilometres and corresponds with the interpreted trace of the Malahara Fault, seen here on a digital elevation model.

4.3.4 Melange zones, petroleum seeps and geothermal springs

No tectonic melange zones were encountered during fieldwork in the area, and melange has not been mapped in this region in previous literature.

Two small oil seeps are located 7 km west of Lake Iralalaru (Audley-Charles 1968), which were reported to Audley-Charles by Leme (pers. comm. 1962). They consist of oil stains and odours in Pleistocene Poros Limestone, and are most likely sourced from underlying Triassic or Permian formations. These seeps occur along strike of the Mehara fault (**Fig. 103**), which bounds the northern edge of the lake, and may be exploiting a continuation or splay of this fault zone as a conduit to the surface.

Norconsult (2006) reported springs in Malahara, located on the Malahara Fault that bounds the southern edge of the lake. It is not specified whether these are geothermal springs or otherwise,

but they are described as supporting evidence for the presence of the Malahara Fault in this location. The presence of springs and seeps associated with faults around Lake Iralalaru supports the interpreted fault locations and suggests, particularly in the case of the seeps, that these are deep structures that penetrate the thickness of the Lautem Plateau.

4.3.5 Structural model

Lake Iralalaru comprises a morphologically distinctive rhomboidal basin within a plateau of synorogenic limestones Pleistocene and younger in age (**Fig. 103**). The lake is bound by large, linear faults along its northern and southern edges which strike 070° and are associated in places with springs and seeps. Adjacent and parallel to the eastern edge of Lake Iralalaru is the Paitchau Range, comprising a horst block of northwest dipping Gondwana Megasequence limestones. The Paitchau Range is juxtaposed against the Lautem Plateau and Lake Iralalaru by a northwest dipping normal fault striking 025°, parallel to the eastern edge of the lake basin, and is surrounded by a number of other faults of similar strike to its north and east.

After finding evidence for large scale left lateral strike-slip deformation parallel to Timor Island at Mount Mundo Perdido, Benincasa *et al.* (2012) suggested that Lake Iralalaru may represent a pull-apart basin formed at a releasing fault stepover within a related strand of a plate-boundary parallel left-lateral strike-slip fault system. This was based on a strong resemblance to pull-apart structures developed at releasing fault stepovers in analogue models (Dooley & McClay 1997) and documented strike-slip systems elsewhere (Mann 2007).

Analogue modelling of transtensional pull-apart basins by Wu *et al.* (2009) provides further evidence supporting such a structural model at Lake Iralalaru. Wu *et al.* (2009) uses scaled sandbox models to investigate the 4D evolution of pull-apart basins formed above underlapping releasing stepovers in strike-slip fault systems. In an experimental model of a 30° underlapping releasing fault stepover, pure strike-slip motion (i.e. basement displacement parallel to the trace of the PDZ) results in the formation of a basin with a geometry identical to that observed at Lake Iralalaru (**Fig. 107**).

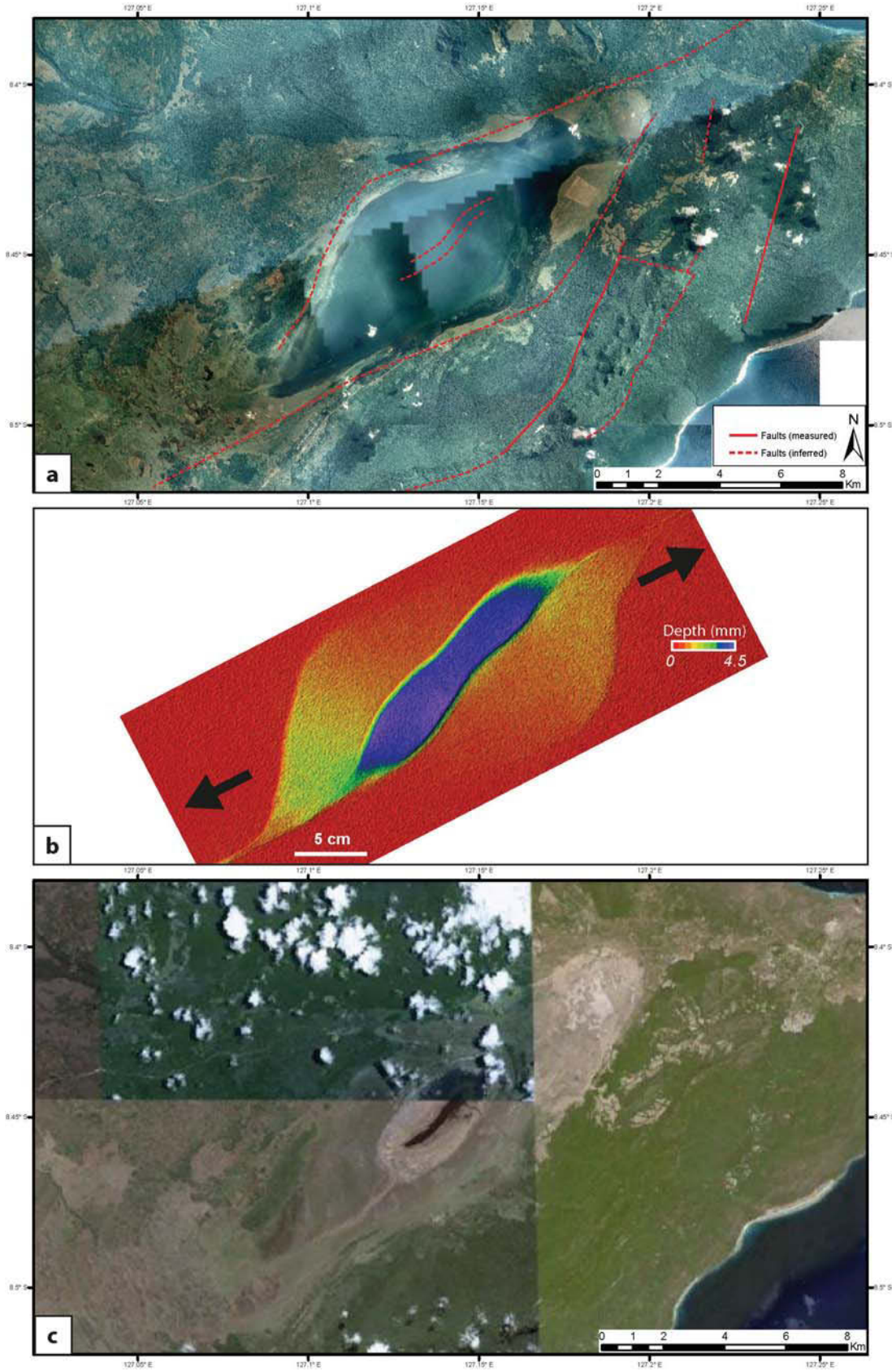

Fig. 107 (a) Aerial photo of Lake Iralalaru in the wet season, with interpreted fault architecture. (b) Image of a transtensional pull-apart basin developed in a scaled sandbox model of a 30° underlapping releasing fault stepover experiencing pure strike-slip, modified after Wu *et al.* (2009). The geometry of the structure is identical to that observed at Lake Iralalaru. (c) Aerial photo of Lake Iralalaru in the dry season, taken from Google Earth, at the same scale as image in (a). A deep, narrow and elongate depression in the centre of the larger, rhomboidal basin is evident in both the analogue model and aerial photograph, at the same orientation.

Both the modelled basin and the Lake Iralalaru basin are flat-bottomed rhomboids, slightly longer than they are wide. The modelled basin is bound by steeply dipping (80–90° dip) oblique-extensional faults on each side subparallel to its long axis, while Lake Iralalaru is similarly bound along its northern and southern edges by the Mehara and Malahara faults. In the model these oblique-extensional faults curve towards the PDZ on the opposite side of the stepover, to become slightly shallower dipping (35–65° dip) normal faults which bound the short ends of the basin, and which intersect the PDZs here at an acute angle of approximately 50°. A similar normal fault bounds the eastern end of Lake Iralalaru basin along the north-western edge of the Paitchau Range. Oriented at 025°, this fault forms an approximately ~45° acute angle with the 070° striking Mehara and Malahara faults, very similar to the 50° angle evident in the sandbox model. Fault systems comprising a number of subparallel, sometimes terraced, oblique-extensional faults are common on the margins of pure strike-slip pull-apart basins (Wu *et al.* 2009) and this is possibly evident in the number of subparallel 020°-030° striking faults around the Paitchau Range.

Directly above the stepover in the centre of the basin, the sandbox model produces a pair of long, linear, oblique-extensional faults with opposing dip polarity which link the PDZs at either end. These faults form a deep, narrow and elongate central graben within the larger, shallower rhomboidal basin, which strikes at approximately 27° oblique to the trace of the PDZs (**Fig. 107b**). An identical feature is visible on aerial photographs of Lake Iralalaru in the dry season, when most of the basin is exposed (**Fig. 107c**). In the centre of the shallow, larger rhomboidal basin is a deep, linear elongate depression which still holds water, striking at approximately 045°, 25° oblique to the Mehara and Malahara faults.

4.4 The Matebian Range

Situated approximately 20 km east of the Ossu fatus, the Matebian Range is one of the largest structural features in East Timor; at over 20 km long it almost bisects Timor Island from the north to south coast (**Figs 86, 108a**). The main part of the range begins to rise from the surrounding land less than 5 km inland of the north coast (**Fig. 108b**), and strikes south-southwest for approximately 20 km, with the high peaks of Matebian Mane (~1500 m) and Matebian Feto (2376) m at the southern end (**Fig. 109**). This main part of the range is 6-7 km wide and displays extremely steep, high scarps along its north-western edge, 700-800 m tall, which extend upwards to the highest points of the range. The topography on the top of the Matebian Range is rugged but generally dips east to southeast (**Fig. 108b**), with the south-eastern edge of the range bounded by much more irregular topography and smaller scarps 200-300 m in height. This main part of the range is mostly bounded along its southern edge by south-southeast facing scarps that strike approximately 070°.

However, at this point the western edge of the range abruptly changes strike from south-southwest to southeast, and a narrow extension of the Matebian Range continues south-eastward towards for a further 11 km (**Fig. 109**). This lesser part of the range comprises a narrow central ridge less than 1 km across, surrounded by irregular topography with more gradual slopes. The height of this southeast-trending extension decreases sharply from over 1900 m in the north where it joins the main part of the Matebian Range, to 1100-1200 m in its middle and south-eastern parts. This extension of the Matebian range terminates less than 4 km inland of the south coast of Timor Island.

Immediately east of the Matebian Range lies the Legumau Range, which begins less than 2 km east of the south-eastern corner of the main section of Matebian (**Fig. 109**). From here it strikes east-northeast for a distance of approximately 20 km, parallel to the south-southeast facing scarps that bound the southern edge of Matebian. At less than 5 km wide the Legumau Range is a long and narrow landform, with a fairly consistent height 1000-1100 m a.s.l. along its length, reaching just over 1200 at its highest point. Legumau is not a fatu-style range; rather it exhibits gentle, hilly topography with gradual slopes to the north and south.

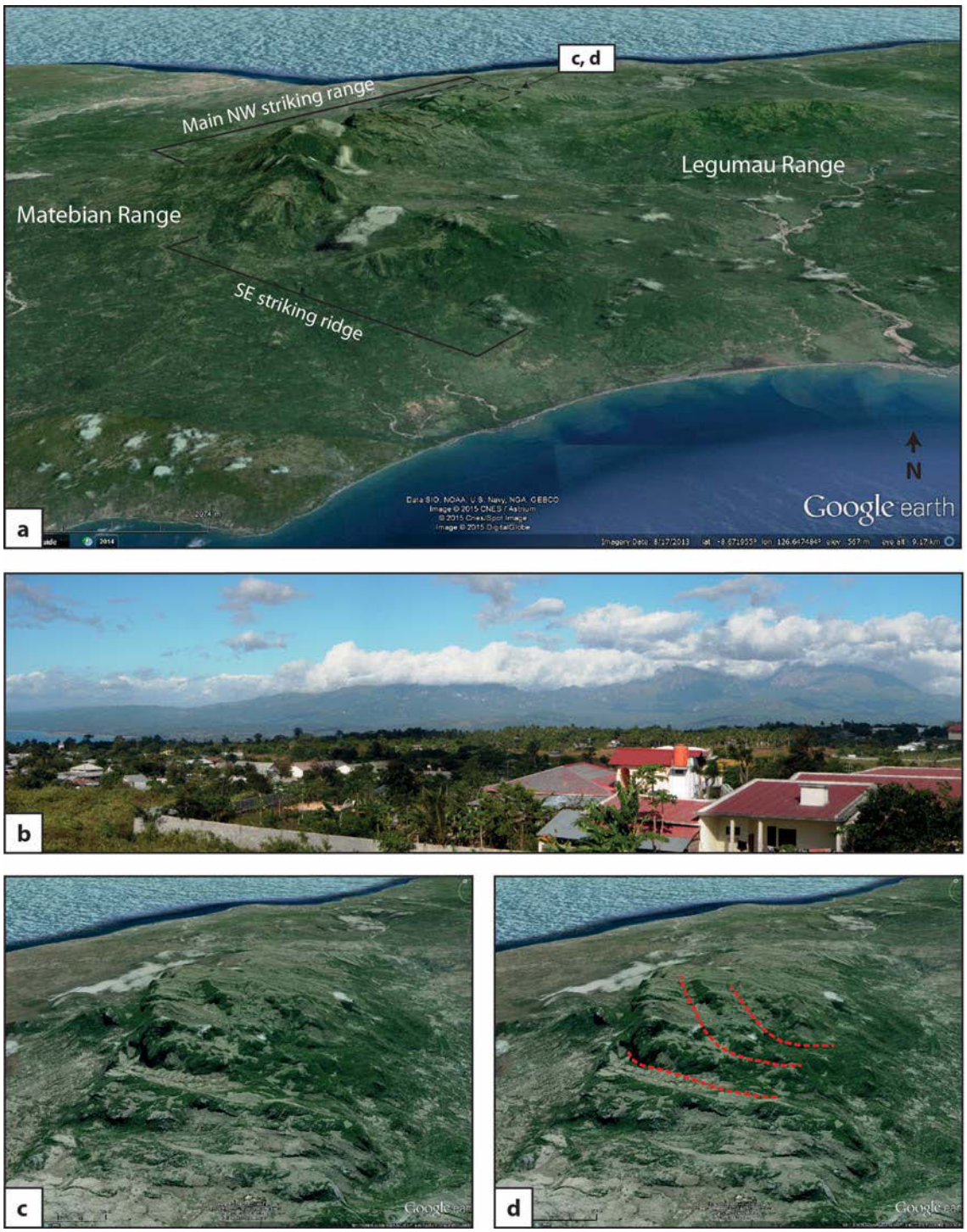

Fig. 108 ↑ (a) Google Earth image of the Matebian Range, facing north (eye altitude 9.2 km). Together, the two main sections of the range nearly bisect Timor Island from south to north. The (b) Profile of the Matebian Range (facing southeast). Beginning near the north coast of Timor Island (left of frame) it extends south-southwest for over 20 km. (b) Uninterpreted and (c) interpreted images from Google Earth, looking north-northeast along strike of the northern part of Matebian Range (eye altitude 3.9 km). At this large scale, bedding appears to dip southeast, displaying steep northwest facing cliffs (left of frame) and more gentle, southeast facing dip-slopes (right of frame).

Fig. 109 → (a) Aerial photo of the Matebian Range with interpreted structure. (b) Digital elevation model of the Matebian Range with interpreted structure. Faults shown with solid lines have been observed and measured in the field; those shown with dashed lines have been interpreted from aerial photographs. Arrows indicate fault striae where observed and measured on major faults.

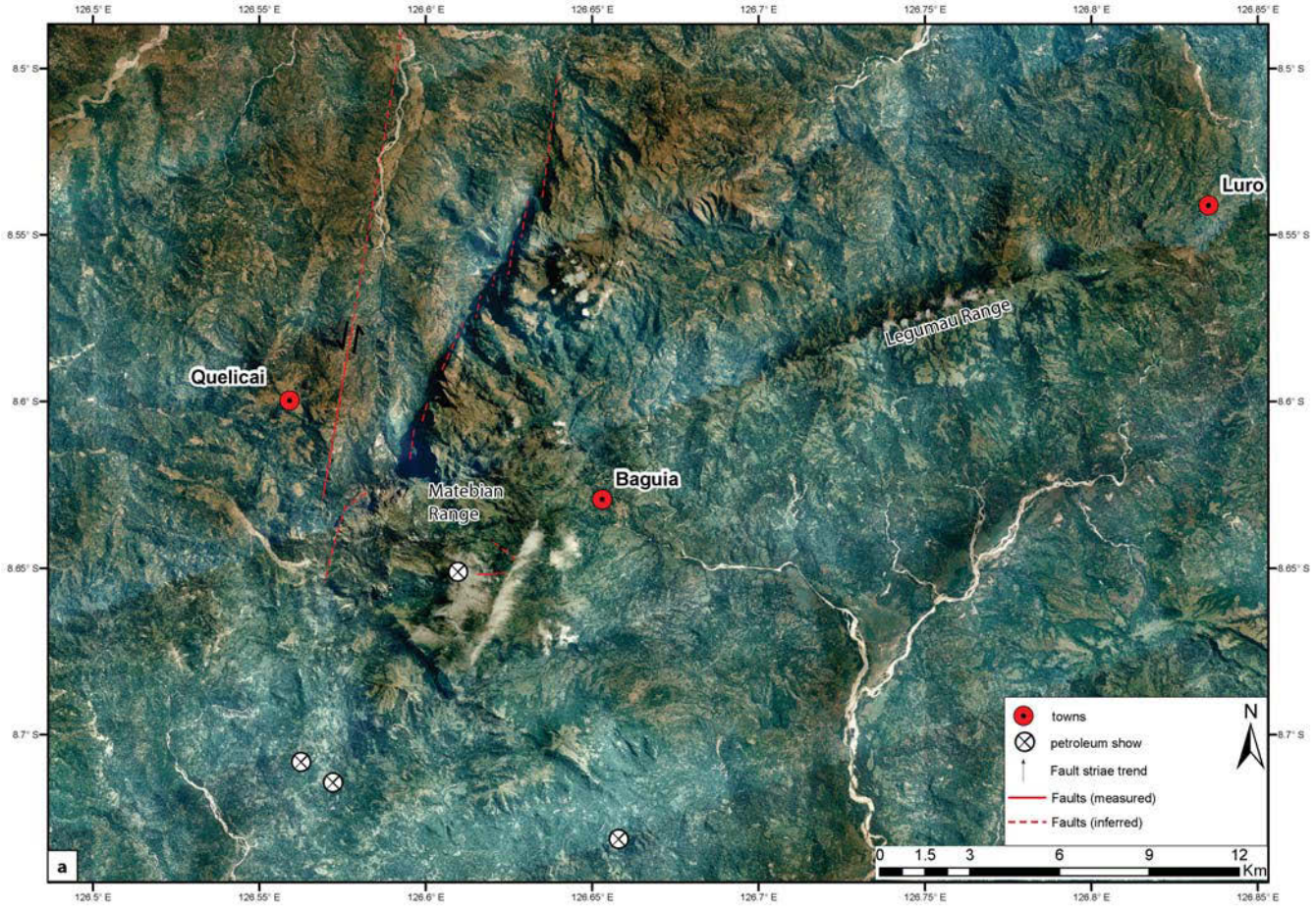
126.5° E
126.55° E
126.6° E
126.65° E
126.7° E
126.75° E
126.8° E
126.85° E
8.5° S
8.55° S
8.6° S
8.65° S
8.7° S
Luro
Legumau Range
Quelicai
Matebian Range
Baguia
towns
petroleum show
Fault striae trend
Faults (measured)
Faults (inferred)
N
0 1.5 3 6 9 12 Km
a

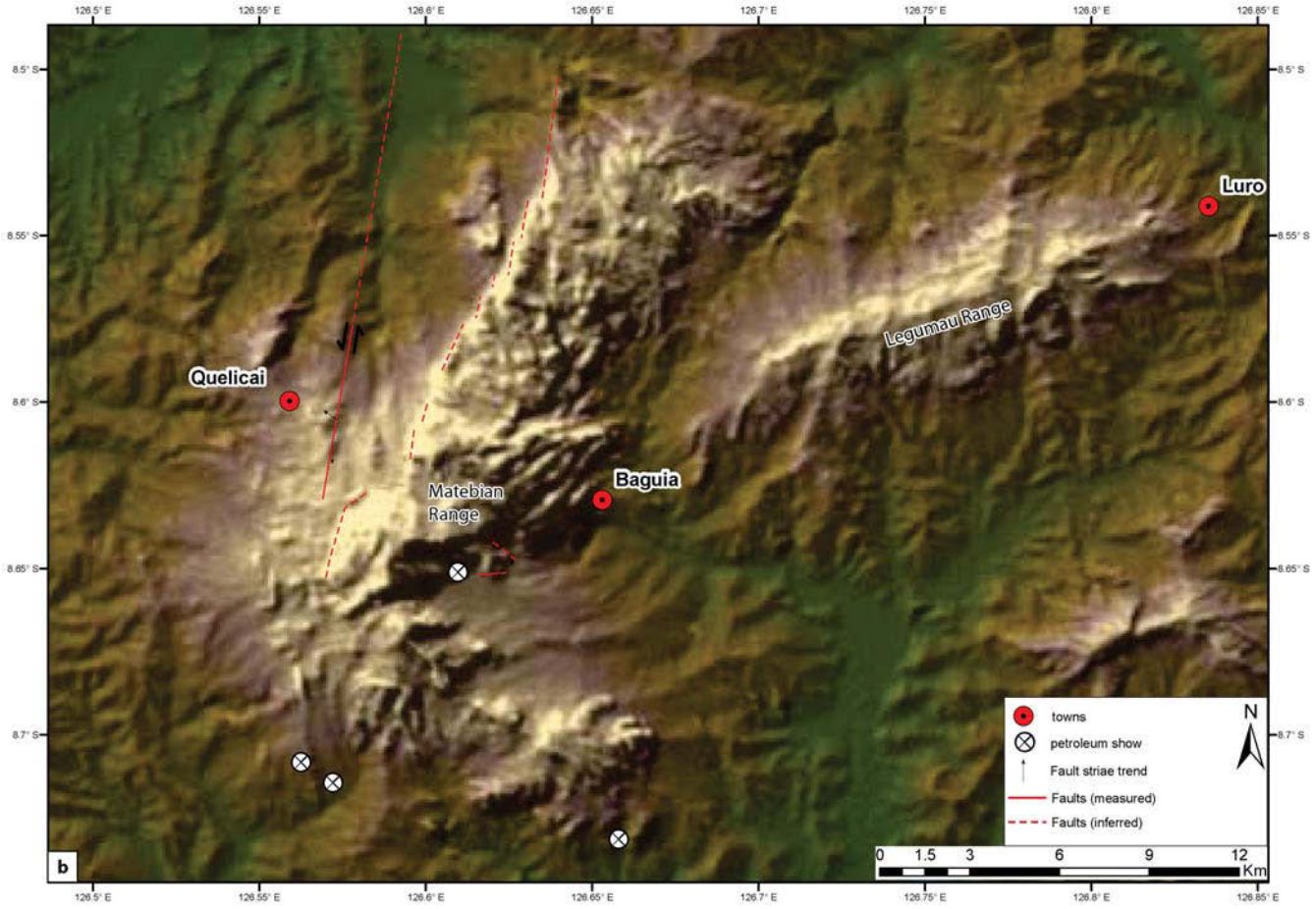
126.5° E
126.55° E
126.6° E
126.65° E
126.7° E
126.75° E
126.8° E
126.85° E
8.5° S
8.55° S
8.6° S
8.65° S
8.7° S
Luro
Legumau Range
Quelicai
Matebian Range
Baguia
towns
petroleum show
Fault striae trend
Faults (measured)
Faults (inferred)
N
0 1.5 3 6 9 12 Km
b

4.4.1 Distribution of stratigraphy

The structurally highest, central regions of the Matebian Range could not be sampled by this study. Unfortunately, little information is found in the literature regarding the composition of the rocks that comprise the high peaks of the range, as access is difficult due to both dangerous terrane and regard for cultural sensitivities (Matebian is a sacred mountain in Timorese culture). As a result, samples at the Matebian Range have often been collected from the lower reaches of the massif under the high cliffs, at around 1200 m or less (e.g. Harris 2006; Standley & Harris 2009). These samples have generally been of Lower Miocene larger foraminiferal limestone (Audley-Charles 1968; Harris 2006), akin to the Booi Group limestones (Banda Megasequence) that comprise the lower cliffs around Mount Mundo Perdido and Mount Laritame.

Rocks comprising the high western cliffs of the Matebian Range have been described as massive grey-weathering, cream-coloured calcilutite with no obvious bedding or fossils (Duffy *et al.* 2013, Harris pers. comm. 2013). This description is far more similar to Australian affinity limestones of the Gondwana or Australian Margin megasequences than it is to fossiliferous limestones of the Booi Group (**Fig. 84**). The high eastern cliffs of the Matebian Range, where sampled by this study, comprise mainly limestones of the Australian Margin Megasequence, with the highest point sampled, a cliff face at ~ 1000 m above sea level, belonging to the Gondwana Megasequence (**Fig. 110**). Pelagites of the Australian Margin Megasequence have previously been mapped in the high, central regions of the Matebian Range by Audley-Charles (1968) (as two small klippen of his 'Borolalo Limestone'), and more recently by Partoyo *et al.* (1995) as extensive but discontinuous patches of outcrop throughout the top of the range (**Fig. 110**). The Australian Margin Megasequence was deposited as a thin (several hundred metres thick) succession unconformably above the Gondwana Megasequence (Haig & McCartain 2007). Digital terrane models from Google Earth appear to show bedding on the top of the Matebian Range dipping east to southeast, particularly in the northern regions of the range (**Fig. 108**). Therefore, if the Matebian Range is covered by a thin, discontinuous veneer of Australian Margin Megasequence limestones it is likely that limestones of the upper part of the Gondwana Megasequence, e.g. the Perdido Limestone, may be exposed in the high western regions of the

range. The Perdido Limestone is consistent with the descriptions of the western cliffs of the Matebian Range given by previous authors (Duffy *et al.* 2013, Harris pers. comm. 2013), and similar relationships of Australian Margin Megasequence pelagites closely associated with, and appearing to overlie, the Perdido Limestone are also present at Mound Mundo Perdido.

Immediately below the western scarp of the Matebian Range this study mapped extensive outcrop of Triassic Aitutu Group mudstones and limestones of the Gondwana Megasequence (**Fig. 110**), with some Permian rocks encountered in overlying float.

Two and a half kilometres west of the scarp is a high-angle north-northeast trending fault which separates Triassic lithologies from the Permian Cribas Group (**Fig. 110**).

Rocks of the Banda Megasequence (the Lolotoi Group, the Barique Group and the Booi Group – previously mapped as 'Cablac Limestone') have been mapped extensively around the edges and lower reaches of the Matebian massif (Audley-Charles 1968; Partoyo *et al.* 1995; Harris 2006; Standley & Harris 2009). These lithologies were not encountered at the Matebian Range by this study; however their mapped extents are consistent with relationships observed at the Ossu fatus, where Banda Megasequence units at low structural levels are juxtaposed against Australian affinity units that comprise the massif, separated by high angle faults.

The Legumau Range has previously been mapped as Permian (Audley-Charles 1968; Partoyo *et al.* 1995) however it was not sampled by this study.

Fig. 110 → Interpreted geological map of the Matebian Range, showing the distribution of lithologies and main geological structures. Geology outside of mapped areas is modified after Partoyo *et al.* (1995) using aerial photographs. SM = Synorogenic Megasequence, BM = Banda Megasequence, AM = Australian Margin Megasequence, GM = Gondwana Megasequence. Faults shown with solid lines have been observed and measured in the field; those shown with dashed lines have been interpreted from aerial photographs. Strike and dip of bedding is shown where measured.

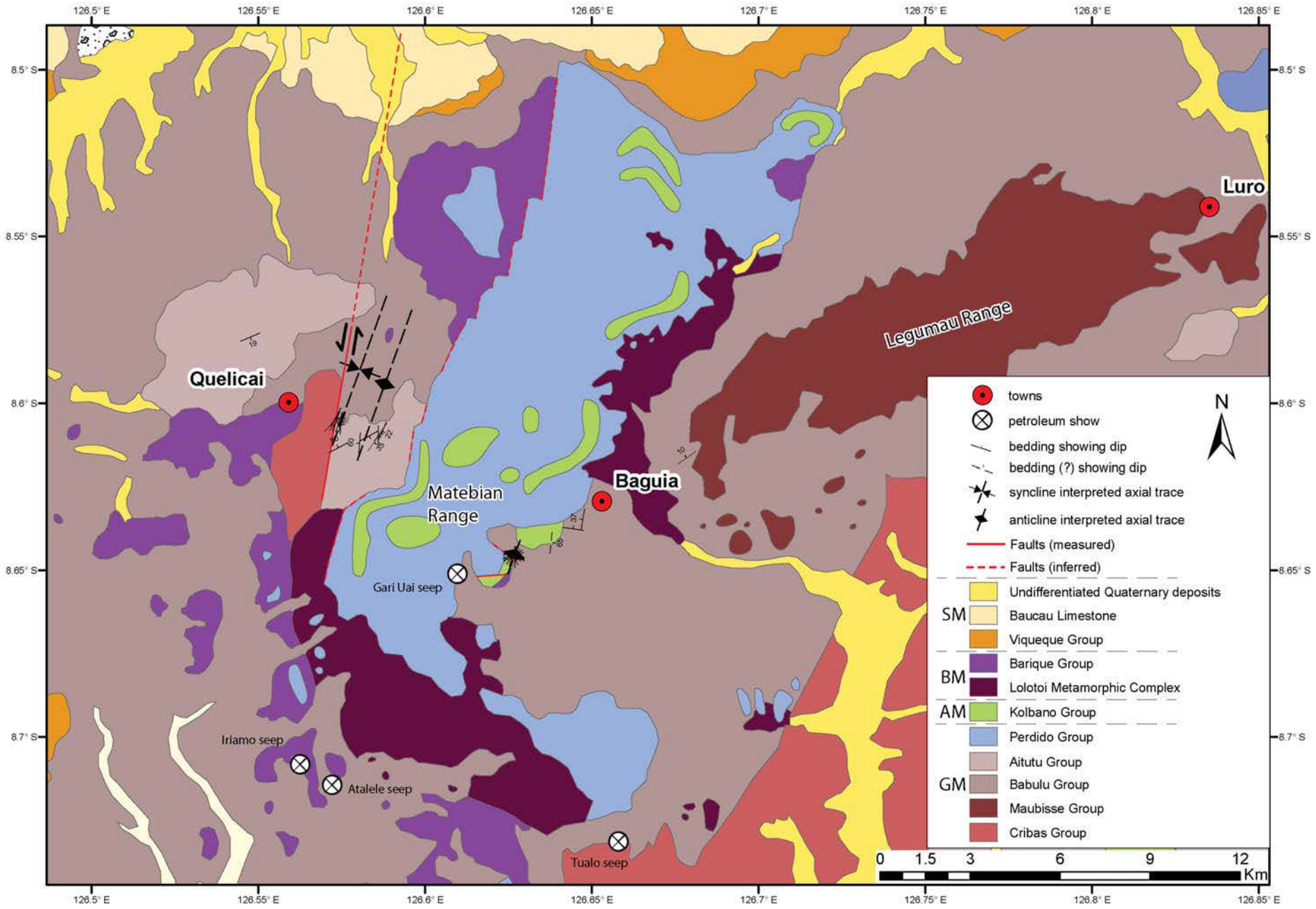
126.5° E
126.55° E
126.6° E
126.65° E
126.7° E
126.75° E
126.8° E
126.85° E
8.5° S
8.55° S
8.6° S
8.65° S
8.7° S
Quelicai
Matebian Range
Baguia
Luro
Legumau Range
Gari Uai seep
Iriamo seep
Atalele seep
Tualo seep
towns
petroleum show
bedding showing dip
bedding (?) showing dip
syncline interpreted axial trace
anticline interpreted axial trace
Faults (measured)
Faults (inferred)
Undifferentiated Quaternary deposits
SM
Baucau Limestone
Viqueque Group
Barique Group
BM
Lolotoi Metamorphic Complex
AM
Kolbano Group
Perdido Group
Aitutu Group
GM
Babulu Group
Maubisse Group
Cribas Group
N
0 1.5 3 6 9 12
Km

4.4.2 Faulting

The most prominent structural feature of the Matebian Range is the extensive scarp that bounds the western edge of the massif (**Figs 108, 109, 110, 111**). Nearly 20 km long and up to 800 m in height, it is the largest limestone scarp in East Timor. Although not visited in the field by this study, observations of extensive fault breccia along the face of the scarp have been made by previous workers (Harris pers. comm. 2013). The scarp dips steeply to the west and strikes north-northeast at approximately 030°, consistent with the north-northwest fault trend seen throughout the Ossu fatus and sub-parallel to the eastern scarps of Mount Laritame and the Mount Ariana ridge. Detail of the Matebian scarp however, particularly in aerial photographs, shows it to comprise a series of smaller, right stepping scarps striking ~010°, generally 0.5-4 km in length (**Fig. 111a, b**).

Elsewhere in the Matebian Range, scarps are also consistent with fault trends seen throughout the Ossu fatus. Scarps which bound the eastern edge of the Matebian Range are lower and less well defined than those on the west of the massif. However, a distinct lineament is evident on the digital elevation model (**Fig. 109b**), particularly in the northern part of the range, which trends 050°, consistent with the 030°– 050° fault trend observed around Ossu. The steep south-southeast facing scarps which bound the southern edge of the main Matebian massif strike at 070° (**Fig. 109**), consistent with the 060°– 070° Ossu trend. At the Matebian Range, this lineament continues east and extends along the southern edge of the Legumau Range. Likewise, the ridge which extends southeast from the south of the Matebian Range has a strike of approximately 130° (**Fig. 109**), very close to the 100°– 120° trend observed around Ossu.

These large-scale lineaments, clearly visible in aerial photography and digital elevation models, are supported by field observations at several locations within the study area. At AB498, approximately 2.5 km west of Matebian's western scarp, a large fault plane is exposed by recent landslips (**Fig. 112a**). This fault plane dips steeply east at 70°, and its strike of 010° parallels the en-echelon fault planes of the Matebian scarp. Prominent fault striae plunge shallowly towards 180°, indicating predominantly strike-slip movement on this fault. Kinematic indicators

a
b
c
8.5° S
8.55° S
8.6° S
8.65° S
126.6° E
126.65° E
0 1 2 4 6 8 Km

including secondary fractures at a small angle to the fault wall (**Fig. 112b**) and crescentic fractures (**Fig. 112c**) point to sinistral, slightly transpressional movement on this fault (following the criteria of Petit 1987, **Fig. 112d**), consistent with interpreted left-lateral movement on the main Matebian scarp. At AB478 the fault plane outcrops over a strike length of approximately 20 m, juxtaposing Permian Cribas Group rocks on the west of the fault with the Triassic Aitutu Group, which extend east from this point to the base of the Matebian scarp. Extending the fault north along strike the fault trace separates mapped outcrops of Permian and Triassic rocks for nearly one kilometre, evidence that this fault likely represents a major structure.

On the southern edge of the main Matebian massif at AB530, fault planes are observed within Perdido Group limestones dipping approximately 55° to the north and striking at around 085°, slightly oblique to the 070° trend of the southern scarps of the massif (**Fig. 112e**). Striae measured on these faults plunge towards 050° indicating a strong component of obliquity to movement in this region also.

Definitive kinematic indicators were not observed on these fault planes, so these striae could be interpreted as either right-lateral transtensional or left lateral transpressional. However, given that these fault planes dip north and are associated with south facing scarps and the uplifted massif to the north, it is likely that they represent transpressional structures.

Remaining structural lineaments on the eastern edge of the massif, the southeast trending extension to the Matebian Range and the Legumau Range were not visited in the field by this study. Rocks of the Lolotoi Metamorphic Complex (Banda Megasequence) have previously been mapped at lower structural levels along the eastern edge of the Matebian Range (Audley-Charles 1968; Partoyo *et al.* 1995; Harris 2006; Standley & Harris 2009), forming a sub-linear strip 500-1500 m wide below and parallel to the eastern cliffs of the massif.

Fig. 111 ← (a) Uninterpreted and (b) interpreted aerial photograph of the Matebian scarp. The main scarp comprises a series of smaller, right stepping scarps striking ~010°. (c) cf. right stepping R shears in a left lateral distributed strike-slip experiment, modified from Schreurs (2003).

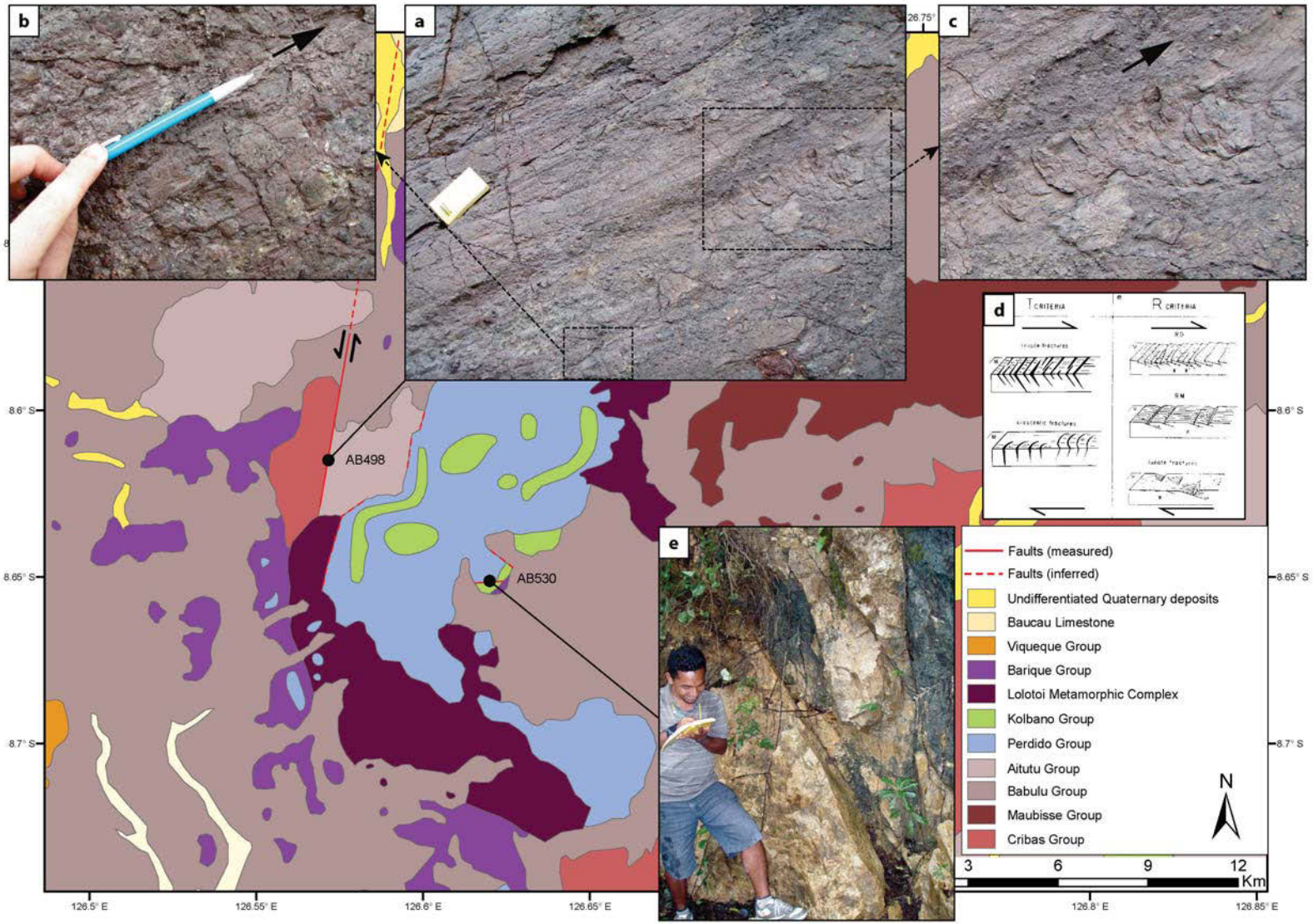
b
a
c
d
e
T CRITERIA
R CRITERIA
AB498
AB530
8.6° S
8.65° S
8.7° S
126.5° E
126.55° E
126.6° E
126.65° E
126.8° E
126.85° E
Faults (measured)
Faults (inferred)
Undifferentiated Quaternary deposits
Baucau Limestone
Viqueque Group
Barique Group
Lolotoi Metamorphic Complex
Kolbano Group
Perdido Group
Aitutu Group
Babulu Group
Maubisse Group
Cribas Group
N
3
6
9
12
Km

It is likely that here, as at the Ossu fatus, these cliffs represent high angle fault scarps juxtaposing the Banda Megasequence rocks against the Australian affinity limestones of the massif. The strong topographic lineament of Matebian's southeast trending extension and its orientation subparallel to fault trends observed in the Ossu fatus suggest that this ridge may also be structurally controlled. This is supported by the presence of several oil and gas seeps located at the base of the ridge along its south-western edge, possibly exploiting structures related to this lineament (see below **Chapter 4.4.4 Melange zones, petroleum seeps and geothermal springs**). Detailed fieldwork in this area would be needed to support this hypothesis. The Legumau Range has previously been mapped as an overthrust unit of Permian Maubisse Group limestone (Gondwana Megasequence) (Audley-Charles 1968) although no thrust contacts have been recorded. The Legumau Range lacks the obvious high angle faults and typical, steep-sided, fatu-style morphology of the other mountains investigated in this study.

Permian Maubisse Group limestone is not rheologically dissimilar to the Mesozoic and Cenozoic limestones that comprise most of the other fatus mapped in this study, and are known to form fatu-style massifs elsewhere on Timor Island (Molengraaf 1912; 't Hoen & van Es 1925; Wittouck 1937; Tappenbeck 1940; Gageonnet & Lemoine 1958). The fact that the Legumau Range lacks typical fatu-style morphology possibly points to differences in its genesis.

Fig. 112 ← (a) Facing west, field photograph of striated fault plane at AB498. Large fault striae plunge shallowly towards 180°. A5 field notebook for scale. Breakouts show low angle secondary R fractures (b) and crescentic T fractures (c) following the criteria of Petit (1987) (d). Fault striae and secondary fractures indicate sinistral, slightly transpressional movement on this fault. (e) Facing west, field photograph of a fault plane developed in Perdido Group limestones at AB530, dipping approximately 55° to the north.

4.4.3 Folding

On the western edge of the Matebian Range, bedding was measured at 15 locations within the Gondwana Megasequence Aitutu Group mudstone and limestone succession where it outcrops between the massive limestones of the Matebian massif and the Permian rocks west of the AB478 fault. A contoured stereonet plot of bedding within the Aitutu Group describes open, upright folding with axial planes striking at approximately 020°, and hinges plunging shallowly towards ~200° (**Fig. 113a**). This data is supported by observations of large, antiformal fold closures in the field, with hinges plunging south-southwest (**Fig. 113b**). Mapped axial traces are sub-parallel to the western scarp of the Matebian Range (**Fig. 110**)

On the eastern side of the Matebian Range, minor outcrop scale folding is observed within Noni Group (Indian Ocean Megasequence) cherts and mudstones at AB526. Here, 12 bedding measurements were recorded (over a metre-scale range as opposed to the kilometre-scale measurements locations within the Aitutu Group) and plotted on a contoured stereonet (**Fig. 113c**). This stereonet plot is remarkably similar to that of measurements from the western side of the Matebian Range; describing an open, upright fold with an axial plane striking north-northeast and a hinge plunging shallowly towards ~195°. This is very limited data however, sourced from only one field locality, so conclusions cannot be drawn regarding correlation with the folding on the western side of the range.

4.4.4 Melange zones, petroleum seeps and geothermal springs

Zones of tectonic melange were not encountered during the limited mapping of this study. Audley-Charles (1968) previously mapped the Matebian Range as being encircled by his 'Bobonaro Melange' that was interpreted as occupying the lowlands surrounding the massif. However, this study has observed that the 'Bobonaro Melange' surrounding fatus elsewhere in East Timor actually comprises Triassic mudstones and sandstones of the Babulu Group with tectonic melange confined to distinct structural zones, and this may be the case around the Matebian Range also.

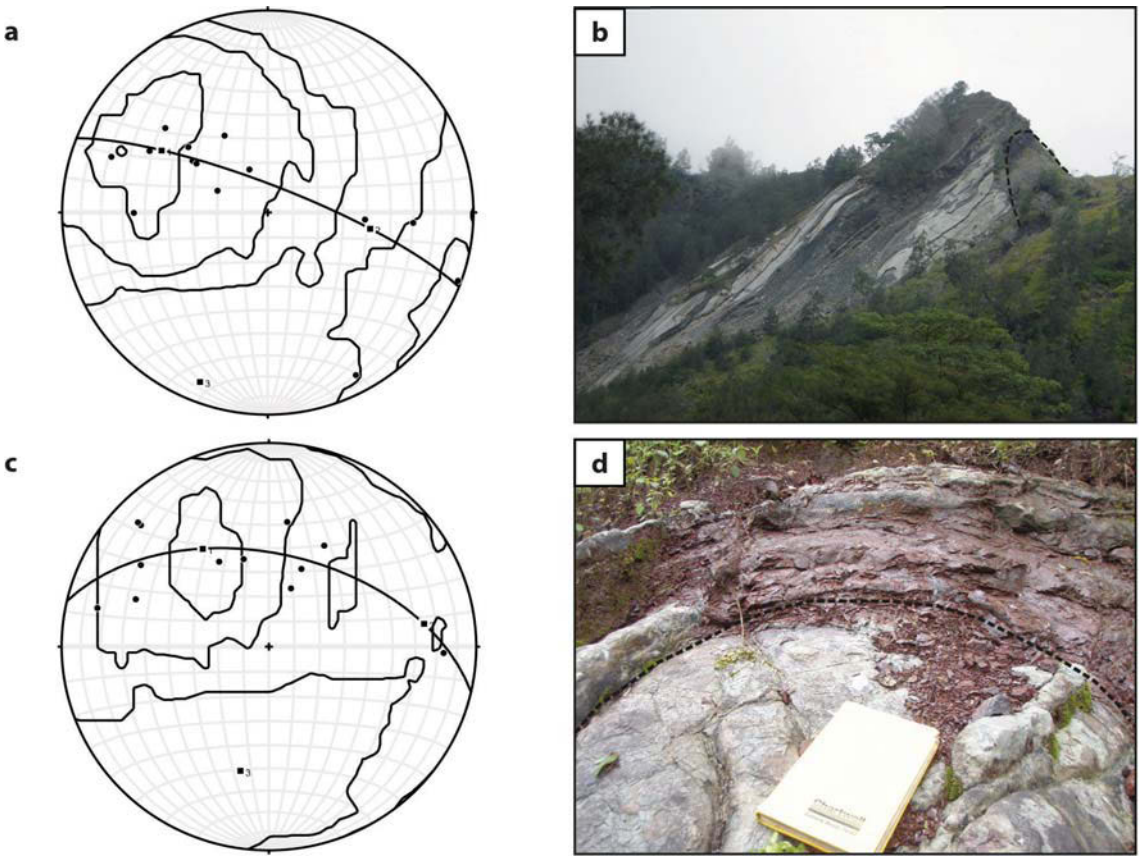

Fig. 113. (a) Contoured stereonet plot of Aitutu Group bedding on the western side of the Matebian Range, with data points representing poles to bedding. Kamb contour interval = 2 sigma, π-circle oriented 291°/79°SW, π-axis 11°→202°. (b) Facing east, large, antiformal fold closures are observed in the field, with hinges plunging south-southwest. This particular hinge formed a prominent hill protruding approximately 50 m from the surrounding landscape. (c) Contoured stereonet plot of Noni bedding at AB526 on the western side of the Matebian Range with data points representing poles to bedding. Kamb contour interval = 2 sigma, π-circle oriented 283°/52°SW, π-axis 38°→193°. The stereonet is quite similar to measurements from the western side of the range, with hinges plunging south-southwest and axial traces sub-parallel to the Matebian scarp. (d) Facing south-southwest, looking down the hinge of a fold developed in Noni Group cherts and mudstones at AB526. A5 notebook for scale.

A number of oil and gas seeps have been recorded by previous workers around the southern parts of the Matebian Range (**Fig. 110**). The Gari Uai oil seep is located below the scarp that bounds the southern edge of the range, at its eastern end, within mudstone near the contact between the limestone cliffs (Audley-Charles 1968). This was once a burning gas seep, and though it is now extinguished it still bears an oil smell. Several oil and gas seeps have also been recorded along the southern edge of the southeast trending extension of the Matebian Range.

These include the Atalele gas seep and Iriamo oil seep emanating from mudstones below the south-western end of the ridge, and the Tualo gas seep, thought to be related to faulting within Permian Cribas Group rocks below the south-eastern tip of the ridge (Audley-Charles 1968).

No geothermal springs were encountered by this study.

4.4.5 Structural model

In common with the Ossu fatus, the Matebian Range comprises a central uplifted core of Australian affinity rocks, with Banda Megasequence units confined to the outskirts of the massif at lower structural levels, separated by high angle faults (**Fig. 110**). These high angle faults dominate the massif and control its morphology, typical of fatus throughout East Timor (**Fig. 109**). At the Matebian Range, the largest of these faults is the north-northwest trending structure that bounds the western edge of the range (**Fig. 108**). This linear, steeply dipping fault exhumes the Australian affinity rocks of the massif and tilts them eastwards. Uplifted Australian Margin Megasequence rocks are now extensively exposed in the higher parts of the range and down to its eastern edge. Older, Gondwana Megasequence limestones are present underneath the thin veneer of Australian Margin Megasequence rocks, they are observed by this study in the eastern parts of the Matebian Range and some observations suggest they may comprise the high cliffs on the west of the range (Duffy 2013 pers. comm., Harris 2013 pers. comm.), although this needs to be confirmed by further fieldwork.

A large left lateral component of movement is strongly evident on this western fault scarp, with the scarp comprising a series of smaller, right-stepping en-echelon Riedel (R) faults oriented at 20° to the main fault trace (**Fig. 111**). This fault distribution is typical of classic Reidel experiments, where experimental models of strike-slip along a vertical basement fault produce a series of en-echelon Reidel shears (R shears) striking at an angle of approximately 15°-20° to the trace of the basement fault (with the exact angle dependent on the internal friction of the material above the fault, but generally between 8°-23° eg. Tchalenko 1970; Naylor *et al.* 1986; Schreurs 2003; Atmaoui *et al.* 2006). The right-stepping en-echelon array at Matebian is indicative of left-lateral movement (**Fig. 111**). Interpreted left-lateral movement here is

supported by the presence of a major left-lateral strike slip fault observed west of the scarp at AB478 which has produced a large fault scarp (**Fig. 112**) and juxtaposes Triassic and Permian rocks for up to a kilometre (**Fig. 110**). If the fault scarp on the western edge of the massif represents the principle displacement zone (PDZ) of left lateral movement at the Matebian Range, it can be seen that all major structural lineaments of the Matebian Range conform to expected fault orientations in a left lateral Riedel shear array (**Fig. 114**).

The main fault scarp strikes north-northeast at approximately 030°, with individual en-echelon segments striking at 010°, representing R shears. The fault at AB478 also represents an R shear, striking at 010°, 20° counter-clockwise to the PDZ. If this fault trace is extrapolated north from AB478 it coincides with a major lineament formed by the Mau Fui River, which flows along the fault trace at 010° for approximately 8 km before draining into a large delta. This correlation may imply that the mapped extent of the fault at AB478 is part of a much larger 010° trending structure.

The southwest trending ridge which forms the southern extension of the Matebian Range is oriented at 130°, which intersects the R shears at 120°, and conforms exactly to an expected Riedel conjugate (R′) orientation in a left lateral strike-slip system. Gas seeps along the southern edge of this ridge may be associated with the structures controlling this lineament. Fault scarps bounding the eastern edge of the Matebian Range strike at approximately 050°. This conforms to the expected P shear orientation in a left lateral system, which form 20° clockwise from the main PDZ.

According to the classic Riedel shear model, compressional structures such as reverse faults and folds should be expected to occur perpendicular to maximum strain, at an orientation which bisects the obtuse angle between the R and R′ orientations. However as displacement increases these structures will often rotate towards shallower angles with respect to the main PDZ, particularly in locations proximal to the PDZ (Dooley & Schreurs 2012). In the case of the left lateral system at the Matebian Range, folds and thrusts should form at an orientation which bisects R at 010° and R′ at 130°, i.e. 070°. At the Matebian Range this is exactly the orientation

at which we see the large structural lineament that extends from the southern scarps of the range and continues along strike through the linear Legumau Range. Therefore, reverse faults associated with the southern scarps of the range are consistent with their expected orientation in the Riedel shear model. It has been noted that the Legumau Range lacks the high-angle bounding faults responsible for the steep-sided morphology typical of the fatu-style massifs of East Timor. The Legumau Range could possibly be interpreted as resulting from a fold with an axial plane at the 070° orientation. The range may represent Permian limestones in the exhumed core of an anticline striking 070°, with overlying Triassic mudstones located to the north and south. This model of the Legumau Range is consistent with a Riedel shear interpretation of other major lineaments at the Matebian Range; however it is unable to be substantiated without further fieldwork. Mapped folds within the Aitutu Group below the western scarp of the Matebian Range strike at 020°, sub-parallel to the PDZ (**Fig. 110**). These folds may represent structures related to strike-slip, rotated into parallelism with the PDZ near the scarp. Alternatively, they could represent drag folds associated with normal displacement along the western edge of the massif. However, folding is ubiquitous and sometimes chaotic throughout the Aitutu Group in East Timor, and ultimately more than the 15 data points of this study would be needed to understand the causes for folding in the Aitutu Group at the Matebian Range.

Fig. 114 → Digital elevation model of the Matebian Range with interpreted structure. If the right-stepping Matebian scarp is interpreted as the principle displacement zone of a left-lateral strike-slip fault striking 030°, then the 010° strike-slip fault at AB478 and it's possible continuation along the Mai Fui River lineament may represent an R shear, 20° counter-clockwise to the PDZ. (b) All major structural lineaments of the Matebian Range conform to expected fault orientations in a left lateral Riedel shear array. See text for detail.

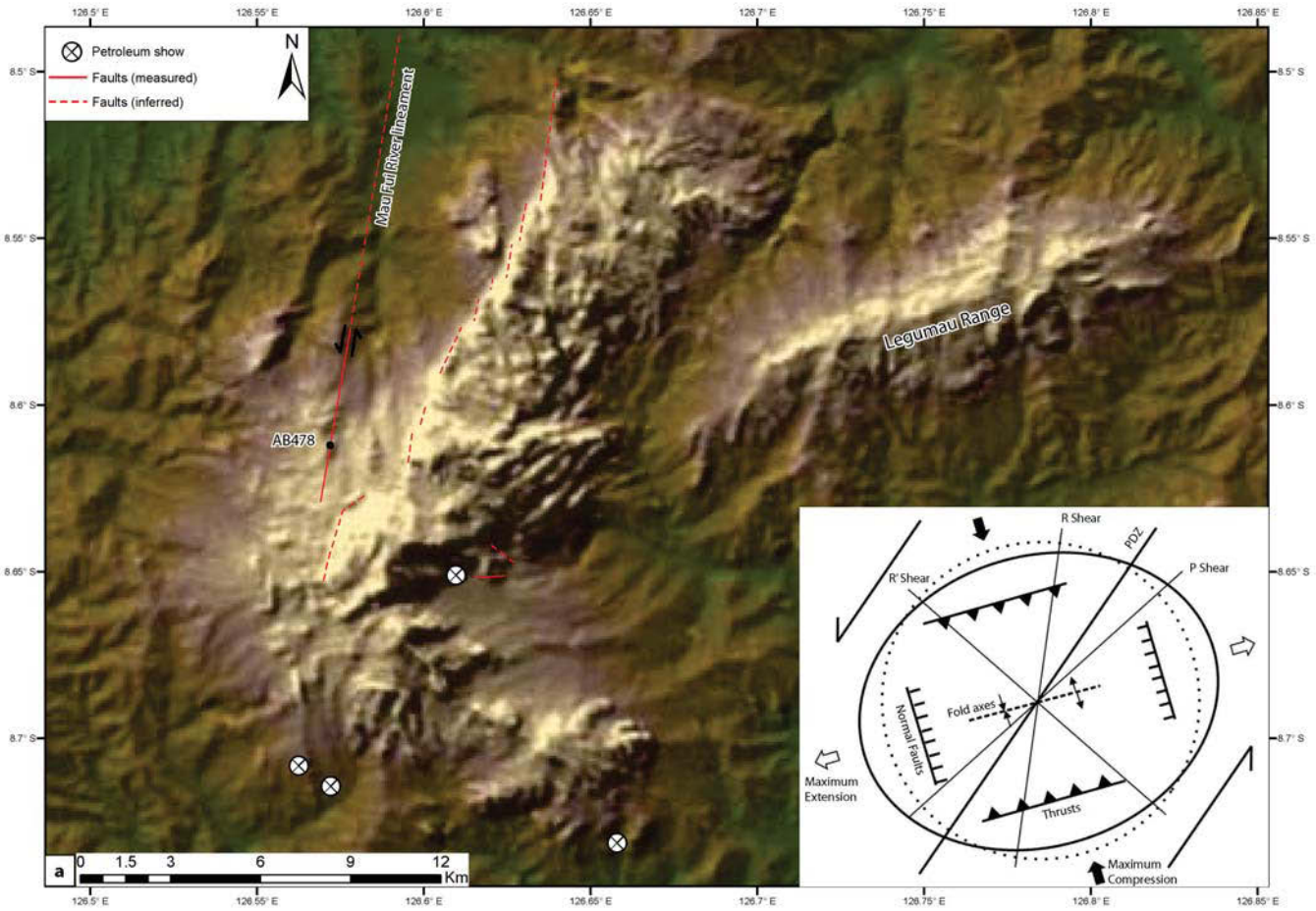
126.5° E
126.55° E
126.6° E
126.65° E
126.7° E
126.75° E
126.8° E
126.85° E
8.5° S
8.55° S
8.6° S
8.65° S
8.7° S
Petroleum show
Faults (measured)
Faults (inferred)
N
Mau Fui River lineament
Legumau Range
AB478
R Shear
PDZ
P Shear
R' Shear
Fold axes
Normal Faults
Thrusts
Maximum Extension
Maximum Compression
a
0 1.5 3 6 9 12 Km

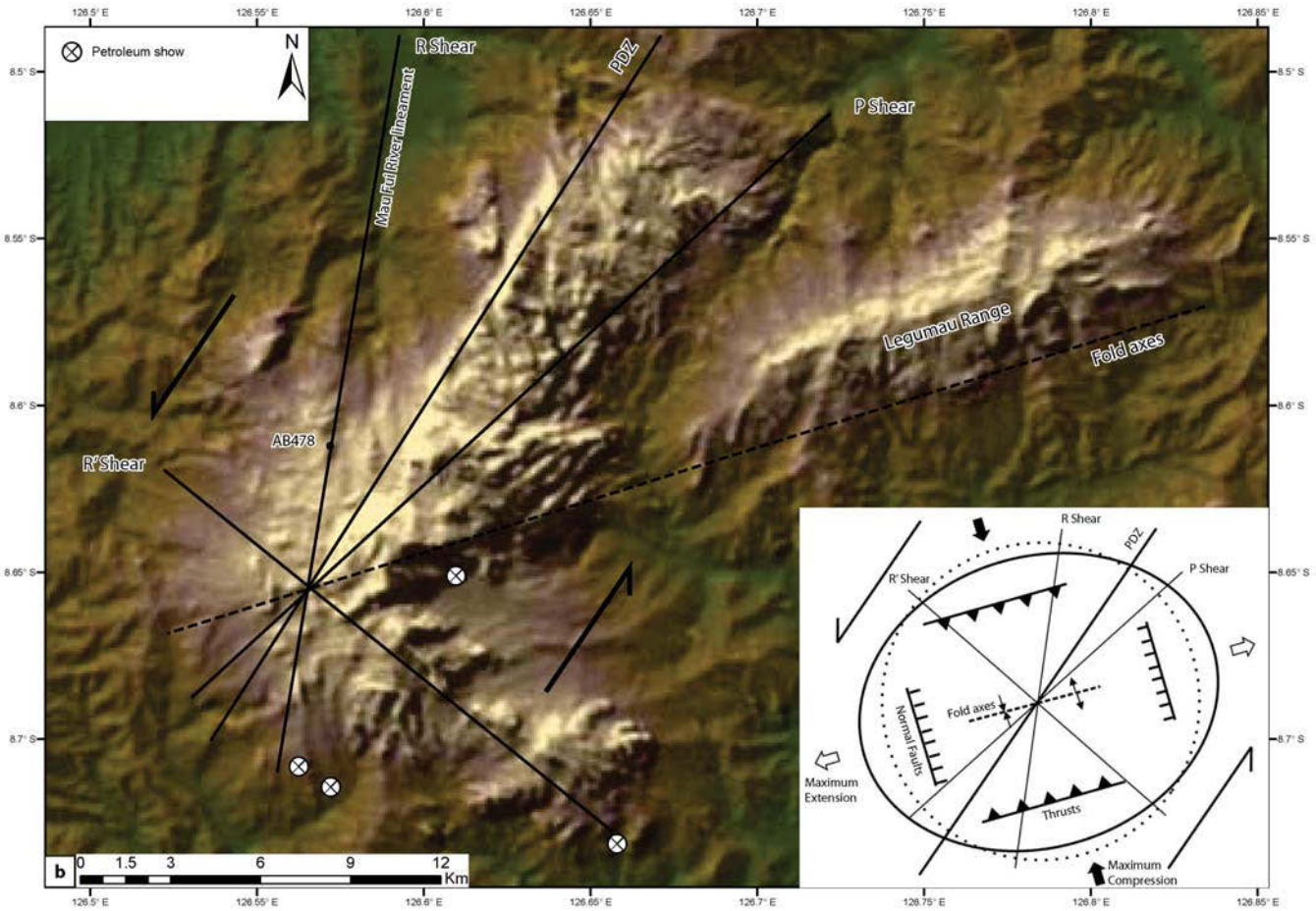
126.5° E
126.55° E
126.6° E
126.65° E
126.7° E
126.75° E
126.8° E
126.85° E
8.5° S
8.55° S
8.6° S
8.65° S
8.7° S
Petroleum show
N
R Shear
PDZ
P Shear
Mau Fui River lineament
Legumau Range
Fold axes
AB478
R' Shear
Normal Faults
Thrusts
Maximum Extension
Maximum Compression
b
0 1.5 3 6 9 12 Km

4.5 Mount Loelako, the Saburai Range and the Maliana basin

Timor Island is a long, narrow, boomerang-shaped island. The western half of the island, comprising the Indonesian province of West Timor and the East Timorese enclave of Oecussi, strikes at approximately 055°, whereas the eastern half the island, comprising East Timor, strikes at approximately 070°. In the centre of the island, at the border between West Timor and East Timor, the island has a pronounced bend, and it is here that we find the Maliana basin and its surrounding fatus Mount Loelako and Mount Saburai (**Fig. 2**).

The Maliana basin is the lowest, flattest part of Timor Island outside of the coastal plains (**Fig. 86**). The basin is approximately 15 km wide and over 25 km long, with its long axis oriented north-northeast (**Fig. 115**). Widest in the south, the Maliana basin narrows to the north where the rivers that drain the basin exit through a gap in the basin margin approximately 3-4 km wide. The flat floor of the basin has a slight gradient from 200 m above sea level in the southeast to less than 100 m in the northwest. The margins of the basin are sharply defined on a digital elevation model (**Fig. 115b**). The western basin margin, striking 020°-030°, and southern basin margin, striking approximately 115°, both comprise low, eroded hills of predominantly friable lithologies, rising to 500-600 m above sea level. The eastern basin margin strikes at approximately 030°-035° in the south, but curves around to approximately 015°-020° in the north. Along this eastern edge of the Maliana basin the flat basin floor meets moderately sloping margins, which rapidly increase in gradient towards the high, steep sided limestone fatus of Mount Loelako and the Saburai Range, which rise to nearly 2000 m above sea level and dominate the landscape east of the basin. Major rivers define the margins of the basin along its western, eastern and southern boundaries.

Mount Loelako forms a long, narrow limestone ridge, approximately 6 km long and no more than 1 km wide at its base (**Fig. 115**). Near vertical cliffs on either side rise up to 1920 m above sea level and meet to form a narrow crest along the top of the mountain, in some places only a few metres wide (**Fig. 116**). Mount Loelako has a unique orientation amongst the fatus of East Timor, which elsewhere strike approximately east-west (Mount Mundo Perdido, Mount Bibileu, the Builo Range), or northeast-southwest (Mount Laritame, the Paitchau Range, Mount

Matebian, Mount Taroman, the Saburai Range; **Fig. 86**). In contrast Mount Loelako strikes approximately 000°, however it is slightly warped along its length, so that the northern and southern ends of the ridge are offset slightly to the northwest-southeast, striking approximately 150°. Mount Loelako shows an asymmetry in topography along a west to east profile across the fatu (**Fig. 116**). From the eastern edge of the Maliana basin at approximately 200 m above sea level, the base of Mount Loelako forms a gradual hill which increases in gradient as it slopes upwards to the bottom of the high, west-facing cliffs which form the crest of the fatu, with the base of the cliffs at approximately 1400 m above sea level. On the eastern side of Mount Loelako the base of the cliffs are much lower, situated at approximately 1000-1100 m above sea level. The topography underneath the eastern cliffs is eroded by drainage leading down to the basin below, forming a number of ridges and gullies between massif and the north trending Aitasiola River, approximately 3 km east of Mount Loelako.

One kilometre north of Mount Loelako is Mount Lesululi, a small massif approximately 2.5 km wide from east to west and less than 1 km from north to south (**Fig. 115**). Triangular in plan view, Mount Lesululi has high cliffs on its southern and western edges which rise to a maximum altitude of 1244 m, while the top of the mountain slopes down gradually towards the north and northeast. Viewed from a distance Mount Lesululi looks like a disjointed part of Mount Loelako, however morphologically it is quite dissimilar.

The southern edge of Mount Lesululi comprises an east-west oriented scarp 2.5 km long, which contrasts sharply with the north-south orientation of the adjacent Mount Loelako fatu (**Fig. 115b**). To the east of Mounts Loelako and Lesululi lies the narrow, north-south trending Marobo basin (named for the Marobo River situated east of Mount Lesululi which drains this basin to the north), which parallels the eastern edge of the much larger Maliana basin (**Fig. 115**).

Fig. 115 → (a) Aerial photo of Mount Loelako and the Saburai Range with interpreted structure. (b) Digital elevation model of the two fatus with interpreted structure. Faults shown with solid lines have been observed and measured in the field; those shown with dashed lines have been interpreted from aerial photographs. Arrows indicate fault striae where observed and measured on major faults.

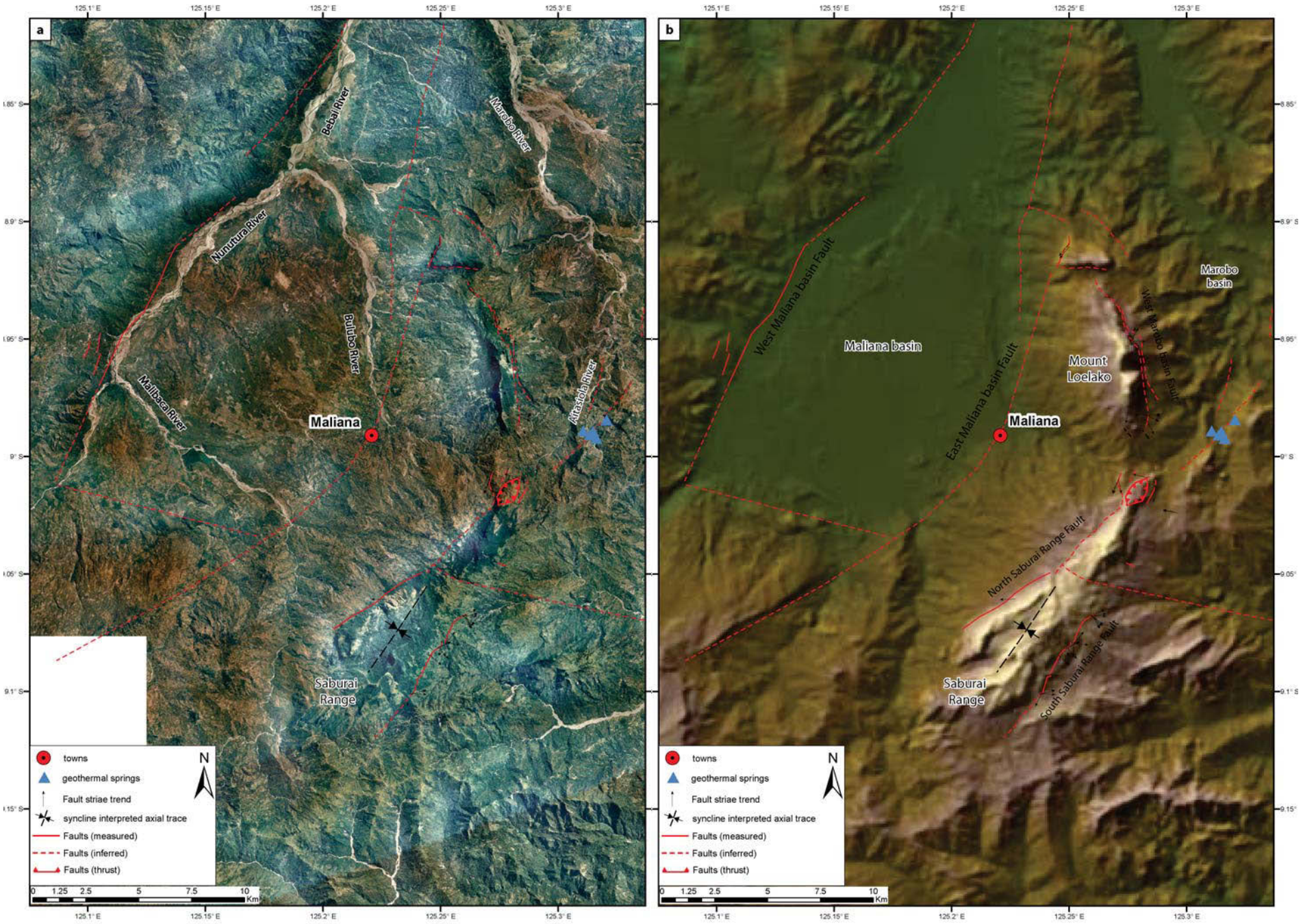
a
b
125.1° E
125.15° E
125.2° E
125.25° E
125.3° E
8.85° S
8.9° S
8.95° S
9° S
9.05° S
9.1° S
9.15° S
Bebal River
Marobo River
Nunutura River
Bulubo River
Mallbaca River
Airastoh River
Maliana
Saburai Range
West Maliana basin Fault
Maliana basin
East Maliana basin Fault
Mount Loelako
Marobo basin
West Marobo basin Fault
North Saburai Range Fault
South Saburai Range Fault
towns
geothermal springs
Fault striae trend
syncline interpreted axial trace
Faults (measured)
Faults (inferred)
Faults (thrust)
N
0 1.25 2.5 5 7.5 10 Km

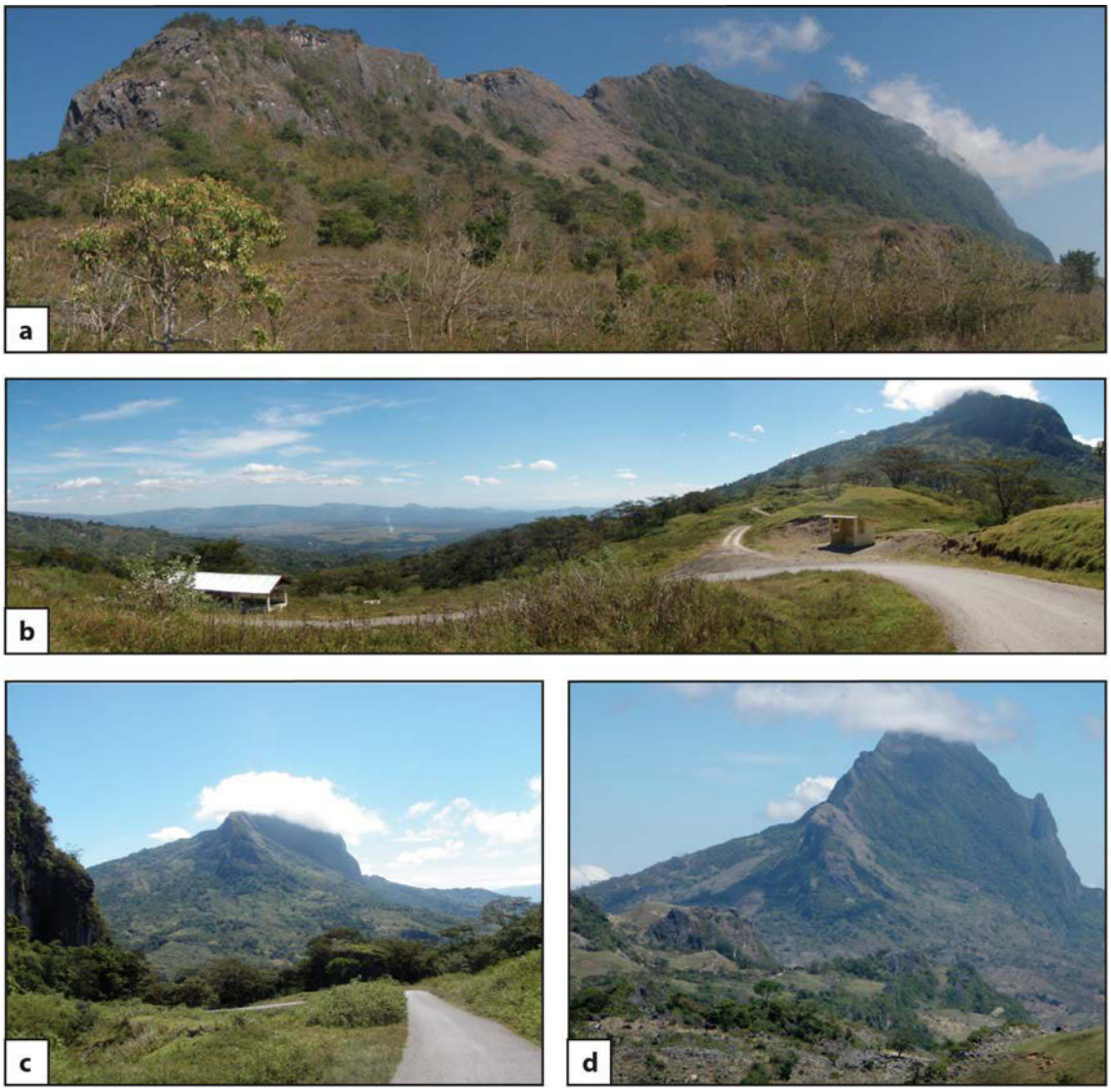

Fig. 116. (a) Facing northwest at the eastern side of Mount Loelako, the steep, narrow ridge extends out to the north. (b) Facing northwest looking over the Maliana basin (left of frame) from the saddle between Mount Loelako and the Saburai Range. Topography slopes up from the eastern margin of the basin to meet Mount Loelako (right of frame). (c, d) Facing north, looking at the southern tip of Mount Loelako. The asymmetric topographic profile of the ridge is evident, with the base of the cliffs on the eastern side much lower than on the west. The slight sinuosity of the ridge is also visible from this perspective, with the southern tip curving around to the southeast.

In contrast to the low, flat Maliana basin that is bound on all sides by well-defined topographic lineaments, the Marobo basin has an irregular outline scored by ridges and gullies (**Fig. 115**). The centre of the basin is occupied by a narrow, flat floodplain 1-2 km wide at the basin's centre, which decreases in altitude from approximately 400 m above sea level east of Mount

Loelako, to less than 100 m 13 km north of Mount Lesululi, where the Marobo River turns west to meet the Bebai River draining north from the Maliana basin (**Fig. 115**).

Situated 2 km south of the southern tip of Mount Loelako is the northern tip of the Saburai Range, with the two high fatu-ridges separated by a narrow gap approximately 2 km wide comprising a lower saddle approximately 800 m above sea level (**Fig. 115**). The Saburai Range forms a 15 km long, elongate triangle shape in plan view, pointing northeast, only a few hundred metres wide at its tip near Mount Loelako, but over 4.5 km wide at its widest point in the south-west of the range (**Fig. 115**). The wide, southern part of the Saburai Range comprises two, high sub-parallel ridges (**Fig. 115**). The western ridge rises to over 1600 m and strikes approximately 050°-060° for a distance of approximately 5 km, while the larger eastern ridge rises to over 1900 m and strikes 040°-050° for a distance of approximately 7 km. These two ridges are separated by a narrow basin approximately 4 km long but no more than 1 km wide, which sits at an altitude of 1500-1600m above sea level (**Fig. 115**). Where the Saburai Range narrows to the northeast it comprises a single ridge, less than 2 km wide and over 1700 m in height, which extends for nearly 6 km (**Fig. 115**). This north-eastern ridge is separated from the two ridges to the southwest by a saddle at approximately 1500 m altitude, which extends south into the southern elevated basin (**Fig. 115**, see also **Chapter 3 Fig. 68a**). The north-western Saburai ridge strikes approximately 030°, and is parallel and adjacent to the south-eastern edge of the Maliana basin. The Saburai Range is bound by steep cliffs along both its south-eastern and north-western edges, although they are higher and steeper where they face the Maliana basin to the northwest. Here, the limestone cliffs are over 600 m high, with their base situated at 1000-1000 m above sea level. From the base of these cliffs, gradual slopes extend down towards the floor of the Maliana basin, situated approximately 5 km to the northwest, displaying a very similar topography to the slopes on the western side of Mount Loelako (**Fig. 115**).

4.5.1 Distribution of stratigraphy

Figure 117 shows an interpreted geological map of Mount Loelako, the Saburai Range and the Maliana basin. The flat floor of the Maliana basin is mostly covered by soil, alluvium and recent

surficial deposits. However in the south-eastern parts of the basin where the basin floor is topographically highest (200-250 m a.s.l.), small incised rivers and streams expose well bedded Viqueque Group mudstones and sandstones of the Synorogenic Megasequence (**Fig. 118a**). Just southwest of the Maliana township where these units are first encountered, bedding dips consistently 20°-30° to the northwest, with strikes ranging from 025°-065°. Bedding gets steeper moving south towards the Saburai Range where dips increase to up to 45°, while strikes rotate slightly clockwise to around 070°-080°. Sampled Viqueque Group exposures are oldest where they are closest to the Saburai Range, and young towards the north-northeast. It is likely that underneath the surficial layers of alluvium and soil the Viqueque Group is present throughout most of the Maliana basin, and is now exposed in the southeast due to uplift and tilting (see **Chapter 3.11 The Maliana basin**).

The Maliana basin is bound along its western and eastern edges by rocks of the Gondwana Megasequence. The western margin of the Maliana basin is defined by the Nunutura River, which juxtaposes the Synorogenic Megasequence deposits that comprise the basin fill with Gondwana Megasequence rocks of the western basin margin. On the eastern bank of the river lies the flat basin floor, comprising alluvium and surficial deposits most likely overlying synorogenic Pleistocene Viqueque Group lithologies, while the river's western bank rises quickly into an eroded, hill topography of low broken hills comprising predominantly 'broken formation facies' Triassic Babulu Group mudstones (**Fig. 118b**). Some outcrops of Viqueque Group limestone are also present along this western margin, generally juxtaposed against Babulu Group mudstones by normal faults that parallel the basin margin. Booi Group limestones of the Banda Megasequence were also observed forming one of the small hills 2.5 km northwest of the north-western basin margin, overlying Babulu Group mudstones, and it is possible that other topographic highs along the basin margin may also be capped by these rocks.

On the eastern edge of the Maliana basin, alluvial and synorogenic deposits give way to Gondwana Megasequence lithologies along a lineament that strikes approximately 020°, extending from the southwest corner of Mount Lesululi down through the Maliana township and then curving slightly west towards 030° to parallel the strike of the Saburai Range. Although the

exact contact was not observed in the field, this lineament separating sample points of Synorogenic and Gondwana megasequence lithologies also mostly corresponds to the topographic rise surrounding the basin, where the flat basin floor abruptly transitions into west to northwest facing inclines which slope upwards to the base of the western cliffs of Mount Lesululi, Mount Loelako, and the Saburai Range. To the north, around Mount Lesululi and Mount Loelako, these slopes comprise interbedded limestones and mudstones of the Aitutu Group (**Fig. 84**), while to the south near the Saburai Range outcrop on these slopes is most commonly Babulu Group (**Fig. 84**) lithologies. On the high parts of the slopes near Mount Lesululi and Mount Loelako, limestone beds within the Aitutu Group become thicker and contain some facies transitional between the basinal Aitutu Group and the shallow water Bandeira Group (**Fig. 84**) limestones that comprise the high cliffs of all three fatus (**Fig. 119a**).

At Mount Lesululi, the Bandeira Group limestones comprising the fatu dip moderately north to slightly northwest, and the sloping northern side of this fatu likely represents a dip slope. Bedding within the Bandeira Group is also responsible for the spectacular morphology of Mount Loelako, which comprises a 'hogback' ridge of subvertically bedded, north-south striking, well bedded Bandeira Group limestones. Bedding dips steeply to the east, with bedding planes forming the steep eastern cliff faces of Mount Loelako. Here, large slabs of rock are visible breaking off along bedding planes (**Fig. 119b**) to produce extensive scree-fans at the base of the cliffs, and the broken ends of limestone beds rise sub-vertically from the top of Mount Loelako to produce the narrow crest of the ridge (**Fig. 119c, d**). Gentle folding within these limestone beds is also responsible for the slight sinuosity in strike of the Loelako ridge, particularly at its northern and southern ends (**Fig. 116c, d**).

Fig. 117 → Interpreted geological map of the Maliana basin and surrounding fatus, showing the distribution of lithologies and main geological structures. Geology outside of mapped areas is modified after Partoyo *et al.* (1995) using aerial photographs. SM = Synorogenic Megasequence, BM = Banda Megasequence, GM = Gondwana Megasequence. Faults shown with solid lines have been observed and measured in the field; those shown with dashed lines have been interpreted from aerial photographs. Strike and dip of bedding is shown where measured. shown in dashed red have been interpreted from aerial photographs. Arrows indicate fault striae where observed and measured on major faults.

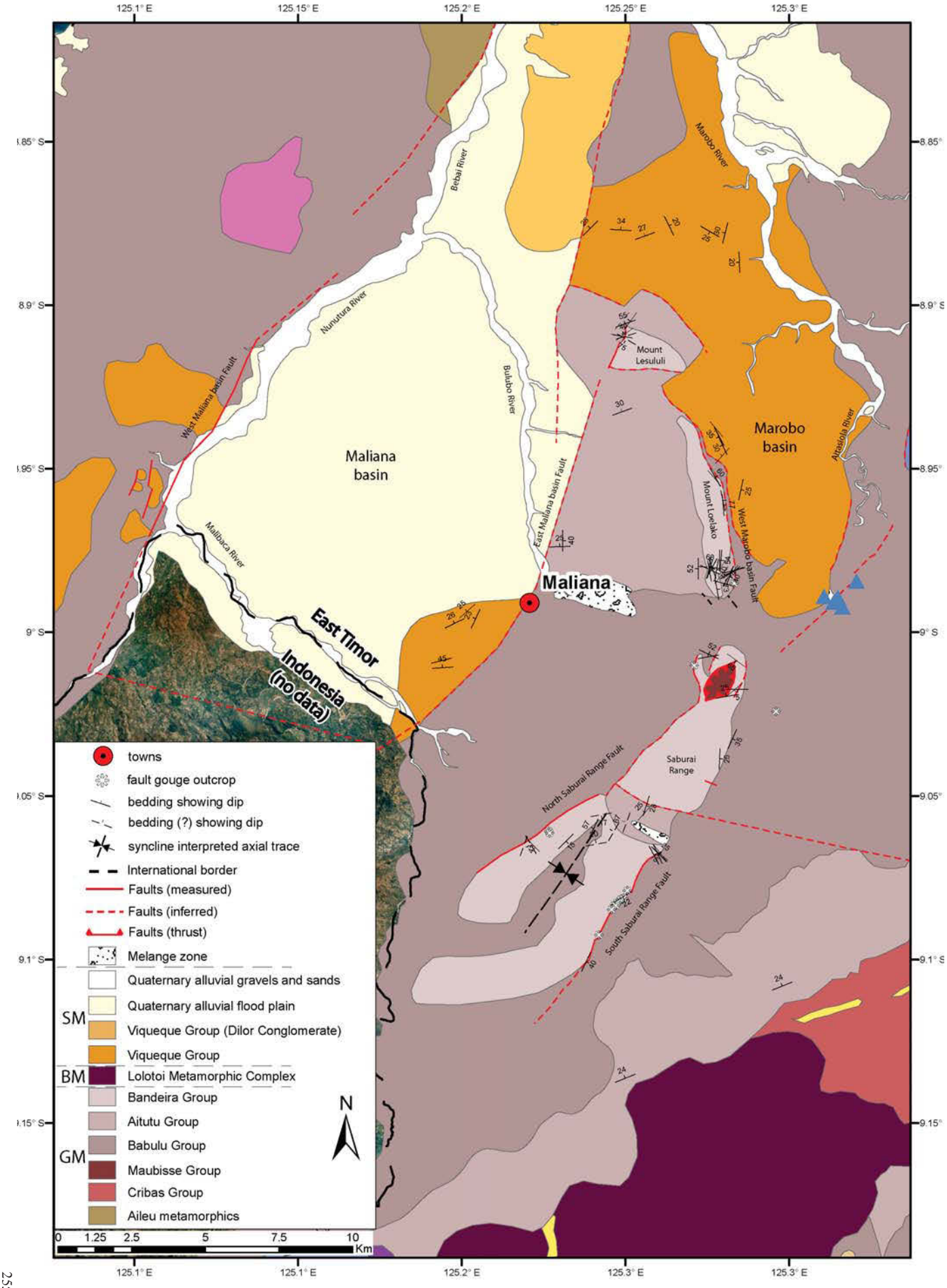
125.1° E
125.15° E
125.2° E
125.25° E
125.3° E
8.85° S
8.9° S
8.95° S
9° S
9.05° S
9.1° S
9.15° S
Bebai River
Marobo River
Nunutura River
Mount Lesululi
West Maliana basin Fault
Bulubo River
Maliana basin
Marobo basin
Atasiola River
East Maliana basin Fault
Mount Loelako
West Marobo basin Fault
Malibaca River
Maliana
East Timor
Indonesia
(no data)
North Saburai Range Fault
Saburai Range
South Saburai Range Fault
towns
fault gouge outcrop
bedding showing dip
bedding (?) showing dip
syncline interpreted axial trace
International border
Faults (measured)
Faults (inferred)
Faults (thrust)
Melange zone
Quaternary alluvial gravels and sands
Quaternary alluvial flood plain
SM
Viqueque Group (Dilor Conglomerate)
Viqueque Group
BM
Lolotoi Metamorphic Complex
Bandeira Group
Aitutu Group
Babulu Group
GM
Maubisse Group
Cribas Group
Aileu metamorphics
N
0 1.25 2.5 5 7.5 10
Km

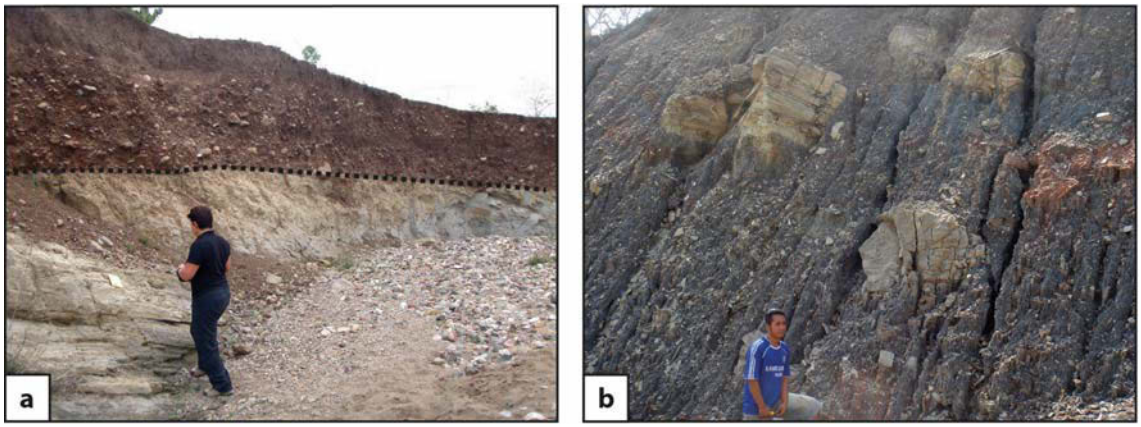

Fig. 118. (a) An incised river in the southeast corner of the Maliana basin has exposed this angular unconformity, with recent alluvial deposits overlying shallow dipping Viqueque Group sandstones and mudstones. It is likely that the Viqueque Group is present beneath alluvium and surficial deposits throughout much of the basin. (b) 'Broken-formation facies' Babulu Group mudstones which comprise the heavily eroded eastern edge of the Maliana basin.

Along the eastern edge of Mount Loelako, and particular in the southeast, bedding within the Bandeira Group limestones of the massif becomes thinner and in places grades back into interbedded limestones and mudstones of the Aitutu Group, with some transitional Bandeira-Aitutu facies present (see **Chapter 3.9 Mount Loelako**), similar to those high on the slopes below the western cliffs of the massifs. The synorogenic Viqueque Group abuts Mount Loelako and Mount Lesululi along the eastern edges of both massifs.

At Mount Loelako however, Viqueque Group rocks are not observed extending all the way up to the eastern cliff faces. Babulu Group mudstones of the Gondwana Megasequence occupy a gap of 100-700 m between the cliffs of the massif and mapped Viqueque Group rocks to the west (**Figs 117, 120a**), although outcrop is sporadic as these mudstones are recessive and extensively covered by debris fans and thick layers of scree.

The Viqueque Group adjacent to Mount Loelako comprises mudstones, sandstones and conglomerates that strike sub-parallel to the massif and dip 25°-40° west, towards the east facing cliffs (**Fig. 120b, c**). Viqueque Group outcrop here is up to 1000 m above sea level, separated from similar Viqueque Group rocks in the Maliana basin west of Mount Loelako by over 800 m of vertical separation.

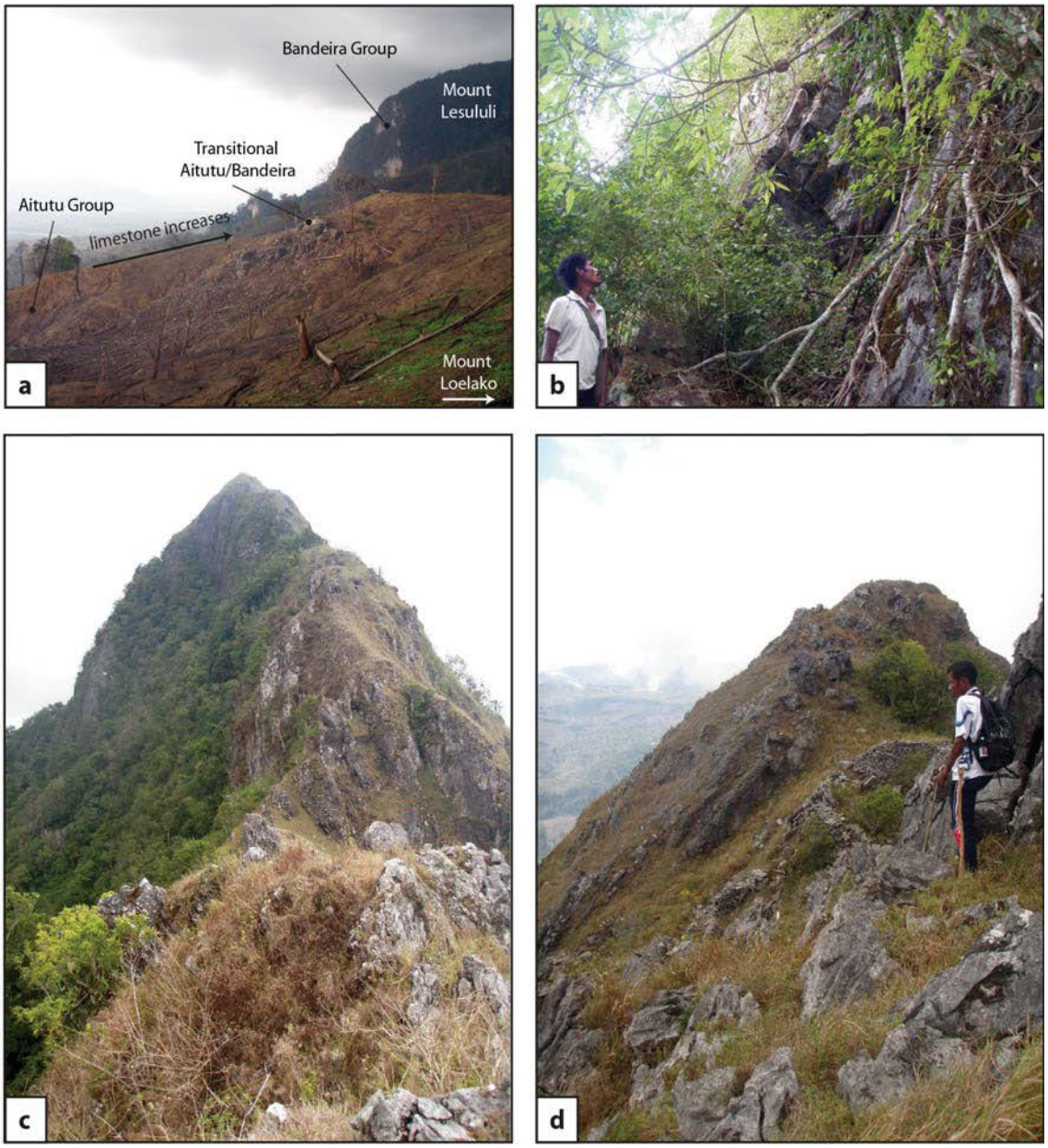

Fig. 119. (a) Facing north, the Maliana basin (left of frame) is bound on it eastern edge by well bedded mudstones and limestones of the Aitutu Group, which slope upwards towards Mount Lesululi and Mount Loelako (right of frame). The Aitutu Group becomes more limestone dominated moving up the slope, as mudstone decreases and limestone beds become thicker and more fossiliferous. High on the slope, close to the base of the fatus, thick limestone beds of facies transitional between the Aitutu and Bandeira Groups form limestone caps above mudstone dominated hills. (b) Subvertically bedded Bandeira Group limestones forming the high east-facing cliff faces of Mount Loelako (c) Facing north and (d) facing south from the top of Mount Loelako, the broken ends of bedding planes (dipping steeply to the east) protrude from the top of Mount Loelako's high crest.

Fig. 120. (a) Facing west, grey Babulu Group mudstones (foreground) are observed outcropping in some localities immediately below the east facing cliffs of mount Loelako (background). Outcrop is thinly bedded and chaotically deformed (b) The western edge of the Marobo basin facing south, with the eastern cliffs of Mount Loelako in the right of frame. The Viqueque Group here dips southwest, towards the east-facing cliffs of Mount Loelako. (c) Facing west, well bedded Viqueque Group mudstones and sandstones (foreground) fill the Marobo basin east of Mount Loelako (background), comprising a package of rocks over 700 m thick which forms the heavily eroded topography leading down towards the Aitasiola River. They are seen here also dipping shallowly to the southwest.

The Viqueque Group extends east of Mount Loelako for approximately 5 km, comprising the heavily eroded landscape which slopes down towards the Aitasiola River, and most likely represents a package of rocks over 700 m thick. Its mapped extent continues around the northern margin of Mount Lesululi, where strikes change to an east-west direction with bedding dipping 25°-35° north.

The main ridges which form the Saburai Range fatu (the single ridge forming the northern part and the two sub-parallel ridges which form the southern part) also comprise Bandeira Group

limestones, although a small 50-60 m thick klippe of Permian Maubisse Group rocks overlies approximately 1 square kilometre of the northern tip of the range (**Figs 117, 121a**). The Saburai Range appears to continue the lineament of Mount Loelako directly to the south; however the Bandeira Group limestones comprising the northern part of the Saburai Range have opposing dip polarity to those comprising Mount Loelako. At Mount Loelako they dip very steeply to the east, while those comprising the northern ridge of the Saburai Range dip moderately to the northwest (**Fig. 121b, c**).

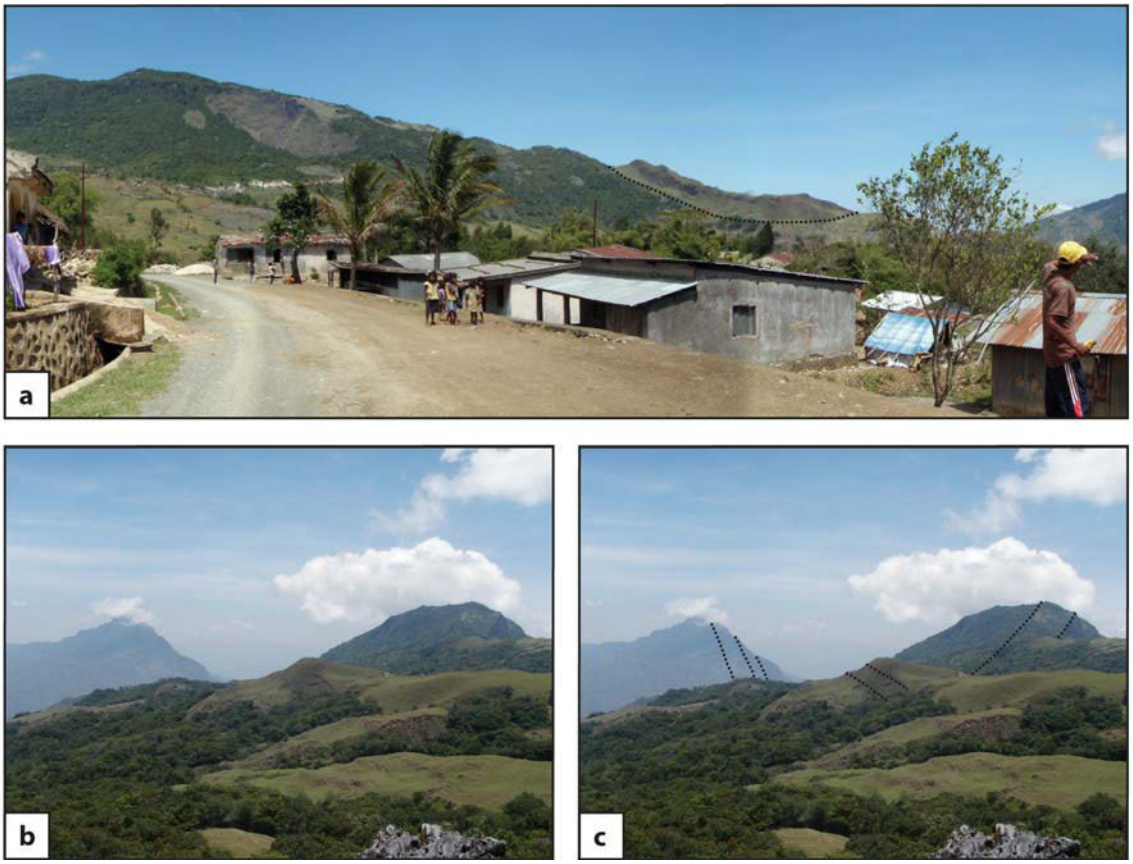

Fig. 121. (a) Facing northwest, a 50-60 m thick klippe of Permian Maubisse Group sandstones and breccias overlies Triassic Bandeira Group limestones at northern tip of the Saburai range. (b) Uninterpreted and (c) interpreted image facing northwest, this picture is taken from the top of the Saburai Range, near the northern tip of the south-western Saburai ridge. In the foreground lies the grassy, hilly topography of the saddle that separates the northern and southern parts of the Saburai range; the southeast dipping bedding along the northern edge of the saddle (centre) is consistent with the bedding in the south-western ridge, underneath the photographer. To the right of frame is the high northern ridge of the Saburai Range, dipping northwest, and to the left of frame in the distance lies Mount Loelako, with bedding dipping steeply to the east.

Bandeira Group limestones comprising the southern ridges of the Saburai Range dip shallowly inwards towards the long axis of the fatu. Bedding in the east southern ridge dips shallowly to the northwest, similar to the orientation of bedding in the northern Saburai Range, while the bedding in the west southern ridge dips shallowly to the southeast. It is possible that these southern ridges may represent the limbs of a syncline, with a northeast-southwest trending fold axial trace oriented parallel to the range. Mudstone is the dominant lithology within the narrow basin between the two southern ridges of the Saburai range and outcrop is rare and recessive. However, two samples from the northern end of this basin belong to the Babulu Group, which may stratigraphically overly the Bandeira Group that comprises the ridges (see **Chapter 3.10 The Saburai Range**).

The saddle comprising the lower, central part of the Saburai Range is immediately distinguishable from the surrounding upper reaches of the range due to its gentle, hilly morphology and grassy vegetation, contrasting with the steep cliffs and jungle of the ridges to the north and south. Outcrop here consists of interbedded limestones and mudstones of the Aitutu Group. The contact of these rocks with the northern ridge was not observed, however they appear to grade into the thick limestone beds of the Bandeira Group to the south, and transitional, shallow water facies are evident within some beds (see **Chapter 3.10 The Saburai Range**). On the eastern side of this saddle is a small zone of tectonic melange containing igneous rocks most likely Permian in origin.

4.5.2 Faulting

At a regional scale, the Maliana basin and surrounding fatus are dominated by northwest to north-northwest trending faults that parallel the orientations of Mound Loelako and the Saburai Range. Bounding the western edge of the Maliana basin, the West Maliana Basin Fault strikes at approximately 025°-030°, and separates the flat, topographically low, Pliocene – Recent basin fill from the higher, eroded, Gondwana Megasequence mudstones of the western basin margin. This study interprets the trace of the main bounding fault as aligning closely with the course of the Nunutura River, as the river is observed to juxtapose the young basin fill on its east bank

with the Gondwana Megasequence on its west bank (**Fig. 117**). At the southwest corner of the Maliana basin, Plio-Pleistocene Viqueque Group limestones of the Synorogenic Megasequence are observed in places overlying the Gondwana Megasequence mudstones comprising the elevated basin margin (**Fig. 117**). Heading east towards the Nunutura River and down into the Maliana basin, a series of faults are observed in roadside outcrop which are parallel to the main trace of the West Maliana Basin Fault. These are subvertical faults that drop down blocks of Plio-Pleistocene Viqueque Group limestones to the east against Triassic Babulu Group mudstones to the west (**Fig. 122**), and are therefore interpreted as extensional faults (either normal or transtensional). These faults most likely form part of the larger scale extensional fault system bounding the western edge of the basin.

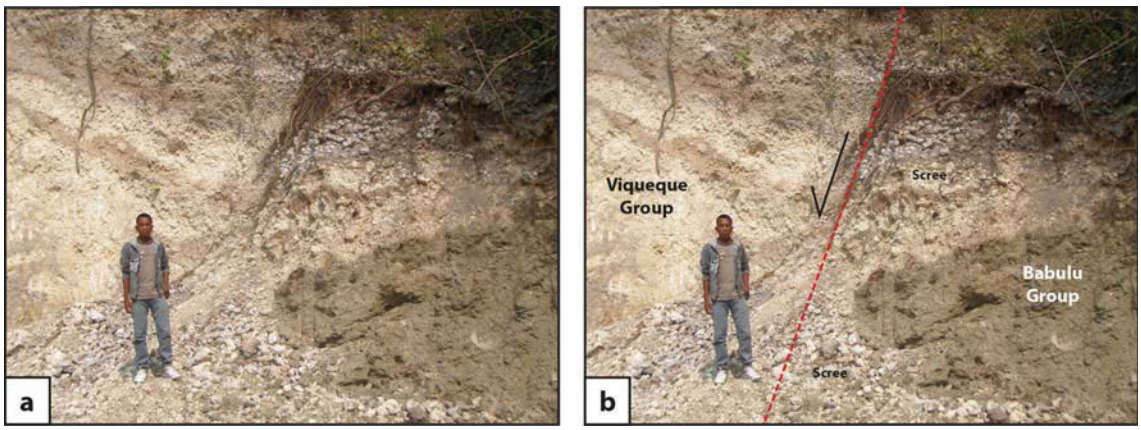

Fig. 122. Facing south, yellow-white Pleistocene Viqueque Group limestones (left) faulted against grey Triassic Babulu Group mudstones (right) along high angle normal faults that parallel the western margin of the Maliana basin. Overlying the grey Babulu Group mudstones are blocks of limestone and fault gouge that have fallen from the fault zone.

On the eastern edge of the Maliana basin the trace of the main bounding fault is inferred to be co-incident with the base of the topographic rise along the eastern edge of the basin, where the flat basin floor begins to slope upwards towards Mount Lesululi, Mount Loelako, and the Saburai Range (**Fig. 115a**). This topographic lineation is observed to juxtapose Pliocene – Recent basin fill against Triassic Gondwana Megasequence Aitutu Group and Babulu Group rocks that comprise the slopes beneath the fatus. The East Maliana Basin Fault strikes approximately 040° in the south, parallel to the Saburai Range, and curves around to the north

to strike 000°-020° alongside Mounts Loelako and Lesululi (**Figs 115, 117**). The west-facing scarp of Mount Lesululi most likely represents a segment or splay of this basin-bounding fault. Drag folds and prominent south-plunging fault striae measured on the scarp indicate that the East Maliana Basin Fault, at least at this location, has undergone left-lateral, transtensional movement (**Fig. 123**). Together, the West Maliana Basin Fault and East Maliana Basin Fault are interpreted as extensional faults of opposing polarity, accommodating subsidence of the Maliana basin and its synorogenic fill between Gondwana Megasequence rocks which comprise the margins of the basin. These are likely high-angle faults due to their linear fault traces at surface, although the East Maliana Basin Fault particularly displays a distinct S-shaped sinuosity.

Unlike the western face of Mount Lesululi, the west-facing cliffs of Mount Loelako do not necessarily represent a fault scarp. Traversing east from the East Maliana Basin Fault to the west-facing scarp of Mount Loelako, the east-dipping Triassic succession grades from basinal Aitutu Group interbedded limestones and mudstones (mudstone-dominated at the base of the slope, becoming increasingly limestone dominated towards Mount Loelako), through to transitional Aitutu/Bandeira Group limestones near the base of the scarp, and finally into the indurated, subvertically-bedded Bandeira Group shallow water limestones which make up the Mount Loelako ridge (**Fig. 116a**, also see **Chapter 3.9 Mount Loelako**). The western edge of Mount Loelako has most likely been eroded back from the basin-bounding East Maliana Basin Fault, with the more friable, mudstone-rich Aitutu Group lithologies closer to the fault more easily removed than the indurated Bandeira Group limestones that now comprise Mount Loelako. It is possible that faulting parallel to the East Maliana Basin Fault has amplified topography at the scarp, however faults were not directly observed as they were at Mount Lesululi.

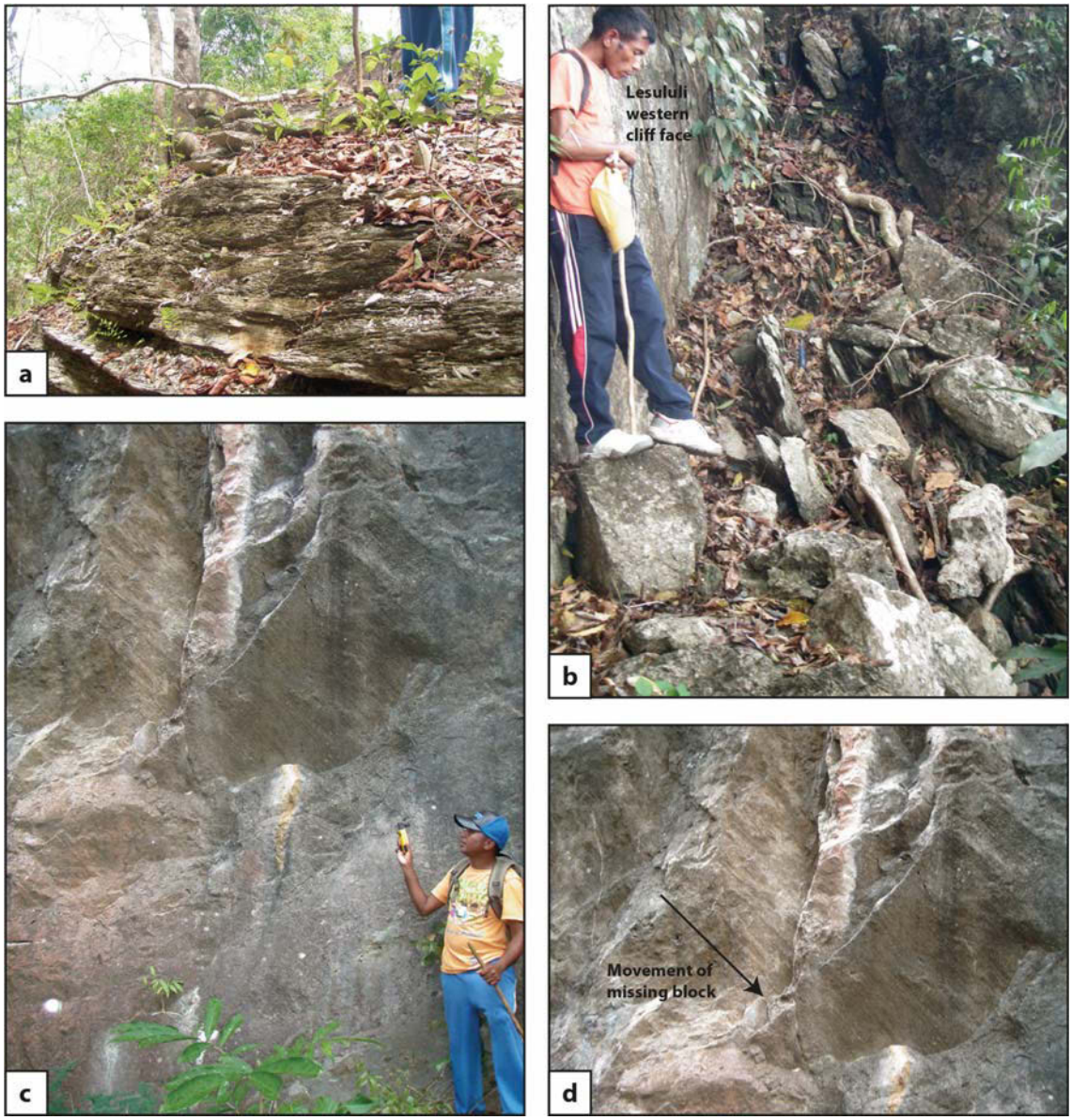

Fig. 123. (a) Interbedded limestones and fissile mudstones approximately 50 m west of the western scarp of Mount Lesululi. Bedding in this area here dips approximately 50° to the north or northwest, and is fairly consistent until within < 10 m of the cliff face (b, facing south) where it is seen to be dragged up sharply to parallel the cliff face which dips at approximately 85° west. (c) Facing east, large striae are visible on the cliff face, plunging towards the south. This cliff face is interpreted as a west dipping, transtensional fault, producing a drag fold in the more ductile, mudstone rich lithologies of the hanging wall as they have been displaced downwards and towards the south against the indurated limestones of Mount Lesululi. (d) Close up of striae on the cliff face showing the interpreted direction of movement of the hanging wall.

A major east-west trending structural discontinuity separates the moderately northwest-dipping limestones of Mount Lesululi from the steeply eastward-dipping to subvertical limestones of Mount Loelako. Based on mapped relationships an east-west trending fault may be interpreted at the southern edge of Mount Lesululi, possibly exhuming the mountain on its southern scarp and tilting bedding back towards the north, however fault outcrops were not directly observed in the field.

The West Marobo Basin Fault bounds the eastern edge of Mount Loelako. Striking due north at the southern end of the Mount Loelako ridge, the fault curves around to the north-northwest at Mount Loelako's northern tip. This fault juxtaposes the gently westwards dipping, Plio-Pleistocene Viqueque Group of the Marobo basin against the subvertically-bedded, Triassic lithologies of Mount Loelako. North-east dipping fault planes (**Fig. 124 a, b**) and thick outcrops of fault gouge (**Fig. 124 c, d**) along the eastern edge of Mount Loelako are associated with the West Marobo Basin Fault; however the fault trace appears to be largely covered with scree shed from the cliffs on this side of the fatu. The Mount Loelako and Mount Lesululi fatus form the highest points of a Triassic horst block between the Maliana basin and Marobo basin, bound on either side by steeply-dipping, north-striking faults.

The Saburai Range begins 2 km south of Mount Loelako and extends to the southwest. It is the only location in this study where thrusting is observed directly – a klippe of Permian Maubisse Group rocks overly Triassic Bandeira Groups limestones at the northern tip of the range, separated by a thrust which dips shallowly to the north (**Fig. 121a**).

The Saburai Range is bound by steep-dipping fault scarps along its north-western and south-eastern edges, parallel to the strike of the range. The North Saburai Range Fault strikes 050°-060°, and dips steeply towards the northwest. Extensively brecciated and recrystallised limestone associated with this fault is common outcropping on the scarp above Saburai village (**Fig. 125a**), and is also observed at the northern tip of the range near the Maliana-Bobonaro road (**Fig. 125b, c**). Fault planes observed within fault breccia near Saburai village strike ~050°, and dip 60-75° towards the northwest, with striae plunging 55°→268°. Near the Maliana-

Bobonaro road sub-vertical fault planes form steep cliffs striking ~015° (**Fig. 125b, c**), and display prominent striae plunging 65°→200° and 70°→205° (**Fig. 125d**). Striae at both these locations therefore indicate left-lateral, transtensional movement most likely associated with the opening of the Maliana basin, and are consistent with movement of the East Maliana Basin Fault observed at Mount Lesululi.

The South Saburai Range Fault bounds the south-eastern edge of the Saburai Range, striking ~030° and dipping steeply towards the southeast. Abundant evidence of the South Saburai Range Fault can be observed along the road south to Lolotoi and Fatululik (**Fig. 126**) which parallels the structural lineament along south-eastern edge of the range (**Fig. 115**).

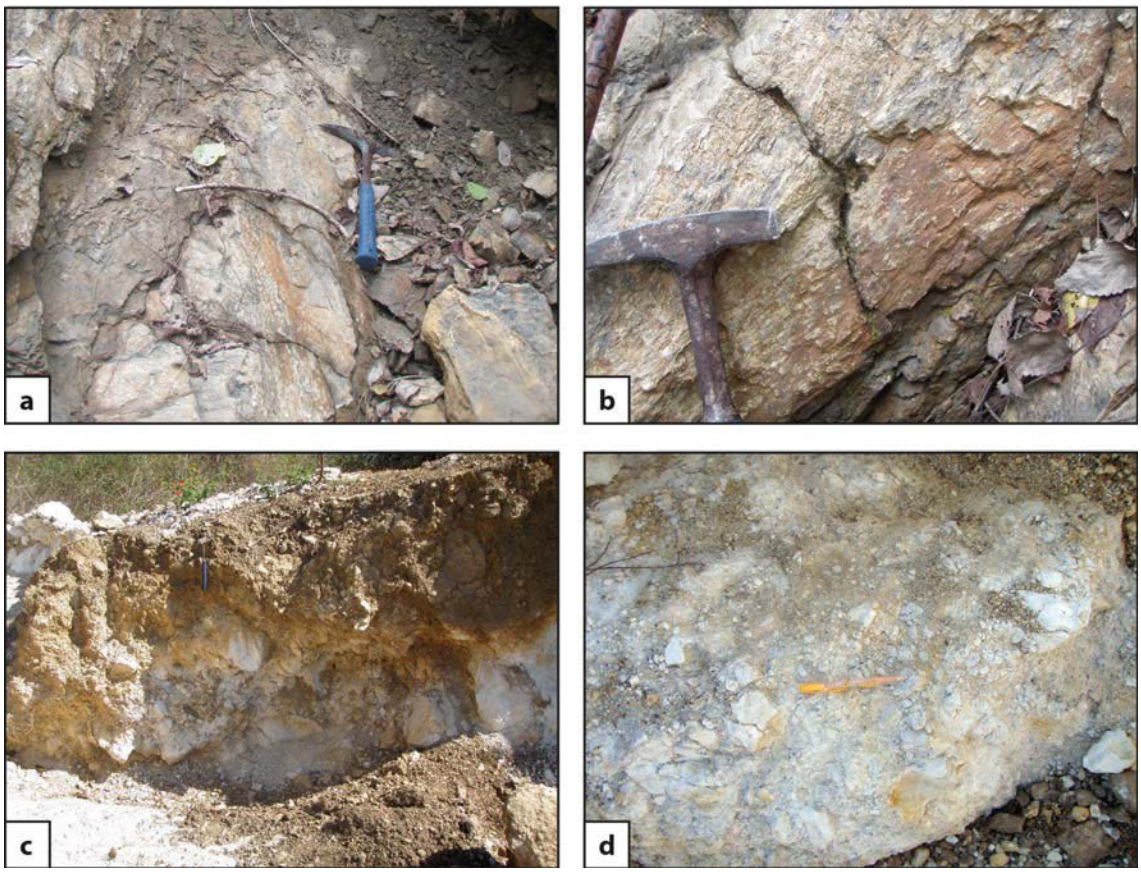

Fig. 124. (a) Hammer sits on an outcrop-scale fault plane at AB479, which dips to the right of frame. Such northeast dipping fault planes along the eastern edge of Mount Loelako are most likely related to the West Marobo Basin Fault. (b) East-plunging striae on this fault plane indicate movement of the hanging wall to the east, co-incident to the opening of the basin. (c) Thick outcrops of fault gouge 10-20 m in width are also found along the lineament of the East Marobo Basin Fault, such as this outcrop at AB639, hammer for scale. These outcrops comprise broken, recrystallized limestone (d) and attest to prolonged periods of brittle shear.

Extensive fault gouge is observed at over a dozen mapped locations, often several metres to tens of metres in thickness (**Fig. 126**, see **Fig. 117** map for fault gouge locations). Several north to northeast striking fault planes are observed associated with this fault gouge (**Fig. 126**). Fault striae generally plunge east to northeast, consistent with left-lateral movement observed on the North Saburai Range fault (**Fig. 126**).

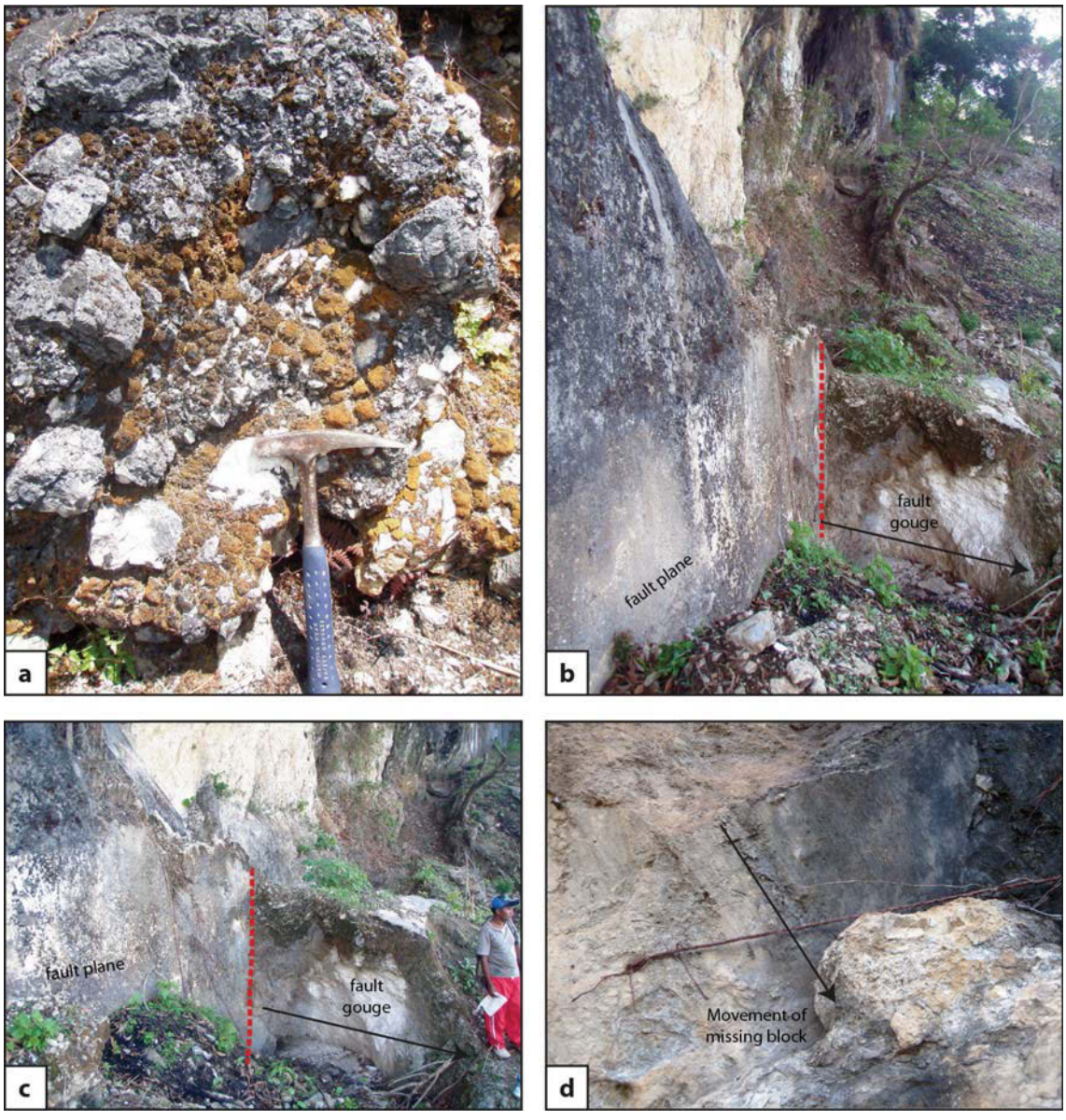

Fig. 125. (a) Fault breccia associated with the North Saburai Range Fault at AB681, near Saburai village. The breccia contains a range of angular, recrystallised limestone clasts 1 < 100 mm in size. Hammer for scale. (b) Subvertical fault planes associated with the North Saburai Range Fault at AB730, fault breccia several metres in thickness in present on the hanging wall. (c) The fault plane at AB730, with field assistant for scale. (d) At AB730, prominent striae plunge towards the southwest, indicating left-lateral, transtensional movement.

Together, the North Saburai Range Fault and the South Saburai Range Fault create a horst block similar to the Loelako horst, and it appears to be a southerly extension of the same structure. However, as discussed there is a significant change in dip between the Bandeira Group limestones at the southern tip of Mount Loelako and the northern tip of the Saburai Range (**Chapter 4.5.1**, **Fig. 121b**), and there may be a significant east-west trending structural discontinuity between the two horsts, similar to that between Mounts Loelako and Lesululi. Outcrop of tectonic melange is observed at AB742, ~4 km due west of the saddle between the Saburai Range and Mount Loeloko, which may be related to this inferred structural zone.

Plotting outcrop scale observations supports the interpretation of regional- and fatu-scale lineaments at the Maliana basin and surrounding fatus (**Fig. 127**). Dominant fault trends at Saburai strike 20°-50° (**Fig. 127a**), which is consistent with the structural lineament of the range itself, and the interpreted North Saburai Range and South Saburai Range faults (**Fig. 115**). Fault trends at Mounts Loelako and Lesululi are slightly more varied (albeit from a smaller sample size). The north-south trend of Loelako is clearly visible in the plot, along with other strong trends at 150° and 300° (**Fig. 127b**). There is also a sub-ordinate east-west trend that may be associated with the east-west trending structural discontinuities between the three fatus. With the exception of the 300° trend at Mount Loelako, both fault plots correlate well with expected Riedel fault orientations in a zone of left-lateral shear (**Fig. 127c, d**). At Mount Loelako, the PDZ would be oriented ~005°, while to the south at the Saburai Range the PDZ moves around to ~050°. Fault striae dominantly plunge east-southeast or west-northwest (**Fig. 127e**), which is consistent with the opening of the Maliana basin in these directions.

Fig. 126 → (a) A steeply dipping fault plane at AB611, striking 052°. Fault striae plunging 65°→074° are consistent with left-lateral, transtensional movement. (b) A large fault plane at AB687 strikes ~040° and dips 50-60° southeast. (c) Several generations of striae on this fault surface at AB687 are consistent with dip-slip and left-lateral movement. (d) Fault gouge several meters thick at AB688. Steeply dipping planes within the gouge strike 035°. (e) Fault planes at AB756 are oriented 060°/50°SE, striae at this outcrop indicate dip-slip movement. (f) Another outcrop of fault gouge at AB690. Planes within the gouge are oriented 044°/55°SE. (g) A very large thickness of fault gouge exposed at AB761. (h) A fault plane at AB761 is oriented 020°/64°SE – the hanging wall rock comprises brecciated, recrystallised limestone. (i) Close up picture of the fault gouge at AB761 illustrating it's unconsolidated, sandy texture.


a
b
c
d
e
f
g
h
i

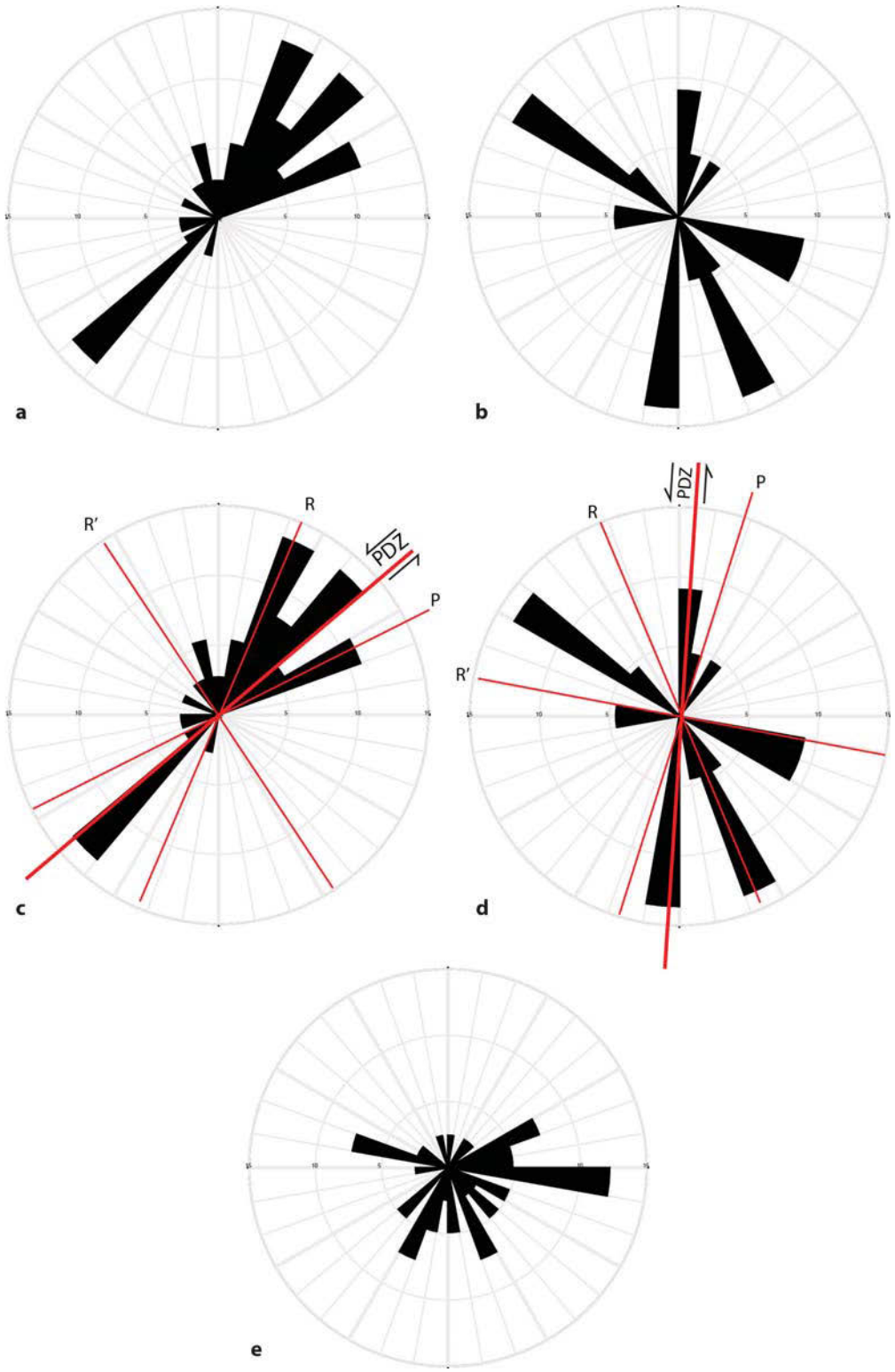

Fig. 127. (a) Rose diagram plotting the strikes of all measured fault planes at the Saburai Range (n=51). (b) Rose diagram plotting the strikes of all measured fault planes at Mount Loelako (n=25). (c) Overlay of expected Riedel fault orientations in a zone of left-lateral shear with measured fault planes at the Saburai Range. If the PDZ is oriented ~050° dominant fault trends correspond with expected Riedel shear and P shear orientations. (d) Overlay of expected Riedel fault orientations in a zone of left-lateral shear with measured fault planes at Mounts Loelako and Lesululi. If the PDZ is oriented ~005° dominant fault trends (with the exception of the 300° trend) correspond with expected Riedel shear, Riedel conjugate shear and P shear orientations. (e) Rose diagram potting the trends of all measured fault striae in the Maliana basin and surrounding fatus (n=41). East-southeast and west-northwest trends are dominant, with subordinate trends at 060°, 150°, and 200°.

Subordinate fault striae directions plot trending 060°, 150°, and 200° (**Fig. 127e**). The 060° and 200° trends are sub-parallel to the margins of the Maliana basin, and may be associated with strike-slip movement at these bounding faults.

4.5.3 Folding

Babulu Group mudstones appear to overlie Bandeira Group limestones at the top of the southern Saburai Range, with these mudstones occupying a depression approximately 1 km wide in the centre of, and parallel to, the strike of the range (**Chapter 3.10.1 The Saburai Range – Grey mudstones with sandstone interbeds**), (**Figs 115, 117**). Bandeira Group limestones comprising the ridges on either side of this depression dip shallowly inwards towards the long axis of the massif. It is possible that this distribution and geometry of stratigraphy may represent syncline, with a northeast-southwest trending fold axial trace oriented parallel to the range. Indurated Bandeira Group limestones in the limbs of the syncline now form high ridges, truncated by faults that bound the edges of the Saburai Range, with recessive, Babulu Group mudstones exposed in the centre of the fold.

As described in '**Chapter 4.5.2 Faulting'**, drag folding is observed in mudstone rich Aitutu Group lithologies where they are faulted against the indurated Bandeira Group limestones of Mount Lesululi, at the East Maliana Basin Fault (**Fig. 123a, b**). Folding is observed as a marked increase in dip within approximately 10 m of the fault scarp that bounds the western edge of the fatu. Dip increases sharply from approximately 50° up to 85°, where the limestone and mudstone beds have been dragged into parallelism with the fault scarp of the cliff face.

Folding is also observed in interbedded Babulu Group mudstones and sandstones at the southern tip of Mount Loelako. At AB420 folding is tight and recumbent, with axial planes oriented 280°/42°/NE and fold hinges plunging 25°→322°. Similar fold styles are observed in the Babulu Group approximately 850 m east, at AB450. Axial planes here were measured at 280°/30°/NE, with fold hinges plunging 20°→320°. It is possible that this folding may related to the potential zone of deformation between Mount Loelako and the Saburai Range, although

more data would need to mapped in this location to be certain, as folding is widespread throughout Triassic lithologies in Timor as a result of older, collisional processes.

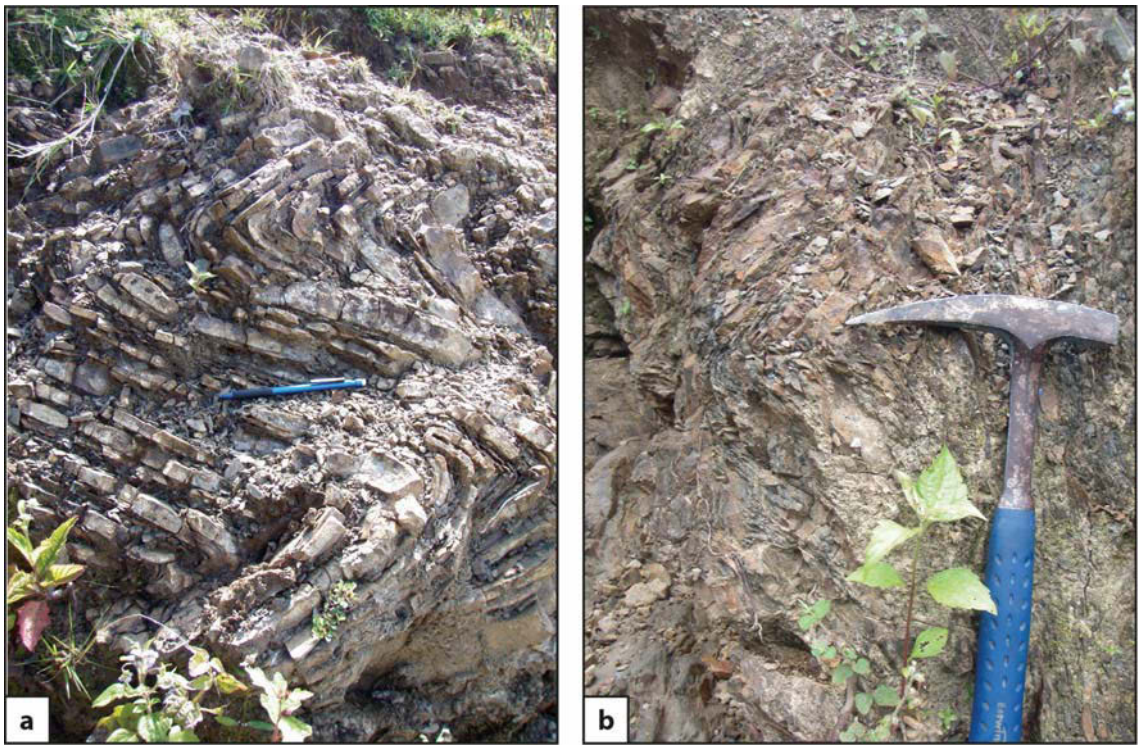

Fig. 128. (a) Tightly folded, thin beds of Babulu Group sandstones at AB420, approximately 400 m southeast of the southern tip of Mount Loelako. Pen for scale. (b) Similarly folded interbedded sandstones and mudstones of the Babulu Group at AB450, approximately 250 m southwest of the southern tip of Mount Loelako. Tip of hammer points to fold hinge.

4.5.4 Melange zones, petroleum seeps and geothermal springs

Bobonaro village, the type section of the Bobonaro Scaly Clay of Audley-Charles (1968), is situated 5 km east of the Saburai Range (**Fig. 86**), and many areas around the Maliana basin were originally mapped as this melange lithology – including all of the western edge of the basin, the lower hills to the west and North of Mount Loelako, and the eastern edge of the Marobo basin. This study has found that most of these areas comprise Triassic lithologies attributable to the Babulu Group or Aitutu Group.

Isolated zones of tectonic melange were observed in a small number of locations. At the saddle that separates the northern and southern sections of the Saburai Range a zone of melange is observed approximately 300 m wide, comprising volcanic cobbles and boulders (most likely Permian in origin, see **Chapter 3.10.5 The Saburai Range – Igneous rocks**) within a matrix of red/green/grey scaly mud (**Fig. 129**). This melange zone is observed to extend approximately 1300 m from the flank of the range up into the central part of the saddle. Tectonic melange is also observed at AB742, ~4 km due west of the saddle between the Saburai Range and Mount Loelako. Outcrop here comprises a variety of angular blocks from centimetre scale to several metres in size, with sandstones and volcanics being the most common, within a matrix of red/grey scaly mudstone.

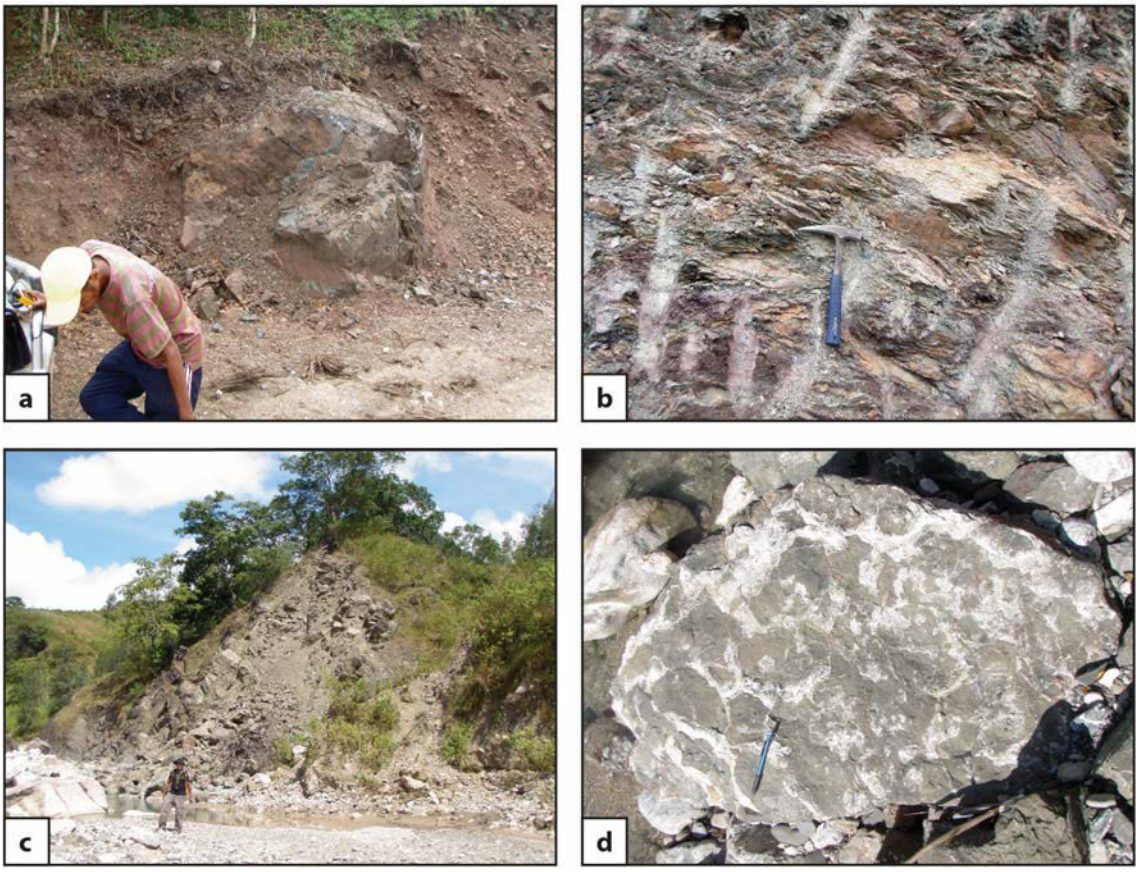

Fig. 129. (a) A large volcanic boulder within a melange zone at AB692, on the eastern flank of the Saburai Range. (b) The matrix of the melange at AB692 comprises red/green/grey scaly mudstone. Hammer for scale. (c) A dislocated block of pillow basalt tens of metres in size within a melange zone near the Marobo Hot Springs. (d) A broken piece of the pillow basalt block showing well defined pillow structures. Pen for scale.

Large blocks of varied, exotic lithologies are also found associated with geothermal springs along the Aitasiola River, at the eastern edge of the Marobo basin. These include large, dislocated blocks of pillow basalt, which are associated with melange zones elsewhere in Timor (e.g. Haig & Bandini 2013).

Several geothermal springs are found along the eastern edge of the Marobo basin, including the well-known Marobo Hot Springs. Temperatures reach 47°C and the springs discharge at a rate of 10 kg/s (Lawless *et al.* 2005). In a non-volcanic setting such as Timor Island such temperatures must require water circulation through faults reaching considerable depth.

4.5.5 Structural model

The Maliana basin displays an extremely distinctive topography, with a large, flat, elongate basin 200 m above sea level surrounded by rugged terrain on either side, with the high fatus of Mounts Lesululi, Loelako and the Saburai Range to the east and southeast (**Fig. 115**). The Plio-Pleistocene to Recent fill of the Maliana basin is juxtaposed against the Triassic, Gondwanan lithologies of the basin margins on very large, high-angle faults which strike north to northwest, with the East Maliana Basin Fault displaying an S-shaped, sinuous fault trace (**Fig. 117**). The Marobo basin east of Mount Loelako is a secondary basin containing similar age Viqueque Group basin fill (**Fig. 117**), however it currently occupies an elevation 800 m vertically higher than the Maliana basin. The Marobo basin is also bound by large, north to northwest striking high angle faults, with the eastern fault the site of geothermal springs sourced from considerable depths. Mounts Lesululi, Loelako and the Saburai Range comprise Triassic horst blocks on the eastern and south-eastern margins of the Maliana basin (**Fig. 117**). The morphology and structure of these fatus are dominated by high angle faults, although the distinctive morphology of Mount Loelako may be largely due to its stratigraphy, and resistance to erosion of the sub-vertically bedded, indurated Bandeira Group limestones that make up its central ridge.

Consistent with other areas mapped in this study, oblique movement is observed on the majority of faults in the Maliana region. Along the western edge of the Maliana basin, fault striae in a number of locations indicate left-lateral, transtensional movement (**Figs 123, 125, 126**). Fault

orientations from Mounts Lesululi, Loelako and the Saburai Range show configurations matching Riedel orientations in a zone of left-lateral shear, further supporting an interpretation of left-lateral movement along this margin (**Fig. 127**). Abundant outcrop of fault gouge along major fault traces, with thicknesses up to tens of metres, is consistent with sustained periods of brittle shear (**Figs 124, 125, 126**).

A possible way of producing such a basin – bound by high-angle, oblique-slip faults – is a releasing bend or step-over within a zone of strike-slip. These pull-apart basins form topographically low, fault-bounded depressions that are commonly the sites of marine embayments, inland lakes and closed topographic depressions, surrounded by uplifted and deeply eroded basement rocks (Mann 2007). The structural architecture of the Maliana basin is similar to that of analogue models of transtensional structures within strike-slip zones (**Fig. 130**).

Dooley *et al.* (2004; 2007) used a sandbox apparatus to model transtensional pull-apart systems having varying mechanical stratigraphies, including a dual layer model to represent a brittle-ductile transition. In their dual-layer models, the final geometry of the basin consists of an elongate graben, with a cross-basin fault zone which diverges around a plunging horst block or blocks, which divide the pull-apart system into multiple grabens (Dooley & Schreurs 2012). The horst blocks form as a result of differential extension between the central graben and the outer sidewall faults, and multiple depocentres may undergo differing amounts of subsidence as active faults switch. Faults bounding the horst blocks are somewhat listric and sole-out into the ductile layer, while basin bounding faults penetrate the full depth of the structural pile.

Fig. 130 → (a) Uninterpreted and (b) interpreted comparison of a digital elevation model of the Maliana basin region (left) with pull-apart basins developed in analogue models of transtensional systems having dual-layer mechanical stratigraphies (right, modified after Dooley & Schreurs 2012). The analogue models develop internal plunging horst blocks, which divide the pull-apart system into multiple grabens. These may be equivalent to the Saburai Range and Mount Loelako structures, with Mount Loelako particularly surrounded by deep synorogenic basins to its east and west.

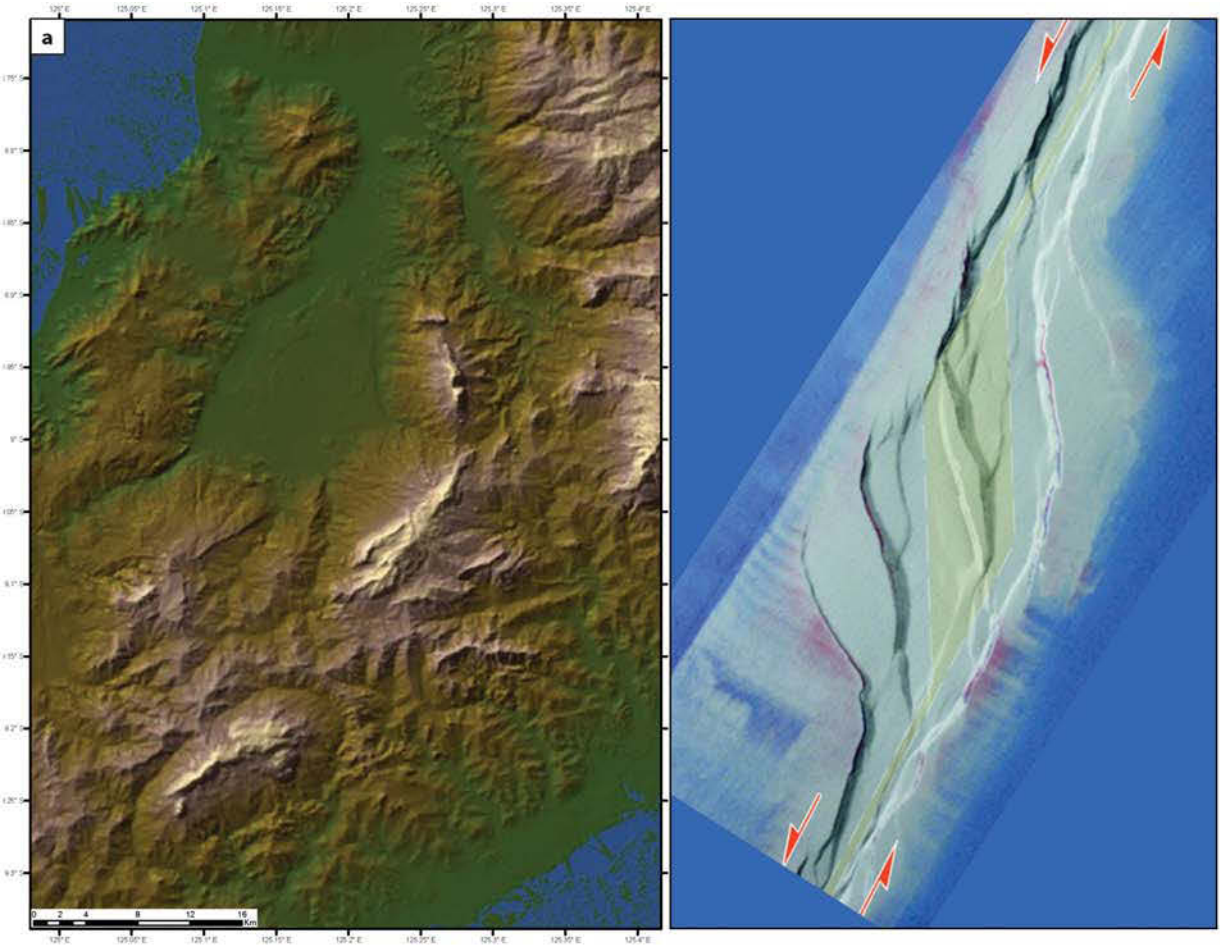
a

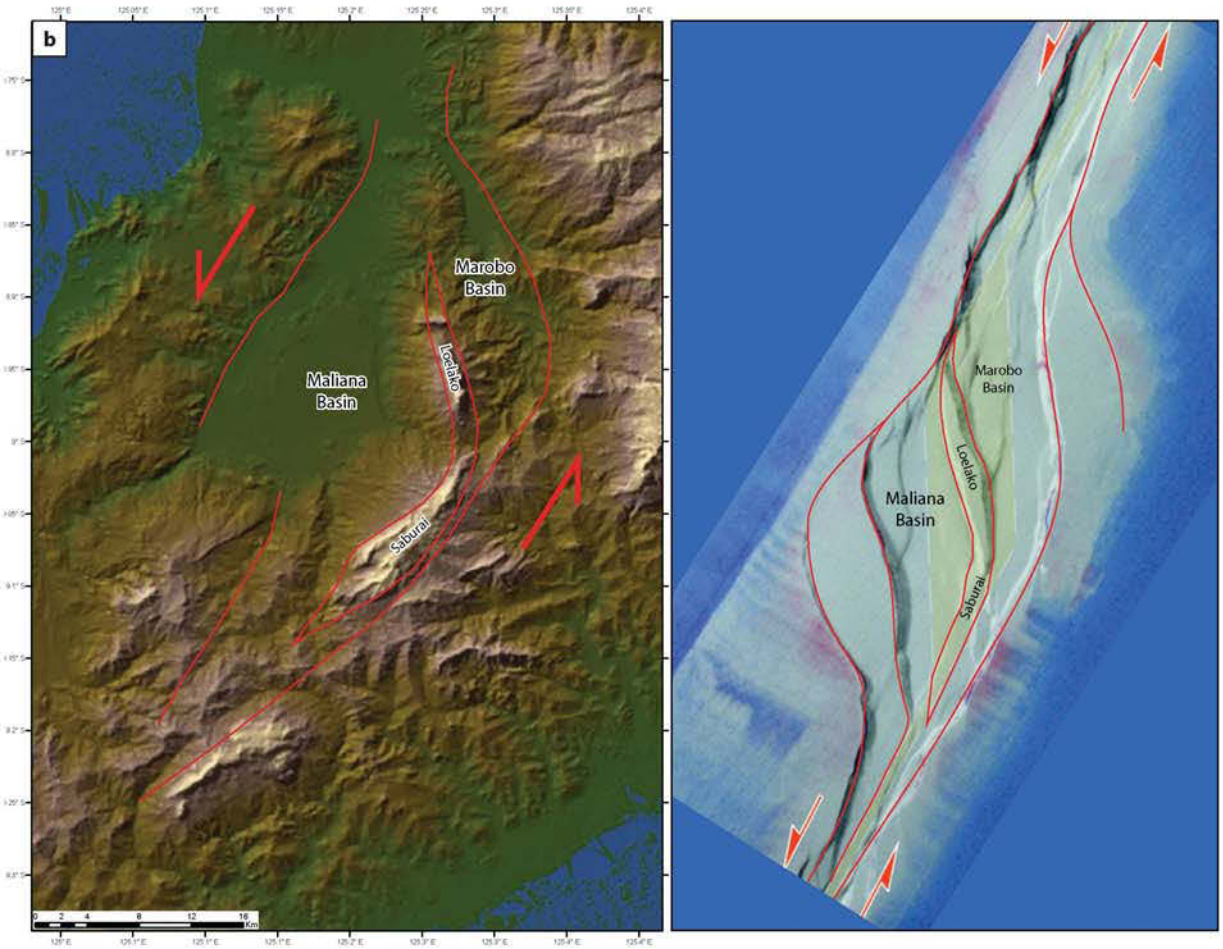
b
Marobo Basin
Maliana Basin
Loelako
Saburai
Marobo Basin
Loelako
Maliana Basin
Saburai

Likewise, the Maliana basin system consists of an elongate graben bound by major transtensional faults. Cross-basin faults diverge around the Lesululi-Loelako-Saburai horst sequence, which divides the two contemporaneous depocentres of the Maliana and Marobo basins that have undergone differential vertical movement (**Figs 115, 117**).

The initial 3-D geometry of the brittle–ductile transition in the dual-layer model has a major impact on the internal deformation within the basin, determining the localization of intrabasin subsidence and the number of internal horsts and grabens formed (Dooley & Schreurs 2012). At the Maliana basin, thick successions of Triassic and Jurassic mudstones are present within the structural pile, possibly at multiple levels due to original shortening, and likely exhibit a complex post-collisional geometry. These lithologies are observed to deform in a ductile fashion throughout Timor, producing broken-formation deformation (Harris *et al.* 1998), zones of tectonic melange (e.g. Haig & McCartain 2010; Benincasa *et al.* 2012; Haig & Bandini 2013, this study), and mud volcanos (Barber *et al.* 1986). Their presence within a strike-slip system at the Maliana basin may be responsible for producing the distinct horsts and multiple depocentres analogous to the sandbox models of Dooley *et al.* (2004; 2007). While faults bounding the Lesululi-Loelako-Saburai horst sequence may sole out into intermediate ductile layers, the basin bounding faults (West Maliana Basin Fault and East Marobo Basin Fault) penetrate deeper into the structural pile, as evidenced by the deep-sourced Marobo Hot Springs.

The Maliana basin is also of similar size and geometry to other known structures along active strike-slip faults. The Salina del Fraile structure is a pull-apart basin developed in Tertiary–Quaternary(?) sediments near Salar de Antofalla in the northern Argentinean Andes (Dooley & McClay 1997). The structure at Salina del Fraile shows strong similarities to the Maliana basin (**Fig. 131**). It has an elongate, rhombic geometry, with a flat to very gently dipping basin floor, and well-developed oblique-slip extensional basin sidewall fault systems (Dooley & McClay 1997). Although the Salina del Fraile structure does not show the internal horst blocks evident in the Maliana basin system and in the dual-layer analogue models above, it otherwise displays a very similar gross geometry and fault architecture to the Maliana basin (**Fig. 131**).

The prominent north-south striking, subvertical bedding of Mount Loelako is an anomaly in East Timor, where an east-northeast trending collision zone has produced folds and thrusts largely sub-parallel to this structural grain elsewhere on the island. However, the models of Dooley *et al.* (2004; 2007) do show some tilting of horsts developed within pull-apart basins, and tilting of the Loelako horst may be expected given the large amounts of differential vertical movement which have occurred on either side, in the Maliana and Marobo basins. Furthermore, rotation of blocks around vertical axes is common within zones of strike-slip (Ryan & Coleman 1992) and in analogue models the presence of a ductile zone at depth allows for even greater fault-block rotation than what is seen in single-layer models (Dooley & Schreurs 2012), so the present-day north-south striking bedding may have been rotated into position. Therefore if the Maliana basin does represent a strike-slip system, it provides some potential solutions to the anomaly of Mount Loelako.

Fig. 131 → Digital elevation model of the Maliana basin region (left) compared with Salina del Fraile (left), a pull-apart structure developed at a releasing bend on a left-lateral strike-slip fault system in the northern Argentinean Andes (modified after Dooley & McClay 1997). Rotating the Salina del Fraile map slightly clockwise so that it is broadly aligned with the Maliana basin, it bears a strong resemblance to the interpreted structure on the digital elevation model. Both structures have comparable scale, morphology, fault architecture and distribution of stratigraphy.

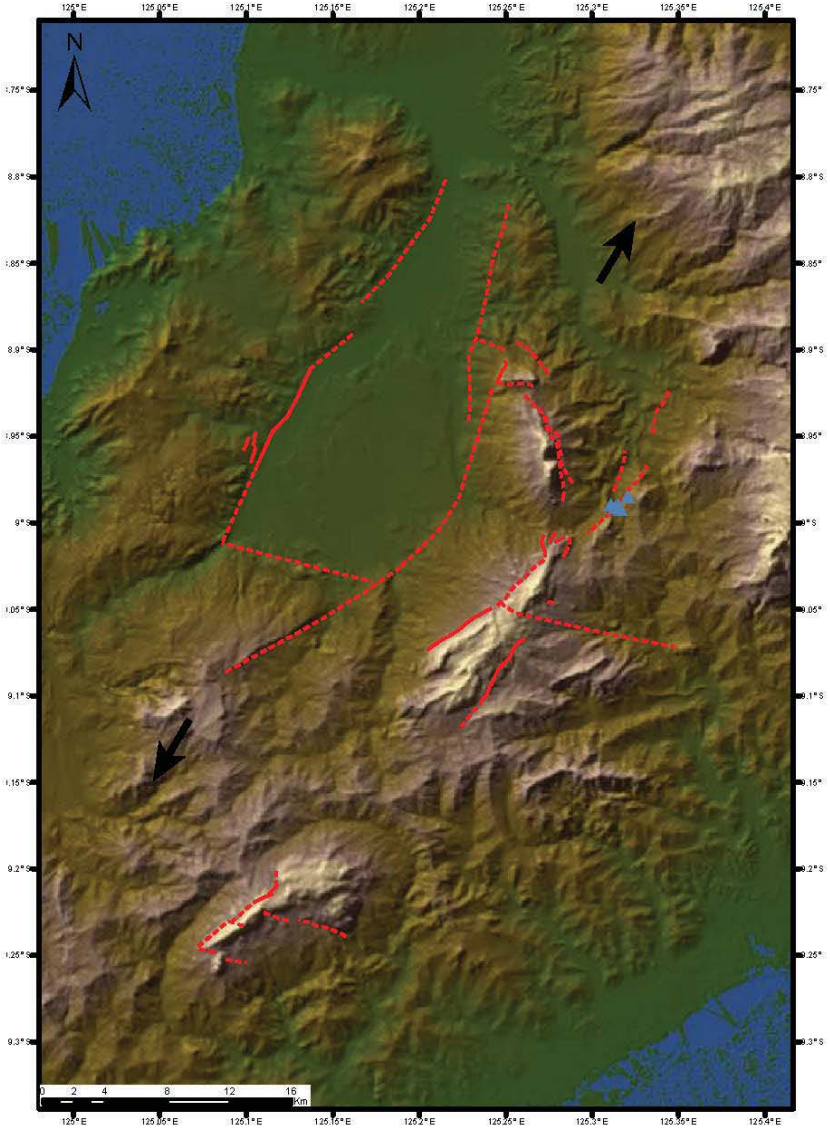
N
125°E
125.05°E
125.1°E
125.15°E
125.2°E
125.25°E
125.3°E
125.35°E
125.4°E
8.75°S
8.8°S
8.85°S
8.9°S
8.95°S
9°S
9.05°S
9.1°S
9.15°S
9.2°S
9.25°S
9.3°S
0 2 4 8 12 16
Km

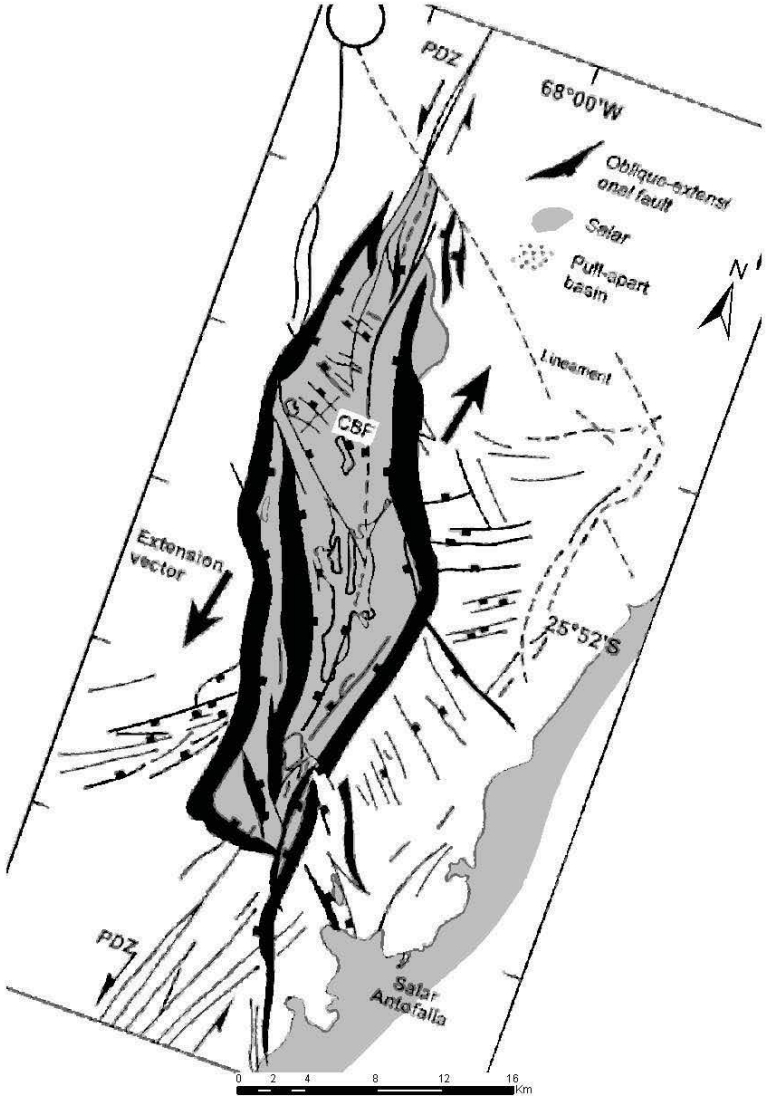
PDZ
68°00'W
Oblique-extensional fault
Salar
Pull-apart basin
N
Lineament
CBF
Extension vector
25°52'S
PDZ
Salar Antofalla
0 2 4 8 12 16
Km

4.6 Mount Taroman

Mount Taroman is a large massif in the southwest corner of East Timor, which rises to nearly 1800 m and dominates the topography northwest of the major coastal town of Suai (**Fig. 86**). It is oriented northeast-southwest, sub-parallel to the Saburai Range from which it lies directly along strike, with Mount Taroman situated approximately 10 km to the southwest of the Saburai Range (**Fig. 132**). Mount Taroman has a distinct stepped topography, with its upper 600-800 m exhibiting a typical steep-sided, blocky, fatu-like morphology, above lower slopes which grade gently down towards the surrounding topography. This steep-sided upper section comprises a broad, irregularly shaped north-eastern segment, and a narrow south-western ridge approximately 1 km wide, which strikes towards 230° for approximately 7 km (**Fig. 132**).

4.6.1 Distribution of stratigraphy

As at Mount Bibileu, only limited mapping was completed at Mount Taroman, with fieldwork being restricted to a small section of detailed mapping on the north-western flank of the range, and one vehicle traverse around the eastern and south-eastern edge. Where sampled, all of the high cliffs of Mount Taroman comprise Perdido Group limestones of the Gondwana Megasequence, and it is likely that these rocks comprise the bulk of the upper, steep-sided section of the range (**Fig. 133**). Along the north-western flank of range, mudstones and sandstones of the Gondwana Megasequence Babulu Group comprise the lower slopes between the Perdido Group limestone cliffs and the rivers below (**Fig. 133**).

Fig. 132 → (a) Aerial photo of Mount Taroman with interpreted structure. (b) Digital elevation model of Mount Taroman with interpreted structure. Faults shown with solid lines have been observed and measured in the field; those shown with dashed lines have been interpreted from aerial photographs. Arrows indicate fault striae where observed and measured on major faults. Inset – Mount Taroman lies directly along strike from the Saburai Range, after which the lineament can be followed curving to the north through Mount Loelako.

Fig. 133 →→ Interpreted geological map of Mount Taroman, showing the distribution of lithologies and main geological structures. Geology outside of mapped areas is modified after Partoyo *et al.* (1995) using aerial photographs. SM = Synorogenic Megasequence, BM = Banda Megasequence, GM = Gondwana Megasequence. Faults shown with solid lines have been observed and measured in the field; those shown with dashed lines have been interpreted from aerial photographs. Strike and dip of bedding is shown where measured.

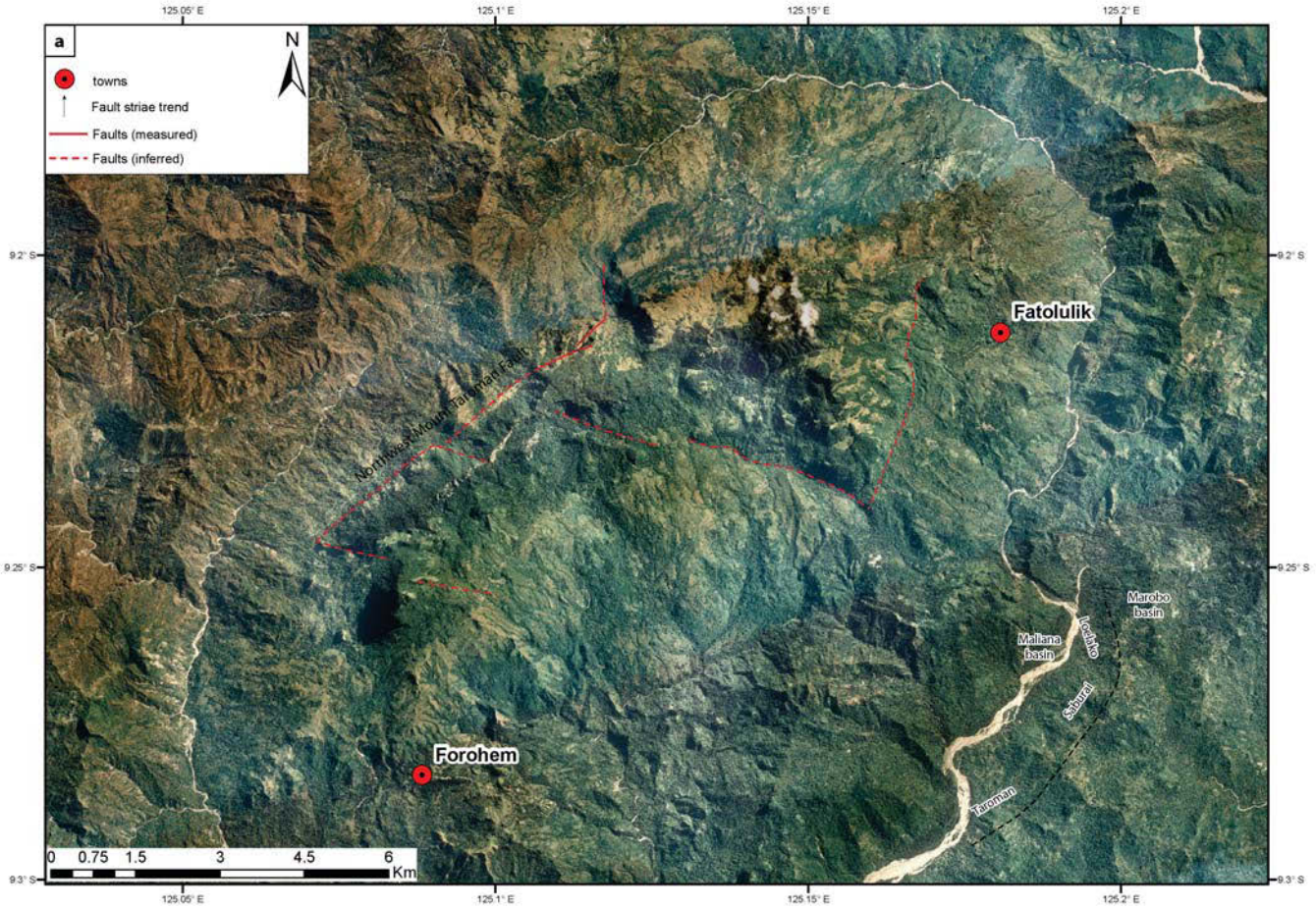
a
N
towns
Fault striae trend
Faults (measured)
Faults (inferred)
125.05° E
125.1° E
125.15° E
125.2° E
9.2° S
9.25° S
9.3° S
Fatolulik
Forohem
Northwest Mount Taroman Fault
Marobo basin
Mallana basin
Loeliko
Saburai
Taroman
0 0.75 1.5 3 4.5 6
Km

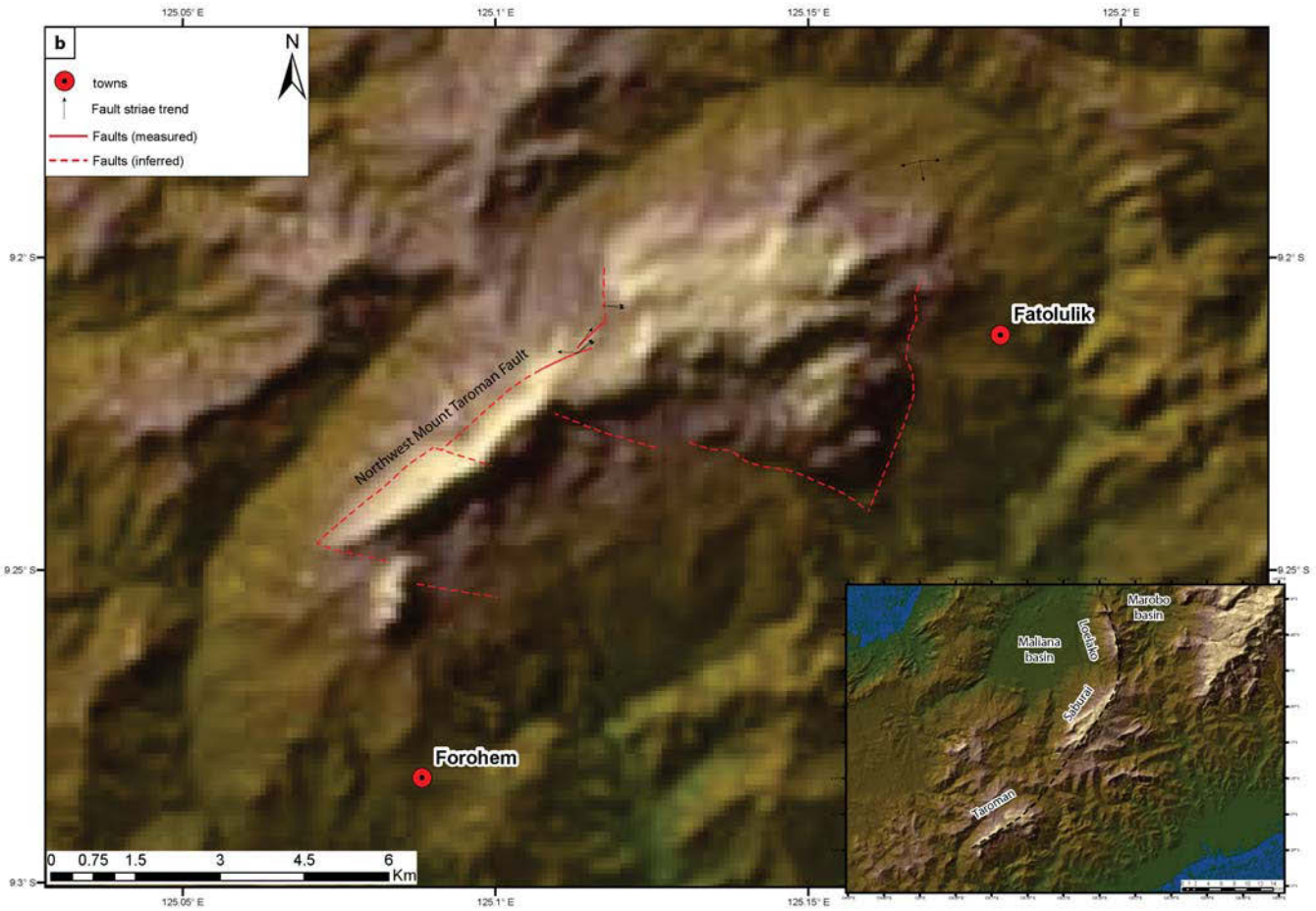
b
N
towns
Fault striae trend
Faults (measured)
Faults (inferred)
125.05° E
125.1° E
125.15° E
125.2° E
9.2° S
9.25° S
9.3° S
Fatolulik
Forohem
Northwest Mount Taroman Fault
Marobo basin
Mallana basin
Loeliko
Saburai
Taroman
0 0.75 1.5 3 4.5 6
Km

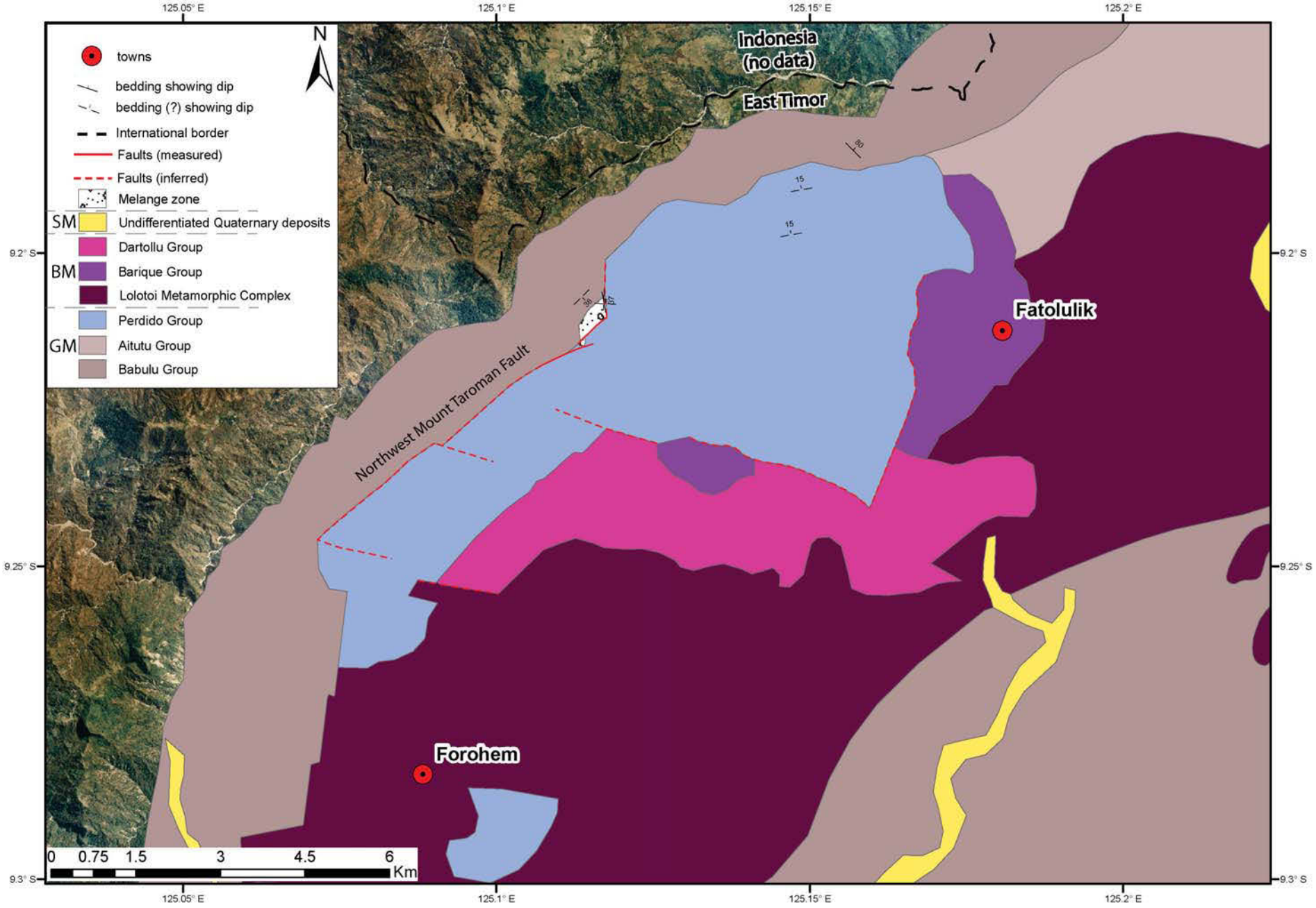
125.05° E
125.1° E
125.15° E
125.2° E
9.2° S
9.25° S
9.3° S
N
towns
bedding showing dip
bedding (?) showing dip
International border
Faults (measured)
Faults (inferred)
Melange zone
SM
Undifferentiated Quaternary deposits
Dartollu Group
BM
Barique Group
Lolotoi Metamorphic Complex
Perdido Group
GM
Aitutu Group
Babulu Group
Indonesia
(no data)
East Timor
Fatolulik
Forohem
Northwest Mount Taroman Fault
0 0.75 1.5 3 4.5 6
Km

Beneath the high cliffs along the eastern flank of Mount Taroman, all outcrop sampled from the lower slopes of the massif comprise igneous and metaphoric rocks of the Banda Megasequence. The Banda Megasequence has also been mapped on the southern flank of Mount Taroman (Barique Group and Dartollu Group lithologies – Audley-Charles 1968; Partoyo *et al.* 1995), however access difficulties prevented sampling of this part of the massif by this study.

4.6.2 Faulting

Two main orientations of structural lineaments are visible on aerial photographs and digital elevation models at Mount Taroman: 050° and 100° (**Fig. 132**). The 050° lineament bounds the north-western edge of the Mount Taroman, and is also the orientation of the long, Perdido Group limestone ridge which extends out towards the southwest of the massif (**Fig. 133**). On a larger scale map, this lineament can be followed up into the Saburai range, which is sub-parallel and directly along strike (**Fig. 132b** - inset). The 100° lineament bounds the southern edge of the main, northern section of Mount Taroman (**Figs 132, 133**). Although not visited in the field by this study, Audley-Charles (1968) mapped this lineament as a fault separating the high Perdido Group limestone cliffs (nee 'Cablac Limestone') from the Banda Megasequence Barique Group and Dartollu Group lithologies below. This orientation can also be seen in minor ~100° striking faults which produce small offsets in the south-western Mount Taroman ridge (**Figs 132, 133**).

On the north-western flank of Mount Taroman, the 050° lineation is visible at several field locations as a major northwest-dipping fault, which separates the Perdido Group limestones of the upper-massif from the Babulu Group mudstones and sandstones below. At AB585 and AB587 a spectacular polished scarp surface is present, covered with friable limestone fault-breccia several metres thick (**Fig. 134**). The scarp is slightly undulating, dipping 30°-45° northwest. At AB585 the scarp strikes ~070° while at AB587 it curves around to 048°, collinear with the main regional lineation. Prominent slip parallel striations, as well as cracks and fissures perpendicular to the slip direction, are visible on the scarp surface (**Fig. 134**). Fault striae are all parallel or sub-parallel to the strike of the plane, indicating strike-slip movement on this surface

(**Fig. 134b, c, d, e**). Tension fractures and gashes are parallel to scarp dip, consistent with strike-slip deformation (**Fig. 134f, g, h**). Kinematic indicators are slightly ambiguous, however where tension fractures appear crescentic in the sense of Petit (1987) they give the impression of left-lateral movement (**Fig. 134h**).

4.6.3 Folding

No evidence of folding was observed at Mount Taroman.

4.6.4 Melange zones, petroleum seeps and geothermal springs

Several outcrops of highly sheared and deformed tectonic melange are observed amidst the mostly recessive geology on the hanging wall of the Northwest Taroman Fault scarp (**Fig. 135**). Lithologies incorporated into the melange include Triassic Bandeira and Aitutu Group limestones of the Gondwana Megasequence, Eocene Kolbano Group limestones of the Australian Margin Megasequence, and schists and igneous mafic rocks of unknown affinity. Clasts sizes range from centimetre scale to boulders several metres in size, with clasts often sheared and deformed. The matrix of the melange is a highly sheared grey to red-green clay. A foliation is present in the clay matrix, oriented subvertically and striking northeast-southwest, sub-parallel to the fault scarp (**Fig. 135c, d**). Kinematic indicators within this melange zone are consistent with left-lateral shear (**Fig. 135e, f**). This zone of sheared melange is observed to extend at least 300-400 m northwest of the scarp, indicating significant a thickness to this structural zone.

No petroleum seeps or geothermal springs were observed during the limited mapping at Mount Taroman.

Fig. 134 → Centre: the Northwest Taroman Fault in outcrop appears as a massive polished scarp dipping to northwest, covered with sheared, limestone fault breccia and friable gouge several metres thick. (a) Closer perspective of the fault, showing fault gouge and breccia being shed as scree from the plane of the fault. The surface of the scarp displays prominent strike-parallel striae (b, c, d, e), often in conjunction with dip-parallel tension fractures (f, g, h), indicating strike-slip movement. (h) Tension fractures in places appear crescentic in the sense of Petit (1987), consistent with left-lateral movement.

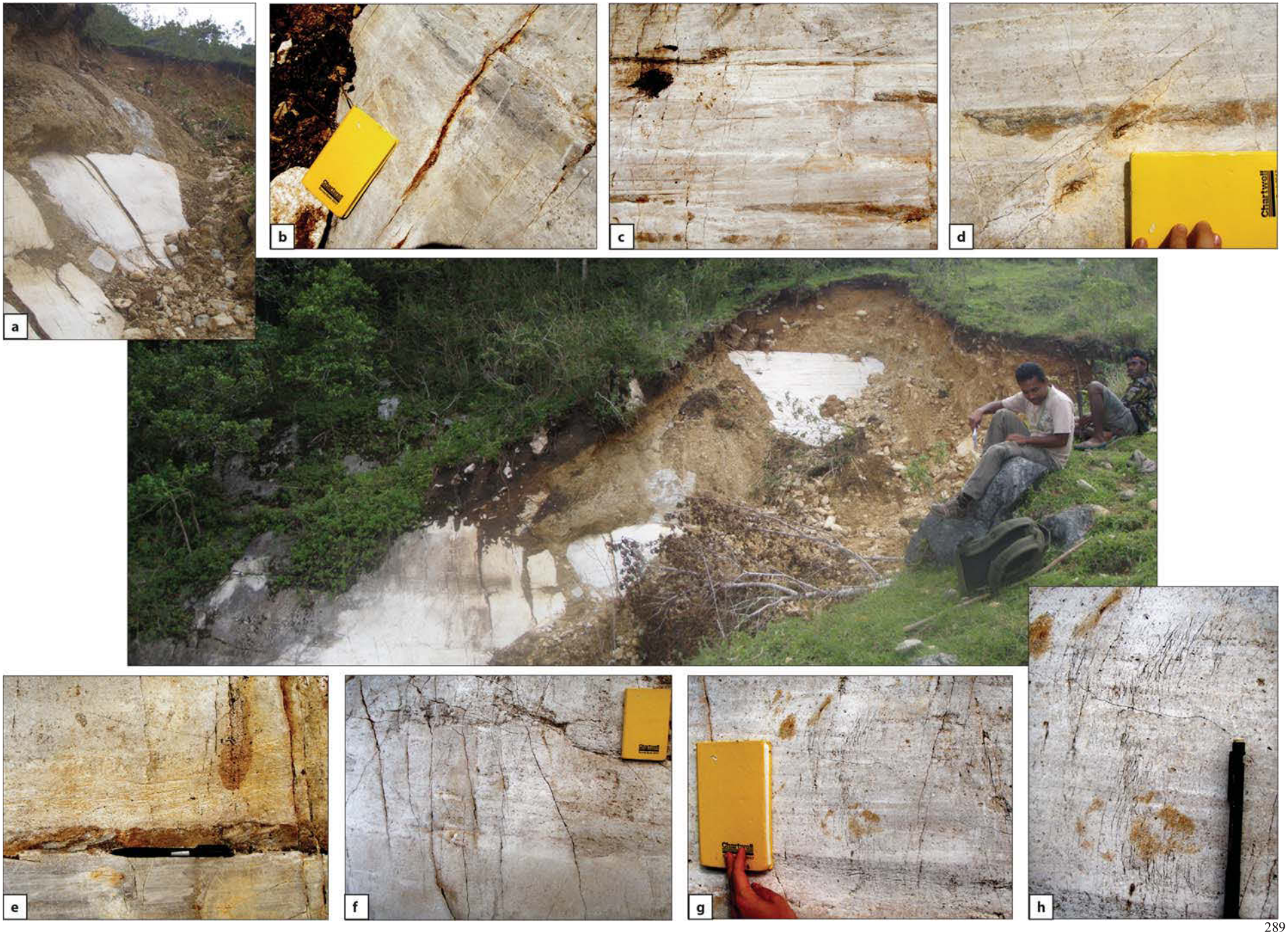
a
b
c
d
e
f
g
h

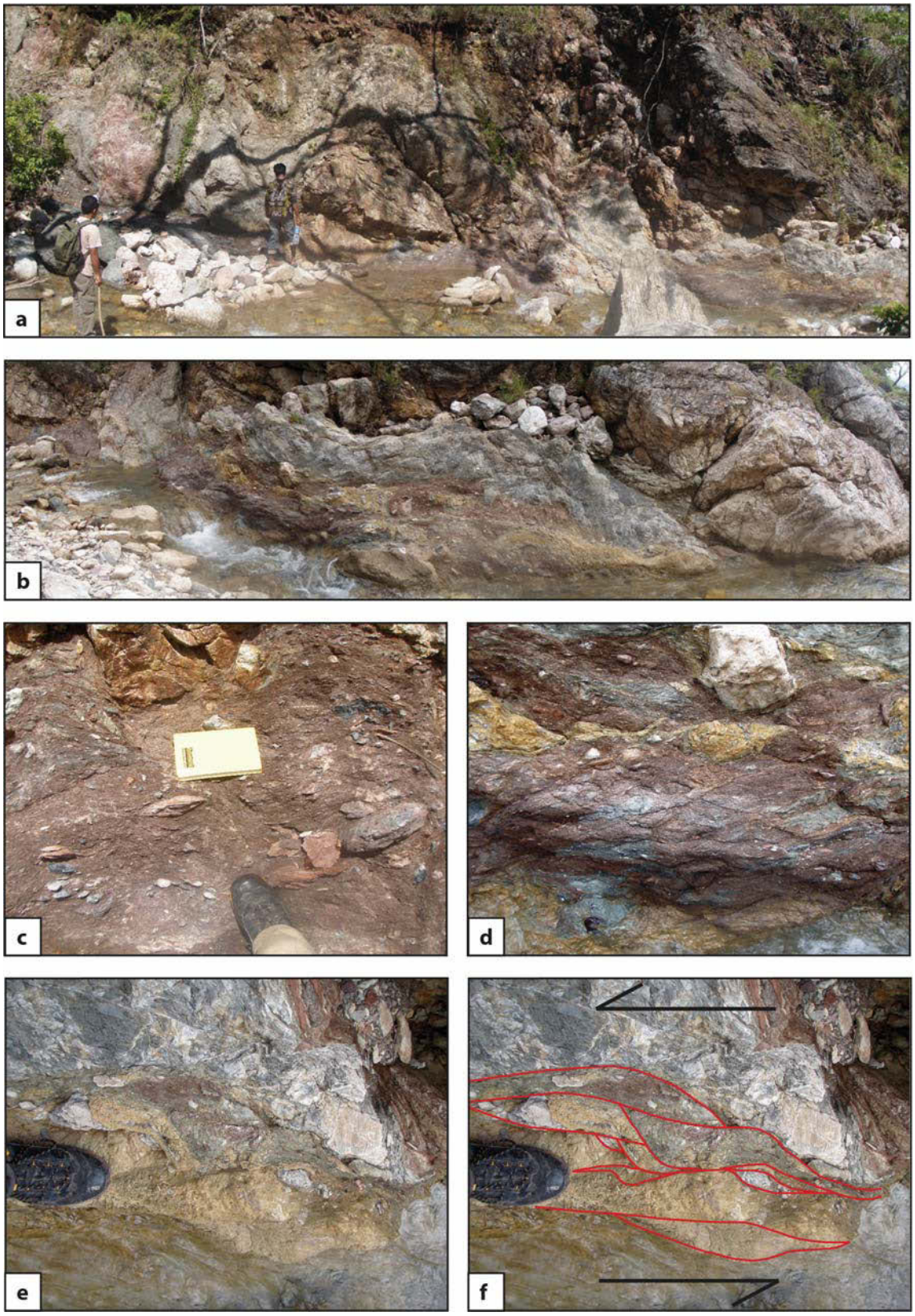

Fig. 135. (a) Sheared tectonic melange observed near the Northwest Taroman Fault, incorporating clasts from ~1 cm to several metres in size, of a range of ages and tectonostratigraphic affinities, within a highly sheared clay matrix. (b) The sheared clay matrix of the melange containing a range of smaller blocks at centre of frame. (c, d) Looking down at the outcrop in plan view, a north-west striking shear fabric is observed in the foliation of the mud matrix, and the alignment of the clasts. (e, f) Kinematic indicators, such as these sheared and offset asymmetric clasts, indicate left-lateral shear.

4.6.5 Structural model

Spectacular evidence of major strike-slip deformation is visible along the northwest flank of Mount Taroman, in the form of a large, polished fault scarp with prominent strike-parallel striations and dip-parallel tension fractures, and a thickness of sheared tectonic melange in the order of several hundred metres. These two structural features are most likely related to the same deformation, with the scarp forming within brittle, Perdido Group limestones and the sheared melange forming within Babulu Group mudstones. The melange zone most likely extends beyond the small, mapped area, and may be present along much of the length of the Northwest Mount Taroman Fault.

This structural zone is present directly along strike from the Saburai Range, and shares the same northeast-southwest orientation. Likewise, indications of left-lateral strike-slip kinematics are present at both the Saburai Range and Mount Taroman, although oblique striae at the Saburai Range suggest transtensional movement while strike-subparallel striae at Mount Taroman are the result of almost pure strike-slip. It is likely that Mount Loelako, the Saburai Range and Mount Taroman are all part of the same zone of left-lateral oblique-slip and strike-slip deformation. The 15 km wide pull-apart structure of the Maliana basin, fault scarps hundreds of metres high along the strike-parallel fatu chain of Mounts Lesululi, Loelako, the Saburai Range and Mount Taroman, and tectonic melange zones several hundred metres thick, all point to this strike-slip zone having undergone significant movement.

Some lithologies present in the Mount Taroman melange zone, such as Kolbano Group limestones of the Australian Margin Megasequence and unknown affinity volcanic rocks, were not observed in outcrop proximal to this zone, and may be sourced from other areas along the fault quite distant to this location.

The zone of left-lateral strike-slip deformation observed by this study extends for over 60 km, from the northern tip of the Maliana basin to the southern tip of Mount Taroman. Timor Island is only 80 km wide in this area from north to south, so it is likely that the zone may cut across the entire island. The island shows a pronounced bend in this area (**Fig. 2**), with the northern

and southern coastlines both exhibiting left-lateral offset, features which may be related to a major zone of strike-slip in this region.

4.7 Summary

All fatus throughout East Timor display a steep-sided, blocky morphology dominated by high, near vertical cliffs up to hundreds of metres in height (e.g. **Fig. 85**), with the largest scarps at Mount Loelako and the Matebian Range reaching nearly 1000 m. When examined closely these cliff faces almost always reveal indicators of movement in the form of fault striae, demonstrating that they fault surfaces (**e.g. Figs 90, 112, 123, 124, 125, 126, 134**). These faults define the boundaries of the fatus and often further divide and segment the fatus internally, juxtaposing rocks of different ages and tectonostratigraphic affinities. The large differential vertical movements accommodated by these faults are spectacularly illustrated at Mount Laritame, where flat-lying terraces of Pleistocene Baucau Limestone have been uplifted to occupy a topographic position 700 m vertically higher than terraces of corresponding age 10 km north on the Baucau Plateau (**Fig. 136**). The Plio-Pleistocene Baucau Limestone observed at Mount Mundo Perdido, Mount Laritame, and the Paitchau Range is the youngest unit displaced (uplifted) by these high-angle faults, suggesting that these faults have been active at least into the early Pleistocene.

Large thicknesses of limestone breccia and fault gouge are associated with these faults in many areas, notably around the Ossu fatus, Mount Loelako and the Saburai Range (e.g. **Figs 124, 125, 126, 134**). These damage zones are in the order of metres to tens of metres in thickness, attesting to prolonged periods of brittle shear indicating large fault displacements. Zones of tectonic melange are observed proximal to some large faults, comprising a chaotic assortment of exotic blocks within a Triassic mud matrix. At Mount Taroman, a melange zone against a major fault has several hundred meters of structural thickness and is observed to be intensely sheared (**Fig. 135**).

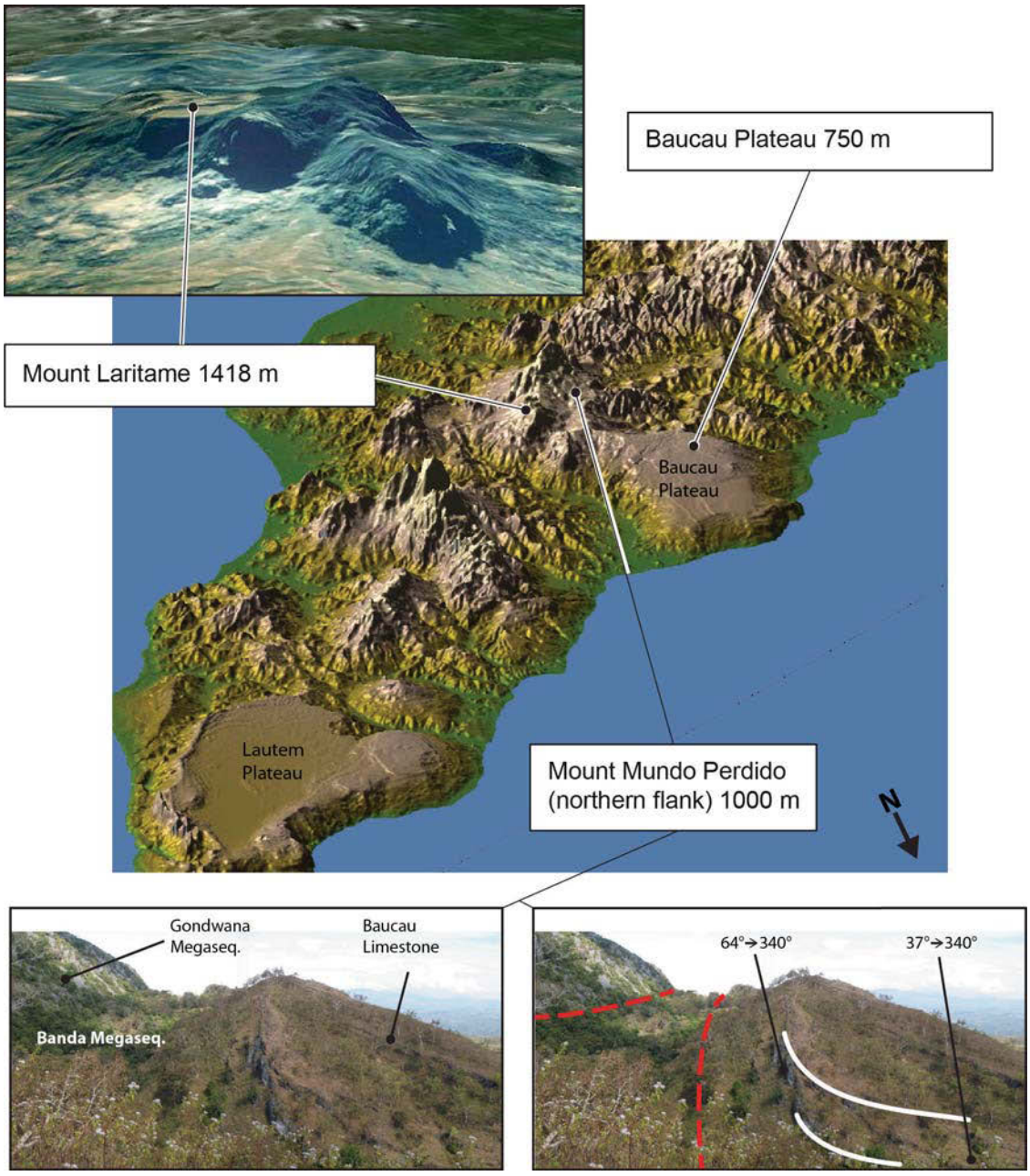

Fig. 136. Differential vertical movements of Pleistocene Baucau Limestone at Mount Mundo Perdido, Mount Laritame and the Baucau Plateau. The Baucau Limestone is a near-shore coral reef succession that has been uplifted since deposition in the Pleistocene. The Baucau Limestone at Mount Mundo Perdido and Mount Laritame have since been vertically displaced by 350 m and over 650 m respectively from the coeval succession at the Baucau Plateau, by movement on high-angle faults. At Mount Laritame this uplift has occurred with no folding or tilting observed, while at Mount Mundo Perdido large drag folds have formed in the Baucau Limestone where they are faulted against the older rocks of the fatu. (modified after Haig 2012c)

Figure 137 summarizes all major faults mapped by this study. Inset (a) shows strike orientations of all 243 fault planes mapped by this study, including minor, outcrop-scale fault planes. Major northwest-southeast oriented strike trends are visible between 020°-050°, and between 060°-070°, with some variation amongst the remainder of the measured fault planes. Inset (b) illustrates strike orientations of 115 measured outcrop fault planes that were large enough in strike length to enable them to be mapped on the 1:5000 scale field maps. Plotting these more dominant faults removes some of the scatter in the rose diagram. The 020°-050° and 060°-070° strike trends are still the prevailing orientations; with minor strike trends also oriented roughly north-south at 000°-010°, east-west at 080°-090°, and northwest-southeast at 140°-150°.

The 020°-050° strike trends are immediately visible in the orientations of the bounding faults of the Maliana basin, the Saburai Range, Mount Taroman, Mount Laritame, the main Matebian Range scarp, the Paitchau Range, and the eastern and western edges of the Lake Iralalaru pull-apart structure . This orientation is also observed in many of the minor, through-going faults which dissect Mount Mundo Perdido.

The 060°-070° trend is sub-parallel to the strike of East Timor itself, which is oriented between 070° at its southern coast and ~080° at its northern coast. Faults which follow this orogen-parallel trend include the northern and southern bounding faults of the Lake Iralalaru pull-apart structure, and the south-eastern bounding faults of Mount Mundo Perdido and Mount Laritame.

The north-south 000°-010° trend comes from measurements around the unusually oriented Mount Loelako, while the east-west 080°-090° trend is seen in bounding and through-going faults at the Ossu fatus and Mount Bibileu. The 140°-150° relates to minor, mapped faults at various locations including Mount Mundo Perdido, the Maliana basin and elsewhere.

Faulting in the fatu limestones has commonly produced huge planes and scarps, many which form the spectacular cliff faces which bound the fatus. Fault surfaces can have differences in appearance depending on the lithologies involved. At Mount Taroman, the main north-western fault juxtaposes limestone against sheared tectonic melange, and has polished, smooth

appearance (**Fig. 134**). Such surfaces are common when limestones are faulted against softer, mud-rich lithologies or volcanics. In faults which juxtapose limestone against limestone, fault planes are often recrystallised and covered with calcite crystals which have infilled the fault zone (e.g. **Figs 90; 124a, b; 126c, e**).

On both types of fault surfaces, kinematic indicators are common. In the case of polished or calcite-overgrown surfaces, striations form when a piece of rock, gouge fragment or mineral grain within a fault plane forms striae, or grooves, as it 'ploughs' through the fault surface during frictional sliding (Petit 1987). The orientation of the resulting striation is parallel to the movement of the fault. This process has been responsible for some spectacular striations observed in East Timor by this study, most notably on fault planes at the Matebian Range (**Fig. 112**) and Mount Taroman (**Fig. 134**) where strike-parallel striations can continue for several metres to tens of metres along the length of a fault plane. On calcite-overgrown surfaces lineations on the plane may be produced by the growth of fibrous minerals which will grow parallel to the direction of fault movement (Petit 1987). This type of movement-parallel mineral lineation is extremely common throughout the limestone faults of East Timor. There were sometimes observed more than one set of striae or mineral lineations on a single fault plane, attesting to multiple episodes of movement with differing vectors (e.g. **Fig. 126c**).

Plotting of all 158 fault striae measured by this study shows two main trend orientations (**Fig. 137c**). The majority of fault striae trend east-northeast to east, sub-parallel to the strike of the East Timor orogen. A second family of fault striae trend south-southwest, oblique to the East Timor orogen and sub-parallel to the major structures of the Matebian Range and the Maliana basin (**Fig. 137c**).

Fig. 137 → Digital elevation model of East Timor showing all faults mapped by this study. Inset rose diagrams show (a) strikes of all faults measured by this study, both map and outcrop scale, (b) strikes of all major, map-scale faults measured by this study and (c) trends of all fault striae measured by this study. (Rose diagram scale is in percent, with the outer edges representing 10% of measured faults)

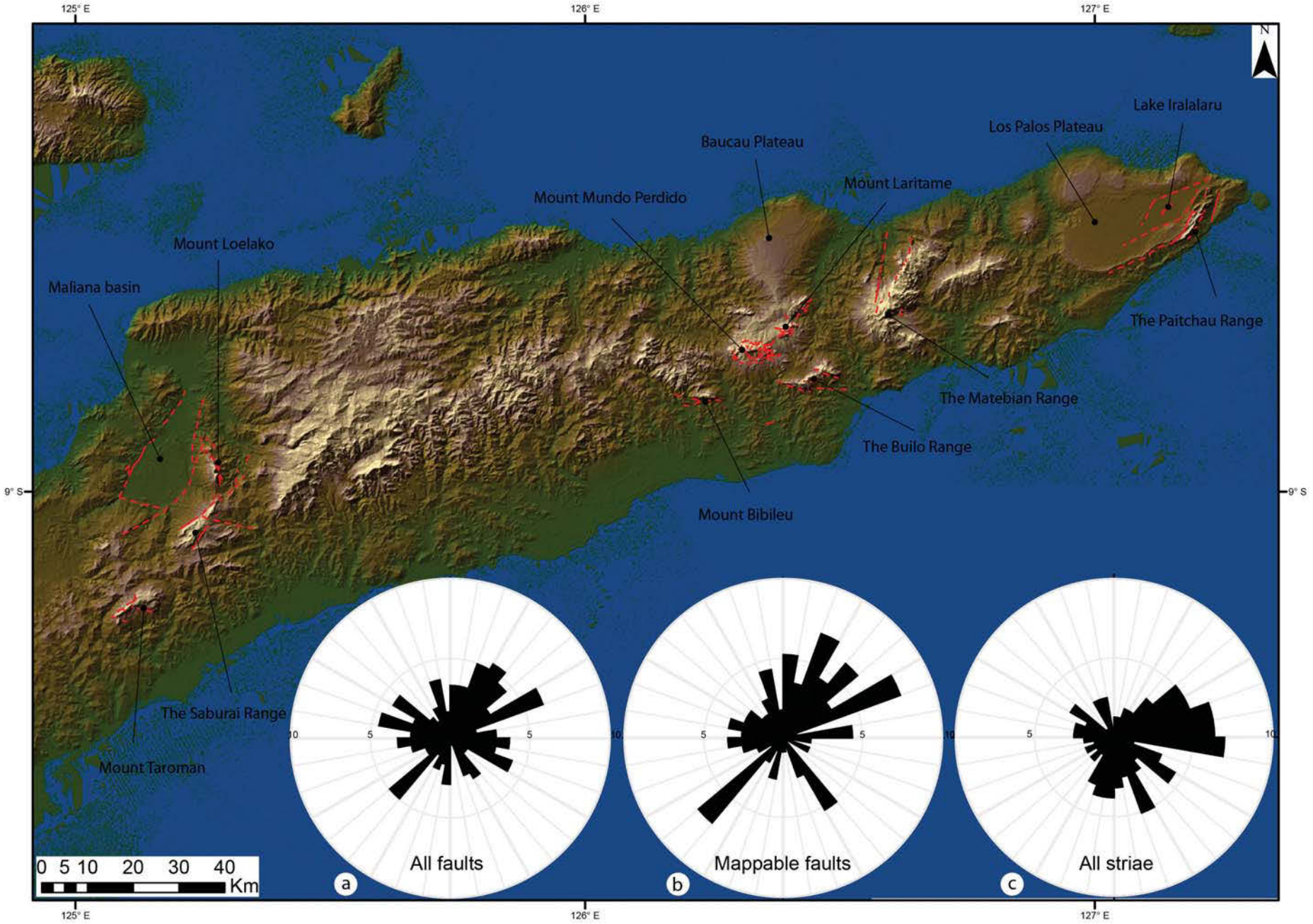
125° E
126° E
127° E
N
9° S
Lake Iralalaru
Los Palos Plateau
Baucau Plateau
Mount Laritame
Mount Mundo Perdido
Mount Loelako
Maliana basin
The Paitchau Range
The Matebian Range
The Builo Range
Mount Bibileu
The Saburai Range
Mount Taroman
0 5 10 20 30 40
Km
a
All faults
b
Mappable faults
c
All striae

Fault striae are able to reveal the direction of fault movement but not the sense, as faults of opposite movement sense will have the same orientation of striae e.g. normal and reverse; sinistral transpressional and dextral transtensional. In order to distinguish between these pairs, further kinematic indicators are required.On some fault planes, kinematic indicators such as tensile fractures, crescentic fractures and accretion steps were used according to Petit (1987) in order to determine the sense of movement on the fault (e.g. **Figs 112b**, **c**; **134h**). Where limestones were faulted against less brittle lithologies such as mudstones or mafic volcanics, shearing is often present in the rheologically softer units. By observing shear fabrics, sigmoidal clasts and other asymmetric deformation within the sheared unit a determination of shear sense, and therefore sense of fault movement, was able to be determined (e.g. **Fig. 135e, f**). However, while it was obvious to determine a sense of dip-slip, strike-slip or oblique-slip movement direction for the majority of faults in this study, movement sense indicators were often far more ambiguous, and only a minority of faults were solved for movement sense.

The vast majority of striae on major, mappable faults are oblique to dip, indicating some component of strike-slip in fault kinematics (**Table 2**). At the outcrop scale we identified 243 fault surfaces from smaller-scale faults throughout the study areas (**Table 2**). Fault striae enabled slip direction interpretations on 142 of the 243 observed fault surfaces, with fault steps, tensile fractures and other kinematic indicators allowing movement sense interpretations on 91 of those 143 faults (**Table 3**). The majority of faults at both outcrop- and map-scale indicate mainly oblique-slip movement (**Table 2, 3**).

Table 4. Classification of major, mappable faults in all study areas. Fault striae indicate a movement direction on 32 of the measured fault surfaces. Kinematic indicators allow a shear sense to be determined on a further 18; indicators included steps and crescentic fractures on limestone fault surfaces, asymmetric deformed clasts within fault zones, and s-c type shear fabrics developed within mudstones. Faults are classified as oblique slip when striae indicate a movement vector with an obliquity greater than 10° from pure strike-slip or pure dip-slip.

Total	Movement indicators		Dip-slip		Strike-slip		Oblique-slip			
	Striae	Kinematic indicators	Normal	Reverse	Dextral	Sinistral	Dextral Normal	Sinistral Reverse	Dextral Reverse	Sinistral Normal
115	78	59	17		9		28		24	
			13	3	0	6	10	8	1	18

Table 5. Classification of all measured fault surfaces in outcrop in all study areas. Fault striae indicate a movement direction on 142 of the measured fault surfaces. Kinematic indicators allow a shear sense to be determined on a further 91; indicators included crescentic and tensile fractures and steps on limestone fault surfaces, asymmetric deformed clasts within fault zones, and s-c type shear fabrics developed within mudstones. Faults are classified as oblique slip when striae indicate a movement vector with an obliquity greater than 10° from pure strike-slip or pure dip-slip.

Total	Movement indicators		Dip-slip		Strike-slip		Oblique-slip			
	Striae	Kinematic indicators	Normal	Reverse	Dextral	Sinistral	Dextral Normal	Sinistral Reverse	Dextral Reverse	Sinistral Normal
243	142	91	23		11		52		56	
			16	3	0	8	19	14	7	24

5. Discussion

5.1 Re-evaluating the fatus

This thesis has presented the results of mapping from a number of limestone fatus in East Timor. The results of this study relative to that of previous work in terms of stratigraphic and structural interpretations are given in **Table 6** and Figure **138**.

In almost all cases the fatus were interpreted by Audley-Charles (1968) as Miocene 'Cablac Limestone', despite many workers over the previous six decades recording units as old as Permian and Triassic as being part of the fatus (Molengraaf 1912; Krumbeck 1921; 't Hoen & van Es 1925; Wittouck 1937; Umbgrove 1938; De Roever 1940; Simons 1940; Tappenbeck 1940; van Voorthuysen 1940; van West 1941; Grunau 1953; Wanner 1956; De Waard 1957; Gageonnet & Lemoine 1958; Romariz & Leme 1967; Grady 1975; Grady & Berry 1977; Brunnschweiler 1978). This interpreted Miocene age became entrained in the literature and incorporated into subsequent geological maps (e.g. Rosidi *et al.* 1979; Bachri & Situmorang 1994; Partoyo *et al.* 1995; Atmaoui *et al.* 2006), and in turn influenced a number of tectonic models. The 'Miocene age Cablac Limestone' fatus of East Timor have since been variably assigned to allochthonous thrust sheets of Asiatic affinity (Audley-Charles 2004; Harris 2006), carbonate build-ups on the outer Australian continental margin (Charlton 2002b), or in situ patch reefs formed after collision but before orogenesis (Audley-Charles & Carter 1972).

However, recent work has re-evaluated the age of the limestone lithologies that dominate the fatus. On the basis of robust biostratigraphic determinations and detailed field mapping Haig *et al.* (2007), Haig *et al.* (2008) and Keep *et al.* (2009) have documented a Late Triassic–Early Jurassic (i.e. not Miocene) age for the Bahaman facies at Cablac Mountain Range. This study now extends that determination to all of the other limestone fatus in East Timor.

In addition, this study documents a number of extensive, young, high-angle faults that dismember the original collisional geometries and control the present-day juxtaposition of stratigraphic units and also control the location of fluid-driven deposits (e.g. oil and gas seeps, melange zones, hot springs). Again these high-angle faults were recognised by previous workers

(Schneeberger 1961; Romariz & Leme 1967; Grady 1975; Grady & Berry 1977; Chamalaun & Grady 1978; Berry & Grady 1981a, b) but not significantly incorporated into previous tectonic models (e.g. Audley-Charles 1968; Reed *et al.* 1996; Harris 2011; see **Chapter 2.2.1** for discussion of tectonic models).

The first part of this discussion examines implications of the stratigraphic determinations of this study, particularly for the Perdido Group, the Bandeira Group, the Booi Group and mud-dominated Triassic lithologies (both structural melange and 'broken formation'). The discussion then examines the significance of late, high-angle faults and the dominance of strike-slip in East Timor, and presents a structural model incorporating the dominant strike-slip mechanisms determined in **Chapter 4**. Finally this chapter explores the implications of the findings of this study for previous tectonic models of Timor, and also explores relationships with adjacent parts of the collisional system, particularly adjacent part of the Outer Banda Arc and the Australian North West Shelf.

5.2 Stratigraphic evaluation

The results of this study support the revisions to the tectonostratigraphic framework of East Timor made by recent studies (Haig & McCartain 2007; Haig *et al.* 2007; Haig *et al.* 2008; Keep *et al.* 2009; Haig & McCartain 2010; Keep & Haig 2010; Haig 2012a; Haig & McCartain 2012; Haig & Bandini 2013), while making some important new findings (**Fig. 138**, **Table 6**).

Fig. 138 → Geological maps constructed by this study (inset), compared with the reconnaissance map of Audley-Charles (1968) (background), on which most geological maps of East Timor are based (e.g. Rosidi *et al.* 1979; Bachri & Situmorang 1994; Partoyo *et al.* 1995; Atmaoui *et al.* 2006). (a) The Maliana basin and surrounding fatus of Mount Loelako and the Saburai Range (**Chapters 3.8, 3.9, 3.10, 4.5**). (b) The Matebian Range (**Chapters 3.7, 4.4**). (c) The Paitchau Range and Lake Iralalaru (**Chapters 3.6, 4.3**). (d) Mount Taroman (**Chapters 3.11, 4.6**). (e) Mount Bibileu (**Chapters 3.5, 4.2**). (f) The Ossu fatus: Mount Mundo Perdido, Mount Laritame and the Builo Range (**Chapters 3.2, 3.3, 3.4, 4.1**).

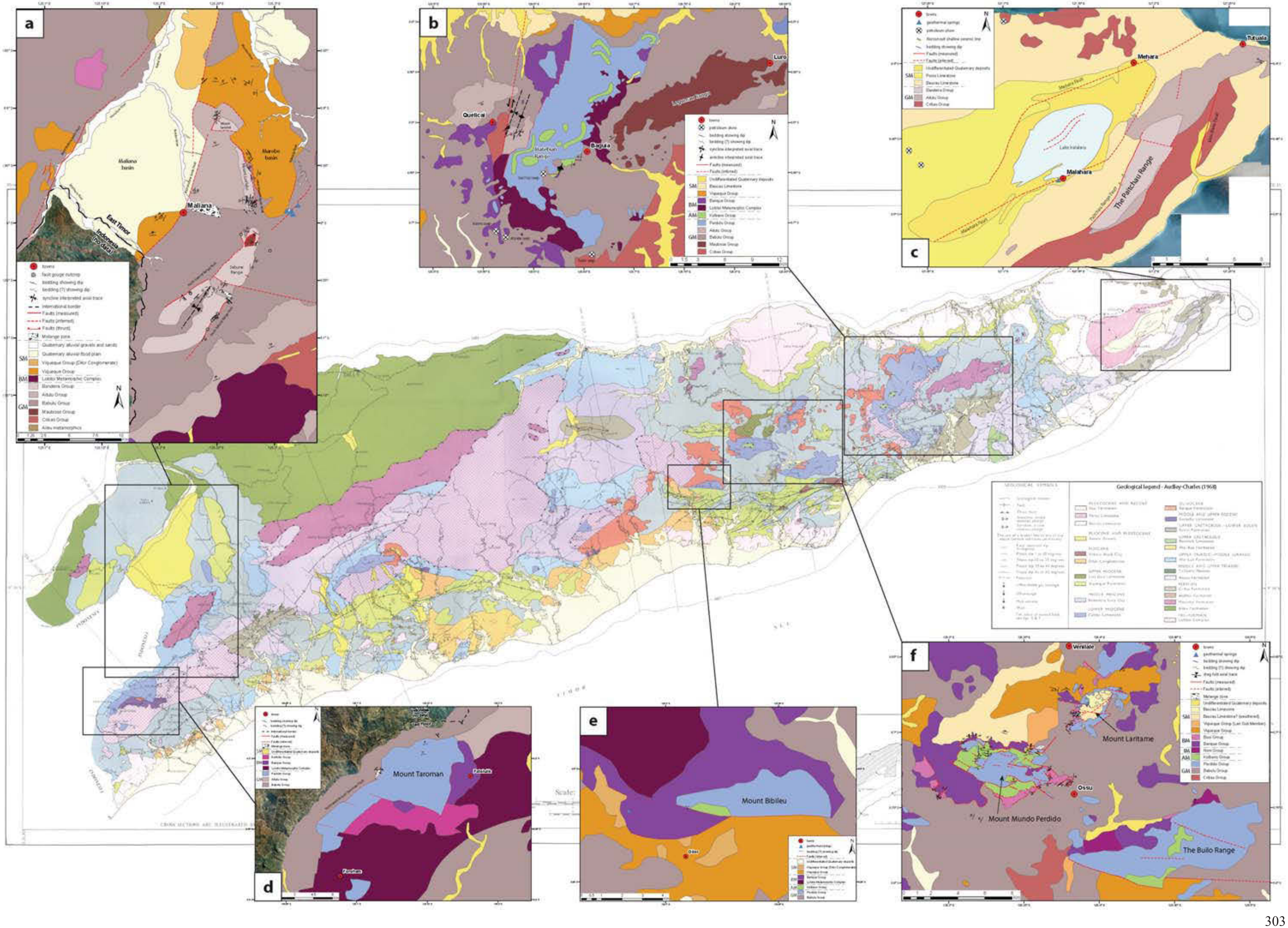
a
Maliana
Maliana basin
Marobo basin
East Timor
Indonesia (no data)
Quaternary alluvial gravels and sands
Quaternary alluvial flood plain
Viqueque Group (Dilor Conglomerate)
Viqueque Group
Lolotoi Metamorphic Complex
Bandeira Group
Aitutu Group
Babulu Group
Maubisse Group
Cribas Group
Aileu metamorphics
b
Quelicai
Baguia
Luro
Undifferentiated Quaternary deposits
Baucau Limestone
Viqueque Group
Barique Group
Lolotoi Metamorphic Complex
Kolbano Group
Perdido Group
Aitutu Group
Babulu Group
Maubisse Group
Cribas Group
c
Tutuala
Mehara
Malahara
Lake Iralalaro
The Paitchau Range
Undifferentiated Quaternary deposits
Poros Limestone
Baucau Limestone
Bandeira Group
Aitutu Group
Cribas Group
Geological legend - Audley-Charles (1968)
d
Mount Taroman
e
Mount Bibileu
Ossu
f
Venilale
Mount Laritame
Ossu
Mount Mundo Perdido
The Builo Range

Table 6. Summary of the revised stratigraphic and structural interpretations of the fatus of East Timor made by this study.

Fatu	Previous stratigraphic interpretation	Previous structural interpretation	Revised stratigraphic interpretation	Revised structural interpretation
Mount Mundo Perdido	Miocene shallow water limestones of Asiatic affinity	Erosional remnants of a thrust sheet of Asiatic affinity, overthrust from the north	A range of lithologies including Triassic-Jurassic interior-rift basin deposits, Cretaceous to Oligocene pelagites, limestones and volcanics of Asiatic affinity, and Plio-Pleistocene synorogenic deposits	A transpressional pop-up structure within a larger zone of east-west oriented sinistral strike-slip.
Mount Laritame	Miocene shallow water limestones of Asiatic affinity	Erosional remnants of a thrust sheet of Asiatic affinity, overthrust from the north	Mainly Triassic-Jurassic interior-rift basin deposits. Minor Cretaceous to Oligocene pelagites, and limestones and volcanics of Asiatic affinity, around the outskirts of the massif. Overlain by extensive, flat-lying Pleistocene synorogenic reef-limestones.	Most likely a transpressional pop-up structure related to the same larger zone of east-west oriented sinistral strike-slip observed at Mount Mundo Perdido.
The Builo Range	Miocene shallow water limestones of Asiatic affinity	Erosional remnants of a thrust sheet of Asiatic affinity, overthrust from the north	Mainly Triassic-Jurassic interior-rift basin deposits, overlain by some Cretaceous to Oligocene pelagites. Jurassic, proto-Indian Ocean affinity mudstones, wackestones and radiolarian cherts along the northern margin of the range	Most likely a transpressional pop-up structure related to the same larger zone of east-west oriented sinistral strike-slip observed at Mount Mundo Perdido.
Mount Bibileu	Miocene shallow water limestones of Asiatic affinity	Erosional remnants of a thrust sheet of Asiatic affinity, overthrust from the north	Triassic-Jurassic interior-rift basin deposits and Eocene carbonate pelagites. Limestones and volcanics of Asiatic affinity comprise lower foothills at western end	An Australian affinity massif exhumed along a high angle, probably transpressional fault along its southern scarp. Possibly related to pop-up structures at Mount Mundo Perdido, Mount Loelako and the Builo Range
The Paitchau Range	Late Triassic – Early Jurassic basinal facies limestones of Australian affinity	The exposed southern limb of a syncline	Triassic, shallow water limestones of Australian affinity.	The uplifted southern margin of a pull-apart basin developed in a zone of east-west oriented sinistral strike-slip.
The Matebian Range	Miocene shallow water limestones of Asiatic affinity	The upper portion of a large nappe of Asiatic affinity, overthrust from the north	Shallow water carbonates of Australian affinity overlain by carbonate pelagites (in part Eocene and Oligocene)	An uplifted core of Australian affinity rocks, exhumed and tilted eastwards by a major west-northwest dipping left-lateral transtensional fault.
Mount Loelako	Miocene shallow water limestones of Asiatic affinity	A klippe remaining from a thrust sheet of Asiatic affinity, overthrust from the north	Triassic, shallow water limestones of Australian affinity.	A horst of subvertically bedded limestones, tilted and exhumed as part of a major, north-northwest trending left-lateral strike-slip system cross-cutting Timor Island in this region
The Saburai Range	Permian shallow water limestones and volcanics of Asiatic (Audley-Charles 1978) or later Australian (Audley-Charles & Harris 1990) affinity	A massive nappe of Permian limestone overthrust on to Jurassic mudstones	Triassic, shallow water limestones of Australian affinity, overlain on its northern tip by a small klippe of Permian sandstones and breccias	A horst of Australian affinity limestones, uplifted and exhumed as part of a major, north-northwest trending left-lateral strike-slip system cross-cutting Timor Island in this region
Mount Taroman	Miocene shallow water limestones of Asiatic affinity	The upper portion of a large nappe of Asiatic affinity, overthrust from the north	Triassic-Jurassic, shallow water limestones of Australian affinity.	The southernmost horst in a strike-parallel chain of uplifted Australian-affinity limestones, most likely related to a major, north-northwest trending left-lateral strike-slip system cross-cutting Timor Island in this region

5.2.1 The Perdido Group

Mount Mundo Perdido, Mount Laritame and the Builo Range were mapped by Audley-Charles (1968) (**Fig. 138**), and similarly by most following authors (e.g. Partoyo *et al.* 1995; Harris 2006) as coherent blocks of Miocene 'Cablac Limestone', deposited unconformably in parts on to Oligocene Barique Formation (mapped in places around the outskirts of the fatus), with Mount Mundo Perdido overlain by a small klippe of Cretaceous 'Borolalo Limestone', equivalent to the Kolbano beds within the tectonostratigraphic framework of this study (**Fig. 9**).

This study has shown that, like the Cablac Mountain Range (Haig *et al.* 2008; Keep *et al.* 2009), most of the high peaks at Mundo Perdido and Mount Laritame are Late Triassic – Early Jurassic, based on the presence of foraminiferal species Duotaxis and Siphovalvulina. In addition, the presence of *Lituosepta* sp. has further confined the age of these Bahaman facies limestones, at least in part, to the upper Lower Jurassic (Pliensbachian). The Bahaman-facies limestones of the Builo Range are similarly assigned to the Perdido Group, and it likely forms the majority of this range previously mapped as 'Cablac Limestone'. This study has also mapped Perdido Group limestones forming significant parts of Mount Bibileu and Mount Taroman, both previously mapped as Miocene 'Cablac Limestone' (Audley-Charles 1968; Partoyo *et al.* 1995; Harris 2006) with similar lithofacies also likely present at Mount Matebian (see **Chapter 4.2.1 The Matebian Range – distribution of stratigraphy**).

5.2.2 The Bandeira Group

First described at the Bandeira Gorge near Atsabe (Brisbout 2010; Haig 2012b), this Carnian-Norian shallow water carbonate group has now been widely mapped throughout East Timor by this study. The Paitchau Range in eastern East Timor, originally mapped as 'Aitutu Formation' (Audley-Charles 1968; Partoyo *et al.* 1995) is recognised by this study as largely comprising Bandeira Group lithologies, which are transitional with the basinal-facies Aitutu Group in places around its base. Mount Loelako, previously mapped as Miocene 'Cablac Limestone' (Audley-Charles 1968; Partoyo *et al.* 1995; Harris 2006) and interpreted as belong to the same Asiatic-derived thrust sheet as the Ossu fatus, the Matebian Range, Mount Bibileu and Mount

Taroman, is found by this study to comprise a ridge of subvertically bedded Bandeira Group limestones. Southwest along strike from Mount Loelako, the Saburai Range has previously been mapped as a massive nappe of Permian limestone (Gageonnet & Lemoine 1958; Audley-Charles 1968; Partoyo *et al.* 1995). This study has observed a small Permian nappe at the northern tip of the Saburai Range; however the majority of the Saburai Range comprises Triassic, Bandeira Group lithologies like those at Mount Loelako.

The finding that fatus across East Timor, previously mapped as predominantly Miocene in age, are in fact dominated by Late Triassic to Early Jurassic lithologies of the Perdido Group and the Bandeira Group, is one of the main contributions of this study. With the Perdido Group first documented at the Cablac Mountain Range (Haig et al. 2008; Keep et al. 2009), and the Bandeira Group at the Bandeira Gorge near Atsabe (Brisbout 2010; Haig 2012b), the results of this thesis extend the identification of these Gondwana Megasequence groups to all of the major fatus studied across East Timor. This significantly changes our understanding of the geological evolution of East Timor.

5.2.3 The Booi Group

Benincasa *et al.* (2012) first mapped the Booi Group earliest Miocene larger foraminiferal limestone (and associated mudstone and sandstone) in East Timor, following the identification of Booi Group limestone in clasts within the Cablac crush breccia by Haig *et al.* (2008 – as Booi limestone). This study has further observed Booi Group limestones at Mount Laritame, and Booi Group mudstones and sandstones at the Builo Range.

Booi Group rocks are associated with Barique Group volcanics at all of the Ossu fatus, and at Mount Mundo Perdido appear to stratigraphically overly the Barique Group (**Fig. 18**). Petrological and geochemical analyses suggest that Barique Group volcanics most likely originated in an island arc type environment (Standley & Harris 2009; Benincasa *et al.* 2012 Appendix B). The stratigraphic succession of Barique Group and overlying Booi Group probably represents the remains of an old Paleogene arc emplaced as part of the Banda Megasequence during collision with the Australian continent (**Fig. 84**). At the Builo Range,

Banda Megasequence lithologies are also associated with Noni Group rocks of the Indian Ocean Megasequence, and both of these non-Australian affinity terranes may have been concurrently overthrust on to Timor during Neogene collision (**Fig. 84**). It is significant that the Banda Megasequence and Indian Ocean Megasequence are found at lower topographic levels around the outskirts of Mundo Perdido, Mount Laritame, the Builo Range, Mount Bibileu, and most likely the Matebian Range, separated from the older, Australian lithologies which comprise the centre of the fatus by high-angle faults. This attests to differential uplift within the fatus and supports their interpretation as being exhumed on high-angle, transpressional and transtensional faults.

5.2.4 The extent of mud-dominated Triassic lithologies

Since the mapping Audley-Charles (1968) (**Fig. 138**), many following geological maps of East Timor (e.g. Rosidi *et al.* 1979; Bachri & Situmorang 1994; Partoyo *et al.* 1995) show the majority of the mud-dominated lithologies of East Timor as a separate unit such as the 'Bobonaro Scaly Clay' or 'Bobonaro Melange'. Since Barber *et al.* (1986) recognised the melange as sourced from Australian affinity units, many of these 'melange' areas have been more correctly mapped as belonging to the Gondwana Megasequence, rather than a separate tectonostratigraphic unit, although mapping of a 'Banda Melange' around fatus is still widespread (e.g. Harris *et al.* 1998; Audley-Charles 2011; Harris 2011). This study has followed Haig and McCartain (2010) in distinguishing between zones of true tectonic melange, usually found along linear structural zones, and units characterised by 'broken-formation' deformation, in which original 'broken' bedding can be readily identified as belonging to a parent rock type. In all the localities visited by this study, the majority of areas originally mapped as 'Bobonaro Melange' or 'Banda Melange' can be identified as stratigraphy belonging to recognised Triassic mud-dominated Gondwana Megasequence rock units, either mudstones and sandstones of the Babulu Group or mudstones and limestones of the Aitutu Group (**Fig. 9**). In areas affected by 'broken formation' deformation, these mudstone-dominated lithologies contain no blocks which are exotic in age or tectonostratigraphic affinity.

Haig and McCartain (2010) documented that limited areas of true structural melange, including exotic blocks, occur along linear structural zones, a finding extended by this study. Such zones occur proximal to areas of transtensional faulting, most notably at Mount Mundo Perdido, near Mount Loelako and the Saburai Range (including near the Marobo Hot Springs), and also at Mount Taroman. These melange zones often incorporate igneous components including large volcanic boulders, in some cases several metres square (see **Fig. 129, Chapter 4** for an example). The proximity of linear zones of tectonic melange to mapped high-angle oblique-slip faults emphasizes the structural controls on these zones of true melange as opposed to the broad expanses of broken formation mud-dominated lithologies.

Contacts between the shallow-water Triassic-Jurassic fatu limestones (Bandeira Group and Perdido Group) and the basinal, mud dominated units surrounding them are generally seen to be high-angle faults. However in some locations, most notably at Mount Loelako, gradational stratigraphic relationships occur between basinal and shallow water facies, with differential erosion producing the spectacular morphology on Loelako's western flank. Other workers have previously described the same gradational contacts between the fatu limestones and surrounding mud-dominated units in both West (De Waard 1957) and East Timor (Wanner 1956).

5.2.5 Implications for structural models

This study has shown that the major fatus of East Timor are not Miocene shallow water limestones of Asiatic affinity, as mapped by Audley-Charles (1968) and others (e.g. Rosidi *et al.* 1979; Partoyo *et al.* 1995; Harris 2011). Rather, all of the fatus visited by this study have their high, central regions dominated by Australian affinity lithologies: either Triassic Banderia Group limestones or Triassic-Jurassic Perdido Group limestones of the Gondwana Megasequence, which are in some places overlain by carbonate pelagites of the Australian Margin Megasequence. In this respect, this study agrees with the observations of many authors prior to Audley-Charles (1968) who described the fatus as comprising mostly Mesozoic, Australian affinity limestones in both West (Molengraaf 1912; Wanner 1913; Umbgrove 1938; De Roever 1940; Simons 1940; Tappenbeck 1940; van Voorthuysen 1940; van West 1941; De

Waard 1957) and East Timor (Hirschi 1907; Wittouck 1937; Wanner 1956; Brunnschweiler 1978), and is consistent with the re-evaluation of the 'Cablac Limestone' at its type section by Haig *et al.* (2008). With this stratigraphic reinterpretation of all major fatus previously mapped as 'Cablac Limestone', in conjunction with areas formerly mapped as 'Bobonaro' or 'Banda Melange' recognised here as either Triassic mud-dominated Babulu Group or Aitutu Group units, this study has dramatically increased the mapped extent of Australian affinity lithologies in East Timor.

With the reinterpretation of the age and tectonostratigraphic affinity of the fatu limestones, it no longer follows that they occupy such high topographic positions as a result of being overthrust on to the developing orogen from the Asian side of the plate boundary during collision. In fact, with the exception of a small Permian klippe at the northern tip of the Saburai Range, no thrust structures were directly observed at any of the fatus visited, and this study has found no evidence that the fatus of East Timor represent the remains of a thrust sheet. This is again consistent with the observations of many previous workers who did not agree with an overthrust interpretation of the fatus (e.g. Wanner 1956; Schneeberger 1961; Romariz & Leme 1967; Grady 1975; Grady & Berry 1977; Brunnschweiler 1978). Rather, every fatu in East Timor is dominated by large high-angle faults, which often dissect the fatus and define their steep-sided, blocky morphology.

At the Ossu fatus, rocks of the Banda Megasequence are juxtaposed against those of the Gondwana and Australian Margin Megasequences. However, the Banda Megasequence rocks, originally emplaced at the top of the structural pile (Harris 2006) are now found at lower structural levels around the outskirts of the fatus. They are juxtaposed by high-angle faults against the Australian affinity rocks which dominate the central regions of the Ossu fatus. This attests to differential uplift within the mountain ranges, a structural style that has previously been observed within the fatus by other workers (e.g. van Bemmelen 1949; Schneeberger 1961; Romariz & Leme 1967). At all the fatus visited by this study, it appears as if differential movement along high angle faults is responsible for exhuming old, Australian affinity rocks

from deep within the structural pile and uplifting them to their present-day, high topographic positions.

5.3 Strike slip in East Timor

Chapter 4 discussed the ubiquity of strike-slip and oblique-slip faulting at and around the fatus of East Timor. Strike-slip and oblique-slip structures occur throughout the study areas at all scales. The relationships are summarised on **Figure 139** opposite and below.

At the Ossu fatus (**Fig. 139**), all three fatus are dominated by high-angle faults, with oblique movement observed on the majority of fault surfaces (**Tables 2, 3, Chapter 4**), and oblique-reverse faults are present at Mount Mundo Perdido and Mount Laritame (**see also Figs 90, 91, 92, Chapter 4**). The morphology, fault architecture and stratigraphic distribution at these fatus show striking similarity to pop-up structures developed within analogue models of restraining bends and stepovers in strike-slip fault systems (Benincasa *et al.* 2012, **Chapter 4.1.5 The Ossu fatus – Structural model**). At Mount Mundo Perdido positive flower structures are observed on strike-faults in outcrop (**Fig. 93, Chapter 4**), the fault architecture and kinematics of which strongly mimic that observed throughout the Ossu fatus at map scale.

At the Paitchau Range, Lake Iralalaru (**Fig. 139**) represents a distinctive rhomboidal basin over 10 km long, bound by high angle faults, which strongly resembles both analogue model and real-world examples (Mann 2007; Wu *et al.* 2009) of pull-apart structures formed at releasing fault stepovers.

At the Matebian Range (**Fig. 139**), the main fault scarp comprises a series of right-stepping en-echelon Riedel segments oriented at 20° to the main fault trace, indicative of left lateral movement (see also **Fig. 111, Chapter 4**). Most major lineaments at the Matebian Range are in fact consistent with expected fault orientations in a Riedel model of left-lateral shear.

Fig. 139. Summary of all major strike-slip systems interpreted in East Timor by this study. The black dashed line oriented at 070° represents the axis of the East Timor orogen. The strike-slip systems interpreted at the Ossu fatus, Lake Iralalaru and Mount Taroman are all parallel to this axis. The strike-slip systems at the Maliana basin and Mount Matebian are oriented oblique to the orogen and possibly represent Riedel orientations.

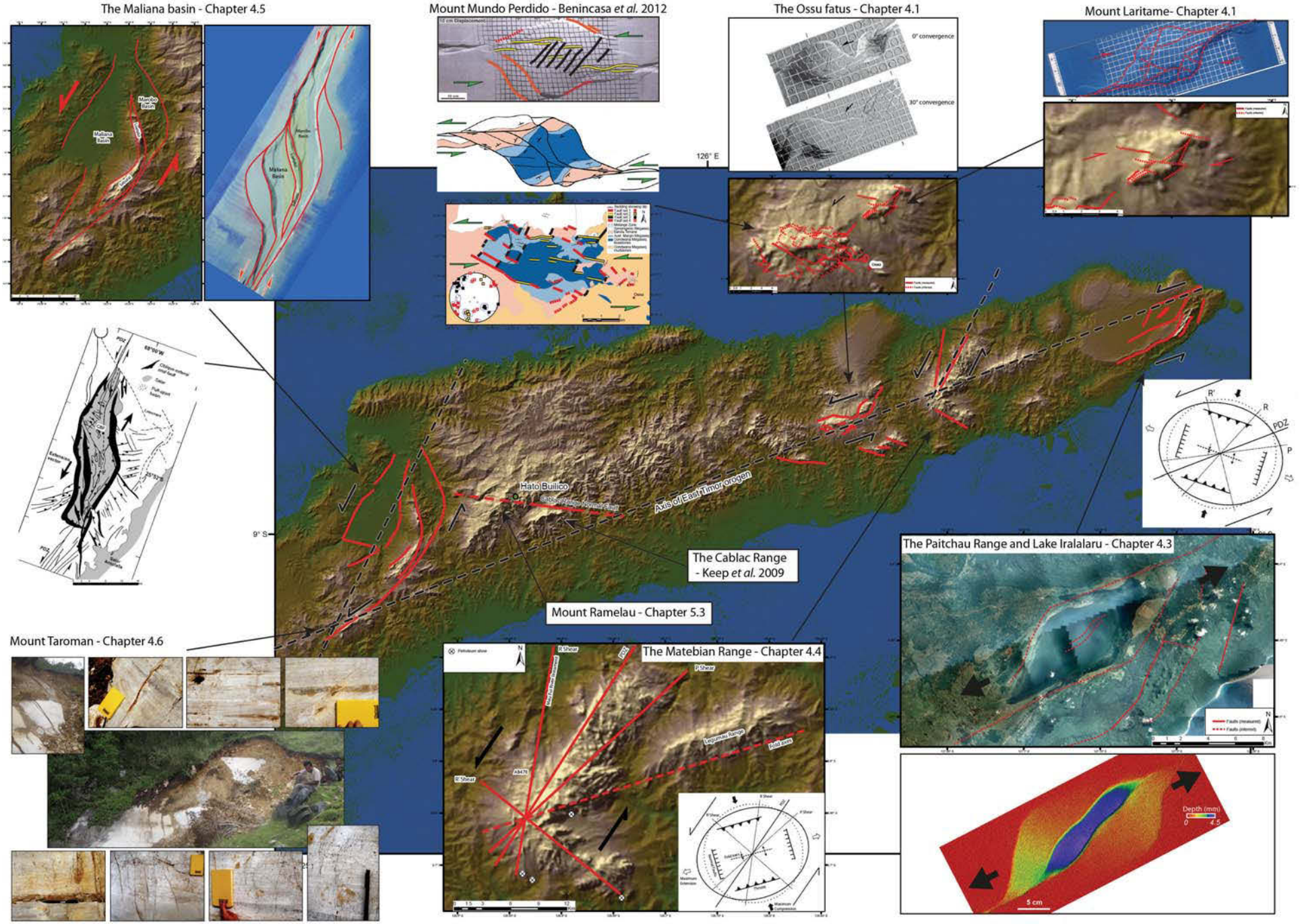
The Maliana basin - Chapter 4.5
Mount Mundo Perdido - Benincasa et al. 2012
The Ossu fatus - Chapter 4.1
Mount Laritame- Chapter 4.1
0° convergence
30° convergence
126° E
9° S
Hato Builico
Axis of East Timor orogen
The Cablac Range
- Keep et al. 2009
Mount Ramelau - Chapter 5.3
The Paitchau Range and Lake Iralalaru - Chapter 4.3
Mount Taroman - Chapter 4.6
The Matebian Range - Chapter 4.4
R'
R
PDZ
P
Depth (mm)
0
4.5
5 cm

A major north-northeast striking strike-slip fault observed in outcrop, just west of the main fault scarp, displaying prominent strike-parallel fault striae, supports the interpretation of left-lateral shear at the Matebian Range.

In the Maliana region (**Fig. 139**), strike-slip and oblique-slip displacement occurs on the majority of mapped fault surfaces. The Maliana basin forms a large, flat, elongate depression bound by high-angle, oblique-slip faults, typical of a releasing bend or step-over within a zone of strike-slip. The structural architecture of the Maliana basin, Marobo basin and associated fatus correlates well with structures formed in analogue models of transtensional pull-apart systems with varying mechanical stratigraphies, which produce multiple depocentres separated by distinct horsts (**see also Fig. 130, Chapter 4**). Southwest along strike of the Maliana basin system, Mount Taroman (**Fig. 139**) forms an elongate fatu bound by a major zone of left-lateral strike-slip along its north-western edge. Strike-slip at Mount Taroman is evidenced by a large polished fault plane exhibiting spectacular strike-parallel striae, and an associated tectonic melange zone several hundred metres thick with sub-vertical foliation and deformed clasts displaying asymmetries consistent with left-lateral shear.

At Mount Laritame, Mount Bibileu, Lake Iralalaru, and the Marobo basin near Maliana, geothermal springs are associated with interpreted strike-slip fault traces, generally the largest, basin-bounding or fatu-bounding faults. This infers that these steep faults extend to the considerable depths required to heat water to temperatures of 40°-60°C. At Lake Iralalaru and the Matebian Range, oil and gas seeps recorded by previous authors also coincide with interpreted fault traces may also be utilising the same faults as fluid conduits.

Chapter 4 also presented possible models to explain the distinctive morphology of the fatus and associated basins in the study areas using analogues of strike-slip systems. If the fatus and basins studied are features related to restraining or releasing bends and stepovers in zones of strike-slip, they represent strike-slip deformation in two major orientations. Firstly, an east-northeast, or orogen-parallel, orientation is broadly shared by the strike-slip systems interpreted at the Ossu fatus, Mount Bibileu, and Lake Iralalaru. Secondly, a northeast, or orogen-oblique,

orientation is shared by the strike-slip systems interpreted at the Maliana region and the Matebian Range. The two main orientations are also reflected in the main trends of fault striae measured throughout the study areas (**Fig. 137**, inset c).

Given the varying geometries of interpreted strike-slip structures in and around the fatus of East Timor, various underlying fault geometries have been proposed, including variations on left- and right-stepping local systems, and underlapping systems, sometimes with a degree of obliquity. Subtle differences at each fatu reflects different fault strands or Reidel types within a larger-scale system. **Figure 139** details these observations, showing the nature of the interpreted strike-slip system through East Timor. We interpret that strike-slip dominates the late stages of the orogen as currently exposed in East Timor, related to oblique convergence and subsequent collision of the Australian Plate with the Banda Arc. In this model we extend the interpreted strike-slip faults between the fatus mapped in this study and incorporate previous data from Mount Mundo Perdido (Benincasa et al. 2012) and data from other fatus such as Cablac Mountain Range (**Fig. 139**) (Haig *et al.* 2008; Keep *et al.* 2009) from work that preceded this study.

The presence of pop-up structures in restraining bends causing differential uplift and exposing Gondwana-related lithologies as the structurally and topographically highest points of the fatus may also apply to other regions of East Timor that were not mapped as part of this study. For example, the highest topographic point in East Timor, Mt. Ramelau (**Fig. 139**), occurs in close proximity to the Cablac Mountain Range, and extends to 2986 m above sea level. Exposure along the path to the peak from the village of Hato Builico (**Fig. 139**) display numerous outcrops of weathered basaltic materials, in places estimated by Audley-Charles (1968) to be over 500 m thick, which preserve pillow basalts in places (Keep pers. comm. 2014). Audley-Charles attributed the thick succession of basic eruptive rocks forming Timor's highest peak to the Permian Maubisse Formation. This therefore represents another example of some of the oldest stratigraphic units in Timor (again of Australian affinity) being exposed at the structurally and topographically highest levels. Although the recessive nature of Mount Ramelau (and of other nearby basaltic outcrops at the Cablac Mountain Range – see Keep *et al.* 2009) does not

allow for identification of obvious fault scarps, it is clear from the SRTM image (**Fig. 139**) that the location of Mount Ramelau coincides with a strong northeast-trending structural lineament that parallels the westerly-adjacent East and West Maliana Basin faults and is along strike from the interpreted fault at Mount Taroman (**Fig. 139**). Given the hypothesis presented in this thesis that strike-slip dominates the young deformation of East Timor, exposing older Australian-related lithologies at topographically and structurally high levels, it seems likely that a similar interpretation could be applied to Mount Ramelau. There is no other presented explanation for why the interpreted Permian age basalts exposed on Mount Ramelau should be the topographically highest point in East Timor when presumably they formed the base of the structural pile during initial shortening.

5.4 Strike-slip at convergent margins

Orogen-parallel strike-slip occurs commonly at convergent margins. Jarrard (1986) estimates that over 50% of subduction zones are accompanied by strike-slip faults that parallel the plate boundary. Beck (1986) further considers that the proportion is probably higher, as the presence and intensity of strike-slip faulting at convergent margins is often difficult to recognise, even with detailed mapping. Fitch (1972) was the first to propose a model for oblique convergence between plates, where any fraction of slip parallel to the plate margin results in strike-slip movements on subvertical faults parallel to the plate boundary. Jarrard (1986) has since shown that the primary factor controlling the presence of plate-boundary parallel strike-slip faulting is coupling between the plates, and that strongly oblique convergence is not required. Active strike-slip faulting is currently observed within subduction zones with near-perpendicular convergence, such as at the Atacama fault zone in northern Chile (Jarrard 1986; see Benincasa *et al.* 2012 for comparison of structures formed at the Atacama fault zone with Mount Mundo Perdido).

In East Timor, the locking of the subduction zone and the transition from subduction to collision has resulted in a strongly coupled system. Therefore, even without a large component of obliquity zones of plate-margin parallel strike-slip should be expected (Jarrard 1986). The overall NNE convergence direction of Australia with respect to the Pacific and Eurasian plates

(Genrich *et al.* 1996) has long been thought to have generated strike-slip motion at the plate boundary (Nelson 1993; Keep *et al.* 1998; Shuster *et al.* 1998; Ainsworth *et al.* 2000; de Ruig *et al.* 2000; Harrowfield *et al.* 2003; Harrowfield & Keep 2005; Bourget *et al.* 2012). However, occurrences of strike-slip on the Australian part of the margin are limited to local structures (Ainsworth *et al.* 2000; de Ruig *et al.* 2000; Keep *et al.* 2000), with the majority of strike-slip thought to be accommodated at the collision front, on Timor Island (Harrowfield *et al.* 2003). The structures documented in this thesis may be the evidence of plate-boundary parallel strike-slip in East Timor that has been suggested by previous workers.

North-northeast oriented strike-slip systems have previously been postulated in East Timor (Audley-Charles 1985; Charlton *et al.* 1991), and even included in regional scale maps (e.g. Audley-Charles 2004), however this study is the first to observe and document examples in the field. Audley-Charles (1985) used the results of previous mapping in conjunction with seismic data from shallow focus earthquakes to infer the presence of north-northeast oriented strike-slip in the Timor region. Charlton *et al.* (1991) mapped small north-northeast striking wrench faults *ca.* 2 km in strike length at Kolbano, in southern West Timor (see locality **Fig. 140**), and discussed the presence of a series of larger scale zones of strike-slip of the same orientation cutting across western Timor Island. He described strike-slip faulting as of great importance in controlling structural relationships. North-northeast striking zones of strike-slip are thought to have developed in several places in the Timor region as transfer zones accommodating differing rates of convergence within the collision zone (McCaffrey 1989; Genrich *et al.* 1996; Nugroho *et al.* 2009).

McCaffrey (1989) modelled this differential shortening across Timor Island using fault plane solutions of shallow-focus earthquakes. He interpreted three zones of north-northeast oriented strike slip in the vicinity of Timor Island: subparallel to the west coast of West Timor separating Rote Island from Timor Island, in the centre of Timor Island through the Maliana basin, and off the coast adjacent to the eastern tip of Timor Island (**Fig. 140**). In the central zone through the Maliana basin region McCaffrey (1989) also noted shallow earthquakes showing left-lateral, strike-slip on NE-trending, vertical fault planes (McCaffrey 1989, 1996). Evidence for this

north-northwest trending strike-slip zone extending north from the Maliana basin up through the Wetar Strait can be seen on the seafloor in sidescan sonar and seismic reflection data (Masson *et al.* 1991). Masson *et al.* (1991) mapped a complex zone of left-lateral strike-slip extending south from between the islands of Alor and Wetar, around Atauro Island, and then almost cutting across the entire island of Timor at a north-northeast orientation along the western edge of the Maliana basin (**Fig. 140**). Clear evidence of left lateral movement on the sea floor includes ridges offset by north-trending faults and pull-apart basins bound by prominent fault traces (Masson *et al.* 1991).

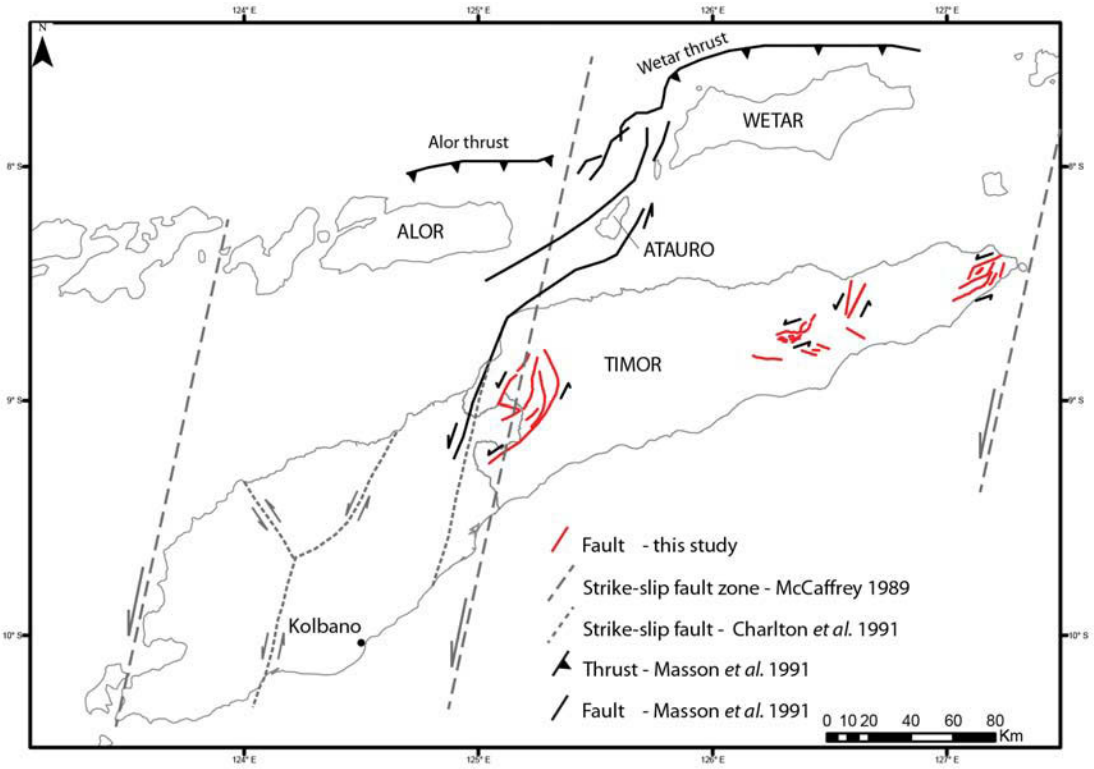

Fig. 140. Dotted lines show strike-slip faulting mapped in West Timor as described by Charlton *et al.* (1991). Dashed lines show north-northeast trending zones of left-lateral strike slip interpreted across Timor Island by McCaffrey using fault plane solutions of shallow focus earthquakes. Solid black lines are faults interpreted by Masson *et al.* (1991) from shallow-focus earthquakes and sea-floor bathymetry. A major zone of left-lateral strike-slip extends north-northeast through the centre of Timor Island, northeast diverging around the island of Atauro, and, then north-northeast along the west coast of Wetar to the Wetar Thrust. This major left-lateral fault zone is interpreted by Masson *et al.* (1991) to extend along the western margin of the Maliana basin, interpreted by this study (solid red lines) as a left-lateral pull-apart structure, and causes several tens of kilometres of offset at the north-coast of Timor Island.

The identification of outcrop and regional scale strike-slip faults in this study therefore provides solid field evidence for previously postulated deformation. Interestingly, despite being hypothesized onshore and identified offshore, the presence or significance of late, high-angle strike-slip faults has been largely overlooked in the development of tectonic models for East Timor (see discussion in **Chapter 2.2.1**).

5.5 Tectonic models

Throughout the history of geological work on East Timor, numerous tectonic models have been proposed to explain its structural evolution, many based on literature analysis and offshore geophysics with little or even no fieldwork or mapping beyond reconnaissance scale (see **Chapter 2.2** for discussion). This body of often opposing concepts and ideas has led to confusion and fuelled controversy.

This study has mapped several areas of East Timor in detail, and in doing so has gathered enough data to confidently revise the stratigraphy of many of the fatus and surrounding areas (**Chapter 3**). Furthermore, potential structural models for these specific areas have been tentatively proposed based on stratigraphic distributions, fault architecture and kinematics, and geomorphological expressions (**Chapter 4**). In this section the most common types of tectonic models present in the literature are discussed in the context of the findings of this study.

5.5.1 Thin-skinned tectonic model

The model presented by Harris (2011) (**Fig. 141**) is the latest iteration of the overthrust-type model proposed by Audley-Charles (1968) and developed by subsequent workers (e.g. Carter *et al.* 1976; Barber *et al.* 1977; Sopaheluwakan *et al.* 1989; Harris 1991; Sani *et al.* 1995; Villeneuve *et al.* 1999). Harris (2011) presents a thin-skinned tectonic model, with the deforming orogen largely separated from the down-going slab by a large scale decollement which links the Timor Trough in the south to where Australian crust meets the Banda Forearc on a south-dipping thrust system under the northern edge of Timor Island. Above the decollement, Gondwana Megasequence rocks form fault-propagation folded thrust sheets 1–3 km thick that are stacked and duplexed to repeat various parts of the Permian to Jurassic

sequence. Above this duplex zone there is a second decollement level, situated close to the Gondwanan breakup unconformity in Jurassic to Early Cretaceous mudstones (Breen *et al.* 1986; Karig *et al.* 1987; Masson *et al.* 1991), and further lubricated by melange sourced from remobilisation and diapirism of overpressured Triassic muds in the underlying Gondwana Megasequence. Imbricate thrusts of Australian Margin Megasequence sediments are stacked and accreted to the front of the orogenic wedge above this upper decollement, along the south coast of Timor and down into the Timor Trough. Further to the north, a large nappe of Banda Megasequence rocks from the Banda Forearc are overthrust and emplaced on top of this zone of melange.

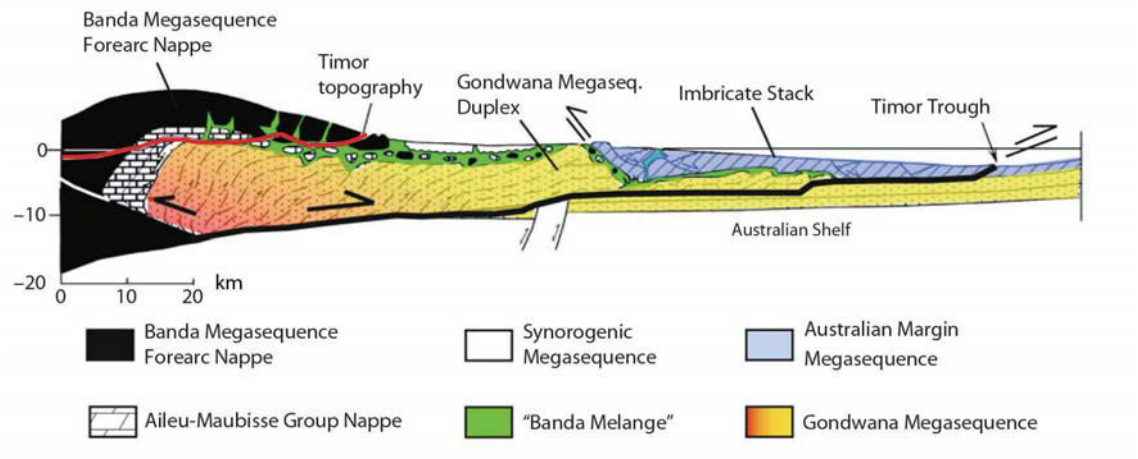

Fig. 141. Thin skinned tectonic model of Harris (2011). It describes the imbrication of the Australian Margin Megasequence on the south coast, coupled with a duplexed succession of Gondwana Megasequence rocks above a large-scale decollement that extends from the Timor Trough to the upper part of the down-going slab. A large thickness of Banda Megasequence units have been overthrust from the north over a layer of melange. Figure modified after Harris (2011).

This model assumes that uplift in the Timor orogen is predominantly from crustal shortening through the development of multiple detachments and duplex systems. The model therefore invokes the presence of a continuous decollement extending from the Timor Trough down to the subducting slab. As this model is based on maps which interpret most of the fatus as Asiatic affinity, it illustrates the presence of a very large Banda Megasequence nappe, emplaced on to an almost continuous unit of 'Banda Melange' which is present overlying all deformed

Gondwanan units. The re-interpretation of the fatus as Australian-derived calls into question the kinematics of this overthrust model, as they cannot be part of a Banda Megasequence nappe.

The stylised series of thrust slices proposed by the thin-skinned tectonic model (e.g. Harris 1991; Harris *et al.* 1998; Harris 2011) is difficult to reconcile on the ground. With the exception of the small klippe of Permian rocks present at the Saburai Range, no thrust structures were directly observed in any of the study areas. Neither was any large-scale repetition of stratigraphy observed at any of the fatus, with the Ossu fatus in particular appearing antiformal in stratigraphic distribution. This study has also observed that Australian Margin Megasequence units are not just confined to the front of the developing orogen. They have been mapped by this study as far north as Mount Mundo Perdido, Mount Laritame, and the Matebian Range where, in some locations, they appear to overly rocks of the upper Gondwana Megasequence. The presence of uninterrupted decollements at the Timor collision front has been questioned by previous authors (Keep *et al.* 2005), and the mapping of Australian Margin Megasequence rocks apparently still in conformable stratigraphic relationships with underlying units may mean that large scale decollements have been discontinuous in time or extent.

The stratigraphic re-evaluation of the fatus of East Timor by this study means that the mapped extent of the Banda Megasequence is far less than has been previously interpreted. Furthermore, this study has found no evidence for a continuous unit of 'Banda Melange' on which the Banda Megasequence has been emplaced upon, as depicted in the model of Harris (2011). Most outcrops of 'melange' are broken and deformed, but still stratigraphically distinct, units of Gondwana Megasequence mudstones and sandstones. True tectonic melange, containing a range of exotic lithologies, has only been encountered within distinct structural zones, generally associated with transtensional faulting.

The tectonic model of Harris (2011) also does not take into account strike-slip faulting, either plate-boundary parallel or oblique to the orogen. Harris (2011) states that there is little evidence of strike-slip geomorphic features in the region and few strike-slip fault plane solutions. This

study has presented new data to support the existence of geomorphic features attributable to strike-slip deformation.

5.5.2 Thick-skinned tectonic model

Although thin-skinned tectonic models have dominated the literature on East Timor (e.g. Audley-Charles 1968; Barber *et al.* 1977; Audley-Charles 1986a; Charlton *et al.* 1991; Harris 1991, 2006; Audley-Charles 2011), invoking large-scale decollements and significant material overthrust from the Asian side of the plate boundary, models such as those proposed by Grady (1975), Grady and Berry (1977) and Chamalaun and Grady (1978) have interpreted Timor Island as comprising entirely Australian affinity stratigraphy, with uplift occurring on basement involved faults - possibly as the result of isostatic rebound following detachment of the down-going slab. Charlton (2002b) re-examined the evidence for basement involved thrusting in Timor, and concluded that there is a contrast in deformation style between West and East Timor. While a thin-skinned style of thrusting is dominant in West Timor, compression in East Timor was accommodated by the development of basement involved thrust structures and through the inversion of pre-collisional graben bounding faults.

Charlton (2002b) based this model on an investigation of the stratigraphic relationships between the Lolotoi Metamorphic Complex and the Australian affinity stratigraphic succession. Although the Lolotoi Metamorphic Complex is generally interpreted as the basement rocks of the Banda Megasequence, equivalent to the Mutis Complex in West Timor (Audley-Charles 1968; Barber & Audley-Charles 1976; Audley-Charles 1986a; Audley-Charles & Harris 1990; Harris 1991, 2006; Audley-Charles 2011), concluded that the Mutis and Lolotoi complexes may not be direct equivalents, and that the Lolotoi Metamorphic Complex that comprises the Lolotoi and Laclubar massifs most likely represents upthrust Australian continental basement. Charlton (2002b) mapped several stratigraphic contacts between the Lolotoi and overlying Australian affinity limestones, and used structural and stratigraphic relationships to interpret the bounding faults of the massifs in places to be high-angle reverse faults or listric normal faults, rather than low angle thrusts. Charlton (2002b) also presented seismic data which places the Lolotoi

Metamorphic Complex at more than 4 km below the subsurface near the south coast of Timor, a position more consistent with an Australian basement unit than a thrust sheet emplaced at the top of the structural pile.

Charlton proposed that there were fundamental differences between the pre-collisional passive margin architecture of West and East Timor (Charlton 2002a; Charlton *et al.* 2002). Wheras West Timor formed a relatively unstructured basin, East Timor was higher and heavily structured with horsts and grabens formed during the breakup of Gondwana. During collision, the thick Permian to Jurassic basin fill and overlying passive margin sequence in West Timor accommodated shortening by development on a thin-skinned fold and thrust belt. However, shortening in East Timor was accommodated by the inversion of former basinal grabens between horst blocks, and the development of basement-involved thrusts, bringing basement rocks up to high structural positions where they are now exhumed at surface.

The thick-skinned model of Charlton (2002b) predicts a large-scale fault architecture in East Timor dominated by steeply dipping, basement involved structures, rather than the shallow imbrication and large overthrust nappes proposed by the thin-skinned model Harris (2011). In this respect Charlton (2002b) is consistent with the detailed mapping of this study, which has documented extensive high-angle faulting throughout all field areas controlling the present-day juxtaposition of stratigraphic units, in many cases sourcing hot fluids and hydrocarbons from deep within the structural pile, together with a lack of observable thrust contacts.

Charlton (2002b) suggests that the heavily structured and block-faulted pre-collisional margin in the location of East Timor had blocks shortened on basement involved thrusts during collision, in many cases re-activating formerly extensional basement faults that were parallel to the developing orogen. However, basin margins that were perpendicular or highly oblique to the collision zone retained their pre-collisional horst-graben structure without significant inversion. These orogen-oblique faults accommodate significant amounts of strike-slip, allowing differences in shortening between adjacent horsts and grabens. This is consistent with large-

scale orogen-oblique strike-slip systems mapped by this study at the Maliana basin and the Matebian Range.

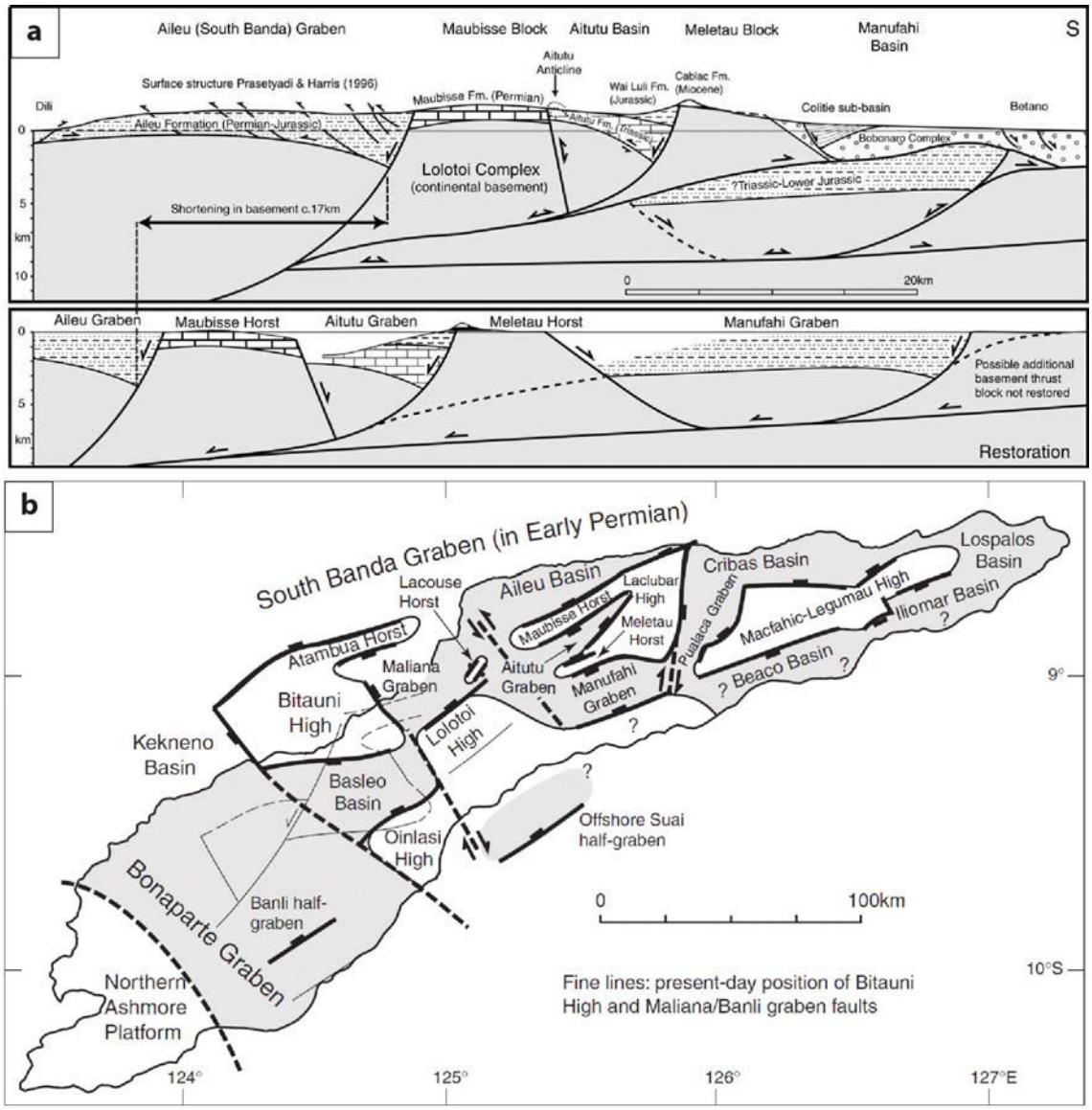

Fig. 142. (a) The thick-skinned model of Charlton (2002b) proposes a pre-collisional horst and graben structure, shortened during collision by the development of large-scale basement involved thrusts and the inversion of original graben-bounding extensional faults. The lower cross-section illustrates a potential pre-collisional horst and graben configuration (figure from Charlton 2002b). (b) Plan view of proposed pre-collisional horsts and grabens in East Timor. Graben-bounding faults parallel to the orogen would undergo significant inversion during shortening. However, graben-bounding faults that are highly oblique or perpendicular to the developing orogen would undergo significant amounts of strike-slip displacement as they accommodate differences in shortening between adjacent horsts and grabens (figure from Charlton 2002a).

The thick-skinned model of Charlton (2002b) is dependent on the premise that the Lolotoi Metamorphic Complex represents Australian basement rocks. However, detailed geochemistry by Standley and Harris (2009) show that the age and thermal history of the Lolotoi Metamorphic Complex is inconsistent with an origin on the Australian margin, and closely matches that of other metamorphic units from the Great Indonesian arc such as the Mutis Complex in West Timor. Furthermore, overlying igneous rocks have arc-related geochemical affinities, which demonstrate that the Lolotoi Metamorphic Complex was near, or part of, a volcanic arc during the Oligocene (Standley & Harris 2009). Therefore, the thick-skinned model of Charlton (2002b) is difficult to reconcile with geochemical data.

5.5.3 Extrusion model

Duffy *et al.* (2013) integrated observations of strike-slip faulting throughout East Timor with the tectonic model of Harris (2011). Duffy *et al.* (2013) identified a predominance of NW-SE oriented dextral-normal faults and NE-SW oriented sinistral-normal faults throughout the East Timor orogen, at scales ranging from outcrop to ~100 km. These faults are interpreted as non-Andersonian conjugate faults accommodating extrusion sub-parallel to the Banda Arc (Duffy *et al.* 2013). Extruded crust is bound by two interpreted orogen-parallel strike-slip systems on the northern and southern sides of Timor Island, exhibiting normal-sinistral and normal-dextral kinematics, respectively. Orogen-oblique structures such as the Matebian Range fault are interpreted as high-angle Riedel shears between the two main fault zones, dipping towards their master faults and linking at depth, accommodating most of the extrusion (Duffy *et al.* 2013). Duffy *et al.* (2013) interpreted extrusion (and associated pervasive strike-slip structures) as a currently active process. This is supported by recent earthquake central-moment-tensor solutions which show that active thrusts are mostly confined to the deformation front south of Timor, whilst the remaining earthquakes under Timor Island are predominantly dominantly strike and normal slip (Duffy *et al.* 2013 fig. 14).

Following the interpretation of Mount Mundo Perdido as a strike-slip structure (Benincasa *et al.* 2012), Duffy *et al.* (2013) supports the findings of large-scale strike-slip deformation – both

orogen-parallel and orogen-oblique –throughout East Timor. The mapping of Duffy *et al.* (2013) (who mapped subsequently to Benincasa, in some of the same locations) also interprets the Matebian Range Fault as a major left-lateral fault, and the Marobo basin near Maliana as being bound by major transtensional structures accommodating up to several kilometres of vertical displacement.

In other areas such as Mount Mundo Perdido, Duffy *et al.* (2013) interprets the fatu as a displaced horst block within a right-lateral strike-slip system, based on faults observed at two field locations, whereas Benincasa *et al.* (2012) interprets a restraining bend based on detailed mapping at a number of localities in and around the fatu over a period of several months. The difference in interpretation relates to the level of detail mapped. At Mount Mundo Perdido observed kinematic interpretations at single outcrops can be inconsistent as fault surfaces display striae of multiple orientations, both steep and gently dipping, indicating multiple phases of slip. Therefore, although dextral faults are present and were mapped by Duffy *et al.* (2013) and Benincasa *et al.* (2012), Benincasa *et al.* (2012) interpreted Mount Mundo Perdido as a left-lateral structure based on correlations of fault architecture, asymmetries in morphology and geological distributions with left-lateral pop-up structures produced in analogue models of strike slip systems, and real world examples of left-lateral pop-up structures elsewhere in the world.

In the extrusion model brittle surface extension is coupled to ductile extrusion at depth. This study has proposed a similar brittle-ductile transition as responsible for the unique morphology of the Maliana basin area (Chapter 4.5.5 Structural model), resulting from thick successions of Triassic and Jurassic mudstones within the structural pile. Duffy *et al.* (2013) compares the interpreted structural architecture of East Timor with extrusion documented at larger scales in the European Alps and Tibet. This model provides a unique perspective on the structural evolution of East Timor, and is consistent with this study in interpreting widespread, large-scale strike-slip faulting within the orogen that are most likely an integral part of the collision kinematics.

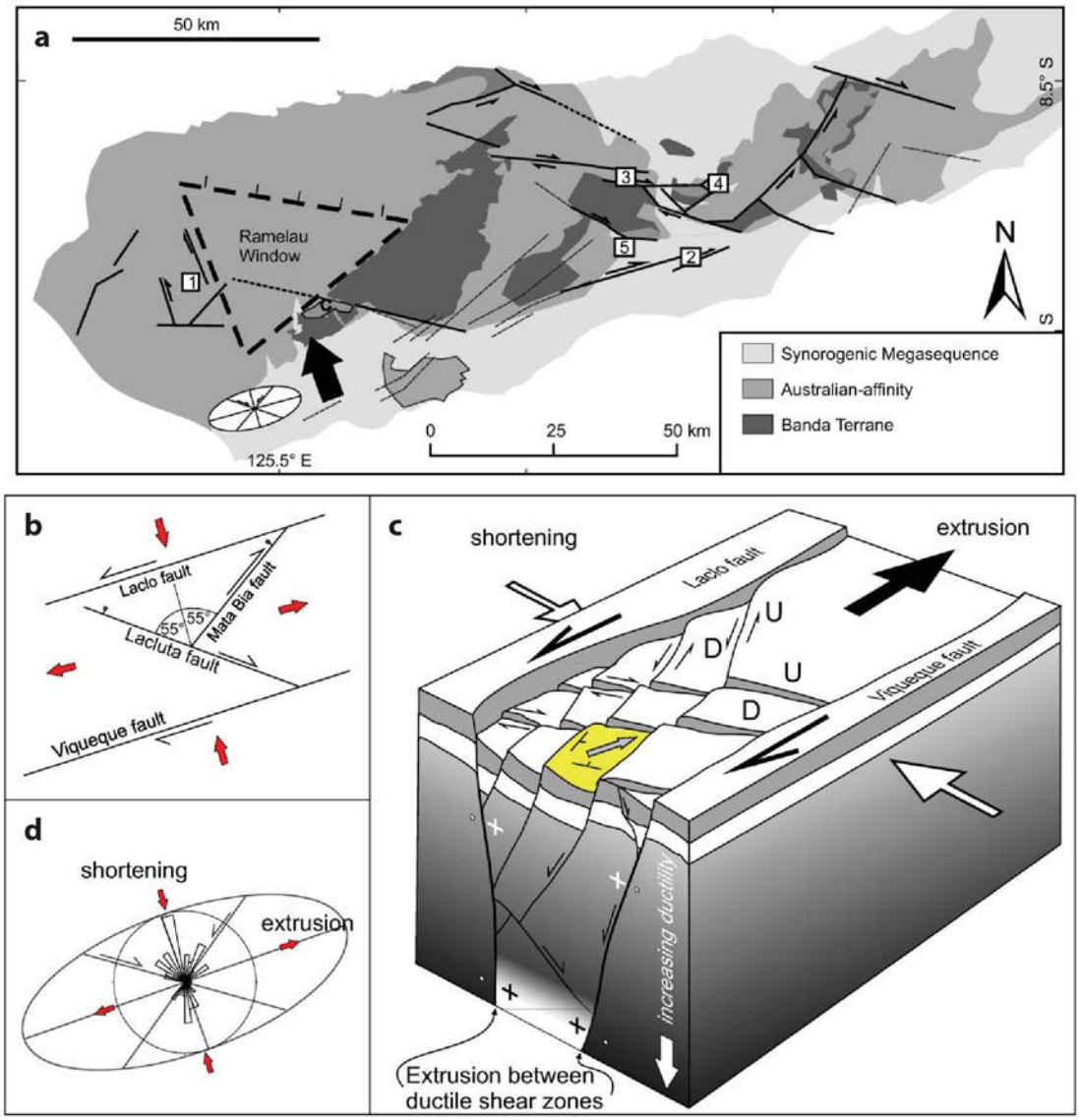

Fig. 143. (a,) Duffy *et al.* (2013) identified a predominance of strike-slip faulting throughout East Timor. (b, c, d) The extrusion model of Duffy *et al.* (2013) proposes that the Timor orogen is being extruded between two interpreted orogen-parallel strike-slip systems on the northern and southern sides of Timor Island. Riedel shears dip towards these fault systems, and create a series of fault-bounded blocks that are tilted back in the extrusion direction. (figures from Duffy *et al.* 2013).

5.6 Relationships with the adjacent Outer Banda Arc and the Australian North West Shelf

5.6.1 North West Shelf

The proposed collisional age of post 9.8 Ma favoured by this and other studies (Haig & McCartain 2007; Keep & Haig 2010; Haig 2012a) contrasts interpretations by other workers, and a full discussion of this issue can be found in Keep and Haig (2010). For the purposes of this study, the identification of late, high-angle strike slip faults dismembering the original collisional geometries supports the conclusions of Haig *et al.* (2008), Keep *et al.* (2009) and Keep and Haig (2010) of distinct phases of orogenesis, with late deformation identified in this study forming as part of a post 4.5 Ma phase of uplift and exhumation (Keep & Haig 2010).

The overall NNE convergence direction of Australia with respect to the Pacific and Eurasian plates (Genrich *et al.* 1996) has produced strong left-lateral shear in Papua New Guinea (Ali & Hall 1995; Packham 1996). This prompted Veevers and Powell (1984) to first postulate that the oblique convergence would not only generate strong left-lateral shear along the northern Australian margin, but that it would also induce a torque on the Australian continent causing it to rotate in a counter clockwise direction. Later workers, using mainly seismic data from the North West Shelf petroleum provinces, agreed with the hypothesis that a strong left-lateral shear should occur along Australia's northern margin as a consequence of oblique collision (e.g. Nelson 1993; Keep *et al.* 1998; Shuster *et al.* 1998), a hypothesis supported by the 1997 Cockatoo Island M6.3 earthquake that generated strike-slip fault plane solutions (reported in Castillo *et al.* 2000). Nelson (1993) documented what he believed to wrench structures in the Bonaparte Basin, immediately to the south of Timor Island, using interpreted 2D seismic data (**Fig. 144f**). He further attributed young inversion of these structures to the collision of the Australian Plate with the Banda Arc and documents a number of reactivated flower structures that appear to breach the surface. Keep *et al.* (1998), also using 2D seismic data, provided examples of reactivation and inversion of pre-existing faults during Neogene deformation in the Bonaparte and Carnarvon basins. They correlated a number of important tectonic events across the region, defining a significant, region-wide (Papua New Guinea, Sumba, the North West

Shelf and the Ninetyeast Ridge) event at ~ 8 Ma, with the onset of strike-slip at 3 Ma. The timing of these events on the North West Shelf correlate extremely well with the timing of tectonic pulses on Timor, proposed as post 9.8 Ma collision with uplift commencing around 3.3 Ma (Keep & Haig 2010). Further, Keep *et al.* (2000) document a 180 km-long strike-slip system in the Barcoo Sub-basin of the Browse Basin (**Fig. 144g**). This Barcoo Fault system (Keep *et al.* 2000) includes both restraining and releasing bends. Reactivation and inversion during the Neogene to Recent has caused the seafloor to be uplifted and domed over this structure, indicating that deformation is extremely young. Keep *et al.* (2000) link this deformation to regional pulses of deformation coincident with stages of deformation in Timor. Shuster *et al.* (1998) inferred strike-slip pull-apart basins in Timor Sea (Bonaparte Basin), suggesting that both the Malita Graben and Cartier Trough represented pull-apart basins generated from left-lateral motion on left-stepping en echelon faults (**Fig. 144c**), a conclusion also supported by de Ruig *et al.* (2000).

Estimates of crustal shortening in the Timor Sea (Harrowfield *et al.* 2003) concluded that overall shortening across the Timor Sea was only in the region of 1%, and that strike-slip deformation of the North West Shelf in response to oblique convergence must be accommodated outboard of the margin in Timor.

Fig. 144 → (a) Overview of the bathymetric and main physiographic elements of the North West Shelf of Australia and adjoining Banda Arc. Main basins are labelled, continent-ocean boundary shown as a white dashed line. White boxes represent locations where evidence for left-lateral strike slip deformation has been documented: 1. = Roti multibeam bathymetry survey of TGS Nopec; 2. = the northern Bonaparte, including the Malita Graben and Cartier Trough; 3. = Jamdena multibean survey of TGS Nopec; 4. = southern Bonaparte Basin including the Jabiru Field; 5. = Barcoo Sub-basin of the Browse Basin. Inset shows the overall plate tectonic setting of this region. (b) Detail from the Roti multibeam survey showing seafloor bathymetry of rhomboidal basins, with seismic line across this structure illustrating flower-type geometries (Holloway 2013). (c) left-lateral strike slip interpretation of Shuster *et al.* (1998) across the northern Bonaparte Basin. (d) Detail from the Jamdena multibeam survey, showing multiple rhomboidal basinal structures at the seafloor, and (e) seismic data across the structures indicating young reactivation and inversion (Auguston 2012). (f) Seismic image from Nelson (1993) showing interpreted flower structures from left-lateral deformation near the Jabiru Field. (g) Lynher-Lombardina strike-slip system of the Barcoo Sub-basin, modified from Keep *et al.* (2000).

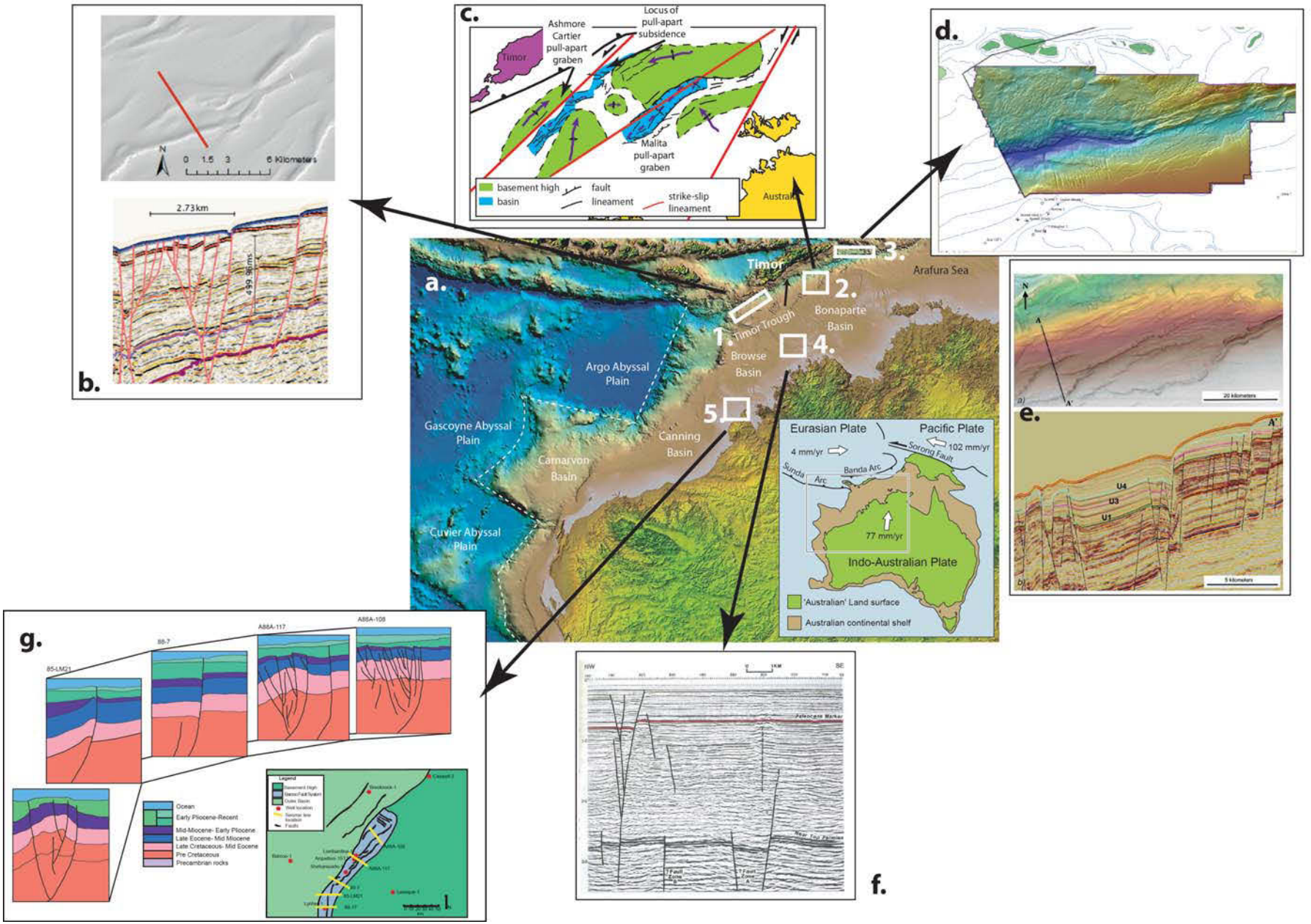
a.
b.
c.
d.
e.
f.
g.
Timor
Arafura Sea
Timor Trough
Bonaparte Basin
Browse Basin
Argo Abyssal Plain
Gascoyne Abyssal Plain
Cuvier Abyssal Plain
Carnarvon Basin
Canning Basin
1.
2.
3.
4.
5
Eurasian Plate
Pacific Plate
Indo-Australian Plate
4 mm/yr
102 mm/yr
77 mm/yr
Sorong Fault
Sunda Arc
Banda Arc
'Australian' Land surface
Australian continental shelf
2.73km
0 1.5 3 6 Kilometers
Ashmore Cartier pull-apart graben
Locus of pull-apart subsidence
Malita pull-apart graben
basement high
basin
fault
lineament
strike-slip lineament
U4
U3
U1
Ocean
Early Pliocene-Recent
Mid-Miocene- Early Pliocene
Late Eocene- Mid Miocene
Late Cretaceous- Mid Eocene
Pre Cretaceous
Precambrian rocks

Left-lateral deformation in the Timor Sea was further documented by Bourget *et al.* (2012) who suggest that left-lateral strike-slip on this section of the margin continued into the Pliocene and Pleistocene, causing fault scarps on the sea floor. A deformation event at 2 Ma is also supported by Langhi *et al.* (2011) who document oblique extensional reactivation at this time.

More recently, Auguston (2012) and Holloway (2013) used high resolution multibeam images of the seafloor to identify present-day deformation processes at the north-eastern (Jamdena, **Fig. 144d**) and south-western (Roti, **Fig. 144b**) ends of the Timor Trough respectively. Seafloor multibeam images from both areas show rhomboidal structures, mainly basinal, consistent not only with pull-apart basin geometries in general, but also consistent with orientations seen in Timor, especially that of Lake Iralalaru. In the Jamdena data set (Auguston 2012), seismic data across the rhomboidal basins show the boundary lineaments to be faults, with deformation and uplift consistent with strike-slip deformation (**Fig. 144d**). Further, the faults bounding the rhomboidal basins appear heavily modified by pockmarks indicating fluid flow along these faults (Auguston 2012, fig. 17). Almost identical structures of the same orientations occur further to the southwest along the Timor Trough, adjacent to and south of Roti Island, off the south-western coast of Timor Island (Holloway 2013). Geometries include classic rhomboidal pull-apart shapes, as well as en-echelon faults and splay tips in map view (**Fig. 144b**). Accompanying seismic data across these structures shows flower structures at shallow crustal levels, reaching and offsetting the sea floor.

Therefore, left-lateral strike-slip deformation has been documented from around not only the Timor Sea immediately south of Timor Island, but also to the northeast and southwest along the Timor Trough, from the Neogene to the present day. Earthquake focal mechanism solutions support the presence of strike-slip in the region (Castillo *et al.* 2000), with a recent study indicating that over 70% of present-day earthquakes recorded for the study display strike-slip or strongly oblique-slip focal mechanisms (Revets *et al.* 2009). It seems that the intensity of deformation decreases away from the central zone of deformation parallel to the strike of East Timor, with instances of strike-slip on the North West Shelf of smaller scale and more sparsely distributed than on Timor Island.

5.6.2 Outer Banda Arc

The geology of Timor Island differs vastly from that of its counterparts both to the west and east along the Outer Banda Arc. To the west, the island of Sumba (**Fig. 145**) is recognised to occupy a unique position, representing an isolated sliver of probable continental (Abdullah *et al.* 2000) or arc crust (Lytwyn *et al.* 2001) occupying a forearc position (Audley-Charles 1985). Suggestions as to its origin include those who believe Sumba represents a sliver of Australian affinity (Audley-Charles 1975; Pigram & Panggabean 1984; Hartono 1990), and those that believe that it has Eurasian-Indonesian affinities and moved to its present position from the northeast (Hamilton 1979; van der Werff *et al.* 1994; Lee & Lawver 1995; Vroon *et al.* 1996; Rutherford *et al.* 2001). Authors agree that the forearc basement is non-oceanic (van der Werff *et al.* 1994), probably derived from arc sources (Lytwyn *et al.* 2001) and possibly underplated by Australian continental crust during collision circa 8 Ma (Keep *et al.* 2003). Authors also seem to agree that Sumba appeared to move into its present position relatively quickly (Hall 1996; Rutherford *et al.* 2001) and began to occupy its present position by approximately 7 Ma (Wensink & van Bergen 1995; Rutherford *et al.* 2001). Geologically the island hosts plutonic, volcanic and volcaniclastic rocks recording arc volcanism from ca 86 Ma to 31 Ma (Rutherford *et al.* 2001), and shows little internal deformation (van der Werff *et al.* 1994; Wensink & van Bergen 1995; Rutherford *et al.* 2001). Therefore both in terms of lithology, deformation and tectonic history, Sumba Island bears no resemblance at all to Timor Island. This is due largely to the fact that it did not form in place but was seemingly transported from elsewhere, probably from the northeast near present-day Alor and Wetar (Rutherford *et al.* 2001) and is not part of the orogenic system that formed Timor.

To the east of Timor lie a number of small islands including Leti, Moa, Sermata, Dai, with Tanimbar forming the end of this chain as the Banda Arc begins to bend around the Weber Deep (**Fig. 145**). These islands, sometimes referred to as the Timor-Tanimbar islands, occur in the non-volcanic Outer Banda Arc and expose a very young, high P/T metamorphic belt (Kaneko *et al.* 2007). This metamorphic belt includes high P/T rocks both in West Timor (Sopaheluwakan 1990) and East Timor (Berry & McDougall 1986), all of which were formed

prior to collision (Kaneko *et al.* 2007). Geological mapping in the smaller islands (Leti, Moa, Sermata, Dai and Laibobar; **Fig. 145**) show them to be dominated by a combination of schistose metamorphic units, gabbros and peridotites, with a cover of Quaternary limestones. Only Leti Island preserves a sliver of unmetamorphsed continental shelf rocks (Kaneko *et al.* 2007). Estimates of 1 km thickness of crystalline rocks are thought to have been extruded as a thin sheet during collision, sandwiched between underlying continental shelf sediments and overlying ophiolites (Kaneko *et al.* 2007). Whilst Kaneko *et al.* (2007) present a subduction origin and subsequent emplacement of this metamorphic belt, their pre-collision ages and the absence of any significant unmetamorphosed Australian-derived rocks, fatus or recognised high-angle faults make comparisons of the deformation presented in this study with deformation on any of these easterly adjacent islands extremely difficult.

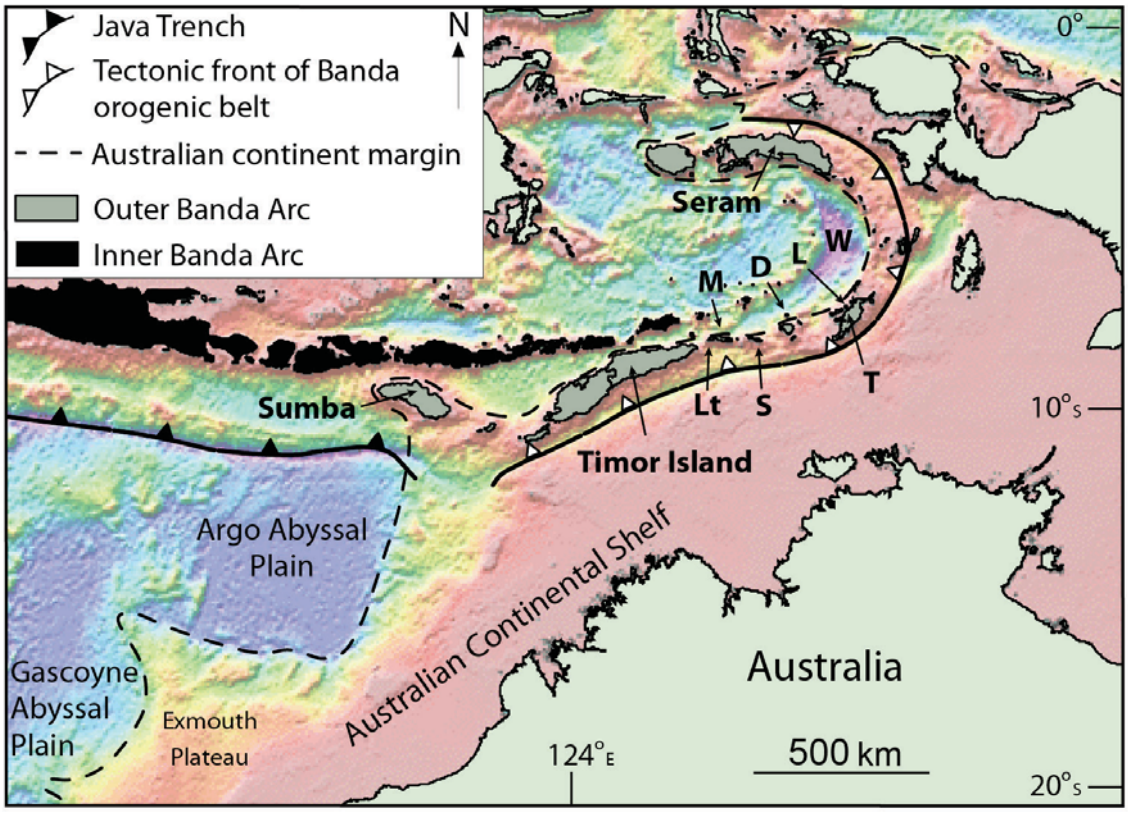

Fig. 145. Location map illustrating the tectonic setting of Timor Island and the main physiographic elements of the region, showing the locations of the main islands of the Outer Banda Arc. Lt = Leti, M = Moa, S = Sermata, D = Dai, L = Laibobar, T = Tanimbar, W = the Weber Deep.

Seram Island occupies a tectonic position to the northeast of Timor, almost at the cessation of curvature of the Banda Arc, and to the north of the Weber Deep (**Fig. 145**). Often portrayed as Timor's 'mirror-image' (Audley-Charles *et al.* 1979) the island in fact exposes granulite facies metamorphism, volcanism and anatexis (Pownall *et al.* 2013), indicating that the tectonic evolution of the Banda Arc is not symmetrical, and inferring that Seram has a tectonic history that diverges from that of Timor.

Similarities exist between Timor and Seram in terms of size, shape and overall elevation (**Fig. 146**) (Pairault *et al.* 2003) and in aspects of the geology, however this is somewhat confused by the large number of stratigraphic schemes (at least 10) proposed for Seram, and the changing names of equivalent formations (see Pownall *et al.* 2013 for an overview). One of the most striking differences in geology is that Seram preserves granulites, representing the youngest ultrahigh-temperature granulites in the world (Pownall *et al.* 2014). This granulite complex includes lithologies such as widespread peridotites (spinel lherzolites) not documented on Timor, which are thought to represent a migmatitic-ultramafic core complex exhumed on low-angle detachments (Pownall *et al.* 2014). Above metamorphic basement, Lower Triassic to Middle Jurassic shallow water carbonates and shales (of various names, including the Manusela Formation and Asinipe Limestone) occupy the 300 m-high Mansuela Mountains, which form a prominent west-northwest trending ridge along the centre of Seram (Pownall *et al.* 2013, fig. 3). Valley fill adjacent to the Mansuela Mountains comprises Triassic to Jurassic dark-grey, deep-water clays, silts and micaceous sandstones (e.g. Tjokrosapoetro & Budhitrisna 1982; de Smet & Barber 1992). Whilst the ages and lithologies correlate well with some mapped units on Timor (e.g. the Late Triassic Babulu Group and Bandeira Group) the confusion in terminology and complications from differences in interpretation of some units (for example, the allochthonous/autochthonous designations applied by Audley-Charles *et al.* 1979), and the interpretation of coeval facies (Tjokrosapoetro & Budhitrisna 1982; de Smet & Barber 1992) as different terranes (Audley-Charles *et al.* 1979), make direct comparison difficult. A detailed correlation is beyond the scope of this study.

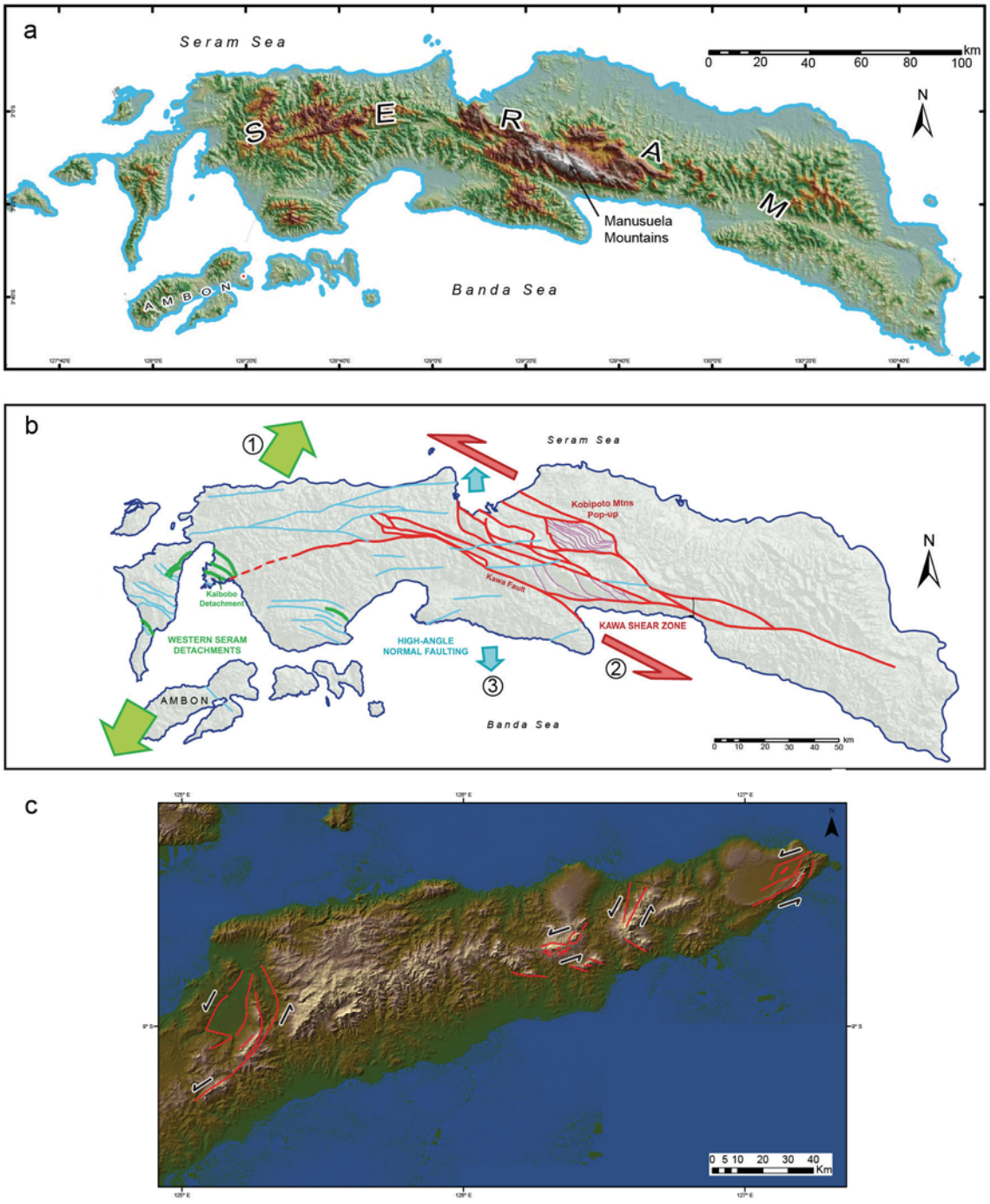

Fig. 146. (a) Digital elevation model of Seram, from Pownall *et al.* (2013) (b) Structural map of Seram from Pownall *et al.* (2013), showing detachment faults (green), high-angle normal faults (blue), strike-slip faults (red), and faults within the Kobipoto Mountains strike-slip pop-up structure (magenta). A major left-lateral strike-slip system is extensive throughout eastern and central Seram, generating pop-up structures in Triassic carbonates to form the central mountain ranges. (c) Digital elevation model of East Timor, at the same scale, showing the left-lateral strike-slip systems identified by this study.

However, the most striking resemblance between Timor and Seram is the identification of an extensive, strike-parallel (120°), left-lateral strike-slip system, the Kawa Fault system, that occupies eastern and central Seram, and bounds the highest mountain ranges (3000 m plus) that contain Lower Triassic to Middle Jurassic shallow water carbonates and shales. A number of smaller, strike-parallel faults occur within this zone (Pownall *et al.* 2013), which juxtaposes metamorphic basement against fault gouges and breccias to the north, and is interpreted to be a major lithospheric feature of immense significance in the recent tectonic evolution of Seram. This left-lateral system has generated a number of pop-up structures that form topographically high areas, much like those documented in this study. Pownall *et al.* (2013) attribute left-lateral strike slip to a combination of slab rollback and Riedel shearing in response to extension, which they believe exposes the core complexes of granulite material. Absolute ages are not presented in Pownall *et al.* (2013), although they refer to the age of the Kawa Fault System as "recent", assisting in exposing the world's youngest (Pliocene) ultrahigh-temperature rocks.

5.7 Summary

The re-interpretation of all of the fatus of East Timor as containing Australian-derived lithologies, and the documentation of a number of high-angle faults with restraining and releasing geometries, changes our understanding of the tectonic evolution of Timor. This study found limited evidence for original thrust geometries, and instead asserts that young strike-slip deformation has dismembered pre-existing thrust stacks, creating the chain of high limestone fatus across East Timor. Further, the change in interpreted age of the limestones comprising these fatus from Miocene to largely Triassic-Jurassic means that tectonic interpretations that attribute the fatu limestones to the over-riding plate, as part of an extensive Banda thrust sheet, must also be examined. This change in interpretation also means that the extent of any previously postulated Banda thrust sheet has diminished considerably, as many of the lithologies have been shown to be of Australian derivation.

Interpretations of young strike-slip in East Timor correlate well with reports of young, left-lateral reactivation deformation across the Timor Sea and Browse Basin of the southerly adjacent North West Shelf of Australia, with intensity of deformation decreasing to the south.

Along strike the notion of strike-slip deformation in East Timor cannot readily be compared to either Sumba or the Timor-Tanimbar islands to the east, but significant similarities in deformation style occur in both Timor and Seram. However, the older geological and tectonic histories of these islands must have differed to produce the markedly different lithologies found on Seram to those on Timor. The significance of slab-rollback as proposed for Seram has not yet been tested for Timor, and will require significant additional work, especially on the Australian-derived metamorphic complexes.

6. Conclusions and recommendations for further work

6.1 Conclusions

The main conclusions of this study are:

1) The fatus of East Timor, previously widely interpreted as containing Miocene-age limestones, have been shown to contain mainly Triassic and Jurassic lithologies of the Australian-derived Gondwana and Australian Margin megasequences. This finding alone significantly changes any tectonic interpretations that attributed these limestones to a Banda nappe;
2) Late, high-angle faults dominate the topography of East Timor and bound all of the fatus, which themselves represent some of the highest topography in Timor. These faults display multiple oblique-slip fault striae, and fault orientations and directions of slip are consistent in all cases with left-lateral strike-slip fault zones creating restraining and releasing bends;
3) This late, left-lateral shear on Timor Island represents a recent deformation event, creating the fatus as pop-up structures and some of the larger basinal areas as pull-apart structures in an overall system comprised of Riedel orientations relative to a main deformation zone;
4) Interpretations of strike-slip in East Timor correlate well with both the southerly-adjacent North West Shelf, and with Seram.

6.2 Recommendations for further work

The reinterpretation of significant extents of the stratigraphy of East Timor, along with the identification of extensive strike-slip deformation throughout the half-island, raises questions about the stratigraphy and recent structural history of other islands in the Outer Banda Arc. However, modern, detailed biostratigraphic ages for use in stratigraphic correlation are needed, particularly in West Timor and Seram. As these islands have been mapped at different times by different workers there is a lack of coherency to the stratigraphic frameworks, leading to confusion and controversy (see discussion in Pownall *et al.* 2013 for an example from Seram).

For this study (and others, for example Haig *et al.* 2008) to identify supposedly Miocene-age limestones as predominantly Triassic in age illustrates how a lack of robust biostratigraphy and an over-reliance on lithostratigraphic schemes for correlations can be problematic. Given the discrepancies in the previous lithostratigraphic schemes of East Timor identified by this study and others (e.g. Haig & McCartain 2007; Haig *et al.* 2008; Keep & Haig 2010; Haig 2012a), it is likely that stratigraphic interpretations and ages in other parts of the Outer Banda Arc may require revision.

As our understanding of tectonic mechanisms becomes more sophisticated and we appreciate the complicated interactions between different tectonic elements, a robust stratigraphic framework will be crucial to 'ground-truthing' elements of the geology in the field. For example, the slab-rollback model proposed for Seram (Pownall *et al.* 2013) may have regional significance throughout the Outer Banda Arc, including East Timor. However, once again detailed biostratigraphy is necessary to constrain the ages of detachment faulting, exhumation, extension, and strike-slip events, as Pownall *et al.* (2013) fail to provide ages for the deformation events they propose. It is also of note that significant slab-rollback throughout the arc (e.g. Spakman & Hall 2010; Pownall *et al.* 2013) may be incompatible with certain tectonic models proposed for East Timor (e.g. the extrusion model of Duffy *et al.* 2013).

The tectonics of Southeast Asia, and the complex interplay between various tectonics elements, has been the source of many decades of research, and will continue to be so for a long time to come. Hopefully this thesis provides the necessary constraints to anchor tectonic models for at least a small part of the system.

7. References

'T HOEN C. W. A. P. & VAN ES L. J. C. 1925. De Opsporingen naar Delfstoffen op het Eiland Timor. *Jaarboek van het Mijnwezen in Nederlandsch-Indie* **1925**, 1-80.

'T HOEN C. W. A. P. & ZIEGLER K. 1917. Verslag over de resultaten van geol. mijnb. verkenningen in Z. W. Celebes. *Jaarboek van het Mijnwezen in Nederlandsch-Indie* **1917**, 253-263.

ABDULLAH C. I., RAMPNOUX J. P., BELLON H., MAURY R. C. & SOERIA-ATMADJA R. 2000. The evolution of Sumba Island (Indonesia) revisited in the light of new data on the geochronology and geochemistry of the magmatic rocks. *Journal of Asian Earth Sciences* **18**, 533-546.

AINSWORTH B. R., BOSSCHER H. & NEWALL M. J. 2000. Forward stratigraphic modelling of forced regressions: evidence for the genesis of attached and detached lowstand systems. *Geological Society, London, Special Publications* **172**, 163-176.

ALI J. R. & HALL R. 1995. Evolution of the boundary between the Philippine Sea Plate and Australia: palaeomagnetic evidence from eastern Indonesia. *Tectonophysics* **251**, 251-275.

ATMAOUI N., KUKOWSKI N., STÖCKHERT B. & KÖNIG D. 2006. Initiation and development of pull-apart basins with Riedel shear mechanism: insights from scaled clay experiments. *International Journal of Earth Sciences* **95**, 225-238.

AUDLEY-CHARLES M. G. 1962. *The Geology of Portuguese Timor*. Report to Timor Oil Ltd, Sydney, Australia.

AUDLEY-CHARLES M. G. 1965a. A Miocene gravity slide deposit from eastern Timor. *Geol. Mag.* **102**, 267-276.

AUDLEY-CHARLES M. G. 1965b. *The Petroleum Prospects of Portuguese Timor*. Report to Timor Oil Ltd, Sydney, Australia.

AUDLEY-CHARLES M. G. 1968. The Geology of Portugese Timor. Geological Society of London, Memoir 4. *Geological Society of London*.

AUDLEY-CHARLES M. G. 1975. The Sumba fracture: A major discontinuity between eastern and western Indonesia. *Tectonophysics* **26**, 213-228.

AUDLEY-CHARLES M. G. 1978. Indonesian and Philippine archipelagoes. *In:* Moullade M. & Nairn A. E. M. eds., *The Phanerozoic Geology of the World*, Vol. Vol. 2, pp 165-207, Elsevier, Amsterdam.

AUDLEY-CHARLES M. G. 1981. Geometrical problems and implications of large scale overthrusting in the Banda Arc–Australian margin collision zone. *In:* McClay K. ed., *Thrust and Nappe Tectonics: Geological Society of London Special Publication*, Vol. 9, pp 407–416.

AUDLEY-CHARLES M. G. 1985. The Sumba enigma: is Sumba a diapiric fore-arc nappe in process of formation? *Tectonophysics* **119**, 435-439.

AUDLEY-CHARLES M. G. 1986a. Rates of Neogene and Quaternary tectonic movements in the Southern Banda Arc based on micropalaeontology. *Journal of the Geological Society of London* **143**, 161-175.

AUDLEY-CHARLES M. G. 1986b. Timor-Tanimbar Trough: the foreland basin of the evolving Banda orogen. *Special Publication of the Association of Sedimentologists* **8**, 91-102.

AUDLEY-CHARLES M. G. 1991. Tectonics of the New Guinea area. *Annual Review of Earth and Planetary Sciences* **19**, 17-41.

AUDLEY-CHARLES M. G. 2004. Ocean trench blocked and obliterated by Banda forearc collision with Australian proximal continental slope. *Tectonophysics* **389**, 65-79.

AUDLEY-CHARLES M. G. 2011. Tectonic post-collision processes in Timor. *Geological Society, London, Special Publications* **355**, 241-266.

AUDLEY-CHARLES M. G., CARTER D. G. & BARBER A. J. 1974. Stratigraphic basis for tectonic interpretations of the Outer Banda Arc, Eastern Indonesia. *Proceedings Indonesian Petroleum Association, Third Annual Convention*, 25-44.

AUDLEY-CHARLES M. G. & CARTER D. J. 1972. Palaeogeographical significance of some aspects of Palaeogene and early neogene stratigraphy and tectonics of the Timor Sea region. *Palaeogeography, Palaeoclimatology, Palaeoecology* **11**, 247-264.

AUDLEY-CHARLES M. G., CARTER D. J., BARBER A. J., NORVICK M. S. & TJOKROSAPOETRO S. 1979. Reinterpretation of the geology of Seram: implications for the Banda Arcs and northern Australia. *Journal of the Geological Society* **136**, 547-566.

AUDLEY-CHARLES M. G. & HARRIS R. A. 1990. Allochthonous terranes of the Southwest Pacific and Indonesia. *Philosophical Transactions of the Royal Society of London* **331**, 571-587.

AUGUSTON A. 2012. Using seafloor bathymetry and seismic data to test models for recent to modern sedimentation in the Timor Sea. Honours Thesis, University of Western Australia, Perth (unpubl.).

BACHRI S. & SITUMORANG R. L. 1994. Geological map of the Dili Sheet, East Timor, Scale 1:250,000. *Geological Research and Development Centre, Bandung*.

BARBER A. J. & AUDLEY-CHARLES M. G. 1976. The significance of the metamorphic rocks of Timor in the development of the Banda Arc, eastern Indonesia. *Tectonophysics* **30**, 119-128.

BARBER A. J., AUDLEY-CHARLES M. G. & CARTER D. J. 1977. Thrust tectonics in Timor. *Journal of the Geological Society of Australia* **1**, 51-62.

BARBER A. J., TJOKROSAPOETRO S. & CHARLTON T. R. 1986. Mud volcanoes, shale diapirs, wrench faults, and melanges in accretionary complexes, eastern Indonesia. *AAPG Bulletin* **70**, 1729-1741.

BARKHAM S. J. 1993. The structure and stratigraphy of the Permo-Triassic carbonate formations of West Timor, Indonesia. M.Sc. thesis, University of London (unpubl.).

BATHURST R. G. C. 1975. *Carbonate Sediments and their Diagenesis*. Elsevier Scentific Publishing Company, Amsterdam.

BECK M. E., JR 1986. Model for Late Mesozoic-Early Tertiary tectonics of coastal California and western Mexico and speculation on the origin of the San Andreas fault. *Tectonics* **5**, 49-64.

BENINCASA A., KEEP M. & HAIG D. W. 2012. A restraining bend in a young collisional margin: Mount Mundo Perdido, East Timor. *Australian Journal of Earth Sciences* **59**, 859-876.

BERRY R. F. & GRADY A. E. 1981a. The age of the major orogenesis in Timor. *Geological Research and Development Centre Republic of Indonesia Special Publication* **2**, 171-181.

BERRY R. F. & GRADY A. E. 1981b. Deformation and Metamorphism of the Aileu Formation, North Coast, East Timor and Its Tectonic Significance. *Journal of Structural Geology* **3**, 143-167.

BERRY R. F. & MCDOUGALL I. 1986. Interpretation of 40Ar/39Ar and K/Ar dating evidence from the Aileu Formation, East Timor, Indonesia. *Chemical Geology* **59**, 43-58.

BIRD P. R. 1987. The Geology of the Permo-Trias of Kekneno, West Timor. PhD thesis, University of London (unpubl.).

BIRD P. R. & COOK S. E. 1991. Permo-Triassic successions of the Kekneno area, West Timor: implications for palaeogeography and basin evolution. *Journal of Southeast Asian Earth Sciences* **6**, 359-371.

BORGES G. 2010. The Stratigraphy of Mount Laritame, Timor Leste. Honours Thesis, University of Western Australia, Perth (unpubl.).

BOUDAGHER-FADEL M. K. 2008. *Evolution and Geological Significance of Larger Benthic Foraminifera* (Developments in Palaeontology & Stratigraphy, Vol. 21). Elsevier, Amsterdam.

BOUDAGHER-FADEL M. K., ROSE E. P. F., BOSEENCE D. W. J. & LORD A. R. 2001. Lower Jurassic foraminifera and calcified microflora from Gilbraltar, Western Mediterranean. *Palaeontology* **44**, 601-621.

BOURGET J., AINSWORTH B. R., BACKE G. & KEEP M. 2012. Tectonic evolution of the northern Bonaparte Basin: impact on continental shelf architecture and sediment distribution during the Pleistocene. *Australian Journal of Earth Sciences* **in press February 2012**.

BREEN N. A., SILVER E. A. & HUSSONG D. M. 1986. Structural styles of an accretionary wedge south of the island of Sumba, Indonesia, revealed by SeaMARC II side scan sonar. *Geological Society of America Bulletin* **97**, 1250-1261.

BRISBOUT L. 2010. Stratigraphy and sedimentology of the Gondwanan Megasequence, Bandeira Gorge, Timor Leste. Honours Thesis, University of Western Australia, Perth (unpubl.).

BROUWER H. A. 1939. Exploration in the Lesser Sunda Islands. *The Geographical Journal* **94**, 1-10.

BROUWER H. A. 1942. Summary of the geological results of the expedition. *In:* Brouwer H. A. ed., *Geological Expedition of the University of Amsterdam to the Lesser Sunda Islands in the South Eastern Part of the Netherlands East Indies 1937*, Vol. 4, pp 345-401, N. V. Noord- Hollandsche Uitgevers Maatschappij, Amsterdam.

BRUNNSCHWEILER R. O. 1978. Notes on the geology of eastern Timor. *Bulletin Australia Bureau of Mineral Resources Geology and Geophysics* **192**, 9-18.

BÜCKING H. 1902. Beiträge zur Geologie von Celebes. *Samml. geol. Reichsmus. Leiden* **7**, 29-207.

CARTER D. J., AUDLEY-CHARLES M. G. & BARBER A. J. 1976. Stratigraphical analysis of island arc-continental margin collision in eastern Indonesia. *Journal of the Geological Society of London* **132**, 179-198.

CASTILLO D. A., BISHOP D. J., DONALDSON I., KUEK D., DE RUIG M. J., TRUPP M. & SHUSTER M. W. 2000. Trap integrity in the Laminaria High-Nancar Trough Region, Timor Sea: Prediction of fault seal failure using well-constrained stress tensors and fault surfaces interpreted from 3D seismic. *The APPEA journal* **40**, 151-173.

CHAMALAUN F. H. & GRADY A. E. 1978. The tectonic development of Timor: a new model and its implications for petroleum exploration. *APEA Journal* **18**, 102-108.

CHAMALAUN F. H., LOCKWOOD K. & WHITE A. 1976. The Bouguer gravity field and crustal structure of Eastern Timor. *Tectonophysics* **30**.

CHARLTON T. R. 1990. Mesozoic-Tertiary stratigraphy of the Kolbano area, southern West Timor. *Bull. Geol. Res. Dev. Centre* **14**, 38-58.

CHARLTON T. R. 2000. Tertiary evolution of the Eastern Indonesia Collision Complex. *Journal of Asian Earth Sciences* **18**, 603-631.

CHARLTON T. R. 2002a. The petroleum potential of East Timor. *APEA Journal* **42**, 351-369.

CHARLTON T. R. 2002b. The structural setting and tectonic significance of the Lolotoi, Laclubar and Aileu metamorphic massifs, East Timor. *Journal of Asian Earth Sciences* **20**, 851-865.

CHARLTON T. R., BARBER A. J. & BARKHAM S. T. 1991. The Structural Evolution of the Timor Collision Complex, Eastern Indonesia. *Journal of Structural Geology* **13**, 489-500.

CHARLTON T. R., BARBER A. J., HARRIS R. A., BARKHAM S. T., BIRD P. R., ARCHBOLD N. W., MORRIS N. J., NICOLL R. S., OWEN H. G., OWENS R. M., SORAUF J. E., TAYLOR P. D., WEBSTER G. D. & WHITTAKER J. E. 2002. The Permian of Timor: stratigraphy, palaeontology and palaeogeography. *Journal of Asian Earth Sciences* **20**, 719-774.

CHARLTON T. R., BARBER A. J., MCGOWAN A. J., NICOLL R. S., RONIEWICZ E., COOK S. E., BARKHAM S. T. & BIRD P. R. 2009. The Triassic of Timor: Lithostratigraphy, chronostratigraphy and palaeogeography. *Journal of Asian Earth Sciences* **36**, 341-363.

CHARLTON T. R. & WALL D. 1994. New biostratigraphic results from the Kolbano area, southern West Timor: Implications for the Mesozoic--Tertiary stratigraphy of Timor. *Journal of Southeast Asian Earth Sciences* **9**, 113-122.

DAVYDOV V. I., HAIG D. W. & MCCARTAIN E. 2013. A latest Carboniferous warming spike recorded by a fusulinid-rich bioherm in Timor Leste: Implications for East Gondwana deglaciation. *Palaeogeography, Palaeoclimatology, Palaeoecology* **376**, 22-38.

DAVYDOV V. I., HAIG D. W. & MCCARTAIN E. 2014. Latest Carboniferous (late Gzhelian) fusulinids from Timor Leste and their paleobiogeographic affinities. *Journal of Paleontology* **88**, 588-605.

DE ROEVER W. P. 1940. Geological investigations in the southwestern Moetis Region (Netherlands Timor). *In:* Brouwer H. A. ed., *Geological Expedition of the University of Amsterdam to the Lesser Sunda Islands in the South Eastern Part of the Netherlands East Indies 1937*, Vol. 2, pp 101-344, N.V. Noord-Hollandsche Uitgevers Maatschappij, Amsterdam.

DE ROEVER W. P. 1942. *Olivine-basalts and their alkaline differentiates in the permian of Timor*. Noord-Hollandsche Uitg. Maatsch, Amsterdam.

DE RUIG M. J., TRUPP M., BISHOP D. J., KUEK D. & CASTILLO D. A. 2000. Fault architecture and the mechanics of fault reactivation in the Nancar Trough/Laminaria area of the Timor Sea, northern Australia. *The APPEA journal* **40 (1)**, 174-193.

DE SMET M. E. M. & BARBER A. J. 1992. *Report on the Geology of Seram (Unpublished Report)*. *Geological Research in Southeast Asia*. University of London.

DE SMET M. E. M., FORTUIN A. R., TROELSTRA S. R., VAN MARLE L. J., KARMINI M., TJOKROSAPOETRO S. & HADIWASASTRA S. 1990. Detection of collision-related vertical movements in the Outer Banda Arc (Timor, Indonesia), using micropaleontological data. *Journal of Southeast Asian Earth Sciences* **4**, 337-356.

DE WAARD D. 1957. Contributions to the geology of Timor: XII. The third Timor geological expedition, preliminary results. *Madjalah Ilmu Alam Untuk Indonesia (Indonesian Journal for Natural Science)* **113**, 7-42.

DOOLEY T. & MCCLAY K. 1997. Analog modeling of pull-apart basins. *AAPG Bulletin* **81**, 1804-1826.

DOOLEY T., MCCLAY K. & BONORA M. 1999. 4D Evolution of segmented strike-slip fault systems: applications to NW Europe. *In:* Fleet A. J. & Boldy S. A. R. eds., *Petroleum Geology of Northwest Europe: Proceedings of the 5th Conference*, The Geological Society, London.

DOOLEY T., MONASTERO F. C., HALL B., MCCLAY K. & WHITEHOUSE P. 2004. Scaled Sandbox Modeling of Transtensional Pull-Apart Basins - Applications to the Coso Geothermal System. *Geothermal Resources Council Transactions* **28**, 637-641.

DOOLEY T., MONASTERO F. C. & MCCLAY K. 2007. Effects of A Weak Crustal Layer in a Transtensional Pull-Apart Basin: Results from a Scaled Physical Modeling Study. *American Geophysical Union, Fall Meeting,* abstract #V53F-04.

DOOLEY T. P. & SCHREURS G. 2012. Analogue modelling of intraplate strike-slip tectonics: A review and new experimental results. *Tectonophysics* **574–575**, 1-71.

DUFFY B., QUIGLEY M., HARRIS R. & RING U. 2013. Arc-parallel extrusion of the Timor sector of the Banda arc-continent collision. *Tectonics* **32**, 641-660.

ELY K. S., SANDIFORD M., HAWKE M. L., PHILLIPS D., QUIGLEY M. & REIS J. E. D. 2011. Evolution of Ataúro Island: Temporal constraints on subduction processes beneath the Wetar zone, Banda Arc. *Journal of Asian Earth Sciences* **41**, 477-493.

FITCH T. J. 1972. Plate Convergence, Transcurrent Faults, and Internal Deformation Adjacent to Southeast Asia and the Western Pacific. *J. Geophys. Res.* **77**, 4432-4460.

FITCH T. J. & HAMILTON W. 1974. Reply to a discussion by M.G. Audley-Charles & J. Milsom. *Journal of Geophysical Research* **79**, 4982-4985.

FLÜGEL E. 2004. *Microfacies of Carbonate Rocks*. Springer, Berlin.

FORTUIN A. R., ROEP T. B. & SUMOSUSASTRO P. A. 1994. The Neogene sediments of east Sumba, Indonesia—products of a lost arc? *Journal of Southeast Asian Earth Sciences* **9**, 67-79.

FORTUIN A. R., VAN DER WERFF W. & WENSINK H. 1997. Neogene basin history and paleomagnetism of a rifted and inverted forearc region, on- and offshore Sumba, Eastern Indonesia. *Journal of Asian Earth Sciences* **15**, 61-88.

FUGAGNOLI A. & BROGLIO C. L. 1998. Revised biostratigraphy of Lower Jurassic shallow water carbonates from the Venetian Prealps (Calcari Grigi, Trento Platform, northern Italy). *Studi Trentini di Scienze Naturali – Acta Geologica* **73**.

FUGAGNOLI A., GIANNETTI A. & RETTORI R. 2003. A new foraminiferal genus (Miliolina) from the Early Jurassic of the Southern Alps (Calcari Grigi Formation, northeastern Italy). *Revista Española de Micropaleontología* **35**, 43-50.

GAGEONNET R. & LEMOINE M. 1958. Contribution à la connaissance de la géologie de la province portugaise de Timor. *Ensaios e Documentos Ministério do Ultramar Junta de Investigações do Ultramar* **48**, 7-134.

GENRICH J. F., BOCK Y., MCCAFFREY R., CALAIS E., STEVENS C. W. & SUBARYA C. 1996. Accretion of the southern Banda arc to the Australian plate margin determined by Global Positioning System measurements. *Tectonics* **15**, 288-295.

GONZÁLEZ D., PINTO L., PEÑA M. & ARRIAGADA C. 2012. 3D deformation in strike-slip systems: Analogue modelling and numerical restoration. *Andean geology* **39**, 295-316.

GRADY A. E. 1975. A reinvestigation of thrusting in Portuguese Timor. *Journal of the Geological Society of Australia* **2**, 223-227.

GRADY A. E. & BERRY R. F. 1977. Some Palaeozoic-Mesozoic stratigraphic-structural relationships in East Timor and their significance in the tectonics of Timor. *Journal of the Geological Society of Australia* **24**, 203-214.

GRUNAU H. R. 1953. Geologie von Portugiesisch Ost-Timor. Eine kurze Übersicht. *Eclogae Geologicae Helveticae* **46**, 29-37.

GRUNAU H. R. 1956. Zur geologie von Portugiesisch Ost-Timor. *Mitteilungen Naturforschende Gesellschaft Bern* **13**, 11-18.

HAIG D. W. 2009. *Stratigraphic framework for geological mapping in the Viqueque - Ossu - Venilale regions of East Timor* (Eni Australia Report). (unpubl.), Perth.

HAIG D. W. 2012a. Palaeobathymetric gradients across Timor during 5.7–3.3 Ma (latest Miocene–Pliocene) and implications for collision uplift. *Palaeogeography, Palaeoclimatology, Palaeoecology* **331–332**, 50-59.

HAIG D. W. 2012b. Stratigraphic reconstruction of Timor Leste. *1st International Congress of Geology of East Timor,* Dili.

HAIG D. W. 2012c. Timor collision and uplift: critical stratigraphic evidence. *34th International Geological Congress,* Brisbane.

HAIG D. W. & BANDINI A. N. 2013. Middle Jurassic Radiolaria from a siliceous argillite block in a structural melange zone near Viqueque, Timor Leste: Paleogeographic implications. *Journal of Asian Earth Sciences* **75**, 71-81.

HAIG D. W. & MCCARTAIN E. 2007. Carbonate pelagites in the post-Gondwana succession (Cretaceous-Neogene) of East Timor. *Australian Journal of Earth Sciences* **54**, 875-897.

HAIG D. W. & MCCARTAIN E. 2010. Triassic organic-cemented siliceous agglutinated foraminifera from Timor-Leste: conservative development in shallow-marine environments. *Journal of Foraminiferal Research* **40**, 366-392.

HAIG D. W. & MCCARTAIN E. 2012. Intraspecific variation in Triassic Ophthalmidiid Foraminifera from Timor. *Revue de Micropaléontologie* **55**, 39-52.

HAIG D. W., MCCARTAIN E., BARBER L. & BACKHOUSE J. 2007. Triassic-Lower Jurassic foraminiferal indices for Bahaman-type carbonate-bank limestones, Cablac Mountain, East Timor. *Journal of Foraminiferal Research* **37**, 248-264.

HAIG D. W., MCCARTAIN E., KEEP M. & BARBER L. 2008. Re-evaluation of the Cablac Limestone at its type area, East Timor: Revision of the Miocene stratigraphy of Timor. *Journal of Asian Earth Sciences* **33**, 366-378.

HAIG D. W., MCCARTAIN E., MORY A. J., BORGES G., DAVYDOV V. I., DIXON M., ERNST A., GROFLIN S., HÅKANSSON E., KEEP M., SANTOS Z. D., SHI G. R. & SOARES J. 2014. Postglacial Early Permian (late Sakmarian–early Artinskian) shallow-marine carbonate

deposition along a 2000 km transect from Timor to west Australia. *Palaeogeography, Palaeoclimatology, Palaeoecology* **409**, 180-204.

HAILE N. S. 1974. An unusual unconformity of radiolarian chert on schist and gneiss east of Pangkajene, southwest arm, Sulawesi (Abstract). *Geol. Soc. Malaysia Newsl.* **52**, 21-22.

HAILE N. S., BARBER A. J. & CARTER D. J. 1979. Mesozoic cherts on crystalline schists in Sulawesi and Timor. *Journal of the Geological Society* **136**, 65-70.

HALL R. 1996. Reconstructing Cenozoic SE Asia. *Geological Society, London, Special Publications* **106**, 153-184.

HALL R. 2002. Cenozoic geological and plate tectonic evolution of SE Asia and the SW pacific: computer-based reconstructions, model and animations. *Journal of Asian Earth Sciences* **20**, 353-431.

HALL R. 2011. Australia–SE Asia collision: plate tectonics and crustal flow. *Geological Society, London, Special Publications* **355**, 75-109.

HALL R. & WILSON M. E. J. 2000. Neogene sutures in eastern Indonesia. *Journal of Asian Earth Sciences* **18**, 781-808.

HAMILTON W. 1979. Tectonics of the Indonesian region. *United States Geological Survey, Professional Paper* **1078**.

HARRIS R., KAISER J., HURFORD A. & CARTER A. 2000. Thermal history of Australian passive margin cover sequences accreted to Timor during Late Neogene arc-continent collision, Indonesia. *Journal of Asian Earth Sciences* **18**, 47-69.

HARRIS R. & LONG T. 2000. The Timor Ophiolite, Indonesia; model or myth? *Geological Society of America Special Paper* **349**, 321-330.

HARRIS R. A. 1991. Temporal distribution of strain in the active Banda orogen: a reconciliation of rival hypotheses. *Journal of Southeast Asian Earth Sciences* **6**, 373-386.

HARRIS R. A. 2006. Rise and fall of the Eastern Great Indonesian arc recorded by the assembly, dispersion and accretion of the Banda Terrane, Timor. *Gondwana Research* **10**, 207-231.

HARRIS R. A. 2011. The Nature of the Banda Arc–Continent Collision in the Timor Region. *In*, *Arc-Continent Collision*, pp 163-211, Springer Berlin Heidelberg.

HARRIS R. A. & AUDLEY-CHARLES M. G. 1987. Taiwan and Timor neotectonics; a comparative review. *Chung Kuo Ti Ch'ih Hsueh Hui Chuan Kan = Memoir of the Geological Society of China* **9**, 45-61.

HARRIS R. A., SAWYER R. K. & AUDLEY-CHARLES M. G. 1998. Collisional melange development: geologic associations of active melange-forming processes with exhumed melange facies in the western Banda orogen, Indonesia. *Tectonics* **17**, 458-479.

HARROWFIELD M., CUNNEEN J., KEEP M. & CROWE W. 2003. Early-stage orogenesis in the Timor Sea region, NW Australia. *Journal of the Geological Society* **160**, 991-1001.

HARROWFIELD M. & KEEP M. 2005. Tectonic modification of the Australian North-West Shelf; episodic rejuvenation of long-lived basin divisions. *Basin research* **17**, 225-239.

HARTONO H. M. S. 1990. Late Cenozoic tectonic development of the Southeast Asian continental margin in the Banda Sea area. *Tectonophysics* **181**, 267-276.

HIRSCHI H. 1907. Zur geologie und geographie von Portugiesisch-Timor, Geologische Mitteilungen aus dem Indo-Australischen Archipel. *Nueues Jahrbuch für Geologie und Paläontologie, Abhandlungen* **24**, 460-474.

HOCKING R. M., MOORS H. T. & VAN DE GRAAFF J. E. 1987. Geology of the Carnarvon Basin, Western Australia. *Geological Survey of Western Australia Bulletin* **133**, 1-289.

HOLLOWAY V. 2013. Modern deformation in the Rote area, Timor: insights from a combined seafloor bathymetry and seismic investigation. Honours Thesis, University of Western Australia, Perth (unpubl.).

HONTHAAS C., REHAULT J.-P., MAURY R. C., BELLON H., HEMOND C., MALOD J.-A., CORNEE J.-J., VILLENEUVE M., COTTEN J., BURHANUDDIN S., GUILLOU H. & ARNAUD N. 1998. A Neogene back-arc origin for the Banda Sea basins: geochemical and geochronological constraints for the Banda ridges (East Indonesia). *Tectonophysics* **298**, 297-317.

JARRARD R. D. 1986. Relations among subduction parameters. *Reviews of geophysics* **24**, 217-234.

KANEKO Y., MARUYAMA S., KADARUSMAN A., OTA T., ISHIKAWA M., TSUJIMORI T., ISHIKAWA A. & OKAMOTO K. 2007. On-going orogeny in the outer-arc of the Timor-Tanimbar region, eastern Indonesia. *Gondwana Research* **11**, 218-233.

KARIG D. E., BARBER A. J., CHARLTON T. R., KLEMPERER S. & HUSSONG D. M. 1987. Nature and distribution of deformation across the Banda Arc–Australian collision zone at Timor. *Geological Society of America Bulletin* **98**, 18-32.

KEEP M., BARBER L. & HAIG D. W. 2009. Deformation of the Cablac Mountain Range, East Timor: An overthrust stack derived from an Australian continental terrace. *Journal of Asian Earth Sciences* **35**, 150-166.

KEEP M., BECK L. & BEKKERS P. 2005. Complex modified thrust systems along the southern margin of East Timor. *APPEA Journal* **45**, 297-310.

KEEP M., BISHOP A. & LONGLEY I. 2000. Neogene wrench reactivation of the Barcoo Sub-basin, Northwest Australia; implications for Neogene tectonics of the northern Australian margin. *Petroleum Geoscience* **6**, 211-220.

KEEP M., CLOUGH M. C. & LANGHI L. 2002. Neogene structural and tectonic evolution of the Timor Sea region, NW Australia. *In:* Keep M. & Moss S. J. eds., *The Sedimentary Basins of Western Australia 3*, pp 341-354, Proceedings of the Petroleum Exploration Society of Australia, Perth.

KEEP M. & HAIG D. W. 2010. Deformation and exhumation in Timor: Distinct stages of a young orogeny. *Tectonophysics* **483**, 93-111.

KEEP M., LONGLEY I. & JONES R. 2003. Sumba and its effect on Australia's northwestern margin. *Geological Society of Australia Special Publication* **22**, 303-312.

KEEP M., POWELL C. M. & BAILLIE P. W. 1998. Neogene deformation of the North West Shelf, Australia. *In:* Purcell P. G. & Purcell R. R. eds., *The Sedimentary Basins of Western Australia 2: Proceedings of the Petroleum Exploration Society of Australia*, pp 81-91, Perth.

KRUMBECK L. 1921. Die Brachiopoden, Lamellibranchiaten und Gastropoden der Trias von Timor. I. Stratigraphischer Teil. *In:* Wanner J. ed., *Paläontologie von Timor nebst kleineren Beiträgen zur Paläontologie einiger anderer Inseln des Ostindischen Archipels. Ergebnisse der Expeditionen G.A.F. Molengraaff, J. Wanner und F. Weber*, Vol. 10, pp 1-142, Stuttgart.

LANGHI L., CIFTCI N. B. & BOREL G. D. 2011. Impact of lithospheric flexure on the evolution of shallow faults in the Timor foreland system. *Marine Geology* **284**, 40-54.

LAWLESS J. V., LOVELOCK B. G. & USSHER G. N. 2005. Geothermal Potential of East Timor. *World Geothermal Congress 2005,* Antalya, Turkey.

LEE T.-Y. & LAWVER L. A. 1995. Cenozoic plate reconstruction of Southeast Asia. *Tectonophysics* **251**, 85-138.

LONGLEY I. M., BUESSENCHUETT C., CLYDESDALE C. J., CUBITT R. C., DAVIS M. K., JOHNSON N. M., MARSHALL A. P., MURRAY R., SOMERVILLE T. B., SPRY & THOMPSON N. B. 2002. The North West Shelf – a Woodside perspective. *In:* Keep M. & Moss S. J. eds., *The Sedimentary basins of Western Australia 3. Proceedings of the Petroleum Exploration Society of Australia, Perth*, pp 27-87.

LYTWYN J., RUTHERFORD E., BURKE K. & XIA C. 2001. The geochemistry of volcanic, plutonic and turbiditic rocks from Sumba, Indonesia. *Journal of Asian Earth Sciences* **19**, 481-500.

MANN P. 2007. Global catalogue, classification and tectonic origins of restraining- and releasing bends on active and ancient strike-slip fault systems. *In:* Cunningham W. D. & Mann P. eds., *Tectonics of Strike-Slip Restraining and Releasing Bends*, Vol. 290, pp 13-142, The Geological Society, Special Publications, London.

MARKS P. 1961. The succession of nappes in the western Miomaffo area of the island of Timor; a possible key to the structure of Timor. *Proceedings of the Pacific Science Congress* **12**, 306-310.

MASSON D. G., MILSOM J., BARBER A. J., SIKUMBANG N. & DWIYANTO B. 1991. Recent tectonics around the island of Timor, eastern Indonesia. *Marine and Petroleum Geology* **8**, 35-49.

MCCAFFREY R. 1989. Seismological constraints and speculations on Banda arc tectonics. *Netherlands Journal of Sea Research* **24**, 141-152.

MCCAFFREY R. 1996. Slip partitioning at convergent plate boundaries of SE Asia. *Geological Society, London, Special Publications* **106**, 3-18.

MCCAFFREY R., MOLNAR P., ROECKER S. W. & JOYODIWIRYO Y. S. 1985. Microearthquake Seismicity and Fault Plane Solutions Related to Arc-Continent Collision in the Eastern Sunda Arc, Indonesia. *J. Geophys. Res.* **90**, 4511-4528.

MCCARTAIN E., BACKHOUSE J., HAIG D. W., BALME B. E. & KEEP M. 2006. Gondwanan-related Late Permian palynoflora, foraminiferas and lithofacies from the Wailuli Valley, Timor Leste. *N. Jb. Geol. Palaont. Abh.* **240**, 53-80.

MCCLAY K. & BONORA M. 2001. Analog models of restraining stepovers in strike-slip fault systems. *AAPG Bulletin* **85**, 223-260.

MCROBERTS C. A. 1993. Systematics and Biostratigraphy of Halobiid Bivalves from the Martin Bridge Formation (Upper Triassic), Northeast Oregon. *Journal of Paleontology* **67**, 198-210.

METCALFE I. 2011. Palaeozoic–Mesozoic history of SE Asia. *Geological Society, London, Special Publications* **355**, 7-35.

MILSOM J. 2000. Stratigraphic constraints on suture models for eastern Indonesia. *Journal of Asian Earth Sciences* **18**, 761-779.

MOLENGRAAF G. A. F. 1912. De fatoe's van Timor. *Geologische Mijnbouwkundig Genootschap voor Nederland en Koloniën, Geologische Sectie, verslag der voordrachten, van 1912 - 1914, gehouden op de Wetenschappelijke Vergaderingen*.

NAYLOR M. A., MANDL G. & SUPESTEIJN C. H. K. 1986. Fault geometries in basement-induced wrench faulting under different initial stress states. *Journal of Structural Geology* **8**, 737-752.

NELSON A. 1993. Wrench and inversion structures in the Timor Sea region. *Petroleum Exploration Society of Australia Journal* **21**, 3-30.

NORCONSULT 2006. *Final Report*. *Iralalaru Hydrpower Project - Feasibility Study*. The Norwegian Water Resources and Energy Directorate (NVE).

NUGROHO H., HARRIS R., LESTARIYA A. W. & MARUF B. 2009. Plate boundary reorganization in the active Banda Arc–continent collision: Insights from new GPS measurements. *Tectonophysics* **479**, 52-65.

PACKHAM G. 1996. Cenozoic SE Asia: reconstructing its aggregation and reorganization. *Geological Society, London, Special Publications* **106**, 123-152.

PAIRAULT A. A., HALL R. & ELDERS C. F. 2003. Structural styles and tectonic evolution of the Seram Trough, Indonesia. *Marine and Petroleum Geology* **20**, 1141-1160.

PARTOYO E., HERMANTO B. & BACHRI S. 1995. Geological Map of Baucau Quadrangle, East Timor, Scale 1:250 000. *Geological Research and Development Centre, Bandung*.

PETIT J. P. 1987. Criteria for the sense of movement on fault surfaces in brittle rocks. *Journal of Structural Geology* **9**, 597-608.

PIGRAM C. J. & PANGGABEAN H. 1984. Rifting of the northern margin of the Australian continent and the origin of some microcontinents in Eastern Indonesia. *Tectonophysics* **107**, 331-353.

POWNALL J. M., HALL R., ARMSTRONG R. A. & FORSTER M. A. 2014. Earth's youngest known ultrahigh-temperature granulites discovered on Seram, eastern Indonesia. *Geology*.

POWNALL J. M., HALL R. & WATKINSON I. M. 2013. Extreme extension across Seram and Ambon, eastern Indonesia: evidence for Banda slab rollback. *Solid Earth* **4**, 277-314.

PRICE N. J. & AUDLEY-CHARLES M. G. 1987. Tectonic collision processes after plate rupture. *Tectonophysics* **140**, 121-129.

PURDY E. G. 1963a. Recent calcium carbonate facies of the Great Bahama Bank. 1. Petrography and reaction groups *Journal of Geology* **71**, 334-355.

PURDY E. G. 1963b. Recent calcium carbonate facies of the Great Bahama Bank. 2. Sedimentary facies. *Journal of Geology* **71**, 472-497.

REED D. L. 1985. Structure and stratigraphy of the eastern Sunda Forearc, Indonesia: geologic consequences of arc-continent collision. PhD thesis, University of California, Santa Cruz (unpubl.).

REED T. A., DE SMET M. E. M., HARAHAP B. H. & SJAPAWI A. 1996. Structural and depositional history of East Timor. *Proceedings of the Indonesian Petroleum Association* **25**, 297-312.

REVETS S. A., KEEP M. & KENNETT B. L. N. 2009. NW Australian intraplate seismicity and stress regime. *Journal of Geophysical Research: Solid Earth* **114**, B10305.

RICHARD P. D., NAYLOR M. A. & KOOPMAN A. 1995. Experimental models of strike-slip tectonics. *Petroleum Geoscience* **1**, 71-80.

RICHARDSON A. N. & BLUNDELL D. J. 1996. Continental collision in the Banda Arc. *In:* Hall R. & Blundell D. J. eds., *Tectonic evolution of southeast Asia. Geological Society Special Publication*, Vol. 106, pp 47-60.

ROMARIZ C. & LEME J. D. A. 1967. Subsidios para a petrografia timorense. Calcario de Fato. *Garcia de Orta* **15**, 111-112.

ROOSMAWATI N. & HARRIS R. 2009. Surface uplift history of the incipient Banda arc-continent collision: Geology and synorogenic foraminifera of Rote and Savu Islands, Indonesia. *Tectonophysics* **479**, 95-110.

ROSIDI H. M. O., SUWITOPIROYO K. & TJOKROSAPOETRO S. 1979. Geological map Kupang–Atambua Quadrangle, Timor, Scale 1:250,000. *Geological Research and Development Centre, Bandung*.

RUTHERFORD E., BURKE K. & LYTWYN J. 2001. Tectonic history of Sumba Island, Indonesia, since the Late Cretaceous and its rapid escape into the forearc in the Miocene. *Journal of Asian Earth Sciences* **19**, 453-479.

RYAN H. F. & COLEMAN P. J. 1992. Composite transform-convergent plate boundaries: description and discussion. *Marine and Petroleum Geology* **9**, 89-97.

SANI K., JACOBSEN M. L. & SIGIT R. 1995. The thin-skinned thrust structures of Timor. *Proceedings of the Indonesian Petroleum Association* **24**, 277-293.

SAWYER R. K., SANI K. & BROWN S. 1993. The stratigraphy and sedimentology of West Timor, Indonesia. *Proceedings of the Indonesian Petroleum Association, 22nd Annual Convention*, 533-574.

SCHELLART W. P. & NIEUWLAND D. A. 2003. 3D evolution of a pop-up structure above a double basement strike-slip fault: some insights from analogue modelling. *Geological Society, London, Special Publications* **212**, 169-179.

SCHLAGINTWEIT F. & VELIĆ I. 2012. Foraminiferan tests and dasycladalean thalli as cryptic microhabitats for thaumatoporellacean algae from Mesozoic (Late Triassic–Late Cretaceous) platform carbonates. *Facies* **58**, 79-94.

SCHNEEBERGER W. F. 1961. *Resume of the geology and petroleum prospects of Portuguese Timor*. Ball Associates, Report to Timor OIl.

SCHREURS G. 2003. Fault development and interaction in distributed strike-slip shear zones: an experimental approach. *Geological Society, London, Special Publications* **210**, 35-52.

SEPTFONTAINE M. 1988. Towards an evolutionary classification of Jurassic lituolids (Foraminifera) in carbonate platform environment. . *Revue de Paléobiologie* **Special Volume 2**, 229-256.

SHUSTER M. W., EATON S., WAKEFIELD L. L. & KLOOSTERMAN H. J. 1998. Neogene tectonics, Greater Timor Sea, offshore Australia: implications for trap risk. *The APPEA journal* **38**, 351-379.

SIMONS A. L. 1940. Geological investigations in N. E. Netherlands Timor. *In:* Brouwer H. A. ed., *Geological Expedition of the University of Amsterdam to the Lesser Sunda Islands in the South Eastern Part of the Netherlands East Indies 1937*, Vol. 1, pp 110-213, N. V. Noord-Hollandsche Uitgevers Maatschappij, Amsterdam.

SOPAHELUWAKAN J. 1990. Ophiolite Obduction in the Mutis Complex, Timor, Eastern Indonesia: An Example of Inverted, Isobaric, Medium-High Pressure metamorphism. University of Amsterdam, PhD Thesis (unpubl.).

SOPAHELUWAKAN J., HELMERS H., TJORKROSAPOETRO S. & NILA E. S. 1989. Medium pressure metamorphism with inverted thermal gradient associated with ophiolite nappe emplacement in Timor. *Netherlands Journal of Sea Research* **24**, 333-343.

SPAKMAN W. & HALL R. 2010. Surface deformation and slab-mantle interaction during Banda arc subduction rollback. *Nature Geosci* **3**, 562-566.

STANDLEY C. E. & HARRIS R. 2009. Tectonic evolution of forearc nappes of the active Banda arc-continent collision: Origin, age, metamorphic history and structure of the Lolotoi Complex, East Timor. *Tectonophysics* **479**, 66-94.

TAPPENBECK D. 1940. Geologie des Mollogebirges und einiger benachbarter gebiete (Niederländisch Timor). *In:* Brouwer H. A. ed., *Geological Expedition of the University of Amsterdam to the Lesser Sunda Islands in the South Eastern Part of the Netherlands East Indies 1937*, Vol. 1, pp 1-105, N. V. Noord-Hollandsche Uitgevers Maatschappij, Amsterdam.

TCHALENKO J. S. 1970. Similarities between Shear Zones of Different Magnitudes. *Geological Society of America Bulletin* **81**, 1625-1640.

TJOKROSAPOETRO S. & BUDHITRISNA T. 1982. Geology and tectonics of the northern Banda Arc. *Geological Research and Development Centre, Bandung* **Special Publication 6**, 1-17.

UMBGROVE J. H. F. 1938. Geological history of the East Indies. *AAPG Bulletin* **22**, 1-70.

VAN BEMMELEN R. W. 1949. *The Geology of Indonesia*. The Hague (Government Publishing Office).

VAN BEMMELEN R. W. 1970. *The geology of Indonesia* (2nd edition). Martinus Nijhoff, The Hague.

VAN DER WERFF W., KUSNIDA D., PRASETYO H. & VAN WEERING T. C. E. 1994. Origin of the Sumba forearc basement. *Marine and Petroleum Geology* **11**, 363-374.

VAN MARLE L. J. 1991a. *Eastern Indonesian, late Cenozoic smaller benthic foraminifera / L.J. van Marle* (Verhandelingen der Koninklijke Nederlandse Akademie van Wetenschappen, Afd. Natuurkunde. Eerste reeks ; d. 34). North-Holland, Amsterdam.

VAN MARLE L. J. 1991b. Late Cenozoic palaeobathymetry and geohistory analysis of Central West Timor, eastern Indonesia. *Marine and Petroleum Geology* **8**, 22-34.

VAN VOORTHUYSEN J. H. 1940. Geological investigations in the Amfoan District (Northwest Timor). *In:* Brouwer H. A. ed., *Geological Expedition of the University of Amsterdam to the Lesser Sunda Islands in the South Eastern Part of the Netherlands East Indies 1937*, Vol. 2, pp 345-367, N.V. Noord-Hollandsche Uitgevers Maatschappij, Amsterdam.

VAN WEST F. P. 1941. Geological investigations in the Miomaffo region (Netherlands Timor). *In:* Brouwer H. A. ed., *Geological Expedition of the University of Amsterdam to the Lesser Sunda Islands in the South Eastern Part of the Netherlands East Indies 1937*, Vol. 3, pp 1-131, N.V. Noord-Hollandsche Uitgevers Maatschappij, Amsterdam.

VEEVERS J. J. & POWELL C. M. 1984. Dextral shear within the eastern Indo-Australian plate. *In:* Veevers J. J. ed., *Phanerozoic Earth History of Australia*, pp 102-103, Clarendon Press, Oxford.

VILLENEUVE M., HARSOLUMKSO A. H., CORNEE J. J. & BELLON H. 1999. Structure of West Timor (Indonesia) along a north–south cross section. *Geologie Mediterraneenne* **26**, 127-142.

VON STEIGER H. 1915. Petrografische beschrijving van einige gesteenten uit de onderafdeeling Pangkajene en het Landscap Tanette. *Jaarboek van het Mijnwezen in Nederlandsch-Indie* **1913**.

VROON P. Z., VAN BERGEN M. J. & FORDE E. J. 1996. Pb and Nd isotope constraints on the provenance of tectonically dispersed continental fragments in east Indonesia. *Geological Society, London, Special Publications* **106**, 445-453.

WANNER J. 1913. Geologie von Westtimor. *Geologische Rundschau* **4**, 136-150.

WANNER J. 1956. Zur Stratigraphie von Portugiesisch Timor. *Zeitschrift der Deutschen Geologische Gesellschaft* **108**, 109-140.

WENSINK H. & HARTOSUKOHARDJO S. 1990. Paleomagnetism of younger volcanics from Western Timor, Indonesia. *Earth and Planetary Science Letters* **100**, 94-107.

WENSINK H. & VAN BERGEN M. J. 1995. The tectonic emplacement of Sumba in the Sunda-Banda Arc: paleomagnetic and geochemical evidence from the early Miocene Jawila volcanics. *Tectonophysics* **250**, 15-30.

WITTOUCK S. F. 1937. *Exploration of Portuguese Timor*. Report of Allied Mining Corp. To Asia Investment Co. Ltd., Amsterdam (Kolff).

WITTOUCK S. F. 1938. Exploration of Portuguese Timor. *The Geographical Journal* **92**, 343-350.

WU J. E., MCCLAY K., WHITEHOUSE P. & DOOLEY T. 2009. 4D analogue modelling of transtensional pull-apart basins. *Marine and Petroleum Geology* **26**, 1608-1623.

Appendix I

Sample locations and descriptions

Location_No	Lat	Long	Region	Sample_type	Field_Description	Rock_Description	Benthic_foraminifera	Planktonic_foraminifera	OtherBioclasts	Facies	Age	Group	Megasequence	Date
12_10_08_4	-8.70495	126.36222	Mundo Perdido	limestone		Packstone with abundant planktonic foraminifera, rare benthic foraminifera (mainly Rotaliida), mollusc fragments, coralline algae, coral debris; bed of planktonic foraminiferal limestone above 143147		Planktonic foraminifera: Globorotalia truncatulinoides, Globorotalia tosaensis		upper bathyal zone	Planktonic foraminiferal Zone N22r; mid Pleistocene within 2.02–0.63 Ma interval (Keep & Haig 2010, fig. 6)	Viqueque Group - Lari Guti Member	Synorogenic Megasequence	12/10
12_10_08_5	-8.70495	126.36222	Mundo Perdido	limestone		Packstone with abundant planktonic foraminifera, rare benthic foraminifera (mainly Rotaliida); lowest bed of fine planktonic foraminiferal limestone in outcrop section		Planktonic foraminifera: Globorotalia truncatulinoides, Globorotalia tosaensis		upper bathyal zone	Planktonic foraminiferal Zone N22r; mid Pleistocene within 2.02–0.63 Ma interval (Keep & Haig 2010, fig. 6)	Viqueque Group - Lari Guti Member	Synorogenic Megasequence	12/10
12_10_08_7	-8.71150	126.35525	Mundo Perdido	limestone		Wackestone with scattered planktonic foraminifera		Planktonic foraminifera: Dicarinella sp., Praeglobotruncana sp.		middle bathyal to abyssal	Late Cretaceous (Turonian)	Kolbano Group	Australian Margin Megasequence	12/10
14_10_08_1_A	-8.73067	126.36735	Mundo Perdido	limestone		Collected on south side of gully: Wackestone with common thaumatoporellacean algae.			Thaumatoporcellacean algae.	innermost neritic.	probably Early Jurassic	Perdido Group	Gondwana Megasequence	14/10
14_10_08_1_B	-8.73067	126.36735	Mundo Perdido	limestone		Collected on north side of gully: Packstone to wackestone with large corals, abundant benthic foraminifera (mainly Rotaliida including larger types), rare small planktonic foraminifera,	Larger benthic foraminifera (in limestone clasts): Eulepidina, primitive Lepidocyclina (Nephrolepidina), Spiroclypeus.	Planktonic foraminifera (in matrix): ?Globigerinoides primordius		Inner neritic	Larger benthic foraminiferal Upper Te Letter Stage (Adams, 1970); planktonic zone N4 or N5 (Kennett & Srinivasan, 1983); latest Oligocene or earliest Miocene	Booi Group	Banda Megasequence	14/10
14_10_08_2	-8.73067	126.36735	Mundo Perdido	limestone		Packstone to wackestone with abundant benthic foraminifera (mainly Rotaliida including larger types), coralline algae and coral debris	Larger benthic foraminifera (in limestone clasts): Eulepidina, primitive Lepidocyclina (Nephrolepidina), Spiroclypeus.				Larger benthic foraminiferal Upper Te Letter Stage (Adams, 1970); latest Oligocene - earliest Miocene	Booi Group	Banda Megasequence	14/10
14_10_08_3	-8.72922	126.36575	Mundo Perdido	limestone		Ooid grainstone with micritic intraclasts; very rare thaumatoporellacean algae scattered recrystallized mollusc debris, very rare echinoid spines and plates, very rare indeterminant benthic foraminifera			Thaumatoporcellacean algae		Probably Early Jurassic	Perdido Group	Gondwana Megasequence	14/10
14_10_08_7	-8.72910	126.36582	Mundo Perdido	limestone		Wackestone with rare planktonic foraminifera (including keeled forms), rare benthic foraminifera (Rotaliida)		Helvetoglobotruncana helvetica, Marginotruncana marginata, Dicarinella spp.		middle bathyal to abyssal	Upper Turonian (Turonian)	Kolbano Group	Australian Margin Megasequence	14/10
14_10_08_8	-8.72910	126.36715	Mundo Perdido	mudstone		Friable grey mudstone		Globorotalia kugleri, Globigerinoides primordius			Planktonic foraminiferal zone N4 (Kennett & Srinivasan 1983); Larger benthic foraminiferal Upper Te Letter Stage (Adams, 1970); earliest Miocene	Booi Group	Banda Megasequence	14/10
14_10_08_9	-8.71702	126.36592	Mundo Perdido	limestone		Ooid grainstone with rare carbonate-cemented agglutinated foraminifera	Siphovalvulina variabilis				Probably Early Jurassic	Perdido Group	Gondwana Megasequence	14/10
8_11_08_04	-8.70575	126.36175	Mundo Perdido	limestone		Planktonic foraminiferal packstone with very rare smaller benthic foraminifera (Rotaliida); collected 2.7 m above base of outcrop section		Globorotalia truncatulinoides, Globorotalia tosaensis		upper bathyal zone	Planktonic foraminiferal Zone N22r; mid Pleistocene within 2.02–0.63 Ma interval (Keep & Haig 2010, fig. 6)	Viqueque Group - Lari Guti Member	Synorogenic Megasequence	8/11
8_11_08_08	-8.70575	126.36175	Mundo Perdido	limestone		Calcirudite with large corals, coralline algal debris, mollusc fragments, common benthic foraminifera (mainly Rotaliida including larger types), scattered planktonic foraminifera; lithic fragments. From base of large channel cut into section	Nummulites venosus, Schlumbergerella, Cycloclypeus	Globorotalia truncatulinoides, Globorotalia tosaensis.		upper bathyal zone	Planktonic foraminiferal Zone N22r; mid Pleistocene within 2.02–0.63 Ma interval (Keep & Haig 2010, fig. 6)	Viqueque Group - Lari Guti Member	Synorogenic Megasequence	8/11

Location_No	Lat	Long	Region	Sample_type	Field_Description	Rock_Description	Benthic_foraminifera	Planktonic_foraminifera	OtherBioclasts	Facies	Age	Group	Megasequence	Date
8_11_08_09	-8.70575	126.36175	Mundo Perdido	limestone		Packstone with abundant benthic foraminifera (mainly rotaliids including larger types), coralline algae, mollusc debris; about 1 m above base of large channel cut into section	Nummulites venosus, Schlumbergerella, Cycloclypeus	Globorotalia truncatulinoides, Globorotalia tosaensis.		upper bathyal zone	Planktonic foraminiferal Zone N22r; mid Pleistocene within 2.02–0.63 Ma interval (Keep & Haig 2010, fig. 6)	Viqueque Group - Lari Guti Member	Synorogenic Megasequence	8/11
8_11_08_13	-8.70575	126.36175	Mundo Perdido	limestone		Calcirudite with large corals, abundant planktonic foraminifera, rare benthic foraminifera (mainly Rotaliida); 13.2 m above base of exposed measured section	Schlumbergerella	Globorotalia truncatulinoides, Globorotalia tosaensis.		upper bathyal zone	Planktonic foraminiferal Zone N22r; mid Pleistocene within 2.02–0.63 Ma interval (Keep & Haig 2010, fig. 6)	Viqueque Group - Lari Guti Member	Synorogenic Megasequence	8/11
8_11_08_15	-8.70575	126.36175	Mundo Perdido	limestone		Packstone with abundant planktonic foraminifera, rare benthic foraminifera (mainly Rotaliida); 21.7 m above base of exposed measured section		Globorotalia truncatulinoides, Globorotalia tosaensis		upper bathyal zone	Planktonic foraminiferal Zone N22r; mid Pleistocene within 2.02–0.63 Ma interval (Keep & Haig 2010, fig. 6)	Viqueque Group - Lari Guti Member	Synorogenic Megasequence	8/11
8_11_08_16	-8.70575	126.36175	Mundo Perdido	limestone		Packstone with abundant planktonic foraminifera, rare benthic foraminifera (mainly Rotaliida); 22.5 m above base of exposed measured section		Globorotalia truncatulinoides, Globorotalia tosaensis		upper bathyal zone	Planktonic foraminiferal Zone N22r; mid Pleistocene within 2.02–0.63 Ma interval (Keep & Haig 2010, fig. 6)	Viqueque Group - Lari Guti Member	Synorogenic Megasequence	8/11
8_11_08_17	-8.70575	126.36175	Mundo Perdido	limestone		Packstone with abundant planktonic foraminifera, rare benthic foraminifera (mainly Rotaliida); 22.6 m above base of exposed measured section at base of coarser limestone unit		Globorotalia truncatulinoides, Globorotalia tosaensis. Benthic foraminifera: Schlumbergerella, Nummulites venosus		upper bathyal zone	Planktonic foraminiferal Zone N22r; mid Pleistocene within 2.02–0.63 Ma interval (Keep & Haig 2010, fig. 6)	Viqueque Group - Lari Guti Member	Synorogenic Megasequence	8/11
8_11_08_18	-8.70575	126.36175	Mundo Perdido	limestone		Packstone/calcirudite with coral debris, coralline algae, mollusc debris, common planktonic foraminifera, rare benthic foraminifera (mainly Rotaliida); 28 m above base of exposed measured section		Globorotalia truncatulinoides, Globorotalia tosaensis. Benthic foraminifera: Schlumbergerella, Nummulites venosus		upper bathyal zone	Planktonic foraminiferal Zone N22r; mid Pleistocene within 2.02–0.63 Ma interval (Keep & Haig 2010, fig. 6)	Viqueque Group - Lari Guti Member	Synorogenic Megasequence	8/11
8_11_08_28	-8.71942	126.36739	Mundo Perdido	limestone		Wackestone/packstone with abundant benthic foraminifera (mainly Rotaliida, including larger types), abundant planktonic foraminifera, coralline algae	Eulepidina, primitive Lepidocyclina (Nephrolepidina), Spiroclypeus	Globigerinoides primordius.			Larger benthic foraminiferal Upper Te Letter Stage (Adams, 1970); planktonic zone N4 or N5 (Kennett & Srinivasan 1983); latest Oligocene or earliest Miocene	Booi Group	Banda Megasequence	8/11
8_11_08_32	-8.72342	126.36708	Mundo Perdido	mudstone		Mudstone with abundant planktonic foraminiferaand rare benthic foraminifera (mainly Orders Buliminida, Lagenida)		Globorotalia kugleri, Globigerinoides primordius			Planktonic Zone N4; Larger benthic foraminiferal Upper Te Letter Stage (Adams, 1970); latest Oligocene or earliest Miocene	Booi Group	Banda Megasequence	8/11
8_11_08_33	-8.72342	126.36708	Mundo Perdido	limestone		Packstone with abundant planktonic foraminifera; rare benthic foraminifera (mainly Rotaliida, including larger types), rare coralline algal debris	Spiroclypeus	Globorotalia kugleri, Globoquadrina binaiensis, Globigerinoides primordius.			Planktonic Zone N4; Larger benthic foraminiferal Upper Te Letter Stage (Adams, 1970); latest Oligocene or earliest Miocene	Booi Group	Banda Megasequence	8/11
8_11_08_34	-8.72342	126.36708	Mundo Perdido	limestone		Wackestone with scattered benthic foraminifera (mainly Order Rotaliida, including larger types) and planktonic foraminifera	Eulepidina, primitive Lepidocyclina (Nephrolepidina), Spiroclypeus				Larger benthic foraminiferal Upper Te Letter Stage (Adams, 1970); latest Oligocene - earliest Miocene	Booi Group	Banda Megasequence	8/11

Location_No	Lat	Long	Region	Sample_type	Field_Description	Rock_Description	Benthic_foraminifera	Planktonic_foraminifera	OtherBioclasts	Facies	Age	Group	Megasequence	Date
9_11_08_9	-8.72419	126.36722	Mundo Perdido	limestone		Wackestone with scattered benthic foraminifera (mainly Order Rotaliida, including larger types); coralline algal debris	primitive Lepidocyclina (Nephrolepidina), Spiroclypeus	Globigerinoides primordius, Globoquadrina binaiensis			Larger benthic foraminiferal Upper Te Letter Stage (Adams, 1970); planktonic zone N4 (Kennett & Srinivasan 1983) ; latest Oligocene or earliest Miocene	Booi Group	Banda Megasequence	9/11
9_11_08_10	-8.72442	126.36769	Mundo Perdido	limestone		Wackestone with common planktonic foraminifera, rare benthic foraminifera (mainly Order Rotaliida, including larger types)	Spiroclypeus	Globorotalia kugleri, Globoquadrina binaiensis, Globigerinoides primordius			Planktonic foraminiferal zone N4 (Kennett & Srinivasan 1983; Larger benthic foraminiferal Upper Te Letter Stage (Adams, 1970); latest Oligocene or earliest Miocene	Booi Group	Banda Megasequence	10/11
9_11_08_12	-8.72442	126.36769	Mundo Perdido	limestone		Packstone with abundant planktonic foraminifera; fragmented larger benthic foraminifera	Spiroclypeus	Globigerinoides primordius or Globigerina praebulloides, Dentoglobigerina altispira, Globoquadrina venezuelana			Larger benthic foraminiferal Upper Te Letter Stage (Adams, 1970): latest Oligocene or earliest Miocene	Booi Group	Banda Megasequence	11/11
9_11_08_14	-8.73042	126.36839	Mundo Perdido	limestone		Wackestone with rare thaumatoporellacean algae and very rare carbonate-cemented agglutinated foraminifera	? Siphovalvulina sp.		Thaumatoporellacean algae: Thaumatoporella ?parvovesiculifera (micritized)		Probably Early Jurassic	Perdido Group	Gondwana Megasequence	12/11
9_11_08_15	-8.73042	126.36839	Mundo Perdido	limestone		Wackestone and peloidal grainstone with common carbonate-cemented agglutinated foraminifera and scattered thaumatoporellacean algae (including cryptoendoliths; see Schlangintweit and Velić 2011); dasycladale algae	Siphovalvulina variabilis, "Planisepta" compressa.		Thaumatoporellacean algae: Thaumatoporella ?parvovesiculifera (micritized).		Early Jurassic (Sinemurian-Pliensbachian)	Perdido Group	Gondwana Megasequence	13/11
9_11_08_16	-8.73322	126.36867	Mundo Perdido	limestone		Wackestone with abundant benthic foraminifera (mainly Order Rotaliida, including larger types), scattered small planktonic foraminifera, abundant coralline algae, coral debris	primitive Lepidocyclina (Nephrolepidina), Spiroclypeus	Globigerinoides primordius or Globigerina praebulloides			Larger benthic foraminiferal Upper Te Letter Stage (Adams, 1970); latest Oligocene - earliest Miocene	Booi Group	Banda Megasequence	14/11
9_11_08_17	-8.73322	126.36867	Mundo Perdido	limestone		Laminated fine calcarenite with very thin layers of coarse sand composed of fragmented larger benthic foraminifera (Order Rotaliida) and scattered small planktonic foraminifera	primitive Lepidocyclina (Nephrolepidina), Spiroclypeus.				Larger benthic foraminiferal Upper Te Letter Stage (Adams, 1970); latest Oligocene - earliest Miocene	Booi Group	Banda Megasequence	15/11
9_11_08_18	-8.73322	126.36867	Mundo Perdido	limestone		Packstone composed mainly of larger benthic foraminifera (Order Rotaliida)	Eulepidina, primitive Lepidocyclina (Nephrolepidina), Spiroclypeus.				Larger benthic foraminiferal Upper Te Letter Stage (Adams, 1970); latest Oligocene - earliest Miocene	Booi Group	Banda Megasequence	16/11
9_11_08_19	-8.73353	126.36922	Mundo Perdido	breccia		Limestone breccia; clasts of wackestone, peloidal grainstone; wackestone contains rare carbonate-cemented agglutinated foraminifera and thaumatoporellacean algae; peloidal grainstone contains common carbonate-cemented agglutinated foraminifera	Siphovalvulina variabilis, "Planisepta" compressa, Meandrovoluta asiagoensis		Thaumatoporellacean algae: Thaumatoporella ?parvovesiculifera (micritized).		Early Jurassic (Sinemurian-Pliensbachian)	Perdido Group	Gondwana Megasequence	17/11
9_11_08_20	-8.73428	126.36853	Mundo Perdido	breccia		Limestone breccia; clasts of wackestone, peloidal grainstone; wackestone contains rare carbonate-cemented agglutinated foraminifera, thaumatoporellacean (including cryptoendoliths; see Schlagintweit and Velić 2011) and dasycladale algae; peloidal grainstone contains common carbonate-cemented agglutinated foraminifera	Siphovalvulina variabilis, Meandrovoluta asiagoensis		Thaumatoporellacean algae: Thaumatoporella ?parvovesiculifera (micritized). Dasycladale algae: Palaeodasycladus mediterraneus.		Early Jurassic (Sinemurian-Pliensbachian)	Perdido Group	Gondwana Megasequence	18/11

Location_No	Lat	Long	Region	Sample_type	Field_Description	Rock_Description	Benthic_foraminifera	Planktonic_foraminifera	OtherBioclasts	Facies	Age	Group	Megasequence	Date
9_11_08_21	-8.73994	126.36397	Mundo Perdido	limestone		Wackestone with rare thaumatoporellacean algae. Breccia with clasts of wackestone and peloidal grainstone with rare carbonate-cemented agglutinated foraminifera.	Siphovalvulina variabilis.		Thaumatoporellacean algae: Thaumatoporella ?parvovesiculifera		Early Jurassic	Perdido Group	Gondwana Megasequence	19/11
AB001	-8.69940	126.33767	Mundo Perdido	mudstone	synorogenic mudstone	Calcareous mudstone with common benthic foraminifera (Elphidium, Lugdunum, Siphogenerina dominate); common planktonic foraminifera (most <0.5 mm maximum dimension; Globigerinoides, Globorotalia, Neogloboquadrina, Pulleniatina, Sphaeroidinella).	Brizalina, Cibicidoides, Amphistegina	Globorotalia truncatulinoides, Globorotalia tosaensis, Globigerinoides immaturus, Globigerinoides ruber, Neogloboquadrina dutertrei, Pulleniatina obliquiloculata		outer neritic zone	Zone N22r; mid Pleistocene within 2.02–0.63 Ma interval (Keep & Haig 2010, fig. 6)	Viqueque Group - Lari Guti Member	Synorogenic Megasequence	
AB002	-8.69940	126.33767	Mundo Perdido	limestone	synorogenic limestone	Packstone with abundant rotaliid foraminifera (including Amphistegina, Elphidium, Schlumbergerella, Homotrema, Cycloclypeus); very rare planktonic foraminifera (Globigerinoides); echinoid spines, coralline algae,and coral debris	Schlumbergerella				Pleistocene (following range for Schlumbergella) given by Loeblich & Tappan, 1987)	Baucau Limestone	Synorogenic Megasequence	
AB003	-8.70620	126.34752	Mundo Perdido	mudstone	mud with rounded quartz and other lithics, possibly alluvial	Mudstone with abundant planktonic foraminifera (including Globigerinoides, Globorotalia, Neogloboquadrina, Orbulina), and abundant benthic foraminifera (with Rotalinoides, Amphistegina, Elphidium, Heterolepa, Lugdunum, Lenticulina, Hoeglundina most conspicuous). Evidence of some reworking from older Pliocene. Rare high-spired gastropods and delicate echinoid spines also present.	Brizalina, Pseudorotalia, Amphistegina, Baggina, Lenticulina	Globorotalia truncatulinoides, Globorotalia tosaensis, Orbulina universa, Globigerinoides immaturus, Globigerinoides conglobatus, Globigerinoides ruber, Globigerinoides sacculifer, Globorotalia ungulata (sinistral), Globigerinoides extremus, Neogloboquadrina dutertrei, Globigerinoides elongatus		outer neritic zone	Zone N22r; mid Pleistocene within 2.02–0.63 Ma interval (Keep & Haig 2010, fig. 6)	Viqueque Group - Lari Guti Member	Synorogenic Megasequence	
AB004	-8.70552	126.35192	Mundo Perdido	unconsolidated	sand, mud, large rounded lithics	Coarse partly friable calcarenite with very rare benthic foraminifera	Elphidium crispum, Amphistegina sp.				Pleistocene	?Baucau Limestone	?Synorogenic Megasequence	
AB005	-8.72988	126.36760	Mundo Perdido	limestone	Booi limestone	Foraminiferal wackestone. Common benthic foraminifera including "larger" Rotaliida, coralline algae	primitive Lepidocyclina (Nephrolepidina); Spiroclypeus			inner neritic zone	Te Letter Stage; latest Oligocene or Earliest Miocene	Booi Group	Banda Megasequence	
AB006	-8.72922	126.36710	Mundo Perdido	limestone	fossiliferous limestone, very large corals	Limestone conglomerate; clasts with corals, coralline algae; common benthic foraminifera (mainly rotaliids and very rare miliolids), and mollusc fragments; matrix with similar foraminifera plus very rare planktonic foraminifera (indeterminant) and rare larger benthic rotaliids	primitive Lepidocyclina (Nephrolepidina)		Colonial corals	inner neritic zone	Probably Te Letter Stage; probably latest Oligocene or earliest Miocene	Booi Group	Banda Megasequence	
AB007	-8.72917	126.36702	Mundo Perdido	limestone	Booi limestone	Packstone with abundant benthic foraminifera (mainly rotaliids including larger types), coral debris, coralline algae	primitive Lepidocyclina (Nephrolepidina); Spiroclypeus			inner neritic zone	Te Letter Stage; latest Oligocene or earliest Miocene interval	Booi Group	Banda Megasequence	
AB008	-8.73407	126.36667	Mundo Perdido	limestone	Booi limestone	Packstone with abundant benthic foraminifera (mainly larger rotaliids), coral debris, coralline algae.	Spiroclypeus			inner neritic zone	Te Letter Stage; latest Oligocene or earliest Miocene interval	Booi Group	Banda Megasequence	

Location_No	Lat	Long	Region	Sample_type	Field_Description	Rock_Description	Benthic_foraminifera	Planktonic_foraminifera	OtherBioclasts	Facies	Age	Group	Megasequence	Date
AB009	-8.72905	126.36575	Mundo Perdido	limestone	Australian margin pelagite	Wackestone with rare minute hyaline foraminifera (mainly planktonic types)		Poorly preserved globotruncaniids - including Marginotruncana pseudolinneiana or Globotruncana linneiana; Heterohelix sp., Hedbergella sp.		middle bathyal to abyssal	Late Cretaceous	Kolbano Group	Australian Margin Megasequence	
AB010	-8.72887	126.36607	Mundo Perdido	no sample	Booi limestone							Booi Group	Banda Megasequence	
AB011	-8.72915	126.36588	Mundo Perdido	no sample	Booi limestone							Booi Group	Banda Megasequence	
AB012	-8.72908	126.36558	Mundo Perdido	limestone	possible Perdido Limestone	Wackestone, highly fractured with calcite veins, with common thaumatoporellacean algae (including cryptoendoliths), rare prismatic shell fragments of bivalves, and very rare carbonate-cemented agglutinated foraminifera	Siphovalvulina variabilis		Thaumatoporellacean algae: Thaumatoporella ?parvovesiculifera (micritized)	innermost neritic	probably Early Jurassic	Perdido Group	Gondwana Megasequence	
AB013	-8.72908	126.36558	Mundo Perdido	limestone	Possible Australian margin pelagite	Wackestone with rare minute hyaline foraminifera (probably mainly planktonic types); extensively stylolitized		?Hedbergella sp., ?Praeglobotruncana sp., ?Heterohelix sp.		middle bathyal to abyssal	Probably Late Cretaceous (Cenomanian or Turonian)	Kolbano Group	Australian Margin Megasequence	
AB014	-8.72935	126.36570	Mundo Perdido	contact	?Fault							observation point		
AB015	-8.72955	126.36585	Mundo Perdido	limestone	Booi limestone	Wackestone with intraclasts. Intraclasts include packstone containing benthic rotaliid foraminifera (including larger types), coral debris, and coralline alga. Matrix of minute rod-shaped particles	Lepidocyclina (Nephrolepidina), Spiroclypeus			inner neritic zone	Intraclasts belong to Te Letter Stage, latest Oligocene or earliest Miocene	Booi Group	Banda Megasequence	
AB016	-8.72965	126.36592	Mundo Perdido	limestone	Perdido Limestone	Ooid grainstone with rare carbonate-cemented agglutinated foraminifera	Siphovalvulina variabilis			innermost neritic zone	probably Early Jurassic	Perdido Group	Gondwana Megasequence	
AB017	-8.72988	126.36620	Mundo Perdido	no sample	Perdido Limestone							Perdido Group	Gondwana Megasequence	
AB018	-8.72995	126.36607	Mundo Perdido	volcanic	Melange zone	Clasts are very weathered mafic volcanics and mafic volcanic Breccia						Melange zone	Melange zone	
AB019	-8.73077	126.36668	Mundo Perdido	no sample	Perdido Limestone							Perdido Group	Gondwana Megasequence	
AB020	-8.73067	126.36698	Mundo Perdido	no sample	Fault	Fault zone containing large competent blocks of Booi Limestone >50 m in size						Booi Group	Banda Megasequence	
AB021	-8.73068	126.36723	Mundo Perdido	limestone	Perdido Limestone	Wackestone with common dasycladale algae with cryptoendolithic thaumatoporellacean algae; very rare carbonate-cemented agglutinated foraminifera	Siphovalvulina variabilis		Dasycladale algae: Palaeodasycladus mediterraneus. Thaumatoporellacean algae: Thaumatoporella ?parvovesiculifera (micritized)	innermost neritic zone	Early Jurassic	Perdido Group	Gondwana Megasequence	
AB022	-8.73057	126.36700	Mundo Perdido	mudstone	Banda mudstone?	Mudstone with abundant planktonic foraminifera (Globigerina, Globorotalia, Globigerinoides, Globoquadrina, Catapsydrax) and rare benthic foraminifera (mainly Order Buliminida)		Globoquadrina binaiensis, Globoquadrina dehiscens (very rare), Globoquadrina venezuelana, Globigerina praebulloides, Globigerinoides primordius, Globigerina ciperoenis, Globorotalia kugleri		upper bathyal	Zone N4b (Kennett & Srinivasan 1983); earliest Miocene	Booi Group	Banda Megasequence	

Location_No	Lat	Long	Region	Sample_type	Field_Description	Rock_Description	Benthic_foraminifera	Planktonic_foraminifera	OtherBioclasts	Facies	Age	Group	Megasequence	Date
AB023	-8.73057	126.36700	Mundo Perdido	breccia	limestone breccia	Breccia with clasts including wackestone with corals, coralline algae and benthic rotaliid foraminifera (including larger types); and wackestone with abundant small planktonic foraminifera.	(1) Spiroclypeus margaritatus, primitive Lepidocyclina (Nephrolepidina) sp.	(2) Globigerina praebulloides – Globigerinoides primordius, Globorotalia kugleri	Coral debris, corraline algae	(1) inner neritic zone. (2) outer neritic	(1) Te Letter Stage; latest Oligocene or earliest Miocene; (2) Zone 4, latest Oligocene or earliest Miocene	Booi Group	Banda Megasequence	
AB024	-8.73085	126.36747	Mundo Perdido	no sample	Perdido Limestone			Lepidocyclina (Nephrolepidina) sp.				Perdido Group	Gondwana Megasequence	
AB025	-8.73027	126.36768	Mundo Perdido	mudstone	grey mudstone	Barren residue					Unknown	Unknown	Unknown	
AB026	-8.73023	126.36860	Mundo Perdido	contact	?Fault							observation point		
AB027	-8.75798	126.32160	Mundo Perdido	limestone	Australian margin pelagite	Wackestone with rare planktonic foraminifera (mainly minute low trochospiral forms with spherical chambers); very rare benthic foraminifera (?Dorothia and trochospiral Rotaliida)		Hedbergella/Blefuscuiana spp.		middle bathyal to abyssal	Late Early Cretaceous (probably Aptian-Albian, based on absence of keeled planktonics)	Kolbano Group	Australian Margin Megasequence	
AB028	-8.75582	126.31635	Mundo Perdido	limestone	well bedded, fossiliferous, muddy layers, possible synorogenic	Oncoidal, cortoidal, gastrpodal grainstone with some cryptoendolithic thaumatoporellacean algae			Gastropods, chambered sponges, Thaumatoporellacean algae	innermost neritic zone	Probably Early Jurassic based on presence of these forms in "bahaman facies" elsewhere in Timor	Perdido Group	Gondwana Megasequence	
AB029	-8.74305	126.29315	Mundo Perdido	limestone	Booi limestone	Wackestone with common benthic foraminifera (including larger rotaliids), very rare small planktonics (Globigerina or Globigerinoides), coral debris, coralline algae	Spiroclypeus, primitive Lepidocyclina (Nephrolepidina)			mid neritic	Te Letter Stage; latest Oligocene to earliest Miocene	Booi Group	Banda Megasequence	
AB030	-8.75665	126.32555	Mundo Perdido	limestone	possible Perdido	Peloidal-ooid grainstone and wackestone with thaumatoporellacean algae, rare punctate brachiopod shell debris, very rare ostracods, very rare carbonate-cemented agglutinated foraminifera	? Siphovalvulina variabilis		Thaumatoporellacean algae: Thaumatoporella ?parvovesiculifera	innermost neritic	Early Jurassic	Perdido Group	Gondwana Megasequence	
AB031	-8.75650	126.32983	Mundo Perdido	limestone	possible Perdido							?Perdido Group	?Gondwana Megasequence	
AB032	-8.72405	126.36732	Mundo Perdido	conglomerate	possible Booi beds	Packstone-wackestone with coral debris, benthic foraminifera (including larger rotaliids), rare small planktonic foraminifera, coralline algae	Spiroclypeus, primitive Lepidocyclina (Nephrolepidina)			mid neritic	Te Letter Stage; within the latest Oligocene to Earliest Miocene interval	Booi Group	Banda Megasequence	
AB033	-8.72405	126.36732	Mundo Perdido	conglomerate	possible Booi beds	Conglomerate with clasts of foraminiferal coral packstone-wackestone in mud matrix; common benthic foraminifera (mainly Rotaliida including larger types), rare planktonic foraminfiera in clasts, abundant in mud matrix	primitive Lepidocyclina (Nephrolepidina), Eulepidina, Spiroclypeus	Globigerinoides primordius		mid neritic	Te Letter Stage; Zone N4 or N5 (Kennett & Srinivasan 1983); latest Oligocene or earliest Miocene	Booi Group	Banda Megasequence	
AB034	-8.72405	126.36732	Mundo Perdido	limestone	possible Booi beds	Foraminiferal packstone with abundant benthic foraminifera (mainly Rotaliida including larger types); patches of finer-grained packstone with darker matrix and common small planktonic foraminifera; coralline algae present	Eulepidina, primitive Lepidocyclina (Nephrolepidina), Spiroclypeus	Globigerina praebulloides – Globigerinoides primordius Globigerina gr. ciperoensis		outer neritic zone	Te Letter Stage; within the latest Oligocene to Earliest Miocene interval	Booi Group	Banda Megasequence	
AB035	-8.72405	126.36732	Mundo Perdido	limestone	possible Booi beds	Clast: packstone with very abundant planktonic foraminifera and fragmented rotaliid foraminifera	Cycloclypeus (small fragments)	Globigerina praebulloides – Globigerinoides primordius Globoquadrina binaiensis Globoquadrina venezuelana Dentoglobigerina altispira Globigerina gr. Ciperoensis		upper bathyal	Within the interval of Zones P22 - N5 (Kennett & Srinivasan 1983); late Oligocene -earliest Miocene	Booi Group	Banda Megasequence	

Location_No	Lat	Long	Region	Sample_type	Field_Description	Rock_Description	Benthic_foraminifera	Planktonic_foraminifera	OtherBioclasts	Facies	Age	Group	Megasequence	Date
AB036	-8.72405	126.36732	Mundo Perdido	mudstone	possible Booi beds	Mudstone with abundant planktonic foraminfiera and rare benthic foraminfiera (mainly Order Buliminida)	Nodosaria sp.	Globoquadrina venezuelana, Globigerinoides primordius, Globigerina praebulloides, Globorotalia kugleri		upper bathyal	Zone N4 (Kennett & Srinivasan 1983); latest Oligocene or earliest Miocene	Booi Group	Banda Megasequence	
AB037	-8.72405	126.36732	Mundo Perdido	limestone	possible Booi beds	Packstone with abundant planktonic foraminifera and benthic foraminifera (mostly rotaliids including larger types and mostly fragmented)	Lepidocyclina (Nephrolepidina) sp.	Globigerina praebulloides – Globigerinoides primordius Globoquadrina binaiensis Globoquadrina venezuelana Dentoglobigerina altispira ? Globorotalia kugleri Globigerina gr. Ciperoensis		outer neritic or upper bathyal	Within the interval of Zones P22 - N5 (Kennett & Srinivasan 1983); late Oligocene -earliest Miocene	Booi Group	Banda Megasequence	
AB038	-8.72405	126.36732	Mundo Perdido	limestone	possible Booi beds	Packstone with abundant planktonic foraminifera and benthic foraminifera (mostly rotaliids including larger types and mostly fragmented)	small hyaline morphotypes including probable Cibicides sp. ? fragment of Cycloclypeus sp.	Globigerina gr. ciperoensis Globigerina praebulloides – Globigerinoides primordius Globorotalia kugleri Globoquadrina binaiensis Dentoglobigerina sp.		outer neritic or upper bathyal	Zone N4 (Kennett & Srinivasan 1983); latest Oligocene or earliest Miocene	Booi Group	Banda Megasequence	
AB039	-8.72405	126.36732	Mundo Perdido	limestone	possible Booi beds	Packstone with abundant benthic foraminifera (mostly Rotaliida including larger types), abundant coral debris, coralline algae, echinoderm debris.	?Eulepidina, primitive Lepidocyclina (Nephrolepidina), Spiroclypeus, Miogypsinoides			inner neritic	Te Letter Stage; latest Oligocene or earliest Miocene interval	Booi Group	Banda Megasequence	
AB040	-8.72437	126.36618	Mundo Perdido	no sample	Graded beds of mudstone within limestone							Booi Group	Banda Megasequence	
AB041	-8.72510	126.36570	Mundo Perdido	limestone	Booi limestone	Stylobreccia with clasts of packstone containing coral debris, common benthic foraminifera (mostly rotaliids including larger types), common coralline algae, rare planktonic foraminifera	primitive Lepidocyclina (Nephrolepidina), Spiroclypeus			neritic	Larger benthic foraminiferal Upper Te Letter Stage (Adams, 1970); latest Oligocene or earliest Miocene interval	Booi Group	Banda Megasequence	
AB042	-8.72582	126.36532	Mundo Perdido	limestone	Perdido Limestone	Stylobreccia with clasts of wackestone and peloidal grainstone; rare thaumatoporellacean algae in wackestone			Thaumatoporellacean algae	innermost neritic	Clasts are probably Early Jurassic	Perdido Group	Gondwana Megasequence	
AB043	-8.72507	126.36538	Mundo Perdido	breccia	possible Perdido	Stylobreccia with clasts of wackestone, grainstone including skeletal and ooid-peloidal grainstone. Wackestone contains scattered mollusc fragments and rare thaumatoporellacean algae. Grainstone contains rare carbonate-cemented agglutinated foraminifera.	?Siphovalvulina variabilis, Gaudryina sp.		Thaumatoporellacean algae: Thaumatoporella ?parvovesiculifera (micritized)	innermost neritic	Clasts are probably Early Jurassic	Perdido Group	Gondwana Megasequence	
AB044	-8.72433	126.36480	Mundo Perdido	no sample	Perdido Limestone							Perdido Group	Gondwana Megasequence	
AB045	-8.72455	126.36432	Mundo Perdido	limestone	Possible Australian margin pelagite	Wackestone with patches of ooid grainstone (? burrow infills), with rare thaumatoporellacean algae, rare carbonate-cemented agglutinated foraminifera	Calcite-cemented agglutinated foraminifera: Duotaxis metula, Meandrovoluta asiagoensi, Siphovalvulina variabilis		Thaumatoporellacean algae: Thaumatoporella ?parvovesiculifera (micritized); Chambered sponges	innermost neritic	Early Jurassic (probably Pleinsbachian)	Perdido Group	Gondwana Megasequence	

Location_No	Lat	Long	Region	Sample_type	Field_Description	Rock_Description	Benthic_foraminifera	Planktonic_foraminifera	OtherBioclasts	Facies	Age	Group	Megasequence	Date
AB046	-8.72423	126.36390	Mundo Perdido	no sample	Perdido Limestone							Perdido Group	Gondwana Megasequence	
AB047	-8.72433	126.36338	Mundo Perdido	limestone	possible Perdido	Wackestone with common mollusc fragments, rare ostracods (with valves intact), rare echinoid spines; very rare carbonate-cemented agglutinated foraminifera	? Siphovalvulina sp.			innermost neritic	Probably Early Jurassic	Perdido Group	Gondwana Megasequence	
AB048	-8.72323	126.36617	Mundo Perdido	no sample	Booi beds							Booi Group	Banda Megasequence	
AB049	-8.71155	126.36420	Mundo Perdido	fault gouge	fault rock				Rare chambered sponges		Probably Late Triassic or Early Jurassic	Perdido Group	Gondwana Megasequence	
AB050	-8.71187	126.36250	Mundo Perdido	mudstone	grey mudstone	Barren of forams, much woody material, mica and fragmented megaspores					Unknown	Unknown	Unknown	
AB051	-8.71187	126.36250	Mundo Perdido	sandstone	well bedded sandstone within grey mudstone	fg sandstone, small flecks of mica and organic particles, no fossils visible					Unknown	Unknown	Unknown	
AB052	-8.71308	126.36295	Mundo Perdido	limestone	Perdido Limestone							Perdido Group	Gondwana Megasequence	
AB053	-8.71387	126.36173	Mundo Perdido	limestone	pink, sandy fissile rock, very weathered	Red wackestone with scattered rare deformed planktonic foraminifera. Clast in conglomerate.		Deformed foraminifera appear to be large Globigerina spp. of Globigerina yeguaensis-Globigerina pseudovenezuelana-Globigerina venezuelana type		middle bathyal to abyssal	Probably Late Eocene or Oligocene	Kolbano Group	Australian Margin Megasequence	
AB054	-8.71455	126.35953	Mundo Perdido	limestone	Perdido Limestone	Ooid grainstone with rare carbonate-cemented agglutinated foraminifera, very rare nodosariid foraminifera , very rare thaumatoporellacean algae	Duotaxis sp., ? Siphovalvulina sp.			innermost neritic	Late Triassic or Early Jurassic	Perdido Group	Gondwana Megasequence	
AB055	-8.71455	126.35953	Mundo Perdido	breccia	many angular clasts and recrystallised calcite and qtz	Calcite cemented breccia, angular clasts 1-5mm, not stylotised, unable to determin nature of clasts with peel. In TS angular clasts are consist entirely of quartz and calcite.					Unknown	Unknown	Unknown	
AB056	-8.71455	126.35953	Mundo Perdido	limestone	grey clast within AB055	Pale grey wackestone with very rare nodosariid foraminifera (incuding Dentalina sp, Lenticulina sp..) and in some layers common mollusc-shell "filaments"	nodosariids	"Molluscan "filaments" probably derived from the very small pelagic stages of bivalves (see Flugel 2004, p. 524-528)		probably outer neritic or upper bathyal	Probably Late Triassic (based on similar fossil association in conodont-dated wackestones elsewhere in Timor)	Aitutu Group	Gondwana Megasequence	
AB057	-8.71427	126.35915	Mundo Perdido	conglomerate	angular clasts of limestone, qtz and lithics	Extensively brecciated and recystallised, no internal structure or fossils visible in clasts, no identifiable biogenic grains. Completely recrystallised in TS also. Quartz/calcite breccia, no biogenic grains visible.					Unknown	Unknown	Unknown	
AB058	-8.71402	126.35887	Mundo Perdido	sandstone	deformed and broken indurated sandstone	fg sandstone, some faint traces of forams visible?			Radiolaria Indeterminate spicules		Probably Late Triassic (lithofacies correlation)	?Aitutu Group	Gondwana Megasequence	
AB059	-8.71403	126.35887	Mundo Perdido	limestone	foliated limestone	Wackestone with rare planktonic foraminifera		Globigerina yeguaensis-Globigerina pseudovenezuelana-Globigerina venezuelana lineage dominant		middle bathyal to abyssal	Probably Early to Middle Oligocene (see Bolli and Saunders 1985)	Kolbano Group	Australian Margin Megasequence	
AB060	-8.71403	126.35887	Mundo Perdido	mudstone	veins of mudstone squeezed up around sandstone blocks	Barren residue					Unknown	Unknown	Unknown	
AB061	-8.70895	126.36067	Mundo Perdido	sandstone	Fine grained sandstone	Planktonic foraminiferal packstone with very rare smaller benthic foraminifera (Rotaliida)		Hantkenina sp., Globigerinatheka sp., Morozovelloides sp. Acarinina spp.		bathyal	Middle Eocene	Un-named Eocene Banda	?Banda Megasequence	

Location_No	Lat	Long	Region	Sample_type	Field_Description	Rock_Description	Benthic_foraminifera	Planktonic_foraminifera	OtherBioclasts	Facies	Age	Group	Megasequence	Date
AB062	-8.71132	126.35397	Mundo Perdido	limestone	Australian margin pelagite	Wackestone with scattered planktonic foraminifera		Dicarinella spp. (including morphotypes with convex spiral sides similar to D. imbricata)		middle bathyal to abyssal	Late Cretaceous (Turonian)	Kolbano Group	Australian Margin Megasequence	
AB063	-8.71260	126.35402	Mundo Perdido	limestone	Australian margin pelagite	Fine grained foliated carbonate rock, no forams visible in peel						Kolbano Group	Australian Margin Megasequence	
AB064	-8.71302	126.35377	Mundo Perdido	limestone	Perdido Limestone	Wackestone with scattered mollusc (bivalve) fragments, rare thaumatoporellacean algae, rare echinoiderm plate debris			Thaumatoporellacean algae: Thaumatoporella ?parvovesiculifera (micritized)	innerm ost neritic	Probably Early Jurassic	Perdido Group	Gondwana Megasequence	
AB065	-8.71472	126.35222	Mundo Perdido	conglomerate	Breccia within a huge linear feature that cuts across the whole landscape	Possible gully fill conglomerate? One small clast is a planktonic foraminiferal wackestone. The forams are indistinct but seem to be Cenozoic rather than Cretaceous types (perhaps Oligocene?) Another clast is a wackestone with ?calcispheres or radiolaria and seems similar to Late Triassic Aitutu Formation limestones. Definite ooid rich Perdido Limestone in here also		Globigerina yeguaensis-Globigerina pseudovenezuelana-Globigerina venezuelana lineage dominant		middle bathyal to abyssal	Oligocene	Kolbano Group	Australian Margin Megasequence	
AB066	-8.71552	126.35255	Mundo Perdido	limestone	possible Perdido?	Wackestone with scattered planktonic forams (mostly fragments)						Kolbano Group	Australian Margin Megasequence	
AB067	-8.73167	126.36757	Mundo Perdido	no sample	Booi limestone							Booi Group	Banda Megasequence	
AB068	-8.73183	126.36762	Mundo Perdido	limestone	Booi limestone	Packstone/wackestone with abundant benthic foraminifera (mainly Rotallida including larger types); abundant coralline algae; rock is highly fractured	primitive Lepidocyclina (Nephrolepidina); Spiroclypeus			inner neritic	Larger benthic foraminiferal Upper Te Letter Stage (Adams, 1970); latest Oligocene or earliest Miocene	Booi Group	Banda Megasequence	
AB069	-8.73190	126.36750	Mundo Perdido	limestone	possibly Booi limestone	Packstone/wackestone with rare benthic foraminifera (mainly Rotaliida including larger types); common coralline algae; coral; mollusc fragments; rock is highly fractured	Primitive Lepidocyclina (Nephrolepidina) sp. Homotrema sp. Spiroclypeus		Coralline algae Mollusc debris	inner neritic	Larger benthic foraminiferal Upper Te Letter Stage (Adams, 1970); latest Oligocene - earliest Miocene	Booi Group	Banda Megasequence	
AB070	-8.73233	126.36743	Mundo Perdido	breccia	very poorly sorted, clasts 10mm - 1m	Poorly sorted conglomerate, clasts are packstone or wackestone with scattered benthic foraminifera (mainly Rotaliida including larger types), coral debris, coralline algae, mollusc fragments	primitive Lepidocyclina (Nephrolepidina); Spiroclypeus			inner neritic	Larger benthic foraminiferal Upper Te Letter Stage (Adams, 1970); latest Oligocene - earliest Miocene	Booi Group	Banda Megasequence	
AB071	-8.73253	126.36660	Mundo Perdido	no sample	Perdido Limestone							Perdido Group	Gondwana Megasequence	
AB072	-8.73418	126.36570	Mundo Perdido	sandstone	grey sandstone, possibly Banda Terrane	Barren peel, nothing visible but fg qtz, no identifiable biogenic grains					Unknown	Unknown	Unknown	
AB073	-8.73465	126.36282	Mundo Perdido	no sample	Perdido Limestone							Perdido Group	Gondwana Megasequence	
AB074	-8.73027	126.36768	Mundo Perdido	unknown	clast within red mudstone	vfg, peel is not enlightening... No identifiable biogenic grains observed					Unknown	Unknown	Unknown	
AB075	-8.73027	126.36768	Mundo Perdido	mudstone	red mudstone	Red mudstone with poorly preserved deformed planktonic foraminifera (Globigerina, Globoquadrina)		Globigerina ciperoensis; Globoquadrina sp. (?ancestral to G. dehiscens), ?Globigerinatheka, ?Globoquadrina venezuelana, ?Globigerina praebulloides, ?Globigerinoides primordius		bathyal	Latest Oligocene or earliest Miocene	Booi Group	Banda Megasequence	
AB076	-8.73027	126.36768	Mundo Perdido	mudstone	grey mudstone	Barren residue					Unknown	Unknown	Unknown	

Location_No	Lat	Long	Region	Sample_type	Field_Description	Rock_Description	Benthic_foraminifera	Planktonic_foraminifera	OtherBioclasts	Facies	Age	Group	Megasequence	Date
AB077	-8.73057	126.36700	Mundo Perdido	mudstone	grey mudstone	Mudstone with abundant planktonic foraminifera (Globigerina, Globorotalia); rare bethonic smaller foraminifera (mostly Buliminida)		Globoquadrina venezuelana, Globigerina praebulloides, Globigerinoides primordius, Globigerina ciperoenis, Globorotalia kugleri		upper bathyal	N4 planktonic foraminifera zone (Kennett & Srinivasan, 1983); earliest Miocene	Booi Group	Banda Megasequence	
AB078	-8.72995	126.36607	Mundo Perdido	conglomerate	range of different clasts in a mud matrix	Clast appears to be composed entirely of recrystallised calcite?					Unknown	Unknown	Unknown	
AB079	-8.73057	126.36700	Mundo Perdido	breccia	limestone stylobreccia	Breccia (clast-supported) composed of limestone clasts with a mud matrix. Clasts are packstone/wackestone with benthic foraminifera (mainly Rotaliida including larger types), coral debirs, coralline algae, and very rare minute planktonic foraminifera. Mud matrix has scattered minute planktonic foraminifera	Eulepidina sp., Spiroclypeus margaritatus, primitive Lepidocyclina (Nephrolepidina) sp.	some small planktics in matrix ?Globigerinoides primordius	Coral debris, corraline algae	mid neritic	Larger benthic foraminiferal Upper Te Letter Stage (Adams, 1970); latest Oligocene - earliest Miocene; all clasts appear coeval. Matrix is similar age	Booi Group	Banda Megasequence	
AB079B	-8.73057	126.36700	Mundo Perdido	breccia	limestone stylobreccia	Coral/coralline algal limestone (?framestone) with packstone/wackestone matrix containing scattered benthic foraminifera (mainly Rotaliida including larger types) and fragmented coralline algae	Lepidocyclina (Eulepidina) sp. Spiroclypeus margaritatus, Lepidocyclina (Nephrolepidina) sp.	some small planktics	Coral debris, corraline algae	inner neritic	Larger benthic foraminiferal Upper Te Letter Stage (Adams, 1970); latest Oligocene - earliest Miocene	Booi Group	Banda Megasequence	
AB080	-8.73057	126.36700	Mundo Perdido	conglomerate	limestone clasts in a mud matrix, possible gully fill	Clast-supported conglomerate containing clasts of packstone containing benthic foraminifera (mainly Rotaliida including larger types), common fragmented coralline algae; very rare minute planktonic foraminifer. Matrix of mudstone with rare minute planktonic foraminifera	Eulepidina, primitive Lepidocyclina (Nephrolepidina), Spiroclypeus	Globigerinoides primordius		mid neritic	Larger benthic foraminiferal Upper Te Letter Stage (Adams, 1970); latest Oligocene - earliest Miocene; all clasts appear coeval. Matrix is of similar age	Booi Group	Banda Megasequence	
AB081			Mundo Perdido	mudstone	mudstone	Mudstone with abundant planktonic foraminifera (Globorotalia, Globigerinoides, Pulleniatina, Neogloboquadrina, Globigerinella, Globigerina) and benthic smaller foraminifera (with Lugdunum, Siphogenerina, Lenticulina, Heterolepa, Rotalinoides, Elphidium, Amphistegina conspicuous); planktonic:benthic = 50%	Heterolepa spp., Lenticulina spp., Siphogenerina spp., Brizalina spp., Pseudorotalia	Globorotalia truncatulinoides, Globorotalia tosaensis, Globorotalia menardii, Globorotalia ungulata, Orbulina universa, Neogloboquadrina dutertrei, Globigerinoides ruber, Globigerinoides quadrilobatus		outer neritic zone	Planktonic foraminiferal Zone N22r; mid Pleistocene within 2.02–0.63 Ma interval (Keep & Haig 2010, fig. 6)	Baucau Limestone	Synorogenic Megasequence	
AB082	-8.70895	126.36067	Mundo Perdido	mudstone	red mud from large block in melange	Red mudstone with abundant planktonic foraminifera (including Hantkenina, Globigerinidae, Morozovelloides, Turborotalia, Globigerinatheka); very rare benthic foraminifera (mainly smaller Rotaliida)		Hantkenina compressa, Morozovelloides crassatus, Turborotalia cerroazulensis		bathyal zone	Within interval E11 to E13; late Middle Eocene (Berggren & Pearson et al., 2006)	Un-named Eocene Banda	?Banda Megasequence	
AB083	-8.70895	126.36067	Mundo Perdido	sandstone	sandstone from large block in melange	Planktonic foraminiferal packstone with very rare smaller benthic foraminifera (Rotaliida)		Morozovella spp. or Morozovelloides spp., Acarinina spp.		bathyal zone	Early or Middle Eocene	Un-named Eocene Banda	?Banda Megasequence	
AB084	-8.70888	126.36030	Mundo Perdido	mudstone	lithified grey mudstone	Mudstone with abundant planktonic foraminifera and rare benthic foraminfiera (including Oridorsalis, Bolivinita)		Globorotalia tosaensis, Sphaeroidinella dehsicens, Pulleniatina obliquiloculata (dextral)		bathyal	Planktonic foraminiferal Zone N21, 3.10-2.02 Ma (Keep & Haig 2010)	Viqueque Group	Synorogenic Megasequence	

Location_No	Lat	Long	Region	Sample_type	Field_Description	Rock_Description	Benthic_foraminifera	Planktonic_foraminifera	OtherBioclasts	Facies	Age	Group	Megasequence	Date
AB085	-8.70888	126.36030	Mundo Perdido	mudstone	grey mudstone	Mudstone with abundant planktonic foraminifera (Globigerinoides, Globorotalia, Pulleniatina, Orbulina, Neogloboquadrina) and rare benthic foraminifera (including Oridorsalis),	Uverigina hispida, Bolivinita quadrilatera	Globorotalia tosaensis, Sphaeroidinella dehsicens, , Globigerinoides pistulosus, Globorotalia tumida (sinistral), Pulleniatina praecursos (sinistral), Globigerinoides elongatus, Globigerinoides ruber, Globigerinoides immaturus, Globigerinoides quadrilobatus, Globigerinoides sacculifer, Orbulina universa, Neogloboquadrina humerosa		bathyal zone	N21; Late Pliocene	Viqueque Group	Synorogenic Megasequence	
AB086	-8.70888	126.36030	Mundo Perdido	mudstone	grey mudstone							Babulu Group	Gondwana Megasequence	
AB087	-8.73437	126.36850	Mundo Perdido	limestone	Perdido Limestone	Stylobreccia with clasts of wackestone and rare ooid grainstone; wackestone with scattered thaumatoporellacean algae and very rare carbonare-cemented agglutinated foraminifera; grainstone with rare carbonate-cemented agglutinated foraminifera	Wackstone: Siphovalvulina variabilis. Grainstone: Siphovalvulina sp.		Wackstone: Thaumatoporella ?parvovesiculifera (micritized)	innermost neritic	Early Jurassic	Perdido Group	Gondwana Megasequence	
AB088	-8.73515	126.37217	Mundo Perdido	mudstone	grey mudstone	Mudstone with well preserved palynomorphs (pollen, spores, dinocysts, acritarchs, prasinophyte algae)			Pollen: Minutosaccus crenulatus, Corollina meyeriana, Enzonalaporites vigens, Samaropollenites speciosus, Rimaesporites aquilonalis. Spores: Cycadopites stonei, Leptolepidites argentaeaformis. Dinocysts: Wanneria listeri, Suessia swabiana, Rhaetogonyaulax wigginsii	shallow-marine	Probably lowest Minutosaccus crenulatus Zone; Late Triassic (probably Norian); (Palynomorph determinations and zonation by Matthew Dixon, pers. com. October 2009)	Babulu Group	Gondwana Megasequence	
AB089	-8.73515	126.37217	Mundo Perdido	sandstone	fine grained sandstone	Fine grained sandstone with abundant woody fragments						Babulu Group	Gondwana Megasequence	
AB090	-8.73470	126.37368	Mundo Perdido	limestone	Booi limestone	Packstone consisting of densely packed highly fragmented skeletal debris and scattered planktonic foraminifera (including Globigerinoides) and benthic foraminifera (mainly Rotaliida including larger types) with mud matrix	primitive Lepidocyclina (Nephrolepidina) sp. Cycloclypeus sp. Spiroclypeus sp.	Globigerinoides primordius – Globigerina praebulloides			Larger benthic foraminiferal Upper Te Letter Stage (Adams, 1970); latest Oligocene - earliest Miocene	Booi Group	Banda Megasequence	
AB091	-8.73412	126.37458	Mundo Perdido	no sample	Booi limestone							Booi Group	Banda Megasequence	
AB092	-8.73307	126.37547	Mundo Perdido	no sample	Booi limestone							Booi Group	Banda Megasequence	
AB093	-8.73300	126.37590	Mundo Perdido	volcanic	mafic volcanic	50% plag laths up to 10 mm, 25% interstitial opx and cpx, 25% volcanic glass. Finer grained areas, possibly due to volatile exsolution? Dolerite						Barique Group	Banda Megasequence	
AB094	-8.73568	126.37418	Mundo Perdido	no sample	mafic volcanics within melange							Melange zone	Melange zone	

Location_No	Lat	Long	Region	Sample_type	Field_Description	Rock_Description	Benthic_foraminifera	Planktonic_foraminifera	OtherBioclasts	Facies	Age	Group	Megasequence	Date
AB095	-8.73407	126.37292	Mundo Perdido	limestone	Booi limestone	Wackestone with common coral and encrusting coralline algal debris and benthic foraminifera (mainly Rotaliida including larger types)	primitive Lepidocyclina (Nephrolepidina), Spiroclypeus; indeterminate acervulinids		Coral (forming most of peel)		Larger benthic foraminiferal Larger benthic foraminiferal Upper Te Letter Stage (Adams, 1970); latest Oligocene - earliest Miocene	Booi Group	Banda Megasequence	
AB096	-8.73307	126.37547	Mundo Perdido	no sample	Booi limestone							Booi Group	Banda Megasequence	
AB097	-8.73192	126.37717	Mundo Perdido	no sample	Fault							Booi Group	Banda Megasequence	
AB098	-8.73202	126.37807	Mundo Perdido	mudstone	grey mudstone	Barren residue					Unknown	Unknown	Unknown	
AB099	-8.73210	126.37843	Mundo Perdido	no sample	Booi limestone							Booi Group	Banda Megasequence	
AB100	-8.72933	126.37912	Mundo Perdido	no sample	Booi limestone							Booi Group	Banda Megasequence	
AB101	-8.72967	126.38015	Mundo Perdido	mudstone	mudstone	Mudstone with common planktonic foraminifera (Dentoglobigerina, Globigerinoides, Globigerina), and very poorly preserved (recrystallized) benthic foraminifera (Rotaliida and Buliminida)	?Miogypsina, ?Lepidocyclina	Globigerinoides altiaperatura, Globigerinoides subquadratus, Globigerinoides triloba, Globigerinoides sicanus, Dentoglobigerinoides altispira		outer neritic or upper bathyal	Planktonic foraminifera zone N5 or N6 (Kennett & Srinivasan, 1983); Early Miocene	Booi Group	Banda Megasequence	
AB102	-8.72967	126.38015	Mundo Perdido	unknown	clast within mudstone						Unknown	Unknown	Unknown	
AB103	-8.72970	126.38083	Mundo Perdido	no sample	grey mudstone - Babulu Formation							Babulu Group	Gondwana Megasequence	
AB104	-8.72970	126.38085	Mundo Perdido	contact	Fault							observation point		
AB105A	-8.72940	126.38247	Mundo Perdido	breccia	Limestone breccia on fault at AB105: clast type A	(A) Breccia containing wackestone, packstone and grainstone with benthic foraminifera (carbonate-cemented agglutinated types), common thaumatoporellacean algae, rare dasycladale algae	(A) Siphovalvulina variabilis, Meandrovoluta asiagoensis.		(A) Thaumatoporellacean algae: Thaumatoporella ?parvovesiculifera.	(A) innermost neritic.	(A) Early Jurassic, Sinemurian-Pliensbachian (Haig et al., 2007)	Perdido Group	Gondwana Megasequence	
AB105B	-8.72940	126.38247	Mundo Perdido	breccia	Limestone breccia on fault at AB105: clast type B	(B) Packstone with abundant benthonic foraminifera (mostly Rotaliida including larger types)	(B) primitive Lepidocyclina (Nephrolepidina), Spiroclypeus			(B) inner neritic	(B) Larger benthic foraminiferal Upper Te Letter Stage (Adams, 1970); latest Oligocene - earliest Miocene	Booi Group	Banda Megasequence	
AB106	-8.72940	126.38315	Mundo Perdido	mudstone	well bedded mudstone	Barren residue					Unknown	Unknown	Unknown	
AB107	-8.72940	126.38315	Mundo Perdido	mud	grey mud	Barren residue					Unknown	Unknown	Unknown	
AB108	-8.72940	126.38315	Mundo Perdido	mud	red mud	Barren residue					Unknown	Unknown	Unknown	
AB109	-8.72940	126.38315	Mundo Perdido	volcanic	volcanic clasts within melange	Very poor thin section. Brecciated texture. Minor cpx and plag visible.						Melange zone	Melange zone	
AB110	-8.73603	126.37720	Mundo Perdido	clast	volcanic breccia within melange	very weathered and altered. Glass, calcite and minor plag visible. Volcaniclastic						Melange zone	Melange zone	
AB111	-8.73472	126.37782	Mundo Perdido	limestone	Booi limestone	Wackestone with framented bioclasts including coralline algae, benthic foraminfiera (mainly Rotaliida including larger types), echinoderm plates	Foraminifera: Lepidocyclina (Nephrolepidina)			inner neritic	Larger benthic foraminiferal Upper Te Letter Stage (Adams, 1970); latest Oligocene - earliest Miocene	Booi Group	Banda Megasequence	
AB112	-8.73432	126.37838	Mundo Perdido	no sample	Booi limestone							Booi Group	Banda Megasequence	
AB113	-8.73233	126.37917	Mundo Perdido	limestone	Booi limestone	Wackestone with foraminifera (mainly Rotaliida including common larger types), coralline algae and coral debris	Foraminifera: Lepidocyclina (Nephrolepidina)			inner neritic	Larger benthic foraminiferal Upper Te Letter Stage (Adams, 1970); latest Oligocene - earliest Miocene	Booi Group	Banda Megasequence	
AB114	-8.73267	126.38033	Mundo Perdido	no sample	Booi limestone							Booi Group	Banda Megasequence	

Location_No	Lat	Long	Region	Sample_type	Field_Description	Rock_Description	Benthic_foraminifera	Planktonic_foraminifera	OtherBioclasts	Facies	Age	Group	Megasequence	Date
AB115	-8.73253	126.38160	Mundo Perdido	no sample	Booi limestone							Booi Group	Banda Megasequence	
AB116	-8.73170	126.38208	Mundo Perdido	contact	Fault							observation point		
AB117	-8.73252	126.38207	Mundo Perdido	contact	Fault							observation point		
AB118	-8.73450	126.37942	Mundo Perdido	no sample	Booi limestone							Booi Group	Banda Megasequence	
AB119	-8.70182	126.32353	Mundo Perdido	limestone	synorogenic	Porous limestone with common benthic foraminifera (mainly Rotaliida including larger types) and coralline algae	Gypsina sp. Calcarina sp. Schlumbergerella floresiana Operculina sp.		Coralline algae Mollusc fragments	inner neritic	Pleistocene (following range for Schlumbergella given by Loeblich & Tappan, 1987)	Baucau Limestone	Synorogenic Megasequence	
AB120	-8.70477	126.32148	Mundo Perdido	limestone	Perdido Limestone	Wackestone with scattered mollusc (bivalve) fragments, rare thaumatoporellacean algae, rare echinoiderm plate debris, rare carbonate-cemented agglutinated foraminifera	Siphovalvulina sp.., Everticyclammina sp.		Thaumatoporellacean algae: Thaumatoporella? parvovesiculifera	innermost neritic	Early Jurassic	Perdido Group	Gondwana Megasequence	
AB121	-8.70472	126.32058	Mundo Perdido	no sample	Perdido Limestone							Perdido Group	Gondwana Megasequence	
AB122	-8.70505	126.32067	Mundo Perdido	limestone	Australian margin pelagite	Scree: wackestone with very rare planktonic foraminifera (deformed, fragmented) and very rare small benthic foraminifera (Order Rotaliida)		large ?Globigerina sp.		middle bathyal to abyssal	Cenozoic, probaby Late Eocene or Oligocene	Kolbano Group	Australian Margin Megasequence	
AB123	-8.70662	126.32333	Mundo Perdido	no sample	Perdido Limestone							Perdido Group	Gondwana Megasequence	
AB124	-8.70638	126.32377	Mundo Perdido	sandstone	within alluvium	Fine grained sandstone, unable to find anything to determine age	nodosariids (indeterminate)		Radiolaria or calcispheres		Probable Late Triassic or Early Jurassic	?Aitutu Group	Gondwana Megasequence	
AB125	-8.70705	126.32393	Mundo Perdido	volcanic	fine sandstone (?) in a red mud matrix	Most likely an extremely weathered mafic volcanic. Too weathered to analyse properly. Barren residue					Unknown	Unknown	Unknown	
AB126	-8.70705	126.32393	Mundo Perdido	mud	red mud matrix of AB125	Barren residue					Unknown	Unknown	Unknown	
AB127	-8.70728	126.32388	Mundo Perdido	no sample	AM pelagite							Kolbano Group	Australian Margin Megasequence	
AB128	-8.70678	126.32443	Mundo Perdido	limestone	Australian margin pelagite?	Peloid grainstone with rare benthic foraminifera (mainly nodosariids including uniserial types and Lenticulina, and very rare glomospiral miliolids and carbonate-cemented agglutinated types)	Lenticulina sp. Nodosaria sp. Pseudonodoaria sp. Cryptoseptida sp. small indeterminate calcite-cemented agglutinated forams [In second peel: Duotaxis or Siphovalvulina sp.]		Ostracods	Innermost neritic	Benthic foraminiferal assemblage is consistent with a Late Triassic or Early Jurassic age.	Perdido Group	Gondwana Megasequence	
AB129	-8.70757	126.32383	Mundo Perdido	unknown	fine sandstone ?	vfg massive appearance in peel. No bioclasts visible. Possibly more silicified and less weathered sample of AB130						?Perdido Group	?Gondwana Megasequence	
AB130	-8.70757	126.32383	Mundo Perdido	unknown	very porous fine sandstone??	peels and residue contains undetermined ovoid objects. Possibly silicified and very weathered bahaman facies limestone						?Perdido Group	?Gondwana Megasequence	
AB131	-8.70757	126.32383	Mundo Perdido	mud	red/grey mud matrix of AB129 & 130	Barren residue					Unknown	Unknown	Unknown	
AB132	-8.70755	126.32347	Mundo Perdido	limestone	Perdido Limestone	Wackestone, fractured and stylotised, with scattered thaumatoporellacean algae and rare carbonate-cemented agglutinated foraminifera	? Siphovalvulina		Thaumatoporellacean algae: Thaumatoporella ?parvovesiculifera	innermost neritic	Early Jurassic	Perdido Group	Gondwana Megasequence	
AB133	-8.70870	126.32350	Mundo Perdido	unknown	sandstone within red mud	fg radiolarite. Foliated and bioturbated with abundant burrows						?Aitutu Group	?Gondwana Megasequence	
AB134	-8.70622	126.32510	Mundo Perdido	no sample	AM pelagite	possible not in situ						Kolbano Group	Australian Margin Megasequence	

Location_No	Lat	Long	Region	Sample_type	Field_Description	Rock_Description	Benthic_foraminifera	Planktonic_foraminifera	OtherBioclasts	Facies	Age	Group	Megasequence	Date
AB135	-8.70550	126.32648	Mundo Perdido	limestone	very fine grained friable porous calcareous sandstone	Friable calcarenite with common benthic foraminifera (Rotaliida and Textulariida)	Calcarina spengleri, Clavulina pacifica, Textularia sp., Calcarinid, Elphidium		echinoid spines, ostracods	innermost neritic	Pleistocene	Baucau Limestone	Synorogenic Megasequence	
AB136	-8.70510	126.32660	Mundo Perdido	limestone	synorogenic	Very porous, fossiliferous limestone with coral fragments, benthic foraminifera (Rotaliida), mollusc fragments, echinoid spines	Neorotalia, Elphidium				Pleistocene	Baucau Limestone	Synorogenic Megasequence	
AB137	-8.70170	126.32708	Mundo Perdido	no sample	Baucau Limestone							Baucau Limestone	Synorogenic Megasequence	
AB138	-8.70450	126.32688	Mundo Perdido	limestone	synorogenic	Very porous, fossiliferous limestone with coralline algae and benthic foraminifera (mainly Rotaliida, including larger types)	Schlumbergerella				Pleistocene (following range for Schlumbergella given by Loeblich & Tappan, 1987)	Baucau Limestone	Synorogenic Megasequence	
AB138A	-8.70450	126.32688	Mundo Perdido	coral	within AB138						Unknown	Unknown	Unknown	
AB139	-8.71062	126.32138	Mundo Perdido	no sample	AM pelagite	possibly not in situ						Kolbano Group	Australian Margin Megasequence	
AB140	-8.71093	126.32032	Mundo Perdido	no sample	AM pelagite	possibly not in situ						Kolbano Group	Australian Margin Megasequence	
AB141	-8.71150	126.31977	Mundo Perdido	no sample	Perdido Limestone							Perdido Group	Gondwana Megasequence	
AB142	-8.71200	126.31988	Mundo Perdido	limestone	Perdido Limestone	Ooid grainstone with very rare carbonate-cemented agglutinated foraminifera, very rare dasycladale algae	Siphovalvulina variabilis. Dasycladale algae: Palaeodasycladus mediterraneus.		Dasycladale algae: Palaeodasycladus mediterraneus.	innermost neritic	Early Jurassic	Perdido Group	Gondwana Megasequence	
AB143	-8.71235	126.31998	Mundo Perdido	no sample	red mud and fine sandstone	Same lithology as AB129-131						?Perdido Group	?Gondwana Megasequence	
AB144	-8.71422	126.32030	Mundo Perdido	no sample	Perdido Limestone	not in situ						?Perdido Group	?Gondwana Megasequence	
AB145	-8.71467	126.32032	Mundo Perdido	limestone	Australian margin pelagite	fg pelagite, abundant tiny specks are most likely forams						Kolbano Group	Australian Margin Megasequence	
AB146	-8.71585	126.31993	Mundo Perdido	no sample	AM pelagite	possibly not in situ						Kolbano Group	Australian Margin Megasequence	
AB147	-8.71617	126.31935	Mundo Perdido	no sample	AM pelagite							Kolbano Group	Australian Margin Megasequence	
AB148	-8.71642	126.31893	Mundo Perdido	observation	photograph	Looking west - contact between AMM to east and GM to west						observation point		
AB149	-8.71750	126.31942	Mundo Perdido	no sample	Perdido Limestone	possible fault						Perdido Group	Gondwana Megasequence	
AB150	-8.71753	126.31942	Mundo Perdido	limestone	possible Australian margin pelagite?	Limestone breccia/conglomerate with clasts of wackestone containing scattered thaumatopellacean algae, and peloidal grainstone with rare carbonate-cemented agglutinated foraminifera	Siphovalvulina sp.		Thaumatoporellacean algae: Thaumatoporella ?parvovesiculifera (micritized)	innermost neritic	Early Jurassic	Perdido Group	Gondwana Megasequence	
AB151	-8.71778	126.31887	Mundo Perdido	limestone	Perdido Limestone	Bad peel, affected by saw marks, hand specimen certainly looks Triassic						Perdido Group	Gondwana Megasequence	
AB152	-8.71895	126.31788	Mundo Perdido	no sample	AM pelagite							Kolbano Group	Australian Margin Megasequence	
AB153	-8.72032	126.31845	Mundo Perdido	no sample	Perdido Limestone	not in situ						?Perdido Group	?Gondwana Megasequence	
AB154	-8.72055	126.31833	Mundo Perdido	limestone	dark grey fine grained carbonate. No GPS available, 50m south of AB153	Bioturbated wackestone with abundant recrystallized radiolarian, common sponge spicules, rare ostracod valves, and very rare carbonate-cemented agglutinated foraminifera. "Patches" of peloidal grainstone lacking radiolaria	Siphovalvulina variabilis		Radiolaria or calcispheres Spicules (sponges)	basinal facies, either outer neritic or upper bathyal; evidence of downslope transport from inner neritic platform facies (e.g. peloids, Siphovalvulina).	Late Triassic or Early Jurassic	Aitutu Group	Gondwana Megasequence	
AB155	-8.72112	126.31833	Mundo Perdido	volcanic	volcanic in scree at top of mountain. Still no GPS. Approx 50m south of AB154	Very altered but remnant textures of large plag laths up to 2 mm						Barique Group	Banda Megasequence	
AB156	-8.72308	126.31880	Mundo Perdido	no sample	red mud and fine sandstone	Same lithology as AB157A & AB157B					Unknown	Unknown	Unknown	
AB157A	-8.72327	126.31907	Mundo Perdido	mud	red mud	Barren residue					Unknown	Unknown	Unknown	

Location_No	Lat	Long	Region	Sample_type	Field_Description	Rock_Description	Benthic_foraminifera	Planktonic_foraminifera	OtherBioclasts	Facies	Age	Group	Megasequence	Date
AB157B	-8.72327	126.31907	Mundo Perdido	sandstone	sandstone within red mud	extensively stylotised and completely recrystallised, no bioclasts visible					Unknown	Unknown	Unknown	
AB158	-8.72317	126.31907	Mundo Perdido	limestone	Australian margin pelagite	Bad peel, affected by saw marks						Kolbano Group	Australian Margin Megasequence	
AB159	-8.72408	126.31908	Mundo Perdido	limestone	Perdido Limestone	Ooid grainstone with rare carbonate-cemented agglutnated foraminifera, very rare Lenticulina , very rare thaumatoporellacean algae	Siphovalvulina variabili		Thaumatoporellacean algae: Thaumatoporella ?parvovesiculifera (micritized)	innermost neritic	Early Jurassic	Perdido Group	Gondwana Megasequence	
AB160	-8.72411	126.31908	Mundo Perdido	limestone	Perdido Limestone	Ooid grainstone with rare carbonate-cemented agglutinated foraminifera; scattered mollusc (bivalve) fragments and echinoid plates	Siphovalvulina variabilis			innermost neritic	Early Jurassic	Perdido Group	Gondwana Megasequence	
AB161	-8.71620	126.32303	Mundo Perdido	limestone	very weathered fine grained limestone with a pervasive foliation	Planktonic foraminiferal packstone		Globigerina yeguaensis-Globigerina pseudovenezuelana-Globigerina venezuelana lineage dominant		middle bathyal to abyssal	Oligocene	Kolbano Group	Australian Margin Megasequence	
AB162	-8.71525	126.32407	Mundo Perdido	no sample	AM pelagite							Kolbano Group	Australian Margin Megasequence	
AB163	-8.71357	126.32390	Mundo Perdido	no sample	AM pelagite							Kolbano Group	Australian Margin Megasequence	
AB164	-8.71325	126.32388	Mundo Perdido	no sample	AM pelagite							Kolbano Group	Australian Margin Megasequence	
AB165	-8.71182	126.32352	Mundo Perdido	limestone	fine grained cream coloured chalky limestone. AMM?	Wackestone with scattered rare planktonic foraminifera (some deformed and fragmented)		Planktonic foraminifera: Globigerina yeguaensis-Globigerina pseudovenezuelana-Globigerina venezuelana lineage; ? Globigerina selli		middle bathyal to abyssal	Oligocene	Kolbano Group	Australian Margin Megasequence	
AB166	-8.71112	126.32197	Mundo Perdido	no sample	red mud and fine sandstone	Same lithology as AB157A & AB157B					Unknown	Unknown	Unknown	
AB167	-8.73990	126.35515	Mundo Perdido	no sample	Booi limestone							Booi Group	Banda Megasequence	
AB168	-8.74023	126.35575	Mundo Perdido	no sample	grey mudstone - Babulu Formation							Babulu Group	Gondwana Megasequence	
AB169	-8.74003	126.35652	Mundo Perdido	no sample	Booi limestone							Booi Group	Banda Megasequence	
AB170	-8.73638	126.35835	Mundo Perdido	breccia	unconsolidated very poorly sorted angular limestone clasts	Oncoidal grainstone; very rare thaumatoporellacean algae			Thaumatoporellacean algae: Thaumatoporella ?parvovesiculifera (micritized)	innermost neritic	Probably Early Jurassic	Perdido Group	Gondwana Megasequence	
AB171	-8.73672	126.35827	Mundo Perdido	contact	Fault							observation point		
AB172	-8.73592	126.35887	Mundo Perdido	limestone	Perdido Limestone	Bahaman facies ooid grainstone						Perdido Group	Gondwana Megasequence	
AB173	-8.73567	126.36047	Mundo Perdido	limestone	Booi limestone	Wackestone with common benthic foraminifera (including larger rotaliids), very rare small planktonics (Globigerina or Globigerinoides), coral debris, coralline algae	?Eulepidina, primitive Lepidocyclina (Nephrolepidina), Spiroclypeus			mid neritic	Larger benthic foraminiferal Upper Te Letter Stage (Adams, 1970); latest Oligocene - earliest Miocene	Booi Group	Banda Megasequence	
AB174	-8.73572	126.35997	Mundo Perdido	limestone	Booi limestone	Packstone with abundant sponge spicules and benthic foraminifera (mainly Rotaliida, including fragmented larger types, and Miliolida)	Lepidocyclina (Nephrolepidina); Spiroclypeus or Cycloclypeus (fragment only)			neritic	Larger benthic foraminiferal Upper Te Letter Stage (Adams, 1970); latest Oligocene - earliest Miocene	Booi Group	Banda Megasequence	
AB175	-8.73683	126.36138	Mundo Perdido	observation	photograph	Looking 295 from this point - photo and sketch						observation point		
AB176	-8.73950	126.36323	Mundo Perdido	unknown	fine grained porous rock within red mud	fg sandstone, no fossils visible. No identifiable biogenic grains observed					Unknown	Unknown	Unknown	

Location_No	Lat	Long	Region	Sample_type	Field_Description	Rock_Description	Benthic_foraminifera	Planktonic_foraminifera	OtherBioclasts	Facies	Age	Group	Megasequence	Date
AB177	-8.73968	126.36345	Mundo Perdido	breccia	unconsolidated very poorly sorted angular limestone clasts	Wackestone with common thaumatoporellacean algae, very rare carbonate-cemented agglutinated foraminifera	Siphovalvulina variabilis.		Thaumatoporellacean algae: Thaumatoporella ?parvovesiculifera (micritized)	innermost neritic	Early Jurassic	Perdido Group	Gondwana Megasequence	
AB178	-8.74258	126.29340	Mundo Perdido	no sample	very well bedded indurated extensively veined white limestone	same lithology as AB179					Earliest Miocene	Booi Group	Banda Megasequence	
AB179	-8.74200	126.29415	Mundo Perdido	limestone	very well bedded indurated extensively veined white limestone	Wackestone with rare deformed benthic foraminifera (including larger rotaliids), coralline algae; foraminifera	Spiroclypeus sp. Lepidocyclina (Nephrolepidina) sp.		Coralline algae	inner neritic	Larger benthic foraminiferal Upper Te Letter Stage (Adams, 1970); latest Oligocene - earliest Miocene	Booi Group	Banda Megasequence	
AB180	-8.74162	126.29475	Mundo Perdido	no sample	mafic volcanic - scree	scree						Barique Group	Banda Megasequence	
AB181	-8.74000	126.29522	Mundo Perdido	volcanic	mafic volcanic breccia	Very weathered and altered. Glass, calcite plag and minor pyroxene visible. Volcaniclastic						Barique Group	Banda Megasequence	
AB182	-8.74015	126.29547	Mundo Perdido	no sample	Booi limestone							Booi Group	Banda Megasequence	
AB183			Mundo Perdido	limestone	strange deformed bed of Booi, could be coral? No GPS signal	Extensively veined, has some kind of internal structure but I'm not sure what it is, could be coral?						Booi Group	Banda Megasequence	
AB184			Mundo Perdido	limestone	Booi limestone. No GPS signal	Bad peel, affected by saw marks	Lepidocyclina (Nephrolepidina) sp. Cycloclypeus sp. Homotrema sp.		Coral debris Coralline algae Echinoid spines		Lower Miocene	Booi Group	Banda Megasequence	
AB185	-8.73790	126.29768	Mundo Perdido	no sample	Booi limestone	Cliffs og Booi on west bank, 70% of alluvium in stream is mafic volcanic						Booi Group	Banda Megasequence	
AB186	-8.73745	126.29808	Mundo Perdido	volcanic	mafic volcanic	Similar to AB093 but much coarser grained. VERY altered. Not much of original minerals left but seems to be remnant textures of plag laths with interstitial pyroxene. Plag is extensively sericitised. Abundant biotite (after pyroxene?). Apatite needles and small zircons. Dolerite.						Barique Group	Banda Megasequence	
AB187	-8.73790	126.29877	Mundo Perdido	no sample	mafic volcanics	same lithology as AB186						Barique Group	Banda Megasequence	
AB188	-8.73707	126.29812	Mundo Perdido	no sample	mafic volcanics	same lithology as AB186						Barique Group	Banda Megasequence	
AB189	-8.73615	126.29907	Mundo Perdido	no sample	mafic volcanics	same lithology as AB186						Barique Group	Banda Megasequence	
AB190	-8.73615	126.29922	Mundo Perdido	no sample	mafic volcanics	same lithology as AB186						Barique Group	Banda Megasequence	
AB191			Mundo Perdido	no sample	mafic volcanics. No GPS signal	same lithology as AB186						Barique Group	Banda Megasequence	
AB192			Mundo Perdido	no sample	mafic volcanics. No GPS signal	same lithology as AB186						Barique Group	Banda Megasequence	
AB193	-8.73635	126.29873	Mundo Perdido	no sample	mafic volcanics	same lithology as AB186						Barique Group	Banda Megasequence	
AB194	-8.73635	126.29417	Mundo Perdido	no sample	mafic volcanics	same lithology as AB186						Barique Group	Banda Megasequence	
AB195	-8.73768	126.29060	Mundo Perdido	no sample	Booi limestone							Booi Group	Banda Megasequence	
AB196	-8.73767	126.29060	Mundo Perdido	no sample	Booi limestone	Contact with Babulu Group						Booi Group	Banda Megasequence	
AB197	-8.73548	126.29432	Mundo Perdido	no sample	mafic volcanics	same lithology as AB186						Barique Group	Banda Megasequence	
AB198	-8.73337	126.29373	Mundo Perdido	no sample	mafic volcanics	same lithology as AB186						Barique Group	Banda Megasequence	
AB199	-8.73193	126.29465	Mundo Perdido	no sample	mafic volcanics	same lithology as AB186						Barique Group	Banda Megasequence	
AB200			Mundo Perdido	no sample	Booi limestone. No GPS signal	possibly a Booi - Lolotoi contact						Booi Group	Banda Megasequence	
AB201	-8.73250	126.29280	Mundo Perdido	contact	Fault	Booi - Barique contact						observation point		
AB202			Mundo Perdido	contact	Fault. No GPS signal	Booi - Barique contact						observation point		

Location_No	Lat	Long	Region	Sample_type	Field_Description	Rock_Description	Benthic_foraminifera	Planktonic_foraminifera	OtherBioclasts	Facies	Age	Group	Megasequence	Date
AB203	-8.73523	126.29377	Mundo Perdido	contact	Fault	Booi - Barique contact						observation point		
AB204	-8.73307	126.29290	Mundo Perdido	contact	Fault	same location as AB201: Booi - Barique contact						observation point		
AB205	-8.72457	126.30532	Mundo Perdido	contact	Fault	same lithology as AB206						observation point		
AB206A	-8.72317	126.30622	Mundo Perdido	limestone	chalky, foliated limestone	Wackestone with rare planktonic foraminifera, some silicified; rare radiolaria		Catapsydrax dissimilis, Globigerina pseudovenezuelana, Globorotalia opima nana		middle bathyal to abyssal	Probably early or middle Oligocene	Kolbano Group	Australian Margin Megasequence	
AB207	-8.72317	126.30622	Mundo Perdido	limestone	Perdido Limestone	Ooid grainstone with very rare carbonate-cemented agglutinated foraminifera	Siphovalvulina variabilis			innermost neritic	Probably Early Jurassic	Perdido Group	Gondwana Megasequence	
AB208	-8.72317	126.30622	Mundo Perdido	limestone	deformed limestone	Wackestone , highly fractured and veined, with common Inoceramus prisms, very rare benthic foraminifera (Order Lagenida including Lenticulina), and rare calpionellids(?), very rare radiolaria			?Calpionellids (? Calpionella alpina)	middle bathyal to abyssal	Possibly latest Jurassic or earliest Cretaceous	Kolbano Group	Australian Margin Megasequence	
AB209	-8.72317	126.30622	Mundo Perdido	unknown	grey friable carbonate	Wackestone with scattered Inoceramus prisms, very rare benthic foraminifera (Order Lagenida including Lenticulina), and rare calpionellids(?)			?Calpionellids (? Calpionella alpina)	middle bathyal to abyssal	Possibly latest Jurassic or earliest Cretaceous	Kolbano Group	Australian Margin Megasequence	
AB210	-8.72317	126.30622	Mundo Perdido	limestone	deformed limestone	Scree: Wackestone with rare planktonic foraminifera (including keeled forms)		Globotruncana linneiana, Globotruncanita stuarti		middle bathyal to abyssal	Late Creatceous (Campanian or early Maastrichtian)	Kolbano Group	Australian Margin Megasequence	
AB211	-8.72317	126.30622	Mundo Perdido	volcanic	basalt	fg plag, glass, very altered pyroxene. Oscillatory zoning within plag phenocrysts. Very high phenocryst concentration. Basaltic volcaniclastic.						Barique Group	Banda Megasequence	
AB212	-8.73605	126.27962	Mundo Perdido	unknown	weathered volcanic?	completely weathered - nothing left but clay.						Barique Group	Banda Megasequence	
AB213	-8.73517	126.27965	Mundo Perdido	mud	mudstone	Barren residue					Unknown	Unknown	Unknown	
AB214	-8.73060	126.28668	Mundo Perdido	contact	Contact	soil changes colour at this point. East soil is red (volcanics), west soil is grey (limestones)						observation point		
AB215	-8.73048	126.28982	Mundo Perdido	volcanic	sheared and brecciated mafic volcanic	fg plag in a matrix of volcanic glass - volcaniclastic						Barique Group	Banda Megasequence	
AB216	-8.72762	126.29142	Mundo Perdido	metamorphic	mafic schist	vfg qtz and calcite. Larger qtz grains have interlocking sutured grain boundaries. Large quartz grains apper to be in pretectonic veins. Similar texture to clast in AB286, may be a sheared version						Barique Group	Banda Megasequence	
AB217	-8.73038	126.28757	Mundo Perdido	observation	observation	130m away bearing 350 are high cliffs that look like Booi						observation point		
AB218	-8.69915	126.33742	Mundo Perdido	no sample	Synorogenic limestone	same lithology as AB001 & AB002						Viqueque Group - Lari Guti Member	Synorogenic Megasequence	
AB219	-8.70052	126.33698	Mundo Perdido	limestone	synorogenic	Packstone with benthic foraminifera (mainly Rotaliida including larger types) and rare planktonic foraminifera; coralline algae, mollusc fragments	Amphistegina sp. Schlumbergerella floresiana Elphidium sp. Gypsina sp.	Globorotalia tumida Pulleniatina obliquiloculata – P. finalis Globigerinoides sacculifer Globorotalia truncatulinoides	Coralline algae Echinoid spines Mollusc debris Bryozoan debris	inner neritic	Pleistocene (following range for Schlumbergella given by Loeblich & Tappan, 1987)	Baucau Limestone	Synorogenic Megasequence	
AB220	-8.70170	126.33880	Mundo Perdido	no sample	Synorogenic limestone	same lithology as AB219						Baucau Limestone	Synorogenic Megasequence	
AB221	-8.70437	126.34025	Mundo Perdido	mud	alluvium or synorogenic?	Barren residue					Unknown	Unknown	Unknown	
AB222	-8.70682	126.34122	Mundo Perdido	contact	Contact	170 contact between synorogenic limestone (west) & alluvium (east)						observation point		
AB223	-8.70782	126.34017	Mundo Perdido	no sample	Synorogenic limestone							Baucau Limestone	Synorogenic Megasequence	
AB224	-8.70895	126.33987	Mundo Perdido	no sample	Synorogenic limestone	on west of gully striking 035						Baucau Limestone	Synorogenic Megasequence	
AB225	-8.70933	126.34013	Mundo Perdido	unknown	very weathered clast within AB226	These clasts appear to be lignite. Need to determine age of AB226					Unknown	Unknown	Unknown	

Location_No	Lat	Long	Region	Sample_type	Field_Description	Rock_Description	Benthic_foraminifera	Planktonic_foraminifera	OtherBioclasts	Facies	Age	Group	Megasequence	Date
AB226	-8.70933	126.34013	Mundo Perdido	mud	orange/grey mud containing mafic volcanic clasts	Barren residue					Unknown	Unknown	Unknown	
AB227	-8.71007	126.33992	Mundo Perdido	no sample	mafic schist	same lithology as AB228						Barique Group	Banda Megasequence	
AB228	-8.71043	126.33998	Mundo Perdido	metamorphic	mafic schist	Recrystallised, foliated qtz and calcite with sutured grain boundaries. Qtz >> calcite						Barique Group	Banda Megasequence	
AB229	-8.71095	126.34027	Mundo Perdido	no sample	mafic schist	same lithology as AB228, just boulders up gully from this point						Barique Group	Banda Megasequence	
AB230	-8.71073	126.34065	Mundo Perdido	mud	dark grey mud containing volcanic clasts	Barren residue					Unknown	Unknown	Unknown	
AB231	-8.71073	126.34065	Mundo Perdido	volcanic	volcanic clasts within AB230	fg qtz, plag and calcite. volcaniclastic						Barique Group	Banda Megasequence	
AB232	-8.71072	126.34063	Mundo Perdido	no sample	mafic schist	same lithology as AB228						Barique Group	Banda Megasequence	
AB233	-8.70845	126.33947	Mundo Perdido	no sample	Synorogenic limestone	Synorogenic Limestone north of this point						Baucau Limestone	Synorogenic Megasequence	
AB234	-8.71058	126.34053	Mundo Perdido	mud	red mud containing clasts of mafic volcanics	Red mudstone with very rare planktonic foraminifera		Globigerinatheka index		bathyal	Middle or Late Eocene	?Barique Group	Banda Megasequence	
AB235	-8.71073	126.34083	Mundo Perdido	mud	dark grey mud at lolotoi-limestone contact	Barren residue					Unknown	Unknown	Unknown	
AB236	-8.71073	126.34083	Mundo Perdido	shale	foliated and folded shale	Red wackestone with abundant planktonic foraminifera		Morozovella velascoensis		middle bathyal to abyssal	Late Paleocene or earliest Eocene (within range of Zones P3b-E2; Berggren & Pearson et al., 2006)	Kolbano Group	Australian Margin Megasequence	
AB237	-8.71073	126.34083	Mundo Perdido	breccia	fault breccia containing clasts of limestone & ?mafics	(one foram specimen only observed in wackestone clast in breccia)	buliminid				Cretaceous or Cenozoic	Kolbano Group	Australian Margin Megasequence	
AB238	-8.71157	126.33998	Mundo Perdido	limestone	possible Perdido	Peloidal-ooid grainstone and wackestone with rare thaumatoporellacean algae, rare carbonate-cemented agglutinated foraminifera	? Siphovalvulina sp.		Chambered sponges; Thaumatoporellacean algae: Thaumatoporella ?parvovesiculifera (micritized)	innermost neritic	Early Jurassic	Perdido Group	Gondwana Megasequence	
AB239	-8.71185	126.34060	Mundo Perdido	no sample	Perdido Limestone	same lithology as AB238						Perdido Group	Gondwana Megasequence	
AB240	-8.71233	126.34010	Mundo Perdido	limestone	deformed and foliated limestone	Deformed and partially recrystallised wackestone with common planktonic foraminifera		Globigerina yeguaensis-Globigerina pseudovenezuelana-Globigerina venezuelana lineage		middle bathyal to abyssal	Probably Oligocene	Kolbano Group	Australian Margin Megasequence	
AB241	-8.71273	126.33948	Mundo Perdido	no sample	Perdido Limestone	contact between AB240 to north and Perdido Limestone to south						Perdido Group	Gondwana Megasequence	
AB242	-8.70100	126.32243	Mundo Perdido	no sample	Synorogenic limestone							Baucau Limestone	Synorogenic Megasequence	
AB243	-8.70379	126.31882	Mundo Perdido	no sample	Synorogenic limestone							Baucau Limestone	Synorogenic Megasequence	
AB244	-8.70482	126.31835	Mundo Perdido	no sample	Perdido Limestone	not in situ						?Perdido Group	?Gondwana Megasequence	
AB245	-8.70307	126.31533	Mundo Perdido	limestone	synorogenic limestone	Packstone with common benthic foraminifera (mainly Rotaliida including larger types), very rare planktonic foraminifera, coralline algae, coral debris, lithic fragments	Nummulites venosus, Cycloclypeus, Amphistegina sp. Operculina sp. Schlumbergerella floresiana	Globorotalia tumida, Pulleniatina obliquiloculata, Globigerinoides sp.	Coralline algae Echinoid spines Mollusc debris	mid neritic	Pleistocene	Baucau Limestone	Synorogenic Megasequence	
AB246	-8.70367	126.31583	Mundo Perdido	volcanic	very weathered mafic volcanic	very weathered. Fg plag, glass and iron oxide						Barique Group	Banda Megasequence	
AB247	-8.70262	126.31545	Mundo Perdido	no sample	synorogenic limestone							Baucau Limestone	Synorogenic Megasequence	
AB248	-8.70228	126.31555	Mundo Perdido	limestone	lithic rich synorogenic limestone	Packstone with benthic foraminifera (mainly Rotaliida including larger types), mollusc fragments, coralline algae, coral debris, bryozoan fragments	Nummulites venosus			neritic	Pleistocene	Baucau Limestone	Synorogenic Megasequence	
AB249			Mundo Perdido	travertine							Holocene	Recent surficial deposits	Recent surficial deposits	

Location_No	Lat	Long	Region	Sample_type	Field_Description	Rock_Description	Benthic_foraminifera	Planktonic_foraminifera	OtherBioclasts	Facies	Age	Group	Megasequence	Date
AB250	-8.70398	126.31552	Mundo Perdido	no sample	very weathered mafic volcanic	same lithology as AB246						Barique Group	Banda Megasequence	
AB251	-8.70427	126.31612	Mundo Perdido	no sample	very weathered mafic volcanic	same lithology as AB246						Barique Group	Banda Megasequence	
AB252	-8.70433	126.31645	Mundo Perdido	no sample	very weathered mafic volcanic	same lithology as AB246						Barique Group	Banda Megasequence	
AB253	-8.70367	126.31748	Mundo Perdido	no sample	very weathered mafic volcanic	same lithology as AB246						Barique Group	Banda Megasequence	
AB254	-8.70455	126.31622	Mundo Perdido	no sample	very weathered mafic volcanic	same lithology as AB246						Barique Group	Banda Megasequence	
AB255	-8.70510	126.31532	Mundo Perdido	no sample	very weathered mafic volcanic	same lithology as AB246, slightly more schistose						Barique Group	Banda Megasequence	
AB256	-8.70507	126.31417	Mundo Perdido	metamorphic	mafic schist	Compositionally layered qtz and calcite. Kink bands visible within foliation						Barique Group	Banda Megasequence	
AB257	-8.70688	126.31018	Mundo Perdido	no sample	very weathered mafic volcanic	same lithology as AB246						Barique Group	Banda Megasequence	
AB258			Mundo Perdido	no sample	very weathered mafic volcanic . No GPS signal	same lithology as AB246, pile of boulders overlying it at this point						Barique Group	Banda Megasequence	
AB259	-8.70727	126.30877	Mundo Perdido	limestone	Booi limestone	Wackestone with common benthic foraminifera (including larger rotaliids), very rare small planktonics (Globigerina or Globigerinoides), coral debris, coralline algae	primitive Lepidocyclina (Nephrolepidina); Spiroclypeus			inner neritic	Larger benthic foraminiferal Upper Te Letter Stage (Adams, 1970); latest Oligocene - earliest Miocene	Booi Group	Banda Megasequence	
AB260	-8.70615	126.30867	Mundo Perdido	conglomerate	mystery conglomerate. Holocene?	Matrix: Wackestone with scattered coralline algae, mollusc fragments, benthic foraminifera (mainly Rotaliida). Clast: Oncoid-peloid grainstone	Nummulites venosus (in matrix), acervulinids (indeterminate), Operculina sp., small indeterminate rotaliids		Coralline algae Coral debris Mollusc debris	neritic	Pleistocene	Baucau Limestone	Synorogenic Megasequence	
AB261	-8.70242	126.31998	Mundo Perdido	no sample	very weathered mafic volcanic	same litholgy as AB246, VERY weathered						Barique Group	Banda Megasequence	
AB262	-8.70338	126.31880	Mundo Perdido	no sample	very weathered mafic volcanic	same litholgy as AB246						Barique Group	Banda Megasequence	
AB263	-8.70292	126.31788	Mundo Perdido	limestone	synorogenic, basal beds overlying lolotoi. Lithic rich.	Porous white limestone containing shell fragments, benthic foraminifera (mainly Rotaliida including larger types), coralline algae, and clasts of mafic igneous rock.	Nummulites venosus, Schlumbergerella, Cycloclypeus, Amphistegina sp., Operculina sp., Elphidium sp.	Globorotalia tumida, Pulleniatina obliquiloculata	Sessile bivalve shell fragments (either mussel, pecten or oyster) Bryozoan fragments Echinoid spines	mid neritic	Pleistocene	Baucau Limestone	Synorogenic Megasequence	
AB264	-8.70570	126.31017	Mundo Perdido	limestone	synorogenic, basal beds overlying lolotoi. Lithic rich.	Very porous yellow limestone with benthic foraminifera (mainly Rotaliida) and some planktonic foraminifera, lithic fragments	Nummulites venosus, Amphistegina sp.	Globorotalia tumida Globigerinoides sacculifer Pulleniatina obliquiloculata Sphaeroidinellopsis seminula or Sphaeroidinella dehsicens	Echinoid spines	mid neritic	Pleistocene	Baucau Limestone	Synorogenic Megasequence	
AB265	-8.70683	126.31045	Mundo Perdido	no sample	very weathered mafic volcanic	same lithology as AB246, pile of boulders overlying it at this point						Barique Group	Banda Megasequence	
AB266	-8.70707	126.30938	Mundo Perdido	no sample	very weathered mafic volcanic	same lithology as AB246, bearing 340 from this point is a gully separating Booi to the west with Baucau Limestone to the east						Barique Group	Banda Megasequence	
AB267	-8.70770	126.30768	Mundo Perdido	no sample	mafic schist	same lithology as AB256						Barique Group	Banda Megasequence	
AB268	-8.70867	126.30667	Mundo Perdido	no sample	very weathered mafic volcanic	same lithology as AB246						Barique Group	Banda Megasequence	
AB269	-8.71017	126.30645	Mundo Perdido	no sample	very weathered mafic volcanic	same lithology as AB246						Barique Group	Banda Megasequence	
AB270	-8.71232	126.31107	Mundo Perdido	limestone	Turonian Australian margin pelagite	Packstone with abundant fragmented ? Inoceramus prisms, and minute calpionellids(?)			?Calpionellids (? Calpionella alpina)	middle bathyal to abyssal	Possibly latest Jurassic or earliest Cretaceous	Kolbano Group	Australian Margin Megasequence	

Location_No	Lat	Long	Region	Sample_type	Field_Description	Rock_Description	Benthic_foraminifera	Planktonic_foraminifera	OtherBioclasts	Facies	Age	Group	Megasequence	Date
AB271	-8.70887	126.32732	Mundo Perdido	volcanic	Slightly schistose mafic volcanic	fg qtz, plag and calcite. Volcaniclastic. Extensive calcite alteration.						Barique Group	Banda Megasequence	
AB272	-8.71018	126.32823	Mundo Perdido	no sample	Slightly schistose mafic volcanic	same lithology as AB271						Barique Group	Banda Megasequence	
AB273	-8.71318	126.33028	Mundo Perdido	no sample	AM pelagite	scree						?Kolbano Group	?Australian Margin Megasequence	
AB274	-8.71642	126.32532	Mundo Perdido	limestone	Australian margin pelagite	Wackestone with scattered Inoceramus prisms, very rare benthic foraminifera (Order Lagenida including Lenticulina), and rare calpionellids(?)			?Calpionellids (? Calpionella alpina)	middle bathyal to abyssal	Possibly latest Jurassic or earliest Cretaceous	Kolbano Group	Australian Margin Megasequence	
AB275	-8.71900	126.32503	Mundo Perdido	no sample	Perdido Limestone	possibly not in situ						Perdido Group	Gondwana Megasequence	
AB276	-8.72323	126.32295	Mundo Perdido	limestone	Australian margin pelagite?	Ooid grainstone with rare carbonate-cemented agglutinated foraminifera and rare hyaline foraminifera (Order Lagenidae including Lenticulina)	Siphovalvulina sp.		Chambered sponges	innermost neritic	Early Jurassic	Perdido Group	Gondwana Megasequence	
AB277	-8.72368	126.32320	Mundo Perdido	no sample	AM pelagite	no access, sighted in						Kolbano Group	Australian Margin Megasequence	
AB278	-8.71542	126.32598	Mundo Perdido	limestone	Australian margin pelagite	Wackestone with rare planktonic foraminifera (large Globigerina spp.)		Planktonic foraminifera: Globigerina yeguaensis-Globigerina pseudovenezuelana-Globigerina venezuelana lineage; ? Globigerina selli		middle bathyal to abyssal	Probably Oligocene	Kolbano Group	Australian Margin Megasequence	
AB279	-8.71432	126.32653	Mundo Perdido	limestone	Australian margin pelagite	Bad peel, no forams visible		Globigerina venezuelana – G. tripartita			Probably Oligocene	Kolbano Group	Australian Margin Megasequence	
AB280	-8.71393	126.32600	Mundo Perdido	limestone	Australian margin pelagite	Packstone with mollusc fragments (including Inoceramus prisms), Belemnite guard, common calpionellids(?) in fine-grained layers	small nodosariids		?Calpionellids (? Calpionella alpina)	middle bathyal to abyssal	Possibly latest Jurassic or earliest Cretaceous	Kolbano Group	Australian Margin Megasequence	
AB281	-8.71393	126.32600	Mundo Perdido	limestone	Possible Perdido	Bad peel, affected by saw marks			Prismatic calcite debris from sessile bivalve shells (e.g. Inoceramus) Echinoid spine fragments indeterminate nodosariid forams.		?earliest Cretaceous or Late Jurassic	Kolbano Group	?Australian Margin Megasequence	
AB282	-8.71120	126.32803	Mundo Perdido	no sample	AM pelagite							Kolbano Group	Australian Margin Megasequence	
AB283	-8.72382	126.36608	Mundo Perdido	sandstone								Booi Group	Banda Megasequence	
AB284	-8.72382	126.36608	Mundo Perdido	mudstone	grey mudstone	grey mudstone with common poorly preserved planktonic foraminifera, and rare benthic foraminifera		Globigerina ciperoensis, Globigerina praebulloides, Globigerina venezuelana		outer neritic or upper bathyal	Late Oligocene	Booi Group	?Banda Megasequence	
AB285	-8.73425	126.36128	Mundo Perdido	limestone	Possible Perdido	Wackestone with patches of ooid grainstone (? burrow infill); rare carbonate-cemented agglutinated foraminifera	? Siphovalvulina sp.			innermost neritic	Probably Early Jurassic	Perdido Group	Gondwana Megasequence	
AB286	-8.72810	126.35245	Mundo Perdido	volcanic	mafic volcanic - basalt	Vfg qtz, plag, glass and calcite. Lithic fragments within a fine grained matrix, flow layering visible around some clasts. Ignimbritic? Pyroclastic deposit? Definitely volcaniclastic.						Barique Group	Banda Megasequence	
AB287	-8.72815	126.35248	Mundo Perdido	no sample	basalt boulders	same lithology as AB286, possibly not in situ						Barique Group	Banda Megasequence	
AB288	-8.71783	126.35362	Mundo Perdido	no sample	red chert	same lithology as AB309						Kolbano Group	?Australian Margin Megasequence	
AB289	-8.72800	126.35237	Mundo Perdido	no sample	very weathered mafic volcanic							Barique Group	Banda Megasequence	
AB290	-8.72425	126.35287	Mundo Perdido	no sample	very weathered mafic volcanic							Barique Group	Banda Megasequence	
AB291	-8.72398	126.35310	Mundo Perdido	no sample	very weathered mafic volcanic							Barique Group	Banda Megasequence	

Location_No	Lat	Long	Region	Sample_type	Field_Description	Rock_Description	Benthic_foraminifera	Planktonic_foraminifera	OtherBioclasts	Facies	Age	Group	Megasequence	Date
AB292	-8.72395	126.35238	Mundo Perdido	limestone	Perdido Limestone	Wackestone with rare thaumatoporellacean algae, very rare carbonate-cemented agglutinated foraminifera	? Siphovalvulina		Thaumatoporellacean algae: Thaumatoporella ?parvovesiculifera (micritized)	innermost neritic	Early Jurassic	Perdido Group	Gondwana Megasequence	
AB293	-8.72373	126.35148	Mundo Perdido	no sample	Perdido Limestone							Perdido Group	Gondwana Megasequence	
AB294	-8.72283	126.35102	Mundo Perdido	no sample	very weathered mafic volcanic?							Unknown	Unknown	
AB295	-8.72285	126.35013	Mundo Perdido	limestone	limestone breccia from fault zone	No identifiable biogenic grains in the oolitic limestone						Perdido Group	Gondwana Megasequence	
AB296	-8.72285	126.35013	Mundo Perdido	volcanic	sheared rock from fault zone	Sheared, deformed bahaman facies limestone containing clasts of altered igneous material within shear planes						Perdido Group	Gondwana Megasequence	
AB297	-8.72285	126.35013	Mundo Perdido	fault gouge	fault rock	Extensively sheared and recrystallised. Mostly clays, quartz and calcite. No biogenic grains visible					Unknown	Unknown	Unknown	
AB298	-8.72285	126.35013	Mundo Perdido	limestone	fault rock	Extensively brecciated, dolomitized oolitic/oncolitic limestone. Some oncolites appear to be nucleated on angular quartz grains and lithic fragments.			Indeterminate mollusc debris (rare)			Perdido Group	Gondwana Megasequence	
AB299	-8.72285	126.35013	Mundo Perdido	?limestone	sheared rock from fault zone	Poor thin section but contains deformed ?ooids. Sheared bahaman facies limestone?						?Perdido Group	?Gondwana Megasequence	
AB300	-8.72285	126.35013	Mundo Perdido	limestone	limestone from fault zone	Ooid peloid grainstone with rare gastropods, thaumatoporellacean algae, carbonate-cemented agglutinated foraminifera	? Siphovalvulina		Thaumatoporellacean algae: Thaumatoporella ?parvovesiculifera (micritized)	innermost neritic	Early Jurassic	Perdido Group	Gondwana Megasequence	
AB301	-8.72285	126.35013	Mundo Perdido	?limestone	fault rock	Dolomitized bahaman facies ooid packstone/wackestone, containing ooids and also what appears to be abundant lithogenic material (sand?). This rock was right on the fault plane but appears undeformed and can see no evidence of any volcanic clasts in the peel. Innermost neritic			Gastropod debris		Late Triassic or Early Jurassic (by local lithofacies correlation)	Perdido Group	Gondwana Megasequence	
AB302	-8.72285	126.35013	Mundo Perdido	limestone	limestone from reverse fault plane	Extensively brecciated and recystallised, dolomitized oolitic limestone. No identifiable bioclasts observed. Minor ?lithic fragments.						Perdido Group	Gondwana Megasequence	
AB303A	-8.72278	126.34972	Mundo Perdido	breccia	limestone breccia from base of huge cliffs at fault zone, clast type A	(A) wackestone with minute planktonic foraminifera		Clast type A: planktonic foraminifera - Blefuscuiana sp. or Hedbergella sp. Globigerinelloides sp..			Clast type A: Early Cretaceous (probably late Aptian – early Albian)	Kolbano Group	Australian Margin Megasequence	
AB303B	-8.72278	126.34972	Mundo Perdido	breccia	limestone breccia from base of huge cliffs at fault zone, clast type B	(B) peloidal – oolitic grainstone with rare thaumatoporellacean algae			Clast type B: Thaumatoporellacean algae - Thaumatoporella ?parvovesiculifera		Clast type B: Early Jurassic	Perdido Group	Gondwana Megasequence	
AB304	-8.72383	126.34808	Mundo Perdido	observation	soil	probably overlying mafic volcanics?						observation point		
AB305	-8.72768	126.34720	Mundo Perdido	observation	soil	probably overlying mafic volcanics?						observation point		
AB306	-8.72910	126.34717	Mundo Perdido	observation	scree	mixed scree of Perdido Limestone and mafic volcanics						observation point		
AB307	-8.73205	126.34632	Mundo Perdido	observation	contact	N-S striking gully separating Perdido Limestone (west) from dark grey volcanic mud and mafic volcanics (east) (volcanics are same lithology as AB319)						observation point		
AB308	-8.73403	126.34767	Mundo Perdido	observation	soil	probably overlying mafic volcanics						observation point		
AB309	-8.73488	126.35080	Mundo Perdido	chert	red chert	No bioclasts visible, possibly cherty base of Australian Margin Megasequence?					Unknown	?Kolbano Group	?Australian Margin Megasequence	
AB310	-8.73767	126.35715	Mundo Perdido	no sample	Booi limestone							Booi Group	Banda Megasequence	

Location_No	Lat	Long	Region	Sample_type	Field_Description	Rock_Description	Benthic_foraminifera	Planktonic_foraminifera	OtherBioclasts	Facies	Age	Group	Megasequence	Date
AB311	-8.73668	126.35437	Mundo Perdido	no sample	VERY red soil	likely overlying red chert						Kolbano Group	?Australian Margin Megasequence	
AB312	-8.73203	126.34633	Mundo Perdido	contact	contact	see description						observation point		
AB313	-8.73203	126.34633	Mundo Perdido	limestone	GM limestone	Peloidal grainstone with common thaumatoporellacean algae			Thaumatoporellacean algae: Thaumatoporella ?parvovesiculifera (micritized)	innermost neritic	Probably Early Jurassic	Perdido Group	Gondwana Megasequence	
AB314	-8.73203	126.34633	Mundo Perdido	breccia	Breccia containing mostly clasts of limestone and abundant black chert	No identifiable biogenic grains observed. Extensively recrystallised, no biogenic grains or even any remnant textures observed					Unknown	Unknown	Unknown	
AB315	-8.73203	126.34633	Mundo Perdido	limestone	fg extensively stylotised pink pelagite	Wackestone with rare planktonic foraminifera (including keeled forms) and very rare hyaline benthic foraminifera (Lagenidae - Lenticulina)	indeterminate hyaline trochospiral types	Globotruncana spp., Globigerinelloides sp.		middle bathyal to abyssal	Late Cretaceous (post-Turonian)	Kolbano Group	Australian Margin Megasequence	
AB316	-8.73203	126.34633	Mundo Perdido	shale	red shale	Red packstone with very abundant planktonic foraminifera		Morozovella spp. (including M. velascoensis), Acarinina spp.		middle bathyal to abyssal	Late Paleocene or earliest Eocene (within range of Zones P4-E2, Berggren & Pearson et al., 2006)	Kolbano Group	Australian Margin Megasequence	
AB317	-8.73023	126.34550	Mundo Perdido	mud	grey mud containing mostly clasts of mafic volcanics. Could be either erosional remnants of volcanics or a melange zone on Perdido mud	Barren residue, all mafic volcanic fragments					Unknown	Unknown	Unknown	
AB318	-8.73245	126.34287	Mundo Perdido	limestone	fg extensively stylotised pink pelagite	Red wackestone with rare poorly preserved planktonic foraminifera	indeterminate hyaline trochospiral types	poorly preserved keel forms belonging either to Dicarinella or Globotruncana		middle bathyal to abyssal	Late Cretaceous	Kolbano Group	Australian Margin Megasequence	
AB319	-8.73273	126.34182	Mundo Perdido	volcanic	clast of mafic volcanic within grey mud	Vfg qtz and very minor plag in a glassy matrix, calcite veining, rare mica. Ferruginous stylolites? May be a volcanic sandstone. Rutile needles and other inclusions are present in quartz.						Melange zone	Melange Zone	
AB320	-8.73350	126.34130	Mundo Perdido	no sample	Perdido Limestone							Perdido Group	Gondwana Megasequence	
AB321	-8.73277	126.33938	Mundo Perdido	limestone	fg extensively stylotised pink pelagite	Wackestone with very rare planktonic foraminifera (deformed, fragmented) and very rare benthic foraminifera (Order Rotaliida)	indeterminate hyaline trochospiral involute types	indeterminant keeled globotruncanid. Benthic foraminfiera: Eponides-like form		middle bathyal to abyssal	Late Cretaceous	Kolbano Group	Australian Margin Megasequence	
AB322			Mundo Perdido	no sample	fg extensively stylotised pink pelagite							Kolbano Group	Australian Margin Megasequence	
AB323	-8.73205	126.33720	Mundo Perdido	no sample	GM & AMM limestones. Loose boulders or blocks in melange?							?Melange zone	?Melange zone	
AB324	-8.73373	126.33772	Mundo Perdido	no sample	Perdido Limestone							Perdido Group	Gondwana Megasequence	
AB325	-8.73607	126.34105	Mundo Perdido	no sample	GM limestone							Perdido Group	Gondwana Megasequence	
AB326	-8.73477	126.34427	Mundo Perdido	no sample	observation							observation point		
AB327	-8.70618	126.35195	Mundo Perdido	no sample	Synorogenic limestone - Lari Guti							Viqueque Group - Lari Guti Member	Synorogenic Megasequence	
AB328	-8.71020	126.35068	Mundo Perdido	no sample	soil	grassy plains and abundant eucalypts, mixed scree of GM & AMM						?Kolbano Group	?Australian Margin Megasequence	
AB329	-8.71108	126.35005	Mundo Perdido	volcanic	orange soil containing abundant mafic volcanics weathered to various degrees	vfg and altered volcanic sandstone. Similar texture to AB319. Variable grainsize - appears graded from one side of the thin section to the other						Barique Group	Banda Megasequence	
AB330	-8.71203	126.35050	Mundo Perdido	no sample	red chert	possibly base of AMM						?Kolbano Group	?Australian Margin Megasequence	

Location_No	Lat	Long	Region	Sample_type	Field_Description	Rock_Description	Benthic_foraminifera	Planktonic_foraminifera	OtherBioclasts	Facies	Age	Group	Megasequence	Date
AB331	-8.71437	126.35165	Mundo Perdido	limestone	Extremely weathered and brecciated pelagite	Wackestone with rare planktonic foraminifera (large Globigerina spp.)		Globigerina yeguaensis-Globigerina pseudovenezuelana-Globigerina venezuelana lineage		middle bathyal to abyssal	Probably Oligocene	Kolbano Group	Australian Margin Megasequence	
AB332	-8.71470	126.35172	Mundo Perdido	limestone	Australian Margin pelagite	Wackestone with scattered rare planktonic foraminifera (some deformed, fragmented and/or partially silicified)		Globigerina spp.		middle bathyal to abyssal	Probably Oligocene	Kolbano Group	Australian Margin Megasequence	
AB333	-8.71283	126.35177	Mundo Perdido	no sample	weathered mafic volcanics	same lithology as AB329						Barique Group	Banda Megasequence	
AB334	-8.71165	126.35217	Mundo Perdido	limestone	Synorogenic limestone - Lari Guti	Porous limestone with common benthic foraminifera (mainly Rotaliida including larger types), rare planktonic forms, and coralline algae	Nummulites venosus, ?Calcarina sp. Operculina sp.	Globigerinoides sp.	Coralline algae	neritic	Pleistocene	Baucau Limestone	Synorogenic Megasequence	
AB400	-8.88271	126.37744	Viqueque	observation	Contact of block with melange clay, east-west striking fault							observation point		15/04
AB401	-8.88280	126.37752	Viqueque	no sample	radiolarite (senso stricto) 5 15 cm beds of siliceous radiolarite, with 1 - 5 cm interbeds of shale. Likely a block in melange							Melange zone	Melange zone	15/04
AB402	-8.81007	126.38052	Builo	no sample	large outcrop of Aitutu Formation. Alternating beds of shale and calcilutite. Halobia-type shell filaments (Triassic), plus ?calcispheres or ?rads. Biomicrite or calcilutite. Possible a block in melange							Aitutu Group	Gondwana Megasequence	16/04
AB403	-8.76490	126.36651	Builo	no sample	Aitutu Formation. Debris slides, overturned bedding							Aitutu Group	Gondwana Megasequence	16/04
AB404	-8.64596	126.43288	Laritame	breccia	Venilale hot springs. Perdido Group limestone and breccia. Breccia is possibly hydrothermal rather than a fault breccia	Breccia clasts are ooid packstones and grainstones						Perdido Group	Gondwana Megasequence	16/04
AB405	-8.47385	127.14804	Paitchau	limestone	High cliffs south of the road to Malahara. Baucau Limestone	Rudstone comprising a range of fauna including coral, algal material, bryozoans, and diverse and abundant foraminifera	miliolids, gypsinids	Globigerinoides				Baucau Limestone	Synorogenic Megasequence	18/04
AB417	-9.02413	125.29604	Saburai	fault gouge	Massive fault gouge. Limestone clasts 1 - 50 mm within a fg clayey-sandy matrix	Angular clasts of limestone and calcite. No fossils visible					Unknown	Unknown	Unknown	28/05
AB418	-9.00888	125.28381	Saburai	limestone	Grey indurated limestone, large shell fragments up to 10 mm	Highly recrystallised, contains abundant large shell fragments, algal growths and nodules, and rare forams	duostominids		Gastropods, ostracods, echinoids, algal growths and nodules		Triassic	Bandeira Group	Gondwana Megasequence	28/05
AB419A	-9.00713	125.27528	Saburai	mudstone	Interbedded mudstone and sandstone, sandstone beds 1 - 30 mm	Residue mainly lithic fragments (vfg qtz sandstone?) abundant sulfides, some replacing organic forms (mostly gastropods and bivalves). One large foram (22, possibly contamination?)			Sulfides replacing gastropods and bivalves		Mesozoic	?Babulu Group	Gondwana Megasequence	28/05
AB419B	-9.00713	125.27528	Saburai	sandstone	Interbedded mudstone and sandstone, sandstone beds 1 - 30 mm	No biogenic grains visible in peel					Unknown	?Babulu Group	?Gondwana Megasequence	28/05
AB420A	-8.99068	125.28273	Loelako	?volcanic sandstone	massive ?clast of ?volcanic sandstone within deformed sandstone/mudstone beds	No biogenic grains visible					Unknown	Unknown	Unknown	29/05
AB420B	-8.99068	125.28273	Loelako	sandstone	thinly bedded folded and deformed interbedded mudstone/sandstone	No forams visible in residue - but a lot of clumps					Unknown	?Babulu Group	?Gondwana Megasequence	29/05
AB420C	-8.99068	125.28273	Loelako	mudstone	thinly bedded folded and deformed interbedded mudstone/sandstone	Barren residue - no biogenic grains					Unknown	?Babulu Group	?Gondwana Megasequence	29/05
AB421	-8.98186	125.28337	Loelako	mudstone	grey mudstone with small (≈ 0.1 mm) black flecks	Barren residue - no biogenic grains					Unknown	?Babulu Group	?Gondwana Megasequence	29/05
AB422A	-8.98149	125.28351	Loelako	limestone	Interbedded orange ?limestone and mudstone	Radiolarian wackestone. Abundant radiolaria but no forams visible			Abundant radiolaria, very rare ?bivalve filaments		?Triassic	?Aitutu Group	Gondwana Megasequence	29/05
AB422B	-8.98149	125.28351	Loelako	mudstone	Interbedded orange ?limestone and mudstone	Barren residue - no biogenic grains. Abundant feldspar					?Triassic	?Aitutu Group	Gondwana Megasequence	29/05
AB423	-8.97122	125.28448	Loelako	mudstone	fissile grey mudstone	Barren residue - no biogenic grains. Grains mostly subrounded, mostly lithics.					Unknown	?Babulu Group	?Gondwana Megasequence	29/05
AB424A	-8.97206	125.28382	Loelako	limestone	Grey massive limestone	Silicified and dolomitised, no biogenic grains visible in peel					Unknown	Unknown	Unknown	29/05
AB424B	-8.97206	125.28382	Loelako	limestone	Orange limestone with abundant chert nodules	Abundant very fine spheroid, conical and rod-shaped grains, possibly radiolaria, in a micritic matrix			?radiolaria		Unknown	Unknown	Unknown	29/05

Location_No	Lat	Long	Region	Sample_type	Field_Description	Rock_Description	Benthic_foraminifera	Planktonic_foraminifera	OtherBioclasts	Facies	Age	Group	Megasequence	Date
AB425	-8.97952	125.28349	Loelako	limestone	Massive dark grey limestone	Wackestone, many tiny grains visible but none identifiable as forams -more peels needed?					Unknown	Unknown	Unknown	29/05
AB426	-8.98634	125.32083	Bobonaro Springs	mudstone	Grey-brown friable mudstone. Tiny white grains which are possibly forams	Residue almost entirely comprises poorly preserved radiolaria spherules, some rare ?forams	Dentolina, Conglophragmium canningensis		Radiolaria		Late Triassic (Carnian-Rhaetian)	Transitional Aitutu/Babulu Group	Gondwana Megasequence	30/05
AB427	-8.98928	125.31389	Bobonaro Springs	limestone	Red-grey limestone with abundant calcite veining	Wackestone containing radiolaria and possibly a few very small forams			Radiolaria		?Triassic	Melange zone	Melange zone	30/05
AB428	-8.98863	125.31288	Bobonaro Springs	volcanic	Pillow basalt, abundant well defined pillows							Melange zone	Melange zone	30/05
AB429	-8.69568	126.37840	Laritame	no sample	Perdido Group Limestone overlying AM pelagite							Perdido Group	Gondwana Megasequence	2/06
AB430	-8.69575	126.37823	Laritame	no sample	Perdido Group Limestone overlying AM pelagite							Perdido Group	Gondwana Megasequence	2/06
AB431	-8.69576	126.37885	Laritame	no sample	Perdido Group Limestone overlying AM pelagite							Perdido Group	Gondwana Megasequence	2/06
AB432	-8.69532	126.37917	Laritame	no sample	Perdido Group Limestone							Perdido Group	Gondwana Megasequence	2/06
AB433	-8.64582	126.43293	Laritame	limestone	Extremely brecciated limestone, ?hydrothermal	Breccia clasts are ooid packstones and grainstones						Perdido Group	Gondwana Megasequence	3/06
AB434	-8.66997	126.34167	Laritame	chalk	Foraminiferal friable chalk, abundant globular forams	Abundant forams in residue						Viqueque Group - Batu Putih Member	Synorogenic Megasequence	3/06
AB435	-8.67235	126.42076	Laritame	chalk	Foraminiferal friable chalk, abundant globular forams	Abundant forams in residue						Viqueque Group - Batu Putih Member	Synorogenic Megasequence	3/06
AB436	-8.67242	126.42303	Laritame	mudstone	Foraminiferal sandy mud. Very friable. Abundant globular planktonic forams. Perhaps a shallower synorogenic facies?	Abundant forams in residue						Viqueque Group	Synorogenic Megasequence	3/06
AB437	-8.65833	126.41634	Laritame	mudstone	Grey vfg mudstone. Possible Viqueque?	Abundant forams in residue						Viqueque Group	Synorogenic Megasequence	3/06
AB438	-8.65417	126.39128	Laritame	no sample	Large flat, smooth fault surface with huge striae, Booi Limestone							Booi Group	Banda Megasequence	3/06
AB439	-8.65420	126.39128	Laritame	sandstone	Sandstone blocks surrounded by mud. Qtz rich plus diverse grains of other material. Coarse grained but quite friable - recent?	Residue is predominantly subangular qtz and lithic fragments, no bioclasts visible					Unknown	Unknown	Unknown	3/06
AB440	-8.67823	126.37318	Laritame	limestone	Fossiliferous wackestone with abundant shelly fragments	Sandstone containing bryozoan clasts 2-5 mm in a muddy, sandy matrix with abundant forams.		?Morozovella		Shallow water, mid neritic	?Eocene	Un-named Eocene Banda	Banda Megasequence	4/06
AB441	-8.67842	126.37543	Laritame	no sample	Very weathered volcaniclastic. Angular clasts of very iron rich rock							Barique Group	Banda Megasequence	4/06
AB442	-8.67851	126.37601	Laritame	no sample	Very weathered volcaniclastic. Angular clasts of very iron rich rock							Barique Group	Banda Megasequence	4/06
AB443	-8.67769	126.37644	Laritame	no sample	Mafic volcanics and volcanic breccias							Barique Group	Banda Megasequence	4/06
AB444	-8.68234	126.38863	Laritame	no sample	Perdido Group Limestone							Perdido Group	Gondwana Megasequence	4/06
AB445	-8.66532	126.32072	Oso Wala	volcanic	Fine grained mafic rock, mm - cm scale layering							?Barique Group	?Banda Megasequence	5/06
AB446A	-8.66533	126.32095	Oso Wala	volcanic	Green-grey crystalline mafic rock, exhibits a fine foliation? ?metamorphosed							?Barique Group	?Banda Megasequence	5/06
AB446B	-8.66533	126.32095	Oso Wala	volcanic	Green-grey crystalline mafic rock, exhibits a fine foliation? ?metamorphosed							?Barique Group	?Banda Megasequence	5/06
AB446C	-8.66533	126.32095	Oso Wala	volcanic	Green-grey crystalline mafic rock, exhibits a fine foliation? ?metamorphosed. This example appears folded?							?Barique Group	?Banda Megasequence	5/06
AB447	-8.68335	126.38879	Laritame	no sample	First appearance of Baucau Limestone which appears to be in situ							Baucau Limestone	Synorogenic Megasequence	6/06
AB448	-8.68655	126.39561	Laritame	?volcanic	Scree sample found on Baucau Limestone at plateau at top of Laritame. Strange, iron-rich rock. Balls of iron 1-2 mm in size in an orange ?iron-oxide matrix. Sediment? Weathered volcanic?							Baucau Limestone	Synorogenic Megasequence	6/06
AB449	-8.95180	125.37078	Bobonaro Springs	observation	p345-347 looking west towards Loelako, Bedding on the eastern side of Loelako dips 15-20° towards S-SSE							observation point		10/06
AB450A	-8.98977	125.27487	Loelako	sandstone	thinly bedded folded and deformed interbedded mudstone/sandstone - as at AB420	Residue contains some rare foram tests and test fragments					Unknown	?Babulu Group	?Gondwana Megasequence	11/06

Location_No	Lat	Long	Region	Sample_type	Field_Description	Rock_Description	Benthic_foraminifera	Planktonic_foraminifera	OtherBioclasts	Facies	Age	Group	Megasequence	Date
AB450B	-8.98977	125.27487	Loelako	sandstone	thinly bedded folded and deformed interbedded mudstone/sandstone - as at AB420	fg sandstone, no biogenic grains visible. Thin section needed to identify minerals.					Unknown	?Babulu Group	?Gondwana Megasequence	11/06
AB451	-8.98736	125.27351	Loelako	no sample	Bandeira Group Limestone in scree							Bandeira Group	Gondwana Megasequence	11/06
AB452A	-8.98661	125.27469	Loelako	limestone	Wackestone with abundant small grains of ?	Fossiliferous wackestone. Shell fragments, foraminera, ?algae	miliolids (Karaburunia)		ostracods, algal nodules		Late Triassic	Bandeira Group	Gondwana Megasequence	11/06
AB452B	-8.98661	125.27469	Loelako	limestone	Fine grained grey limestone, chert nodules	Shelly wackestone with rare small forams and ostracods. Very recrystallised	miliolids				Late Triassic	Bandeira Group	Gondwana Megasequence	11/06
AB453	-8.98661	125.27556	Loelako	observation	Edge of steep gully separating sandstone/mudstone on southeast from huge limestone cliffs on northwest							observation point		12/06
AB454	-8.98128	125.27472	Loelako	observation	Entering jungle, possible lithology change? Abundant limestone scree							observation point		12/06
AB455	-8.98044	125.27566	Loelako	limestone	Grey massive limestone, extensively recrystallised	Micritic limestone with rare forams	miliolids		Coralline algae??		Late Triassic	Bandeira Group	Gondwana Megasequence	12/06
AB456	-8.98043	125.27578	Loelako	limestone	Massive grey limestone	Micritic limestone, very few biogenic grains visible			Gastropods, echinoids		?Late Triassic	?Bandeira Group	?Gondwana Megasequence	12/06
AB457	-8.98029	125.27580	Loelako	no sample	Same outcrop as AB456						?Late Triassic	?Bandeira Group	?Gondwana Megasequence	12/06
AB458	-8.97983	125.27543	Loelako	no sample	Same outcrop as AB456						?Late Triassic	?Bandeira Group	?Gondwana Megasequence	12/06
AB459	-8.97957	125.27559	Loelako	limestone	Massive grey limestone, small brac/bivalve ≈ 10 mm	Extensively recrystallised and dolomitised limestone containing some rare forams	duostominids, miliolids		ostracods		Late Triassic	Bandeira Group	Gondwana Megasequence	12/06
AB460	-8.97918	125.27569	Loelako	no sample	As at AB456-459						?Late Triassic	?Bandeira Group	?Gondwana Megasequence	12/06
AB461	-8.97931	125.27274	Loelako	no sample	As at AB420/AB450							?Babulu Group	?Gondwana Megasequence	12/06
AB462A	-8.98065	125.27182	Loelako	sandstone	Interbedded sandstone/mudstone. Sandstone is friable and qtz rich	fg well sorted subrounded micaceous qtz sandstone, no biogenic grains visible					Neogene	?Viqueque Group	Synorogenic Megasequence	12/06
AB462B	-8.98065	125.27182	Loelako	mudstone	Interbedded sandstone/mudstone	Similar residue to AB462A but less abundant mica and contains some very rare planktonic forams (just 9 tests/test fragments in entire residue - a.v. 1 per picking tray!)		Globorotalia (sinistral), Globigerinoides		outer neritic/upper bathyal	Neogene	?Viqueque Group	Synorogenic Megasequence	12/06
AB463	-8.98095	125.27942	Loelako	observation	see notebook for bearings from this point to Loelako features							observation point		13/06
AB464	-8.97812	125.27958	Loelako	limestone	Very weathered white, crystalline, sugary limestone	Extensively recrystallised, one cm thick bed of shell & echinoid fragments - shallow water? No smaller biogenic grains visible					?Late Triassic	?Bandeira Group	?Gondwana Megasequence	13/06
AB465	-8.97805	125.27927	Loelako	limestone	Very well bedded white limestone	Extensively recrystallised, similar litholgy to AB464 but without the larger shell fragments					?Late Triassic	?Bandeira Group	?Gondwana Megasequence	13/06
AB466	-8.97800	125.27906	Loelako	no sample	Same lithology as AB465, exposed fault surface						?Late Triassic	?Bandeira Group	?Gondwana Megasequence	13/06
AB467	-8.98278	125.27974	Loelako	mudstone	Grey, friable, micaceous sandy mudstone	Residue comprises predominantly mafic lithic grains. No biogenic grains visible.					Unknown	Unknown	Unknown	13/06
AB468	-8.98557	125.27989	Loelako	limestone	Medium bedded grey limestone, abundant halobia type filaments, some sulphides, bioturbated	Wackestone with abundant shell fragments (bivalves, brachiopods, gastropods), small nodosariids. Transitional facies between Bandeira and Aitutu facies	nodosariids, Lenticulina (diverse but not strongly ornamented), miliolids		bivalves, brachiopods, gastropods, crinoids, ostracods		Triassic	Transitional Bandeira/Aitutu	Gondwana Megasequence	13/06
AB469	-8.98692	125.27844	Loelako	limestone	Grey medium bedded wackestone with tiny < 0.2 mm grains (?forams). Abundant chert nodules. Could be siliceous	Bivalve packstone with rare small forams. Transitional facies between Bandeira and Aitutu facies			bivalves, brachiopods		Triassic	Transitional Bandeira/Aitutu	Gondwana Megasequence	13/06
AB470	-8.95790	125.28507	Loelako	observation	Caixa Postal bearing 280							observation point		14/06
AB471	-8.95923	125.28142	Loelako	limestone	Well bedded grey limestone with abundant small, round grains	vfg rock containing radiolaria. Abundant dolomite rhombs, concentrated in cm scale layers			sponge spicules		Unknown	Unknown	Unknown	14/06
AB472	-8.95966	125.28071	Loelako	limestone	Massive grey limestone, abundant shell fragments and other large fossils	Fossiliferous wackestone, abundant shell fragments and algal material			Gastropods, punctate brachiopods, ?chambered sponge,		Late Triassic	Bandeira Group	Gondwana Megasequence	14/06
AB473	-8.95976	125.28027	Loelako	limestone	Pink, sugary, recrystallised limestone	Highly dolomitised. No biogenic grains visible.					Unknown	Unknown	Unknown	14/06

Location_No	Lat	Long	Region	Sample_type	Field_Description	Rock_Description	Benthic_foraminifera	Planktonic_foraminifera	OtherBioclasts	Facies	Age	Group	Megasequence	Date
AB474	-8.96113	125.28029	Loelako	limestone	Base of giant cliffs. Subvertically bedded grey limestone.	Floatstone. Distinct bedding visible. Bed 1 contains grains 1 - 2 mm. Bed 2 contains grains < 0.2 mm.	Aulotortus, Duostomina		crinoids, shell fragments, large gastropods, coral, intact ostracods, algal nodules		Late Triassic	Bandeira Group	Gondwana Megasequence	14/06
AB475	-8.96149	125.28024	Loelako	no sample	Highest point we can climb. Same lithology as AB474						Late Triassic	Bandeira Group	Gondwana Megasequence	14/06
AB476	-8.95931	125.28329	Loelako	conglomerate	Range of different rounded - subrounded clasts (2 - 100 mm) including limestone, mudstone, qtz, in a sandy-mud matrix. River deposit? Abundant in scree along this path						?Quaternary	Recent surficial deposits	Recent surficial deposits	14/06
AB477A	-8.98174	125.28316	Loelako	limestone	Interbedded, indurated grey limestones and friable mudstones. Limestone beds 5 - 50 cm, one mudstone bed > 100 cm. Some halobia type filaments visible in limestone beds.	Stylotised wackestone. Abundant calcispheres & radiolaria. One foram in peel (?nodosarid)			calcispheres, radiolaria, echinoid debris, rare ostracods		Triassic	Aitutu Group	Gondwana Megasequence	15/06
AB477B	-8.98174	125.28316	Loelako	mudstone	Interbedded, indurated grey limestones and friable mudstones. Limestone beds 5 - 50 cm, one mudstone bed > 100 cm.	Abundant feldspar. Some rare foram tests and test fragments.					Triassic	Aitutu Group	Gondwana Megasequence	15/06
AB478	-8.98217	125.28309	Loelako	limestone	Grey limestone with abundant large fossils, mostly bivalves. Also some sulphides	Majority of peel is fg micrite with a ≈ 1 cm shelly bed visible at the top. Abundant stylolites. Contains calcispheres & radiolaria. Rare forams (?nodosarids). Will use large bivalves to date			Halorella (braciopods)		Triassic	Aitutu Group	Gondwana Megasequence	15/06
AB479	-8.98218	125.28281	Loelako	limestone	Very well bedded limestone with thin mudstone interbeds. Aitutu?	Extensively stylotised and veined micrite containing calcispheres and rare ostracods			Calcispheres, ostracods		?Triassic	?Aitutu Group	?Gondwana Megasequence	15/06
AB480	-8.98245	125.28218	Loelako	no sample	Still many large bivalves in scree rocks						?Triassic	?Aitutu Group	?Gondwana Megasequence	15/06
AB481	-8.98246	125.28212	Loelako	no sample	as at AB479, last outcrop before emerging from gully						?Triassic	?Aitutu Group	?Gondwana Megasequence	15/06
AB482	-8.98298	125.28225	Loelako	limestone	Thickly bedded white crystalline limestone	Completely recrystallised and dolomitised, no biogenic grains visible					Unknown	Unknown	Unknown	15/06
AB483	-8.98086	125.28334	Loelako	limestone	Thickly bedded white crystalline limestone	Highly recrystallised and dolomitised. Some remnant duotaxis visible?					Unknown	Unknown	Unknown	15/06
AB484	-8.75446	126.44965	Builo	mudstone	Large outcrop of grey-brown mudstone, containing small white flecks (forams?). Outcrop is deformed with abundant veins and small faults.	Abundant planktonic forams in 150 micron residue		Globigerinoides triloba, Globorotalia kugleri			Oligocene-Miocene boundary	Booi Group	Banda Megasequence	21/06
AB485	-8.74616	126.46346	Builo	limestone	well bedded grey wackestone with abundant chert nodules and cherty beds	Micritic limestone containing radiolaria and possibly some small forams					Unknown	?Noni Group	?Proto Indian Ocean Megasequence	21/06
AB486	-8.74567	126.46315	Builo	limestone	white wackestone (small ?forams within a mud sized matrix). Less chert than AB485	Micritic limestone containing vfg skeletal fragments possibly including forams	ornamented nodosariids, rare carbonate cemented agglutinated forms		Bivalves, ostracods, ?radiolaria		?Jurassic	?Noni Group	?Proto Indian Ocean Megasequence	21/06
AB487A	-8.77688	126.39175	Builo	mudstone	Interbedded **red-grey mudstone** and friable, white porous fine sandstone. Some ?siliceous looking layers. Bedding 5 - 15 cm. Extensively folded and faulted - bedding is chaotic.	Rare radiolaria in 150 micron residue.						?Noni Group	?Proto Indian Ocean Megasequence	22/06
AB487B	-8.77688	126.39175	Builo	sandstone	Interbedded red-grey mudstone and **friable, white porous fine sandstone**. Some ?siliceous looking layers. Bedding 5 - 15 cm. Extensively folded and faulted - bedding is chaotic.	Radiolarite. Abundant radiolaria in residue and peel, one possible foram (40)						?Noni Group	?Proto Indian Ocean Megasequence	22/06
AB487C	-8.77688	126.39175	Builo	unknown	Interbedded red-grey mudstone and friable, white porous fine sandstone. **Some ?siliceous looking layers.** Bedding 5 - 15 cm. Extensively folded and faulted - bedding is chaotic.	Siliceous layers are likely altered radiolarite						?Noni Group	?Proto Indian Ocean Megasequence	22/06
AB488A	-8.76563	126.41127	Builo	mudstone	Interbedded **mudstone** and fine sandstone/siltstone, similar to AB487. Well defined bedding.	Abundant forams and radiolaria in residue, only forams picked.						?Booi Group	?Banda Megasequence	22/06
AB488B	-8.76563	126.41127	Builo	siltstone	Interbedded mudstone and **fine sandstone/siltstone**, similar to AB487. Well defined bedding.	vfg sandstone, no biogenic grains visible						?Booi Group	?Banda Megasequence	22/06

Location_No	Lat	Long	Region	Sample_type	Field_Description	Rock_Description	Benthic_foraminifera	Planktonic_foraminifera	OtherBioclasts	Facies	Age	Group	Megasequence	Date
AB489A	-8.74801	126.38820	Builo	mudstone	Interbedded **mudstone** and sandstone. Sandstone beds display hummocky cross bedding and load clasts at base. See sketch.	63 micron residue contains radiolaria and some very small, elongate, tubular forams. Also rare conodonts.	Pseudonodosaria, Dentalina sp., Astacolus sp., all unornamented		conodonts		Late Triassic	?Babulu Group	Gondwana Megasequence	22/06
AB489B	-8.74801	126.38820	Builo	sandstone	Interbedded mudstone **and sandstone**. Sandstone beds display hummocky cross bedding and load clasts at base. See sketch.	vfg sandstone, no biogenic grains visible						?Babulu Group	Gondwana Megasequence	22/06
AB490	-8.75706	126.39331	Builo	no sample	Ooid wackestone							Perdido Group	Gondwana Megasequence	22/06
AB491A	-8.60725	126.57100	Quelecai	sandstone	fg, grey, **?volcanic sandstone** with pervasive slatey cleavage. Contains some large clasts of ?volcanic sandstone/breccia	vfg ?sandstone					?Permian	?Cribas Group	?Gondwana Megasequence	3/07
AB491B	-8.60725	126.57100	Quelecai	?sandstone	fg, grey ?volcanic sandstone with pervasive slaty cleavage. Contains some large **clasts of ?volcanic sandstone/breccia**	Very well graded rock. Grades from cg biogenic and lithogenic clasts in a muddy, sandy matrix into a vfg sandstone containing a few fine bivalve filaments and other fg skeletal fragments. Contains a few rare forams. Clasts are possibly from many different ages, Triassic, Eocene, ?Permian...			bivalves, rhynchonellid brachiopods, crinoids, echinoids, bryozoans		?Permian	?Cribas Group	?Gondwana Megasequence	3/07
AB492	-8.60796	126.56995	Quelecai	no sample	Similar to AB491 but finer grained and very slatey cleavage. No clasts.						?Permian	?Cribas Group	?Gondwana Megasequence	3/07
AB493	-8.60866	126.56984	Quelecai	mudstone	Grey, fissile mudstone	Abundant radiolaria in residue. Some forms look similar to forams but are likely just rads stuck together					?Permian	?Cribas Group	?Gondwana Megasequence	3/07
AB494A	-8.60974	126.57055	Quelecai	?turbidite	Well bedded red-green sandstone and **graded ?volcanic flows.**	Very well graded turbidite containing abundant bryozoans and very well preserved Colaniella	Colaniella		Fenestrate bryozoans, echinoids		Late Permian	?Cribas Group	Gondwana Megasequence	3/07
AB494B	-8.60974	126.57055	Quelecai	sandstone	Well bedded red-green **sandstone** and graded ?volcanic flows.						Late Permian	?Cribas Group	Gondwana Megasequence	3/07
AB495	-8.61092	126.57333	Quelecai	mudstone	Micaceous mudstone with very thin (< 5 mm) sandstone interbeds.	Some radiolaria and rare very small forams								3/07
AB496	-8.61559	126.57559	Quelecai	conglomerate	Conglomerate grading into sandstone, containing shells and many limestone clasts in a sandy matrix.	Very poorly sorted subangular limestone and mudstone clasts in a muddy, sandy matrix. Clasts contain abundant bryozoans, large shell fragments and rare forams. Clasts are possibly from many different ages, Triassic, Eocene, ?Permian...			Bryozoans					3/07
AB497	-8.61280	126.57378	Quelecai	limestone	Well bedded **limestone** (beds 10 - 30 cm) and mudstone (beds < 70 cm). Limestone is grey, highly indurated with a slightly concoidal fracture (siliceous?). Tiny dark specs visible which may be rads. Cut by abundant large (≈ 10 mm) calcite veins.	Wackestone containing abundant vf high relief grains (?sand) and very small forams	nodosariids, ?Atsabella				Triassic	Aitutu Group	Gondwana Megasequence	3/07
AB498	-8.61260	126.57195	Quelecai	?volcanic	?Volcanic breccia						?Permian	?Cribas Group	?Gondwana Megasequence	3/07
AB499	-8.61319	126.57823	Quelecai	igneous	?pillow basalt						?Permian	?Cribas Group	?Gondwana Megasequence	4/07
AB500	-8.61187	126.57996	Quelecai	limestone	Well bedded limestone and mudstone. Limestone is grey, indurated and contains halobia filaments.	Wackestone containing thin bivalve filaments commonly concentrated in beds, rare small forams	miliolids, Atsabella		Bivalve filaments		Triassic	Aitutu Group	Gondwana Megasequence	4/07
AB501	-8.61030	126.58347	Quelecai	no sample	Same as AB500						Triassic	Aitutu Group	Gondwana Megasequence	4/07
AB502	-8.60929	126.58643	Quelecai	observation	See notebook for sketch of observations from this point							observation point		4/07
AB503A	-8.60993	126.58359	Quelecai	mudstone	dark grey mudstone	Rare forams and radiolaria. Abundant sulfides.								4/07
AB503B	-8.60993	126.58359	Quelecai	igneous	pillow basalt in scree						?Permian	?Cribas Group	?Gondwana Megasequence	4/07
AB504	-8.61518	126.57493	Quelecai	mudstone	dark grey mudstone	Rare forams, rare radiolaria (fewer than previous samples), some rare echinoid spines?								4/07
AB505	-8.61248	126.57413	Quelecai	observation	See notebook for sketch of observations from this point							observation point		4/07

Location_No	Lat	Long	Region	Sample_type	Field_Description	Rock_Description	Benthic_foraminifera	Planktonic_foraminifera	OtherBioclasts	Facies	Age	Group	Megasequence	Date
AB506	-8.61094	126.57320	Quelecai	mudstone	grey mudstone with small (≈ 0.1 mm) black flecks	very rare forams and radiolaria, abundant qtz in this sample. Bryozoan is contamination								4/07
AB507	-8.61060	126.57275	Quelecai	igneous	appears to be an eruptive, ?pyroclastic rock rather than pillow basalt.	Pillow breccia								4/07
AB508	-8.61025	126.57284	Quelecai	sandstone	Medium grained sandstone. In block at base of landslide. Contains qtz and a variety of other grains. Mostly subrounded and poorly sorted.	No biogenic grains visible in peel or residue, residue comprises predominantly subangular lithic fragments					Unknown	Unknown	Unknown	4/07
AB509	-8.60660	126.57227	Quelecai	no sample	mudstone									5/07
AB510	-8.60642	126.57233	Quelecai	observation	See notebook for structural observations made from this point							observation point		5/07
AB511	-8.60610	126.57371	Quelecai	no sample	Mudstone with sandstone interbeds									5/07
AB512	-8.60563	126.57360	Quelecai	limestone	Interbedded grey, indurated, fg **limestone** and grey, fg mudstone. Limestone is bioturbated, and contains tiny dark specs which may be rads.	Radiolarite containing bivalve filaments, echinoid fragments and rare nodosarids	nodosariids, Lenticulina		Radiolaria, bivalve filaments, echinoid fragments		Late Triassic	Aitutu Group	Gondwana Megasequence	5/07
AB513	-8.60596	126.57436	Quelecai	limestone	Interbedded mudstone and **fossiliferous limestone.** Limestone contains ?forams and ?shell fragments.	Ooid packstone containing shell fragments and many small forams including Lenticulina. Packstone-mudstone contact shows rip-up clasts of mudstone, this bed is likely a debris slide transporting shallow water fauna to within Aitutu mudstones	Lenticulina, Opthalmidium		peloids		Late Triassic	Transitional Bandeira/Aitutu	Gondwana Megasequence	5/07
AB514	-8.60581	126.57455	Quelecai	no sample	same as AB513						Late Triassic	Transitional Bandeira/Aitutu	Gondwana Megasequence	5/07
AB515A	-8.60557	126.57476	Quelecai	?limestone	Interbedded **limestone** and mudstone	Indurated mudstone? too porous for useful peel					Unknown	Unknown	Unknown	5/07
AB515B	-8.60557	126.57476	Quelecai	mudstone	Interbedded limestone and **mudstone**	Abundant small forams	Diverse assemblage of organic cemented agglutinated foraminifera, lagenids and robertinids. Species include Cryptoseptida oberhauseri, Duostomina biconvexa, Dentalina sp.				Carnian to Early Norian	Transitional Bandeira/Aitutu	Gondwana Megasequence	5/07
AB516	-8.60451	126.57361	Quelecai	limestone	Well bedded pink-grey wackestone. Abundant small grains which are most likely forams.	Extensively recrystallised and dolomitised but many ghosts of forams visible					Unknown	Unknown	Unknown	5/07
AB517	-8.60645	126.57247	Quelecai	mudstone	mudstone with thin sandstone interbeds	Abundant forams, mainly benthic with rare planktonic	Diverse assemblage of organic cemented agglutinated foraminifera, lagenids and robertinids. Species include Cryptoseptida oberhauseri, Duostomina biconvexa				Carnian to Early Norian	Transitional Bandeira/Aitutu	Gondwana Megasequence	5/07
AB518	-8.60635	126.56752	Quelecai	igneous	Course grained mafic - intermediate boulders in scree						?Permian	?Cribas Group	?Gondwana Megasequence	5/07
AB519	-8.60677	126.56457	Quelecai	no sample	Extremely weathered and deformed red and grey ?volcanics. Remnant igneous textures visible. Very weathered - looks superficially like mud.						?Permian	?Cribas Group	?Gondwana Megasequence	5/07
AB520	-8.60895	126.58690	Quelecai	no sample	Course grained weathered igneous rocks - see notebook for sketch						?Permian	?Cribas Group	?Gondwana Megasequence	6/07
AB521	-8.60893	126.58695	Quelecai	no sample	Grey mudstone with thin beds (5 - 20 cm) of indurated grey ?limestone, which appears slightly siliceous. Tiny specs which are possible rads. Prevented by locals from sampling.							?Aitutu Group	?Gondwana Megasequence	6/07

Location_No	Lat	Long	Region	Sample_type	Field_Description	Rock_Description	Benthic_foraminifera	Planktonic_foraminifera	OtherBioclasts	Facies	Age	Group	Megasequence	Date
AB522	-8.60857	126.58746	Quelecai	no sample	Same as AB 521 but indurated beds are thinner.							?Aitutu Group	?Gondwana Megasequence	6/07
AB523	-8.60795	126.58774	Quelecai	observation	See notebook for sketch of observations from this point							observation point		6/07
AB524	-8.60733	126.58907	Quelecai	observation	From around this point the bedrock changes from mudstones to volcanics, heading towards the mountain.							observation point		6/07
AB525	-8.58057	126.54772	Quelecai	limestone	Will bedded, siliceous limestone with thin mudstone	Radiolarian wackestone			Abundant radiolaria		Triassic	Aitutu Group (by	Gondwana	7/07
AB526A	-8.64601	126.62655	Baguia	chert	Interbedded **red chert** and red mudstone. Abundant small transparent spheres (rads?) in the red chert. No visible bioclasts in the mudstone but it does have an oily sheen. Bedding 5 - 10 cm. Outcrop is folded into a roughly anticlinal structure - see notebook for sketch.	Radiolarian chert with rare ?bivalve filaments			Abundant radiolaria, rare ?bivalve filaments		?Jurassic	?Noni Group	?Proto Indian Ocean Megasequence	8/07
AB526B	-8.64601	126.62655	Baguia	mudstone	Interbedded red chert and **red mudstone**. Abundant small transparent spheres (rads?) in the red chert. No visible bioclasts in the mudstone but it does have an oily sheen. Bedding 5 - 10 cm. Outcrop is folded into a roughly anticlinal structure - see notebook for sketch.						?Jurassic	?Noni Group	?Proto Indian Ocean Megasequence	8/07
AB527	-8.64595	126.62607	Baguia	mudstone	Grey massive, deformed mudstone. No bioclasts visible. Next to outcrop are two large boulders of black basalt.	Barren residue					Unknown	Unknown	Unknown	8/07
AB528	-8.64657	126.62610	Baguia	limestone	Extensively recrystallised and stylotised limestone. Few clasts of original limestone remaining but what is there appears to be a light grey foraminiferal wackestone.	Samples consists mostly of large calcite crystals but has small clasts of wackestone containing abundant planktonic foraminifera		Morozovella, Acarinina			early Eocene	Kolbano Group	Australian Margin Megasequence	8/07
AB529	-8.65336	126.62354	Baguia	no sample	Very weathered red-green ?volcanics/?metavolcanics									8/07
AB530	-8.65148	126.62193	Baguia	limestone	Orange-grey ooid packstone	?peloid packstone containing rare small forams	Lenticulina				?Triassic	?Bandeira Group	Gondwana Megasequence	8/07
AB531	-8.64153	126.63850	Baguia	limestone	Yellow-white thickly-bedded limestone. Abundant small grains, ?forams.	Wackestone containing abundant, very well preserved radiolaria and planktonic foraminifera. Some small cm scale chert nodules		Globigerinoides	Abundant radiolaria		?Oligocene	Kolbano Group	Australian Margin Megasequence	8/07
AB532	-8.63711	126.64435	Baguia	?sandstone	Blue-grey ?sandstone. Contains abundant small transparent grains (rads?) along with small black flecks. Rare mudstone interbeds < 10 cm. Sandstone beds ≥ 1 m	No biogenic grains visible in peel					Unknown	Unknown	Unknown	8/07
AB533	-8.63465	126.64681	Baguia	?sandstone	Similar blue-grey sandstone as AB532 but finer grained, less obvious fossils and thinner bedding	Siliceous rock possibly containing some radiolaria			?radiolaria		Unknown	Unknown	Unknown	8/07
AB534	-8.62919	126.65095	Baguia	observation	See field notebook for sketch of observations from this point.							observation point		8/07
AB535A	-8.83025	126.21319	Bibileu	limestone	Scree - white wackestone, extensively stylotised with small, elongate forams	Extensively stylotised micritic rock containing some rare forams and ?shell fragments			?shell fragments, brachiopods		?Triassic	?Bandeira or ?Perdido Group	Gondwana Megasequence	10/10
AB535B	-8.83025	126.21319	Bibileu	limestone	Scree - Pink, foliated wackestone. Extensively stylotised with pervasive foliation	Foliated wackestone containing abundant radiolaria and planktonic foraminifera. Rads are very well preserved but most forams are crushed and deformed		Acarinina			early to mid ?Eocene	Kolbano Group	Gondwana Megasequence	10/10
AB536	-8.82766	126.21032	Bibileu	no sample	Volcanic breccia - clasts 1 - 20 cm. Too weathered to sample							?Barique Group	?Banda Megasequence	10/10
AB537	-8.82787	126.21056	Bibileu	conglomerate	Fresh, white, large, spheroid grains (5 - 10 mm) in a grey/brown muddy, sandy matrix. Spheroid grains are mostly of chaotic orientation. Debris flow?	Foraminiferal muddy wackestone containing many larger benthic forams. Very shallow water carbonate platform	Alveolina, Nummulites, rotalids, miliolids				middle Eocene	Dartollu/Barique Group	Banda Megasequence	10/10
AB538	-8.82310	126.21236	Bibileu	observation	From the car until this point has all been Barique Formation							observation point		11/10
AB539	-8.82125	126.21186	Bibileu	observation	Scree here is all limestone. No bedrock visible but volcanics are absent from scree at this point.							observation point		11/10
AB540	-8.81996	126.21004	Bibileu	no sample	Volcanic breccia - very weathered							?Barique Group	?Banda Megasequence	11/10
AB541	-8.81678	126.20964	Bibileu	limestone	White, hard, crystalline limestone. Faint traces of ?ooids visible	Recrystallised ooid grainstone. Abundant micritised ooids and some larger shell fragments, a few ghosts of forams visible			Ooids, shell fragments including gastropods,			Perdido Group (by lithofacies correlation)	Gondwana Megasequence	11/10

Location_No	Lat	Long	Region	Sample_type	Field_Description	Rock_Description	Benthic_foraminifera	Planktonic_foraminifera	OtherBioclasts	Facies	Age	Group	Megasequence	Date
AB542	-8.81616	126.20856	Bibileu	limestone	Extensively deformed and recrystallised purple-brown limestone. Possibly Perdido Group?	Extensively recrystallised and dolomitised ooid packtone/grainstone containing abundant shell debri including gastropods			large shell fragments including gastropods, pectin bivalves, ostracods			Perdido Group (by lithofacies correlation)	Gondwana Megasequence	11/10
AB543	-8.81772	126.22132	Bibileu	limestone	Foliated, recrystallised yellow-white limestone	Stylotised and veined wackestone containing abundant planktonic foraminifera and well preserved radiolaria. Similar fauna to AB535B but this rock is more crystalline, less foliated		Acarinina, Morozovella	Abundant well preserved radiolaria		early-middle Eocene	Kolbano Group	Australian Margin Megasequence	11/10
AB544	-8.81964	126.22000	Bibileu	limestone	Pink, foliated limestone. Foliations ≈ 1 cm. No bioclasts visible under hand lens	Stylotised, foliated wackestone containing abundant radiolaria and rare planktonic foraminifera			Abundant radiolaria		early-middle Eocene	Kolbano Group	Australian Margin Megasequence	11/10
AB545	-8.81941	126.18077	Bibileu	sandstone	Brown/white fg-mg sandstone. Porous and friable. A range of grain types including small, rounded qtz grains, and small, rounded black grains which may be igneous in origin.	Foraminiferal sandstone		Morozovella			latest Paleocene - early Eocene	Un-named Eocene Banda	Banda Megasequence	12/10
AB546	-8.81877	126.18081	Bibileu	observation	All scree on this hill is igneous - appears basaltic. A few metres up the hill from this point these rocks are found in situ.							observation point		12/10
AB547	-8.81808	126.18377	Bibileu	observation	Hot springs approx. 50 m south of this point (not allowed to see their origin). All scree here is volcanic with rare limestone boulders. Alluvium in this stream is all black volcanics and schist.							observation point		12/10
AB548	-8.47405	127.18015	Paitchau	limestone	South side of La Mainina swallow hole. Extremely vegetated with rare outcrop of Baucau limestone. Bedding not visible.	Highly silicified and altered fossiliferous limestone, contains one large bivalve ~25 mm, with abundant ghosts of foraminifera						Baucau Limestone	Synorogenic Megasequence	14/10
AB549	-8.49098	127.17594	Paitchau	limestone	Scree. Large boulders of indurated, grey wackestone. Rare transparent circular to ovoid grains ≈ 1 mm in size.	Recrystallised packstone/bindstone with abundant algal material and some forams					Late Triassic	Bandeira Group	Gondwana Megasequence	15/10
AB550	-8.49064	127.17624	Paitchau	observation	No GPS signal. Approx. 50 m NE of AB549. Baucau Limestone disappears from scree at this point. All scree here is indurated grey wackestone as at AB549. Very close to contact.							observation point		15/10
AB551	-8.48134	127.18511	Paitchau	limestone	At drill hole AB1. Indurated grey wackestone. Sample taken from outcrop 3 m from hole.	Packstone comprising algal nodules and growths, ooids, large shell fragments and abundant foraminifera	Duostomina,		Thaumatoporellacean algae		Late Triassic	Bandeira Group	Gondwana Megasequence	15/10
AB552	-8.40952	127.29011	Paitchau	limestone	Medium bedded grey limestone and interbedded chert. Chert beds 5 - 10 cm. Possible halobia filaments visible? Looks superficially like Aitutu Formation.	Highly recrystallised and dolomitised wackestone containing radiolaria and some thin bivalve filaments						Aitutu Group (by lithofacies correlation)	Gondwana Megasequence	16/10
AB553	-8.40738	127.28833	Paitchau	no sample	Baucau Limestone							Baucau Limestone	Synorogenic Megasequence	16/10
AB554	-8.39826	127.27156	Paitchau	limestone	Well bedded white/brown wackestone Abundant transparent circular grains in a mud matrix. Bedding 10 - 20 cm. Outcrop is yellow/white with patches of pink.	Wackestone with abundant planktonic forams, including Morozovella		Morozovella			Early to Mid ?Eocene	Kolbano Group	Australian Margin Megasequence	16/10
AB555	-8.39853	127.26960	Paitchau	limestone	Very well bedded limestone with thin mudstone interbeds. Bedding 10 - 30 cm. Aitutu?	Cherty limestone with thin mudstone interbeds containing radiolaria, thin bivalve filaments and foraminifera. Possibly some shallow water fauna washed down	nodosariids, lagenoides		ostracods		Triassic	Aitutu Group	Gondwana Megasequence	16/10
AB556	-8.44861	127.19106	Paitchau	limestone	Scree. Large boulder of foliated foraminiferal wackestone. Many bulbous, chambered forams and possible Morozovella?	Foraminiferal wackestone/packstone. Abundant planktonic foraminifera including Morozovella		Globorotalia limbata, Dentoglobigerina altispira			N14-N15	Kolbano Group	Australian Margin Megasequence	17/10
AB557A	-8.45156	127.19093	Paitchau	limestone	Scree sample from base of mountain, collected about 100 m south of this point. Ooid grainstone.	Wackestone comprising algal nodules, gastropods and other large shell fragments, ooids and benthic forams	Duostomina, Aulotortus		Algal nodules, gastropods, shell debris, ooids		Late Triassic	Bandeira Group	Gondwana Megasequence	17/10
AB557B	-8.45156	127.19093	Paitchau	limestone	Scree sample from base of mountain, collected about 100 m south of this point. Wackestone.	Extensively recrystallised wackestone, rare ?forams			?gastropods		Late Triassic	Bandeira Group	Gondwana Megasequence	17/10
AB558	-8.44946	127.19135	Paitchau	limestone	No GPS signal. Southern edge of Mt Neliki. Fg calcilutite	Brecciated wackestone/packstone containing algal nodules, ooids, benthic forams			Algal nodules, ooids		Late Triassic	Bandeira Group	Gondwana Megasequence	17/10
AB559	-8.44532	127.19314	Paitchau	limestone	No GPS signal. Sample is ≈ 50 m bearing 115 from this point. Grey calcilutite, no bioclasts visible	Completely recrystallised and dolomitised, some ghosts of ooids and forams?						Bandeira Group	Gondwana Megasequence	17/10
AB560	-8.98892	125.31335	Bobonaro Springs	no sample	sheared melange outcrop							Melange zone	Melange zone	20/10

Location_No	Lat	Long	Region	Sample_type	Field_Description	Rock_Description	Benthic_foraminifera	Planktonic_foraminifera	OtherBioclasts	Facies	Age	Group	Megasequence	Date
AB561	-9.04036	125.27917	Saburai	no sample	Interbedded white/grey limestone and dark grey shale. Limestone beds 20 - 40 cm. Shale beds 5 - 10 cm. Possible Aitutu.							?Aitutu Group	?Gondwana Megasequence	21/10
AB562	-9.05390	125.26306	Saburai	observation	See notebook for sketch of observations from this point							observation point		21/10
AB563	-9.06221	125.26133	Saburai	no sample	large blocks of igneous (volcanogenic sediments?) in melange							?Melange zone	?Melange zone	21/10
AB564	-9.07802	125.25417	Saburai	observation	Large, flat plane of cliff (fault?)							observation point		21/10
AB565	-9.08156	125.24873	Saburai	fault gouge	limestone fault gouge	No biogenic grains visible in peel					Unknown	Unknown	Unknown	21/10
AB566	-9.09353	125.24155	Saburai	observation	Fault plane							observation point		21/10
AB567	-9.26167	125.07603	Taroman	limestone	Weakly bedded limestone with very abundant chert. Some blocks appear very deformed and recrystallised	Siliceous rock containing abundant radiolaria, also some ?bivalve filaments concentrated in thin beds			radiolaria, ?bivalve filaments		Triassic	Aitutu Group	Gondwana Megasequence	21/10
AB568	-9.20469	125.11344	Taroman	sandstone	fg-mg brown sandstone. Rounded to subrounded grains of qtz, fspr, mica, and some rare tiny grains which are possibly forams? Minor cross bedding	No biogenic grains visible in peel					Unknown	?Babulu Group	?Gondwana Megasequence	23/10
AB569	-9.20493	125.11730	Taroman	limestone	Grey ooid packstone/wackestone. Contains ooids and shell debris	Ooid packstone/grainstone. Dolomitised cement, some rare forams?						Perdido/Bandeira Group	Gondwana Megasequence	24/10
AB570	-9.20719	125.11818	Taroman	no sample	ooid grainstone - Perdido Group Limestone							Perdido Group	Gondwana Megasequence	24/10
AB571	-9.20759	125.11787	Taroman	observation	On the edge of an enormous grassy plain between two ridges. Gully strikes = SE. No limestone outcrop							observation point		24/10
AB572A	-9.20782	125.11742	Taroman	?schist	Weathered red/green ?chlorite schist.						Unknown	?Melange zone	?Melange zone	24/10
AB572B	-9.20782	125.11742	Taroman	siltstone	siltstone/sandy mudstone? Gritty grey rock containing some rounded, white grains	Sandy mudstone. White grains look possible micritic					Unknown	?Melange zone	?Melange zone	24/10
AB572C	-9.20782	125.11742	Taroman	?limestone	Deformed limestone? Contains chert nodules - possible AMM	Peel is entirely silica and calcite, no biogenic grains					Unknown	?Melange zone	?Melange zone	24/10
AB572D	-9.20782	125.11742	Taroman	?schist	Clast from shear zone - ?chlorite schist	Highly deformed, No biogenic grains					Unknown	?Melange zone	?Melange zone	24/10
AB572E	-9.20782	125.11742	Taroman	?limestone	Clast from shear zone - Chert/siliceous limestone						Unknown	?Melange zone	?Melange zone	24/10
AB572F	-9.20782	125.11742	Taroman	limestone	Clast from shear zone - limestone with angular, cherty nodules						Unknown	?Melange zone	?Melange zone	24/10
AB572G	-9.20782	125.11742	Taroman	?limestone	Clast from shear zone - limestone?	Foraminiferal wackestone/packstone. Abundant planktonic foraminifera		Acarinina, Morozovella			Early-early middle Eocene	Kolbano Group	Australian Margin Megasequence	24/10
AB572H	-9.20782	125.11742	Taroman	schist	Clast from shear zone - schist							?Melange zone	?Melange zone	24/10
AB572I	-9.20782	125.11742	Taroman	limestone	pink limestone with cherty nodules	Foliated pink wackestone containing abundant radiolaria, recrystallised ?bivalve filaments and rare foraminifera	Lenticulina		radiolaria, ostracods		Triassic	Transitional Bandeira/Aitutu	Gondwana Megasequence	24/10
AB573	-9.20767	125.11735	Taroman	limestone	Grey, deformed, stylotised limestone with abundant chert. Possibly AMM? No bedding visible	Mostly a stockwork of calcite and quartz veins with some limestone clasts, but no visible biogenic grains. Limestone clast comprise mainly micritised peloids					Triassic	?Transitional Bandeira/Aitutu	Gondwana Megasequence	24/10
AB574A	-9.20779	125.11742	Taroman	sandstone	Interbedded **grey sandstone** and dark grey mudstone. **Sandstone beds 10 - 30 cm**. Mudstone beds 20 - 60 cm. Similar to AB575 but with much mudstone beds are much thicker here compared to sandstone beds	Some vfg shell fragments and very rare forams visible in peel. One rad and some very rare forams in residue.					Late Triassic	Babulu Group	Gondwana Megasequence	24/10
AB574B	-9.20779	125.11742	Taroman	mudstone	Interbedded grey sandstone and **dark grey mudstone**. Sandstone beds 10 - 30 cm. **Mudstone beds 20 - 60 cm**. Similar to AB575 but with much mudstone beds are much thicker here compared to sandstone beds	Abundant very small, planispiral forams. Very little teperature maturity - low burial	Dentalina, Pseudonodosaria, Glomospirella	Globotruncana (contamination?)	Ostracods, conodonts		Late Triassic	Babulu Group	Gondwana Megasequence	24/10
AB575A	-9.20752	125.11737	Taroman	sandstone	**Thick beds of grey sandstone/marl (< 1 m)**, interbedded with thin (20 - 30 cm) beds of grey mudstone	Muddy sandstone composed predominantly of bryozoan and crinoid debri			Bryozoans, crinoids		?Triassic	Possible debris slide from Bandeira into Babulu	Gondwana Megasequence	24/10
AB575B	-9.20752	125.11737	Taroman	mudstone	Thick beds of grey sandstone/marl (< 1 m), interbedded with **thin (20 - 30 cm) beds of grey mudstone**	Barren residue, mainly lithic (mafic igneous?) fragments						?Babulu Group	?Gondwana Megasequence	24/10
AB576	-9.20823	125.11717	Taroman	no sample	On this side of the river, under grass and soil, is all weathered schist							?Melange zone	?Melange zone	24/10
AB577	-9.20758	125.11686	Taroman	no sample	At this point, to the NW of the shear zone in the river, bedrock all looks like in situ limestones (same cherty, ?AMM limestone as at AB573)							?Bandeira Group	?Gondwana Megasequence	24/10

Location_No	Lat	Long	Region	Sample_type	Field_Description	Rock_Description	Benthic_foraminifera	Planktonic_foraminifera	OtherBioclasts	Facies	Age	Group	Megasequence	Date
AB578	-9.20758	125.11670	Taroman	no sample	Tiny, very weathered outcrop of the same shear zone?? Weathered ?schist containing clasts of weathered??? Foliation strikes ≈ E-W. Check on map							?Melange zone	?Melange zone	24/10
AB579	-9.20655	125.11735	Taroman	observation	Large fault at this point - however no evidence left in situ to measure - recent landslip							observation point		24/10
AB580	-9.20971	125.11701	Taroman	no sample	"pinnacle" hill in the middle of a grassy plain (which has mostly been mud and schist). This hillside is made of very weathered igneous, mafic rock. Is now mostly iron oxides and secondary minerals. Possible remnant textures of pillows. This valley is possibly one big melange zone?							?Melange zone	?Melange zone	25/10
AB581A	-9.21157	125.11657	Taroman	limestone	Large, weathered outcrop of very indurated, fractured and stylotised **yellow/white pelagite (AB581A)**, with some minor grey pelagite (AB581B). Wackestone with some very small transparent grains which are possibly forams.	Completely dolomitised, no biogenic grains visible					Unknown	Unknown	Unknown	25/10
AB581B	-9.21157	125.11657	Taroman	limestone	Large, weathered outcrop of very indurated, fractured and stylotised yellow/white pelagite (AB581A), with some minor **grey pelagite (AB581B)**. Wackestone with some very small transparent grains which are possibly forams.	Completely recrystallised, no biogenic grains visible					Unknown	Unknown	Unknown	25/10
AB582	-9.21313	125.11624	Taroman	no sample	top of hill - very weathered but looks like same pelagite as at AB581						Unknown	Unknown	Unknown	25/10
AB583	-9.21458	125.11581	Taroman	mudstone	pale grey/yellow goethite stained mudstone	No biogenic grains visible, barren residue also					Unknown	Unknown	Unknown	25/10
AB584	-9.21447	125.11383	Taroman	no sample	Orange/grey iron stained mud containing clasts (1 - 30 cm) of very weathered fg-mg igneous material. No clasts contain qtz, just weathered feldspars and fe & mg oxides. Mud looks and feels just like saprolitic clay.						Unknown	?Melange zone	?Melange zone	25/10
AB585	-9.21524	125.11316	Taroman	observation	Giant fault plane, top section recently exposed by landslip. Juxtaposes limestones on the SE with mudstones on the NW. Two main directions of slip but dominantly SW. See notebook for observations							observation point		25/10
AB585A	-9.21524	125.11316	Taroman	limestone	Limestone from face of fault. Grey, very recrystallised	Completely recrystallised, no biogenic grains visible					Unknown	Unknown	Unknown	25/10
AB585B	-9.21524	125.11316	Taroman	fault gouge	Fault gouge from just above face of fault	Ooid packstone/grainstone. Dolomitised cement.						?Perdido Group (by lithofacies correlation)	Gondwana Megasequence	25/10
AB585C	-9.21524	125.11316	Taroman	?limestone	Rounded clast from within orange mud. The mud may be the gouge itself??	Highly recrystallised ?wackestone. Occasional large shell fragments and rare forams	Lenticulina				?Latest Triassic	?Aitutu Group	Gondwana Megasequence	25/10
AB585D	-9.21524	125.11316	Taroman	mudstone	Orange/grey mud from around clasts	Some rare forams in residue, including ?duostomina cast (6)					Late Triassic - Early Jurassic			25/10
AB586	-9.21409	125.11311	Taroman	limestone	Ridge front is ooid packstone - Perdido Group Limestone. Grey, indurated, massive limestone. Across the other side of the gully, to the SE, across the fault, is what looked like AMM	Ooid packstone/grainstone. Large ooids.						Perdido Group (by lithofacies correlation)	Gondwana Megasequence	25/10
AB587	-9.21385	125.11362	Taroman	no sample	Probably the same fault as at AB585							observation point		25/10
AB588	-9.21192	125.11391	Taroman	schist	weathered to various degrees from the surface, with dark black mafic schist exposed at the base by a landslip	No biogenic grains visible					Unknown	?Melange zone	?Melange zone	25/10
AB589	-9.21002	125.11448	Taroman	no sample	more weathered schist at this point. Most likely underlies most of the grassy plains						Unknown	?Melange zone	?Melange zone	25/10
AB590A	-9.20720	125.11387	Taroman	sandstone	Interbedded grey sandstone and red mudstone in path. Looks superficially similar to AB574. **AB590A is mg sandstone, subangular clasts of a variety of types including lithic fragments and possible bioclasts. Bedding 5 - 20 cm.** AB590B is red mudstone, bedding ≈ 50 cm.	Highly siliceous, no biogenic grains visible in peel					Unknown	?Babulu Group	?Gondwana Megasequence	25/10

Location_No	Lat	Long	Region	Sample_type	Field_Description	Rock_Description	Benthic_foraminifera	Planktonic_foraminifera	OtherBioclasts	Facies	Age	Group	Megasequence	Date
AB590B	-9.20720	125.11387	Taroman	mudstone	Interbedded grey sandstone and red mudstone in path. Looks superficially similar to AB574. AB590A is mg sandstone, subangular clasts of a variety of types including lithic fragments and possible bioclasts. Bedding 5 - 20 cm. **AB590B is red mudstone, bedding ≈ 50 cm.**	Barren residue					Unknown	?Babulu Group	?Gondwana Megasequence	25/10
AB591	-9.20588	125.11443	Taroman	no sample	possible fg volcanic sediment. Too weathered to sample						Unknown	Unknown	Unknown	25/10
AB592	-9.18304	125.14609	Taroman	no sample	interbedded fg micaceous sandstone and grey mudstone. Very weathered. Possible BabuluFormation. Looks similar to Babulu Formation on ridge south of Loelako							?Babulu Group	?Gondwana Megasequence	26/10
AB593	-9.18096	125.15288	Taroman	no sample	same broken facies ?Babulu Formation as at AB592							?Babulu Group	?Gondwana Megasequence	26/10
AB594	-9.18343	125.15708	Taroman	chert	Very weathered red chert or red ?siliceous mudstone. Well bedded (5 - 10 cm). Rock is vfg, looks like red chert but breaks apart to the touch - possibly just very weathered? Thin beds (< 1 cm) of red mud are found between cherty beds	No biogenic grains visible in peel					Unknown	?Noni Group	?Proto Indian Ocean Megasequence	26/10
AB595	-9.18210	125.16236	Taroman	no sample	same broken facies ?Babulu Formation as at AB592							?Babulu Group	?Gondwana Megasequence	26/10
AB596	-9.18458	125.16788	Taroman	?limestone	Lumps of grey limestone in an orange, gritty, clayey matrix. Possibly a huge fault gouge. See notebook	Ooid wackestone. Abundant large shell fragments and ooids however most smaller grains are very poorly preserved. Abundant layered algal growths around larger grains. Some rare forams visible. Very muddy matrix.			Ooids, gastropods, large shell fragments, layered algal growths			?Perdido Group (by lithofacies correlation)	?Gondwana Megasequence	26/10
AB597	-9.18874	125.17236	Taroman	no sample	possibly a very weathered volcanic sediment. Looks like a dark grey fg sandstone. No bedding visible - just a massive, weathered outcrop. Brown-red in colour - iron rich? Some coarser grained regions of this outcrop show what could be relict igneous textures - but are very weathered							?Barique Group	?Banda Megasequence	26/10
AB598	-9.19241	125.17417	Taroman	?volcanic	weathered basalt or possible volcanic sediment. Fg mafic rock							?Barique Group	?Banda Megasequence	26/10
AB599	-9.19538	125.17539	Taroman	no sample	very weathered red/green ?schist							?Lolotoi Metamorphic Complex	?Banda Megasequence	26/10
AB600	-9.19618	125.17656	Taroman	no sample	weathered, fg basalt. Some pillows visible. Too weathered to sample.							?Barique Group	?Banda Megasequence	26/10
AB601	-9.20155	125.18106	Taroman	no sample	another "pinnacle" hill of weathered pillow basalt at this point.							?Barique Group	?Banda Megasequence	26/10
AB602	-9.20972	125.18062	Taroman	no sample	Heading SW down the road from this point are exposed blocks of mafic volcanics and volcanic breccia, red limestones, sandstone blocks, conglomerates, and clasts of metamorphics, all ranging in size from 10 cm to 2 m. Melange zone.							Melange zone	Melange zone	26/10
AB603	-9.22063	125.18082	Taroman	no sample	more weathered mafic rocks. Volcanics (basalts?) or volcanic sediments.							?Barique Group	?Banda Megasequence	26/10
AB604	-9.22155	125.18038	Taroman	no sample	very sheared green/red/purple clay? Melange? No blocks just these clays. Some of the more competent parts look like schist							?Lolotoi Metamorphic Complex	?Banda Megasequence	26/10
AB605	-9.22915	125.17067	Taroman	no sample	more of the same red/green clay							?Lolotoi Metamorphic Complex	?Banda Megasequence	26/10
AB606	-9.22990	125.17035	Taroman	no sample	"pinnacle" hill of fg-mg intermediate igneous rock amongst melange muds							?Barique Group	?Banda Megasequence	26/10
AB607	-9.23028	125.17039	Taroman	observation	end of the road! Still looks like red/green/purple clays							?Lolotoi Metamorphic Complex	?Banda Megasequence	26/10

Location_No	Lat	Long	Region	Sample_type	Field_Description	Rock_Description	Benthic_foraminifera	Planktonic_foraminifera	OtherBioclasts	Facies	Age	Group	Megasequence	Date
AB608	-9.20299	125.17842	Taroman	observation	walking in west from the road to look at a hill. From the road, including this point, is weathered mafic volcanics. Some minor scattered limestone scree.							?Barique Group	?Banda Megasequence	26/10
AB609	-9.20324	125.17790	Taroman	no sample	At the base of hill. All weathered fg mafic volcanics. Another "pinnacle" Some remnant pillow textures?							?Barique Group	?Banda Megasequence	26/10
AB610	-9.20335	125.17554	Taroman	limestone	sheared and recrystallised yellow limestone	Completely recrystallised and dolomitised, no biogenic grains visible					Unknown	Unknown	Unknown	26/10
AB611A	-9.10091	125.23808	Saburai	breccia	dark grey, brecciated limestone	Completely recrystallised and dolomitised, no biogenic grains visible					Unknown	Unknown	Unknown	26/10
AB611B	-9.10091	125.23808	Saburai	limestone	Red, crystalline limestone. Non-brecciated example of AB611A taken a few metres up the road to the NE of fault	Completely recrystallised and dolomitised, no biogenic grains visible					Unknown	Unknown	Unknown	26/10
AB611C	-9.10091	125.23808	Saburai	mudstone	grey, micaceous mudstone, taken a few metres down the road to the SW of fault	Abundant small sulfide casts of grains made up of many tiny spheres, abundant small, tubular/branch-like forms,	Dentolina		Echinoderm fragments		Late Triassic-Jurassic	?Babulu Group	Gondwana Megasequence	26/10
AB612	-9.08338	125.24674	Saburai	fault gouge	soft, powdery limestone fault gouge	Completely recrystallised, no biogenic grains visible					Unknown	Unknown	Unknown	26/10
AB613	-8.95230	125.36579	Lacao	ENI sample	Malaya marica packstone, base of AMM						Tithonian to Kimmeridgian (Upper Jurassic)	Oe Baat Formation	Australian Margin Megasequence	31/05
AB614	-8.96515	125.37965	Lacao	ENI sample	Grey mudstone with 10-20 cm interbeds of indurated fg, green-grey ?sandstone. Sandstone shows signs of bioturbation						Late Triassic (Carnian-Norian)	?Babulu Group (mud dominated)	Gondwana Megasequence	31/05
AB615	-8.96523	125.37969	Lacao	ENI sample	Undulating fault plane on the surface of a large limestone block near AB614							observation point		31/05
AB616	-9.11214	125.29517	Bazol River	ENI sample	Dark grey massive mudstone containing vfg flecks of ?mica. Outcrop at least 5-6 m thick and probably much thicker.							?Babulu Group	Gondwana Megasequence	1/06
AB617	-9.10772	125.29766	Bazol River	ENI sample	Intrusion of diapir of Babulu Group muds. This point is the southern contact of the Babulu mudstone with river gravels (see field notebook for sketch)							?Babulu Group	Gondwana Megasequence	1/06
AB618	-9.13595	125.24969	Bazol River	ENI sample	Very well bedded limestone, bedding 5-15 cm							Aitutu Group	Gondwana Megasequence	2/06
AB619	-9.13487	125.24358	Bazol River	Observation	Bearing 285 are the "Three Sisters" see field notebook for sketch							observation point		2/06
AB620	-9.09046	125.34164	Bazol River	ENI sample	Hol Mesil gas seep. Gas emanating from Babulu Group badlands, grey mudstone with broken formation sandstone. A craggy peak called "Taswa" is situated above the Babulu Group muds.							Babulu Group	Gondwana Megasequence	2/06
AB621	-9.03143	125.30644	Bazol River	Observation	Looking south from the road the eastern edge of a ridge has dropped down against a fault. See field notebook for sketch.							observation point		2/06
AB623	-8.95095	125.10094	Maliana Basin	contact	Contact of Viqueque Formation (east) with Bobonaro Formation (west)- see field notebook for sketch.							observation point		12/10
AB624	-8.95006	125.10338	Maliana Basin	No sample	Babulu has reappeared a few hundred metres down the road							Babulu Group	Gondwana Megasequence	12/10
AB625	-8.95074	125.10495	Maliana Basin	contact	Mudstone goes back into limestone							observation point		12/10
AB626	-8.95235	125.10820	Maliana Basin	contact	Back into mudstone again							observation point		12/10
AB627	-8.92077	125.21752	Maliana Basin	Mudstone	Deformed, well bedded grey mudstone. Thinly interbedded, mudstone dominated. Mudstone beds 1-3 cm, sandstone beds < 1 cm	Residue is barren except for two small branch-like structures and one possible foram. Possibly reworked					Unknown	Unknown	Unknown	13/10
AB628	-8.93390	125.24271	Lesululi	No sample	Fissile, brown, weathered mudstone. Looks similar to unit on the SW of Loelako but no sandstone beds visible at this location. Very weathered.									13/10
AB629	-8.93228	125.24432	Lesululi	No sample	A large outcrop (big hill) of similar brown mudstone but contains abundant Aitutu-like blocks. Not in situ as it looks like the whole hillside has slipped but must be close.							?Aitutu Group	Gondwana Megasequence	13/10

Location_No	Lat	Long	Region	Sample_type	Field_Description	Rock_Description	Benthic_foraminifera	Planktonic_foraminifera	OtherBioclasts	Facies	Age	Group	Megasequence	Date
AB630	-8.93218	125.24901	Lesululi	Limestone	At the top of the mudstone hill is an outcrop of very well bedded (5-20 cm) grey limestone. Interbedded mudstones are generally < 1 cm. Looks similar to Aitutu Formation. Depositional contact with mudstones below, mudstones at lower levels transition up to this limestone "cap" on the hill.	Extensively recrystalised and stylotised wackestone containing ?bivlve filaments and rare small ?forams	lagenoides, Lenticulina		Ostracods, calcispheres, ?bivalve filaments		Triassic	Aitutu or Bandeira Group	Gondwana Megasequence	13/10
AB631	-8.92748	125.25689	Lesululi	Limestone	Another topographic high with well bedded limestone "cap" as at AB630	Fossiliferous wackestone containing large gastropods, well preserved bryozoa and abundant algal material	duostominids		Large gastropods, bryozoans, algal growths		late Triassic	Bandeira Group	Gondwana Megasequence	13/10
AB632	-8.92287	125.26324	Lesululi	Limestone	Scree. Very fossiliferous grey limestone	Algal bindstone? Similar facies to AB631 but with more abundant algae, less forams	nodosariids		Gastropods, echinoids, brachiopod fragments, bryozoans, abundant and diverse algal material, stromatoporoid algae, coral		Late Triassic	Bandeira Group	Gondwana Megasequence	13/10
AB633	-8.92081	125.26599	Lesululi	Limestone	Scree from the base of the south facing cliffs of Lesululi. Fossiliferous grey wackestone. Possible ?forams. See notebook for sketch of east side of Loelako from this point.	Algal bindstone? Abundant algal nodules and growths (mostly recrystallised) with smal forams within interstitial material	miliolids, duostominids, Endothyra, Duotaxis		Thaumatoporellacean algae, stromatoporoid algae		Late Triassic	Bandeira Group	Gondwana Megasequence	13/10
AB634	-8.92032	125.26609	Lesululi	Limestone	Scree from higher up the scree slope. Grey, fossiliferous wackestone/packstone. Looks similar to Perdido Limestone but no ooids. Some small ?bivalves very well preserved ≈ 5 mm in size	Highly recrystallised ?wackestone containing large algal growths, with shell fragments, ?ooids and abundant small forams	Aulotortus, Duostomina, miliolids		Brachiopods, ostracods		Late Triassic	Bandeira Group	Gondwana Megasequence	13/10
AB635	-8.92147	125.26713	Lesululi	No sample	Very thick > 20 m succession of orange mud, gravel and cobble beds. Top of Viqueque?							?Viqueque Group	Synorogenic Megasequence	13/10
AB636	-8.92594	125.25811	Lesululi	Limestone	Scree. Similar dark-grey Aitutu-like facies but this rock has small, round chert nodules ≈ 10 cm in size.	Packstone containing abundant bivalve filaments, small nodosarids and other forams, and other fine shelly debri	nodosariids, Lenticulina		Ostracods, abundant bivalve filaments,		Late Triassic	Aitutu Group	Gondwana Megasequence	13/10
AB637	-8.92664	125.25737	Lesululi	Mudstone	Orange, fissile mudstone, slightly micaceous? This lithology comprises most of the lowlands around this area, which are "capped" by well bedded limestone.	Very small volume of residue containing no biogenic grains					Unknown	Unknown	Unknown	13/10
AB638	-9.00947	125.24199	Saburai	Observation	Road up to and including this point heading out of Maliana is grey mudstone. Bearing 215 from this point is a large block ≈ 20 m in size, looks like limestone through binoculars, probably fallen.							observation point		14/10
AB639	-8.98510	125.28325	Loelako	Fault gouge	On the right side of the road heading north is a large outcrop of fault gouge at least 10-20 m in size. Broken, recrystallised limestone.	Completely recrystallised, no biogenic grains visible					Unknown	Unknown	Unknown	14/10
AB640A	-8.95648	125.28576	Loelako	Sandstone	Brown-grey interbedded mudstone and **friable muddy sandstone**. Sandstone beds 5-40 cm. Forams visible in mudstone.	Subangular qtz and lithic fragments (abundant schist). No biogenic grains.						Viqueque Group	Synorogenic Megasequence	14/10
AB640B	-8.95648	125.28576	Loelako	Mudstone	Brown-grey interbedded **mudstone** and friable muddy sandstone. Sandstone beds 5-40 cm. Forams visible in mudstone.	Abundant planktonic forams. Globoginoides, probably the same age as AB641B		Globigerinoides			Above N20, probably the same age as AB641B	Viqueque Group	Synorogenic Megasequence	14/10
AB641A	-8.94572	125.27936	Loelako	Sandstone	Brown-grey interbedded mudstone and **friable muddy sandstone**. Sandstone beds 20-100 cm. Forams visible in mudstone.	Subangular qtz and lithic fragments (abundant schist). No biogenic grains.						Viqueque Group	Synorogenic Megasequence	14/10
AB641B	-8.94572	125.27936	Loelako	Mudstone	Brown-grey interbedded **mudstone** and friable muddy sandstone. Sandstone beds 20-100 cm. Forams visible in mudstone.	Abundant planktonic and some benthic foraminifera. Number 9 truncorotalia tosaensis . Deep water.					N21-N22 Latest Pliocene Early Pleistocene	Viqueque Group	Synorogenic Megasequence	14/10
AB642	-8.94295	125.27942	Loelako	No sample	Well bedded sandstone with thin mudstone beds < 10 cm							Viqueque Group	Synorogenic Megasequence	14/10
AB643	-8.94043	125.27811	Loelako	No sample	Well bedded sandstone 10-40 cm with interbedded mudstone beds 5-10 cm							Viqueque Group	Synorogenic Megasequence	14/10
AB644	-8.93830	125.27741	Loelako	Conglomerate	Interbedded sandstone and gravel/pebble/cobble conglomerate	Clasts are mainly vfg igneous material, with some rare mudstone/slate and some clasts of calcisphere/bivalve limestone similar to that at AB477-479. Clasts of both Aitutu Group and Bandeira Group present						?Viqueque Group	?Synorogenic Megasequence	14/10
AB645	-8.94930	125.28216	Loelako	No sample	Interbedded sandstone and mudstone							Viqueque Group	Synorogenic Megasequence	14/10

Location_No	Lat	Long	Region	Sample_type	Field_Description	Rock_Description	Benthic_foraminifera	Planktonic_foraminifera	OtherBioclasts	Facies	Age	Group	Megasequence	Date
AB646	-8.95022	125.28019	Loelako	Mudstone	Dark grey/purple mudstone, micaceous with abundant black carbonaceous flecks < 1 mm. Chaotically deformed. Thinly bedded, mudstone beds ≈ 1 cm with thin sandstone laminae ≈ 1 mm	Barren residue, no biogenic grains visible						?Babulu Group	?Gondwana Megasequence	14/10
AB647	-8.95104	125.27966	Loelako	Observation	See notebook for sketch and pictures of the eastern side of Loelako							observation point		14/10
AB648	-8.95129	125.27929	Loelako	Limestone	Scree at Loelako. Grey/white fossiliferous packstone/wackestone with large spherical to ovoid grains < 30 mm.	Rock consist of large algal nodules 10-30 mm, with some small forams within interstitial material. Highly dolomitised cement	lagenoides, Aulotortus		Algal nodules, gastropods		Late Triassic	Bandeira Group	Gondwana Megasequence	14/10
AB649	-8.94996	125.28283	Loelako	No sample	Same conglomerate as at AB644							?Viqueque Group	?Synorogenic Megasequence	14/10
AB650	-8.97082	125.28459	Loelako	No sample	Grey/green/purple scaly clay with chaotic, broken sandstone blocks							Babulu Group	Gondwana Megasequence	14/10
AB651	-8.98294	125.27396	Loelako	Limestone	Scree at Loelako. Massive grey limestone. Interesting internal structure - looks like an ooid grainstone/packstone? May be the inside of a coral?	Packstone containing ooids, abundant algal material, large shell fragments and small benthic forams	miliolids (Karaburunia)		Gastropods, echinoids, brachiopods		Late Triassic	Bandeira Group	Gondwana Megasequence	15/10
AB652	-8.98059	125.27684	Loelako	No sample	Close to AB457 (2010). Well bedded grey limestone, bedding 5-30 cm.						?Late Triassic	?Bandeira Group	?Gondwana Megasequence	15/10
AB653	-8.98016	125.27602	Loelako	Limestone	Well bedded grey limestone, bedding 5-30 cm. Limestone is white on fresh surface and looks very sugary and recrystallised	Completely recrystallised and dolomitised, no biogenic grains visible					Unknown	Unknown	Unknown	15/10
AB654	-8.98038	125.27603	Loelako	Limestone	Interbedded dark grey limestone, bedding 5-100 cm. Contains shell filaments and other small biogenic grains.	Algal bindstone? Containing shelly debri, ?calcispheres and small forams	nodosariids		Algal material, ostracods, calcispheres, small shell fragments		Triassic	Transitional Bandeira/Aitutu	Gondwana Megasequence	15/10
AB655	-8.98087	125.27618	Loelako	Limestone	One of the southern peaks of Loelako. Interbedded grey limestone, bedding 10-100 cm. Fresh rock is white, sugary and recrystallised.	Completely recrystallised and dolomitised, no biogenic grains visible					Unknown	Unknown	Unknown	15/10
AB656	-8.98114	125.27618	Loelako	Limestone	Similar well bedded grey limestone to AB655 but much less recrystallised. Well bedded grey wackestone with some cherty nodules.	Extensively recrystallised but apears to be a packstone containing crinoids, large shell fragments, possibly faint traces of ooids and rare small forams. Lagoonal facies	Endothyra		Crinoids, shell fragments, ostracods, ?ooids, gastropods		Late Triassic	Bandeira Group	Gondwana Megasequence	15/10
AB657	-8.98056	125.27696	Loelako	Limestone	Well bedded grey limestone, bedding 40-100 cm. Fresh rock is dark grey with some cherty layers.	Packstone mainly consisting of very abundant small shell (?bivalve) filaments	nodosariids, Endothyra		Bivalves, ostracods, punctate brachiopods, ?crinoid fragments		Triassic	Transitional Bandeira/Aitutu	Gondwana Megasequence	15/10
AB658	-8.98096	125.27839	Loelako	Limestone	Medium bedded grey limestone. Bedding 30-200 cm	Wackestone containing abundant large shell fragments, mainly ?brachiopods. Apears similar to AB656 & 657 but much larger grain size and much less recrystallised.			Large brachiopods, crinoids, echinoids		Late Triassic	Bandeira Group	Gondwana Megasequence	15/10
AB659	-8.99325	125.20143	Maliana Basin	Mudstone	Well bedded **mudstones**, muddy sandstones and sandstones. Constant shallow dip.	300 µ residue contains abundant gastropods, bivalves, benthic foraminifera and some larger planktonic forms. 150 µ residue contains more abundant small planktonic forms. One crab claw. Outer neritic. Top of Viqueque					Neogene	Viqueque Group	Synorogenic Megasequence	16/10
AB670	-8.99697	125.19775	Maliana Basin	Mudstone	Well bedded shallow dipping mudstones and sandstones	Residue is mostly qtz and lithic grains with some rare foraminifera					Neogene	Viqueque Group	Synorogenic Megasequence	16/10
AB671A	-9.00814	125.19374	Maliana Basin	Sandstone	Very weathered outcrop of well bedded mudstone and **friable sandstone**. **Sandstone contains subangular quartz grains and lithic fragments.** Some of the mudstone contains thin sand laminae.	Residue comprises qtz and lithic fragments, predominantly schist. No biogenic grains visible.						Viqueque Group	Synorogenic Megasequence	16/10
AB671B	-9.00814	125.19374	Maliana Basin	Mudstone	Very weathered outcrop of **well bedded mudstone** and friable sandstone. Sandstone contains subangular quartz grains and lithic fragments. **Some of the mudstone contains thin sand laminae.**	Abundant foraminifera					Neogene	Viqueque Group	Synorogenic Megasequence	16/10
AB672	-9.01029	125.19410	Maliana Basin	Mudstone	Interbedded grey mudstones	Diverse and highly abundant foraminifera. 150 µ residue comprises approx 80% planktonic forams (31-40)		Globorotalia tosaensis, Globorotalia truncatulinoides			N22 - Pleistocene	Viqueque Group	Synorogenic Megasequence	16/10

Location_No	Lat	Long	Region	Sample_type	Field_Description	Rock_Description	Benthic_foraminifera	Planktonic_foraminifera	OtherBioclasts	Facies	Age	Group	Megasequence	Date
AB673	-9.03364	125.19715	Maliana Basin	Limestone	Isolated pinnacle hill approx. 50 m in size. Could possibly be a very old fallen block. Dense, white/grey calcilutite. Looks similar to Perdido Limestone but no biogenic grains visible in hand specimen.						?Eocene	?Kolbano Group	?Australian Margin Megasequence	16/10
AB674	-9.03682	125.20461	Maliana Basin	Mudstone	Thinly bedded soft grey mudstone, indurated white sandstone. Bedding generally < 10 cm. Bioturbation visible in siltstone. Looks similar to Aitutu Formation but with thinner bedding overall and more mud.	Brown wackestone with abundant radiolaria and very thin shell filaments (?halobia) concentrated in thin beds < 1 cm. Deep water facies			radiolaria, shell filaments (?halobia)		Triassic	Transitional Aitutu/Babulu Group	Gondwana Megasequence	16/10
AB675	-9.03956	125.20817	Maliana Basin	?Sandstone	Weathered, dark grey ?sandstone in excavated roadside gully. Iron rich with very red soil overlying. No visible bedding.	Sample quite porous so peel is poor quality. No biogenic grains visible. Some lath-like grains, potentially an igneous rock.					Unknown	Unknown	Unknown	16/10
AB676	-9.06027	125.22150	Saburai	Observation	Location of Saburai village							observation point		17/10
AB677	-9.06507	125.22139	Saburai	Limestone	Medium to thick bedded (30 cm < 2 m) dense grey limestone at base of north-facing cliffs. Calcilutite with no biogenic grains visible in hand specimen.	Very dense ?ooid wackestone. Some recrystallised foraminifera but most are just outlines with no internal structure remaining	miliolids				Triassic	Bandeira Group	Gondwana Megasequence	17/10
AB678	-9.06531	125.22057	Saburai	Limestone	Dense, grey fossiliferous limestone. Very hard. Contains small round grains < 3 mm in size (?crinoid x-sections). Medium to thick bedding, 0.4-1.5 m. Very large block surrounded by scree, possibly not in situ.	Very dense wackestone. Contains ooids, shell fragments and some ghosts of forams					Triassic	Bandeira Group	Gondwana Megasequence	17/10
AB679	-9.06546	125.21952	Saburai	Limestone	Medium to thick bedded dense grey limestone. Packstone/grainstone made up of many small < 1 mm spherical grains.	Interbedded ooid packstone and wackestone. Some ghosts of forams but most internal structure is recrystallised	miliolids, Endothyra				Triassic	Bandeira Group	Gondwana Megasequence	17/10
AB680	-9.06362	125.21937	Saburai	Observation	Facing 125° from this point bedding at the top of the massif seems to have an apparent dip of ≈ 10° → 220°. Standing on a scree slope at this point.							observation point		17/10
AB681	-9.06071	125.22666	Saburai	Fault gouge	Entire hillside at this point appears to be fault breccia and gouge.	No biogenic grains visible					Unknown	Unknown	Unknown	17/10
AB682	-9.00910	125.28394	Saburai	Limestone	Road outcrop on pass between Saburai massif and Loelako massif. Northern most of Saburai massif.	Completely recrystallised, some rare ghosts of larger biogenic grains			?ostracods, ?gastropods		Unknown	Unknown	Unknown	18/10
AB683	-9.02675	125.29963	Saburai	Volcanic	A pinnacle hill of pillow basalt being mined for road base.									18/10
AB684A	-9.03865	125.27926	Saburai	Limestone	Well bedded **limestone** and mudstone. **Very indurated grey limestone beds 10-100 cm.** Fissile grey mudstone beds < 1 < 30 cm. **Limestone beds are heavily bioturbated - looks similar to Aitutu Formation**	Ooid grainstone containing small benthic forams	Endothyra, miliolids (Karaburunia)				Triassic	Bandeira Group	Gondwana Megasequence	18/10
AB684B	-9.03865	125.27926	Saburai	Mudstone	Well bedded limestone and **mudstone**. Very indurated grey limestone beds 10-100 cm. **Fissile grey mudstone beds < 1 < 30 cm**. Limestone beds are heavily bioturbated - looks similar to Aitutu Formation	Rare forams, mostly globular planktonic forms					Triassic	Bandeira Group	Gondwana Megasequence	18/10
AB685	-9.04592	125.27603	Saburai	No sample	Same lithology as AB684. A fold on a thrust fault? See notebook for sketch.						Triassic	Bandeira Group	Gondwana Megasequence	18/10
AB686	-9.05313	125.25679	Saburai	Limestone	Top of Saburai ridge at Timor Telecom tower. Well bedded limestone and mudstone. Highly bioturbated. Same lithology from the main road to this point.	Muddy wackestone containing abundant radiolaria, rare small forams and abundant fine, angular, sometimes square to oblong shaped grains	Lenticulina		radiolaria		Late Triassic	Aitutu Group	Gondwana Megasequence	18/10
AB687	-9.06777	125.25970	Saburai	Limestone	Fault plane with interbedded limestones and mudstones. Same lithology as AB684.	Muddy wackestone containing shell filaments and very small forams	miliolids, nodosariids, Lenticulina		bivalve filaments		Triassic	Transitional Bandeira/Aitutu	Gondwana Megasequence	18/10
AB688	-9.07890	125.25066	Saburai	Fault gouge	Massive limestone fault gouge. White gouge crumbling to yellow sand.						Unknown	Unknown	Unknown	18/10
AB689	-9.08179	125.24859	Saburai	No sample	Fault gouge.						Unknown	Unknown	Unknown	18/10
AB690	-9.08256	125.24748	Saburai	Fault gouge	Very friable limestone fault gouge.	No biogenic grains visible					Unknown	Unknown	Unknown	18/10
AB691	-9.09252	125.24188	Saburai	No sample	Fault gouge						Unknown	Unknown	Unknown	18/10
AB692	-9.06421	125.26025	Saburai	Volcanic	Large outcrop of volcanic rock along the road. Green/grey, fine grained basaltic vesicular eruptive rock. Seems to be associated with a very deformed, schistose-looking red/green/grey scaly clay. This point marks the southern extent of volcanic outcrop.							?Melange zone	?Melange zone	18/10

Location_No	Lat	Long	Region	Sample_type	Field_Description	Rock_Description	Benthic_foraminifera	Planktonic_foraminifera	OtherBioclasts	Facies	Age	Group	Megasequence	Date
AB693	-9.06170	125.26172	Saburai	No sample	Large outcrop of volcanic rock along the road. Green/grey, fine grained basaltic vesicular eruptive rock. Seems to be associated with a very deformed, schistose-looking red/green/grey scaly clay. This point marks the northern extent of volcanic outcrop.							?Melange zone	?Melange zone	18/10
AB694	-9.03266	125.28298	Saburai	Mudstone	Thinly interbedded mudstone (bedding 1-5 cm) and micaceous sandstone (bedding ≈ 1 mm). Bedding gently folded and slightly undulating.	Two main types of planktonic forams present. Globular type (3-21) far more common than planispiral type (1-2). Possibly contamination?								19/10
AB695	-9.05461	125.25578	Saburai	?mudstone	Well bedded mudstones with indurated interbeds 2-10 cm. Not limestone - no HCl rxn	No biogenic grains visible					Unknown	?Babulu Group	?Gondwana Megasequence	19/10
AB696	-9.05562	125.25449	Saburai	No sample	Medium to thinly bedded sandstone with occasional thin mudstone laminae < 1 mm. Huge boulders here are strewn chaotically, most are not in situ but would represent the remains of resistant sandstone beds at this point.							?Babulu Group	?Gondwana Megasequence	19/10
AB697	-9.05795	125.25218	Saburai	No sample	Blocks of mafic volcanic rocks < 1 m in size within red/brown mud. Volcanics are slightly vesicular and look similar to those at AB692. Strong striations are observed on the sides of many blocks and are evidence of shearing and movement among blocks.							?Melange zone	?Melange zone	19/10
AB698	-9.05786	125.24978	Saburai	Limestone	Interbedded grey limestone and chert. Limestone beds 10-20 cm, chert beds ≈ 5 cm. May not be in situ at this point but probably is. Also good view of Loelako from this point, see notebook for sketch.	Appears similar forams to AB687 but muddier facies, more recrystallised						Transitional Bandeira/Aitutu	Gondwana Megasequence	19/10
AB699A	-9.06065	125.24577	Saburai	Limestone	Medium to thickly bedded fossiliferous white limestone. Roughly spheroid white grains 0.5-2 mm in size with no internal structure. Need to peel. This outcrop possibly not in situ but if not have definitely fallen from cliffs above. AB699 A & B taken from two different beds.	Ooid grainstone? Very small pryramid-shaped forams	Gandinella				Triassic	Bandeira Group	Gondwana Megasequence	19/10
AB699B	-9.06065	125.24577	Saburai	Limestone	Medium to thickly bedded fossiliferous white limestone. Roughly spheroid white grains 0.5-2 mm in size with no internal structure. Need to peel. This outcrop possibly not in situ but if not have definitely fallen from cliffs above. AB699 A & B taken from two different beds.	Ooid grainstone containing small ?benthic forams	duostominids, Gandinella				Triassic	Bandeira Group	Gondwana Megasequence	19/10
AB700	-9.05906	125.24703	Saburai	Observation	Facing 310° from this point the bedding in the bluff at the cliff top appears to be dipping shallowly back towards the south?							observation point		19/10
AB701	-8.87614	125.23908	Cailaco	Mudstone	Grey mudstone with thin interbeds of orange sandstone ≈ 1 cm. Constant shallow dip. Mud dominated Viqueque.	Only a very small volume of >150 μ residue but it contains abundant very well preserved planktonic forams. Upper bathyal.	Hyalina baltica				Pleistocene	Viqueque Group	Synorogenic Megasequence	20/10
AB702	-8.87648	125.24864	Cailaco	No sample	Same lithology as AB701, mud dominated Viqueque.							Viqueque Group	Synorogenic Megasequence	20/10
AB703	-8.87848	125.25593	Cailaco	Mudstone	Well bedded mudstone with thin sandstone interbeds, mud dominated Viqueque.	Extremely diverse and abundant range of planktonic and benthic foraminifera (perhaps have not even captured full range in 40 picks). Some quite large benthic forms. Upper bathyal. Preservation suggests infilling and recrystallisation, higher temps	Valvulina pennatula, Bolivina robusta, Pullenia bulloides				Neogene	Viqueque Group	Synorogenic Megasequence	20/10
AB704	-8.87559	125.26357	Cailaco	No sample	Same lithology as AB703, mud dominated Viqueque.							Viqueque Group	Synorogenic Megasequence	20/10
AB705	-8.87802	125.27556	Cailaco	Sandstone	Medium bedded (< 30 cm) muddy sandstone.	Qtz rich residue containing some foraminifera, mostly planktonic. Preservation suggests infilling and recrystallisation, higher temps		Globorotalia			Neogene	Viqueque Group	Synorogenic Megasequence	20/10
AB706	-8.87787	125.28010	Cailaco	Sandstone	Well bedded muddy sandstone 5-30 cm with thin mudstone interbeds generally < 5 cm. Includes one thick (≈ 1 m) bed of melange (landslide deposit?: very poorly sorted pebbles, cobbles and boulders in a mud matrix.)	Diverse subrounded to subangular lithogenic grains, with only a few very rare rads and possible forams found in residue. Pristine forams, low temp	Pseudorotalia				Pleistocene	Viqueque Group	Synorogenic Megasequence	20/10

Location_No	Lat	Long	Region	Sample_type	Field_Description	Rock_Description	Benthic_foraminifera	Planktonic_foraminifera	OtherBioclasts	Facies	Age	Group	Megasequence	Date
AB707	-8.88685	125.28434	Cailaco	Mudstone	Alternating beds of muddy sandstone (5-30 cm), mudstone (5-10 cm) and pebble/cobble beds. Sample taken of black mudstone.	300 µ residue contains a variety of planktonic and benthic forams, 150 µ residue contains only small globular planktonic forms					Neogene	Viqueque Group	Synorogenic Megasequence	20/10
AB708	-8.82047	125.28003	Cailaco	Observation	Directly across the river from this point, bearing 230°, is a very thick outcrop of Viqueque Formation which appears to be dipping shallowly (< 10°) towards the south.							observation point		20/10
AB709	-8.90515	125.24971	Lesululi	Limestone	Fissile brown/grey mudstone with occasional limestone beds up to 1 m thick. Limestone is of similar colour to the mudstone but very indurated. Outcrop is quite deformed with the foliation in the mudstone very folded.	Largely recrystallised, containing many small calcite spheres (?calcispheres). Also contains abundant very fine, high relief grains, likely radiolaria			Radiolaria, ?calcispheres		?Triassic	?Aitutu Group	?Gondwana Megasequence	21/10
AB710	-8.90533	125.25009	Lesululi	Limestone	Similar lithology to AB709 but with limestone beds much more abundant. Bedding clearly visible sub-parallel to the northern face of the mountain, which is now seen to be a dip slope.	Recrystallised wackestone containing abundant, very fine, high releif grains, likely radiolaria. Some rare ?bivalve filaments	nodosariids		ostracods, ?radiolaria		?Triassic	?Aitutu Group	?Gondwana Megasequence	21/10
AB711	-8.90460	125.25122	Lesululi	No sample	Same lithology as AB710						?Triassic	?Aitutu Group	?Gondwana Megasequence	21/10
AB712	-8.90785	125.24570	Lesululi	No sample	A small pinnacle hill of dark grey volcanic rock.									21/10
AB713	-8.90868	125.24905	Lesululi	Limestone	Fossiliferous white limestone, appears similar to Perdido Limestone, faint traces of ooids? Large block tens of metres in size but has possibly fallen from cliffs above	Extensively recrystallised and dolomitised, contains algal noduls and growths, small gastropods and rare, small forams.	rare miliolids		Algal growths, small gastropods, bryozoans		Late Triassic	Bandeira Group	Gondwana Megasequence	21/10
AB714	-8.90847	125.24945	Lesululi	Limestone	Interbedded grey mudstone and limestone similar to that on the north slopes. At this point, appears to be topographically below the limestone of the massif.	Completely recrystallised, no biogenic grains visible					Unknown	Unknown	Unknown	21/10
AB715	-8.90877	125.25002	Lesululi	Limestone	Massive white limestone, sugary and recrystallised but contains some larger fossils: ?shell fragments and ?crinoid stems. Definitely a pervasive foliation a ≈ 1 m scale that looks very much like medium to thick bedding. Also a strange geometric ?jointing pattern similar to that on the east side of Loelako.	Extensively recrystallised and dolomitised, contains faint ghosts of biogenic grains, mainly larger shell fragments but with some rare forams			Algal nodules, brachiopods, ?coral		?Late Triassic	?Bandeira Group	?Gondwana Megasequence	21/10
AB716	-8.90915	125.24979	Lesululi	Limestone	White limestone in scree at base of cliff, a few shell fragments and other fossils visible.	Some larger shell and algal fragments visible in peel but rock shows extensive recrystallsation and dolomitisation. Soe possible rare ghosts of forams			bivalves, echinoids, crinoids		Unknown	Unknown	Unknown	21/10
AB717	-8.90928	125.24997	Lesululi	Mudstone	Fissile, bioturbated mudstone. Contact with limestone cliff at this point. Mudstone is dragged up the face of the cliff in a drag fold.	vfg peel. No identifiable grains.								21/10
AB718	-8.91002	125.24979	Lesululi	Limestone	Massive white limestone cliffs - structural measurements taken	Completely recrystallised and dolomitised, possibly a few rare ghosts of forams visible					Unknown	Unknown	Unknown	21/10
AB719	-8.91097	125.25002	Lesululi	No sample	Massive white limestone cliffs - structural measurements taken							?Bandeira Group	?Gondwana Megasequence	21/10
AB720	-8.91073	125.24955	Lesululi	Limestone	Massive white limestone cliffs	Completely recrystallised and dolomitised, contains some large shell fragments and possibly a few rare ghosts of forams			bivalves			?Bandeira Group	?Gondwana Megasequence	21/10
AB721	-8.95240	125.27793	Loelako	?chert	Sugary white recrystallised limestone with rare thin beds of grey ?chert	Completely recrystallised and dolomitised, no biogenic grains visible					Unknown	Unknown	Unknown	22/10
AB722	-8.95263	125.27752	Loelako	Limestone	Grey limestone, possibly containing small bioclasts , 1 mm	Completely recrystallised and dolomitised, no biogenic grains visible. Dolomite rhombs concentrated in beds					Unknown	Unknown	Unknown	22/10
AB723	-8.95306	125.27765	Loelako	Limestone	Recrystallised grey limestone, contains ghosts of many large fossils > 1 cm including ?gastropods and shell fragments.	Sample is in advanced state of dolomotisation, only the outlines of some larger fossil fragments remain			Crinoids, echinoids, gastropods, punctate brachiopods		?Late Triassic	?Bandeira Group	?Gondwana Megasequence	22/10
AB724	-8.95208	125.27736	Loelako	Limestone	Scree from east side of Loelako. Fossiliferous white limestone	Large algal nodules 5-20 mm with interstitial forams, ooids and shelly debri. Similar to AB648	Duostomina, Gandinella, Aulotortus		Algal nodules, gastropods, ooids,		Late Triassic	Bandeira Group	Gondwana Megasequence	22/10
AB725	-8.95159	125.27722	Loelako	Limestone	Fossiliferous grey limestone, many large fossils ≈ 1 cm. From very large block > 10 m at base of cliffs, probably not in situ but very close to. See notebook and photos for strange geometric planar features on cliff face.	Packstone with abundant shell fragments, echinoids, algal nodules. 5 cm bed at top with abundant large gastropods, echinoids. Quite recrystallised, forams rare and poorly preserved.	?Lenticulina		Abundant gastropods, pentacrinoids, punctate brachiopods, possible ?ammonoids		Triassic	Transitional Bandeira/Aitutu	Gondwana Megasequence	22/10
AB726	-8.95100	125.27712	Loelako	No sample	Limestone displaying many strong lineations						Unknown	Unknown	Unknown	22/10

Location_No	Lat	Long	Region	Sample_type	Field_Description	Rock_Description	Benthic_foraminifera	Planktonic_foraminifera	OtherBioclasts	Facies	Age	Group	Megasequence	Date
AB727	-8.95062	125.27643	Loelako	Limestone	White sugary recrystallised limestone. Similar geometric features as at AB725. See notebook for structural data	Completely recrystallised and dolomitised, no biogenic grains visible					Unknown	Unknown	Unknown	22/10
AB728	-8.95034	125.27627	Loelako	No sample	Fault plane with gouge						Unknown	Unknown	Unknown	22/10
AB729	-9.00964	125.27118	Saburai	No sample	Cliff face close to road on the northern tip of Saburai. Limestone. Structural measurements sighted in						Unknown	Unknown	Unknown	23/10
AB730	-9.01003	125.27104	Saburai	Fault gouge	Gouge from fault plane	No biogenic grains visible					Unknown	Unknown	Unknown	23/10
AB731	-9.00643	125.27557	Saburai	Sandstone	Thinly bedded grey mudstone and **brown/orange sandstone**. Bedding 2-5 cm, gently undulating. Looks similar to outcrop on the south end of Loelako but much less deformed.	No biogenic grains visible					Unknown	?Babulu Group	?Gondwana Megasequence	23/10
AB732	-9.00897	125.28343	Saburai	Limestone	Well bedded limestone.	Shelly wackestone with an extensively recrystallised matrix	Duostomina				Triassic	Bandeira Group	Gondwana Megasequence	23/10
AB733	-9.00921	125.28304	Saburai	No sample	Fault plane developed in same limestone as AB732						Triassic	Bandeira Group	Gondwana Megasequence	23/10
AB734	-9.01788	125.28429	Saburai	Limestone	Thickly bedded white limestone. Bedding 30 cm < 3 m < . Bedding is subhorizontal and dips shallowly (< 5°) towards the south. Bedding truncated by a subvertical fault striking ≈ 210° which runs sub-parallel to the southern scarp of Saburai. Fresh rock is grey and contains abundant shell fragments and small < 1 mm spherical grains. Limestone beds get thinner and grade into mudstone moving west up the hill. Bedding displays gentle, open folding with an approx. east-west axis.	Wackestone containing shell fragments and forams	Lenticulina, Duostomina				Triassic	Bandeira Group	Gondwana Megasequence	23/10
AB735	-9.01789	125.28343	Saburai	Limestone	Well bedded, fine grained, brown/grey limestone. Medium to thinly bedded 5-30 cm	Wackestone containing radiolara and very rare planktonic forams					Unknown	Unknown	Unknown	23/10
AB736	-9.01823	125.28182	Saburai	Limestone	Brown/grey wackestone. Bedding difficult to determine - sub-vertical fabric is probably jointing.	Wackestone containing some benthic forams						?Bandeira Group	?Gondwana Megasequence	23/10
AB737	-9.01903	125.28073	Saburai	Limestone	Limestone-volcanic contact. Limestone is very well bedded (medium bedding < 1 m), brown and fossiliferous with gastropods and abundant shell fragments. Bearing 230 from this point on the opposite side of a gully is a very similar looking outcrop of similar orientation (p929)	Very fossiliferous wackestone	Lenticulina, miliolids		Echinoid spines, gastropods, bryozoans, stromatoporoid algae		Triassic	Bandeira Group	Gondwana Megasequence	23/10
AB738	-9.01895	125.28067	Saburai	Sandstone	Cg sandstone. These boulders have fallen from the unit at the top of the bluff overlying the volcanics, now lie at limestone-volcanic contact	Mostly subrounded, poorly sorted lithic grains with occassional biogenic material.			Calcareous green algae (738_9), crinoids, bryozoans		Permian	Maubisse Group	Gondwana Megasequence	23/10
AB739	-9.02066	125.27469	Saburai	?Volcanic	Weathered volcanic sandstone?. This point is the volcanic-limestone contact at the top of the hill.	Very poorly sorted volcanic sandstone/breccia, rare biogenic grains including coraline algae fragments			coralline algae		Permian	Maubisse Group	Gondwana Megasequence	23/10
AB740	-8.97345	125.22996	Loelako	Limestone	Very well bedded (5-30 cm), dark grey, fg limestone on the western flank of Loelako. Resembles Aitutu Formation.	Wackestone containing radiolaria, shell filaments and rare larger shell fragments. Stylolites common	nodosariids				?Triassic	?Aitutu Group	?Gondwana Megasequence	23/10
AB741	-8.97199	125.23136	Loelako	Limestone	Similar well bedded limestone to AB740, resembling Aitutu Formation. Above this point all outcrop is brown/orange muds with broken sandstone blocks	Brown wackestone with abundant radiolaria and thin shell filaments (?halobia), often with the shell filaments concentrated in thin beds. Rare bulbous planktonic forams					?Triassic	?Aitutu Group	?Gondwana Megasequence	23/10
AB742	-8.98841	125.23463	Maliana Basin	Mudstone	Red/grey scaly mudstone containing an assortment of exotic blocks. Some huge outcrops > 20 m high. Irrigation dam at this point.							?Melange zone	?Melange zone	23/10
AB743	-9.02953	125.21794	Maliana Basin	No sample	Red/grey scaly mudstone with deformed white/brown sandstone beds ≈ 1-2 cm. Mudstone dominated							?Babulu Group	?Gondwana Megasequence	25/10
AB744	-8.99580	125.20395	Maliana Basin	No sample	Mudstones and muddy sandstones in river, Viqueque Formation							Viqueque Group	Synorogenic Megasequence	25/10
AB745	-9.06136	125.22688	Saburai	Fault gouge	Fault gouge from slope	No biogenic grains visible					Unknown	Unknown	Unknown	26/10
AB746	-9.06156	125.22728	Saburai	Observation	See notebook for sketch							observation point		26/10

Location_No	Lat	Long	Region	Sample_type	Field_Description	Rock_Description	Benthic_foraminifera	Planktonic_foraminifera	OtherBioclasts	Facies	Age	Group	Megasequence	Date
AB747	-9.06206	125.22813	Saburai	Limestone	Fossiliferous grey limestone from scree - fallen from cliffs above. See notebook for description of pictures at this point	Fosilliferous wackestone	Endothyra				Triassic	Bandeira Group	Gondwana Megasequence	26/10
AB748	-9.06259	125.22980	Saburai	Limestone	Fossiliferous white wackestone with thick mottled black bands 30-100 cm causing the "bedded" look in the high cliffs (at this point it is mostly huge loose boulders fallen from cliffs above). Limestone from the black bands contain abundant white rhombic crystals (dolomite?)	Peel shows extensive recrystallisation and dolomitisation, very difficult to determine biogenic grains	Aulotortus (25), Siphovalvulina, Duostomina				Triassic	Bandeira Group	Gondwana Megasequence	26/10
AB749A	-9.06413	125.23213	Saburai	Limestone	Contact between **massive, black banded limestones as at AB748 (A, west)** with well bedded limestones and mudstones (B, east). Gully striking 140° from this point is possibly the fault trace. See notebook for sketch of field relationships.	Peel shows extensive recrystallisation and dolomitisation, some larger shell fragments along with some very faint ghosts of other, smaller biogenic grains visible.			ostracods, brachiopods, stromatoporoid algae		Triassic	Bandeira Group	Gondwana Megasequence	26/10
AB749B	-9.06413	125.23213	Saburai	Limestone	Contact between massive, black banded limestones as at AB748 (A, west) with **well bedded limestones and mudstones (B, east)**. Gully striking 140° from this point is possibly the fault trace. See notebook for sketch of field relationships.	?Ooid grainstone, outlines of biogenic grains visible but difficult to identify	Gandinella		punctate brachiopods,		Triassic	Bandeira Group	Gondwana Megasequence	26/10
AB750	-9.06383	125.23283	Saburai	Observation	See notebook for sketch of field relationships							observation point		26/10
AB751	-9.06439	125.23439	Saburai	Observation	Bearing 090 from this point on the opposite side of the mudstone saddle is well bedded limestone oriented ≈ 20° → 350° (sighted in)							observation point		26/10
AB753A	-9.05983	125.24000	Saburai	Sandstone	Very well interbedded grey mudstone and **grey fg micaceous sandstone** of constant steep dip	No biogenic grains visible						?Babulu Group	?Gondwana Megasequence	26/10
AB753B	-9.05983	125.24000	Saburai	Mudstone	Very well interbedded **grey mudstone** and grey fg micaceous sandstone of constant steep dip	Only a few rare biogenic grains in residue including: poorly preserved forams, small black pellets	Ammodiscus		Chondrites trace fossils	Anoxic (Bromley & Ekdale 1984)	?Triassic	?Babulu Group	?Gondwana Megasequence	26/10
AB754	-9.05879	125.24153	Saburai	Mudstone	Weathered friable orange/grey mudstone	Some radiolaria and forams in residue. Bathysyphons, high temp colour, Estacolis (coiled nodosarid)		?Carteriella manelobasensis	Bathysiphons		Triassic	Babulu Group	Gondwana Megasequence	26/10
AB755	-9.05682	125.24315	Saburai	No sample	Gentle, open upright folding in well bedded limestones and mudstones							observation point		26/10
AB756	-9.06777	125.26013	Saburai	No sample	Interbedded limestones and mudstones							?Bandeira Group	Gondwana Megasequence	27/10
AB757A	-9.06747	125.26020	Saburai	No sample	Interbedded limestones and mudstones							?Bandeira Group	Gondwana Megasequence	27/10
AB757B	-9.06745	125.26055	Saburai	No sample	Interbedded limestones and mudstones							?Bandeira Group	Gondwana Megasequence	27/10
AB758	-9.06738	125.26064	Saburai	No sample	Interbedded limestones and mudstones							?Bandeira Group	Gondwana Megasequence	27/10
AB759	-9.06725	125.26086	Saburai	Limestone	Well bedded **limestones** and mudstones, some evidence of gentle folding	Shelly wackestone with abundant echinoid and chrinoid fragments	Pamula		echinoids, crinoids, bryozoans, punctate brachiopods		Triassic	Transitional Bandeira/Aitutu with debris slides	Gondwana Megasequence	27/10
AB760	-9.06819	125.25924	Saburai	No sample	Odd looking "damage zone?". Bedding is abruptly truncated by large blocks with sub-vertical fractures trending 160°. Zone is 6-8 m wide							observation point		27/10
AB761	-9.07921	125.25208	Saburai	No sample	Fault plane partially covered by gouge and breccia							observation point		27/10
AB762A	-9.08126	125.24944	Saburai	Fault gouge	Massive limestone with **fault gouge on surface (A, west)** faulted against sandy mudstone (B, east)						Unknown	Unknown	Unknown	27/10
AB762B	-9.08126	125.24944	Saburai	Mudstone	Massive limestone with fault gouge on surface (A, west) faulted against s**andy mudstone (B, east)**	Some small shell fragments and possibly ?radiolaria visible. Rare foraminifera	nodosariids				?Triassic	?Babulu Group	?Gondwana Megasequence	27/10
AB763	-9.08351	125.24704	Saburai	No sample	fault gouge above road at this point							observation point		27/10
AB764	-9.08470	125.24584	Saburai	Fault gouge	Limestone fault gouge	No biogenic grains visible					Unknown	Unknown	Unknown	27/10
AB765	-9.09352	125.24165	Saburai	No sample	Fault gouge "slide" appears to have a source over the top of the ridge							observation point		27/10

Location_No	Lat	Long	Region	Sample_type	Field_Description	Rock_Description	Benthic_foraminifera	Planktonic_foraminifera	OtherBioclasts	Facies	Age	Group	Megasequence	Date
AB766	-9.09394	125.24099	Saburai	No sample	Gouge slide with no obvious fault, gouge is sitting in front of well bedded limestones and mudstones							observation point		27/10
AB767	-9.10078	125.23839	Saburai	No sample	Very well bedded limestone							observation point		27/10
AB768	-8.92816	125.15197	Maliana Basin	No sample	Friable cobbles gravel and sand - young alluvial deposits						?Quaternary	Recent surficial deposits	Recent surficial deposits	28/10
AB769	-8.80626	125.20977	Maliana Basin	Igneous	Rounded outcrop of course-grained igneous rock (grains < 1 cm) looks slightly porphyritic	Subhedral to anhedral porphyroclasts in a fine grained matrix containing small plagioclase laths								28/10
AB770	-8.78248	125.20636	Maliana Basin	Sandstone	Outcrop/subcrop of large sandstone blocks ≈ 1-2 m in size within light brown mud (recessive - now soil). Hummocky cross bedding visible in some blocks. Bedding shows discontinuity but similar orientations in all blocks. Looks exactly like the sandstone blocks in Bobonaro Formation heading into Maliana from Balibo	Sandstone containing abundant very small, globular planktonic forams - probably contamination					?Triassic	?Babulu Group	Gondwana Megasequence	28/10
AB771	-8.76275	125.19383	Maliana Basin	Igneous	Weathered igneous rock. Possibly part of Aileu but not very metamorphosed. Looks like a fg basaltic rock	fg matrix of plagioclase laths, ?pyroxene and volcanic glass								28/10
AB772	-8.76256	125.19266	Maliana Basin	No sample	Very large sandstone block within the Babulu							?Babulu Group	?Gondwana Megasequence	28/10
AB773	-8.75281	125.18097	Maliana Basin	Igneous	Fg igneous rocks of intermediate composition	Porphyritic igneous rock								28/10
AB774	-8.96392	125.02981	Maliana Basin	No sample	Well bedded purple/grey limestone						Unknown	Unknown	Unknown	28/10
AB775	-8.88506	125.13172	Maliana Basin	No sample	Broken formation sandstone blocks within grey mudstone, similar to outcrop near the Maliana bridge. No exotic blocks observed.							?Babulu Group	?Gondwana Megasequence	29/10
AB776A	-8.88161	125.12688	Maliana Basin	Limestone	White wackestone with abundant shell fragments and distinctive larger Booi limestone forams. Samples are from scree being shed from a small vegetated hill bearing 033° from this point	Wackestone with abundant larger benthic forams, shell and coral fragments, and rarer small planktonic forams	Alveolina				Middle Eocene	Dartollu Group	Banda Megasequence	29/10
AB776B	-8.88161	125.12688	Maliana Basin	Limestone	White wackestone with abundant shell fragments and distinctive larger Booi limestone forams. Samples are from scree being shed from a small vegetated hill bearing 033° from this point	Wackestone with abundant larger benthic forams, shell and coral fragments, and rarer small planktonic forams					Latest Oligocene Earliest Miocene	Booi Group	Banda Megasequence	
AB777	-8.88040	125.11438	Maliana Basin	No sample	Broken formation sandstone blocks within grey mudstone							?Babulu Group	?Gondwana Megasequence	29/10
AB778	-8.85810	125.08575	Maliana Basin	clay	Badlands style outcrop of soft, white/yellow clay containing angular clasts 0.5-3 cm of red chert	Residue composed of red and white angular cherty grains. Abundant radiolarian debri in 150 µ residue (poorly preserved, just small spherules - no spines)					?Mesozoic	Unknown	?Gondwana Megasequence	29/10
AB779	-8.84956	125.07498	Maliana Basin	Limestone	Scree from roadside. Vfg pink/white pelagite - looks like AMM and is possibly related to the red chert	Wackestone containing very small planktonic forams					?Eocene	?Un-named Eocene Banda	?Banda Megasequence	29/10
AB780	-8.84990	125.07217	Maliana Basin	No sample	Outcrop containing very weathered, yellow/white, cg, igneous material; very weathered, red, fractured, fg, igneous material; and very weathered, red, siliceous, cherty mud.									29/10

Appendix II

Structural observations

Location No	Lat	Long	Region	Structure Type	Dip	Dip Direction	Lineation Dip	Lineation Dip Direction	Movement	or	Group	Megasequence	Notes
AB002	-8.69940	126.33767	Mundo Perdido	Bedding	18	008							
AB005	-8.72988	126.36760	Mundo Perdido	Bedding	20	224					Baucau Limestone	Synorogenic Megasequence	
AB013	-8.72908	126.36558	Mundo Perdido	?Fault	65	110					Booi Group	Banda Megasequence	
AB014	-8.72935	126.36570	Mundo Perdido	?Fault	85	205					Kolbano Group	Australian Margin Megasequence	
AB021	-8.73068	126.36723	Mundo Perdido	Fault	60	030	25	052	dextral normal	sinistral reverse	observation point		
AB023	-8.73057	126.36700	Mundo Perdido	Fault	60	030	28	053	sinistral reverse		Perdido Group	Gondwana Megasequence	
AB027	-8.75798	126.32160	Mundo Perdido	Bedding	30	300					Booi Group	Banda Megasequence	
AB028	-8.75582	126.31635	Mundo Perdido	Bedding	26	290					Kolbano Group	Australian Margin Megasequence	
AB029	-8.74305	126.29315	Mundo Perdido	Bedding	18	212					Perdido Group	Gondwana Megasequence	
AB032	-8.72405	126.36732	Mundo Perdido	Bedding	38	115					Booi Group	Banda Megasequence	
AB036	-8.72405	126.36732	Mundo Perdido	Bedding	20	122					Booi Group	Banda Megasequence	
AB040	-8.72437	126.36618	Mundo Perdido	Bedding	35	108					Booi Group	Banda Megasequence	
AB043	-8.72507	126.36538	Mundo Perdido	?Fault	80	130					Perdido Group	Gondwana Megasequence	
AB049	-8.71155	126.36420	Mundo Perdido	Fault plane	74	016	38	092	dextral normal		Perdido Group	Gondwana Megasequence	
AB049	-8.71155	126.36420	Mundo Perdido	Fault plane	74	016	56	074	dextral normal		Perdido Group	Gondwana Megasequence	
AB049	-8.71155	126.36420	Mundo Perdido	Fault plane	74	016	64	062	dextral normal		Perdido Group	Gondwana Megasequence	
AB049	-8.71155	126.36420	Mundo Perdido	Fault plane	62	022					Perdido Group	Gondwana Megasequence	
AB049	-8.71155	126.36420	Mundo Perdido	Fault plane	52	148					Perdido Group	Gondwana Megasequence	
AB049	-8.71155	126.36420	Mundo Perdido	Fault plane	88	352	50	070	dextral normal		Perdido Group	Gondwana Megasequence	
AB049	-8.71155	126.36420	Mundo Perdido	Fault plane	30	092					Perdido Group	Gondwana Megasequence	
AB049	-8.71155	126.36420	Mundo Perdido	Fault plane	47	012					Perdido Group	Gondwana Megasequence	
AB049	-8.71155	126.36420	Mundo Perdido	Fault plane	87	343					Perdido Group	Gondwana Megasequence	
AB049	-8.71155	126.36420	Mundo Perdido	Fault plane	38	293					Perdido Group	Gondwana Megasequence	
AB057	-8.71427	126.35915	Mundo Perdido	?Fault	84	054					Unknown	Unknown	
AB059	-8.71403	126.35887	Mundo Perdido	Bedding	60	030					Kolbano Group	Australian Margin Megasequence	
AB060	-8.71403	126.35887	Mundo Perdido	Bedding	30	020					Unknown	Unknown	
AB062	-8.71132	126.35397	Mundo Perdido	Bedding	55	345					Kolbano Group	Australian Margin Megasequence	
AB063	-8.71260	126.35402	Mundo Perdido	Bedding	50	020					Kolbano Group	Australian Margin Megasequence	
AB066	-8.71552	126.35255	Mundo Perdido	?Fault	75	016					Kolbano Group	Australian Margin Megasequence	

Location No	Lat	Long	Region	Structure Type	Dip	Dip Direction	Lineation Dip	Lineation Dip Direction	Movement	or	Group	Megasequence	Notes
AB072	-8.73418	126.36570	Mundo Perdido	Bedding	15	184					Unknown	Unknown	
AB075	-8.73027	126.36768	Mundo Perdido	?Fault	58	072					Booi Group	Banda Megasequence	
AB079	-8.73057	126.36700	Mundo Perdido	Fault	60	120	20	065	?dextral normal		Booi Group	Banda Megasequence	
AB079B	-8.73057	126.36700	Mundo Perdido	Fault	60	120	20	080	?dextral normal		Booi Group	Banda Megasequence	
AB090	-8.73470	126.37368	Mundo Perdido	Bedding	35	145					Booi Group	Banda Megasequence	
AB091	-8.73412	126.37458	Mundo Perdido	?Fault	20	048					Booi Group	Banda Megasequence	
AB091	-8.73412	126.37458	Mundo Perdido	Bedding	30	145					Booi Group	Banda Megasequence	
AB092	-8.73307	126.37547	Mundo Perdido	Fault plane	85	335	80	020	dextral reverse		Booi Group	Banda Megasequence	
AB092	-8.73307	126.37547	Mundo Perdido	Fault plane	77	132	55	075	sinistral normal		Booi Group	Banda Megasequence	
AB092	-8.73307	126.37547	Mundo Perdido	Fault plane	60	000	40	058	dextral reverse		Booi Group	Banda Megasequence	
AB092	-8.73307	126.37547	Mundo Perdido	Fault plane	80	165					Booi Group	Banda Megasequence	
AB092	-8.73307	126.37547	Mundo Perdido	Fault plane	65	130	60	120	sinistral normal	dextral reverse	Booi Group	Banda Megasequence	
AB092	-8.73307	126.37547	Mundo Perdido	Fault plane	54	124	45	105	sinistral normal	dextral reverse	Booi Group	Banda Megasequence	
AB092	-8.73307	126.37547	Mundo Perdido	Fault plane	55	280	50	350	dextral normal	sinistral reverse	Booi Group	Banda Megasequence	
AB092	-8.73307	126.37547	Mundo Perdido	Fault plane	56	010	40	330	sinistral normal	dextral reverse	Booi Group	Banda Megasequence	
AB095	-8.73407	126.37292	Mundo Perdido	Fault	50	130	10	092	sinistral normal	dextral reverse	Booi Group	Banda Megasequence	
AB096	-8.73307	126.37547	Mundo Perdido	Fault	80	155			sinistral normal		Booi Group	Banda Megasequence	
AB096	-8.73307	126.37547	Mundo Perdido	Fault plane	79	294	58	242	sinistral normal	dextral reverse	Booi Group	Banda Megasequence	
AB096	-8.73307	126.37547	Mundo Perdido	Fault plane	58	126	60	144	dextral normal	sinistral reverse	Booi Group	Banda Megasequence	
AB096	-8.73307	126.37547	Mundo Perdido	Fault plane	49	116	49	116	normal	reverse	Booi Group	Banda Megasequence	
AB096	-8.73307	126.37547	Mundo Perdido	Fault plane	80	198	63	132	sinistral normal	dextral reverse	Booi Group	Banda Megasequence	
AB096	-8.73307	126.37547	Mundo Perdido	Fault plane	49	126	50	116	sinistral normal	dextral reverse	Booi Group	Banda Megasequence	
AB096	-8.73307	126.37547	Mundo Perdido	Fault plane	56	140	54	128	sinistral normal	dextral reverse	Booi Group	Banda Megasequence	
AB096	-8.73307	126.37547	Mundo Perdido	Fault plane	52	150	50	124	sinistral normal	dextral reverse	Booi Group	Banda Megasequence	
AB096	-8.73307	126.37547	Mundo Perdido	Fault plane	39	202	32	166	sinistral normal	dextral reverse	Booi Group	Banda Megasequence	
AB096	-8.73307	126.37547	Mundo Perdido	Fault plane	44	194	38	158	sinistral normal	dextral reverse	Booi Group	Banda Megasequence	
AB096	-8.73307	126.37547	Mundo Perdido	Fault plane	36	178	30	180	normal	reverse	Booi Group	Banda Megasequence	
AB096	-8.73307	126.37547	Mundo Perdido	Fault plane	44	145	40	125	sinistral normal	dextral reverse	Booi Group	Banda Megasequence	
AB096	-8.73307	126.37547	Mundo Perdido	Fault plane	80	158	75	205	dextral normal	sinistral reverse	Booi Group	Banda Megasequence	

Location No	Lat	Long	Region	Structure Type	Dip	Dip Direction	Lineation Dip	Lineation Dip Direction	Movement	or	Group	Megasequence	Notes
AB096	-8.73307	126.37547	Mundo Perdido	Fault plane	40	326	24	274	sinistral normal	dextral reverse			
AB096	-8.73307	126.37547	Mundo Perdido	Fault plane	80	310	79	075	dextral normal	sinistral reverse	Booi Group	Banda Megasequence	
AB096	-8.73307	126.37547	Mundo Perdido	Fault plane	45	154	40	168	dextral normal	sinistral reverse	Booi Group	Banda Megasequence	
AB096	-8.73307	126.37547	Mundo Perdido	Fault plane	80	132	73	086	sinistral normal	dextral reverse	Booi Group	Banda Megasequence	
AB096	-8.73307	126.37547	Mundo Perdido	Fault plane	32	275	32	275	normal	reverse	Booi Group	Banda Megasequence	
AB096	-8.73307	126.37547	Mundo Perdido	Fault plane	70	274	50	026	dextral normal	sinistral reverse	Booi Group	Banda Megasequence	
AB097	-8.73192	126.37717	Mundo Perdido	Fault	50	098	35	060	sinistral normal	dextral reverse	Booi Group	Banda Megasequence	
AB100	-8.72947	126.37912	Mundo Perdido	?Bedding	65	102					Booi Group	Banda Megasequence	
AB104	-8.72970	126.38085	Mundo Perdido	Fault plane	45	004	42	016	dextral normal	sinistral reverse	observation point		
AB104	-8.72970	126.38085	Mundo Perdido	Fault plane	54	018	52	002	sinistral normal	dextral reverse	observation point		
AB104	-8.72970	126.38085	Mundo Perdido	Fault plane	62	018	55	332	sinistral normal	dextral reverse	observation point		
AB104	-8.72970	126.38085	Mundo Perdido	Fault plane	62	018	34	304	sinistral normal	dextral reverse	observation point		
AB104	-8.72970	126.38085	Mundo Perdido	Fault	60	018	54	332	sinistral normal	dextral reverse	observation point		
AB104	-8.72970	126.38085	Mundo Perdido	Fault plane	65	026	56	344	sinistral normal	dextral reverse	observation point		
AB104	-8.72970	126.38085	Mundo Perdido	Fault plane	85	014	15	292	sinistral normal	dextral reverse	observation point		
AB105	-8.72940	126.38247	Mundo Perdido	Fault	70	068	45	108	dextral normal	sinistral reverse	observation point		
AB106	-8.72940	126.38315	Mundo Perdido	Bedding	30	096					Unknown	Unknown	
AB111	-8.73472	126.37782	Mundo Perdido	?Fault	40	345	40	345	?normal		Booi Group	Banda Megasequence	
AB111	-8.73472	126.37782	Mundo Perdido	?Bedding	40	156					Booi Group	Banda Megasequence	
AB112	-8.73432	126.37838	Mundo Perdido	Fault	45	314	36	346	dextral reverse		Booi Group	Banda Megasequence	
AB112	-8.73432	126.37838	Mundo Perdido	Fault plane	60	205	45	250	dextral reverse		Booi Group	Banda Megasequence	
AB112	-8.73432	126.37838	Mundo Perdido	Fault plane	70	182	45	248	dextral reverse		Booi Group	Banda Megasequence	
AB112	-8.73432	126.37838	Mundo Perdido	Bedding	28	126					Booi Group	Banda Megasequence	
AB114	-8.73280	126.38033	Mundo Perdido	Fault plane	74	325	65	295	dextral reverse		Booi Group	Banda Megasequence	
AB114	-8.73280	126.38033	Mundo Perdido	Fault plane	86	157	75	230	dextral normal		Booi Group	Banda Megasequence	
AB114	-8.73280	126.38033	Mundo Perdido	Fault plane	68	327	67	318	dextral reverse		Booi Group	Banda Megasequence	
AB114	-8.73280	126.38033	Mundo Perdido	Fault plane	36	196	35	176	sinistral normal		Booi Group	Banda Megasequence	
AB114	-8.73280	126.38033	Mundo Perdido	Fault plane	36	196	20	126	sinistral normal		Booi Group	Banda Megasequence	
AB114	-8.73280	126.38033	Mundo Perdido	Fault plane	38	184	25	233	dextral normal		Booi Group	Banda Megasequence	

Location No	Lat	Long	Region	Structure Type	Dip	Dip Direction	Lineation Dip	Lineation Dip Direction	Movement	or	Group	Megasequence	Notes
AB114	-8.73280	126.38033	Mundo Perdido	Fault plane	69	218	45	154	sinistral normal				
AB114	-8.73280	126.38033	Mundo Perdido	Fault plane	56	212	56	212	normal		Booi Group	Banda Megasequence	
AB114	-8.73280	126.38033	Mundo Perdido	Bedding	26	215					Booi Group	Banda Megasequence	
AB115	-8.73253	126.38160	Mundo Perdido	Bedding	45	215					Booi Group	Banda Megasequence	
AB117	-8.73252	126.38207	Mundo Perdido	Fault	77	070					Booi Group	Banda Megasequence	
AB118	-8.73463	126.37942	Mundo Perdido	Fault	60	090	56	080	sinistral normal		observation point		
AB118	-8.73463	126.37942	Mundo Perdido	Bedding	30	210					Booi Group	Banda Megasequence	
AB119	-8.70182	126.32353	Mundo Perdido	?Bedding	25	010					Booi Group	Banda Megasequence	
AB120	-8.70477	126.32148	Mundo Perdido	?Fault	85	045					Baucau Limestone	Synorogenic Megasequence	
AB120	-8.70477	126.32148	Mundo Perdido	?Bedding	65	150					Perdido Group	Gondwana Megasequence	
AB128	-8.70678	126.32443	Mundo Perdido	?Bedding	24	000					Perdido Group	Gondwana Megasequence	
AB134	-8.70622	126.32510	Mundo Perdido	Bedding	50	015					Perdido Group	Gondwana Megasequence	
AB138	-8.70450	126.32688	Mundo Perdido	Bedding	10	312					Kolbano Group	Australian Margin Megasequence	
AB140	-8.71093	126.32032	Mundo Perdido	Bedding	25	090					Baucau Limestone	Synorogenic Megasequence	
AB141	-8.71163	126.31977	Mundo Perdido	Fault	90	170					Kolbano Group	Australian Margin Megasequence	
AB143	-8.71235	126.31998	Mundo Perdido	?Fault	90	240					Perdido Group	Gondwana Megasequence	
AB145	-8.71467	126.32032	Mundo Perdido	Bedding	20	235					?Perdido Group	?Gondwana Megasequence	
AB145	-8.71467	126.32032	Mundo Perdido	Fold axial plane	50	088					Kolbano Group	Australian Margin Megasequence	
AB145	-8.71467	126.32032	Mundo Perdido	Fold axis	50	080					Kolbano Group	Australian Margin Megasequence	
AB145	-8.71467	126.32032	Mundo Perdido	Fold axial plane	81	275					Kolbano Group	Australian Margin Megasequence	
AB145	-8.71467	126.32032	Mundo Perdido	Fold axis	34	195					Kolbano Group	Australian Margin Megasequence	
AB146	-8.71585	126.31993	Mundo Perdido	Bedding	15	172					Kolbano Group	Australian Margin Megasequence	
AB147	-8.71630	126.31935	Mundo Perdido	Bedding	45	280					Kolbano Group	Australian Margin Megasequence	
AB149	-8.71750	126.31942	Mundo Perdido	?Fault	90	285	40	194	sinistral	dextral	Perdido Group	Gondwana Megasequence	
AB152	-8.71895	126.31788	Mundo Perdido	Bedding	42	000					Kolbano Group	Australian Margin Megasequence	
AB158	-8.72330	126.31907	Mundo Perdido	Bedding	05	160					Kolbano Group	Australian Margin Megasequence	
AB158	-8.72330	126.31907	Mundo Perdido	Fold axial plane	85	300					Kolbano Group	Australian Margin Megasequence	
AB158	-8.72330	126.31907	Mundo Perdido	Fold axis	10	215					Kolbano Group	Australian Margin Megasequence	
AB161	-8.71620	126.32303	Mundo Perdido	?Bedding	28	194					Kolbano Group	Australian Margin Megasequence	

Location No	Lat	Long	Region	Structure Type	Dip	Dip Direction	Lineation Dip	Lineation Dip Direction	Movement	or	Group	Megasequence	Notes
AB162	-8.71525	126.32407	Mundo Perdido	Bedding	44	024					Kolbano Group	Australian Margin Megasequence	
AB163	-8.71357	126.32390	Mundo Perdido	Bedding	30	006					Kolbano Group	Australian Margin Megasequence	
AB165	-8.71182	126.32352	Mundo Perdido	Bedding	68	002					Kolbano Group	Australian Margin Megasequence	
AB167	-8.73990	126.35515	Mundo Perdido	Bedding	53	173	45	244	dextral normal		Booi Group	Banda Megasequence	
AB169	-8.74003	126.35652	Mundo Perdido	Fault	88	140	88	140	normal		Booi Group	Banda Megasequence	
AB171	-8.73672	126.35827	Mundo Perdido	Fault	65	060	36	125			observation point		
AB171	-8.73672	126.35827	Mundo Perdido	Fault plane	60	074	50	144	sinistral reverse		observation point		
AB171	-8.73672	126.35827	Mundo Perdido	Bedding	22	134					observation point		
AB173	-8.73567	126.36047	Mundo Perdido	?Bedding	35	138					Booi Group	Banda Megasequence	
AB174	-8.73572	126.35997	Mundo Perdido	Bedding	48	150					Booi Group	Banda Megasequence	
AB178	-8.74258	126.29340	Mundo Perdido	Bedding	47	050					Booi Group	Banda Megasequence	
AB179	-8.74200	126.29415	Mundo Perdido	Bedding	50	160					Booi Group	Banda Megasequence	
AB182	-8.74015	126.29547	Mundo Perdido	Fault	44	310	06	015	sinistral reverse		Booi Group	Banda Megasequence	
AB182	-8.74015	126.29547	Mundo Perdido	Fault	80	080			sinistral reverse	dextral normal	Booi Group	Banda Megasequence	
AB182	-8.74015	126.29547	Mundo Perdido	Fault	80	145					Booi Group	Banda Megasequence	
AB183			Mundo Perdido	Bedding	44	322					Booi Group	Banda Megasequence	
AB185	-8.73790	126.29768	Mundo Perdido	?Fault	72	315					Booi Group	Banda Megasequence	
AB185	-8.73790	126.29768	Mundo Perdido	Bedding	47	305	25	255	sinistral normal	dextral reverse	Booi Group	Banda Megasequence	
AB195	-8.73768	126.29060	Mundo Perdido	Bedding	38	250					Booi Group	Banda Megasequence	
AB196	-8.73767	126.29060	Mundo Perdido	?Fault	50	314					Booi Group	Banda Megasequence	
AB201	-8.73263	126.29280	Mundo Perdido	Fault	70	235	52	160			observation point		
AB206	-8.72330	126.30622	Mundo Perdido	Fault	67	200	67	200	sinistral normal	dextral reverse	observation point		
AB206	-8.72330	126.30622	Mundo Perdido	Fault	62	180	25	262	normal	reverse	observation point		
AB219	-8.70052	126.33698	Mundo Perdido	Bedding	34	020					Baucau Limestone	Synorogenic Megasequence	
AB224	-8.70895	126.33987	Mundo Perdido	?Fault	90	125			sinistral reverse	dextral normal	Baucau Limestone	Synorogenic Megasequence	
AB235	-8.71073	126.34083	Mundo Perdido	Fault	78	072					Unknown	Unknown	
AB236	-8.71073	126.34083	Mundo Perdido	Fault	67	128	66	114	reverse		Kolbano Group	Australian Margin Megasequence	
AB236	-8.71073	126.34083	Mundo Perdido	Fault plane	80	116	65	180	sinistral reverse		Kolbano Group	Australian Margin Megasequence	
AB236	-8.71073	126.34083	Mundo Perdido	Fault plane	74	125	65	184	sinistral reverse		Kolbano Group	Australian Margin Megasequence	

Location No	Lat	Long	Region	Structure Type	Dip	Dip Direction	Lineation Dip	Lineation Dip Direction	Movement	or	Group	Megasequence	Notes
AB236	-8.71073	126.34083	Mundo Perdido	Fault plane	76	120	70	178	sinistral reverse				
AB236	-8.71073	126.34083	Mundo Perdido	Fault plane	03	335	03	335	sinistral reverse		Kolbano Group	Australian Margin Megasequence	
AB236	-8.71073	126.34083	Mundo Perdido	Fault plane	24	108	17	154			Kolbano Group	Australian Margin Megasequence	
AB238	-8.71157	126.33998	Mundo Perdido	Fault	52	026			sinistral reverse		Kolbano Group	Australian Margin Megasequence	
AB240	-8.71247	126.34010	Mundo Perdido	Fold axial plane	90	000					Perdido Group	Gondwana Megasequence	
AB241	-8.71273	126.33948	Mundo Perdido	Fault	45	002					Kolbano Group	Australian Margin Megasequence	
AB247	-8.70262	126.31545	Mundo Perdido	Bedding	37	340					Perdido Group	Gondwana Megasequence	
AB259	-8.70727	126.30877	Mundo Perdido	Bedding	34	098					Baucau Limestone	Synorogenic Megasequence	
AB263	-8.70292	126.31788	Mundo Perdido	Bedding	64	340					Booi Group	Banda Megasequence	
AB264	-8.70570	126.31017	Mundo Perdido	Bedding	42	350					Baucau Limestone	Synorogenic Megasequence	
AB270	-8.71232	126.31107	Mundo Perdido	Bedding	45	000					Baucau Limestone	Synorogenic Megasequence	
AB274	-8.71642	126.32532	Mundo Perdido	?Bedding	25	028					Kolbano Group	Australian Margin Megasequence	
AB275	-8.71900	126.32503	Mundo Perdido	?Bedding	65	346					Kolbano Group	Australian Margin Megasequence	
AB276	-8.72323	126.32295	Mundo Perdido	?Bedding	26	215					Perdido Group	Gondwana Megasequence	
AB277	-8.72327	126.32330	Mundo Perdido	?Bedding	20	035					Perdido Group	Gondwana Megasequence	
AB278	-8.71542	126.32598	Mundo Perdido	Bedding	80	006					Kolbano Group	Australian Margin Megasequence	
AB279	-8.71432	126.32653	Mundo Perdido	Bedding	15	088					Kolbano Group	Australian Margin Megasequence	
AB280	-8.71393	126.32600	Mundo Perdido	Bedding	15	000					Kolbano Group	Australian Margin Megasequence	
AB282	-8.71120	126.32803	Mundo Perdido	Bedding	45	004					Kolbano Group	Australian Margin Megasequence	
AB285	-8.73425	126.36128	Mundo Perdido	?Fault	85	236					Kolbano Group	Australian Margin Megasequence	
AB285	-8.73425	126.36128	Mundo Perdido	?Bedding	80	140					Perdido Group	Gondwana Megasequence	
AB293	-8.72373	126.35148	Mundo Perdido	?Fault	90	230					Perdido Group	Gondwana Megasequence	
AB295	-8.72285	126.35013	Mundo Perdido	Fault	80	354	34	050			Perdido Group	Gondwana Megasequence	
AB296	-8.72285	126.35013	Mundo Perdido	Fault plane	27	202	26	234	sinistral reverse		Perdido Group	Gondwana Megasequence	
AB297	-8.72285	126.35013	Mundo Perdido	Fault plane	38	070	34	050	sinistral reverse		Perdido Group	Gondwana Megasequence	
AB310	-8.73767	126.35715	Mundo Perdido	?Fault	84	018			sinistral reverse		Unknown	Unknown	
AB312	-8.73203	126.34633	Mundo Perdido	?Fault	55	172	20	220			Booi Group	Banda Megasequence	
AB313	-8.73203	126.34633	Mundo Perdido	Fault	70	122	29	055	dextral normal	sinistral reverse	observation point		
AB318	-8.73245	126.34287	Mundo Perdido	Bedding	40	010					Perdido Group	Gondwana Megasequence	
											Kolbano Group	Australian Margin Megasequence	

Location No	Lat	Long	Region	Structure Type	Dip	Dip Direction	Lineation Dip	Lineation Dip Direction	Movement	or	Group	Megasequence	Notes
AB321	-8.73277	126.33938	Mundo Perdido	?Fault	74	150			sinistral normal	dextral reverse			
AB325	-8.73607	126.34105	Mundo Perdido	Fault	60	020	17	305			Kolbano Group	Australian Margin Megasequence	
AB325	-8.73607	126.34105	Mundo Perdido	Fault plane	72	298			sinistral		Perdido Group	Gondwana Megasequence	
AB325	-8.73607	126.34105	Mundo Perdido	Fault plane	77	274					Perdido Group	Gondwana Megasequence	
AB325	-8.73607	126.34105	Mundo Perdido	Fault plane	43	152					Perdido Group	Gondwana Megasequence	
AB332	-8.71470	126.35172	Mundo Perdido	Bedding	67	348					Perdido Group	Gondwana Megasequence	
AB400	-8.88271	126.37744	Viqueque	Fault	90	000					Kolbano Group	Australian Margin Megasequence	East-west striking fault separating Viqueque from melange zone
AB402	-8.81007	126.38052	Builo								observation point		
AB417	-9.02413	125.29604	Saburai	Fault plane	55	035					Aitutu Group	Gondwana Megasequence	Possible block in melange
AB417	-9.02413	125.29604	Saburai	Fault plane	50	340	30	280	sinistral normal		Unknown	Unknown	
AB417	-9.02413	125.29604	Saburai	Fault plane	30	310					Unknown	Unknown	
AB417	-9.02413	125.29604	Saburai	Fault plane	51	312	44	282	sinistral normal		Unknown	Unknown	
AB417	-9.02413	125.29604	Saburai	Fault plane	70	310					Unknown	Unknown	
AB419	-9.00713	125.27528	Saburai	Fault plane	57	350					Unknown	Unknown	
AB420B	-8.99068	125.28273	Loelako	Bedding	25	350					Bandeira Group	Gondwana Megasequence	
AB420B	-8.99068	125.28273	Loelako	Fold axial plane	42	010					?Babulu Group	?Gondwana Megasequence	Tight recumbent folds
AB422A	-8.98149	125.28351	Loelako	Fold hinge	25	322					?Babulu Group	?Gondwana Megasequence	Tight recumbent folds
AB429	-8.69568	126.37840	Laritame	Bedding	28	166					?Aitutu Group	Gondwana Megasequence	
AB430	-8.69575	126.37823	Laritame	Fault	60	157					Perdido Group	Gondwana Megasequence	
AB430	-8.69575	126.37823	Laritame	Fault	40	155	19	215	sinistral reverse		Perdido Group	Gondwana Megasequence	
AB430	-8.69575	126.37823	Laritame	Fault	40	155	54	154	reverse		Perdido Group	Gondwana Megasequence	
AB431	-8.69576	126.37885	Laritame	Fault	40	155	39	188	sinistral reverse		Perdido Group	Gondwana Megasequence	
AB431	-8.69576	126.37885	Laritame	Fault	80	130			sinistral		Perdido Group	Gondwana Megasequence	Riedel shears describe sinistral movement on this fault
AB431	-8.69576	126.37885	Laritame	Fault plane	78	070					Perdido Group	Gondwana Megasequence	
AB432	-8.69532	126.43293	Laritame	Fault plane	80	157					Perdido Group	Gondwana Megasequence	
AB438	-8.65417	126.39128	Laritame	Fault	70	150	65	195	sinistral reverse		Perdido Group	Gondwana Megasequence	
AB438	-8.65417	126.39128	Laritame	Fault	34	055	30	095	sinistral reverse	dextral normal	Booi Group	Banda Megasequence	Main fabric
AB444	-8.68234	126.38863	Laritame	Fault	34	055	33	060	sinistral reverse	dextral normal	Booi Group	Banda Megasequence	Secondary fabric
AB449	-8.95180	125.37078	Bobonaro Springs	Observation	90	006	50	070	dextral normal		Perdido Group	Gondwana Megasequence	bedding on the eastern side of Loelako dipping 15-20° towards S-SSE
											observation point		

Location No	Lat	Long	Region	Structure Type	Dip	Dip Direction	Lineation Dip	Lineation Dip Direction	Movement	or	Group	Megasequence	Notes
AB450A	-8.98977	125.27487	Loelako	Fold axial plane	30	010					?Babulu Group	?Gondwana Megasequence	
AB450A	-8.98977	125.27487	Loelako	Fold hinge	20	320					?Babulu Group	?Gondwana Megasequence	
AB453	-8.98661	125.27556	Loelako	Fault	90	245					observation point		Gully at base of cliffs on western side of Loelako
AB456	-8.98043	125.27578	Loelako	Vein	47	008					?Bandeira Group	?Gondwana Megasequence	
AB457	-8.98029	125.27580	Loelako	?Bedding	32	025					?Bandeira Group	?Gondwana Megasequence	
AB458	-8.97983	125.27543	Loelako	Fault plane	60	098	22	190	sinistral reverse	dextral normal	?Bandeira Group	?Gondwana Megasequence	Effectively strike-slip
AB459	-8.97957	125.27559	Loelako	?Bedding	68	005					Bandeira Group	Gondwana Megasequence	
AB462A	-8.98065	125.27182	Loelako	Bedding	52	270					?Viqueque Group	Synorogenic Megasequence	
AB464	-8.97812	125.27958	Loelako	Bedding	57	095					?Bandeira Group	?Gondwana Megasequence	
AB465	-8.97805	125.27927	Loelako	Bedding	54	090					?Bandeira Group	?Gondwana Megasequence	
AB466	-8.97800	125.27906	Loelako	Fault	47	270	35	340	sinistral reverse	dextral normal	?Bandeira Group	?Gondwana Megasequence	
AB467	-8.98278	125.27974	Loelako	Bedding	25	128					Unknown	Unknown	
AB468	-8.98557	125.27989	Loelako	Bedding	20	195					Transitional Bandeira/Aitutu	Gondwana Megasequence	
AB469	-8.98692	125.27844	Loelako	Bedding	73	080					Transitional Bandeira/Aitutu	Gondwana Megasequence	Cliff face is a bedding plane
AB473	-8.95976	125.28027	Loelako	Bedding	55	078					Unknown	Unknown	
AB474	-8.96113	125.28029	Loelako	Bedding	77	085					Bandeira Group	Gondwana Megasequence	Cliff face is a bedding plane
AB477A	-8.98174	125.28316	Loelako	Bedding	34	157					Aitutu Group	Gondwana Megasequence	
AB479	-8.98218	125.28281	Loelako	Bedding	44	144					?Aitutu Group	?Gondwana Megasequence	
AB479	-8.98218	125.28281	Loelako	Bedding	40	130					?Aitutu Group	?Gondwana Megasequence	
AB479	-8.98218	125.28281	Loelako	Fault plane	87	040	40	116	dextral normal		?Aitutu Group	?Gondwana Megasequence	
AB479	-8.98218	125.28281	Loelako	Fault plane	65	035	27	118			?Aitutu Group	?Gondwana Megasequence	
AB479	-8.98218	125.28281	Loelako	Fault plane	60	035	43	092			?Aitutu Group	?Gondwana Megasequence	
AB479	-8.98218	125.28281	Loelako	Fault plane	62	032	44	087			?Aitutu Group	?Gondwana Megasequence	
AB481	-8.98246	125.28212	Loelako	Bedding	35	150					?Aitutu Group	?Gondwana Megasequence	
AB482	-8.98298	125.28225	Loelako	?Bedding	56	116					Unknown	Unknown	
AB482	-8.98298	125.28225	Loelako	Bedding	40	110					Unknown	Unknown	
AB483	-8.98086	125.28334	Loelako	?Fault plane	60	235					Unknown	Unknown	
AB483	-8.98086	125.28334	Loelako	?Fault plane	50	205					Unknown	Unknown	
AB483	-8.98086	125.28334	Loelako	?Fault plane	65	100					Unknown	Unknown	

Location No	Lat	Long	Region	Structure Type	Dip	Dip Direction	Lineation Dip	Lineation Dip Direction	Movement	or	Group	Megasequence	Notes
AB485	-8.74616	126.46346	Builo	Bedding	49	005					?Noni Group	?Proto Indian Ocean Megasequence	
AB485	-8.74616	126.46346	Builo	Fault plane	72	045	55	092	dextral normal		?Noni Group	?Proto Indian Ocean Megasequence	
AB492	-8.60796	126.56995	Quelecai	?Cleavage	26	048					?Cribas Group	?Gondwana Megasequence	
AB497	-8.61280	126.57378	Quelecai	Bedding	80	332					Aitutu Group	Gondwana Megasequence	
AB498	-8.61260	126.57195	Quelecai	Fault	70	100	25	180	sinistral		?Cribas Group	?Gondwana Megasequence	Strike slip linealtions on fault plane at top of landslide. Likely dextral slightly transpressional
AB500	-8.61187	126.57996	Quelecai	Bedding	60	274					Aitutu Group	Gondwana Megasequence	Possibly not in situ
AB501	-8.61030	126.58347	Quelecai	Bedding	36	151					Aitutu Group	Gondwana Megasequence	
AB502	-8.61000	126.58643	Quelecai	Bedding	55	090					observation point		
AB510	-8.60642	126.57233	Quelecai	Bedding	42	130					observation point		
AB511	-8.60610	126.57371	Quelecai	Bedding	55	130							
AB512	-8.60563	126.57360	Quelecai	Bedding	70	110					Aitutu Group	Gondwana Megasequence	
AB513	-8.60596	126.57436	Quelecai	Bedding	39	274					Transitional Bandeira/Aitutu	Gondwana Megasequence	
AB513	-8.60596	126.57436	Quelecai	Fault plane	39	274	21	305			Transitional Bandeira/Aitutu	Gondwana Megasequence	Movement on bedding plane
AB514	-8.60581	126.57455	Quelecai	Bedding	70	110					Transitional Bandeira/Aitutu	Gondwana Megasequence	
AB515	-8.60557	126.57476	Quelecai	Bedding	88	290					Transitional Bandeira/Aitutu	Gondwana Megasequence	
AB516	-8.60451	126.57361	Quelecai	Bedding	55	118					Unknown	Unknown	
AB521	-8.60893	126.58695	Quelecai	Bedding	37	125					?Aitutu Group	?Gondwana Megasequence	
AB522	-8.60857	126.58746	Quelecai	Bedding	22	114					?Aitutu Group	?Gondwana Megasequence	
AB523	-8.61200	126.58500	Quelecai	Bedding	35	125					observation point		
AB523	-8.61200	126.58500	Quelecai	Fold hinge	35	125					observation point		
AB525	-8.58057	126.54772	Quelecai	Bedding	19	157					Aitutu Group (by lithofacies correlation)	Gondwana Megasequence	
AB526	-8.64601	126.62655	Baguia	Bedding	47	208					Aitutu Group (by lithofacies correlation)	Gondwana Megasequence	13 bedding measurements around a fold
AB526	-8.64601	126.62655	Baguia	Bedding	34	202					Aitutu Group (by lithofacies correlation)	Gondwana Megasequence	13 bedding measurements around a fold
AB526	-8.64601	126.62655	Baguia	Bedding	25	200					Aitutu Group (by lithofacies correlation)	Gondwana Megasequence	13 bedding measurements around a fold
AB526	-8.64601	126.62655	Baguia	Bedding	52	188					Aitutu Group (by lithofacies correlation)	Gondwana Megasequence	13 bedding measurements around a fold
AB526	-8.64601	126.62655	Baguia	Bedding	37	164					Aitutu Group (by lithofacies correlation)	Gondwana Megasequence	13 bedding measurements around a fold
AB526	-8.64601	126.62655	Baguia	Bedding	40	150					Aitutu Group (by lithofacies correlation)	Gondwana Megasequence	13 bedding measurements around a fold
AB526	-8.64601	126.62655	Baguia	Bedding	58	110					Aitutu Group (by lithofacies correlation)	Gondwana Megasequence	13 bedding measurements around a fold
AB526	-8.64601	126.62655	Baguia	Bedding	63	123					Aitutu Group (by lithofacies correlation)	Gondwana Megasequence	13 bedding measurements around a fold

Location No	Lat	Long	Region	Structure Type	Dip	Dip Direction	Lineation Dip	Lineation Dip Direction	Movement	or	Group	Megasequence	Notes
AB526	-8.64601	126.62655	Baguia	Bedding	74	103					Aitutu Group (by lithofacies correlation)	Gondwana Megasequence	13 bedding measurements around a fold
AB526	-8.64601	126.62655	Baguia	Bedding	73	272					Aitutu Group (by lithofacies correlation)	Gondwana Megasequence	13 bedding measurements around a fold
AB526	-8.64601	126.62655	Baguia	Bedding	75	134					Aitutu Group (by lithofacies correlation)	Gondwana Megasequence	13 bedding measurements around a fold
AB526	-8.64601	126.62655	Baguia	Bedding	77	134					Aitutu Group (by lithofacies correlation)	Gondwana Megasequence	13 bedding measurements around a fold
AB526	-8.64601	126.62655	Baguia	Fold axial plane	65	263					Aitutu Group (by lithofacies correlation)	Gondwana Megasequence	approx
AB526	-8.64601	126.62655	Baguia	Fold hinge	68	170					Aitutu Group (by lithofacies correlation)	Gondwana Megasequence	approx
AB527	-8.64595	126.62607	Baguia	Cliff face	64	038					Unknown	Unknown	possible stylofabric
AB530	-8.65148	126.62193	Baguia	Fault	54	357	44	050	dextral normal		?Bandeira Group	Gondwana Megasequence	
AB531	-8.64153	126.63850	Baguia	?Bedding	65	096					Kolbano Group	Australian Margin Megasequence	possibly jointing
AB532	-8.63711	126.64435	Baguia	Bedding	70	008					Unknown	Unknown	
AB533	-8.63465	126.64681	Baguia	Bedding	37	279					Unknown	Unknown	
AB534	-8.61600	126.67800	Baguia	Bedding	10	325					observation point		Sighted in
AB541	-8.81678	126.20964	Bibileu	?Bedding	74	184					Perdido Group (by lithofacies correlation)	Gondwana Megasequence	possibly jointing
AB542	-8.81616	126.20856	Bibileu	?Fault plane	27	080					Perdido Group (by lithofacies correlation)	Gondwana Megasequence	
AB542	-8.81616	126.20856	Bibileu	?Fault plane	58	300					Perdido Group (by lithofacies correlation)	Gondwana Megasequence	
AB542	-8.81616	126.20856	Bibileu	?Fault plane	55	195					Perdido Group (by lithofacies correlation)	Gondwana Megasequence	
AB542	-8.81616	126.20856	Bibileu	?Fault plane	30	350					Perdido Group (by lithofacies correlation)	Gondwana Megasequence	
AB542	-8.81616	126.20856	Bibileu	?Fault plane	44	350					Perdido Group (by lithofacies correlation)	Gondwana Megasequence	
AB543	-8.81772	126.22132	Bibileu	Cliff face	34	172					Kolbano Group	Australian Margin Megasequence	foliation subparallel to cliff face - possible stylofabric
AB552	-8.40952	127.29011	Paitchau	Bedding	26	220					Aitutu Group (by lithofacies correlation)	Gondwana Megasequence	
AB554	-8.39826	127.27156	Paitchau	Bedding	45	196					Kolbano Group	Australian Margin Megasequence	
AB555	-8.39853	127.26960	Paitchau	Bedding	10	344					Aitutu Group	Gondwana Megasequence	
AB555	-8.39853	127.26960	Paitchau	Fault							Aitutu Group	Gondwana Megasequence	huge fault quarry, can't access deformed rocks to take measurements
AB559	-8.44600	127.19400	Paitchau	Cliff face	75	310					Bandeira Group	Gondwana Megasequence	
AB561	-9.04036	125.27917	Saburai	Fault plane	40	050					?Aitutu Group	?Gondwana Megasequence	
AB561	-9.04036	125.27917	Saburai	Fold hinge	15	270					?Aitutu Group	?Gondwana Megasequence	
AB564	-9.07802	125.25417	Saburai	Cliff face	90	150					observation point		
AB565	-9.08156	125.24873	Saburai	Fault	72	075	70	065	sinistral normal		Unknown	Unknown	
AB565	-9.08156	125.24873	Saburai	Fault	75	062	75	062	normal		Unknown	Unknown	

Location No	Lat	Long	Region	Structure Type	Dip	Dip Direction	Lineation Dip	Lineation Dip Direction	Movement	or	Group	Megasequence	Notes
AB566	-9.09353	125.24155	Saburai	Fault	70	155					observation point		
AB572B	-9.20782	125.11742	Taroman	Fault plane	60	104	59	096	normal		?Melange zone	?Melange zone	
AB572C	-9.20782	125.11742	Taroman	Fault plane	63	088	63	088	normal		?Melange zone	?Melange zone	
AB573	-9.20767	125.11735	Taroman	?Bedding	45	002					?Transitional Bandeira/Aitutu	Gondwana Megasequence	
AB574A	-9.20779	125.11742	Taroman	Bedding	66	080					Babulu Group	Gondwana Megasequence	
AB575A	-9.20752	125.11737	Taroman	Bedding	37	092					Possible debris slide from Bandeira into Babulu	Gondwana Megasequence	
AB579	-9.20655	125.11735	Taroman	?Fault	40	315					observation point		approximate orientation - sighted in
AB584	-9.21447	125.11383	Taroman	Foliation	53	326					?Melange zone	?Melange zone	foliation within mud
AB585	-9.21524	125.11316	Taroman	Fault	34	336	18	048	dextral normal		observation point		
AB585	-9.21524	125.11316	Taroman	Fault	38	338	12	048	dextral normal		observation point		
AB585	-9.21524	125.11316	Taroman	Fault	37	340	17	048	dextral normal		observation point		
AB585	-9.21524	125.11316	Taroman	Fault	37	340	16	272	sinistral normal	dextral reverse	observation point		secondary lineation
AB585	-9.21524	125.11316	Taroman	Fault	40	340	10	056	dextral normal		observation point		
AB587	-9.21385	125.11362	Taroman	Fault	44	318	10	036	dextral normal		observation point		
AB587	-9.21385	125.11362	Taroman	Fault	30	308					observation point		
AB590A	-9.20720	125.11387	Taroman	?Bedding	36	135					?Babulu Group	?Gondwana Megasequence	
AB594	-9.18343	125.15708	Taroman	Bedding	80	045					?Noni Group	?Proto Indian Ocean Megasequence	
AB596	-9.18458	125.16788	Taroman	Fault	70	175	14	255	dextral normal	sinistral reverse	?Perdido Group (by lithofacies correlation)	?Gondwana Megasequence	Enormous fault gouge > 40m ??? Almost pure strike-slip
AB596	-9.18458	125.16788	Taroman	Fault	60	172	10	086	dextral reverse	sinistral normal	?Perdido Group (by lithofacies correlation)	?Gondwana Megasequence	Enormous fault gouge > 40m ??? Almost pure strike-slip
AB596	-9.18458	125.16788	Taroman	Fault	46	176	45	170	normal		?Perdido Group (by lithofacies correlation)	?Gondwana Megasequence	Enormous fault gouge > 40m ??? Dip-slip
AB611A	-9.10091	125.23808	Saburai	Fault	52	132	36	076	sinistral normal		Unknown	Unknown	
AB611A	-9.10091	125.23808	Saburai	Fault	67	142	58	092	sinistral normal		Unknown	Unknown	
AB611A	-9.10091	125.23808	Saburai	Fault	79	142	65	074	sinistral normal		Unknown	Unknown	
AB613	-8.95230	125.36879	Lacao	Vein	48	070	27	132	dextral normal	sinistral rerverse	Oe Baat Formation	Australian Margin Megasequence	
AB615	-8.96523	125.37969	Lacao	Fault	51	230	40	287	dextral normal		observation point		
AB615	-8.96523	125.37969	Lacao	Fault	36	267	35	270	normal		observation point		
AB617	-9.10772	125.29766	Bazol River	Bedding	24	338					?Babulu Group	Gondwana Megasequence	
AB617	-9.10772	125.29766	Bazol River	Fold hinge	25	252					?Babulu Group	Gondwana Megasequence	
AB617	-9.10772	125.29766	Bazol River	Fault	59	237			normal		?Babulu Group	Gondwana Megasequence	

Location No	Lat	Long	Region	Structure Type	Dip	Dip Direction	Lineation Dip	Lineation Dip Direction	Movement	or	Group	Megasequence	Notes
AB618	9.13595	125.24969	Bazol River	Fold hinge			25	252			Aitutu Group	Gondwana Megasequence	
AB618	9.13595	125.24969	Bazol River	Bedding	24	338					Aitutu Group	Gondwana Megasequence	
AB618	9.13595	125.24969	Bazol River	Fault	59	327			normal		Aitutu Group	Gondwana Megasequence	
AB621	9.03143	125.30644	Bazol River	Observation	84	090			normal		observation point		Fault due south of this GPS
AB623	-8.95095	125.10094	Maliana Basin	Fault	80	090			normal		observation point		
AB625	-8.95074	125.10495	Maliana Basin	Fault	90	100			?normal		observation point		
AB630	-8.93218	125.24901	Lesululi	Bedding	30	340					Aitutu or Bandeira Group	Gondwana Megasequence	
AB633	-8.92081	125.26599	Lesululi	Observation	32	090					Bandeira Group	Gondwana Megasequence	Bedding of Loelako foothills sighted in (Synorogenic Megasequence), bearing 160 from
AB639	-8.98510	125.28325	Loelako	Fault plane	41	198	36	152			Unknown	Unknown	Within Gouge
AB639	-8.98510	125.28325	Loelako	Fault plane	37	208					Unknown	Unknown	Within Gouge
AB639	-8.98510	125.28325	Loelako	Fault plane	42	245					Unknown	Unknown	Within Gouge
AB639	-8.98510	125.28325	Loelako	Fault plane	62	270					Unknown	Unknown	Within Gouge
AB639	-8.98510	125.28325	Loelako	Fault plane	75	198					Unknown	Unknown	Within Gouge
AB639	-8.98510	125.28325	Loelako	Fault plane	62	275	57	300			Unknown	Unknown	Within Gouge
AB640	-8.95648	125.28576	Loelako	Bedding	25	102					Unknown	Unknown	
AB641	-8.94572	125.27936	Loelako	Bedding	26	312					Viqueque Group	Synorogenic Megasequence	
AB642	-8.94295	125.27942	Loelako	Bedding	30	245					Viqueque Group	Synorogenic Megasequence	
AB643	-8.94043	125.27811	Loelako	Bedding	40	242					Viqueque Group	Synorogenic Megasequence	
AB644	-8.93830	125.27741	Loelako	Bedding	35	230					?Viqueque Group	?Synorogenic Megasequence	
AB652	-8.98059	125.27684	Loelako	Bedding	63	118					?Bandeira Group	?Gondwana Megasequence	
AB653	-8.98016	125.27602	Loelako	Bedding	61	098					Unknown	Unknown	
AB654	-8.98038	125.27603	Loelako	Bedding	61	100					Transitional Bandeira/Aitutu	Gondwana Megasequence	
AB655	-8.98087	125.27618	Loelako	Bedding	60	108					Unknown	Unknown	
AB656	-8.98114	125.27618	Loelako	Bedding	60	080					Bandeira Group	Gondwana Megasequence	Signted in
AB657	-8.98056	125.27696	Loelako	Bedding	70	070					Transitional Bandeira/Aitutu	Gondwana Megasequence	
AB658	-8.98096	125.27839	Loelako	Bedding	40	100					Bandeira Group	Gondwana Megasequence	Sighted in
AB659	-8.99325	125.20143	Maliana Basin	Bedding	25	318					Viqueque Group	Synorogenic Megasequence	
AB670	-8.99697	125.19775	Maliana Basin	Bedding	26	334					Viqueque Group	Synorogenic Megasequence	
AB671	-9.00814	125.19374	Maliana Basin	Bedding	35	347					Viqueque Group	Synorogenic Megasequence	

Location No	Lat	Long	Region	Structure Type	Dip	Dip Direction	Lineation Dip	Lineation Dip Direction	Movement	or	Group	Megasequence	Notes
AB672	-9.01029	125.19410	Maliana Basin										
				Bedding	45	356					Viqueque Group	Synorogenic Megasequence	
AB677	-9.06507	125.22139	Saburai										Sighted in, may be slightly shallower in some
				Bedding	60	226					Bandeira Group	Gondwana Megasequence	places
AB678	-9.06531	125.22057	Saburai										
				?Bedding	75	240					Bandeira Group	Gondwana Megasequence	Possibly not in situ
AB679	-9.06546	125.21952	Saburai										
				?Bedding	43	110					Bandeira Group	Gondwana Megasequence	Possibly not bedding, could be a jointing
AB680	-9.06362	125.21937	Saburai										Apparent dip of bedding at the top of the massif
				Observation	10	220					observation point		sighted in from this point
AB681	-9.06071	125.22666	Saburai										
				Fault	58	310	55	268	sinistral normal		Unknown	Unknown	Massive fault breccia on hill side
AB681	-9.06071	125.22666	Saburai										
				Fault	75	318					Unknown	Unknown	Massive fault breccia on hill side
AB684	-9.03865	125.27926	Saburai										
				Bedding	25	092							
AB685	-9.04592	125.27603	Saburai										
				Fault	44	020			reverse		Bandeira Group	Gondwana Megasequence	
AB686	-9.05313	125.25679	Saburai										
				Bedding	28	107					Aitutu Group	Gondwana Megasequence	
AB687	-9.06777	125.25920	Saburai										
				Bedding	18	062					Transitional Bandeira/Aitutu	Gondwana Megasequence	Slightly west of AB687
AB687	-9.06777	125.26030	Saburai										
				Bedding	15	232					Transitional Bandeira/Aitutu	Gondwana Megasequence	Slightly east of AB687
AB687	-9.06777	125.25970	Saburai										
				Fault	50	116					Transitional Bandeira/Aitutu	Gondwana Megasequence	
AB687	-9.06777	125.25970	Saburai										
				Fault	58	132					Transitional Bandeira/Aitutu	Gondwana Megasequence	
AB687	-9.06777	125.25970	Saburai										
				Fault	52	134	45	126	sinistral normal		Transitional Bandeira/Aitutu	Gondwana Megasequence	
AB687	-9.06777	125.25970	Saburai										
				Fault	52	110	50	090	sinistral normal		Transitional Bandeira/Aitutu	Gondwana Megasequence	
AB687	-9.06777	125.25970	Saburai										
				Fault	50	110	45	134	dextral normal		Transitional Bandeira/Aitutu	Gondwana Megasequence	
AB687	-9.06777	125.25970	Saburai										
				Fault	46	098	40	062	sinistral normal		Transitional Bandeira/Aitutu	Gondwana Megasequence	
AB687	-9.06777	125.25970	Saburai										
				Fault	49	109	46	080	sinistral normal		Transitional Bandeira/Aitutu	Gondwana Megasequence	
AB688	-9.07890	125.25066	Saburai										
				Fault plane	70	125	45	190	dextral normal		Unknown	Unknown	Within Gouge
AB689	-9.08179	125.24859	Saburai										
				Fault plane	75	122					Unknown	Unknown	Within Gouge
AB690	-9.08256	125.24748	Saburai										
				Fault plane	55	134					Unknown	Unknown	Within Gouge
AB694	-9.03266	125.28298	Saburai										
				Bedding	35	114							Gently folded and slightly undulating
AB695	-9.05461	125.25578	Saburai										
				Bedding	25	312					?Babulu Group	?Gondwana Megasequence	
AB698	-9.05786	125.24978	Saburai										
				?Bedding	67	290					Transitional Bandeira/Aitutu	Gondwana Megasequence	Possibly not in situ
AB699	-9.06065	125.24577	Saburai										
				?Bedding	70	300					Transitional Bandeira/Aitutu	Gondwana Megasequence	Sighted in
AB700	-9.05625	125.24288	Saburai										
				?Bedding	17	170					observation point		Sighted in
AB701	-8.87614	125.23908	Cailaco										
				Bedding	25	315					Viqueque Group	Synorogenic Megasequence	
AB702	-8.87648	125.24864	Cailaco										
				Bedding	34	003					Viqueque Group	Synorogenic Megasequence	

Location No	Lat	Long	Region	Structure Type	Dip	Dip Direction	Lineation Dip	Lineation Dip Direction	Movement	or	Group	Megasequence	Notes
AB703	-8.87848	125.25593	Cailaco	Bedding	27	340					Viqueque Group	Synorogenic Megasequence	
AB704	-8.87559	125.26357	Cailaco	Bedding	20	064					Viqueque Group	Synorogenic Megasequence	
AB705	-8.87802	125.27556	Cailaco	Bedding	25	210					Viqueque Group	Synorogenic Megasequence	
AB706	-8.87787	125.28010	Cailaco	Bedding	30	284					Viqueque Group	Synorogenic Megasequence	
AB707	-8.88685	125.28434	Cailaco	Bedding	20	268					Viqueque Group	Synorogenic Megasequence	
AB708	-8.82047	125.28003	Cailaco	Observation	10	180					observation point		Bedding sighted in across river
AB709	-8.90515	125.24971	Lesululi	?Bedding	66	130					?Aitutu Group	?Gondwana Megasequence	Not confident measurement, bedding quite deformed
AB710	-8.90533	125.25009	Lesululi	Bedding	55	340					?Aitutu Group	?Gondwana Megasequence	
AB711	-8.90460	125.25122	Lesululi	Bedding	50	306					?Aitutu Group	?Gondwana Megasequence	
AB713	-8.90868	125.24905	Lesululi	?Bedding	50	010					Bandeira Group	Gondwana Megasequence	Foliation quite vague, possibly not bedding
AB714	-8.90847	125.24945	Lesululi	Bedding	55	324					Unknown	Unknown	
AB715	-8.90877	125.25002	Lesululi	?Bedding	40	343					?Bandeira Group	?Gondwana Megasequence	Pervasive foliation - possibly bedding
AB717	-8.90928	125.24997	Lesululi	Fault	85	288			normal				Drag fold against fault - see notebook for sketch
AB718	-8.91002	125.24979	Lesululi	Fault	87	305	63	220	sinistral normal		Unknown	Unknown	
AB719	-8.91097	125.25002	Lesululi	Fault	88	298	50	220	sinistral normal		?Bandeira Group	?Gondwana Megasequence	sighted in
AB719	-8.91097	125.25002	Lesululi	?Bedding	75	210					?Bandeira Group	?Gondwana Megasequence	Pervasive foliation - possibly bedding
AB721	-8.95240	125.27793	Loelako	Bedding	81	060					Unknown	Unknown	
AB722	-8.95263	125.27752	Loelako	Bedding	60	050					Unknown	Unknown	
AB723	-8.95306	125.27765	Loelako	Foliation	46	180					?Bandeira Group	?Gondwana Megasequence	Pervasive blocky fabric caused by 3 intersecting foliations
AB723	-8.95306	125.27765	Loelako	Foliation	70	062					?Bandeira Group	?Gondwana Megasequence	Pervasive blocky fabric caused by 3 intersecting foliations
AB723	-8.95306	125.27765	Loelako	Foliation	80	326					?Bandeira Group	?Gondwana Megasequence	Pervasive blocky fabric caused by 3 intersecting foliations
AB726	-8.95100	125.27712	Loelako	?Fault	80	095	46	008	dextral normal		Unknown	Unknown	Possibly not in situ
AB727	-8.95062	125.27643	Loelako	Foliation	60	185					Unknown	Unknown	Pervasive blocky fabric caused by 3 intersecting foliations
AB727	-8.95062	125.27643	Loelako	Foliation	55	240					Unknown	Unknown	Pervasive blocky fabric caused by 3 intersecting foliations
AB727	-8.95062	125.27643	Loelako	Foliation	66	312					Unknown	Unknown	Pervasive blocky fabric caused by 3 intersecting foliations
AB727	-8.95062	125.27643	Loelako	Fault	62	355					Unknown	Unknown	
AB727	-8.95062	125.27643	Loelako	?Fault plane	65	250	20	175	sinistral normal	dextral reverse	Unknown	Unknown	
AB727	-8.95062	125.27643	Loelako	?Fault plane	62	008	40	093	sinistral reverse	dextral normal	Unknown	Unknown	
AB727	-8.95062	125.27643	Loelako	?Fault plane	85	120	25	030	sinistral normal	dextral reverse	Unknown	Unknown	

Location No	Lat	Long	Region	Structure Type	Dip	Dip Direction	Lineation Dip	Lineation Dip Direction	Movement	or	Group	Megasequence	Notes
AB728	-8.95034	125.27627	Loelako	Fault	67	248					Unknown	Unknown	
AB729	-9.00964	125.27118	Saburai	Fault	80	100	60	170			Unknown	Unknown	
AB730	-9.01003	125.27104	Saburai	Fault	88	285	78	205	sinistral normal		Unknown	Unknown	
AB730	-9.01003	125.27104	Saburai	Fault	88	285	65	200	sinistral normal		Unknown	Unknown	
AB731	-9.00643	125.27557	Saburai	Bedding	52	025					?Babulu Group	?Gondwana Megasequence	
AB732	-9.00897	125.28343	Saburai	Bedding	65	215					Bandeira Group	Gondwana Megasequence	
AB733	-9.00921	125.28304	Saburai	Fault	57	320	50	285	sinistral normal		Bandeira Group	Gondwana Megasequence	
AB734	-9.01788	125.28429	Saburai	Bedding	05	180					Bandeira Group	Gondwana Megasequence	
AB734	-9.01788	125.28429	Saburai	?Fault	90	120					Bandeira Group	Gondwana Megasequence	Abrupt subvertical truncation of bedding subparallel to south scarp of Saburai
AB735	-9.01789	125.28343	Saburai	Bedding	26	140					Unknown	Unknown	
AB736	-9.01823	125.28182	Saburai	?Jointing	70	215					?Bandeira Group	?Gondwana Megasequence	
AB736	-9.01823	125.28182	Saburai	?Fault	90	110					?Bandeira Group	?Gondwana Megasequence	Abrupt truncation by cliff face
AB737	-9.01903	125.28073	Saburai	Bedding	25	350					Bandeira Group	Gondwana Megasequence	
AB740	-8.97345	125.22996	Loelako	Bedding	25	358					?Aitutu Group	?Gondwana Megasequence	
AB741	-8.97199	125.23136	Loelako	Bedding	40	090					?Aitutu Group	?Gondwana Megasequence	
AB744	-8.99580	125.20395	Maliana Basin	Bedding	23	295					Viqueque Group	Synorogenic Megasequence	
AB749B	-9.06413	125.23213	Saburai	Bedding	15	135					Bandeira Group	Gondwana Megasequence	
AB751	-9.06401	125.24088	Saburai	?Bedding	20	350					observation point		Sighted in
AB753	-9.05983	125.24000	Saburai	Bedding	57	295					observation point		
AB756	-9.06777	125.26013	Saburai	Fault	50	150	50	150	normal		?Bandeira Group	Gondwana Megasequence	
AB757A	-9.06747	125.26020	Saburai	Bedding	25	065					?Bandeira Group	Gondwana Megasequence	
AB757B	-9.06745	125.26055	Saburai	Bedding	15	045					?Bandeira Group	Gondwana Megasequence	
AB758	-9.06738	125.26064	Saburai	Fault	60	154	58	156	normal		?Bandeira Group	Gondwana Megasequence	
AB759	-9.06725	125.26086	Saburai	Bedding	25	040					Transitional Bandeira/Aitutu with debris slides	Gondwana Megasequence	Some evidence of gentle folding
AB760	-9.06819	125.25924	Saburai	Foliation	90	070	70	350	sinistral normal	dextral reverse	observation point		Strange "damage zone" - bedding is abruptly truncated bt large blocks with subvertical fractures trending 160
AB760	-9.06819	125.25924	Saburai	Foliation	90	070	80	014	sinistral normal	dextral reverse	observation point		Strange "damage zone" - bedding is abruptly truncated bt large blocks with subvertical fractures trending 161
AB761	-9.07921	125.25208	Saburai	Fault	64	110	62	098	normal		observation point		
AB761	-9.07921	125.25208	Saburai	Fault	64	110	33	040	sinistral normal		observation point		

Location No	Lat	Long	Region	Structure Type	Dip	Dip Direction	Lineation Dip	Lineation Dip Direction	Movement	or	Group	Megasequence	Notes
AB761	-9.07921	125.25208	Saburai	Fault	64	110	34	182	dextral normal		observation point		
AB762A	-9.08126	125.24944	Saburai	Fault	80	152	78	140	sinistral normal		Unknown	Unknown	
AB762B	-9.08126	125.24944	Saburai	Bedding	22	148					?Babulu Group	?Gondwana Megasequence	
AB764	-9.08470	125.24584	Saburai	Fault	43	070	30	132	dextral normal	sinistral reverse	Unknown	Unknown	
AB765	-9.08470	125.24584	Saburai	Fault	87	086					observation point		
AB767	-9.10078	125.23839	Saburai	Bedding	40	115					observation point		
AB767	-9.10078	125.23839	Saburai	Fault	90	136	71	205	dextral normal		observation point		
AB770	-8.78248	125.20636	Maliana Basin	Bedding	30	205					?Babulu Group	Gondwana Megasequence	
AB770	-8.78248	125.20636	Maliana Basin	Bedding	40	146					?Babulu Group	Gondwana Megasequence	
AB772	-8.76256	125.19266	Maliana Basin	?Bedding	62	085					?Babulu Group	?Gondwana Megasequence	Probably a large loose block
AB774	-8.96392	125.02981	Maliana Basin	Fault	70	230	35	295	dextral normal		Unknown	Unknown	

Appendix III

A restraining bend in a young collisional margin: Mount Mundo Perdido, East Timor

A. Benincasa, M. Keep & D. W. Haig (2012): A restraining bend in a young collisional margin: Mount Mundo Perdido, East Timor, Australian Journal of Earth Sciences: An International Geoscience Journal of the Geological Society of Australia, 59:6, 859-876

Including:

Mundo Perdido paper Appendix A - Lithostratigraphic units and age diagnostic fossils recognised at Mount Mundo Perdido

Mundo Perdido paper Appendix B - XRF analysis of volcanic and metamorphic samples.

Candidates contribution: This paper was written by the candidate based on field work completed by the candidate. Myra Keep assisted with editing the paper and David Haig assisted with foraminiferal identification and age determinations.

Australian Journal of Earth Sciences: An International Geoscience Journal of the Geological Society of Australia

Publication details, including instructions for authors and subscription information:
http://www.tandfonline.com/loi/taje20

A restraining bend in a young collisional margin: Mount Mundo Perdido, East Timor

A. Benincasa [a] , M. Keep [a] & D. W. Haig [a]

[a] School of Earth and Environment, University of Western Australia, Perth, 6009, Australia

Version of record first published: 30 Jul 2012

To cite this article: A. Benincasa, M. Keep & D. W. Haig (2012): A restraining bend in a young collisional margin: Mount Mundo Perdido, East Timor, Australian Journal of Earth Sciences: An International Geoscience Journal of the Geological Society of Australia, 59:6, 859-876

To link to this article: http://dx.doi.org/10.1080/08120099.2012.686453

Australian Journal of Earth Sciences (2012) **59**, (859–876)

A restraining bend in a young collisional margin: Mount Mundo Perdido, East Timor

A. BENINCASA*, M. KEEP AND D. W. HAIG

School of Earth and Environment, University of Western Australia, Perth, 6009, Australia.

Mount Mundo Perdido, a 1750 m-high, steep-sided massif situated in the Viqueque district of East Timor, comprises approximately 30 km^2 of complexly juxtaposed rocks deriving from both sides of the collisional plate boundary between the Australian Plate and the Banda Arc. Lithologies include Triassic–Jurassic interior-rift basin deposits, Cretaceous–Oligocene pelagites of Australian passive margin origin, neritic Oligocene–Miocene limestones and volcanics of Asiatic affinity, and Pliocene–Pleistocene synorogenic deposits. Detailed structural mapping shows Mount Mundo Perdido to be dominated by recent, high angle, oblique-slip and strike-slip faults that have been active into the Pleistocene and control the present-day topography. The fault architecture and stratigraphic distribution in the study area are comparable to pop-up structures developed at restraining bends, in this case within an east–west oriented zone of sinistral strike-slip. Our observations, supported by comparisons to scaled sandbox models and to similar pop-up structures developed in strike-slip systems elsewhere in the world, suggest that plate boundary-parallel strike-slip deformation is an integral part of the kinematics within the collisional zone between the Australian and Eurasian/Pacific plates in the Timor region.

KEY WORDS: Mount Mundo Perdido, Timor, collision, strike-slip, restraining bend, high-angle faults, biostratigraphy.

INTRODUCTION

Timor Island, formed at the collisional front between the northern edge of the Australian Plate and the Banda Arc (Figure 1), provides an ideal setting to study the processes of recent orogenesis (e.g. Hall & Wilson 2000; Milsom 2000; Audley-Charles 2004; Harris 2006; Keep & Haig 2010). Collisional shortening juxtaposes rocks of the Australian continental margin against remnants of the pre-collisional arc and synorogenic deposits (Audley-Charles 2004; Harris 2006) (Figure 2). Despite the resulting orogenic pile being described as 'tectonic chaos' (Fitch & Hamilton 1974; Hamilton 1979), biostratigraphic analyses (e.g. Haig & McCartain 2007; Haig *et al.* 2007, 2008; Haig 2012) have allowed documentation of three distinct orogenic phases (Keep & Haig 2010). These include initial shortening with associated diapirism (9.8–5.7 Ma), a tectonic quiet interval possibly representing the time of locking of the subduction zone (5.7–4.5 Ma) and a post-4.5 Ma phase of uplift, unroofing and additional diapirism (Keep & Haig 2010; Haig 2012). Structures developed through early thrusting during phase 1 (e.g. Carter *et al.* 1976; Harris & Audley-Charles 1987) have since been overprinted by later high-angle faulting during phase 3 (Chamalaun & Grady 1978; Charlton *et al.* 1991; Keep & Haig 2010).

Across Timor Island, a strike-parallel chain of steep-sided limestone massifs, known locally as 'fatus' (Figure 2), form high peaks (e.g. 2495 m, Cablac Mountain Range) in both East and West Timor (e.g. Wanner 1913; De Roever 1940; Simons 1940; Tappenbeck 1940; van West 1941; Brouwer 1942; De Waard 1957; Audley-Charles 1968). Bahaman facies oolitic wackestones, packstones and grainstones, that were originally interpreted as shallow water Miocene deposits (Audley-Charles 1968, pp. 25–27) and included in the 'Cablac Limestone,' dominate the fatus and have been variably assigned to allochthonous thrust sheets of Asiatic affinity (Audley-Charles 2004; Harris 2006), carbonate buildups on the outer Australian continental margin (Charlton 2002), or *in situ* patch reefs formed after collision but before orogenesis (Audley-Charles & Carter 1972). More recent detailed field mapping (Haig *et al.* 2007, 2008; Keep *et al.* 2009) documented a Late Triassic–Early Jurassic (i.e. not Miocene) age for the Bahaman facies at Cablac Mountain Range, one of the largest fatus and site of the 'Cablac Limestone' type locality (Audley-Charles 1968, p. 26). To avoid confusion over the use of the term 'Cablac Limestone' or 'Cablac Formation,' which also includes uppermost Oligocene and lowest Miocene limestones referred to by Haig *et al.* (2008, p. 375) as the 'Booi limestone' (here referred to as the 'Booi beds'), we designate the Late Triassic–Early Jurassic Bahaman-facies rocks seen at Cablac Mountain and at all other limestone fatus, including Mount Mundo Perdido, as the Perdido Group with the Mount Mundo Perdido exposures taken as the

*Corresponding author: benina01@student.uwa.edu.au

ISSN 0812-0099 print/ISSN 1440-0952 online
http://dx.doi.org/10.1080/08120099.2012.686453

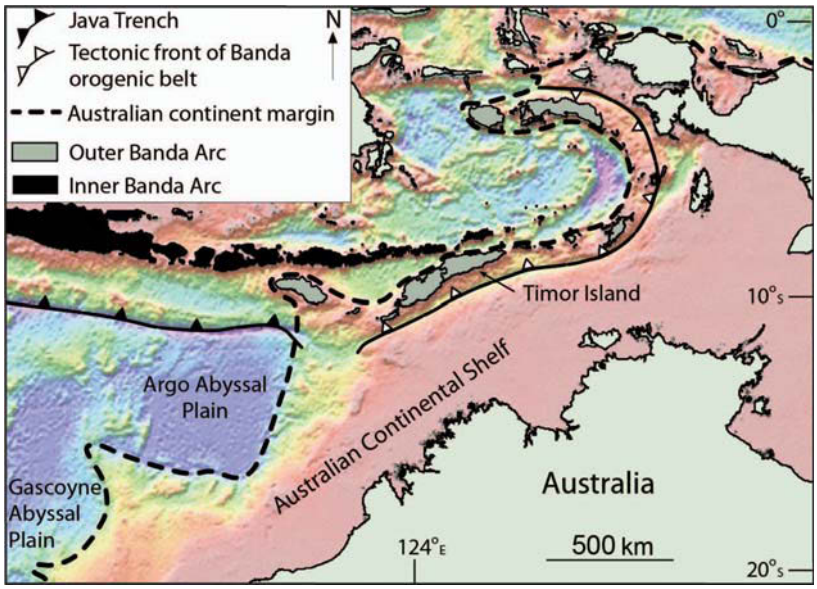

Figure 1 Location map illustrating the tectonic setting of Timor Island and the main physiographic elements of the region, modified from Keep *et al.* 2003. The dashed line around the Outer Banda Arc estimates the position of underthrust Australian continental crust in this region.

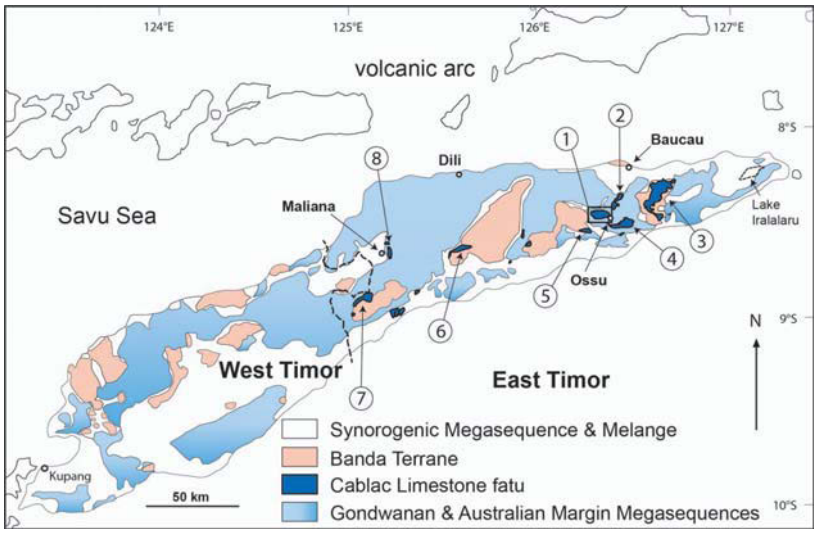

Figure 2 Schematic geological map of Timor Island, illustrating the generalised distribution of the main megasequences and terranes in East and West Timor, modified from Haig *et al.* (2008). The location of the study area containing Mount Mundo Perdido and the town of Ossu is shown (1), along with other massifs originally mapped as Cablac Limestone: Mt Laritame (2), the Matebian Range (3), the Builo Range (4), Mt Bibileo (5), the Cablac Mountain Range (6), Mt Taroman (7), and Mt Loelako (8). The outline of Lake Iralalaru is shown at the eastern tip of the island.

type area (see Appendix 1 for a list of localities typical of the Group). Further work may subdivide the highly deformed Perdido Group into formations.

The revised mapping of Cablac Mountain prompted examination of other fatus in East Timor, in order to assess their age and structural relationships. This paper presents the results of detailed field mapping at Mount Mundo Perdido, a fatu situated 1 km northwest of the town of Ossu (Figure 2) and directly along strike to the east of Cablac Mountain. The morphology of the mountain, with a roughly rhombic outline, steep-sided flanks and a long axis in an east–west orientation, mimics that of Cablac Mountain and other fatus, which all lie in a strike-parallel chain across East Timor. Investigating the development of this fatu, as well as others in the structural chain, may provide insights into the structural evolution of the island.

REGIONAL GEOLOGY

Collision between Australian continental crust and the Banda Arc commenced at approximately 25 Ma in the New Guinea region (collision with the Pacific and Caroline plates) and continued diachronously westwards (Hall 2002; Keep *et al.* 2003). The age for collision in the Timor region has been reviewed by Keep & Haig (2010), Spakman & Hall (2010), Audley-Charles (2011), Hall (2011) and Haig (2012). Detailed stratigraphic evidence (Haig & McCartain 2007; Keep & Haig 2010; Haig 2012) suggests that continental crust, likely an outlying continental plateau (Timor Plateau) resembling present-day Exmouth Plateau, entered the subduction zone in the Timor region during the Late Miocene, between 9.8 Ma and 5.7 Ma, causing disruption in Timor and eventual jamming of the subduction zone at approximately 5.7 Ma. Collision caused subduction to cease, evidenced by a present lack of deep seismic activity and a cessation of volcanism in the arc immediately north of Timor (Chamalaun & Grady 1978; with timing issues discussed by Ely *et al.* 2011, p. 492). Whilst this age for collision, after 9.8 Ma but before 5.7 Ma (Haig & McCartain 2007; Keep & Haig 2010; Haig 2012) is older than some other estimates (e.g. 4 to 2 Ma, Audley-Charles 2004, 2011; Spakman & Hall 2010; Hall 2011), it is consistent with other evidence for a regional event at approximately 8 Ma from both Timor and the adjacent Australian North West Shelf (e.g. Reed 1985; McCaffrey *et al.* 1985; Berry & McDougall 1986; van der Werff *et al.* 1994; Fortuin *et al.* 1994, 1997; Richardson & Blundell 1996; Charlton 2000; Rutherford *et al.* 2001; Keep *et al.* 2002, 2003).

Since collision, Timor Island has undergone uplift and exhumation in excess of 5 km (Keep & Haig 2010) through processes of crustal thickening (Richardson & Blundell 1996) and isostatic rebound following a possible detachment of the down-going slab (Price & Audley-Charles 1987; Audley-Charles 2004; Ely *et al.* 2011). Its emergence possibly had begun by 5.7 Ma (Haig 2012) and the island continues to undergo uplift of around 1.5 mm/year (Audley-Charles 1986).

The tectonostratigraphic framework of Timor includes the Permian to Middle Jurassic Gondwana Megasequence deposited within interior basins of the East Gondwanan rift system (Harris *et al.* 1998; Harris 2006; Haig & McCartain 2007, 2010); Late Jurassic to early Late Miocene Australian Margin Megasequence deposited on the passive margin that, in the vicinity of Timor, subsided to middle bathyal water depths during the Early Cretaceous to form the 'Timor Plateau' (Haig & McCartain 2007; Keep & Haig 2010); Jurassic to Early Miocene Banda Terrane of Asian affinity (Audley-Charles & Harris 1990, Harris 2006, Haig *et al.* 2008); and the Synorogenic Megasequence (Haig & McCartain 2007; Roosmawati & Harris 2009; Haig 2012). The Bobonaro Melange (=Synorogenic Melange) recognised by Harris *et al.* (1998), Haig & McCartain (2007) and Haig *et al.* (2008) is no longer considered a coherent stratigraphic unit. It includes structural melange zones probably caused by diapirism (Barber *et al.* 1986; Harris *et al.* 1998) generated within Triassic clay units (Haig & McCartain 2010; see also Brunnschweiler 1978). However, in many areas, incipient diapirism has resulted in 'broken-formation' deformation (Harris *et al.* 1998) within units that can be identified as particular formations (e.g. much of the Babulu Formation recognised here).

MATERIALS AND METHODS

This study is based on two months of field mapping completed in 2009. A field laboratory was set up in Ossu with equipment for cutting limestones, disaggregation of mudstones and making acetate peels, enabling initial tectonostratigraphic determinations in the field. Additional peels and thin-sections were made at the University of Western Australia, enabling biostratigraphic age determinations of 148 samples (Appendix 1). Thin-sections were made of all volcanic and metamorphic samples, with the least weathered samples selected for XRF analysis (Appendix 2).

Samples of the original rock, along with acetate peels, thin-sections and processed residues, are housed in the collection of the Edward de Courcy Clarke Earth Science Museum at the University of Western Australia. Duplicates of each sample are stored in the Geological Laboratory of the Secretary of Energy and Natural Resources at Hera, East Timor.

THE MUNDO PERDIDO AREA

Mount Mundo Perdido forms an elongate massif (approximately 10 km × 3 km), with its highest peak reaching 1752 m (Figure 3). Early descriptions of high limestone peaks in Timor as 'fatus' (Molengraaf 1912) included the term 'Fatukalke' (Fatu Limestone) in West Timor (Wanner 1913), with Wittouck (1937) describing Mount Mundo Perdido as a 'Fatu type of topography.' Grunau (1953) and Gageonnet & Lemoine (1958) also classified the rocks of Mount Mundo Perdido as 'Fatu Limestone' forming a topographic high of stark relief, terminated by near-vertical cliffs, and lacking stratigraphic continuity with surrounding areas (Gageonnet & Lemoine 1958; Romariz & Leme 1967) (Figure 3c, d). Early work interpreted the Mount Mundo Perdido fatu as an erosional limestone remnant or klippe, despite the absence of any observed thrust contacts (Grunau 1953, Gageonnet & Lemoine 1958), while recording evidence of a complex tectonic history including subvertical faults and differential vertical movements (Romariz & Leme 1967). Upper Cretaceous and Oligocene ages were determined from the presence of the foraminifera *Globotruncana* and *Spiroclypeus* respectively (Grunau 1953; Romariz & Leme 1967). Romariz & Leme (1967) suggested that the fatus developed as isolated coral reefs on an ancient submarine relief during the Cenozoic, whilst also noting the presence of older, Cretaceous very fine-grained carbonates at Mount Mundo Perdido. Similarly Audley-Charles (1968) interpreted Mount Mundo Perdido to be an internally coherent block of his 'Miocene Cablac Limestone' (see above) deposited unconformably in parts on 'Oligocene' volcanics (the Barique Formation

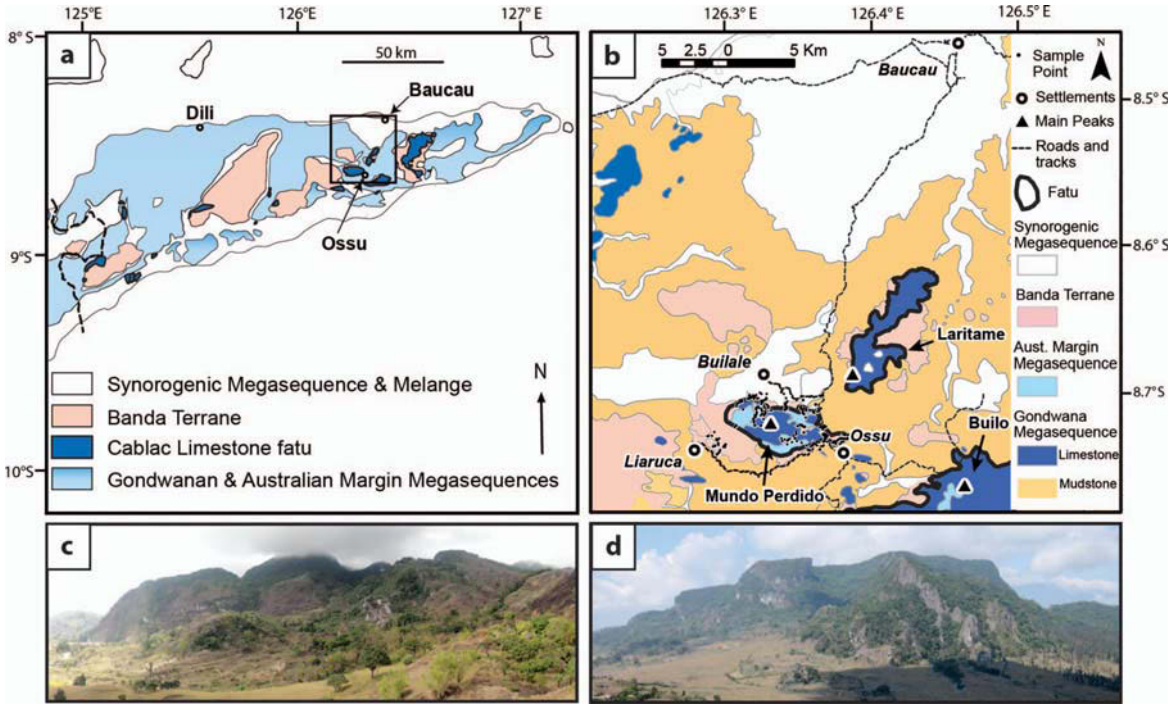

Figure 3 (a) Schematic geological map of East Timor showing the generalised distribution of megasequences and fatus, and outline of the location map (b). (b) Schematic geological map of the Baucau-Ossu region showing the fatus of Mount Mundo Perdido, Mt Laritame and the Builo Range. The geology of Mount Mundo Perdido is based on the present study, with the geology of the surrounding area modified from Partoyo *et al.* (1995). The main road, which runs south from Baucau to Ossu, skirts the eastern side of Mount Mundo Perdido. From here, tracks run west to Builale and Liaruca providing four wheel drive access to the base of Mundo Perdido's northern and southern flanks. Black dots represent sample locations. (c, d) The steep sided, blocky profiles of Mount Mundo Perdido (c, facing W) and Mt Laritame (d, facing ENE).

of Audley-Charles 1968, p. 24), overlain by small klippen of Cretaceous limestone.

From stratigraphic re-evaluation during the present study (Table 1) and mapping of the stratigraphy, Mount Mundo Perdido displays a broadly anticlinal distribution of stratigraphic units (Figure 4). Triassic–Jurassic Gondwana Megasequence limestones dominate the structurally highest, central regions, with younger, Cretaceous to Oligocene limestones of the Australian Margin Megasequence forming the high cliffs on the northern and southern flanks. Banda Terrane units occupy the foothills and lower cliffs, extending up into higher levels only on the eastern side. Therefore, Banda Terrane units now occur only at lower topographic levels at Mount Mundo Perdido. High-angle, oblique-slip faults juxtapose the Banda Terrane rocks against the older Australian-affinity rocks in the higher, central regions of the mountain (Figure 4) and form the sheer-sided limestone cliffs that dominate the topography (e.g. Figure 3c, d). The youngest units in the study area, Pliocene–Pleistocene limestones and mudstones of the Synorogenic Megasequence, abut the massif on its northern flank.

In the study region, there is a difference in structural style between the more highly deformed Gondwana- and Australian Margin Megasequence units and the Booi beds (Banda Terrane). The former generally have steeply inclined bedding of variable strike that in many places are folded and disrupted by small-scale faulting and fracturing. The less deformed Booi beds show more consistency in bedding, commonly dipping between 20 and 50° towards the south (Figures 4a, 5a, b), and are less internally deformed. The focus of this paper is to present an analysis of larger-scale structures on the mountain and its surrounds.

REGIONAL- TO OUTCROP-SCALE DEFORMATION

At the regional scale, late, high-angle faults dominate the topography of Mount Mundo Perdido. These faults obscure structures associated with early shortening, which is now evidenced at Mount Mundo Perdido by the juxtaposition of rocks of the Gondwana- and Australian Margin megasequences against those of the Banda Terrane. These high-angle faults produce near vertical cliffs extending up to several hundred metres in height and up to several kilometres in length for some fault strands (Grunau 1953; Gageonnet & Lemoine 1958; Romariz & Leme 1967) (Figure 3c, d). These striking, near-vertical cliffs, which were mapped both in the field and also from aerial photography, occur along three dominant trends, including a 120°–140° trend, a 110° trend and a 030°–040° trend, with a subordinate fourth trend of 060°–080° (Figure 4). The lateral extent of the

Table 1 Lithostratigraphic units recognised at Mundo Perdido. Additional details on lithology and age-diagnostic fossils are provided in Supplementary Appendix 1.

Unit	Main rock types	Age	Facies
Synorogenic Megasequence			
Baucau Limestone (Audley-Charles 1968)	Medium to thick-bedded, yellow to white porous vuggy packstone and grainstone with corals, coralline algae, and larger rotaliid benthonic foraminifera as main bioclasts	Pleistocene	Neritic carbonate platform associated with coral reefs
Viqueque Formation including Lari Guti Member (Grunau 1956; Gageonnet & Lemoine 1958; Audley-Charles 1968; Haig & McCartain 2007)	Grey mud and sandy mud containing abundant planktonic foraminifera. Lari Guti Member: thin to thick-bedded yellow to white vuggy foraminiferal packstone and grainstone (including planktonic foraminiferal grainstone) with thick beds of coral rudstone in cut and fill channels.	Latest Pliocene to Early Pleistocene in this area (planktonic foraminiferal zones N21–N22). Lari Guti Member: Early Pleistocene (planktonic foraminiferal zone N22). Note: the base of the Viqueque Formation has not been observed in the mapped area.	Middle to Upper Bathyal zone. Lari Guti Member is composed of bioclastic debris-slide deposits that accumulated at water depths of 500–1000 m.
Banda Terrane			
Booi beds (Haig *et al.* 2008—as Booi limestone) (Figure 5a, b)	Medium to thick-bedded white to pale grey packstone and wackestone. Larger benthonic rotaliid foraminifera, coralline algae and corals are the main bioclasts. Thinly bedded grey mudstones with, in places, thin sandstone interbeds. Mudstones contain abundant planktonic and benthonic foraminifera.	Latest Oligocene–earliest Miocene (Upper Te Letter Stage and ?P22–N4–?N5 planktonic foraminiferal zones)	Limestones are neritic; mudstones are outer neritic to upper bathyal
Barique Formation (Audley-Charles 1968) (Figure 5a, b)	Undifferentiated volcanic sandstone and breccia, associated red mudstone, schist, and gabbro. Sandstone contains lithic fragments in a matrix of angular plagioclase crystals and glass, and in places displays flow layering.	No age determinations made of volcanic and igneous rocks in map area. Red mudstone is late Middle Eocene (within planktonic foraminiferal zones E11–E13) Lithostratigraphic correlation to Barique Formation in its type area (Quique River, 20 km southeast of map area) where it is associated with Middle Eocene limestone.	Basaltic to intermediate calc-alkaline plutonic and volcanic rocks of island arc affinity; mudstone is upper bathyal
Australian-Margin Megasequence			
Kolbano Beds (Kolbano facies of Audley-Charles & Carter 1972)	Pink to white carbonate pelagite, grey wackestones with, in places, chert nodules aligned to bedding. Most samples contain abundant planktonic foraminifera. Oldest unit lacks planktonic foraminifera, but has calpionellids, inoceramid prisms, and rare belemnite guards.	Ages determined: (1) latest Jurassic or earliest Cretaceous; (2) Early Cretaceous (late Aptian or early Albian; (3) Late Cretaceous (?Cenomanian, Turonian, Campanian or early Maastrichtian); Paleogene (Late Paleocene or earliest Eocene, ?Late Eocene, Oligocene)	Latest Jurassic or earliest Cretaceous beds: upper bathyal. Aptian and younger units: Middle Bathyal to Abyssal (within 500–3000 m water depth)
Gondwana Megasequence			
Perdido Group	Massive grey oolitic, oncoidal, peloidal, and intraclastic grainstone, packstone and wackestone. Main bioclasts include carbonate-cemented agglutinated foraminifera, dasycladale algae and thaumatoporellacean algae (including cryptoendolithic types—following Schlagintweit & Velić 2012).	Early Jurassic (? Late Triassic). Where the unit can be dated with precision it is Sinemurian–Pleinsbachian.	Inner neritic carbonate platform with restricted marine conditions including higher than normal salinities (Bahaman facies)

(*continued*)

Table 1 (*Continued*).

Unit	Main rock types	Age	Facies
Aitutu Formation (Audley-Charles 1968) Note: this formation is present only in isolated outcrop closely associated with the Perdido Group limestone and is not mapped separately.	Dark grey radiolarian-rich bioturbated wackestone. In places with 'lenses' of reworked pedoidal grainstone. In other outcrop, pelagic bivalve 'filaments' are abundant.	Late Triassic or Early Jurassic. Elsewhere in Timor, the formation has a ?Anisian, Ladinian to Early Jurassic age (Haig & McCartain 2010)	Basinal facies (outer neritic or upper bathyal in rift-basin setting)
Babulu Formation (in map area: mud-dominated facies with 'broken-formation' deformation (Figure 5c) (Bird & Cook 1991)	In map area: mainly mudstone incorporating, in places, small blocks, up to ~2 m thick, of laminated fine to medium quartz sandstone (with swaley and hummocky bedding)	In map area: Late Triassic (probably lowest Minutosaccus crenulatus Zone, Norian). Mudstone and sandstone yields similar palynomorph assemblage.	Prodelta facies (in shallow rift-basin setting)

largest faults was mapped from aerial photographs, the resolution of which did not allow determination of accurate dip directions. However, traces of these structures cut across topography, indicating steep dips, which are verified by field observations of sub-vertical fault planes. Where the lower reaches of these vertical faults were accessible, fault orientations and striae were measured directly on these fault planes (Table 2). The surfaces yielded fault striae, often with multiple orientations, including both gently and steeply plunging, indicating multiple phases of slip on these surfaces, all of which are oblique to dip, indicating some component of strike-slip (Table 2).

At the outcrop scale we identified 111 fault surfaces from smaller-scale faults that displayed both steep and shallow dips (Table 3). Fault striae (Figure 6a, b) enabled slip direction interpretations on 77 of the 111 observed fault surfaces, with fault steps and other kinematic indicators allowing kinematic interpretations on an additional 37 faults (Table 3). The majority of faults at both outcrop- and map-scale indicate mainly oblique-slip movement (Tables 2, 3). We therefore have slip data from over 100 regional- and outcrop-scale fault surfaces in the study area, indicating a strong strike-slip component to the faulting, for multiple slip events, both on steeply and shallowly dipping fault surfaces. Further, these strike-slip indicators indicate a change in movement sense between the highest and lowest structural levels of Mount Mundo Perdido. The highest mapped fault structure, at ~1350 m above sea-level (the highest sample was at ~1760 m above sea-level), indicated reverse-oblique movement (Figure 4). Map-scale drag folds developed in the Lari Guti Member and Baucau Limestone on the northern side of the massif (Figure 4) adjacent to the bounding faults of the massif (Figure 7a, b) are consistent with interpreted reverse-oblique movement. At the lower structural levels, ~600 m above sea-level, motion was interpreted to be normal-oblique, in the southeast part of the area (Figure 4). Given the relatively young age of deformation, as evidenced by the fault-controlled present-day topography, the ~700 m elevation difference equates to an equivalent structural thickness.

In addition, dip domains identified in fault attitude data indicate that at lower structural levels (i.e. in the foothills of Mount Mundo Perdido, ~600 m above sea-level) faults generally dip away from the elongate east–west axis of the mountain, whereas at higher structural levels (~1350 m to ~1760 m above sea-level), faults dip towards the axis of elongation (Figure 4).

The strike-slip interpretations from striae on both regional- and outcrop-scale fault surfaces are supported by the discovery of a multi-domainal strike-slip fault at outcrop scale (Figure 8). This structure, approximately 3 m in height by 5 m in width, shows several domains. The top of the outcrop preserves a positive flower structure, indicating a reverse-oblique sense of displacement. In middle of the structure the multiple strands of the flower merge into a single dominant strand, with a near-vertical dip. Towards the base of the structure, the single strand splays out into a number of smaller faults, with overall net normal displacement, becoming a single steep strand again at the base of the outcrop. The finely bedded nature of the rocks and the numerous contrasting marker layers accentuate the sense of slip at both the upper- and lower-levels of this structure. The reverse-oblique motion at higher structural levels therefore contrasts the net normal (normal-oblique) sense of displacement at the lowest structural levels of the outcrop, separated by a domain of a single-strand, high-angle fault (Figure 8). Movement senses in this outcrop-scale strike-slip fault mimic relationships described above at a larger scale, with faults at high structural levels showing indication of reverse-oblique motion, contrasting interpreted normal-oblique motion at significantly lower structural levels. The presence of these relationships at both scales within the study area, coupled with the hundreds of fault striae measurements, suggest strike-slip has dominated movement on these young faults at all scales.

Minor outcrop-scale folding includes open, upright-to-inclined folds within pelagites of the Australian Margin Megasequence (Figure 8c–f). Axial plane strikes vary and include strikes of 005°, 030° and 090°, with dips ranging from moderate to steep, and plunges ranging from shallow to moderate (Table 4). From their limited exposure it is not clear whether these small-scale folds are related to early (phase 1) contraction or are coeval with strike-slip. Zones of tectonic mélange (Figure 5d) are restricted to areas proximal to extensional/transten-

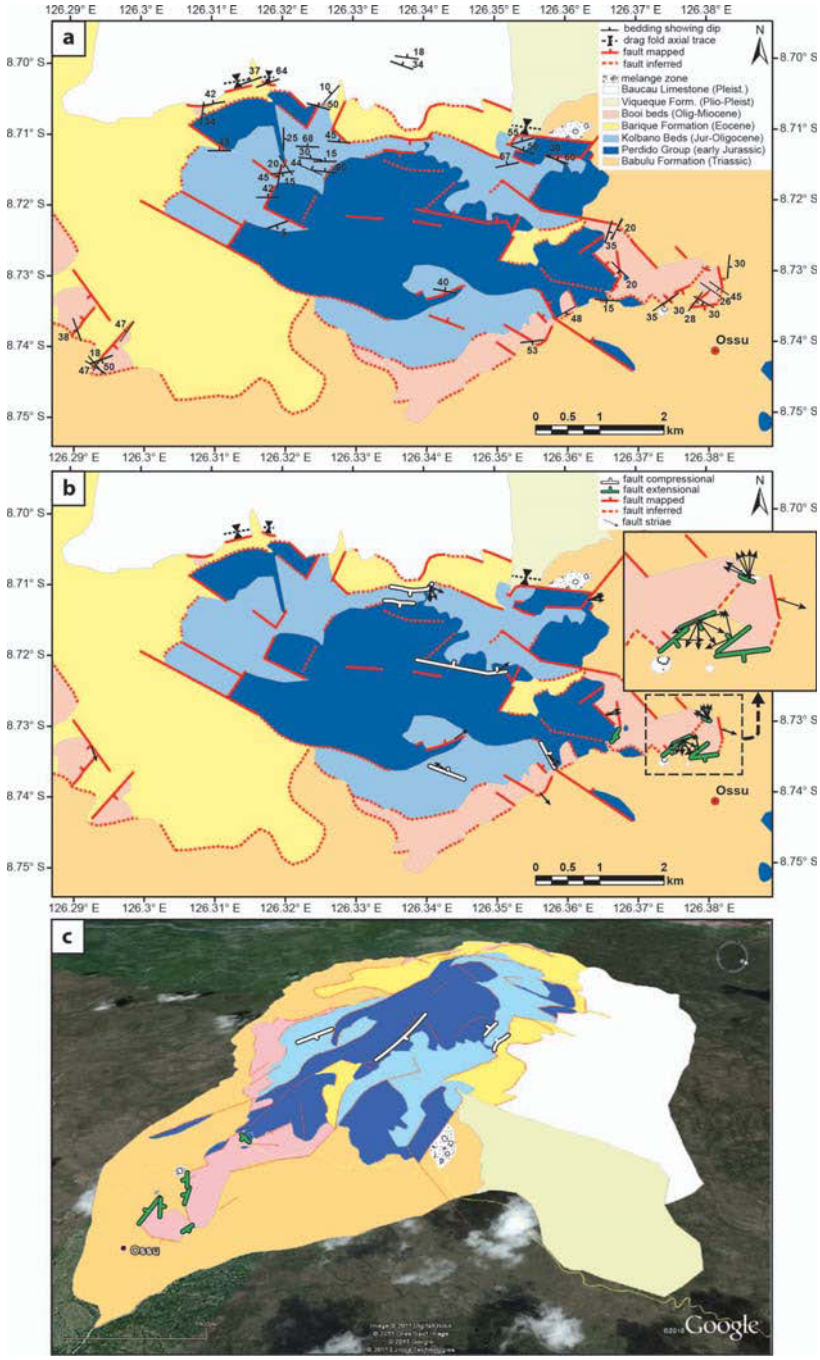

Figure 4 (a) Interpreted geological map of Mount Mundo Perdido, showing the distribution of lithologies, bedding and main geological structures. Legend ages are as determined for samples collected at Mundo Perdido (see Table 1); greater age ranges are recorded for the Viqueque Formation and Kolbano Beds elsewhere in Timor (see Haig & McCartain 2007). Faults shown in solid red have been observed in the field, and show dip directions where measured. Faults shown in dashed red have been interpreted from aerial photographs. (b) Arrows indicate fault striae where observed and measured on major faults. Confirmed compressional faults (white, showing dip direction) are most common in the centre of the massif at high structural levels, where they dip towards the central east–west axis of the mountain range. Confirmed extensional faults (green, showing dip direction) are most common at lower structural levels, where they dip away from the central axis. Inset shows detail of striae recording multiple directions of oblique slip on extensional faults in the southeast corner of the massif. (c) Geological map draped over a Google Earth digital elevation model, looking west-southwest over the massif, showing confirmed extensional and compressional faults..

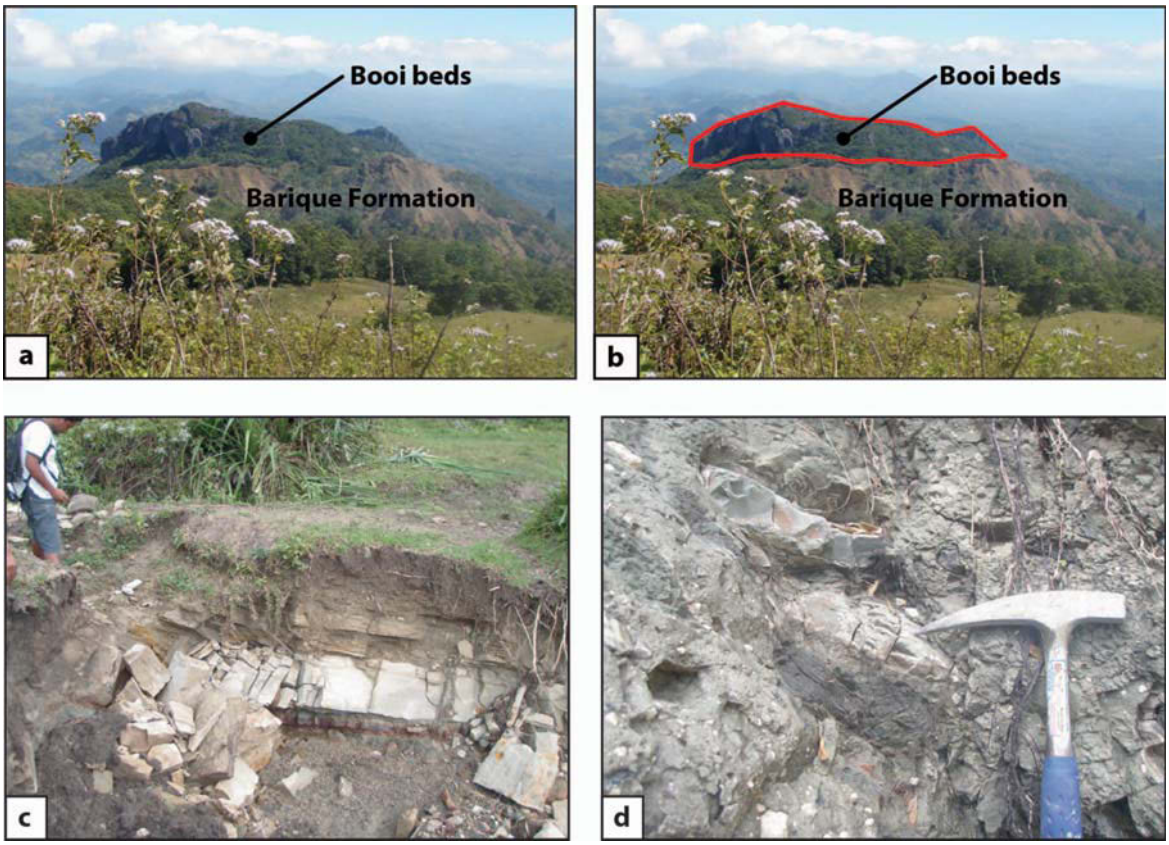

Figure 5 (a, b) Looking south, from high on the southern flank of the massif, over southern exposures of Banda Terrane. Field relationships, most commonly in the northwest and southwest of the study area, often have blocks of Booi beds (highlighted in red on the right) subhorizontally overlying mafic volcanics of the Barique Formation, which may be a stratigraphic contact. (c) A faulted and broken sandstone bed within the Babulu Formation, on the south side of Mount Mundo Perdido. Within the study area, the Babulu Formation is found at most localities originally mapped as 'Bobonaro Scaly Clay' (Audley-Charles 1968), and is distinguished by this study from (d) tectonic melange from within fault zones. Note the chaotic assortment of exotic blocks at this locality from a fault zone in the southwest corner of Mundo Perdido: clasts consist of limestones, mudstones, and mafic volcanics 2 mm to 1 m in size

sional structures in the southwest corner of Mount Mundo Perdido (Figure 4).

The lack of thrust structures or stratigraphic repetition (Grunau 1953; Gageonnet & Lemoine 1958) that are seen further to the west in Timor (e.g. at Mt Cablac as interpreted by Keep *et al.* 2009; and in the Maliana region by Audley-Charles 1968), and the dominance of steep, high-angle, oblique-slip faults throughout the Mount Mundo Perdido area suggests that younger high-angle deformation may overprint earlier shortening in the area (Keep & Haig 2010). The distribution of mapped units, with the oldest rocks (Gondwana- and Australia Margin Megasequence) at the centre of the structure at the highest structural levels and topographic elevations, and the younger rocks (Banda Terrane) around the perimeter of the structure at the lowest structural levels and topographic elevations, suggests differential uplift of the Gondwana and Australian Margin Megasequence rocks relative to the Banda Terrane. Bedding, most often measured within the Booi beds and Australian Margin Megasequence, generally dips away from the central east–west axis of the massif (Figure 4).

The distribution of stratigraphy (Figure 4), along with the pattern of net normal (normal-oblique) faults at lower structural levels, contrasting reverse-oblique faults at higher structural levels, and the presence of flower structures in outcrop, suggests a strike-slip mechanism, possibly a restraining bend, may account for the present-day geological distributions at Mount Mundo Perdido.

A STRIKE-SLIP/RESTRAINING BEND MODEL

Structures at Mount Mundo Perdido strongly mimic those from both analogue models of restraining bends (Dooley *et al.* 1999; McClay & Bonora 2001), and those from restraining bends in documented active and ancient strike-slip fault systems (Mann 2007).

Analogue models for both pure strike-slip faulting above a double basement fault (Schellart & Nieuwland 2003) and for restraining bends (Dooley *et al.* 1999; McClay & Bonora 2001) generate rhomboidal or lozenge shaped uplifts or pop-ups, bounded by oblique-slip

Table 2 Classification of major, mappable faults at Mound Mundo Perdido. Fault striae indicate a movement direction on 23 of the measured fault surfaces. Kinematic indicators allow a shear sense to be determined on a further 12; indicators included steps and crescentic fractures on limestone fault surfaces, asymmetric deformed clasts within fault zones, and s–c type shear fabrics developed within mudstones. Faults are classified as oblique slip when striae indicate a movement vector with an obliquity greater than 10° from pure strike-slip or pure dip-slip.

Total	Movement indicators		Dip-slip		Strike-slip		Oblique-slip			
	Striae	Kinematic indicators	Normal	Reverse	Dextral	Sinistral	Dextral Normal	Sinistral Reverse	Dextral Reverse	Sinistral Normal
45	23	12	5		2		9		7	
			3	1	0	1	2	3	1	1

Table 3 Classification of all measured fault surfaces in outcrop at Mount Mundo Perdido. Fault striae indicate a movement direction on 77 of the measured fault surfaces. Kinematic indicators allow a shear sense to be determined on a further 37; indicators included steps and crescentic fractures on limestone fault surfaces, asymmetric deformed clasts within fault zones, and s-c type shear fabrics developed within mudstones. Faults are classified as oblique slip when striae indicate a movement vector with an obliquity greater than 10° from pure strike-slip or pure dip-slip.

Total	Movement indicators		Dip-slip		Strike-slip		Oblique-slip			
	Striae	Kinematic indicators	Normal	Reverse	Dextral	Sinistral	Dextral Normal	Sinistral Reverse	Dextral Reverse	Sinistral Normal
111	77	37	8		2		31		36	
			3	1	0	1	8	11	7	6

reverse faults, with their upper surfaces dissected by synthetic and antithetic oblique-slip and strike-slip faults (Figure 9a). Narrow positive flower structures in cross-section view broaden and become asymmetric towards the centre of the structure, with the asymmetry switching on either side of the central region. In addition, three distinct sets of faults including bounding faults, faults sub-parallel to the axis of strike-slip, and antithetic through-going faults occur with similar orientation in both the sandbox models and the geological map (Figure 9). The stratigraphic distribution in plan views of sandbox models of restraining bends shows striking similarity to that mapped at Mount Mundo Perdido (Figure 9c). The oldest rock units are found at the centre, with a succession of progressively younger strata exposed moving out towards the edges of the pop-up structure (Figure 9b). Bedding dips away from the centre of the structure, and rotation occurs within some fault-bounded blocks (McClay & Bonora 2001). Both of these models, either the double basement strike-slip fault or the strike-slip restraining bend, could explain the overall geometry of the structure at Mount Mundo Perdido. However, the rhomboidal morphology seen at Mount Mundo Perdido most closely mimics that generated in restraining bend analogue models (McClay & Bonora 2001), rather than the highly elongate structures developed over double basement strike-slip faults (Schellart & Nieuwland 2003).

Cross-sectional views of analogue models of both double basement strike-slip faults and restraining bends (McClay & Bonora 2001; Schellart & Nieuwland 2003) clearly show the pop-up or flower structure at the surface, merging into a narrow fault zone at depth. However, the models do not go any deeper than the narrow fault zone, constrained by the thick sand pack and edge effects from the deformation apparatus. The models therefore only generate structures that would be equivalent to those in the upper part of the structural section at Mount Mundo Perdido–lower structural level structures, such as our domains of normal-oblique offset, are not generated. These models therefore do not fully generate the types of multi-domainal strike-slip faults that occur in outcrop at Mount Mundo Perdido (Figure 8). We believe this may be due to the very young nature of the faults at Mount Mundo Perdido, perhaps preserving stages of deformation that are not preserved in older faults that have undergone additional slip. In addition, episodes of inversion (transpression) on faults within the structure, known to affect mainly the upper parts of structures, could preserve net normal slip on reactivated pre-existing structures that have not exceeded the null point (e.g. Deeks & Thomas 1995; Holford *et al.* 2009; Withjack *et al.* 2010). Therefore, both cross-sectional and map view comparisons of analogue models of strike-slip systems to the structure at Mount Mundo Perdido indicate that strike-slip is a likely mechanism for deformation. A schematic block model of Mount Mundo Perdido, with cross-sections based on the geometries of mapped flower structures, shows the distribution and orientation of mapped stratigraphy and faults in the upper part of the structural section (Figure 10).

We believe that deformation at Mount Mundo Perdido results from uplift in a strike-slip fault zone, likely as part of a restraining bend in that system. Asymmetries in morphology and orientation of dominant fault trends suggest a left-lateral movement sense

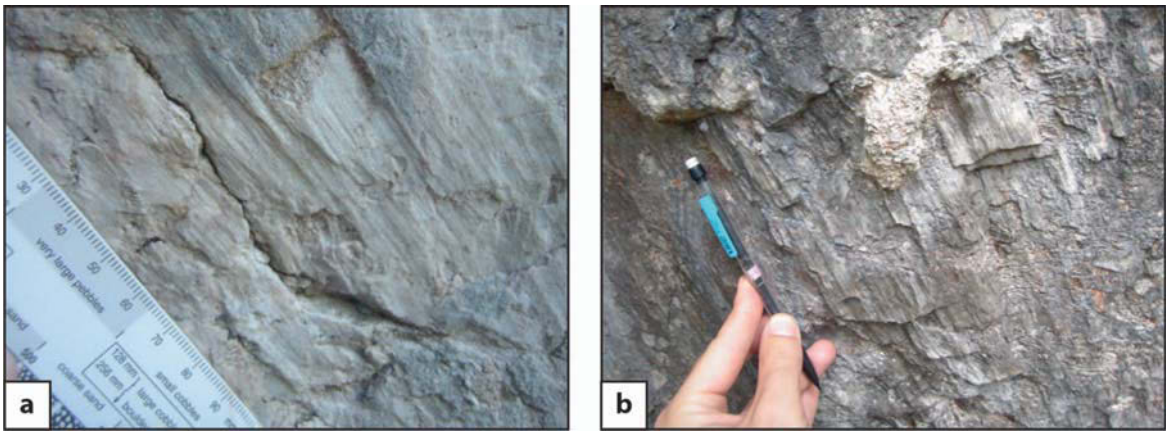

Figure 6 (a) Well-defined fault striae recording oblique movement within limestone of the Booi beds, which forms the lower cliffs at the eastern end of the massif. (b) Fault striae and steps on the hanging wall surface of an oblique-reverse fault developed within Australian Margin Megasequence foraminiferal wackestones, on the northern flank of Mount Mundo Perdido.

(Figure 9). Left-lateral oblique-slip and strike-slip faults have also been observed and measured at Mt Laritame, Mt Taroman, Mt Loelako and around the Maliana basin (Figure 2). The presence of coral-debris slides in the Early Pleistocene Lari Guti Member (Table 1) and fault juxtaposition and drag folds involving the Lari Guti Member and overlying Baucau Limestone (Figure 7) indicates that the uplift was active likely during the Early and Middle Pleistocene.

DISCUSSION

Strike-slip faults in Timor have previously been inferred from shallow-focus earthquakes (Audley-Charles 1985) or extrapolated from smaller structures (2 km-long, northeast-striking wrench faults) in West Timor (Charlton *et al.* 1991). The Mount Mundo Perdido structure documented herein represents the first evidence for large-scale strike-slip faulting documented in East Timor. The length of any principal deformation zone/strike-slip faults in the Mount Mundo Perdido area must logically exceed the approximate 10 km length of the pop-up/flower structure, indicating that the fault zone is of considerable size. This is supported by outcrops of fault gouge along the road near Ossu (documented in Keep & Haig 2010), where fault gouge structural thicknesses of up to 30 m indicate significant fault slip, possibly many tens of metres. No direct measurements of potential fault offset were possible owing to the nature of the terrain and the high erosion rate.

Other examples of potential strike-slip structures occur along strike from Mount Mundo Perdido and may represent the often anastomosing or braided nature of large-scale strike-slip systems (Woodcock & Fischer 1986; Mann 2007). For example, a deformation zone with potential strike-slip geometry occurs at Lake Iralalaru, between Los Palos and Tutuala (Figures 2, 11a). Lake Iralalaru, approximately 90 km along strike from Mount Mundo Perdido, forms a rhomboidal east-northeast-striking basin within Pleistocene Baucau Limestone (Figure 11a) which strongly resembles pull-apart structures developed at releasing bends in analogue models (Dooley & McClay 1997) and documented strip-slip fault systems (Mann 2007). The lake level varies seasonally and during the dry season exhibits an elongate spindle shape, the trend of which parallels one set of faults mapped at Mount Mundo Perdido. The geometry and orientation of Lake Iralalaru, and its proximity to the strike-slip at Mount Mundo Perdido, suggest that young strike-slip faulting is likely extensive, continuing for over 90 km of strike in East Timor. Lake Iralalaru is consistent with a sinistral pull-apart structure/releasing bend in a related fault strand, and it merits further investigation as part of a larger strike-slip system.

Steep topography forming anomalously high peaks, a feature common to restraining bends in both active and ancient strike-slip systems (Mann 2007), may explain the location, elevation and morphology of the chain of 'fatu' limestones that extends across East Timor (Figure 2). Pop-up structures often represent transitory features within the larger fault zone, with slip eventually bypassing or being transferred across them as restraining bends or step-overs impede continued slip along major strike-slip fault systems (Brown *et al.* 1991). As fault displacement increases, bends or step-overs tend to be smoothed out as through-going faults develop that transect the pop-up structures and link the principal zones of deformation (McClay & Bonora 2001). In this way, segments of early-formed uplifted areas may be dissected and transported along the major strike slip zone as a fragmented pop-up (McClay & Bonora 2001). This mechanism may explain the variation in size and orientation of fatu limestones in East Timor, from the extensive Matabian Range of eastern East Timor to the north-trending and smaller Mt Loelako near Maliana (Figure 2).

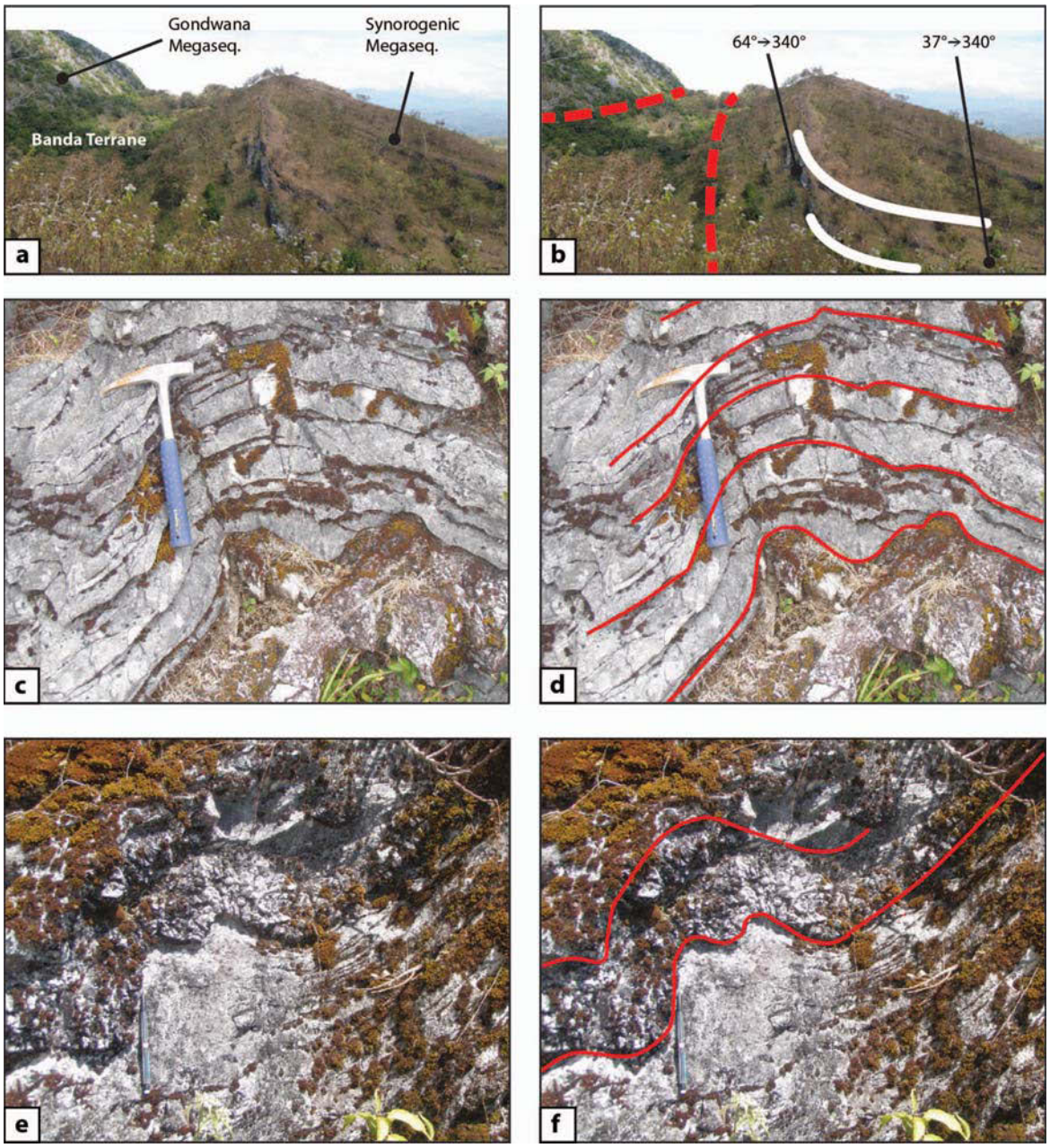

Figure 7 Facing west, uninterpreted (a) and interpreted (b) images of the northern edge of Mundo Perdido show Triassic–Jurassic Gondwana Megasequence limestones of the massif in the top left corner of the frame. They are faulted against volcanics of the Banda Terrane (occupying the gully), which are in turn faulted against much younger Pliocene–Pleistocene synorogenic limestones of the Baucau Limestone (right of frame). Dashed red lines show the interpreted surface traces of the faults on either side of the gully. The measured change in the dip of bedding in the synorogenic units moving north from the fault trace describes a drag fold (white). These large drag folds form a series of small hills that parallel the northern edge of the mountain. Uninterpreted (c) and interpreted (d) images of open, upright folding within an outcrop of Turonian Australian Margin Megasequence pelagite at 144821. Of note is the 'M' fold developed in the fold hinge within the cherty bed at the base of outcrop. Uninterpreted (e) and interpreted (f) images of open, moderately inclined, moderately plunging folding within an outcrop of similar pelagite at 144814. Folding is well defined within cherty layers.

We believe Mount Mundo Perdido resembles a pop-up structure developed within a sharp restraining bend following the classification of Mann (2007); these form at discrete fault step-overs and produce localised rhomboidal topographic uplift aligned along the general trend of major strike-slip faults (Mann 2007; Figure 1c). Given that fault separations at sharp restraining bends are generally less than 15 km (Mann 2007) similar strike-slip

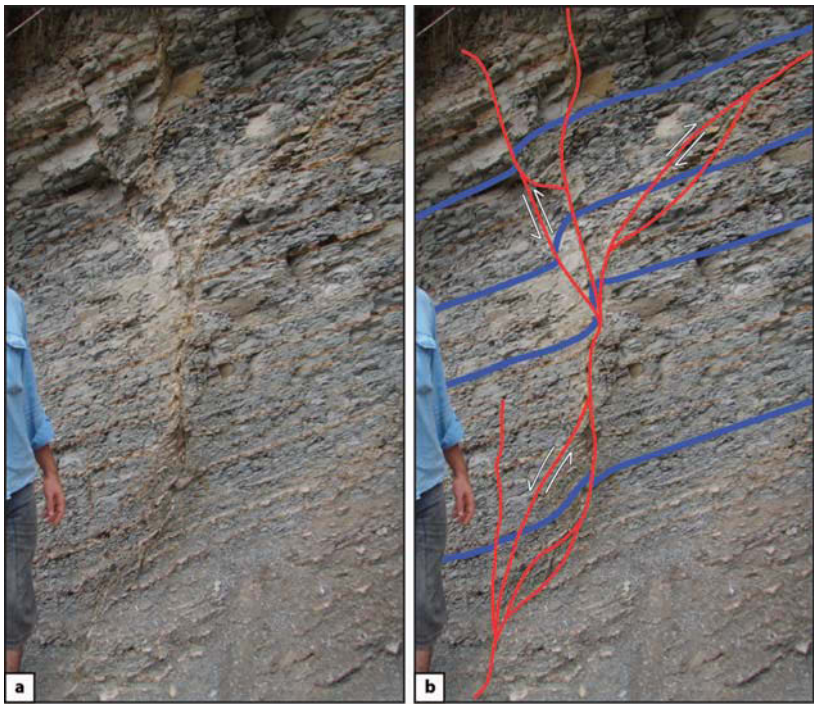

Figure 8 Uninterpreted (a) and interpreted (b) figures of a large, asymmetric flower structure at location 144878, produced by strike-slip movement within grey Banda Terrane mudstones with thin sandstone interbeds. Note the large number of steeply dipping, upwardly diverging fault splays at high structural levels. Corresponding bed-sets have been marked on the outcrop with faults highlighted in red; following bed-sets through the fault zone allows fault movement to be determined. Reverse movement is observed on fault splays at higher structural levels, forming a pop-up structure, while normal movement is observed around the main fault strand at lower structural levels. Drag folds formed against the fault splays in outcrop (b) are replicated at map scale (Figure 7a, b) where the Synorogenic Megasequence is faulted against the older rocks of the massif.

displacement could be expected at Mount Mundo Perdido, although this may represent only a small part of total movement along a larger fault zone within East Timor. The Mount Mundo Perdido structure is of similar size and geometry to other known structures along active strike-slip faults. These include the Villa Vasquez bend in Hispaniola (14 km × 2 km; Mann *et al.* 1999), the Ocotillo Badlands bend in southern California (8 km × 1.5 km; Brown *et al.* 1991; Lutz *et al.* 2006) and the Cerro de la Mica structure in Chile (McClay & Bonora 2001) (Figure 11b). These structures compare favourably in size and morphology to the 10 km × 3 km structure of Mount Mundo Perdido. Shortening and uplift within the Ocotillo Badlands accommodates approximately 15 km of fault displacement (Lutz *et al.* 2006).

The Cerro de la Mica structure forms a pop-up structure at a restraining bend adjacent to the Atacama Fault in Chile, and comprises a short, isolated range of uplifted Paleozoic volcanic and sedimentary rocks (McClay & Bonora 2001). The structure displays a remarkable similarity in morphology, fault architecture and distribution of stratigraphy

Figure 9 (a) Plan view of a pop-up structure, which has formed in a sandbox model of a restraining bend within a strike slip zone, after 10 cm of sinistral displacement (modified from Dooley *et al.* 1999). This structure shows three distinct sets of faults: bounding faults (red), faults subparallel to the axis of strike-slip (yellow), and antithetic through going faults which dissect the pop-up (black). A schematic geological map of Mount Mundo Perdido (c), exhibits very similar fault architecture, with the same three distinct sets of faults also evident in both the map and contoured stereonet fault plot (points represent poles to fault planes). Green arrows show the interpreted sinistral direction of movement around the main structure. (b) An interpreted horizontal section through a sandbox model of a restraining bend within a sinistral strike slip zone, taken from 1 cm below the surface (modified from McClay & Bonora 2001). This modelled 'erosion' has exposed a successive progression of older to younger units, moving outwards from the centre of the structure. The schematic geological map of Mount Mundo Perdido (c) shows a very similar distribution of stratigraphy. The oldest Triassic–Jurassic limestones that occupy the highest peaks in the centre of the mountain (dark blue) are surrounded by, younger, Cretaceous to Oligocene pelagites on the mountain's southern and northern flanks (light blue). A rim of Banda Terrane units (pink), originally at the top of the structural pile, forms the foothills and lower cliffs surrounding the mountain. Bedding generally dips away from the central east–west axis of the structure.

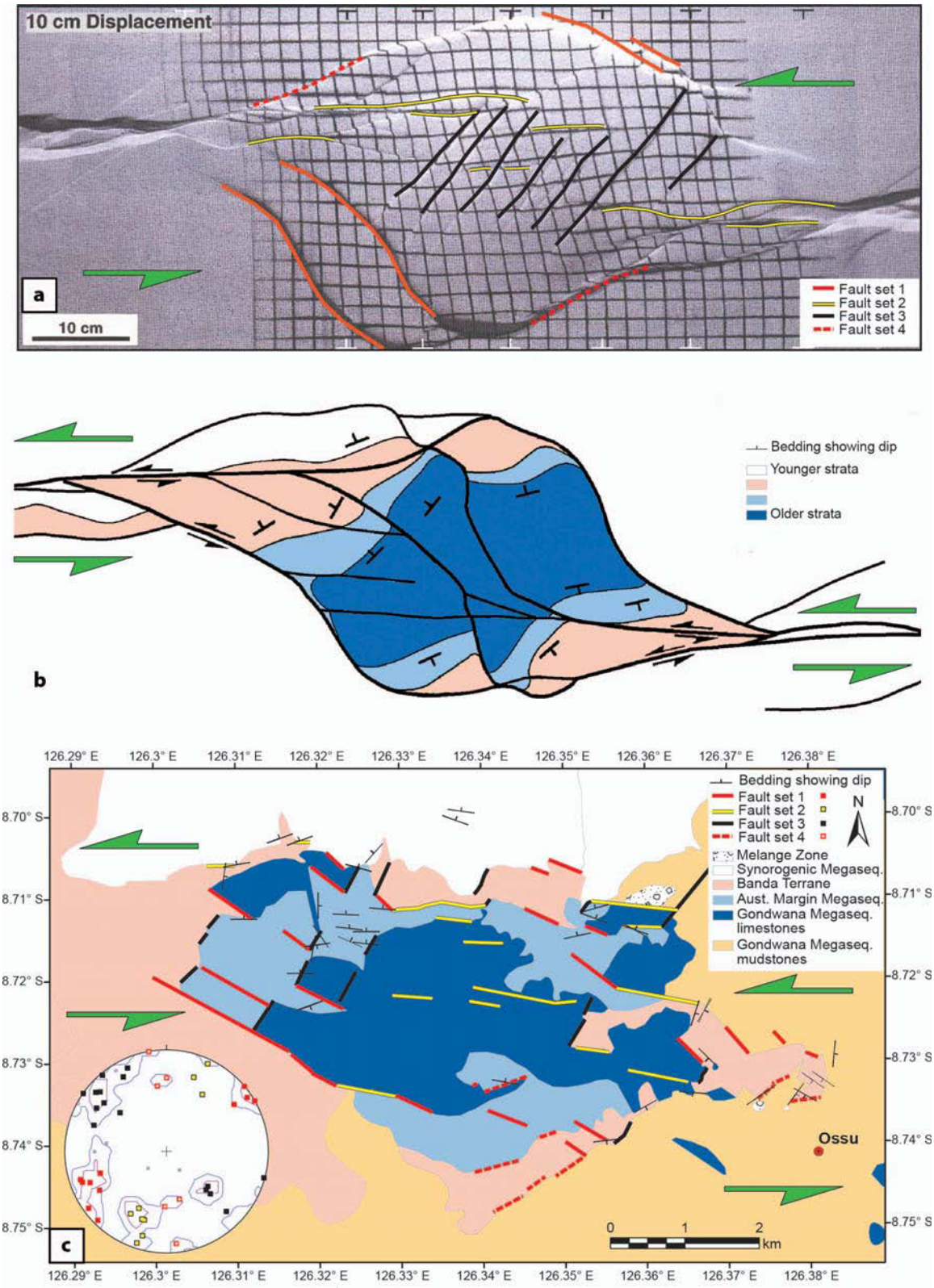

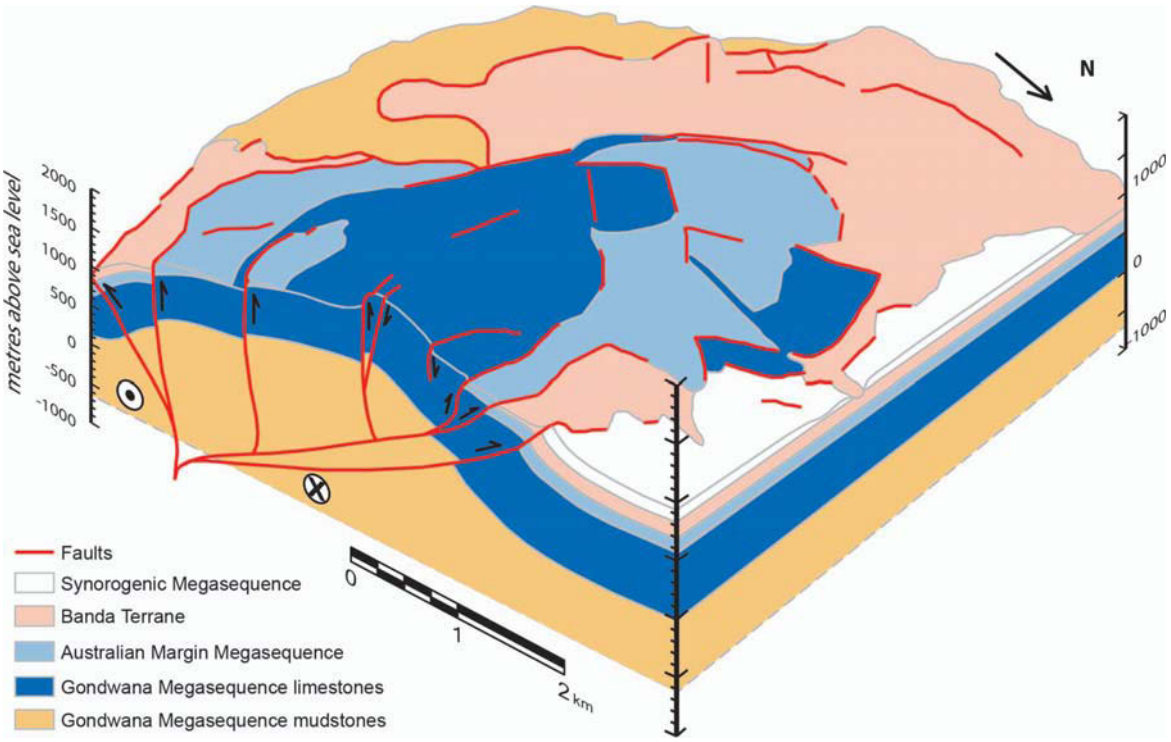

Figure 10 Simplified schematic model of a possible NNE–SSW cross-section through Mount Mundo Perdido, showing the western half of the massif, with subsurface fault architecture based in part on geometries observed in outcrop. The eastern half of the massif (including main extensional faults) has been removed to illustrate the cross-section. Circle signifies movement out of the page, and X signifies movement into the page. The resulting structure exposes the Triassic–Jurassic Cablac Limestone at its centre. Moving north and south towards the edges there is exposed a differential progression through successively younger units separated by high-angle, mostly reverse-oblique faults. Drag folds are visible within the Synorogenic Megasequence along the northern edge of the massif. A layer-cake megasequence stratigraphy is modelled for simplicity, but at Mount Mundo Perdido stratigraphy is likely complicated by earlier episodes of thrusting.

Table 4 Description of folding observed at three locations on Mount Mundo Perdido. All folds are upright, with the exception of one fold at AB145, which has its axial plane inclined. Note the large variation in dip direction of the fold axial planes. The fold axis was not measured at AB240.

Site no.	Approximate fold axial plane		Approximate fold axis		Interlimb angle	Symmetry	Fold Style	Formation	Megasequence
	Dip	Dip Dir	Plunge	Trend					
AB145	50	88	50	80	Open	Symmetric	Parallel	Kolbano beds	Australian Margin Megasequence
AB145	81	275	34	195	Open	Weakly asymmetric	Parallel	Kolbano beds	Australian Margin Megasequence
AB158	85	300	10	215	Open	Symmetric	Parallel	Kolbano beds	Australian Margin Megasequence
AB240	90	0	–	–	Open	Symmetric	Parallel	Kolbano beds	Australian Margin Megasequence

to Mount Mundo Perdido (Figure 11b). Both are rhomboidal and asymmetrical, of comparable scale and height, and they share complex internal structures displaying faults both parallel and oblique to their long axes. Both have similar stratigraphic distributions, and steep bounding faults separate both from the surrounding geology.

Despite their modest size, all of these examples, the Villa Vasquez structure that is part of the Septentrional fault zone (Mann *et al.* 1999), the Ocotillo Badlands structure that is part of the San Jacinto fault zone–San Andreas fault system (Brown *et al.* 1991; Lutz *et al.* 2006) and the Cerro de la Mica structure (McClay & Bonora 2001), occur within crustal-scale fault systems. In fact,

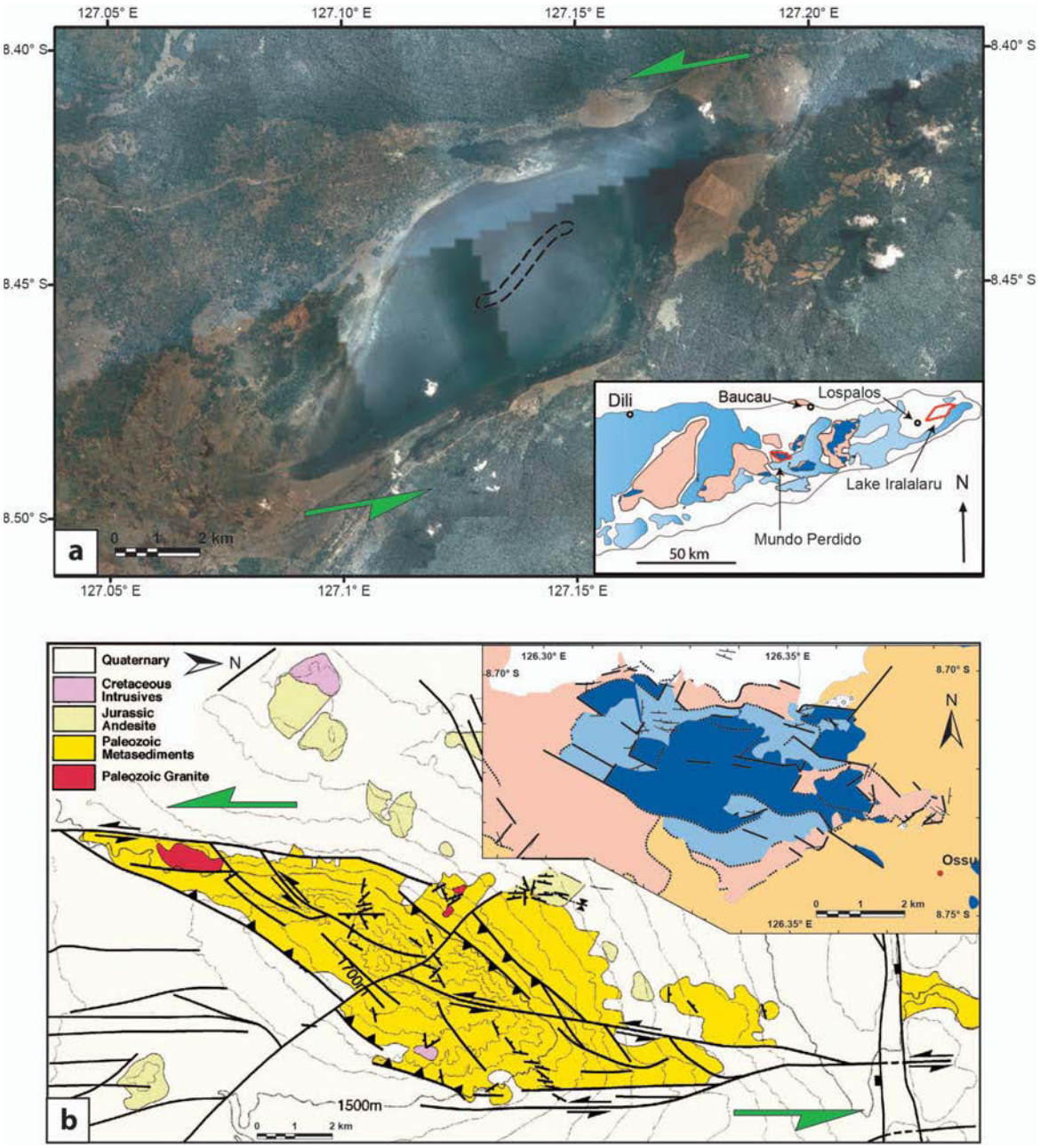

Figure 11 (a) Composite aerial photograph of Lake Iralalaru during the wet season, which exhibits the rhomboidal geometry characteristic of pull-apart basins. The dashed outline represents the elongate, spindle-shaped extent of the lake during the dry season. The basin is situated along strike from Mount Mundo Perdido, is of similar scale, and would require a similar sinistral displacement sense to create its rhomboidal geometry as a pull-apart structure. (b) Cerro de la Mica, a pop-up structure developed at a sinistral restraining bend on the north–south-trending Atacama fault zone, Chile (modified from McClay & Bonora 2001). Rotating the Cerro de la Mica map 90° clockwise so that its north–south fault axis is oriented east–west, it bears a strong resemblance to the interpreted pop-up structure at Mount Mundo Perdido. Both structures have comparable scale, morphology, fault architecture and distribution of stratigraphy.

most of the 49 restraining bends catalogued by Mann (2007) associated with pop-up structures of comparable scale to Mount Mundo Perdido are part of crustal-scale strike-slip fault systems. The possibility of a similar crustal-scale structure in East Timor therefore needs to be investigated. Plate-boundary parallel strike-slip faults of this scale occur adjacent to subduction zones (Beck 1986; Jarrard 1986) owing to coupling between the plates, and do not necessarily require strong obliquity (Jarrard 1986). Near-orthogonal collision produced the

1100 km-long, sinistral Atacama fault zone in northern Chile (Jarrard 1986; Mann 2007).

In East Timor, the transition from subduction to collision and the locking of the subduction zone (Keep & Haig 2010) created a strongly coupled system in which large-scale strike slip deformation may be expected (Jarrard 1986; Mann 2007), as the oblique component of collision is partitioned into zones of plate-boundary parallel strike-slip, as in the Atacama Fault Zone described above. The overall NNE convergence direction of Australia with respect to the Pacific and Eurasian plates (Genrich *et al.* 1996) has long been thought to have generated strike-slip motion at the plate boundary (Nelson 1993; Keep *et al.* 1998; Shuster *et al.* 1998; Ainsworth *et al.* 2000; de Ruig *et al.* 2000; Harrowfield *et al.* 2003; Harrowfield & Keep, 2005; Bourget *et al.* 2012). However, occurrences of strike-slip on the Australian part of the margin are limited to local structures (Ainsworth *et al.* 2000; de Ruig *et al.* 2000; Keep *et al.* 2000), with the majority of strike-slip thought to be accommodated in Timor (Harrowfield *et al.* 2003). The structure at Mount Mundo Perdido documented here and the comparison to other similar structures, which commonly form as parts of crustal-scale strike-slip faults, indicate that local-scale strike slip, and possibly more regional-scale strike-slip, has occurred in East Timor.

CONCLUSIONS

Mount Mundo Perdido comprises a complex assortment of rock types of differing ages and tectonostratigraphic affinities, including Triassic–Jurassic interior rift basin deposits of Gondwanan affinity, Cretaceous–Oligocene pelagites deposited on the Australian passive margin, limestones and island arc volcanics of Asiatic affinity, and Pliocene–Pleistocene synorogenic deposits. The dominant structures include numerous late stage, high-angle, oblique-slip faults, which control the uplift and create prominent drag folds, including within synorogenic limestones where they are faulted against the older rocks of the Mundo Perdido massif. Based on the age of these synorogenic units, deformation at Mount Mundo Perdido is interpreted as Pleistocene.

Fault architecture and stratigraphic distribution support the interpretation of Mount Mundo Perdido as a pop-up structure formed within a strike-slip fault zone, possibly at a restraining bend or step-over in an east–west-striking zone of sinistral strike-slip. This interpretation, supported by similarities to both analogue models and real world examples of sinistral pop-up structures, suggests that large-scale strike-slip deformation may be an integral part of the collision kinematics.

ACKNOWLEDGEMENTS

We thank Eni Australia Ltd for supporting our research in Timor Leste and making this project possible, with special thanks to Tony Heynen and Jose Sabino at Eni Timor Leste for their assistance in Dili. Thank you Norberta da Costa, Director, and all the staff at the National Directorate of Geology and Mineral Resources in the Secretariate for Energy and Natural Resources (SERN) for your continuing support. We thank the Viqueque District Administrator, Ossu Sub-District Administrator, and Sucu Chiefs of Liaruca, Builale and Ossu de Cima for facilitating our fieldwork at Mundo Perdido. Thanks to Eujay McCartian for logistical help during the 2009 field season. We thank Matt Dixon for assistance with palynological determinations, and Mary Gee for assistance with the igneous material. Many thanks to Gilsel Borges, now Geoscientist at Eni Timor Leste; without your assistance and expertise in geological mapping this project would not have been possible. We are very grateful to everyone who assisted in the field, including Januario de Carvalho, Manuel Hornai Gonsalves and Andy Montiero. Finally, we thank the Montiero family, who opened up their home to us while in Ossu with unreserved generosity and hospitality.

REFERENCES

Ainsworth R. B., Bosscher H. & Newall M. J. 2000. Forward stratigraphic modelling of forced regressions: Evidence for the genesis of attached and detached lowstand systems. *Geological Society, London, Special Publications* **172**, 163–176.

Audley-Charles M. G. 1968. The Geology of Portugese Timor. *Memoirs of the Geological Society of London* **4**.

Audley-Charles M. G. 1985. The Sumba enigma: is Sumba a diapiric fore-arc nappe in process of formation? *Tectonophysics* **119**, 435–439.

Audley-Charles M. G. 1986. Rates of Neogene and Quaternary tectonic movements in the Southern Banda Arc based on micropalaeontology. *Journal of the Geological Society of London* **143**, 161–175.

Audley-Charles M. G. 2004. Ocean trench blocked and obliterated by Banda forearc collision with Australian proximal continental slope. *Tectonophysics* **389**, 65–79.

Audley-Charles M. G. 2011. Tectonic post-collision processes in Timor. *Geological Society, London, Special Publications* **355**, 241–266.

Audley-Charles M. G. & Carter D. J. 1972. Palaeogeographical significance of some aspects of Palaeogene and early neogene stratigraphy and tectonics of the Timor Sea region. *Palaeogeography, Palaeoclimatology, Palaeoecology* **11**, 247–264.

Audley-Charles M. G. & Harris R. A. 1990. Allochthonous terranes of the Southwest Pacific and Indonesia. *Philosophical Transactions of the Royal Society of London* **331**, 571–587.

Barber A. J., Tjokrosapoetro S. & Charlton T. R. 1986. Mud volcanoes, shale diapirs, wrench faults, and melanges in accretionary complexes, eastern Indonesia. *AAPG Bulletin* **70**, 1729–1741.

Beck M. E., Jr 1986. Model for Late Mesozoic–Early Tertiary tectonics of coastal California and western Mexico and speculation on the origin of the San Andreas fault. *Tectonics* **5**, 49–64.

Berry R. F. & McDougall I. 1986. Interpretation of $^{40}Ar/^{39}Ar$ and K/Ar dating evidence from the Aileu Formation, East Timor, Indonesia. *Chemical Geology* **59**, 43–58.

Bird P. R. & Cook S. E. 1991. Permo-Triassic successions of the Kekneno area, West Timor: implications for palaeogeography and basin evolution. *Journal of Southeast Asian Earth Sciences* **6**, 359–371.

Bourget J., Ainsworth B. R., Backé G. & Keep M. 2012. Tectonic evolution of the northern Bonaparte Basin: impact on continental shelf architecture and sediment distribution during the Pleistocene. *Australian Journal of Earth Sciences*, doi: 10.1080/08120099.2012.674555.

Brouwer H. A. 1942. Summary of the geological results of the expedition. *In*: Brouwer H. A. ed. *Geological expedition of the University of Amsterdam to the Lesser Sunda Islands in the south eastern part of the Netherlands East Indies 1937*, Vol. 4, pp. 345–401. N.V. Noord-Hollandsche Uitgevers Maatschappij, Amsterdam.

Brown N. N., Fuller D. F. & Sibson R. H. 1991. Paleomagnetism of the Ocotillo Badlands, southern California, and implications for slip transfer through an antidilational fault jog. *Earth and Planetary Science Letters* **102**, 277–288.

Brunnschweiler R. O. 1978. Notes on the geology of eastern Timor. *Bulletin Australia Bureau of Mineral Resources Geology and Geophysics* **192**, 9–18.

Carter D. J., Audley-Charles M. G. & Barber A. J. 1976. Stratigraphical analysis of island arc–continental margin collision in eastern Indonesia. *Journal of the Geological Society of London* **132**, 179–198.

Chamalaun F. H. & Grady A. E. 1978. The tectonic development of Timor: a new model and its implications for petroleum exploration. *APEA Journal* **18**, 102–108.

Charlton T. R. 2000. Tertiary evolution of the Eastern Indonesia Collision Complex. *Journal of Asian Earth Sciences* **18**, 603–631.

Charlton T. R. 2002. The structural setting and tectonic significance of the Lolotoi, Laclubar and Aileu metamorphic massifs, East Timor. *Journal of Asian Earth Sciences* **20**, 851–865.

Charlton T. R., Barber A. J. & Barkham S. T. 1991. The Structural Evolution of the Timor Collision Complex, Eastern Indonesia. *Journal of Structural Geology* **13**, 489–500.

De Roever W. P. 1940. Geological investigations in the southwestern Moetis Region (Netherlands Timor). *In*: Brouwer H. A. ed. *Geological expedition of the University of Amsterdam to the Lesser Sunda Islands in the south eastern part of the Netherlands East Indies 1937*, Vol. 2, pp. 101–344, N.V. Noord-Hollandsche Uitgevers Maatschappij, Amsterdam.

de Ruig M. J., Trupp M., Bishop D., Kuek D. & Castillo D. 2000. Fault architecture and the mechanics of fault reactivation in the Nancar Trough/Laminaria area of the Timor Sea, Northern Australia. *The APPEA Journal* **40**, 174–193.

De Waard D. 1957. Contributions to the geology of Timor: XII. The third Timor geological expedition, preliminary results. *Madjalah Ilmu Alam Untuk Indonesia (Indonesian Journal for Natural Science)* **113**, 7–42.

Deeks N. R. & Thomas S. A. 1995. Basin inversion in a strike-slip regime: the Tornquist Zone, Southern Baltic Sea. *Geological Society, London, Special Publications* **88**, 319–338.

Dooley T. & McClay K. 1997. Analog modeling of pull-apart basins. *AAPG Bulletin* **81**, 1804–1826.

Dooley T., McClay K. & Bonora M. 1999. 4D Evolution of segmented strike-slip fault systems: applications to NW Europe. *In*: Fleet A. J. & Boldy S. A. R. eds. *Petroleum Geology of Northwest Europe: Proceedings of the 5th Conference*, The Geological Society, London.

Ely K. S., Sandiford M., Hawke M. L., Phillips D., Quigley M. & Dos Reis J. E. 2011. Evolution of Ataúro Island: Temporal constraints on subduction processes beneath the Wetar zone, Banda Arc. *Journal of Asian Earth Sciences* **41**, 477–493.

Fitch T. J. & Hamilton W. 1974. Reply to a discussion by M.G. Audley-Charles & J. Milsom. *Journal of Geophysical Research* **79**, 4982–4985.

Fortuin A. R., Roep T. B. & Sumosusastro P. A. 1994. The Neogene sediments of east Sumba, Indonesia—products of a lost arc? *Journal of Southeast Asian Earth Sciences* **9**, 67–79.

Fortuin A. R., van der Werff W. & Wensink H. 1997. Neogene basin history and paleomagnetism of a rifted and inverted forearc region, on- and offshore Sumba, Eastern Indonesia. *Journal of Asian Earth Sciences* **15**, 61–88.

Gageonnet R. & Lemoine M. 1958. Contribution à la connaissance de la géologie de la province portugaise de Timor. *Ensaios e Documentos Ministério do Ultramar Junta de Investigações do Ultramar* **48**, 7–134.

Genrich J., Bock V., McCaffrey R., Calias E. & Stevens C. 1996. Accretion of the southern Banda Arc to the Australian plate margin determined by Global Positioning System measurements. *Tectonics* **15**, 288–295.

Grunau H. R. 1953. Geologie von Portugiesisch Ost-Timor. Eine kurze Übersicht. *Eclogae Geologicae Helveticae* **46**, 29–37.

Grunau H. R. 1956. Zur geologie von Portugiesisch Ost-Timor. *Mitteilungen Naturforschende Gesellschaft Bern* **13**, 11–18.

Haig D. W. 2012. Palaeobathymetric gradients across Timor during 5.7–3.3 Ma (latest Miocene–Pliocene) and implications for collision uplift. *Palaeogeography, Palaeoclimatology, Palaeoecology*, doi:10.1016/j.palaeo.2012.02.032.

Haig D. W. & McCartain E. 2007. Carbonate pelagites in the post-Gondwana succession (Cretaceous–Neogene) of East Timor. *Australian Journal of Earth Sciences* **54**, 875–897.

Haig D. W. & McCartain E. 2010. Triassic organic-cemented siliceous agglutinated foraminifera from Timor-Leste: conservative development in shallow-marine environments. *Journal of Foraminiferal Research* **40**, 366–392.

Haig D. W., McCartain E., Barber L. & Backhouse J. 2007. Triassic–Lower Jurassic foraminiferal indices for Bahaman-type carbonate-bank limestones, Cablac Mountain, East Timor. *Journal of Foraminiferal Research* **37**, 248–264.

Haig D. W., McCartain E. W., Keep M. & Barber L. 2008. Re-evaluation of the Cablac Limestone at its type area, East Timor: Revision of the Miocene stratigraphy of Timor. *Journal of Asian Earth Sciences* **33**, 366–378.

Hall R. 2002. Cenozoic geological and plate tectonic evolution of SE Asia and the SW pacific: computer-based reconstructions, model and animations. *Journal of Asian Earth Sciences* **20**, 353–431.

Hall R. 2011. Australia–SE Asia collision: plate tectonics and crustal flow. *Geological Society, London, Special Publications* **355**, 75–109.

Hall R. & Wilson M. E. J. 2000. Neogene sutures in eastern Indonesia. *Journal of Asian Earth Sciences* **18**, 781–808.

Hamilton W. 1979. Tectonics of the Indonesian region. *United States Geological Survey, Professional Paper* **1078**.

Harris R. 2006. Rise and fall of the Eastern Great Indonesian arc recorded by the assembly, dispersion and accretion of the Banda Terrane, Timor. *Gondwana Research* **10**, 207–231.

Harris R. A. & Audley-Charles M. G. 1987. Taiwan and Timor neotectonics; a comparative review. *Chung Kuo Ti Ch'ih Hsueh Hui Chuan Kan = Memoir of the Geological Society of China* **9**, 45–61.

Harris R. A., Sawyer R. K. & Audley-Charles M. G. 1998. Collisional melange development: geologic associations of active melange-forming processes with exhumed melange facies in the western Banda orogen, Indonesia. *Tectonics* **17**, 458–479.

Harrowfield M. & Keep M. 2005. Tectonic modification of the Australian North-West Shelf; episodic rejuvenation of long-lived basin divisions. *Basin Research* **17**, 225–239.

Harrowfield M., Cunneen J., Keep M. & Crowe W. 2003. Early-stage orogenesis in the Timor Sea region, NW Australia. *Journal of the Geological Society* **160**, 991–1001.

Holford S. P., Turner J. P., Green P. F. & Hillis R. R. 2009. Signature of cryptic sedimentary basin inversion revealed by shale compaction data in the Irish Sea, western British Isles. *Tectonics* **28**, doi:10.1029/2008TC002359.

Jarrard R. D. 1986. Relations among subduction parameters. *Reviews of Geophysics* **24**, 217–234.

Keep M. & Haig D. W. 2010. Deformation and exhumation in Timor: Distinct stages of a young orogeny. *Tectonophysics* **483**, 93–111.

Keep M., Barber L. & Haig D. 2009. Deformation of the Cablac Mountain Range, East Timor: An overthrust stack derived from an Australian continental terrace. *Journal of Asian Earth Sciences* **35**, 150–166.

Keep M., Bishop A. & Longley I. 2000. Neogene wrench reactivation of the Barcoo Sub-basin, northwest Australia: implications for Neogene tectonics of the northern Australian margin. *Petroleum Geoscience* **6**, 211–220.

Keep M., Clough M. C. & Langhi L. 2002. Neogene structural and tectonic evolution of the Timor Sea region, NW Australia. *In*: Keep M. & Moss S. J. eds. *The sedimentary basins of Western Australia 3.* pp. 341–354. Proceedings of the Petroleum Exploration Society of Australia, Perth.

Keep M., Longley I. & Jones R. 2003. Sumba and its effect on Australia's northwestern margin. *Geological Society of Australia Special Publication* **22**, 303–312.

Keep M., Powell C. M. & Baillie P. W. 1998. Neogene deformation of the North West Shelf, Australia. *In*: Purcell P. G. & Purcell R. R. eds. *The sedimentary basins of Western Australia 2,* pp. 81–91. Proceedings of the Petroleum Exploration Society of Australia, Perth.

Lutz A. T., Dorsey R. J., Housen B. A. & Janecke S. U. 2006. Stratigraphic record of Pleistocene faulting and basin evolution in the Borrego Badlands, San Jacinto fault zone, Southern California. *Geological Society of America Bulletin* **118**, 1377–1397.

Mann P. 2007. Global catalogue, classification and tectonic origins of restraining- and releasing bends on active and ancient strike-slip fault systems. *In*: Cunningham W. D. & Mann P. eds. *Tectonics of strike-slip restraining and releasing bends*, pp. 13–142. The Geological Society, Special Publications Vol. 290, London.

MANN P., MCLAUGHLIN P. P. J., VAN DEN BOLD W. A., LAWRENCE S. R. & LAMAR M. E. 1999. Tectonic and eustatic controls on Neogene evaporitic and siliciclastic deposition in the Enriquillo Basin, Dominican Republic. *In*: Mann P. ed. *Caribbean basins, sedimentary basins of the world 4*, pp. 287–342. Elsevier, Amsterdam.

MCCAFFREY R., MOLNAR P., ROECKER S. W. & JOYODIWIRYO Y. S. 1985. Microearthquake Seismicity and Fault Plane Solutions Related to Arc–continent Collision in the Eastern Sunda Arc, Indonesia. *Journal of Geophysical Research* **90**, 4511–4528.

MCCLAY K. & BONORA M. 2001. Analog models of restraining stepovers in strike-slip fault systems. *AAPG Bulletin* **85**, 223–260.

MILSOM J. 2000. Stratigraphic constraints on suture models for eastern Indonesia. *Journal of Asian Earth Sciences* **18**, 761–779.

MOLENGRAAF G. A. F. 1912. De fatoe's van Timor. *Geologische Mijnbouwkundig Genootschap voor Nederland en Koloniën, Geologische Sectie, verslag der voordrachten, van 1912–1914, gehouden op de Wetenschappelijke Vergaderingen*.

NELSON A. 1993. Wrench and inversion structures in the Timor Sea region. *Petroleum Exploration Society of Australia Journal* **21**, 3–30.

PARTOYO E., HERMANTO B. & BACHRI S. 1995. Geological Map of Baucau Quadrangle, East Timor, Scale 1:250 000. *Geological Research and Development Centre, Bandung*.

PRICE N. J. & AUDLEY-CHARLES M. G. 1987. Tectonic collision processes after plate rupture. *Tectonophysics* **140**, 121–129.

REED D. L. 1985. Structure and stratigraphy of the eastern Sunda Forearc, Indonesia: geologic consequences of arc–continent collision. PhD thesis, University of California, Santa Cruz.

RICHARDSON A. N. & BLUNDELL D. J. 1996. Continental collision in the Banda Arc. *In*: Hall R. & Blundell D. J. eds. *Tectonic evolution of southeast Asia*, pp. 47–60. *Geological Society Special Publication* Vol. 106.

ROMARIZ C. & LEME J. D. A. 1967. Subsidios para a petrografia timorense. Calcario de Fato. *Garcia de Orta* **15**, 111–112.

ROOSMAWATI N. & HARRIS R. 2009. Surface uplift history of the incipient Banda arc–continent collision: Geology and synorogenic foraminifera of Rote and Savu Islands, Indonesia. *Tectonophysics* **479**, 95–110.

RUTHERFORD E., BURKE K. & LYTWYN J. 2001. Tectonic history of Sumba Island, Indonesia, since the Late Cretaceous and its rapid escape into the forearc in the Miocene. *Journal of Asian Earth Sciences* **19**, 453–479.

SCHELLART W. P. & NIEUWLAND D. A. 2003. 3D evolution of a pop-up structure above a double basement strike-slip fault: some insights from analogue modelling. *Geological Society, London, Special Publications* **212**, 169–179.

SCHLAGINTWEIT F. & VELIĆ I. 2012. Foraminiferan tests and dasycladalean thalli as cryptic microhabitats for thaumatoporellacean algae from Mesozoic (Late Triassic–Late Cretaceous) platform carbonates. *Facies* **58**, 79–84.

SIMONS A. L. 1940. Geological investigations in N. E. Netherlands Timor. *In*: Brouwer H. A. ed. *Geological expedition of the University of Amsterdam to the Lesser Sunda Islands in the south eastern part of the Netherlands East Indies 1937*, Vol. 1, pp. 110–213. N. V. Noord-Hollandsche Uitgevers Maatschappij, Amsterdam.

SHUSTER M. W., EATON S., WAKEFIELD L. L. & KLOSTERMAN H. J. 1998. Neogene Tectonics, Greater Timor Sea, Offshore Australia: Implications for Trap Risk. *The APPEA Journal* **38**, 351–379.

SPAKMAN W. & HALL R. 2010. Surface deformation and slab-mantle interaction during Banda arc subduction rollback. *Nature Geoscience* **3**, 562–566.

TAPPENBECK D. 1940. Geologie des Mollogebirges und einiger benachbarter gebiete (Niederländisch Timor). *In*: Brouwer H. A. ed. *Geological expedition of the University of Amsterdam to the Lesser Sunda Islands in the south eastern part of the Netherlands East Indies 1937*, Vol. 1, pp. 1–105. N. V. Noord-Hollandsche Uitgevers Maatschappij, Amsterdam.

VAN DER WERFF W., KUSNIDA D., PRASETYO H. & VAN WEERING T. C. E. 1994. Origin of the Sumba forearc basement. *Marine and Petroleum Geology* **11**, 363–374.

VAN WEST F. P. 1941. Geological investigations in the Miomaffo region (Netherlands Timor). *In*: Brouwer H. A. ed. *Geological expedition of the University of Amsterdam to the Lesser Sunda Islands in the south eastern part of the Netherlands East Indies 1937*, Vol. 3, pp. 1–131. N.V. Noord-Hollandsche Uitgevers Maatschappij, Amsterdam.

WANNER J. 1913. Geologie von Westtimor. *Geologische Rundschau* **4**, 136–150.

WITHJACK M. O., BAUM M. S. & SCHLISCHE R. W. 2010. Influence of pre-existing fault fabric on inversion-related deformation: a case study of the inverted Fundy rift basin, southeastern Canada. *Tectonics* **29**, doi:10.1029/2010TC002744.

WITTOUCK S. F. 1937. *Exploration of Portuguese Timor*. Report of Allied Mining Corp. To Asia Investment Co. Ltd, Amsterdam (Kolff).

WOODCOCK N. H. & FISCHER M. 1986. Strike-slip duplexes. *Journal of Structural Geology*. **8**, 725–735.

Received 7 October 2011; accepted 25 March 2012

SUPPLEMENTARY PAPERS

Appendix 1 Table A1 Lithostratigraphic units and age-diagnostic fossils recognised at Mundo Perdido.
Appendix 2 XRF analysis volcanic and metamorphic samples.

SUPPLEMENTARY APPENDIX A: Description and age determination of samples

Sample types: a.p. = acetate peels; w.r. = washed sediment residue (>150µm); t.s. = thin section

UWA No	Lat	Long	Field Number	Sample type	Rock Description	Age diagnostic fossils	Age and facies	Formation and tectonostratigraphic affinity
143146	-8.70495	126.36222	12_10_08_4	a.p.	Packstone with abundant planktonic foraminifera, rare benthic foraminifera (mainly Rotaliida), mollusc fragments, coralline algae, coral debris; bed of planktonic foraminiferal limestone above 143147	Planktonic foraminifera: *Globorotalia truncatulinoides* , *Globorotalia tosaensis*	Planktonic foraminiferal Zone N22r; mid Pleistocene within 2.02–0.63 Ma interval (Keep & Haig 2010, fig. 6); upper bathyal zone	Lari Guti Member of Viqueque Formation; Synorogenic Megasequence
143147	-8.70495	126.36222	12_10_08_5	a.p., w.r.	Packstone with abundant planktonic foraminifera, rare benthic foraminifera (mainly Rotaliida); lowest bed of fine planktonic foraminiferal limestone in outcrop section	Planktonic foraminifera: *Globorotalia truncatulinoides* , *Globorotalia tosaensis*	Planktonic foraminiferal Zone N22r; mid Pleistocene within 2.02–0.63 Ma interval (Keep & Haig 2010, fig. 6); upper bathyal zone	Lari Guti Member of Viqueque Formation; Synorogenic Megasequence
143149	-8.71150	126.35525	12_10_08_7	a.p.	Wackestone with scattered planktonic foraminifera	Planktonic foraminifera: *Dicarinella* sp., *Praeglobotruncana* sp.	Late Cretaceous (Turonian); middle bathyal to abyssal	Kolbano Beds; Australian Margin Megasequence
143163	-8.73067	126.36735	14_10_08_1	a.p.	(A) Collected on south side of gully: Wackestone with common thaumatoporellacean algae. (B) Collected on north side of gully: Packstone to wackestone with large corals, abundant benthic foraminifera (mainly Rotaliida including larger types), rare small planktonic foraminifera,	(A) Thaumatoporcellacean algae. (B) Larger benthic foraminifera (in limestone clasts): *Eulepidina* , primitive *Lepidocyclina* (*Nephrolepidina*), *Spiroclypeus* . Planktonic foraminifera (in matrix): ?*Globigerinoides primordius*	(A) probably Early Jurassic; innermost neritic. (B) Larger benthic foraminiferal Upper Te Letter Stage (Adams, 1970); planktonic zone N4 or N5 (Kennett & Srinivasan, 1983); latest Oligocene or earliest Miocene; inner neritic	(A) Perdido Group; Gondwana Megasequence. (B) Booi beds; Banda Terrane

UWA No	Lat	Long	Field Number	Sample type	Rock Description	Age diagnostic fossils	Age and facies	Formation and tectonostratigraphic affinity
143164	-8.73067	126.36735	14_10_08_2	a.p.	Packstone to wackestone with abundant benthic foraminifera (mainly Rotaliida including larger types), coralline algae and coral debris	Larger benthic foraminifera (in limestone clasts): *Eulepidina* , primitive *Lepidocyclina* (*Nephrolepidina*), *Spiroclypeus* .	Larger benthic foraminiferal Upper Te Letter Stage (Adams, 1970); latest Oligocene - earliest Miocene	Booi beds; Banda Terrane
143165	-8.72922	126.36575	14_10_08_3	a.p.	Ooid grainstone with micritic intraclasts; very rare thaumatoporellacean algae scattered recrystallized mollusc debris, very rare echinoid spines and plates, very rare indeterminant benthic foraminifera	Thaumatoporcellacean algae	Probably Early Jurassic	Perdido Group; Gondwana Megasequence
143169	-8.72910	126.36582	14_10_08_7	a.p., t.s.	Wackestone with rare planktonic foraminifera (including keeled forms), rare benthic foraminifera (Rotaliida)	Planktonic foraminifera: *Helvetoglobotruncana helvetica* , *Marginotruncana marginata* , *Dicarinella* spp.	Upper Turonian (Turonian); middle bathyal to abyssal	Kolbano Beds; Australian Margin Megasequence
143170	-8.72910	126.36715	14_10_08_8	a.p.	Friable grey mudstone	Planktonic foraminifera: *Globorotalia kugleri* , *Globigerinoides primordius*	Planktonic foraminiferal zone N4 (Kennett & Srinivasan 1983); Larger benthic foraminiferal Upper Te Letter Stage (Adams, 1970); earliest Miocene	Booi beds; Banda Terrane
143171	-8.71702	126.36592	14_10_08_9	a.p.	Ooid grainstone with rare carbonate-cemented agglutinated foraminifera	Foraminifera: *Siphovalvulina variabilis*	Probably Early Jurassic	Perdido Group; Gondwana Megasequence

UWA No	Lat	Long	Field Number	Sample type	Rock Description	Age diagnostic fossils	Age and facies	Formation and tectonostratigraphic affinity
143187	-8.70575	126.36175	8_11_08_04	a.p.	Planktonic foraminiferal packstone with very rare smaller benthic foraminifera (Rotaliida); collected 2.7 m above base of outcrop section	Planktonic foraminifera: *Globorotalia truncatulinoides* , *Globorotalia tosaensis*	Planktonic foraminiferal Zone N22r; mid Pleistocene within 2.02–0.63 Ma interval (Keep & Haig 2010, fig. 6); upper bathyal zone	Lari Guti Member of Viqueque Formation; Synorogenic Megasequence
143191	-8.70575	126.36175	8_11_08_08	a.p.	Calcirudite with large corals, coralline algal debris, mollusc fragments, common benthic foraminifera (mainly Rotaliida including larger types), scattered planktonic foraminifera; lithic fragments. From base of large channel cut into section	Planktonic foraminifera: *Globorotalia truncatulinoides* , *Globorotalia tosaensis* . Benthic foraminifera: *Nummulites venosus* , *Schlumbergerella* , *Cycloclypeus*	Planktonic foraminiferal Zone N22r; mid Pleistocene within 2.02–0.63 Ma interval (Keep & Haig 2010, fig. 6); upper bathyal zone	Lari Guti Member of Viqueque Formation; Synorogenic Megasequence
143192	-8.70575	126.36175	8_11_08_09	a.p.	Packstone with abundant benthic foraminifera (mainly rotaliids including larger types), coralline algae, mollusc debris; about 1 m above base of large channel cut into section	Planktonic foraminifera: *Globorotalia truncatulinoides* , *Globorotalia tosaensis* . Benthic foraminifera: *Nummulites venosus* , *Schlumbergerella* , *Cycloclypeus*	Planktonic foraminiferal Zone N22r; mid Pleistocene within 2.02–0.63 Ma interval (Keep & Haig 2010, fig. 6); upper bathyal zone	Lari Guti Member of Viqueque Formation; Synorogenic Megasequence
143196	-8.70575	126.36175	8_11_08_13	a.p.	Calcirudite with large corals, abundant planktonic foraminifera, rare benthic foraminifera (mainly Rotaliida); 13.2 m above base of exposed measured section	Planktonic foraminifera: *Globorotalia truncatulinoides* , *Globorotalia tosaensis* . Benthic foraminifera: *Schlumbergerella*	Planktonic foraminiferal Zone N22r; mid Pleistocene within 2.02–0.63 Ma interval (Keep & Haig 2010, fig. 6); upper bathyal zone	Lari Guti Member of Viqueque Formation; Synorogenic Megasequence

UWA No	Lat	Long	Field Number	Sample type	Rock Description	Age diagnostic fossils	Age and facies	Formation and tectonostratigraphic affinity
143198	-8.70575	126.36175	8_11_08_15	a.p.	Packstone with abundant planktonic foraminifera, rare benthic foraminifera (mainly Rotaliida); 21.7 m above base of exposed measured section	Planktonic foraminifera: *Globorotalia truncatulinoides* , *Globorotalia tosaensis*	Planktonic foraminiferal Zone N22r; mid Pleistocene within 2.02–0.63 Ma interval (Keep & Haig 2010, fig. 6); upper bathyal zone	Lari Guti Member of Viqueque Formation; Synorogenic Megasequence
143199	-8.70575	126.36175	8_11_08_16	a.p.	Packstone with abundant planktonic foraminifera, rare benthic foraminifera (mainly Rotaliida); 22.5 m above base of exposed measured section	Planktonic foraminifera: *Globorotalia truncatulinoides* , *Globorotalia tosaensis*	Planktonic foraminiferal Zone N22r; mid Pleistocene within 2.02–0.63 Ma interval (Keep & Haig 2010, fig. 6); upper bathyal zone	Lari Guti Member of Viqueque Formation; Synorogenic Megasequence
143200	-8.70575	126.36175	8_11_08_17	a.p.	Packstone with abundant planktonic foraminifera, rare benthic foraminifera (mainly Rotaliida); 22.6 m above base of exposed measured section at base of coarser limestone unit	Planktonic foraminifera: *Globorotalia truncatulinoides* , *Globorotalia tosaensis* . Benthic foraminifera: *Schlumbergerella* , *Nummulites venosus*	Planktonic foraminiferal Zone N22r; mid Pleistocene within 2.02–0.63 Ma interval (Keep & Haig 2010, fig. 6); upper bathyal zone	Lari Guti Member of Viqueque Formation; Synorogenic Megasequence
143201	-8.70575	126.36175	8_11_08_18	a.p.	Packstone/calcirudite with coral debris, coralline algae, mollusc debris, common planktonic foraminifera, rare benthic foraminifera (mainly Rotaliida); 28 m above base of exposed measured section	Planktonic foraminifera: *Globorotalia truncatulinoides* , *Globorotalia tosaensis* . Benthic foraminifera: *Schlumbergerella* , *Nummulites venosus*	Planktonic foraminiferal Zone N22r; mid Pleistocene within 2.02–0.63 Ma interval (Keep & Haig 2010, fig. 6); upper bathyal zone	Lari Guti Member of Viqueque Formation; Synorogenic Megasequence

UWA No	Lat	Long	Field Number	Sample type	Rock Description	Age diagnostic fossils	Age and facies	Formation and tectonostratigraphic affinity
143210	-8.71942	126.36739	8_11_08_28	a.p.	Wackestone/packstone with abundant benthic foraminifera (mainly Rotaliida, including larger types), abundant planktonic foraminifera, coralline algae	Larger benthic foraminifera: *Eulepidina* , primitive *Lepidocyclina* (*Nephrolepidina*), *Spiroclypeus* . Planktonic foraminifera: *Globigerinoides primordius.*	Larger benthic foraminiferal Upper Te Letter Stage (Adams, 1970); planktonic zone N4 or N5 (Kennett & Srinivasan 1983); latest Oligocene or earliest Miocene	Booi beds; Banda Terrane
143214	-8.72342	126.36708	8_11_08_32	w.r.	Mudstone with abundant planktonic foraminiferaand rare benthic foraminifera (mainly Orders Buliminida, Lagenida)	Planktonic foraminifera: *Globorotalia kugleri* , *Globigerinoides primordius*	Planktonic Zone N4; Larger benthic foraminiferal Upper Te Letter Stage (Adams, 1970); latest Oligocene or earliest Miocene	Booi beds; Banda Terrane
143215	-8.72342	126.36708	8_11_08_33	a.p.	Packstone with abundant planktonic foraminifera; rare benthic foraminifera (mainly Rotaliida, including larger types), rare coralline algal debris	Planktonic foraminifera: *Globorotalia kugleri* , *Globoquadrina binaiensis* , *Globigerinoides primordius* . Benthic foraminifera: *Spiroclypeus*	Planktonic Zone N4; Larger benthic foraminiferal Upper Te Letter Stage (Adams, 1970); latest Oligocene or earliest Miocene	Booi beds; Banda Terrane
143216	-8.72342	126.36708	8_11_08_34	a.p.	Wackestone with scattered benthic foraminifera (mainly Order Rotaliida, including larger types) and planktonic foraminifera	Larger benthic foraminifera: *Eulepidina* , primitive *Lepidocyclina* (*Nephrolepidina*), *Spiroclypeus*	Larger benthic foraminiferal Upper Te Letter Stage (Adams, 1970); latest Oligocene - earliest Miocene	Booi beds; Banda Terrane
143226	-8.72419	126.36722	9_11_08_9	a.p.	Wackestone with scattered benthic foraminifera (mainly Order Rotaliida, including larger types); coralline algal debris	Larger benthic foraminifera: primitive *Lepidocyclina* (*Nephrolepidina*), *Spiroclypeus* . Planktonic foraminifera: *Globigerinoides primordius* , *Globoquadrina binaiensis*	Larger benthic foraminiferal Upper Te Letter Stage (Adams, 1970); planktonic zone N4 (Kennett & Srinivasan 1983) ; latest Oligocene or earliest Miocene	Booi beds; Banda Terrane

UWA No	Lat	Long	Field Number	Sample type	Rock Description	Age diagnostic fossils	Age and facies	Formation and tectonostratigraphic affinity
143227	-8.72442	126.36769	9_11_08_10	a.p.	Wackestone with common planktonic foraminifera, rare benthic foraminifera (mainly Order Rotaliida, including larger types)	Planktonic foraminifera: *Globorotalia kugleri* , *Globoquadrina binaiensis, Globigerinoides primordius* . Larger benthic foraminifera: *Spiroclypeus*	Planktonic foraminiferal zone N4 (Kennett & Srinivasan 1983; Larger benthic foraminiferal Upper Te Letter Stage (Adams, 1970); latest Oligocene or earliest Miocene	Booi beds; Banda Terrane
143229	-8.72442	126.36769	9_11_08_12	a.p.	Packstone with abundant planktonic foraminifera; fragmented larger benthic foraminifera	Planktonic foraminifera: *Globigerinoides primordius* or *Globigerina praebulloides* , *Dentoglobigerina altispira* , *Globoquadrina venezuelana* . Larger benthic foraminfiera: *Spiroclypeus*	Larger benthic foraminiferal Upper Te Letter Stage (Adams, 1970): latest Oligocene or earliest Miocene	Booi beds; Banda Terrane
143231	-8.73042	126.36839	9_11_08_14	a.p.	Wackestone with rare thaumatoporellacean algae and very rare carbonate-cemented agglutinated foraminifera	Thaumatoporellacean algae: *Thaumatoporella ?parvovesiculifera* (micritized). Foraminifera: ? *Siphovalvulina* sp.	Probably Early Jurassic	Perdido Group; Gondwana Megasequence
143232	-8.73042	126.36839	9_11_08_15	a.p.	Wackestone and peloidal grainstone with common carbonate-cemented agglutinated foraminifera and scattered thaumatoporellacean algae (including cryptoendoliths; see Schlangintweit and Velić 2011); dasycladale algae	Foraminifera: Siphovalvulina variabilis, "Planisepta" compressa. Thaumatoporellacean algae: Thaumatoporella ?parvovesiculifera (micritized).	Early Jurassic (Sinemurian-Pliensbachian)	Perdido Group; Gondwana Megasequence

UWA No	Lat	Long	Field Number	Sample type	Rock Description	Age diagnostic fossils	Age and facies	Formation and tectonostratigraphic affinity
143233	-8.73322	126.36867	9_11_08_16	a.p., t.s.	Wackestone with abundant benthic foraminifera (mainly Order Rotaliida, including larger types), scattered small planktonic foraminifera, abundant coralline algae, coral debris	Larger benthic foraminifera: primitive *Lepidocyclina* (*Nephrolepidina*), *Spiroclypeus* . Planktonic foraminifera: *Globigerinoides primordius* or *Globigerina praebulloides*	Larger benthic foraminiferal Upper Te Letter Stage (Adams, 1970); latest Oligocene - earliest Miocene	Booi beds; Banda Terrane
143234	-8.73322	126.36867	9_11_08_17	a.p.	Laminated fine calcarenite with very thin layers of coarse sand composed of fragmented larger benthic foraminifera (Order Rotaliida) and scattered small planktonic foraminifera	Larger benthic foraminifera: primitive *Lepidocyclina* (*Nephrolepidina*), *Spiroclypeus* .	Larger benthic foraminiferal Upper Te Letter Stage (Adams, 1970); latest Oligocene - earliest Miocene	Booi beds; Banda Terrane
143235	-8.73322	126.36867	9_11_08_18	a.p., t.s.	Packstone composed mainly of larger benthic foraminifera (Order Rotaliida)	Larger benthic foraminifera: *Eulepidina* , primitive *Lepidocyclina* (*Nephrolepidina*), *Spiroclypeus* .	Larger benthic foraminiferal Upper Te Letter Stage (Adams, 1970); latest Oligocene - earliest Miocene	Booi beds; Banda Terrane
143236	-8.73353	126.36922	9_11_08_19	a.p., t.s.	Limestone breccia; clasts of wackestone, peloidal grainstone; wackestone contains rare carbonate-cemented agglutinated foraminifera and thaumatoporellacean algae; peloidal grainstone contains common carbonate-cemented agglutinated foraminifera	Foraminifera: Siphovalvulina variabilis, "Planisepta" compressa, Meandrovoluta asiagoensis. Thaumatoporellacean algae: Thaumatoporella ?parvovesiculifera (micritized).	Early Jurassic (Sinemurian-Pliensbachian)	Perdido Group; Gondwana Megasequence

UWA No	Lat	Long	Field Number	Sample type	Rock Description	Age diagnostic fossils	Age and facies	Formation and tectonostratigraphic affinity
143237	-8.73428	126.36853	9_11_08_20	a.p.	Limestone breccia; clasts of wackestone, peloidal grainstone; wackestone contains rare carbonate-cemented agglutinated foraminifera, thaumatoporellacean (including cryptoendoliths; see Schlagintweit and Velić 2011) and dasycladale algae; peloidal grainstone contains common carbonate-cemented agglutinated foraminifera	Foraminifera: *Siphovalvulina variabilis* , *Meandrovoluta asiagoensis* . Thaumatoporellacean algae: *Thaumatoporella* ?parvovesiculifera (micritized). Dasycladale algae: *Palaeodasycladus mediterraneus* .	Early Jurassic (Sinemurian-Pliensbachian)	Perdido Group; Gondwana Megasequence
143238	-8.73994	126.36397	9_11_08_21	a.p.	Wackestone with rare thaumatoporellacean algae. Breccia with clasts of wackestone and peloidal grainstone with rare carbonate-cemented agglutinated foraminifera.	Foraminifera: *Siphovalvulina variabilis* . Thaumatoporellacean algae: *Thaumatoporella ?parvovesiculifera*	Early Jurassic	Perdido Group; Gondwana Megasequence
144708	-8.69940	126.33767	AB001	w.r.	Calcareous mudstone with common benthic foraminifera (*Elphidium, Lugdunum, Siphogenerina* dominate); common planktonic foraminifera (most <0.5 mm maximum dimension; *Globigerinoides, Globorotalia, Neogloboquadrina, Pulleniatina, Sphaeroidinella*).	Planktonic foraminifera: *Globorotalia truncatulinoides, Globorotalia tosaensis*	Zone N22r; mid Pleistocene within 2.02–0.63 Ma interval (Keep & Haig 2010, fig. 6); outer neritic zone	Lari Guti Member of Viqueque Formation; Synorogenic Megasequence

UWA No	Lat	Long	Field Number	Sample type	Rock Description	Age diagnostic fossils	Age and facies	Formation and tectonostratigraphic affinity
144709	-8.69940	126.33767	AB002	a.p.	Packstone with abundant rotaliid foraminifera (including *Amphistegina, Elphidium, Schlumbergerella, Homotrema, Cycloclypeus*); very rare planktonic foraminifera (*Globigerinoides*); echinoid spines, coralline algae,and coral debris	Larger benthic foraminifera: Schlumbergerella	Pleistocene (following range for *Schlumbergella*) given by Loeblich & Tappan, 1987)	Baucau Limestone; Synorogenic Megasequence
144710	-8.70620	126.34752	AB003	w.r.	Mudstone with abundant planktonic foraminifera (including *Globigerinoides, Globorotalia, Neogloboquadrina, Orbulina*), and abundant benthic foraminifera (with *Rotalinoides, Amphistegina, Elphidium, Heterolepa, Lugdunum, Lenticulina, Hoeglundina* most conspicuous). Evidence of some reworking from older Pliocene. Rare high-spired gastropods and delicate echinoid spines also present.	Planktonic foraminifera: *Globorotalia truncatulinoides, Globorotalia tosaensis*	Zone N22r; mid Pleistocene within 2.02–0.63 Ma interval (Keep & Haig 2010, fig. 6); outer neritic zone	Lari Guti Member of Viqueque Formation; Synorogenic Megasequence
144711	-8.70552	126.35192	AB004	w.r.	Coarse partly friable calcarenite with very rare benthic foraminifera	Foraminifera: *Elphidium crispum* , *Amphistegina* sp.	Pleistocene	Baucau Limestone; Synorogenic Megasequence
144712	-8.72988	126.36760	AB005	a.p.	Foraminiferal wackestone. Common benthic foraminifera including "larger" Rotaliida, coralline algae	Larger benthic foraminifera: primitive *Lepidocyclina* (*Nephrolepidina*); *Spiroclypeus*	Te Letter Stage; latest Oligocene or Earliest Miocene; inner neritic zone	Booi beds; Banda Terrane

UWA No	Lat	Long	Field Number	Sample type	Rock Description	Age diagnostic fossils	Age and facies	Formation and tectonostratigraphic affinity
144713	-8.72922	126.36710	AB006	a.p.	Limestone conglomerate; clasts with corals, coralline algae; common benthic foraminifera (mainly rotaliids and very rare miliolids), and mollusc fragments; matrix with similar foraminifera plus very rare planktonic foraminifera (indeterminant) and rare larger benthic rotaliids	Larger benthic foraminifera: primitive *Lepidocyclina* (*Nephrolepidina*)	Probably Te Letter Stage; probably latest Oligocene or earliest Miocene; inner neritic zone	Booi beds; Banda Terrane
144714	-8.72917	126.36702	AB007	a.p.	Packstone with abundant benthic foraminifera (mainly rotaliids including larger types), coral debris, coralline algae	Larger benthic foraminifera: primitive *Lepidocyclina* (*Nephrolepidina*); *Spiroclypeus*	Te Letter Stage; latest Oligocene or earliest Miocene interval; inner neritic zone	Booi beds; Banda Terrane
144715	-8.73407	126.36667	AB008	a.p.	Packstone with abundant benthic foraminifera (mainly larger rotaliids), coral debris, coralline algae.	Larger benthic foraminifera: *Spiroclypeus*	Te Letter Stage; latest Oligocene or earliest Miocene interval; inner neritic zone	Booi beds; Banda Terrane
144716	-8.72905	126.36575	AB009	a.p.	Wackestone with rare minute hyaline foraminifera (mainly planktonic types)	Poorly preserved globotruncaniids - including *Marginotruncana pseudolinneiana* or *Globotruncana linneiana; Heterohelix* sp., *Hedbergella* sp.	Late Cretaceous;middle bathyal to abyssal	Kolbano Beds; Australian Margin Megasequence

UWA No	Lat	Long	Field Number	Sample type	Rock Description	Age diagnostic fossils	Age and facies	Formation and tectonostratigraphic affinity
144717	-8.72908	126.36558	AB012	a.p.	Wackestone, highly fractured with calcite veins, with common thaumatoporellacean algae (including cryptoendoliths), rare prismatic shell fragments of bivalves, and very rare carbonate-cemented agglutinated foraminifera	Benthic foraminifera: *Siphovalvulina variabilis.* Thaumatoporellacean algae*: Thaumatoporella ?parvovesiculifera* (micritized)	Probably Early Jurassic; innermost neritic zone	Perdido Group; Gondwana Megasequence
144718	-8.72908	126.36558	AB013	a.p.	Wackestone with rare minute hyaline foraminifera (probably mainly planktonic types); extensively stylolitized	Planktonic foraminifera: ?*Hedbergella* sp., ?*Praeglobotruncana* sp., ?*Heterohel* ix sp.	Probably Late Cretaceous (Cenomanian or Turonian); middle bathyal to abyssal	Kolbano Beds; Australian Margin Megasequence
144719	-8.72955	126.36585	AB015	a.p.	Wackestone with intraclasts. Intraclasts include packstone containing benthic rotaliid foraminifera (including larger types), coral debris, and coralline alga. Matrix of minute rod-shaped particles	Larger benthic foraminifera in intraclasts: *Lepidocyclina (Nephrolepidina), Spiroclypeus*	Intraclasts belong to Te Letter Stage, latest Oligocene or earliest Miocene; inner neritic zone	Booi beds; Banda Terrane
144720	-8.72965	126.36592	AB016	a.p.	Ooid grainstone with rare carbonate-cemented agglutinated foraminifera	Foraminifera: *Siphovalvulina variabilis*	Probably Early Jurassic; innermost neritic zone	Perdido Group; Gondwana Megasequence
144722	-8.73068	126.36723	AB021	a.p.	Wackestone with common dasycladale algae with cryptoendolithic thaumatoporellacean algae; very rare carbonate-cemented agglutinated foraminifera	Foraminifera: *Siphovalvulina variabilis* . Dasycladale algae: *Palaeodasycladus mediterraneus* . Thaumatoporellacean algae: *Thaumatoporella ?parvovesiculifera* (micritized)	Early Jurassic; innermost neritic zone	Perdido Group; Gondwana Megasequence

UWA No	Lat	Long	Field Number	Sample type	Rock Description	Age diagnostic fossils	Age and facies	Formation and tectonostratigraphic affinity
144723	-8.73057	126.36700	AB022	w.r.	Mudstone with abundant planktonic foraminifera (Globigerina, Globorotalia, Globigerinoides, Globoquadrina, Catapsydrax) and rare benthic foraminifera (mainly Order Buliminida)	Planktonic foraminifera: *Globorotalia kugleri* , *Globoquadrina binaiensis* , *Globoquadrina dehiscens* (very rare), *Globigerinoides primordius*	Zone N4b (Kennett & Srinivasan 1983); earliest Miocene; upper bathyal	Booi beds; Banda Terrane
144724	-8.73057	126.36700	AB023	a.p.	Breccia with clasts including wackestone with corals, coralline algae and benthic rotaliid foraminifera (including larger types); and wackestone with abundant small planktonic foraminifera.	(1) Clasts with benthic rotaliid foraminifera: *Spiroclypeus* , primitive *Lepidocyclina (Nephrolepidina*).(2) Clasts with planktonic foraminifera: *Globigerinoides primordius, Globorotalia kugleri*	(1) Te Letter Stage; latest Oligocene or earliest Miocene; inner neritic zone. (2) Zone 4, latest Oligocene or earliest Miocene; outer neritic	Booi beds; Banda Terrane
144726	-8.75798	126.32160	AB027	a.p.	Wackestone with rare planktonic foraminifera (mainly minute low trochospiral forms with spherical chambers); very rare benthic foraminifera (?*Dorothia* and trochospiral Rotaliida)	Planktonic foraminifera: *Hedbergella/Blefuscuiana* spp.	Late Early Cretaceous (probably Aptian-Albian, based on absence of keeled planktonics); middle bathyal to abyssal	Kolbano Beds; Australian Margin Megasequence
144727	-8.75582	126.31635	AB028	a.p.	Oncoidal, cortoidal, gastrpodal grainstone with some cryptoendolithic thaumatoporellacean algae	Thaumatoporellacean algae	Probably Early Jurassic based on presence of these forms in "bahaman facies" elsewhere in Timor; innermost neritic zone	Perdido Group; Gondwana Megasequence

UWA No	Lat	Long	Field Number	Sample type	Rock Description	Age diagnostic fossils	Age and facies	Formation and tectonostratigraphic affinity
144728	-8.74305	126.29315	AB029	a.p.	Wackestone with common benthic foraminifera (including larger rotaliids), very rare small planktonics (*Globigerina* or *Globigerinoides*), coral debris, coralline algae	Larger benthic foraminifera: *Spiroclypeus* , primitive *Lepidocyclina* (*Nephrolepidina*)	Te Letter Stage; latest Oligocene to earliest Miocene; mid neritic	Booi beds; Banda Terrane
144729	-8.75665	126.32555	AB030	a.p.	Peloidal-ooid grainstone and wackestone with thaumatoporellacean algae, rare punctate brachiopod shell debris, very rare ostracods, very rare carbonate-cemented agglutinated foraminifera	Thaumatoporellacean algae: *Thaumatoporella ?parvovesiculifera* (micritized); foraminifera: ? *Siphovalvulina variabilis*	Early Jurassic; innermost neritic	Perdido Group; Gondwana Megasequence
144731	-8.72405	126.36732	AB032	a.p.	Packstone-wackestone with coral debris, benthic foraminifera (including larger rotaliids), rare small planktonic foraminifera, coralline algae	Larger benthic foraminifera: *Spiroclypeus* , primitive *Lepidocyclina* (*Nephrolepidina*)	Te Letter Stage; within the latest Oligocene to Earliest Miocene interval; mid neritic zone	Booi beds; Banda Terrane
144732	-8.72405	126.36732	AB033	a.p.	Conglomerate with clasts of foraminiferal coral packstone-wackestone in mud matrix; common benthic foraminifera (mainly Rotaliida including larger types), rare planktonic foraminfiera in clasts, abundant in mud matrix	Larger benthic foraminifera: primitive *Lepidocyclina* (*Nephrolepidina*), Eulep[idina, *Spiroclypeus* . Planktonic foraminifera: *Globigerinoides primordius* .	Te Letter Stage; Zone N4 or N5 (Kennett & Srinivasan 1983; latest Oligocene or earliest Miocene; mid neritic zone	Booi beds; Banda Terrane

UWA No	Lat	Long	Field Number	Sample type	Rock Description	Age diagnostic fossils	Age and facies	Formation and tectonostratigraphic affinity
144733	-8.72405	126.36732	AB034	a.p.	Foraminiferal packstone with abundant benthic foraminifera (mainly Rotaliida including larger types); patches of finer-grained packstone with darker matrix and common small planktonic foraminifera; coralline algae present	Larger benthic foraminifera: *Eulepidina* , primitive *Lepidocyclina* (*Nephrolepidina*), *Spiroclypeus* . Planktonic foraminifera: *Globigerinoides primordius* .	Te Letter Stage; within the latest Oligocene to Earliest Miocene interval; outer neritic	Booi beds; Banda Terrane
144734	-8.72405	126.36732	AB035	a.p.	Clast: packstone with very abundant planktonic foraminifera and fragmented rotaliid foraminifera	Planktonic foraminifera: *Globoquadrina binaiensis*	Within the interval of Zones P22 - N5 (Kennett & Srinivasan 1983); late Oligocene -earliest Miocene; outer neritic or upper bathyal	Booi beds; Banda Terrane
144735	-8.72405	126.36732	AB036	w.r.	Mudstone with abundant planktonic foraminfiera and rare benthic foraminfiera (mainly Order Buliminida)	Planktonic foraminifera: *Globorotalia kugleri* , *Globigerinoides primordius*	Zone N4 (Kennett & Srinivasan 1983); latest Oligocene or earliest Miocene; upper bathyal	Booi beds; Banda Terrane
144736	-8.72405	126.36732	AB037	a.p.	Packstone with abundant planktonic foraminifera and benthic foraminifera (mostly rotaliids including larger types and mostly fragmented)	Larger benthic foraminifera: primitive *Lepidocyclina (Nephrolepidina*). Planktonic foraminifera: *Globoquadrina binaiensis*	Within the interval of Zones P22 - N5 (Kennett & Srinivasan 1983); late Oligocene -earliest Miocene; outer neritic or upper bathyal	Booi beds; Banda Terrane
144737	-8.72405	126.36732	AB038	a.p.	Packstone with abundant planktonic foraminifera and benthic foraminifera (mostly rotaliids including larger types and mostly fragmented)	Planktonic foraminifera: *Globoquadrina binaiensis, Globorotalia kugleri, Globigerinoides primordius*	Zone N4 (Kennett & Srinivasan 1983); latest Oligocene or earliest Miocene; outer neritic or upper bathyal	Booi beds; Banda Terrane

UWA No	Lat	Long	Field Number	Sample type	Rock Description	Age diagnostic fossils	Age and facies	Formation and tectonostratigraphic affinity
144738	-8.72405	126.36732	AB039	a.p.	Packstone with abundant benthic foraminifera (mostly Rotaliida including larger types), abundant coral debris, coralline algae, echinoderm debris.	Larger benthic foraminifera: ?*Eulepidina* , primitive *Lepidocyclina* (*Nephrolepidina*), *Spiroclypeus, Miogypsinoides*	Te Letter Stage; latest Oligocene or earliest Miocene interval; inner neritic	Booi beds; Banda Terrane
144739	-8.72510	126.36570	AB041	a.p.	Stylobreccia with clasts ofof packstone containing coral debris, common benthic foraminifera (mostly rotaliids including larger types), common coralline algae, rare planktonic foraminifera	Larger benthic foraminifera: primitive *Lepidocyclina* (*Nephrolepidina*), *Spiroclypeus*	Larger benthic foraminiferal Upper Te Letter Stage (Adams, 1970); latest Oligocene or earliest Miocene interval; neritic	Synorogenic breccia: Clasts are of Booi beds); Banda Terrane
144740	-8.72582	126.36532	AB042	a.p.	Stylobreccia with clasts of wackestone and peloidal grainstone; rare thaumatoporellacean algae in wackestone	Thaumatoporellacean algae	Clasts are probably Early Jurassic; innermost neritic	Perdido Group; Gondwana Megasequence
144741	-8.72507	126.36538	AB043	a.p.	Stylobreccia with clasts of wackestone, grainstone including skeletal and ooid-peloidal grainstone. Wackestone contains scattered mollusc fragments and rare thaumatoporellacean algae. Grainstone contains rare carbonate-cemented agglutinated foraminifera.	Thaumatoporellacean algae: *Thaumatoporella* ?*parvovesiculifera* (micritized); foraminifera: ?*Siphovalvulina variabilis* , *Gaudryina* sp.	Clasts are probably Early Jurassic; innermost neritic	Perdido Group; Gondwana Megasequence

UWA No	Lat	Long	Field Number	Sample type	Rock Description	Age diagnostic fossils	Age and facies	Formation and tectonostratigraphic affinity
144742	-8.72455	126.36432	AB045	a.p.	Wackestone with patches of ooid grainstone (? burrow infills), with rare thaumatoporellacean algae, rare carbonate-cemented agglutinated foraminifera	Thaumatoporellacean algae: *Thaumatoporella* ?*parvovesiculifera* (micritized); foraminifera: *Siphovalvulina variabilis*	Early Jurassic; innermost neritic	Perdido Group; Gondwana Megasequence
144743	-8.72433	126.36338	AB047	a.p.	Wackestone with common mollusc fragments, rare ostracods (with valves intact), rare echinoid spines; very rare carbonate-cemented agglutinated foraminifera	Foraminifera: ? *Siphovalvulina* sp.	Probably Early Jurassic; innermost neritic	Perdido Group; Gondwana Megasequence
144748	-8.71387	126.36173	AB053	a.p.	Red wackestone with scattered rare deformed planktonic foraminifera. Clast in conglomerate.	Deformed foraminifera appear to be large *Globigerina* spp. of *Globigerina yeguaensis-Globigerina pseudovenezuelana-Globigerina venezuelana* type	Probably Late Eocene or Oligocene; middle bathyal to abyssal	Kolbano Beds; Australian Margin Megasequence
144749	-8.71455	126.35953	AB054	a.p.	Ooid grainstone with rare carbonate-cemented agglutinated foraminifera, very rare nodosariid foraminifera , very rare thaumatoporellacean algae	Foraminifera: *Duotaxis* sp., ? *Siphovalvulina* sp.	Late Triassic or Early Jurassic; innermost neritic	Perdido Group; Gondwana Megasequence

UWA No	Lat	Long	Field Number	Sample type	Rock Description	Age diagnostic fossils	Age and facies	Formation and tectonostratigraphic affinity
144751	-8.71455	126.35953	AB056	a.p.	Pale grey wackestone with very rare nodosariid foraminifera (incuding *Dentalina* sp, *Lenticulina* sp..) and in some layers common mollusc-shell "filaments"	"Molluscan "filaments" probably derived from the very small pelagic stages of bivalves (see Flugel 2004, p. 524-528) associated with nodosariid foraminifera	Probably Late Triassic (based on similar fossil association in conodont-dated wackestones elsewhere in Timor); probably outer neritic or upper bathyal	Probably Aitutu Formation; Gondwana Megasequence
144754	-8.71403	126.35887	AB059	a.p.	Wackestone with rare planktonic foraminifera	Planktonic foraminifera: *Globigerina yeguaensis-Globigerina pseudovenezuelana-Globigerina venezuelana* lineage dominant	Probably Early to Middle Oligocene (see Bolli and Saunders 1985); middle bathyal to abyssal	Kolbano Beds; Australian Margin Megasequence
144756	-8.70895	126.36067	AB061	a.p.	Planktonic foraminiferal packstone with very rare smaller benthic foraminifera (Rotaliida)	Planktonic foraminifera: *Hantkenina* sp., *Globigerinatheka* sp., *Morozovelloides* sp. *Acarinina* spp.	Middle Eocene; bathyal	Barique Formation ?; Banda Terrane; block in melange zone
144757	-8.71132	126.35397	AB062	a.p.	Wackestone with scattered planktonic foraminifera	Planktonic foraminifera: *Dicarinella* spp. (including morphotypes with convex spiral sides similar to *D. imbricata*)	Late Cretaceous (Turonian); middle bathyal to abyssal	Kolbano Beds; Australian Margin Megasequence
144759	-8.71302	126.35377	AB064	a.p.	Wackestone with scattered mollusc (bivalve) fragments, rare thaumatoporellacean algae, rare echinoiderm plate debris	Thaumatoporellacean algae: *Thaumatoporella* ?*parvovesiculifera* (micritized)	Probably Early Jurassic; innermost neritic	Perdido Group; Gondwana Megasequence

UWA No	Lat	Long	Field Number	Sample type	Rock Description	Age diagnostic fossils	Age and facies	Formation and tectonostratigraphic affinity
144761	-8.71552	126.35255	AB066	a.p.	Wackestone with scattered planktonic forams (mostly fragments	Planktonic foraminifera: *Globigerina yeguaensis-Globigerina pseudovenezuelana-Globigerina venezuelana* lineage dominant	Oligocene;middle bathyal to abyssal	Kolbano Beds; Australian Margin Megasequence
144762	-8.73183	126.36762	AB068	a.p.	Packstone/wackestone with abundant benthic foraminifera (mainly Rotallida including larger types); abundant coralline algae; rock is highly fractured	Larger benthic foraminifera: primitive *Lepidocyclina* (*Nephrolepidina*); *Spiroclypeus*	Larger benthic foraminiferal Upper Te Letter Stage (Adams, 1970); latest Oligocene or earliest Miocene; inner neritic	Booi beds; Banda Terrane
144763	-8.73190	126.36750	AB069	a.p.	Packstone/wackestone with rare benthic foraminifera (mainly Rotaliida including larger types); common coralline algae; coral; mollusc fragments; rock is highly fractured	Larger benthic foraminifera: primitive *Lepidocyclina* (*Nephrolepidina*); Spiroclypeus	Larger benthic foraminiferal Upper Te Letter Stage (Adams, 1970); latest Oligocene - earliest Miocene; inner neritic	Booi beds; Banda Terrane
144764	-8.73233	126.36743	AB070	a.p.	Poorly sorted conglomerate, clasts are packstone or wackestone with scattered benthic foraminifera (mainly Rotaliida including larger types), coral debris, coralline algae, mollusc fragments	Larger benthic foraminifera: primitive *Lepidocyclina* (*Nephrolepidina*), *Spiroclypeus* .	Larger benthic foraminiferal Upper Te Letter Stage (Adams, 1970); latest Oligocene - earliest Miocene; all clasts appear coeval; inner neritic	Booi beds; Banda Terrane
144767	-8.73027	126.36768	AB075	w.r.	Red mudstone with poorly preserved deformed planktonic foraminifera *(Globigerina , Globoquadrina*)	Planktonic foraminifera: *Globigerina ciperoensis; Globoquadrina* sp. (?ancestral to *G. dehiscens*)	Latest Oligocene or earliest Miocene; bathyal	Booi beds; Banda Terrane

UWA No	Lat	Long	Field Number	Sample type	Rock Description	Age diagnostic fossils	Age and facies	Formation and tectonostratigraphic affinity
144769	-8.73057	126.36700	AB077	w.r.	Mudstone with abundant planktonic foraminifera (*Globigerina, Globorotalia*); rare bethonic smaller foraminifera (mostly Buliminida)	Planktonic foraminifera: *Globorotalia kugleri* , *Globigerinoides primordius*	N4 planktonic foraminifera zone (Kennett & Srinivasan, 1983); earliest Miocene; upper bathyal	Booi beds; Banda Terrane
144771	-8.73057	126.36700	AB079A	a.p.	Breccia (clast-supported) composed of limestone clasts with a mud matrix. Clasts are packstone/wackestone with benthic foraminifera (mainly Rotaliida including larger types), coral debirs, coralline algae, and very rare minute planktonic foraminifera. Mud matrix has scattered minute planktonic foraminifera	Larger benthic foraminifera (in limestone clasts): *Eulepidina* , primitive *Lepidocyclina* (*Nephrolepidina*), *Spiroclypeus* . Planktonic foraminifera (in matrix): ?*Globigerinoides primordius*	Larger benthic foraminiferal Upper Te Letter Stage (Adams, 1970); latest Oligocene - earliest Miocene; all clasts appear coeval. Matrix is similar age; mid neritic	Booi beds; Banda Terrane
144772	-8.73057	126.36700	AB079B	a.p.	Coral/coralline algal limestone (?framestone) with packstone/wackestone matrix containing scattered benthic foraminifera (mainly Rotaliida including larger types) and fragmented coralline algae	Larger benthic foraminifera: primitive *Lepidocyclina* (*Nephrolepidina*), *Spiroclypeus*	Larger benthic foraminiferal Upper Te Letter Stage (Adams, 1970); latest Oligocene - earliest Miocene; inner neritic zone	Booi beds; Banda Terrane

UWA No	Lat	Long	Field Number	Sample type	Rock Description	Age diagnostic fossils	Age and facies	Formation and tectonostratigraphic affinity
144773	-8.73057	126.36700	AB080	conglomerate	Clast-supported conglomerate containing clasts of packstone containing benthic foraminifera (mainly Rotaliida including larger types), common fragmented coralline algae; very rare minute planktonic foraminifer. Matrix of mudstone with rare minute planktonic foraminifera	Larger benthic foraminifera: *Eulepidina* , primitive *Lepidocyclina (Nephrolepidina*), *Spiroclypeus* . Planktonic foraminifera: *Globigerinoides primordius* .	Larger benthic foraminiferal Upper Te Letter Stage (Adams, 1970); latest Oligocene - earliest Miocene; all clasts appear coeval. Matrix is of similar age; mid neritic zone	Booi beds; Banda Terrane
144774			AB081	w.r.	Mudstone with abundant planktonic foraminifera (*Globorotalia* , *Globigerinoides* , *Pulleniatina* , *Neogloboquadrina* , *Globigerinella* , *Globigerina*) and benthic smaller foraminifera (with *Lugdunum* , *Siphogenerina* , *Lenticulina* , *Heterolepa* , *Rotalinoides* , *Elphidium* , *Amphistegina* conspicuous); planktonic:benthic = 50%	Planktonic foraminifera: *Globorotalia truncatulinoides* , *Globorotalia tosaensis*	Planktonic foraminiferal Zone N22r; mid Pleistocene within 2.02–0.63 Ma interval (Keep & Haig 2010, fig. 6); outer neritic zone	Baucau Limestone; Synorogenic Megasequence
144775	-8.70895	126.36067	AB082	w.r.	Red mudstone with abundant planktonic foraminifera (including *Hantkenina* , Globigerinidae, *Morozovelloides* , *Turborotalia* , *Globigerinatheka*); very rare benthic foraminifera (mainly smaller Rotaliida)	Planktonic foraminifera: *Hantkenina compressa* , *Morozovelloides crassatus, Turborotalia cerroazulensis*	Within interval E11 to E13; late Middle Eocene (Berggren & Pearson et al., 2006); bathyal zone	Barique Formation ?; Banda Terrane; block in melange zone

UWA No	Lat	Long	Field Number	Sample type	Rock Description	Age diagnostic fossils	Age and facies	Formation and tectonostratigraphic affinity
144776	-8.70895	126.36067	AB083	a.p.	Planktonic foraminiferal packstone with very rare smaller benthic foraminifera (Rotaliida)	Planktonic foraminifera: *Morozovella* spp. or *Morozovelloides* spp., *Acarinina* spp.	Early or Middle Eocene; bathyal	Barique Formation ?; Banda Terrane; block in melange zone
144777	-8.70888	126.36030	AB084	w.r.	Mudstone with abundant planktonic foraminifera and rare benthic foraminfiera (including *Oridorsalis* , *Bolivinita*)	Planktonic foraminifera: *Globorotalia tosaensis*	Planktonic foraminiferal Zone N21, 3.10-2.02 Ma (Keep & Haig 2010); bathyal zone	Viqueque Formation; Synorogenic Megasequence
144778	-8.70888	126.36030	AB085	w.r.	Mudstone with abundant planktonic foraminifera (*Globigerinoides* , *Globorotalia* , *Pulleniatina* , *Orbulina* , *Neogloboquadrina*) and rare benthic foraminifera (including *Oridorsalis*),	Planktonic foraminifera: *Globorotalia tosaensis*	Planktonic foraminiferal Zone N21, 3.10-2.02 Ma (Keep & Haig 2010); bathyal zone	Viqueque Formation; Synorogenic Megasequence
144780	-8.73437	126.36850	AB087	a.p.	Stylobreccia with clasts of wackestone and rare ooid grainstone; wackestone with scattered thaumatoporellacean algae and very rare carbonare-cemented agglutinated foraminifera; grainstone with rare carbonate-cemented agglutinated foraminifera	Wackstone: *Thaumatoporella* ?*parvovesiculifera* (micritized), *Siphovalvulina variabilis* . Grainstone: *Siphovalvulina* sp.	Early Jurassic; innermost neritic	Perdido Group; Gondwana Megasequence

UWA No	Lat	Long	Field Number	Sample type	Rock Description	Age diagnostic fossils	Age and facies	Formation and tectonostratigraphic affinity
144781	-8.73515	126.37217	AB088	pal	Mudstone with well preserved palynomorphs (pollen, spores, dinocysts, acritarchs, prasinophyte algae)	Pollen: *Minutosaccus crenulatus* , *Corollina meyeriana* , *Enzonalaporites vigens* , *Samaropollenites speciosus* , *Rimaesporites aquilonalis* . Spores: *Cycadopites stone* i, *Leptolepidites argentaeaformis* . Dinocysts: *Wanneria listeri* , *Suessia swabiana* , *Rhaetogonyaulax wigginsii*	Probably lowest *Minutosaccus crenulatus* Zone; Late Triassic (probably Norian); shallow-marine (Palynomorph determinations and zonation by Matthew Dixon, pers. com. October 2009)	Babulu Formation (mud-dominated member showing broken-formation deformation); Gondwana Megasequence
144783	-8.73470	126.37368	AB090	a.p.	Packstone consisting of densely packed highly fragmented skeletal debris and scattered planktonic foraminifera (including *Globigerinoides*) and benthic foraminifera (mainly Rotaliida including larger types) with mud matrix	Planktonic foraminifera: *Globigerinoides primordius* . Larger benthic foraminifera: primitive *Lepidocyclina* (*Nephrolepidina*), *Spiroclypeus*	Larger benthic foraminiferal Upper Te Letter Stage (Adams, 1970); latest Oligocene - earliest Miocene	Booi beds; Banda Terrane
144785	-8.73407	126.37292	AB095	a.p.	Wackestone with common coral and encrusting coralline algal debris and benthic foraminifera (mainly Rotaliida including larger types)	Larger benthic foraminifera: primitive *Lepidocyclina* (*Nephrolepidina*), *Spiroclypeus*	Larger benthic foraminiferal Larger benthic foraminiferal Upper Te Letter Stage (Adams, 1970); latest Oligocene - earliest Miocene	Booi beds; Banda Terrane

UWA No	Lat	Long	Field Number	Sample type	Rock Description	Age diagnostic fossils	Age and facies	Formation and tectonostratigraphic affinity
144787	-8.72967	126.38015	AB101	w.r.	Mudstone with common planktonic foraminifera (*Dentoglobigerina* , *Globigerinoides* , *Globigerina*), and very poorly preserved (recrystallized) benthic foraminifera (Rotaliida and Buliminida)	Planktonic foraminifera: *Globigerinoides triloba* , *Globigerinoides subquadratus* , *Globigerinoides altiaperatura*	Planktonic foraminifera zone N5 or N6 (Kennett & Srinivasan, 1983); Early Miocene; outer neritic or upper bathyal	Booi beds; Banda Terrane
144789	-8.72940	126.38247	AB105	a.p.	Breccia with clasts including: (A) Breccia containing wackestone, packstone and grainstone with benthic foraminifera (carbonate-cemented agglutinated types), common thaumatoporellacean algae, rare dasycladale algae; and (B) Packstone with abundant benthonic foraminifera (mostly Rotaliida including larger types)	(A) Foraminifera: *Siphovalvulina variabilis* , *Meandrovoluta asiagoensis* . Thaumatoporellacean algae: *Thaumatoporella ?parvovesiculifera*. (B) Foraminifera: primitive *Lepidocyclina* (*Nephrolepidina*), *Spiroclypeus*	Clast ages: (A) Early Jurassic, Sinemurian-Pliensbachian (Haig et al., 2007); innermost neritic. (B) Larger benthic foraminiferal Upper Te Letter Stage (Adams, 1970); latest Oligocene - earliest Miocene; inner neritic	Synorogenic breccia with clasts of Perdido Group and Booi beds; Synorogenic Megasequence
144795	-8.73472	126.37782	AB111	a.p.	Wackestone with framented bioclasts including coralline algae, benthic foraminfiera (mainly Rotaliida including larger types), echinoderm plates	Foraminifera: primitive *Lepidocyclina* (*Nephrolepidina*)	Larger benthic foraminiferal Upper Te Letter Stage (Adams, 1970); latest Oligocene - earliest Miocene; inner neritic	Booi beds; Banda Terrane
144796	-8.73233	126.37917	AB113	a.p.	Wackestone with foraminifera (mainly Rotaliida including common larger types), coralline algae and coral debris	Foraminifera: *Spiroclypeus* , primitive *Lepidocyclina* (*Nephrolepidina*)	Larger benthic foraminiferal Upper Te Letter Stage (Adams, 1970); latest Oligocene - earliest Miocene; inner neritic	Booi beds; Banda Terrane

UWA No	Lat	Long	Field Number	Sample type	Rock Description	Age diagnostic fossils	Age and facies	Formation and tectonostratigraphic affinity
144797	-8.70182	126.32353	AB119	a.p.	Porous limestone with common benthic foraminifera (mainly Rotaliida including larger types) and coralline algae	Larger benthic foraminifera: *Schlumbergerella*	Pleistocene (following range for *Schlumbergella* given by Loeblich & Tappan, 1987); inner neritic	Baucau Limestone; Synorogenic Megasequence
144798	-8.70477	126.32148	AB120	a.p.	Wackestone with scattered mollusc (bivalve) fragments, rare thaumatoporellacean algae, rare echinoiderm plate debris, rare carbonate-cemented agglutinated foraminifera	Foraminifera: *Siphovalvulina* sp.., *Everticyclammina* sp. Thaumatoporellacean algae: *Thaumatoporella* ? *parvovesiculifera*	Early Jurassic, innermost neritic	Perdido Group; Gondwana Megasequence
144799	-8.70505	126.32067	AB122	a.p.	Scree: wackestone with very rare planktonic foraminifera (deformed, fragmented) and very rare small benthic foraminifera (Order Rotaliida)	Foraminifera: large ?*Globigerina* sp.	Cenozoic, probaby Late Eocene or Oligocene; middle bathyal to abyssal	Kolbano Beds; Australian Margin Megasequence (scree)
144803	-8.70678	126.32443	AB128	a.p.	Peloid grainstone with rare benthic foraminifera (mainly nodosariids including uniserial types and *Lenticulina* , and very rare glomospiral miliolids and carbonate-cemented agglutinated types)	Carbonate-cemented agglutinated foraminifera: ? *Siphovalvulina* /*Duotaxis* .	Probably Easrly Jurassic or Late Triassic. Benthic foraminiferal assemblage is consistent with a Late Triassic or Early Jurassic age. Innermost neritic	Perdido Group; Gondwana Megasequence
144807	-8.70755	126.32347	AB132	a.p.	Wackestone, fractured and stylotised, with scattered thaumatoporellacean algae and rare carbonate-cemented agglutinated foraminifera	Thaumatoporellacean algae: *Thaumatoporella* ?*parvovesiculifera* (micritized). Foraminifera: ? *Siphovalvulina* .	Early Jurassic; innermost neritic	Perdido Group; Gondwana Megasequence

UWA No	Lat	Long	Field Number	Sample type	Rock Description	Age diagnostic fossils	Age and facies	Formation and tectonostratigraphic affinity
144809	-8.70550	126.32648	AB135	w.r.	Friable calcarenite with common benthic foraminifera (Rotaliida and Textulariida)	Benthic foraminifera: *Calcarina spengleri* , *Clavulina pacifica*	Pleistocene; innermost neritic	Baucau Limestone; Synorogenic Megasequence
144810	-8.70510	126.32660	AB136	a.p.	Very porous, fossiliferous limestone with coral fragments, benthic foraminifera (Rotaliida), mollusc fragments, echinoid spines	Benthic foraminifera: *Neorotalia* , *Elphidium*	Pleistocene	Baucau Limestone; Synorogenic Megasequence
144811	-8.70450	126.32688	AB138	a.p.	Very porous, fossiliferous limestone with coralline algae and benthic foraminifera (mainly Rotaliida, including larger types)	Benthic foraminifera: *Schlumbergerella*	Pleistocene (following range for *Schlumbergella* given by Loeblich & Tappan, 1987)	Baucau Limestone; Synorogenic Megasequence
144813	-8.71200	126.31988	AB142	a.p.	Ooid grainstone with very rare carbonate-cemented agglutinated foraminifera, very rare dasycladale algae	Carbonate-cemented agglutinated foraminifera: *Siphovalvulina variabilis* . Dasycladale algae: *Palaeodasycladus mediterraneus* .	Early Jurassic, innermost neritic	Perdido Group; Gondwana Megasequence
144815	-8.71753	126.31942	AB150	a.p.	Limestone breccia/conglomerate with clasts of wackestone containing scattered thaumatopellacean algae, and peloidal grainstone with rare carbonate-cemented agglutinated foraminifera	Thaumatoporellacean algae: *Thaumatoporella* ?*parvovesiculifera* (micritized). Foraminifera: ? *Siphovalvulina* .	Early Jurassic; innermost neritic	Perdido Group; Gondwana Megasequence

UWA No	Lat	Long	Field Number	Sample type	Rock Description	Age diagnostic fossils	Age and facies	Formation and tectonostratigraphic affinity
144817	-8.72055	126.31833	AB154	a.p.	Bioturbated wackestone with abundant recrystallized radiolarian, common sponge spicules, rare ostracod valves, and very rare carbonate-cemented agglutinated foraminifera. "Patches" of peloidal grainstone lacking radiolaria	Foraminifera: *Siphovalvulina variabilis*	Late Triassic or Early Jurassic; basinal facies, either outer neritic or upper bathyal; evidence of downslope transport from inner neritic platform facies (e.g. peloids, *Siphovalvulina*).	Aitutu Formation; Gondwana Megasequence
144822	-8.72408	126.31908	AB159	a.p.	Ooid grainstone with rare carbonate-cemented agglutnated foraminifera, very rare *Lenticulina* , very rare thaumatoporellacean algae	Foraminifera: *Siphovalvulina variabilis* . Thaumatoporellacean algae: *Thaumatoporella ?parvovesiculifera* (micritized). Foraminifera: ? *Siphovalvulina* .	Early Jurassic; innermost neritic	Perdido Group; Gondwana Megasequence
144823	-8.72411	126.31908	AB160	a.p.	Ooid grainstone with rare carbonate-cemented agglutinated foraminifera; scattered mollusc (bivalve) fragments and echinoid plates	Foraminifera: *Siphovalvulina variabilis*	Early Jurassic; innermost neritic	Perdido Group; Gondwana Megasequence
144824	-8.71620	126.32303	AB161	a.p.	Planktonic foraminiferal packstone	Planktonic foraminifera: *Globigerina yeguaensis-Globigerina pseudovenezuelana-Globigerina venezuelana* lineage dominant	Oligocene; middle bathyal to abyssal	Kolbano Beds; Australian Margin Megasequence

UWA No	Lat	Long	Field Number	Sample type	Rock Description	Age diagnostic fossils	Age and facies	Formation and tectonostratigraphic affinity
144825	-8.71182	126.32352	AB165	a.p.	Wackestone with scattered rare planktonic foraminifera (some deformed and fragmented)	Planktonic foraminifera: *Globigerina yeguaensis-Globigerina pseudovenezuelana-Globigerina venezuelana* lineage; ? *Globigerina selli*	Oligocene; middle bathyal to abyssal	Kolbano Beds; Australian Margin Megasequence
144826	-8.73638	126.35835	AB170	a,p,	Oncoidal grainstone; very rare thaumatoporellacean algae	Thaumatoporellacean algae: *Thaumatoporella* ?*parvovesiculifera* (micritized)	Probably Early Jurassic; innermost neritic	Perdido Group; Gondwana Megasequence
144828	-8.73567	126.36047	AB173	a.p.	Wackestone with common benthic foraminifera (including larger rotaliids), very rare small planktonics (Globigerina or Globigerinoides), coral debris, coralline algae	Larger benthic foraminifera: ?*Eulepidina* , primitive *Lepidocyclina* (*Nephrolepidina*), *Spiroclypeus*	Larger benthic foraminiferal Upper Te Letter Stage (Adams, 1970); latest Oligocene - earliest Miocene; mid neritic	Booi beds; Banda Terrane
144829	-8.73572	126.35997	AB174	a.p.	Packstone with abundant sponge spicules and benthic foraminifera (mainly Rotaliida, including fragmented larger types, and Miliolida)	Larger benthic foraminifera in intraclasts: *Lepidocyclina* (*Nephrolepidina*); *Spiroclypeus* or *Cycloclypeus* (fragment only)	Larger benthic foraminiferal Upper Te Letter Stage (Adams, 1970); latest Oligocene - earliest Miocene; neritic	Booi beds; Banda Terrane
144831	-8.73968	126.36345	AB177	a.p.	Wackestone with common thaumatoporellacean algae, very rare carbonate-cemented agglutinated foraminifera	Foraminifera: *Siphovalvulina variabilis* . Thaumatoporellacean algae: *Thaumatoporella* ?*parvovesiculifera* (micritized).	Early Jurassic, innermost neritic	Perdido Group; Gondwana Megasequence

UWA No	Lat	Long	Field Number	Sample type	Rock Description	Age diagnostic fossils	Age and facies	Formation and tectonostratigraphic affinity
144832	-8.74200	126.29415	AB179	a.p.	Wackestone with rare deformed benthic foraminifera (including larger rotaliids), coralline algae; foraminifera	Foraminifera: *Spiroclypeus*	Larger benthic foraminiferal Upper Te Letter Stage (Adams, 1970); latest Oligocene - earliest Miocene; inner neritic	Booi beds; Banda Terrane
144837	-8.72317	126.30622	AB206_a	a.p., a.d.r.	Wackestone with rare planktonic foraminifera, some silicified; rare radiolaria	Planktonic foraminifera: *Catapsydrax dissimilis* , *Globigerina pseudovenezuelana* , *Globorotalia opima nana*	Probably early or middle Oligocene; middle bathyal to abyssal	Kolbano Beds; Australian Margin Megasequence
144838	-8.72317	126.30622	AB207	a.p.	Ooid grainstone with very rare carbonate-cemented agglutinated foraminifera	Foraminifera: *Siphovalvulina variabilis*	Probably Early Jurassic; innermost neritic	Perdido Group; Gondwana Megasequence
144839	-8.72317	126.30622	AB208	a.p., t.s.	Wackestone , highly fractured and veined, with common *Inoceramus* prisms, very rare benthic foraminifera (Order Lagenida including *Lenticulina*), and rare calpionellids(?), very rare radiolaria	?Calpionellids (? *Calpionella alpina*)	Possibly latest Jurassic or earliest Cretaceous; middle bathyal to abyssal	Kolbano Beds; Australian Margin Megasequence
144840	-8.72317	126.30622	AB209	a.p.	Wackestone with scattered *Inoceramus* prisms, very rare benthic foraminifera (Order Lagenida including *Lenticulina*), and rare calpionellids(?)	?Calpionellids (? *Calpionella alpina*)	Possibly latest Jurassic or earliest Cretaceous; middle bathyal to abyssal	Kolbano Beds; Australian Margin Megasequence
144841	-8.72317	126.30622	AB210	a.p.	Scree: Wackestone with rare planktonic foraminifera (including keeled forms)	Planktonicforaminifera: *Globotruncana linneiana* , *Globotruncanita stuarti*	Late Creatceous (Campanian or early Maastrichtian); middle bathyal to abyssal	Kolbano Beds; Australian Margin Megasequence

UWA No	Lat	Long	Field Number	Sample type	Rock Description	Age diagnostic fossils	Age and facies	Formation and tectonostratigraphic affinity
144847	-8.70052	126.33698	AB219	a.p.	Packstone with benthic foraminifera (mainly Rotaliida including larger types) and rare planktonic foraminifera; coralline algae, mollusc fragments	Benthic foraminifera: *Schlumbergerella*	Pleistocene (following range for *Schlumbergella* given by Loeblich & Tappan, 1987); inner neritic	Baucau Limestone; Synorogenic Megasequence
144854	-8.71058	126.34053	AB234	w.r.	Red mudstone with very rare planktonic foraminifera	Planktonic foraminifera: *Globigerinatheka index*	Middle or Late Eocene; bathyal	Barique Formation ?; Banda Terrane
144856	-8.71073	126.34083	AB236	w.r.	Red wackestone with abundant planktonic foraminifera	Planktonic foraminifera: *Morozovella velascoensis*	Late Paleocene or earliest Eocene (within range of Zones P3b-E2; Berggren & Pearson et al., 2006); middle bathyal to abyssall	Kolbano Beds; Australian Margin Megasequence
144858	-8.71157	126.33998	AB238	a.p.	Peloidal-ooid grainstone and wackestone with rare thaumatoporellacean algae, rare carbonate-cemented agglutinated foraminifera	Thaumatoporellacean algae: *Thaumatoporella ?parvovesiculifera* (micritized). Foraminifera: ? *Siphovalvulina* sp.	Early Jurassic; innermost neritic	Perdido Group; Gondwana Megasequence
144859	-8.71233	126.34010	AB240	a.p.	Deformed and partially recrystallised wackestone with common planktonic foraminifera	Planktonic foraminifera: *Globigerina yeguaensis - Globigerina pseudovenezuelana - Globigerina venezuelana* lineage	Probably Oligocene; middle bathyal to abyssal	Kolbano Beds; Australian Margin Megasequence
144860	-8.70307	126.31533	AB245	a.p., t.s.	Packstone with common benthic foraminifera (mainly Rotaliida including larger types), very rare planktonic foraminifera, coralline algae, coral debris, lithic fragments	Benthic foraminifera: *Nummulites venosus* , *Cycloclypeus* . Planktonic foraminifera: *Globorotalia tumida* , *Pulleniatina* sp.	Pleistocene; mid neritic	Baucau Limestone; Synorogenic Megasequence

UWA No	Lat	Long	Field Number	Sample type	Rock Description	Age diagnostic fossils	Age and facies	Formation and tectonostratigraphic affinity
144862	-8.70228	126.31555	AB248	a.p., t.s.	Packstone with benthic foraminifera (mainly Rotaliida including larger types), mollusc fragments, coralline algae, coral debris, bryozoan fragments	Benthic foraminifera: *Nummulites venosus*	Pleistocene; neritic	Baucau Limestone; Synorogenic Megasequence
144865	-8.70727	126.30877	AB259	a.p.	Wackestone with common benthic foraminifera (including larger rotaliids), very rare small planktonics (*Globigerina* or *Globigerinoides*), coral debris, coralline algae	Larger benthic foraminifera in intraclasts: primitive *Lepidocyclina* (*Nephrolepidina*); *Spiroclypeus*	Larger benthic foraminiferal Upper Te Letter Stage (Adams, 1970); latest Oligocene - earliest Miocene; inner neritic	Booi beds; Banda Terrane
144866	-8.70615	126.30867	AB260	a.p.	Matrix: Wackestone with scattered coralline algae, mollusc fragments, benthic foraminifera (mainly Rotaliida). Clast: Oncoid-peloid grainstone	Benthic foraminifera in matrix: *Nummulites venosus*	Pleistocene; inner neritic	Baucau Limestone; Synorogenic Megasequence
144867	-8.70292	126.31788	AB263	a.p., t.s.	Porous white limestone containing shell fragments, benthic foraminifera (mainly Rotaliida including larger types), coralline algae, and clasts of mafic igneous rock.	Benthic foraminifera: *Nummulites venosus* , *Schlumbergerella* , *Cycloclypeus* . Planktonic foraminifera: *Globorotalia tumida* , *Pulleniatina* sp.	Pleistocene; mid neritic	Baucau Limestone; Synorogenic Megasequence
144868	-8.70570	126.31017	AB264	a.p., t.s.	Very porous yellow limestone with benthic foraminifera (mainly Rotaliida) and some planktonic foraminifera, lithic fragments	Benthic foraminifera: *Nummulites venosus.* Planktonic foraminifera: *Globorotalia tumida* ,	Pleistocene; mid neritic	Baucau Limestone; Synorogenic Megasequence

UWA No	Lat	Long	Field Number	Sample type	Rock Description	Age diagnostic fossils	Age and facies	Formation and tectonostratigraphic affinity
144869	-8.71232	126.31107	AB270	a.p.	Packstone with abundant fragmented ? *Inoceramus* prisms, and minute calpionellids(?)	?Calpionellids (? *Calpionella alpina*)	Possibly latest Jurassic or earliest Cretaceous; middle bathyal to abyssal	Kolbano Beds; Australian Margin Megasequence
144871	-8.71642	126.32532	AB274	a.p.	Wackestone with scattered *Inoceramus* prisms, very rare benthic foraminifera (Order Lagenida including *Lenticulina*), and rare calpionellids(?)	?Calpionellids (? *Calpionella alpina*)	Possibly latest Jurassic or earliest Cretaceous; middle bathyal to abyssal	Kolbano Beds; Australian Margin Megasequence
144872	-8.72323	126.32295	AB276	a.p.	Ooid grainstone with rare carbonate-cemented agglutinated foraminifera and rare hyaline foraminifera (Order Lagenidae including *Lenticulina*)	Foraminifera: *Siphovalvulina* sp.	Probably Early Jurassic; innermost neritic	Perdido Group; Gondwana Megasequence
144873	-8.71542	126.32598	AB278	a.p.	Wackestone with rare planktonic foraminifera (large *Globigerina* spp.)	Planktonic foraminifera: *Globigerina yeguaensis* - *Globigerina pseudovenezuelana* - *Globigerina venezuelana* lineage; ? *Globigerina selli*	Probably Oligocene; middle bathyal to abyssal	Kolbano Beds; Australian Margin Megasequence
144875	-8.71393	126.32600	AB280	a.p.	Packstone with mollusc fragments (including *Inoceramus* prisms), Belemnite guard, common calpionellids(?) in fine-grained layers	?Calpionellids (? *Calpionella alpina*)	Possibly latest Jurassic or earliest Cretaceous; middle bathyal to abyssal	Kolbano Beds; Australian Margin Megasequence
144878	-8.72382	126.36608	AB284	mudstone	grey mudstone with common poorly preserved planktonic foraminifera, and rare benthic foraminifera	Planktonic foraminifera: *Globigerina ciperoensis* , *Globigerina praebulloides* , *Globigerina venezuelana*	Late Oligocene; outer neritic or upper bathyal	Booi beds; Banda Terrane

UWA No	Lat	Long	Field Number	Sample type	Rock Description	Age diagnostic fossils	Age and facies	Formation and tectonostratigraphic affinity
144879	-8.73425	126.36128	AB285	a.p.	Wackestone with patches of ooid grainstone (? burrow infill); rare carbonate-cemented agglutinated foraminifera	Foraminifera: ? *Siphovalvulina* sp.	Probably Early Jurassic; innermost neritic	Perdido Group; Gondwana Megasequence
144881	-8.72395	126.35238	AB292	a.p.	Wackestone with rare thaumatoporellacean algae, very rare carbonate-cemented agglutinated foraminifera	Thaumatoporellacean algae: *Thaumatoporella* ?*parvovesiculifera* (micritized). Foraminifera: ? *Siphovalvulina*	Early Jurassic; innermost neritic	Perdido Group; Gondwana Megasequence
144887	-8.72285	126.35013	AB300	a.p.	Ooid peloid grainstone with rare gastropods, thaumatoporellacean algae, carbonate-cemented agglutinated foraminifera	Thaumatoporellacean algae: *Thaumatoporella* ?*parvovesiculifera* (micritized). Foraminifera: ? *Siphovalvulina*	Early Jurassic; innermost neritic	Perdido Group; Gondwana Megasequence
144890	-8.72278	126.34972	AB303	a.p., t.s.	Breccia with two main rock types (A) wackestone with minute planktonic foraminifera (B) peloidal – oolitic grainstone with rare thaumatoporellacean algae	Clast type A: planktonic foraminifera - *Blefuscuiana* sp. or *Hedbergella* sp. *Globigerinelloides* sp.. Clast type B: Thaumatoporellacean algae - *Thaumatoporella* ?*parvovesiculifera*	Clast type A: Early Cretaceous (probably late Aptian – early Albian); Clast type B: Early Jurassic	Synorogenic breccia. Clast type A: Kolbano Beds, Australian Margin Megasequence ; Clast type B: Perdido Group, Gondwana Megasequence
144892	-8.73203	126.34633	AB313	a.p.	Peloidal grainstone with common thaumatoporellacean algae	Thaumatoporellacean algae: *Thaumatoporella* ?*parvovesiculifera* (micritized)	Probably Early Jurassic; innermost neritic	Perdido Group; Gondwana Megasequence

UWA No	Lat	Long	Field Number	Sample type	Rock Description	Age diagnostic fossils	Age and facies	Formation and tectonostratigraphic affinity
144894	-8.73203	126.34633	AB315	a.p.	Wackestone with rare planktonic foraminifera (including keeled forms) and very rare hyaline benthic foraminifera (Lagenidae - *Lenticulina*)	Planktonic foraminifera: *Globotruncana* spp., *Globigerinelloides* sp.	Late Cretaceous (post-Turonian); middle bathyal to abyssal	Kolbano Beds; Australian Margin Megasequence
144895	-8.73203	126.34633	AB316	a.p.	Red packstone with very abundant planktonic foraminifera	Planktonic foraminifera: Morozovella spp. (including M. velascoensis), Acarinina spp.	Late Paleocene or earliest Eocene (within range of Zones P4-E2, Berggren & Pearson et al., 2006); middle bathyal to abyssal	Kolbano Beds; Australian Margin Megasequence
144897	-8.73245	126.34287	AB318	a.p.	Red wackestone with rare poorly preserved planktonic foraminifera	Planktonic foraminifera: poorly preserved keel forms belonging either to *Dicarinella* or *Globotruncana*	Late Cretaceous; middle bathyal to abyssal	Kolbano Beds; Australian Margin Megasequence
144899	-8.73277	126.33938	AB321	a.p.	Wackestone with very rare planktonic foraminifera (deformed, fragmented) and very rare benthic foraminifera (Order Rotaliida)	Planktonic foraminifera: indeterminant keeled globotruncanid. Benthic foraminfiera: *Eponides* -like form	Late Cretaceous; middle bathyal to abyssal	Kolbano Beds; Australian Margin Megasequence
144901	-8.71437	126.35165	AB331	a.p.	Wackestone with rare planktonic foraminifera (large *Globigerina* spp.)	Planktonic foraminifera: *Globigerina yeguaensis* - *Globigerina pseudovenezuelana* - *Globigerina venezuelana* lineage	Probably Oligocene; middle bathyal to abyssal	Kolbano Beds; Australian Margin Megasequence
144902	-8.71470	126.35172	AB332	a.p.	Wackestone with scattered rare planktonic foraminifera (some deformed, fragmented and/or partially silicified)	Planktonic foraminifera: *Globigerina* spp.	Probably Oligocene; middle bathyal to abyssal	Kolbano Beds; Australian Margin Megasequence

UWA No	Lat	Long	Field Number	Sample type	Rock Description	Age diagnostic fossils	Age and facies	Formation and tectonostratigraphic affinity
144903	-8.71165	126.35217	AB334	a.p.	Porous limestone with common benthic foraminifera (mainly Rotaliida including larger types), rare planktonic forms, and coralline algae	Benthic foraminifera: *Nummulites venosus*	Pleistocene; neritic	Baucau Limestone; Synorogenic Megasequence

Additional references (not listed in main reference list of paper):

Adams, C.G., 1970. A reconsideration of the East Indian Letter Classification of the Tertiary. Bulletin of The British Museum (Natural History) Geology, 19, 87-137.

Bolli, H.M. and Saunder, J.B., 1985. Oligocene to Holocene low latitude planktic foraminfiera. In Bolli, H.M., Saunders, J.B., Perch-Nielsen, K. (eds.), Plankton Stratigraphy Volume 1, p. 155-262. Cambridge University Press

Kennett, J.P. and Srinivasan, S., 1983. Neogene Planktonic Foraminifera: A Phylogenetic Atlas. Hutchinson Ross Publishing Company, Stroudsburg, Pennsylvania, 265 p.

Loeblich, A.R.Jr. and Tappan, H., 1987. Foraminiferal Genera and Their Classification. Van Nostrand Reinhold Company, New York, 970 p. ;

Berggren, W.A. and Berggren & Pearson, P.N., 2006. Tropical to subtropical planktonic foraminiferal zonation of the Eocene and Oligocene. Cushman Foundation for Foraminiferal Research Special Publication 41, 29-40.

Supplementary Appendix B: XRF analysis volcanic and metamorphic samples.

Sample	SiO2	Al2O3	CaO	Fe2O3	K2O	MgO	Na2O	P2O5	TiO2	MnO	BaO	SrO	ZrO2	Ni	Nb	Cr2O3	Cu	LOI1000
UNITS	%	%	%	%	%	%	%	%	%	%	ppm	%	ppm	ppm	ppm	ppm	ppm	%
AB093	49	15	10.9	10.1	0.06	8.02	2.98	0.104	1.328	0.24	40	0.03	105	105	30	285	70	2.07
AB186	50.8	10.8	6.83	15.3	0.03	1.95	2.52	0.775	3.076	0.17	50	0.02	655	5	20	-5	20	7.23
AB211	43.2	17.1	14.6	6.23	0.86	3.21	3.09	0.102	0.686	0.29	110	0.04	80	20	30	70	-10	10.1
AB286	13.7	2.79	43.7	1.59	0.18	0.56	0.85	0.055	0.171	0.96	100	0.07	50	10	20	30	-10	35.1
SARM-1	75.7	12.1	0.78	2	4.99	0.06	3.36	0.007	0.089	0.02	130		410	10	50	35		
STD 1.1	75.7	12.1	0.77	1.96	4.94	0.06	3.32	0.007	0.09	0.02	140	-0.01	390	10	60	30	-10	
LOI std 1																		1.34
STD 1.2																		1.36
AB319	57.2	9.33	10.6	6.13	0.31	2.02	2.6	0.08	0.358	0.29	440	0.05	115	30	20	95	-10	10.4
AB329	71	11.1	0.7	6.96	0.38	2.8	2.77	0.11	0.568	0.05	120	0.02	180	95	30	410	-10	3.15
AB329 Rpt	70.9	11.1	0.69	6.95	0.38	2.8	2.77	0.11	0.569	0.05	120	0.02	170	100	30	410	-10	3.15
SARM-2	63.6	17.3	0.68	1.4	15.3	0.46	0.43	0.12	0.043	-0.01	2700		35	5	-10	35	20	
STD 2.1	63.5	17.3	0.67	1.39	15.2	0.46	0.44	0.116	0.043	-0.01	2740	0.01	35	10	20	30	20	
LOI std 2																		5.67
STD 2.2																		5.69
SARM-3	52.4	13.6	3.22	9.91	5.51	0.28	8.37	0.055	0.48	0.77	500	0.54	14900	30	980	15	20	
STD 3.1	52.4	13.6	3.23	9.9	5.48	0.29	8.41	0.053	0.477	0.79	480	0.55	15100	25	990	20	20	
LOI std 3																		10.3
STD 3.2																		10.4
CanMet Ta	74																	
STD 4.1	73.8	14.8	0.37	0.37	1.71	0.06	6.04	0.404	0.022	0.04	80	-0.01	15	-5	180	5	-10	
LOI std 1(2																		1.34
STD 4.2																		1.35
French Iror	16.8	4.27	9.62	43.7	0.21	3.32	0.11	1.4	0.198	0.61	220		160	140		130	20	
STD 5.1	16.8	4.24	9.56	43.8	0.2	3.24	0.13	1.41	0.193	0.62	200	0.04	155	135	20	125	30	
LOI std 2(2																		5.67
STD 5.2																		5.71
SARM 40	3.08	0.41	49.8	2.75	0.03	1.97	0.05	2.05	0.05	0.18								
STD 6.1	3	0.39	50	2.7	0.02	1.94	0.05	2.01	0.047	0.19	510	0.2	125	25	-10	55	-10	
SARM 39 K	33.4	4.29	9.69	9.29	1.04	26.2	0.63	1.46	1.58	0.17	1900	0.17	285	985	110	1810	60	
STD 7.1	33.5	4.24	9.72	9.32	1.06	26.3	0.64	1.47	1.614	0.18	1890	0.18	295	990	100	1830	60	
Sarm-4 No	52.7	16.5	11.5	8.97	0.25	7.5	2.46	0.015	0.2	0.18	110	0.03	35	120		45	10	
STD 8.1	52.6	16.5	11.5	8.94	0.24	7.47	2.44	0.013	0.194	0.19	120	0.03	25	125	10	40	-10	

Sample Preparation

No sample preparation was required on these samples.

Analytical Methods

The samples have been cast using a 12:22 flux to form a glass bead which has been analysed by XRF. Sample to flux ratios and instrument counting times have been adjusted to enhance sensitivity of some elements.

SiO2, Al2O3, CaO, Fe2O3, K2O, MgO, Na2O, P2O5, TiO2, MnO, BaO, SrO, ZrO2, Ni
Nb, Cr2O3, Cu
have been determined by X-Ray Fluorescence Spectrometry

Loss on Ignition has been determined between 105 and 1000 degrees celsius. Results are reported on a dry sample basis.

LOI1000
has been determined Gravimetrically

All

Al2O3	CaO	Fe2O3	K2O	MgO	Na2O	P2O5	TiO2	MnO	BaO	SrO	ZrO2	Ni	Nb	Cr2O3	Cu	LOI1000
%	%	%	%	%	%	%	%	%	ppm	%	ppm	ppm	ppm	ppm	ppm	%
15	10.9	10.1	0.06	8.02	2.98	0.104	1.328	0.24	40	0.03	105	105	30	285	70	2.07
10.8	6.83	15.3	0.03	1.95	2.52	0.775	3.076	0.17	50	0.02	655	5	20	-5	20	7.23
17.1	14.6	6.23	0.86	3.21	3.09	0.102	0.686	0.29	110	0.04	80	20	30	70	-10	10.1
2.79	43.7	1.59	0.18	0.56	0.85	0.055	0.171	0.96	100	0.07	50	10	20	30	-10	35.1
9.33	10.6	6.13	0.31	2.02	2.6	0.08	0.358	0.29	440	0.05	115	30	20	95	-10	10.4
11.1	0.69	6.95	0.38	2.8	2.77	0.11	0.569	0.05	120	0.02	170	100	30	410	-10	3.15

Major(ox%)

Sample	SiO2	Al2O3	CaO	Fe2O3	K2O	MgO	Na2O	P2O5	TiO2	MnO	LOI	Sum of Maj	Maj+LOI		
UNITS	%	%	%	%	%	%	%	%	%	%	%				
AB093	49	15	10.9	10.1	0.06	8.02	2.98	0.104	1.328	0.24	2.07	97.732	99.802	50.03784	1.02118
AB186	50.8	10.8	6.83	15.3	0.03	1.95	2.52	0.775	3.076	0.17	7.23	92.251	99.481		
AB211	43.2	17.1	14.6	6.23	0.86	3.21	3.09	0.102	0.686	0.29	10.1	89.368	99.468		
AB286	13.7	2.79	43.7	1.59	0.18	0.56	0.85	0.055	0.171	0.96	35.1	64.556	99.656		
AB319	57.2	9.33	10.6	6.13	0.31	2.02	2.6	0.08	0.358	0.29	10.4	88.918	99.318		
AB329	70.9	11.1	0.69	6.95	0.38	2.8	2.77	0.11	0.569	0.05	3.15	96.319	99.469		

LOI Normalised

UNITS	%	%	%	%	%	%	%	%	%	%	%						
Sample	**SiO2**	**Al2O3**	**CaO**	**Fe2O3**	**K2O**	**MgO**	**Na2O**	**P2O5**	**TiO2**	**MnO**	**Total**	**TAS class**	**Ti/Zr no.**	**Ti/Zr class**	Na2O+K2O	Na2O+K2O-CaO	Fe/MgO	
AB093	50.03784	15.31771	11.13087	10.31392	0.061271	8.189867	3.043118	0.106203	1.356128	0.245083	99.802	basalt			3.104388	-8.02648		1.259352
AB186	54.78136	11.64643	7.365289	16.49911	0.032351	2.102828	2.7175	0.835739	3.317076	0.183323	99.481	basaltic andesite			2.749851	-4.61544		7.846154
AB211	48.08228	19.03257	16.25003	6.934089	0.957194	3.572781	3.439219	0.113528	0.763529	0.322775	99.468	basalt			4.396413	-11.8536		1.94081
AB286	21.14888	4.306962	67.4603	2.454505	0.277869	0.86448	1.312157	0.084904	0.263975	1.481965	99.656				1.590025	-65.8703		2.839286
AB319	63.89021	10.42125	11.83979	6.846975	0.346258	2.256263	2.9041	0.089357	0.399872	0.323919	99.318	dacite			3.250359	-8.58944		3.034653
AB329	73.2187	11.46301	0.712566	7.177292	0.392427	2.891571	2.86059	0.113597	0.587608	0.051635	99.469	dacite			3.253017	2.540451		2.482143

Sample	AB093	AB186	AB211	AB286	AB319	AB329
SiO2	50.03784	54.78136	48.08228	21.14888	63.89021	73.2187
Al2O3	15.31771	11.64643	19.03257	4.306962	10.42125	11.46301
CaO	11.13087	7.365289	16.25003	67.4603	11.83979	0.712566
Fe2O3	10.31392	16.49911	6.934089	2.454505	6.846975	7.177292
K2O	0.061271	0.032351	0.957194	0.277869	0.346258	0.392427
MgO	8.189867	2.102828	3.572781	0.86448	2.256263	2.891571
Na2O	3.043118	2.7175	3.439219	1.312157	2.9041	2.86059
P2O5	0.106203	0.835739	0.113528	0.084904	0.089357	0.113597
TiO2	1.356128	3.317076	0.763529	0.263975	0.399872	0.587608
MnO	0.245083	0.183323	0.322775	1.481965	0.323919	0.051635

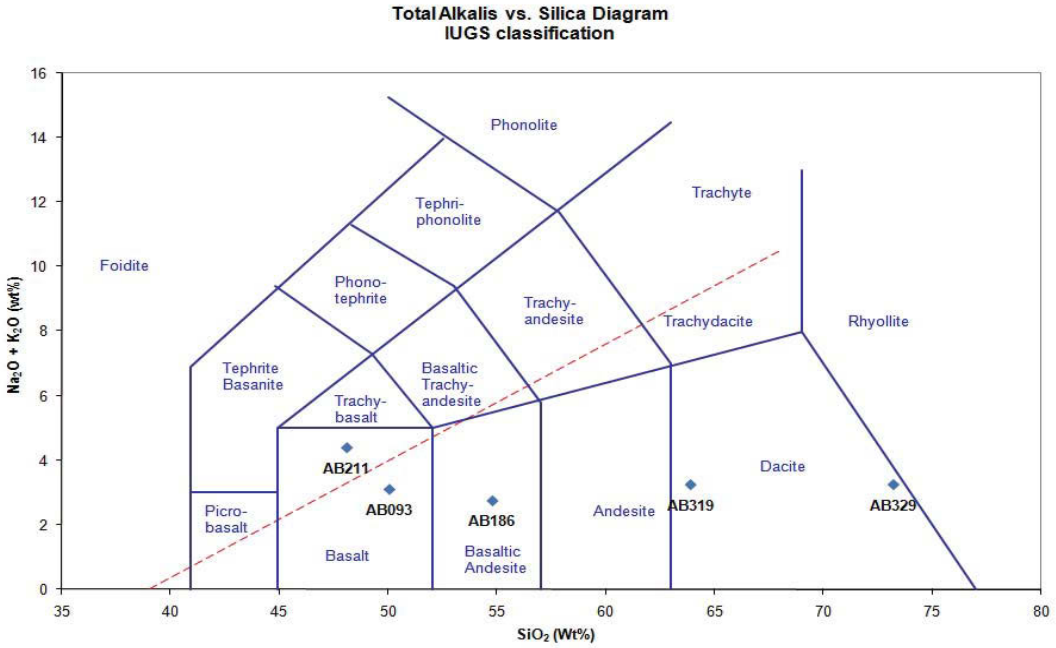

MgO plots

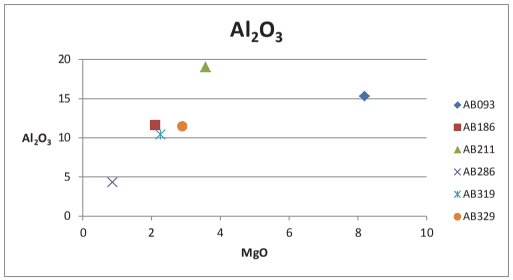

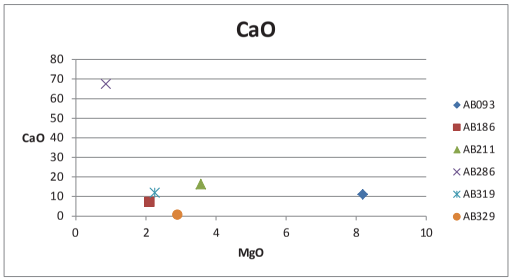

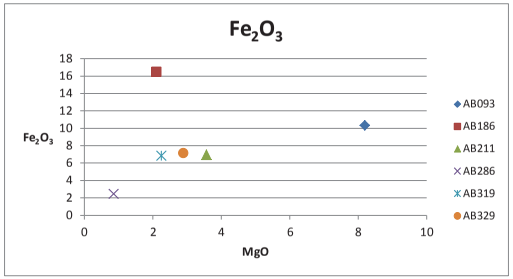

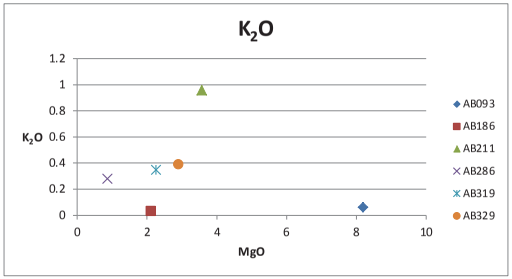

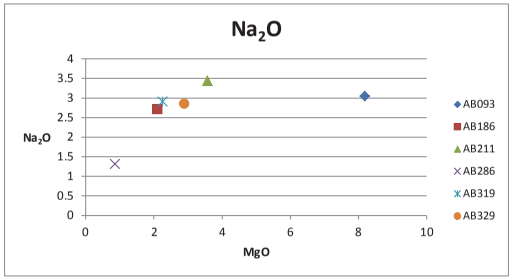

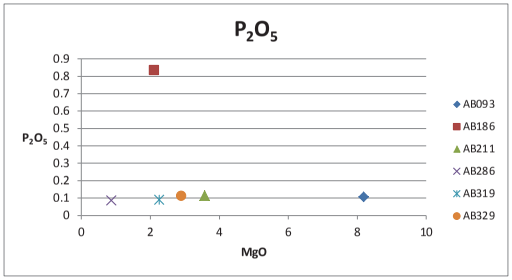

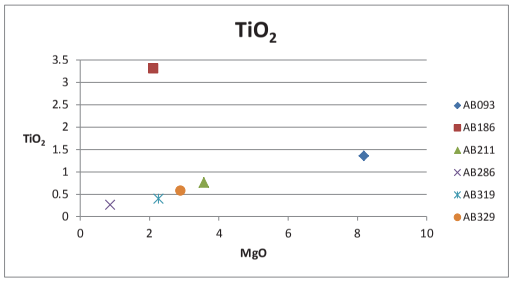

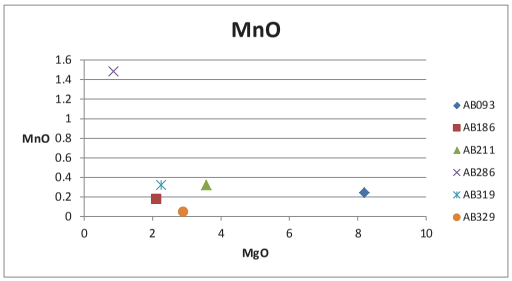

AB093 4x

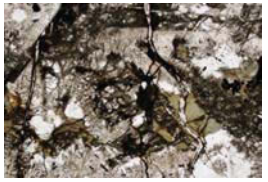

AB186 4x

AB211 4x

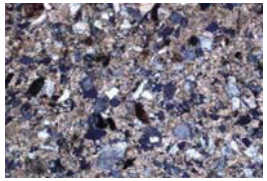

AB286 10x

AB319 10x

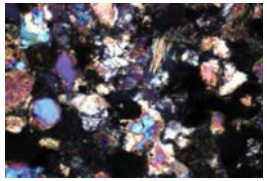

AB329 10x

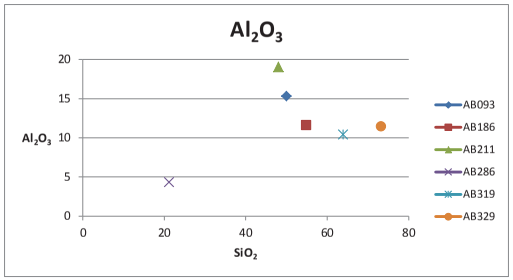
Al2O3
20
15
10
5
0
Al2O3
0
20
40
60
80
SiO2
AB093
AB186
AB211
AB286
AB319
AB329

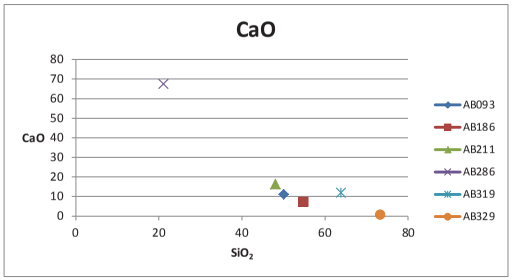
CaO
80
70
60
50
40
30
20
10
0
CaO
0
20
40
60
80
SiO2
AB093
AB186
AB211
AB286
AB319
AB329

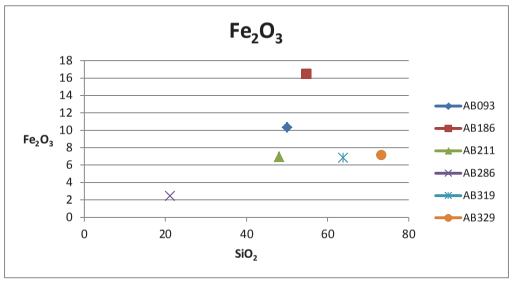
Fe2O3
18
16
14
12
10
8
6
4
2
0
Fe2O3
0
20
40
60
80
SiO2
AB093
AB186
AB211
AB286
AB319
AB329

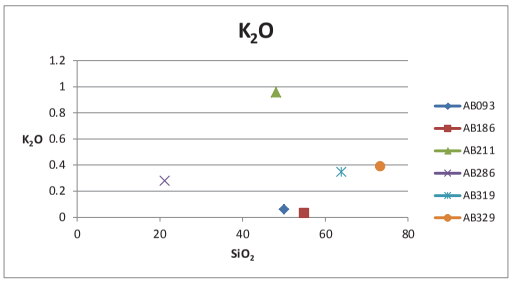
K2O
1.2
1
0.8
0.6
0.4
0.2
0
K2O
0
20
40
60
80
SiO2
AB093
AB186
AB211
AB286
AB319
AB329

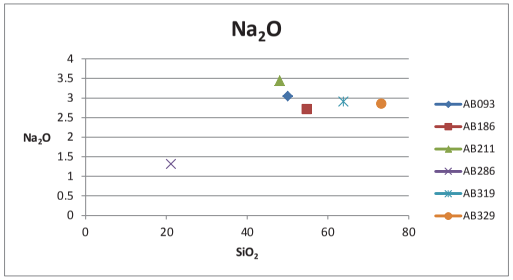
Na2O
4
3.5
3
2.5
2
1.5
1
0.5
0
Na2O
0
20
40
60
80
SiO2
AB093
AB186
AB211
AB286
AB319
AB329

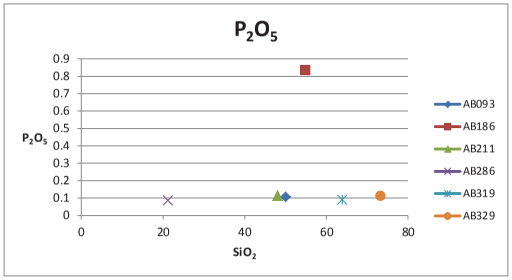
P2O5
0.9
0.8
0.7
0.6
0.5
0.4
0.3
0.2
0.1
0
P2O5
0
20
40
60
80
SiO2
AB093
AB186
AB211
AB286
AB319
AB329

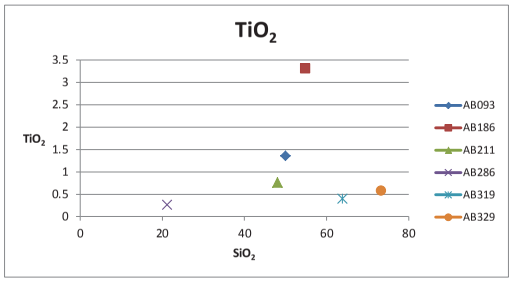
TiO2
3.5
3
2.5
2
1.5
1
0.5
0
TiO2
0
20
40
60
80
SiO2
AB093
AB186
AB211
AB286
AB319
AB329

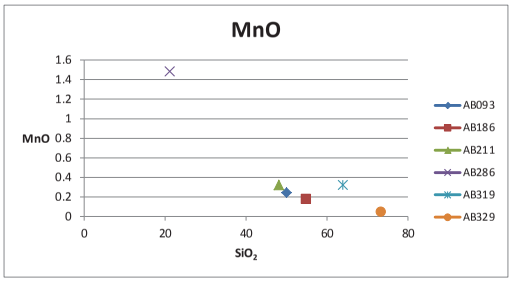
MnO
1.6
1.4
1.2
1
0.8
0.6
0.4
0.2
0
MnO
0
20
40
60
80
SiO2
AB093
AB186
AB211
AB286
AB319
AB329

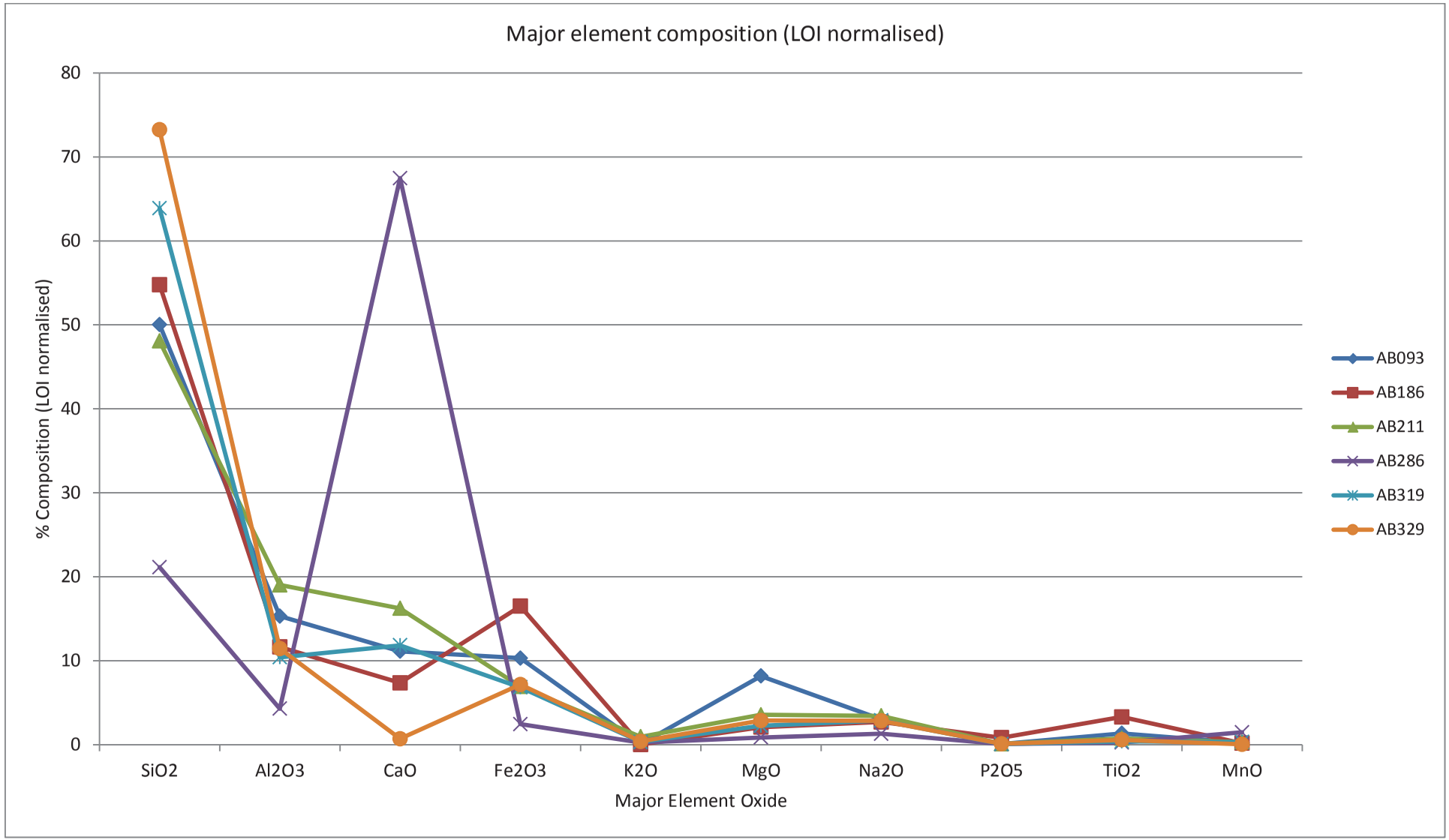
Major element composition (LOI normalised)
% Composition (LOI normalised)
80
70
60
50
40
30
20
10
0
SiO2
Al2O3
CaO
Fe2O3
K2O
MgO
Na2O
P2O5
TiO2
MnO
Major Element Oxide
AB093
AB186
AB211
AB286
AB319
AB329

Minor(ppm)

UNITS	ppm	ppm	ppm	ppm	ppm	ppm	ppm	ppm	Ti/Zr	Ti/Zr	Zr/Ti	Zr/Nb
Sample	Ni	Cu	Cr	Ba	Nb	Sr	Zr	Ti				
AB093	105	70	195	36	30	254	78	8130.12	104.5909	basalt	0.009561	2.591085
AB186	5	20		45	20	169	485	19886.2	41.01067	andesite	0.024384	24.24515
AB211	20		48	98	30	338	59	4577.432	77.28911	basalt	0.012938	1.97416
AB286	10		21	90	20	592	37	1582.557	42.7539	andesite	0.02339	1.850775
AB319	30		65	394	20	423	85	2397.274	28.15829	andesite	0.035514	4.256783
AB329	100		281	107	30	169	126	3522.772	27.99123	andesite	0.035725	4.19509
N-MORB				6	2	90	74	7600	102.7027		0.009737	31.75966
E-MORB				57	8	155	73	6000	82.19178		0.012167	8.795181
OIB				350	48	660	280	17200	61.42857		0.016279	5.833333

Chondrite	11000.000	126.000	2660.000	2.340	0.246	7.800	3.940	Anders E. and Grevesse N. (1989)

"Abundances of the elements: Meteoritic and solar"
Geochimica et Cosmochimica Acta **53**, 197-214.

Rock/Chondrite	Ni	Cu	Cr	Ba	Nb	Sr	Zr
AB093	0.010	0.556	0.073	15.305	121.951	32.523	19.729
AB186	0.000	0.159		19.131	81.301	21.682	123.072
AB211	0.002		0.018	42.089	121.951	43.364	15.032
AB286	0.001		0.008	38.262	81.301	75.886	9.395
AB319	0.003		0.024	168.355	81.301	54.204	21.608
AB329	0.009		0.105	45.915	121.951	21.682	31.942
N-MORB				2.692	9.472	11.538	18.782
E-MORB				24.359	33.740	19.872	18.528
OIB				149.573	195.122	84.615	71.066

"Mean C1 Chondr." of Table 1

Primitive Mantle	1960.000	30.000	2625.000	6.600	0.658	19.900	10.500	M&S 1995

Rock/Primitive Mantle	Ni	Cu	Cr	Ba	Nb	Sr	Zr
AB093	0.054	2.333	0.074	5.426	45.593	12.748	7.403
AB186	0.003	0.667		6.783	30.395	8.498	46.181
AB211	0.010		0.018	14.922	45.593	16.997	5.640
AB286	0.005		0.008	13.566	30.395	29.744	3.525
AB319	0.015		0.025	59.689	30.395	21.246	8.108
AB329	0.051		0.107	16.279	45.593	8.498	11.986
N-MORB				0.955	3.541	4.523	7.048
E-MORB				8.636	12.614	7.789	6.952
OIB				53.030	72.948	33.166	26.667

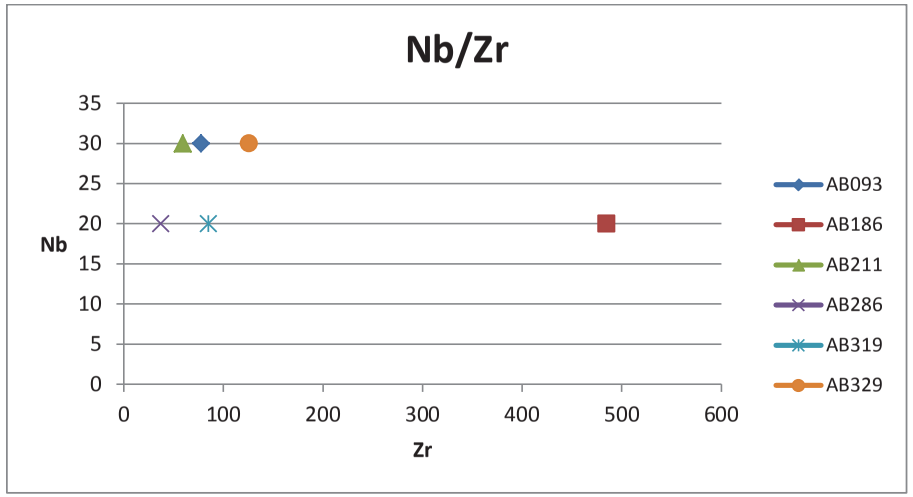
Nb/Zr
Nb
Zr
0
5
10
15
20
25
30
35
0
100
200
300
400
500
600
AB093
AB186
AB211
AB286
AB319
AB329

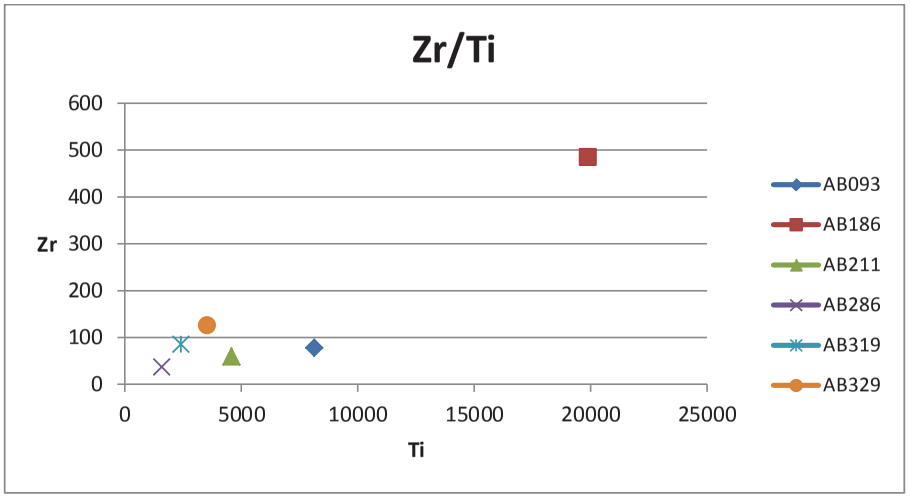
Zr/Ti
Zr
Ti
0
100
200
300
400
500
600
0
5000
10000
15000
20000
25000
AB093
AB186
AB211
AB286
AB319
AB329

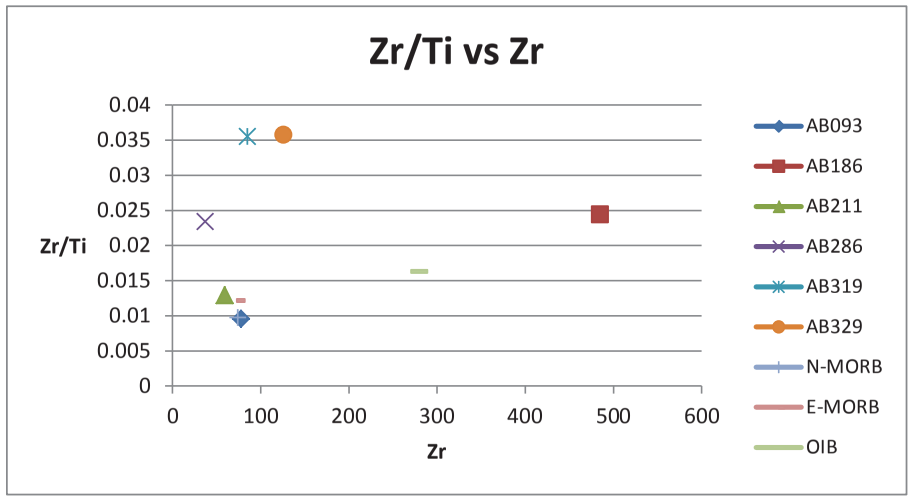
Zr/Ti vs Zr
Zr/Ti
Zr
0
0.005
0.01
0.015
0.02
0.025
0.03
0.035
0.04
0
100
200
300
400
500
600
AB093
AB186
AB211
AB286
AB319
AB329
N-MORB
E-MORB
OIB

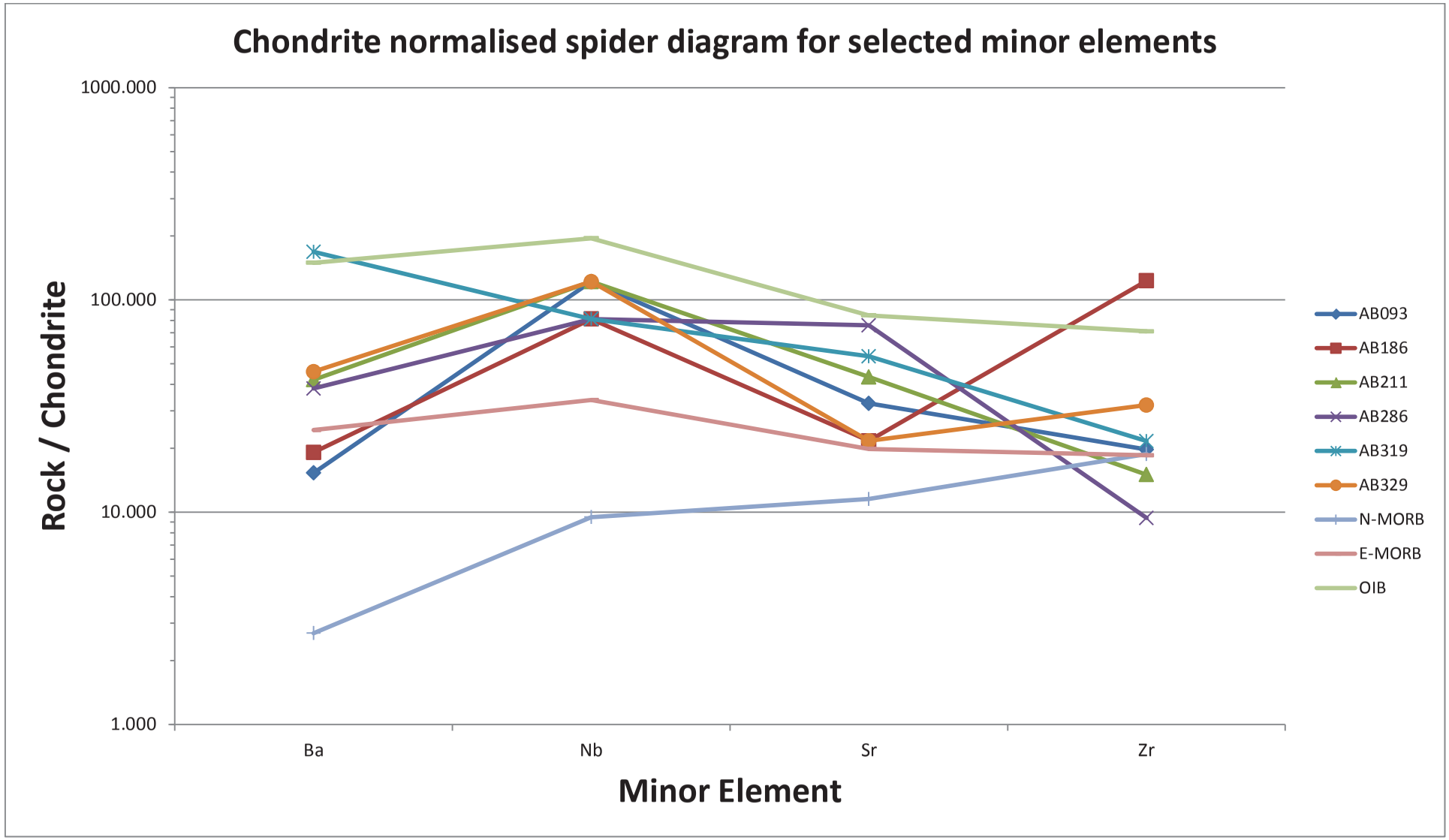
Chondrite normalised spider diagram for selected minor elements
1000.000
100.000
10.000
1.000
Rock / Chondrite
Ba
Nb
Sr
Zr
Minor Element
AB093
AB186
AB211
AB286
AB319
AB329
N-MORB
E-MORB
OIB

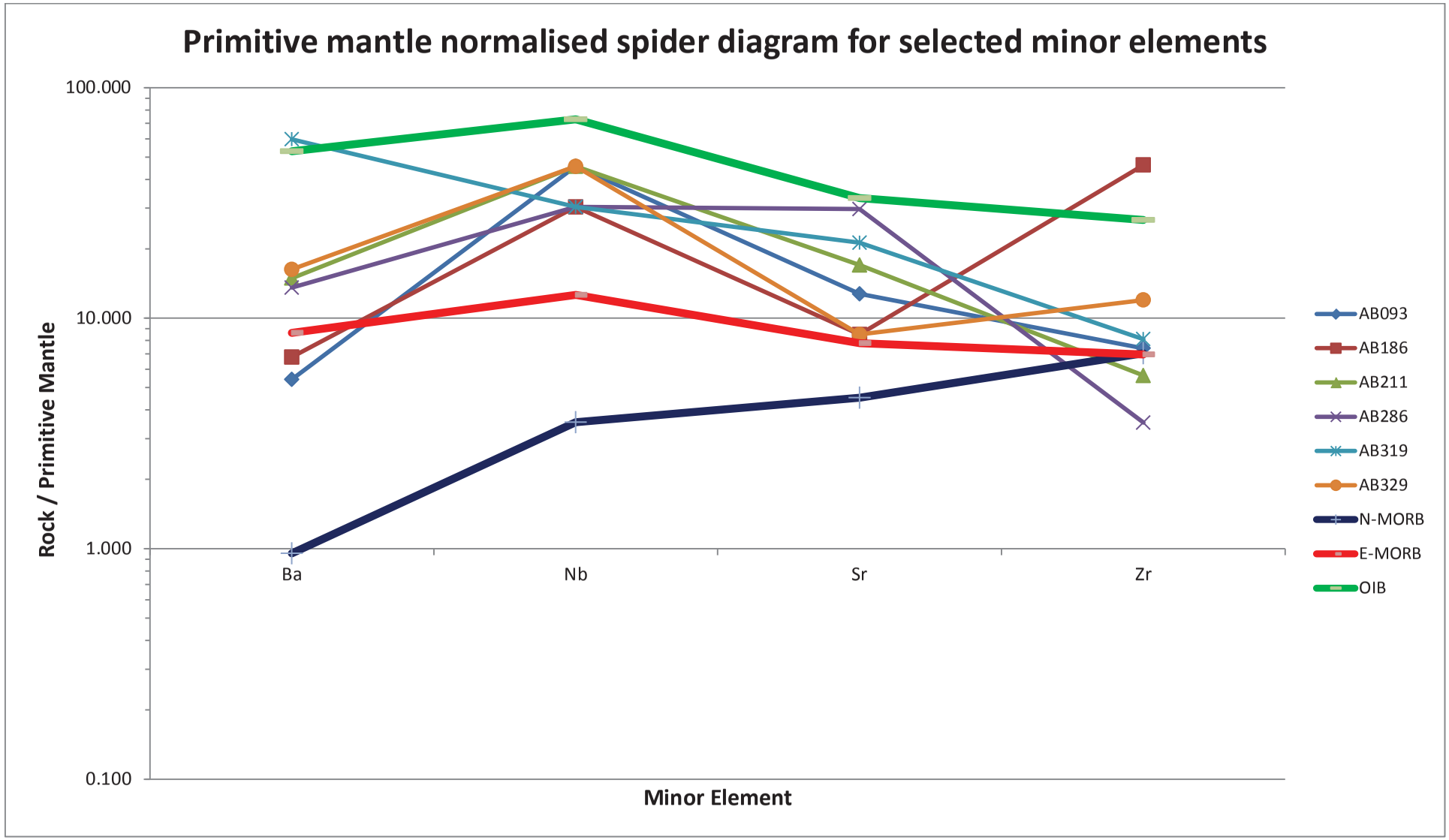
Primitive mantle normalised spider diagram for selected minor elements
100.000
10.000
1.000
0.100
Rock / Primitive Mantle
Ba
Nb
Sr
Zr
Minor Element
AB093
AB186
AB211
AB286
AB319
AB329
N-MORB
E-MORB
OIB

Minor(working)

Sample	SrO	Sr	Sr	BaO	Ba	Nb	ZrO2	Zr	Ni	Cr2O3	Cr	Cu	TiO2	Ti	Ti
UNITS	%	%	ppm	ppm	ppm	ppm	ppm	ppm	ppm	ppm	ppm	ppm	%	%	ppm
AB093	0.03	0.025368	253.677	40	35.8136	30	105	77.73255	105	285	194.997	70	1.356128	0.813012	8130.12
AB186	0.02	0.016912	169.118	50	44.767	20	655	484.9031	5	-5	-3.421	20	3.317076	1.98862	19886.2
AB211	0.04	0.033824	338.236	110	98.4874	30	80	59.2248	20	70	47.894	-10	0.763529	0.457743	4577.432
AB286	0.07	0.059191	591.913	100	89.534	20	50	37.0155	10	30	20.526	-10	0.263975	0.158256	1582.557
AB319	0.05	0.04228	422.795	440	393.9496	20	115	85.13565	30	95	64.999	-10	0.399872	0.239727	2397.274
AB329	0.02	0.016912	169.118	120	107.4408	30	170	125.8527	100	410	280.522	-10	0.587608	0.352277	3522.772

AFM data

UNITS	%	%	%	%	%	%
Sample	Fe2O3	MgO	Na2O+K2O	Na2O	K2O	Total
AB093	10.31392	8.189867	3.104388327	3.043118	0.061271	21.60818
AB186	16.49911	2.102828	2.749851492	2.7175	0.032351	21.35179
AB211	6.934089	3.572781	4.396412586	3.439219	0.957194	14.90328
AB286	2.454505	0.86448	1.590025404	1.312157	0.277869	4.90901
AB319	6.846975	2.256263	3.250358533	2.9041	0.346258	12.3536
AB329	7.177292	2.891571	3.253017058	2.86059	0.392427	13.32188

AFM	F	M	A	
UNITS	%	%	%	%
Sample	Fe2O3	MgO	Na2O+K2O	Total
AB093	47.73157	37.9017	14.36672968	100
AB186	77.27273	9.848485	12.87878788	100
AB211	46.52726	23.97311	29.49962659	100
AB286	50	17.61006	32.38993711	100
AB319	55.42495	18.26401	26.31103074	100
AB329	53.87597	21.70543	24.41860465	100

	%	%	
Fe2O3x0.9	MgO	Na2O+K2O	Total
9.28252957	8.1898666	3.104388	20.5767845
14.8491981	2.1028276	2.749851	19.7018772
6.24067984	3.5727809	4.396413	14.2098733
2.20905471	0.8644798	1.590025	4.66355995
6.16227767	2.2562626	3.250359	11.6688988
6.45956244	2.8915707	3.253017	12.6041502

AFM	F	M	A	
UNITS	%	%	%	%
Sample	Fe2O3x0.9	MgO	Na2O+K2O	Total
AB093	45.111663	39.80149	15.0868486	100
AB186	75.369458	10.67323	13.9573071	100
AB211	43.917913	25.14295	30.93914	100
AB286	47.368421	18.53691	34.0946706	100
AB319	52.809419	19.33569	27.8548866	100
AB329	51.249488	22.94142	25.8090946	100